# Measurement of Gas Composition using Ultrasonic Sensors

**Sihe Wang**

**September, 2017**

**Supervised by: Dr. Daryl R. Williams**

A Thesis Submitted for the Imperial College Degree of Doctor of Philosophy (Ph.D.)

Department of Chemical Engineering

Imperial College London

SW7 2AZ

# Declaration of Originality

I hereby declare that this thesis has been written solely by myself and that it has not been submitted in any previous application for a degree.

I certify that the work in this thesis is entirely my own unless explicitly acknowledged and referenced.

07 September 2017

# Copyright Declaration

The copyright of this thesis rests with the author and is made available under a Creative Commons Attribution Non-Commercial No Derivatives licence. Researchers are free to copy, distribute or transmit the thesis on the condition that they attribute it, that they do not use it for commercial purposes and that they do not alter, transform or build upon it. For any reuse or redistribution, researchers must make clear to others the licence terms of this work.

# Acknowledgements

I would like to express my heartfelt appreciation to my supervisor, Dr. Daryl Williams, for providing me an opportunity to conduct this research, and for all his advice, encouragement and help. I would also like to thank the engineers of Surface Measurement Systems (SMS) Ltd. for their contributions to this project, including Dirk Bruere (electronics and firmware), Paul Collins (mechanical engineering) and Christopher Cawe (PC interface software). I acknowledge the suggestions and assistance given by Prof. Martin Trusler who is my academic mentor. Valuable technical assistance in temperature calibration was provided by Dr. Emmanuel Efika. Sincere thanks are also given to many other members of the Department of Chemical Engineering at Imperial College London and also of SMS Ltd. for the cooperation and advice that I have received.

I am grateful for the financial support of Imperial College London and the China Scholarship Council.

Finally, I would like to sincerely thank my parents, parents-in-law and my wife for their continual encouragement and support during my study in the UK.

# Abstract

An improved experimental apparatus for measuring the speed of sound (SoS) of binary gas mixtures using a single acoustic sensor in an on-line mode is described in this thesis. The SoS sensor has a fixed acoustic path and is operated at a fixed frequency of 121362 Hz. A pair of piezoelectric transducers are used in the sensor as the ultrasound pulse transmitter and receiver, respectively. A single-pulse time of flight (ToF) based approach with a novel wave interpolation algorithm allowed the SoS to be resolved typically better than 1 part in 500,000 at one second measurement intervals. Suitability for precise rapid on-line measurement and simplicity are the two most important factors considered in the selection of SoS determination method.

Real gas SoS is functionally dependent upon gas composition, temperature, pressure and acoustic frequency, which is the fundamental principle of the SoS technique for measuring the composition of binary gas mixtures.

Pure reference gases including Ar, He and $N_2$ were used in the experiment for analysing the SoS measurement uncertainty. For $CO_2/N_2$, the experimental $CO_2$ mole fraction ranged from 0 to 0.3 and the uncertainty[1] of the measured SoS results was estimated to be 0.1%. For any other tested binary gas mixture which consists of water vapour or an organic vapour, including n-hexane, n-heptane, n-octane, n-nonane, n-decane, toluene, cyclohexane, acetone, methyl ethyl ketone, ethyl acetate, methanol, ethanol, isopropanol, dichloromethane, chloroform, 1,2-dichloroethane, m-/o-/p-xylene, ethylbenzene, n-butylamine, limonene and α-pinene, as one component and dry air as the other, the mole fraction of the vapour component in the experiments was in the range from 0 to 95% of the saturated vapour mole fraction (0 to

[1] In this thesis, unless specially noted, uncertainties all refer to the standard uncertainty with a confidence level of 68%.

95%SAT), and the SoS measurement uncertainty was estimated to be 0.14%. The experimental temperature range was from 5 to 55 °C, and each experiment was performed isothermally under atmospheric pressure. The temperature of the gas in the acoustic cavity of the SoS sensor can be measured with an uncertainty of 12.5 m°C by using the calibrated SoS sensor's PT100. With the use of a barometric sensor mounted in the SoS sensor electronics board, a measurement of atmospheric pressure with 0.75 mbar uncertainty can be achieved. The carrier gas, $N_2$ or dry air, was employed as the reference gas in each isothermal experiment for the calibration of the acoustic pathlength.

The true gas composition of the binary gas mixtures was determined using a novel gas density measurement based on Archimedes' Principle. The relationships between gas composition and density was established with an equation of state analysis using the Helmholtz equations stored in the NIST REFPROP software or the Van der Waals equation. Mixture density was measured with an uncertainty of 0.0015 kg/m$^3$. A plot of measured SoS versus composition under different isothermal conditions is given for each investigated mixture.

The deviation between the lossless real gas SoS determined using the NIST REFPROP software and the measured SoS was analysed for the mixtures with available thermodynamic data in the software including $CO_2/N_2$ and n-hexane, n-heptane, n-octane, n-nonane, n-decane, toluene, cyclohexane, water/dry air. Since $CO_2$ is a strongly dispersive gas, the deviation for $CO_2/N_2$ is large and the maximum deviation reaches about 1.8%. For the other mixtures the deviation is below 0.5% and is reasonably small.

By correlating the measured composition with SoS and temperature, SoS measurements allow rapid and real time gas composition determinations. Under atmospheric pressure and within the respective experimental composition ranges, for example for $CO_2/N_2$ at temperatures from 10 to 50 °C, SoS based technique is able to give compositions with an uncertainty of 0.0006 in

mole fraction; for n-heptane/dry air mixtures at temperatures from 25 to 55 °C the uncertainty is between 0.16 and 0.40%SAT.

This thesis also reports the most complete set of SoS data for organic vapour/dry air mixtures yet reported, including twenty-three different organic solvents across a range of temperatures, typically 5 to 55 °C.

This study confirmed the versatility of SoS (ToF) ultrasonic measurements for the rapid and accurate composition measurement of binary gas mixtures for potential deployment in industrial or scientific instrumentation. Manufacture of the SoS sensor is practicable, and the difference in composition measurement uncertainty between a manufactured sensor and the prototype sensor used in this project should be negligible. In comparison with traditional gas composition measurement techniques, this technique is not only robust but also has the potential to be faster, simpler, more cost-effective, more precise and more accurate.

# Table of Contents

List of Symbols ..... 12
List of Abbreviations ..... 18
List of Tables ..... 20
List of Figures ..... 24
CHAPTER 1. Introduction ..... 27
1.1 Overview ..... 27
1.2 Objectives ..... 29
CHAPTER 2. Literature Review and Basic Theories ..... 30
2.1 Traditional On-Line Gas Composition Measurement Techniques ..... 30
2.1.1 Capacitive Humidity Sensors ..... 30
2.1.2 Dew Point Analysers ..... 31
2.1.3 Thermal Conductivity Detectors ..... 33
2.1.4 Flame Ionisation Detectors ..... 35
2.1.5 Fourier Transform Infrared Spectrometers ..... 37
2.1.6 Near-Infrared Spectrometers ..... 39
2.1.7 Summary of the Typical Characteristics of Different On-Line Gas Composition Measurement Techniques ..... 41
2.2 Equations of State (EoSs) for Gases ..... 43
2.2.1 Ideal Gas Law (Ideal Gas EoS) ..... 43
2.2.2 Virial EoS ..... 43
2.2.3 Van Der Waals EoS ..... 44
2.2.4 Basic Mixing Rules ..... 44
2.2.5 H-EoSs for Pure Gases ..... 46
2.2.6 H-EoSs for Gas Mixtures ..... 48
2.3 Fundamental Theory of Speed of Sound ..... 52
2.3.1 The Linearised Propagation of Plane Sound Waves in Non-Dissipative Fluids ..... 52
2.3.2 Ideal Gas and Lossless Real Gas SoS ..... 57
2.3.3 Relaxation Phenomena and Real Gas SoS ..... 59
2.3.3.1 Vibrational and Rotational Relaxation ..... 60
2.3.3.2 Chemical and Structural Relaxation ..... 61
2.3.3.3 Translational Relaxation ..... 62
2.3.4 Summary ..... 62
2.4 SoS Measurement Methods ..... 64

2.4.1 ToF Method ..... 64
2.4.1.1 Ultrasonic Transducers ..... 64
2.4.1.2 Theory for SoS Determination Using ToF Method ..... 65
2.4.1.3 SoS Sensors Based on ToF Method ..... 66
2.4.1.4 Signal Analysis Methods for ToF Determination ..... 67
2.4.1.5 SoS Measurement Error Using ToF Method ..... 70
2.4.1.6 Other Typical Pulse Methods ..... 72
2.4.2 Acoustic Resonance Method ..... 76
2.4.2.1 Spherical Acoustic Resonator ..... 76
2.4.2.2 Cylindrical Acoustic Resonator ..... 79
2.4.3 Interferometry Method ..... 80
2.5 Review of SoS Measurements for Pure Gases ..... 83
2.6 Review of SoS Measurements for Binary Gas Mixtures ..... 88
2.6.1 ToF Method ..... 88
2.6.2 Acoustic Resonance Method and Interferometry Method ..... 92
2.7 Comparisons of Different SoS Measurement Methods ..... 94
CHAPTER 3. Experimental Methods ..... 96
3.1 Mechanical Design for the SoS Sensor ..... 96
3.2 Electronics Design for the SoS Sensor ..... 97
3.3 ToF Signal Analysis Algorithm ..... 99
3.4 Experimental Setup ..... 102
3.5 Temperature Calibration ..... 106
3.6 Microbalance Calibration and Stability Check ..... 108
3.7 Volume Difference Measurement ..... 109
3.8 Experimental Procedure ..... 109
3.9 Materials ..... 115
3.10 Pathlength Calibration ..... 117
CHAPTER 4. Results ..... 118
4.1 Typical Raw Experimental Data for Mass Readings and Measured ToF ..... 118
4.2 Representation of the Experimental Results ..... 120
4.3 Experimental Results ..... 120
CHAPTER 5. Discussion ..... 148
5.1 SoS Measurement Uncertainty and Rate of Change in Pathlength with Temperature ..... 148
5.2 SoS Comparisons ..... 150
5.3 Uncertainty Analysis of Gas Density and Composition Experimental Results ..... 162
5.3.1 Binary Gas Mixtures in Group A ..... 162

5.3.2 Binary Gas Mixtures in Group B ..... 163
5.4 Gas Composition Measurement with an SoS Sensor ..... 165
CHAPTER 6. Conclusions ..... 194
CHAPTER 7. Future Work ..... 198
References ..... 200
Appendix ..... 210
A1. Determination of Real Gas SoS ..... 210
A1.1 Real Gas SoS of Argon and Helium ..... 210
A1.2 Real Gas SoS of Nitrogen ..... 211
A1.3 Real Gas SoS of Dry Air ..... 213
A1.3.1 Ideal Gas SoS of Standard Dry Air ..... 214
A1.3.2 Virial Correction Factor and Lossless Real Gas SoS of Standard Dry Air ..... 215
A1.3.3 Dispersion Correction Factor and Real Gas SoS of Standard Dry Air ..... 216
A1.3.4 Uncertainty Analysis for Real Gas SoS of Standard Dry Air ..... 218
A1.3.5 Real Gas SoS of Experimental Dry Air ..... 219
A2. Photos of Experimental System and SoS sensor ..... 221
A3. Measurement Precision of SoS Sensor ..... 224
A4. Determination of Volume Difference ..... 228
A5. Property Parameters ..... 230
A6. Results ..... 232
A6.1 n-Hexane/dry air ..... 233
A6.2 n-Octane/dry air ..... 239
A6.3 n-Nonane/dry air ..... 246
A6.4 n-Decane/dry air ..... 252
A6.5 Toluene/dry air ..... 256
A6.6 Cyclohexane/dry air ..... 263
A6.7 Water/dry air ..... 269
A6.8 Acetone/dry air ..... 273
A6.9 Methyl ethyl ketone/dry air ..... 278
A6.10 Ethyl acetate/dry air ..... 285
A6.11 Methanol/dry air ..... 292
A6.12 Ethanol/dry air ..... 298
A6.13 Isopropanol/dry air ..... 305
A6.14 Dichloromethane/dry air ..... 312
A6.15 Chloroform/dry air ..... 315
A6.16 1,2-Dichloroethane/dry air ..... 320

A6.17 m-Xylene/dry air ..... 327
A6.18 o-Xylene/dry air ..... 330
A6.19 p-Xylene/dry air ..... 333
A6.20 Ethylbenzene/dry air ..... 336
A6.21 n-Butylamine/dry air ..... 339
A6.22 Limonene/dry air ..... 342
A6.23 α-Pinene/dry air ..... 345

# List of Symbols

| | |
|---|---|
| $A_c$ | Coefficient in the Callendar-Van Dusen equation |
| $a$ | Parameter in the Van der Waals equation of state |
| $B_c$ | Coefficient in the Callendar-Van Dusen equation |
| $b$ | Parameter in the Van der Waals equation of state |
| $C_P$ | Isobaric heat capacity |
| $C_P^o$ | Ideal gas isobaric heat capacity |
| $C_V$ | Isochoric heat capacity |
| $C_{vb}$ | Contribution of molecular vibrational mode to heat capacity |
| $C_V^o$ | Ideal gas isochoric heat capacity |
| $C_{vb}^{\mathrm{N}}$ | Vibrational heat capacity of $N_2$ |
| $C_{vb}^{\mathrm{O}}$ | Vibrational heat capacity of $O_2$ |
| $c$ | Kirchhoff constant |
| $D$ | Thermal diffusivity |
| $d^3\mathbf{X}$ | The volume of a small rectangular parallelepiped element of fluid centered at point $\mathbf{X}$ with sides of $dX_1$, $dX_2$ and $dX_3$ in parallel with the three Cartesian coordinate axes |
| $F_{ij}$ | Adjustable factor |
| $f$ | Regular frequency |
| $f_c$ | Molecular collision frequency |
| $f_{lmn}$ | Resonance frequency of mode $(l, m, n)$ (cylindrical resonator) |
| $f_{ln}$ | Resonance frequency of mode $(l, n)$ (spherical resonator) |
| $f_r$ | Relaxation frequency |
| $f_{r_ro}$ | Rotational relaxation frequency |
| $f_{r_vb}^{\mathrm{N}}$ | Vibrational relaxation frequency of $N_2$ |
| $f_{r_vb}^{\mathrm{O}}$ | Vibrational relaxation frequency of $O_2$ |
| $\mathbf{i}$ | Imaginary unit |
| $K_c$ | Correction factor in the correlation of $W$ to pathlength $L$ and $t_m$ |
| $K_d$ | Dispersion correction factor |
| $K_v$ | Virial correction factor |
| $k$ | Wave number |

| | |
|---|---|
| $k_{ij}$ | Coupling factor ($i \neq j$) |
| $L$ | Propagation distance or pathlength |
| | Cylindrical cavity length |
| $L_0$ | Distance between ultrasound transmitter and receiver |
| $L'$ | Calibrated pathlength |
| $l$ | Resonance mode index |
| $M$ | Molecular weight |
| $m$ | Resonance mode index |
| $m_1$ | Mass of glass sphere |
| $m_2$ | Mass of counterweight |
| $m_d$ | Apparent mass difference between the two sides of microbalance |
| $m_{read}$ | Mass reading |
| $N$ | Total number of different components in a mixture |
| $n$ | Resonance mode index |
| $P$ | Pressure |
| $P^*$ | Reference pressure, 1 atm |
| $P_0$ | Equilibrium pressure of fluid in absence of sound wave |
| $P_1^0$ | Amplitude of variation in pressure in the $X_1$ direction |
| $P_{00}$ | Coefficient in 3-D polynomial equation |
| $P_{10}$ | Coefficient in 3-D polynomial equation |
| $P_{01}$ | Coefficient in 3-D polynomial equation |
| $P_{20}$ | Coefficient in 3-D polynomial equation |
| $P_{11}$ | Coefficient in 3-D polynomial equation |
| $P_{02}$ | Coefficient in 3-D polynomial equation |
| $P_{30}$ | Coefficient in 3-D polynomial equation |
| $P_{21}$ | Coefficient in 3-D polynomial equation |
| $P_{12}$ | Coefficient in 3-D polynomial equation |
| $P_{03}$ | Coefficient in 3-D polynomial equation |
| $P_{40}$ | Coefficient in 3-D polynomial equation |
| $P_{31}$ | Coefficient in 3-D polynomial equation |
| $P_{22}$ | Coefficient in 3-D polynomial equation |
| $P_{13}$ | Coefficient in 3-D polynomial equation |
| $P_{04}$ | Coefficient in 3-D polynomial equation |

| | |
|---|---|
| $P_c$ | Critical pressure |
| $P_{SAT}$ | Saturated vapour pressure |
| $R$ | Universal gas constant |
| $R_0$ | Coefficient in the Callendar-Van Dusen equation |
| $R_T$ | Resistance |
| $r$ | Radius |
| $r_s$ | Radius of sound source |
| $\bar{r}$ | Mean radius of spherical cavity |
| $S$ | Entropy |
| $T$ | Temperature |
| $T^*$ | Reference temperature, 293.15 K |
| $T_0$ | Equilibrium temperature of fluid in absence of sound wave |
| $T_c$ | Critical temperature |
| $T_r$ | Reducing function for mixture temperature |
| $T_{DVS}$ | DVS temperature |
| $T_{SoS}$ | SoS temperature |
| $T'_{SoS}$ | Temperature measured by a manufactured SoS sensor's temperature probe |
| $t$ | Time |
| $t_d$ | Time delay |
| $t_m$ | Measured time of flight |
| $t_m^0$ | Measured time of flight corresponding to the first zero step |
| $t_r$ | Round-trip pulse propagation time |
| $t_s$ | Single-trip pulse propagation time |
| $u$ | Volumetric flow rate |
| $U$ | Uncertainty |
| $U(x)_{SoS}$ | Uncertainty in gas composition measurement using SoS sensor |
| $V$ | Volume |
| $V_1$ | Volume of glass sphere |
| $V_2$ | Volume of counterweight |
| $V_s$ | Volume of spherical cavity |
| $v$ | Flow velocity |
| $v_1^0$ | Amplitude of variation in flow velocity in the $X_1$ direction |
| $W$ | Real gas speed of sound |

| | |
|---|---|
| $W^0$ | Carrier gas real gas SoS corresponding to the first zero step |
| $W_m$ | Measured speed of sound |
| $W_o$ | Ideal gas speed of sound |
| $W_s$ | Isentropic speed of sound |
| $W_t$ | Sound propagation velocity in a cylindrical tube |
| $W_{tr}$ | Real gas speed of sound under the assumption that dispersion could only result from translational relaxation |
| $W_\theta$ | Lossless real gas speed of sound |
| $W_{\theta_N}$ | $W_\theta$ determined using the NIST REFPROP software |
| $W_{\theta_Z}$ | $W_\theta$ determined using the Zuckerwar's method |
| $W_\infty$ | High-frequency-limit speed of sound |
| $W_{\infty_vb}$ | Vibrational relaxation high-frequency-limit speed of sound |
| $X$ | Temperature in 3-D polynomial fitting |
| $\mathbf{X}$ | A point with coordinates ($X_1$, $X_2$, $X_3$) in the Cartesian coordinate system |
| $x$ | Mole fraction |
| $x_{\mathrm{C}}$ | $CO_2$ mole fraction in standard dry air |
| $x'_{\mathrm{C}}$ | $CO_2$ mole fraction in experimental dry air |
| $x_{\mathrm{N}}$ | $N_2$ mole fraction in standard dry air |
| $x'_{\mathrm{N}}$ | $N_2$ mole fraction in experimental dry air |
| $x_{\mathrm{O}}$ | $O_2$ mole fraction in standard dry air |
| $x'_{\mathrm{O}}$ | $O_2$ mole fraction in experimental dry air |
| $x_{SAT}$ | Saturated vapour mole fraction |
| $x_T$ | Target mole fraction |
| $\bar{x}$ | Vector of molar composition |
| $Y$ | Speed of sound in 3-D polynomial fitting |
| $y$ | Mole fraction |
| $Z$ | Gas composition in 3-D polynomial fitting |
| $Z_{ro}$ | Rotational collision number |
| $z$ | Propagation distance |
| $\mathcal{B}$ | Second virial coefficient |
| $\mathcal{B}_\mathcal{P}$ | Second virial pressure coefficient |
| $\mathcal{C}$ | Third virial coefficient |

| | |
|---|---|
| $\mathcal{C}_{\mathcal{P}}$ | Third virial pressure coefficient |
| $\mathcal{F}$ | Second acoustic virial pressure coefficient |
| $\mathcal{G}$ | Third acoustic virial pressure coefficient |
| $\mathcal{H}$ | Helmholtz energy |
| $\mathcal{H}^o$ | Ideal gas Helmholtz energy |
| $\mathcal{H}^r$ | Residual Helmholtz energy |
| $\hbar$ | Reduced Helmholtz energy |
| $\hbar^o$ | Reduced ideal gas Helmholtz energy |
| $\hbar^r$ | Reduced residual Helmholtz energy |
| $\hbar^r{}_{ij}$ | Part of $\Delta\hbar^r{}_{ij}$ |
| $\mathcal{K}$ | Second acoustic virial coefficient |
| $\mathcal{L}$ | Third acoustic virial coefficient |
| $\alpha$ | Absorption coefficient |
| $\beta_{T\,ij}$ | Binary parameter |
| $\beta_{v\,ij}$ | Binary parameter |
| $\gamma$ | Heat capacity ratio |
| $\gamma^o$ | Ideal gas heat capacity ratio |
| $\gamma_{T\,ij}$ | Binary parameter |
| $\gamma_{v\,ij}$ | Binary parameter |
| $\Delta_D$ | Difference between $W_m$ and $W_\theta$ |
| $\Delta'_D$ | Difference between $W_{\theta_Z}$ and $W_{\theta_N}$ |
| $\Delta_{RD}$ | Relative difference between $W_m$ and $W_\theta$ |
| $\Delta'_{RD}$ | Relative difference between $W_{\theta_Z}$ and $W_{\theta_N}$ |
| $\Delta_{RE}$ | Relative error between $W_m$ and $W$ |
| $\Delta f_i$ | The $i$th frequency perturbation term |
| $\Delta m_{read}$ | Change in mass reading |
| $\Delta V$ | Volume difference between the two sides of microbalance |
| $\Delta\hbar^r$ | Departure function |
| $\Delta\hbar^r{}_{ij}$ | Binary subsystem departure function |
| $\delta P$ | Change in pressure of fluid element due to sound propagation |
| $\delta T$ | Change in temperature of fluid element due to sound propagation |
| $\delta t$ | Correction to $t_m$ due to diffraction effect |

| | |
|---|---|
| $\delta\rho$ | Change in density of fluid element due to sound propagation |
| $\varepsilon_r$ | Relaxation strength |
| $\varepsilon_{r_vb}$ | Vibrational relaxation strength |
| $\varepsilon_{r_vb}^{\mathrm{N}}$ | Vibrational relaxation strength of $N_2$ |
| $\varepsilon_{r_vb}^{\mathrm{O}}$ | Vibrational relaxation strength of $O_2$ |
| $\zeta$ | Reduced density |
| $\eta$ | Inverse reduced temperature |
| $\theta_{vb}$ | Characteristic vibrational temperature |
| $\theta_{vb}^{\mathrm{N}}$ | Characteristic vibrational temperature of $N_2$ |
| $\theta_{vb}^{\mathrm{O}}$ | Characteristic vibrational temperature of $O_2$ |
| $\kappa$ | Thermal conductivity |
| $\lambda$ | Wavelength |
| $\mu$ | Dynamic viscosity |
| $\nu$ | Kinematic viscosity |
| $\rho$ | Density |
| $\rho^0$ | Carrier gas density |
| $\rho_0$ | Equilibrium density of fluid in absence of sound wave |
| $\rho_1^0$ | Amplitude of variation in density in the $X_1$ direction |
| $\rho_c$ | Critical density |
| $\rho_r$ | Reducing function for mixture density |
| $\tau_c$ | Collision time between molecules |
| $\tau_r$ | Relaxation time |
| $\tau_{r_ro}$ | Rotational relaxation time |
| $\tau_{r_tr}$ | Translational relaxation time |
| $\upsilon_{ln}$ | The $n$th turning point of the spherical Bessel function of order $l$ |
| $\varphi$ | Phase shift |
| $\chi_{mn}$ | The $n$th turning point of the cylindrical Bessel function of order $m$ |
| $\omega$ | Angular frequency |

# List of Abbreviations

| | |
|---|---|
| 3-D | 3-Dimensional |
| AC | Alternating current |
| ADC | Analog to digital converter |
| CFE | $CO_2$-free experimental dry air |
| CFS | $CO_2$-free standard dry air |
| CW | Constant wave |
| DAC | Digital to analog converter |
| DoF | Degree of freedom |
| DPA | Dew point analyser |
| DVS | Dynamic vapour sorption |
| EA | Experimental dry air |
| EoS | Equation of state |
| FID | Flame ionisation detector |
| FT | Fourier transform |
| GC | Gas chromatograph(y) |
| H-EoS | Helmholtz equation of state (fundamental equation explicit in the Helmholtz energy or the reduced Helmholtz energy) |
| IR | Infrared |
| ITS-90 | International Temperature Scale of 1990 |
| MCU | Microcontroller unit |
| MEA | Monoethanolamine |
| MFC | Mass flow controller |
| MIR | Mid-infrared |
| NIR | Near-infrared |
| OPD | Optical path difference |
| PC | Personal computer |
| PCB | Printed circuit board |
| PID | Proportional-integral-derivative |
| ppb | Parts per billion |
| ppm | Parts per million |
| ppt | Parts per thousand |

| | |
|---|---|
| PRT | Platinum resistance thermometer |
| PVDF | Polyvinylidene fluoride |
| $R^2$ | R-square |
| RH | Relative humidity |
| RMSE | Root mean squared error |
| $RS_1$ | The 1st received signal |
| $RS_2$ | The 2nd received signal |
| SA | Standard dry air |
| SoS | Speed of sound |
| SPRT | Standard platinum resistance thermometer |
| SSE | Sum of squares due to error |
| TCD | Thermal conductivity detector |
| TCXO | Temperature compensated crystal oscillator |
| ToF | Time of flight |
| $TS_0$ | Transmitted signal |
| USB | Universal serial bus |
| %SAT | Percentage of saturated vapour mole fraction (percentage of maximum achievable vapour mole fraction corresponding to 100% saturation at the experimental temperature and pressure) |

# List of Tables

Table 1. General summary of the typical characteristics of different on-line gas composition measurement techniques ..... 42
Table 2. Pure gases with available thermodynamic data in the NIST REFPROP software ..... 47
Table 3. Gas mixtures of interest with available thermodynamic data in the NIST REFPROP software ..... 51
Table 4. Binary subsystems in the gas mixtures of interest with available thermodynamic data in the NIST REFPROP software ..... 51
Table 5. Summary of temperature/pressure/frequency/composition dependences of SoSs and correction factors ..... 63
Table 6. Advantages and disadvantages of typical methods for ToF determination ..... 70
Table 7. Turning points of the spherical Bessel function of zero order ..... 77
Table 8. Reported SoS Measurements for Pure Gases ..... 83
Table 9. Typical characteristics of different SoS measurement methods ..... 95
Table 10. Uncertainty schedule for the calibration of the SoS temperature probe ..... 107
Table 11. Basic experimental information ..... 110
Table 12. Methods used to determine $\rho 0$ and $x$ for the experiments on the binary gas mixtures in Group A (the binary gas mixtures with available thermodynamic data in the NIST REFPROP software) ..... 114
Table 13. Methods used to determine $\rho 0$ and $x$ for the experiments on the binary gas mixtures in Group B (the binary gas mixtures without available thermodynamic data in the NIST REFPROP software) ..... 114
Table 14. Suppliers and purities of materials ..... 116
Table 15. n-Heptane/dry air results (5 °C isotherm) ..... 122
Table 16. n-Heptane/dry air results (15 °C isotherm) ..... 123
Table 17. n-Heptane/dry air results (25 °C isotherm) ..... 124
Table 18. n-Heptane/dry air results (35 °C isotherm) ..... 126
Table 19. n-Heptane/dry air results (45 °C isotherm) ..... 127
Table 20. n-Heptane/dry air results (55 °C isotherm) ..... 128
Table 21. Carbon dioxide/nitrogen results (10 °C isotherm) ..... 129
Table 22. Carbon dioxide/nitrogen results (20 °C isotherm) ..... 130
Table 23. Carbon dioxide/nitrogen results (25 °C isotherm) ..... 131
Table 24. Carbon dioxide/nitrogen results (30 °C isotherm) ..... 132
Table 25. Carbon dioxide/nitrogen results (40 °C isotherm) ..... 133
Table 26. Carbon dioxide/nitrogen results (50 °C isotherm) ..... 134
Table 27. Methods for the determination of $W\theta$ using the NIST REFPROP software ..... 150
Table 28. Comparison between $W\theta_Z$ and $W\theta_N$ at 1 atm ..... 161
Table 29. Fitted 3-D polynomial equation and estimated $UxSoS$ (n-hexane/dry air) ..... 169
Table 30. Fitted 3-D polynomial equation and estimated $UxSoS$ (n-heptane/dry air) ..... 170
Table 31. Fitted 3-D polynomial equation and estimated $UxSoS$ (n-octane/dry air) ..... 171
Table 32. Fitted 3-D polynomial equation and estimated $UxSoS$ (n-nonane/dry air) ..... 172
Table 33. Fitted 3-D polynomial equation and estimated $UxSoS$ (n-decane/dry air) ..... 173
Table 34. Fitted 3-D polynomial equation and estimated $UxSoS$ (toluene/dry air) ..... 174
Table 35. Fitted 3-D polynomial equation and estimated $UxSoS$ (cyclohexane/dry air) ..... 175
Table 36. Fitted 3-D polynomial equation and estimated $UxSoS$ (water/dry air) ..... 176

Table 37. Fitted 3-D polynomial equation and estimated $UxSoS$ (acetone/dry air) ..... 177
Table 38. Fitted 3-D polynomial equation and estimated $UxSoS$ (methyl ethyl ketone/dry air) ..... 178
Table 39. Fitted 3-D polynomial equation and estimated $UxSoS$ (ethyl acetate/dry air) ..... 179
Table 40. Fitted 3-D polynomial equation and estimated $UxSoS$ (methanol/dry air) ..... 180
Table 41. Fitted 3-D polynomial equation and estimated $UxSoS$ (ethanol/dry air) ..... 181
Table 42. Fitted 3-D polynomial equation and estimated $UxSoS$ (isopropanol/dry air) ..... 182
Table 43. Fitted 3-D polynomial equation and estimated $UxSoS$ (dichloromethane/dry air) ..... 183
Table 44. Fitted 3-D polynomial equation and estimated $UxSoS$ (chloroform/dry air) ..... 184
Table 45. Fitted 3-D polynomial equation and estimated $UxSoS$ (1,2-dichloroethane/dry air) ..... 185
Table 46. Fitted 3-D polynomial equation and estimated $UxSoS$ (m-xylene/dry air) ..... 186
Table 47. Fitted 3-D polynomial equation and estimated $UxSoS$ (o-xylene/dry air) ..... 187
Table 48. Fitted 3-D polynomial equation and estimated $UxSoS$ (p-xylene/dry air) ..... 188
Table 49. Fitted 3-D polynomial equation and estimated $UxSoS$ (ethylbenzene/dry air) ..... 189
Table 50. Fitted 3-D polynomial equation and estimated $UxSoS$ (n-butylamine/dry air) ..... 190
Table 51. Fitted 3-D polynomial equation and estimated $UxSoS$ (limonene/dry air) ..... 191
Table 52. Fitted 3-D polynomial equation and estimated $UxSoS$ (α-pinene/dry air) ..... 192
Table 53. Fitted 3-D polynomial equation and estimated $UxSoS$ (carbon dioxide/nitrogen) ..... 193
Table 54. Estimation of dispersion effect for Ar and He ..... 211
Table 55. Estimation of translational dispersion effect for $N_2$ ..... 212
Table 56. Estimation of rotational relaxation time for $N_2$ ..... 212
Table 57. Leading constituents of standard dry air ..... 214
Table 58. Estimation of translational dispersion effect for standard dry air ..... 216
Table 59. Estimation of rotational relaxation frequency ..... 217
Table 60. Details of $\Delta V$ measurement experiment ..... 228
Table 61. Molecular weights and critical constants ..... 230
Table 62. Vapour pressure of liquids ..... 231
Table 63. n-Hexane/dry air results (5 °C isotherm) ..... 233
Table 64. n-Hexane/dry air results (15 °C isotherm) ..... 234
Table 65. n-Hexane/dry air results (25 °C isotherm) ..... 235
Table 66. n-Hexane/dry air results (35 °C isotherm) ..... 237
Table 67. n-Hexane/dry air results (45 °C isotherm) ..... 238
Table 68. n-Octane/dry air results (5 °C isotherm) ..... 239
Table 69. n-Octane/dry air results (15 °C isotherm) ..... 240
Table 70. n-Octane/dry air results (25 °C isotherm) ..... 241
Table 71. n-Octane/dry air results (35 °C isotherm) ..... 243
Table 72. n-Octane/dry air results (45 °C isotherm) ..... 244
Table 73. n-Octane/dry air results (55 °C isotherm) ..... 245
Table 74. n-Nonane/dry air results (15 °C isotherm) ..... 246
Table 75. n-Nonane/dry air results (25 °C isotherm) ..... 247
Table 76. n-Nonane/dry air results (35 °C isotherm) ..... 249
Table 77. n-Nonane/dry air results (45 °C isotherm) ..... 250
Table 78. n-Nonane/dry air results (55 °C isotherm) ..... 251
Table 79. n-Decane/dry air results (25 °C isotherm) ..... 252
Table 80. n-Decane/dry air results (35 °C isotherm) ..... 253
Table 81. n-Decane/dry air results (45 °C isotherm) ..... 254
Table 82. n-Decane/dry air results (55 °C isotherm) ..... 255
Table 83. Toluene/dry air results (5 °C isotherm) ..... 256
Table 84. Toluene/dry air results (15 °C isotherm) ..... 257

Table 85. Toluene/dry air results (25 °C isotherm) ..... 258
Table 86. Toluene/dry air results (35 °C isotherm) ..... 260
Table 87. Toluene/dry air results (45 °C isotherm) ..... 261
Table 88. Toluene/dry air results (55 °C isotherm) ..... 262
Table 89. Cyclohexane/dry air results (15 °C isotherm) ..... 263
Table 90. Cyclohexane/dry air results (25 °C isotherm) ..... 264
Table 91. Cyclohexane/dry air results (35 °C isotherm) ..... 266
Table 92. Cyclohexane/dry air results (45 °C isotherm) ..... 267
Table 93. Cyclohexane/dry air results (55 °C isotherm) ..... 268
Table 94. Water/dry air results (25 °C isotherm) ..... 269
Table 95. Water/dry air results (35 °C isotherm) ..... 270
Table 96. Water/dry air results (45 °C isotherm) ..... 271
Table 97. Water/dry air results (55 °C isotherm) ..... 272
Table 98. Acetone/dry air results (5 °C isotherm) ..... 273
Table 99. Acetone/dry air results (15 °C isotherm) ..... 274
Table 100. Acetone/dry air results (25 °C isotherm) ..... 275
Table 101. Acetone/dry air results (35 °C isotherm) ..... 277
Table 102. Methyl ethyl ketone/dry air results (5 °C isotherm) ..... 278
Table 103. Methyl ethyl ketone/dry air results (15 °C isotherm) ..... 279
Table 104. Methyl ethyl ketone/dry air results (25 °C isotherm) ..... 280
Table 105. Methyl ethyl ketone/dry air results (35 °C isotherm) ..... 282
Table 106. Methyl ethyl ketone/dry air results (45 °C isotherm) ..... 283
Table 107. Methyl ethyl ketone/dry air results (55 °C isotherm) ..... 284
Table 108. Ethyl acetate/dry air results (5 °C isotherm) ..... 285
Table 109. Ethyl acetate/dry air results (15 °C isotherm) ..... 286
Table 110. Ethyl acetate/dry air results (25 °C isotherm) ..... 287
Table 111. Ethyl acetate/dry air results (35 °C isotherm) ..... 289
Table 112. Ethyl acetate/dry air results (45 °C isotherm) ..... 290
Table 113. Ethyl acetate/dry air results (55 °C isotherm) ..... 291
Table 114. Methanol/dry air results (5 °C isotherm) ..... 292
Table 115. Methanol/dry air results (15 °C isotherm) ..... 293
Table 116. Methanol/dry air results (25 °C isotherm) ..... 294
Table 117. Methanol/dry air results (35 °C isotherm) ..... 296
Table 118. Methanol/dry air results (45 °C isotherm) ..... 297
Table 119. Ethanol/dry air results (5 °C isotherm) ..... 298
Table 120. Ethanol/dry air results (15 °C isotherm) ..... 299
Table 121. Ethanol/dry air results (25 °C isotherm) ..... 300
Table 122. Ethanol/dry air results (35 °C isotherm) ..... 302
Table 123. Ethanol/dry air results (45 °C isotherm) ..... 303
Table 124. Ethanol/dry air results (55 °C isotherm) ..... 304
Table 125. Isopropanol/dry air results (5 °C isotherm) ..... 305
Table 126. Isopropanol/dry air results (15 °C isotherm) ..... 306
Table 127. Isopropanol/dry air results (25 °C isotherm) ..... 307
Table 128. Isopropanol/dry air results (35 °C isotherm) ..... 309
Table 129. Isopropanol/dry air results (45 °C isotherm) ..... 310
Table 130. Isopropanol/dry air results (55 °C isotherm) ..... 311
Table 131. Dichloromethane/dry air results (5 °C isotherm) ..... 312
Table 132. Dichloromethane/dry air results (15 °C isotherm) ..... 313

Table 133. Dichloromethane/dry air results (25 °C isotherm) ..... 314
Table 134. Chloroform/dry air results (5 °C isotherm) ..... 315
Table 135. Chloroform/dry air results (15 °C isotherm) ..... 316
Table 136. Chloroform/dry air results (25 °C isotherm) ..... 317
Table 137. Chloroform/dry air results (35 °C isotherm) ..... 319
Table 138. 1,2-Dichloroethane/dry air results (5 °C isotherm) ..... 320
Table 139. 1,2-Dichloroethane/dry air results (15 °C isotherm) ..... 321
Table 140. 1,2-Dichloroethane/dry air results (25 °C isotherm) ..... 322
Table 141. 1,2-Dichloroethane/dry air results (35 °C isotherm) ..... 324
Table 142. 1,2-Dichloroethane/dry air results (45 °C isotherm) ..... 325
Table 143. 1,2-Dichloroethane/dry air results (55 °C isotherm) ..... 326
Table 144. m-Xylene/dry air results (30 °C isotherm) ..... 327
Table 145. m-Xylene/dry air results (40 °C isotherm) ..... 328
Table 146. m-Xylene/dry air results (50 °C isotherm) ..... 329
Table 147. o-Xylene/dry air results (30 °C isotherm) ..... 330
Table 148. o-Xylene/dry air results (40 °C isotherm) ..... 331
Table 149. o-Xylene/dry air results (50 °C isotherm) ..... 332
Table 150. p-Xylene/dry air results (30 °C isotherm) ..... 333
Table 151. p-Xylene/dry air results (40 °C isotherm) ..... 334
Table 152. p-Xylene/dry air results (50 °C isotherm) ..... 335
Table 153. Ethylbenzene/dry air results (30 °C isotherm) ..... 336
Table 154. Ethylbenzene/dry air results (40 °C isotherm) ..... 337
Table 155. Ethylbenzene/dry air results (50 °C isotherm) ..... 338
Table 156. n-Butylamine/dry air results (25 °C isotherm) ..... 339
Table 157. n-Butylamine/dry air results (35 °C isotherm) ..... 340
Table 158. n-Butylamine/dry air results (45 °C isotherm) ..... 341
Table 159. Limonene/dry air results (25 °C isotherm) ..... 342
Table 160. Limonene/dry air results (35 °C isotherm) ..... 343
Table 161. Limonene/dry air results (45 °C isotherm) ..... 344
Table 162. α-Pinene/dry air results (25 °C isotherm) ..... 345
Table 163. α-Pinene/dry air results (35 °C isotherm) ..... 346
Table 164. α-Pinene/dry air results (45 °C isotherm) ..... 347

# List of Figures

Figure 1. Basic information of the NIST REFPROP software ..... 29
Figure 2. Left – Schematic of the sensing part of a capacitive humidity sensor; Right – Various types of probes of capacitive humidity sensors (Rotronic Instrument Corporation [Online]) ..... 31
Figure 3. Left – Schematic of the measurement principle of DPA (Davies et al., 1998); Right – A typical DPA probe (Michell Instruments [Online]) ..... 33
Figure 4. Left – Schematic of a typical GC (BBC GCSE Bitesize Science [Online]); Right – Schematic of the separation process (General Chemistry [Online]) ..... 35
Figure 5. Left – Schematic of the measurement principle of TCD (Christian & O'Reilly, 1986); Right – A typical TCD (AGC Instruments [Online]) ..... 35
Figure 6. Left – Schematic of the measurement principle of FID (Christian & O'Reilly, 1986); Right – A typical FID (GOW-MAC Instrument Co. [Online]) ..... 37
Figure 7. Above – Schematic of Michelson interferometer and associated electronics (Christian & O'Reilly, 1986); Below – Schematic of an FT-IR spectrometer for gas analysis (Gemini Scientific Instruments [Online]) ..... 39
Figure 8. Schematic of a simple dispersive NIR spectrometer (Metrohm AG [Online]) ..... 40
Figure 9. Dispersion effect on $W$ of a vibrational or rotational relaxation process characterised by a single $\tau r$ (x-axis – logarithm of angular frequency; y-axis – square of real gas SoS) ..... 61
Figure 10. Typical cross-sectional structure of piezoelectric ultrasonic transducers ..... 65
Figure 11. Schematic of transducer configuration and ultrasound propagation path in a typical double-transducer SoS-ToF sensor ($TS_0$ – transmitted signal; $RS_1$ – the 1st received signal; $RS_2$ – the 2nd received signal) ..... 66
Figure 12. Schematic of transducer configuration and ultrasound propagation path in a typical single-transducer SoS-ToF sensor ($TS_0$ – transmitted signal; $RS_1$ – the 1st received signal; $RS_2$ – the 2nd received signal) ..... 66
Figure 13. Schematic of a typical amplitude thresholding method with preset signal waveform amplitude thresholds ..... 68
Figure 14. Schematic of a typical fitting method with functions (curves) fitted to waveform envelopes ..... 69
Figure 15. Schematic of a transmitted signal with a phase-reversal marker ..... 69
Figure 16. Dual-path ultrasonic cell (Peleties et al., 2010) ..... 76
Figure 17. The spherical resonator of Moldover et al. (1988) ..... 78
Figure 18. Cylindrical resonator with electronics as used by Younglove & McCarty (1980) ..... 80
Figure 19. The acoustic interferometer (Colclough et al., 1979; Quinn et al., 1976) ..... 82
Figure 20. The ultrasonic gas analysis system (Hallewell et al., 1988) ..... 89
Figure 21. SoS versus $C_2H_6$ concentration in $CH_4$ at 30 °C (Hallewell et al., 1988) ..... 90
Figure 22. SoS versus Ar mole fraction in $N_2$ (Löfqvist et al., 2003) ..... 92
Figure 23. Iterative method for SoS and gas composition determination (Hozumi et al., 1997) ..... 93
Figure 24. Cross-section view of the SoS sensor: 1 – outlet tube; 2, 3 – transducer holders; 4, 5 – ATK120 transducers; 6 – spiral grooved channel; 7 – inlet hole; 8 – woven fiberglass mesh (blue area) ..... 97
Figure 25. 3-D views of the SoS sensor: 1 – outlet tube; 2 – inlet tube; 3 – main body (outer sleeve shown); 4, 5 – transducer holders; 6 – recess for PT100; 7 – spiral grooved channel; 8 – inlet hole; 9 – grooved tube (main body, outer sleeve not shown) ..... 97

Figure 26. SoS sensor electronics board: 1 – USB interface; 2 – MCU; 3 – barometric sensor; 4 – potentiometer; 5 – receiver transducer connector; 6 – transmitter transducer connector; 7 – PT100 connector ..... 99
Figure 27. A typical received signal waveform and detailed views of the zero crossing points (x-axis – time with a unit of 200 ns; y-axis – amplitude with a unit of 3/4095 V) ..... 102
Figure 28. Schematic of DVS based experimental system with SoS sensor ..... 106
Figure 29. A typical procedure for the isothermal experiments on organic vapour/dry air and water vapour/dry air binary gas mixtures ..... 111
Figure 30. The procedure for the experiments on $CO_2/N_2$ binary gas mixtures ..... 112
Figure 31. Raw experimental data for mass readings and measured ToF (n-heptane/dry air at 35 °C) ..... 119
Figure 32. Raw experimental data for mass readings and measured ToF (carbon dioxide/nitrogen at 25 °C) ..... 119
Figure 33. Measured SoS versus composition for n-heptane/dry air binary gas mixture ..... 135
Figure 34. Measured SoS versus composition for carbon dioxide/nitrogen binary gas mixture ..... 135
Figure 35. Measured SoS versus composition for n-hexane/dry air binary gas mixture ..... 136
Figure 36. Measured SoS versus composition for n-octane/dry air binary gas mixture ..... 136
Figure 37. Measured SoS versus composition for n-nonane/dry air binary gas mixture ..... 137
Figure 38. Measured SoS versus composition for n-decane/dry air binary gas mixture ..... 137
Figure 39. Measured SoS versus composition for toluene/dry air binary gas mixture ..... 138
Figure 40. Measured SoS versus composition for cyclohexane/dry air binary gas mixture ..... 138
Figure 41. Measured SoS versus composition for water/dry air binary gas mixture ..... 139
Figure 42. Measured SoS versus composition for acetone/dry air binary gas mixture ..... 139
Figure 43. Measured SoS versus composition for methyl ethyl ketone/dry air binary gas mixture ..... 140
Figure 44. Measured SoS versus composition for ethyl acetate/dry air binary gas mixture ..... 140
Figure 45. Measured SoS versus composition for methanol/dry air binary gas mixture ..... 141
Figure 46. Measured SoS versus composition for ethanol/dry air binary gas mixture ..... 141
Figure 47. Measured SoS versus composition for isopropanol/dry air binary gas mixture ..... 142
Figure 48. Measured SoS versus composition for dichloromethane/dry air binary gas mixture ..... 142
Figure 49. Measured SoS versus composition for chloroform/dry air binary gas mixture ..... 143
Figure 50. Measured SoS versus composition for 1,2-dichloroethane/dry air binary gas mixture ..... 143
Figure 51. Measured SoS versus composition for m-xylene/dry air binary gas mixture ..... 144
Figure 52. Measured SoS versus composition for o-xylene/dry air binary gas mixture ..... 144
Figure 53. Measured SoS versus composition for p-xylene/dry air binary gas mixture ..... 145
Figure 54. Measured SoS versus composition for ethylbenzene/dry air binary gas mixture ..... 145
Figure 55. Measured SoS versus composition for n-butylamine/dry air binary gas mixture ..... 146
Figure 56. Measured SoS versus composition for limonene/dry air binary gas mixture ..... 146
Figure 57. Measured SoS versus composition for α-pinene/dry air binary gas mixture ..... 147
Figure 58. Relative error between $Wm$ and $W$ versus experimental temperature ..... 149
Figure 59. Difference between $Wm$ and $W\theta$ ($\Delta D$) for n-hexane/dry air ..... 152
Figure 60. Relative difference between $Wm$ and $W\theta$ ($\Delta RD$) for n-hexane/dry air ..... 152
Figure 61. Difference between $Wm$ and $W\theta$ ($\Delta D$) for n-heptane/dry air ..... 153
Figure 62. Relative difference between $Wm$ and $W\theta$ ($\Delta RD$) for n-heptane/dry air ..... 153
Figure 63. Difference between $Wm$ and $W\theta$ ($\Delta D$) for n-octane/dry air ..... 154
Figure 64. Relative difference between $Wm$ and $W\theta$ ($\Delta RD$) for n-octane/dry air ..... 154
Figure 65. Difference between $Wm$ and $W\theta$ ($\Delta D$) for n-nonane/dry air ..... 155
Figure 66. Relative difference between $Wm$ and $W\theta$ ($\Delta RD$) for n-nonane/dry air ..... 155
Figure 67. Difference between $Wm$ and $W\theta$ ($\Delta D$) for n-decane/dry air ..... 156

Figure 68. Relative difference between $Wm$ and $W\theta$ ($\Delta RD$) for n-decane/dry air ..... 156
Figure 69. Difference between $Wm$ and $W\theta$ ($\Delta D$) for toluene/dry air ..... 157
Figure 70. Relative difference between $Wm$ and $W\theta$ ($\Delta RD$) for toluene/dry air ..... 157
Figure 71. Difference between $Wm$ and $W\theta$ ($\Delta D$) for cyclohexane/dry air ..... 158
Figure 72. Relative difference between $Wm$ and $W\theta$ ($\Delta RD$) for cyclohexane/dry air ..... 158
Figure 73. Difference between $Wm$ and $W\theta$ ($\Delta D$) for water/dry air ..... 159
Figure 74. Relative difference between $Wm$ and $W\theta$ ($\Delta RD$) for water/dry air ..... 159
Figure 75. Difference between $Wm$ and $W\theta$ ($\Delta D$) for $CO_2/N_2$ ..... 160
Figure 76. Relative difference between $Wm$ and $W\theta$ ($\Delta RD$) for $CO_2/N_2$ ..... 160
Figure 77. 3-D polynomial surface for n-hexane/dry air ..... 169
Figure 78. 3-D polynomial surface for n-heptane/dry air ..... 170
Figure 79. 3-D polynomial surface for n-octane/dry air ..... 171
Figure 80. 3-D polynomial surface for n-nonane/dry air ..... 172
Figure 81. 3-D polynomial surface for n-decane/dry air ..... 173
Figure 82. 3-D polynomial surface for toluene/dry air ..... 174
Figure 83. 3-D polynomial surface for cyclohexane/dry air ..... 175
Figure 84. 3-D polynomial surface for water/dry air ..... 176
Figure 85. 3-D polynomial surface for acetone/dry air ..... 177
Figure 86. 3-D polynomial surface for methyl ethyl ketone/dry air ..... 178
Figure 87. 3-D polynomial surface for ethyl acetate/dry air ..... 179
Figure 88. 3-D polynomial surface for methanol/dry air ..... 180
Figure 89. 3-D polynomial surface for ethanol/dry air ..... 181
Figure 90. 3-D polynomial surface for isopropanol/dry air ..... 182
Figure 91. 3-D polynomial surface for dichloromethane/dry air ..... 183
Figure 92. 3-D polynomial surface for chloroform/dry air ..... 184
Figure 93. 3-D polynomial surface for 1,2-dichloroethane/dry air ..... 185
Figure 94. 3-D polynomial surface for m-xylene/dry air ..... 186
Figure 95. 3-D polynomial surface for o-xylene/dry air ..... 187
Figure 96. 3-D polynomial surface for p-xylene/dry air ..... 188
Figure 97. 3-D polynomial surface for ethylbenzene/dry air ..... 189
Figure 98. 3-D polynomial surface for n-butylamine/dry air ..... 190
Figure 99. 3-D polynomial surface for limonene/dry air ..... 191
Figure 100. 3-D polynomial surface for α-pinene/dry air ..... 192
Figure 101. 3-D polynomial surface for carbon dioxide/nitrogen ..... 193
Figure 102. DVS based experimental system ..... 221
Figure 103. Interior of DVS incubator ..... 222
Figure 104. I – glass sphere; II – counterweight ..... 223
Figure 105. SoS sensor ..... 223
Figure 106. A captured plot of temperature, ToF and RSD in the SoS Sensor Internal Test Program ..... 227
Figure 107. Estimation of $\Delta V$ measurement uncertainty ..... 229

# CHAPTER 1. Introduction

## 1.1 Overview

Current commonly used measurement techniques for determining on-line gas composition do not always satisfy all of the requirements of industrial and process applications. These techniques include capacitive humidity sensing, Fourier transform infrared (FT-IR) spectroscopy, near-infrared (NIR) spectroscopy, dew point analyser (DPA) as well as analysers commonly associated with gas chromatography (GC) which include thermal conductivity detector (TCD) and flame ionisation detector (FID). Capacitive humidity sensors are used for humidity measurement only and thus have limited applications. The most common limitations encountered with the other techniques are that they can be expensive to implement, require complicated calibration processes, long measurement times (up to several minutes), and in some case are not practical for on-line measurements which are crucial for process control and measurement applications.

There are a range of acoustic techniques that have been shown to be useful for measuring gas composition, such as acoustic absorption (Ejakov et al., 2003) and SoS techniques (see Section 2.4). Acoustic absorption can be characterised using a coefficient $\alpha$, which is defined such that the amplitude of a plane wave decreases during the propagation in a medium with distance $z$ in proportional to $\exp(-\alpha z)$ (Trusler, 1991). The absorption of acoustic energy is attributed to the disturbance of the local equilibrium of the medium caused by sound propagation. In comparison with the other types of acoustic techniques, SoS is more popular due to the better established fundamental theory and the availability of higher-quality published reference data. Speed of sound in gases can be measured with the use of ToF, acoustic resonance and

interferometry methods. ToF method is based on pulse propagation, while the latter two methods use constant waves.

This research project focusses on an on-line gas composition measurement technique for binary gas mixtures. Binary composition measurements are crucial for a number of industrial applications including post combustion carbon dioxide capture, reactive gas process control, hydrocarbon gas control for the oil industry and hydrogen/helium gas purity monitoring. For a binary gas mixture, each of the two gas components can be either a pure gas (e.g. $N_2$, dry air) or a pure vapour (e.g. n-heptane, ethanol). It is noteworthy that although dry air consists of multiple gas components such as $N_2$, $O_2$, Ar and $CO_2$, it can still be considered as a pseudo pure gas because the composition is constant.

An ideal on-line process measurement technique should be non-destructive, safe, easy to operate, fast, cost effective, precise and accurate, and only require a simple, robust and easy-to-manufacture measuring system. In order to fulfill these requirements, the SoS sensor deployed in this research project was designed based on a simple type of ToF method and will be shown to be a fast and high resolution measurement technique well suited for process and analytical chemical applications.

In this research project, experiments were performed on a series of binary gas mixtures in order to correlate the measured speed of sound (SoS) by the SoS sensor with composition. The latter was determined from a density measurement according to Archimedes' Principle; the measured density was converted to composition according to an equation of state analysis with the use of the NIST REFPROP software (see Figure 1) or the Van der Waals equation. The thermodynamic data used by the software are calculated according to the Helmholtz fundamental equations of state.

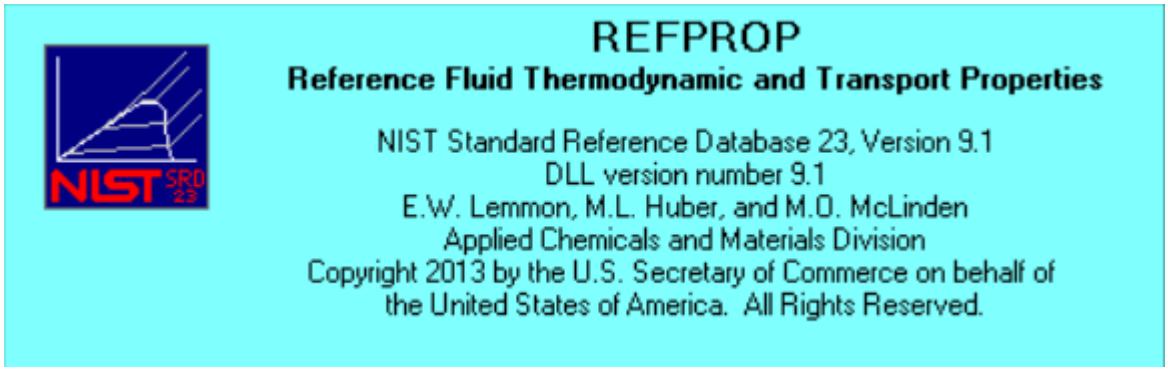



Figure 1. Basic information of the NIST REFPROP software

## 1.2 Objectives

The objectives of this research project are as follows:

1) To develop an apparatus based upon a simple ToF method for on-line gas phase SoS measurement at atmospheric pressure. The apparatus should also be simple, robust, cost effective, easy to operate and manufacture, and be able to provide fast and precise measurement of SoS.
2) To correlate the measured SoS with composition for a wide range of binary gas mixtures at atmospheric pressure and over a range of temperatures.
3) To evaluate the performance of this SoS based gas composition measurement technique.

# CHAPTER 2. Literature Review and Basic Theories

## 2.1 Traditional On-Line Gas Composition Measurement Techniques

### 2.1.1 Capacitive Humidity Sensors

In humidity measurements the requirement is to determine the amount of water vapour in the air for the temperature of interest; therefore, it can be considered as a measurement of composition of a specific type of binary gas mixture (water vapour/dry air). Commonly this measurement is relative humidity, which must be referenced to a measurement temperature (e.g. the relative humidity is 50% at 25 °C). Capacitive humidity sensors are common instruments for humidity measurement in both industries and academic research laboratories (Innovative Sensor Technology [*Online*]; Rotronic Instrument Corporation [*Online*]; Roveti, 2001 [*Online*]). The sensing element of a capacitive humidity sensor is a small capacitor, comprising a thin film of hygroscopic dielectric material deposited between a pair of conductive metal electrodes (see Figure 2). Usually one electrode is attached onto a ceramic, glass or silicon substrate, and the other is porous, allowing moisture to penetrate through and to be absorbed by the dielectric material while protecting it against exposure to contamination and condensation. The dielectric material is typically a polymer or metal oxide with dielectric constant much smaller than that of water vapour. Consequently, as the material absorbs moisture, its dielectric constant should increase, resulting in an incremental change in the sensor capacitance. There is a functional relationship between the amount of moisture absorbed by the material and its capacitance. At equilibrium, the amount of moisture present in the material is dependent on the humidity in the surrounding environment, therefore, by monitoring the sensor capacitance theoretically the humidity can be derived. A resistance thermometer (PT100) is always incorporated into such a sensor for temperature measurement which is necessary for humidity determination. Various types of probes of capacitive humidity sensors are illustrated in Figure 2.

The operating temperature range of such humidity sensors can reach up to 200 °C and down to -100 °C, and the measurement range is always from 0 to 100% relative humidity (RH). Typically, the bulk capacitance is between 0.1 and 0.5 nF at 50% RH and 25 °C, and for a 1% RH change, the variation in capacitance is 0.2 to 0.5 pF. For a 63% RH step change, the

response time generally ranges from 0.5 to 1 min. The typical measurement accuracy is around ± 1% RH from 5 to 95% RH with a simple two-point linear calibration. Capacitive humidity sensors are compact, inexpensive and have excellent stability. However, at high temperatures (> 70 °C) and at high humidity levels (> 50% RH) their long term stability and reliability can be problematic. Furthermore, their performance can be limited by the distance from the sensing part to the electronics owing to the relative small capacitance variations of the former with respect to the capacitive effect of the connecting cables. In addition this type of sensors usually suffer a loss of measurement accuracy at low RH levels. And due to the temperature dependence of the dielectric constant of water vapour, the hygroscopic and dielectric properties of the sensor materials and the capacitance of the connecting cables, compensation for the effect of temperature must be performed for accurate humidity determination.




Figure 2. Left – Schematic of the sensing part of a capacitive humidity sensor; Right – Various types of probes of capacitive humidity sensors (Rotronic Instrument Corporation [*Online*])

### 2.1.2 Dew Point Analysers

Dew point analysers (DPA), also known as optical condensation hygrometers and chilled mirror detectors, are instruments which can be used to determine the composition of a gas system (generally a binary gas mixture in which one gas component is in its vapour phase and thus condensable while the other is not) by directly measuring its dew-point temperature (Davies et al., 1998; General Electric Company [*Online*]; Michell Instruments [*Online*]; Rotronic Instrument Corporation [*Online*]). Taking humid air as an example, its dew point refers to the temperature at which it has to be cooled to reach a saturation state (100% RH) at constant pressure and constant water vapour content wherein drops of dew would form on a local surface. As is shown in Figure 3, for a gas phase sample passing over the metal mirror,

and when the mirror is clean and dry, the light received by the detector which is a reflection off the mirror surface is at its maximum intensity. If the mirror is then gradually chilled by a Peltier thermoelectric cooler until the intensity of the reflected light received by the detector reduces due to the formation of dew on the mirror surface which scatters the incident light, then the dew point temperature is reached. The mirror temperature is monitored by a platinum resistance thermometer (PRT) and at this moment the temperature is recorded as the dew point of the gas system. Then, in theory, if the total gas pressure is known, the dew point temperature can be converted into gas composition either by interpolating the values in the saturated vapour pressure versus temperature table for the condensed pure liquid or by using the corresponding Antoine equation, based in the actual measurement temperature.

Typically, in a laboratory type measurement device, the dew point temperature can be measured with an accuracy of ± 0.1 to 0.2 °C, and the relative humidity of ambient air at around 25 °C and atmospheric pressure can be determined with an accuracy of ± 0.3% RH. It is noteworthy that in RH measurement air temperature should be measured with another thermometer. Limited by the cooling and heating rates, as well as the control loop for the mirror temperature, the response time of this type of instruments is usually relatively long from 30 seconds to a few minutes. Intrinsic to the measurement principle, this technique is not practically applicable to permanent gas mixtures. In reality, DPA is predominantly utilised for humidity measurement, and its application to organic-vapour-contained binary gas mixtures which is very occasional, is often limited by the low surface tensions of organics which increase the difficulty of forming dew (droplets which are non-wetting) on the mirror surface. In terms of humidity measurement, in comparison with the capacitive sensors discusses in Section 2.1.1, this technique is generally more accurate and repeatable, but is more expensive and requires a much cleaner environment and a higher level of maintenance. The technique is especially vulnerable to surface contamination of the mirror which can require ongoing instrument maintenance.




Figure 3. Left – Schematic of the measurement principle of DPA (Davies et al., 1998); Right – A typical DPA probe (Michell Instruments [*Online*])

### 2.1.3 Thermal Conductivity Detectors

Gas chromatographs (GC) are widely used analytical instruments for both identification and quantitation of different components of a mixture (Christian, 1994; Christian & O'Reilly, 1986). The sample of interest should be vapourised before being carried into the chromatographic column if it is not already in gaseous state. The carrier gas, which is known as the mobile phase, is usually a pure chemically inert gas such as helium or nitrogen. Typically, the chromatographic column consists of a tube packed with solid particles on which the liquid stationary phase is coated, or a capillary tube coated with a film of stationary phase on the inside wall. The separation of the sample is achieved based on the different strengths of interaction between different sample components and the stationary phase. A stronger interaction should result in a longer retention time which means it takes longer for the sample component to pass through the column, and vice versa. The separated sample components in the effluent flowing out of the column are detected sequentially using a detector whose response is dependent on their concentrations. The retention time or relative retention time theoretically can be used to identify the different sample components and the area under a chromatographic peak which is proportional to the concentration of the corresponding sample component in both the effluent and the original sample can be used for quantitative analysis. In some cases the peak height is used instead of the area. The schematics of a typical GC and the separation process are shown in Figure 4.

Thermal conductivity detectors (TCD), also called hot wire detectors, are commonly used in GC (Christian, 1994; Christian & O'Reilly, 1986). The schematic of the measurement principle of a typical TCD can be found in Figure 5. The detector has four heated filament wires ($R_1$, $R_2$, $S_1$, $S_2$) arranged in a Wheatstone bridge circuit. $R_1$ and $R_2$ are in the reference cell and the other

two filaments are in the sample cell. The output signal (voltage) across Point 1 and 2 is zeroed when only pure carrier gas flows through both of the two cells. This is the balanced state of the bridge circuit. During measurement, a pure carrier gas stream is passed through the reference cell as reference gas while the effluent gas flowing out of the chromatographic column which is generally a stream of binary gas mixture comprising both the sample component and the carrier gas is passed through the sample cell. Since the temperature of the filaments is dependent on the rate at which heat is transferred by the gas medium to the cell body and the resistance of the filaments is dependent on temperature, the difference in thermal conductivity between the two gas streams will lead to a potential difference across the two points and a non-zero output signal can thus be detected. The intensity of the signal is proportional to the difference in thermal conductivity which is related to the concentration of the sample component in the effluent. The visible output of the signal with respect to time is called chromatogram where the peaks each of which corresponds to a particular sample component can be used for both qualitative and quantitative analyses. Hydrogen or helium is generally preferred as the carrier gas due to their significantly higher thermal conductivity than that of most other gases (typically ten times that of argon, carbon dioxide, nitrogen, air, most organic vapours, etc.) which can facilitate the detection of even a small amount of sample component or a small variation of its concentration in the effluent. Helium is usually more preferred for safety reasons.

TCD is simple, inexpensive, reliable and sensitive to essentially all substances. However, the sensitivity of this type of instruments is limited and this technique generally requires careful calibration. TCD can be used for on-line composition measurement of binary gas mixtures (passed through the sample cell) independently without being connected into a GC, however, because of the measurement principle, there is a requirement for a reference gas to pass through the reference cell which is usually a pure stream of one of the dominant constituent gases. However, as the case in this research project, if the thermal conductivities of the two gas components of a binary mixture under test are relatively close to each other, in which case the difference in thermal conductivity between the two gas streams will be small, no matter what the concentration of the non-reference gas component in the mixture stream is, the resultant measurement accuracy will thus be low. Coupling into a GC (GC-TCD) can in theory solve some of the above problems, but the applicability to on-line measurements will become very limited, and the measurement cost and complexity will be increased dramatically.

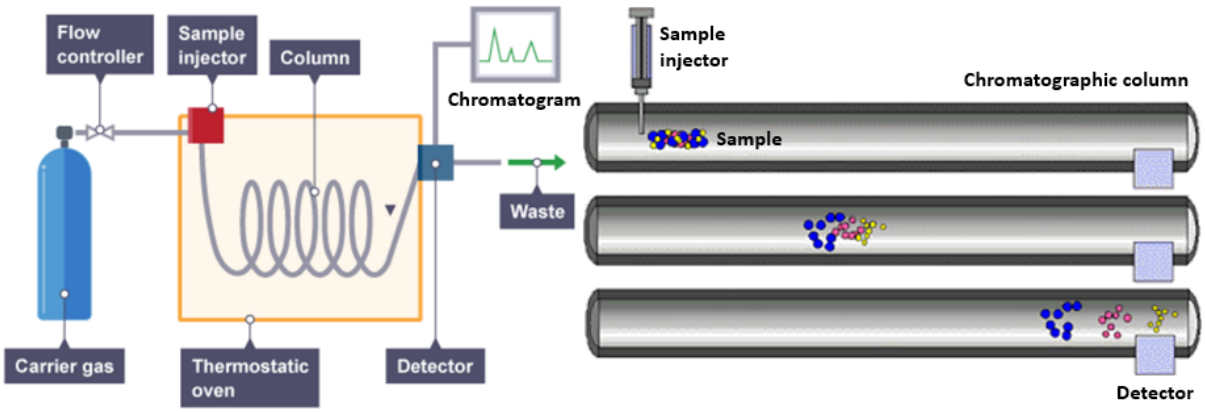



Figure 4. Left – Schematic of a typical GC (BBC GCSE Bitesize Science [*Online*]); Right – Schematic of the separation process (General Chemistry [*Online*])

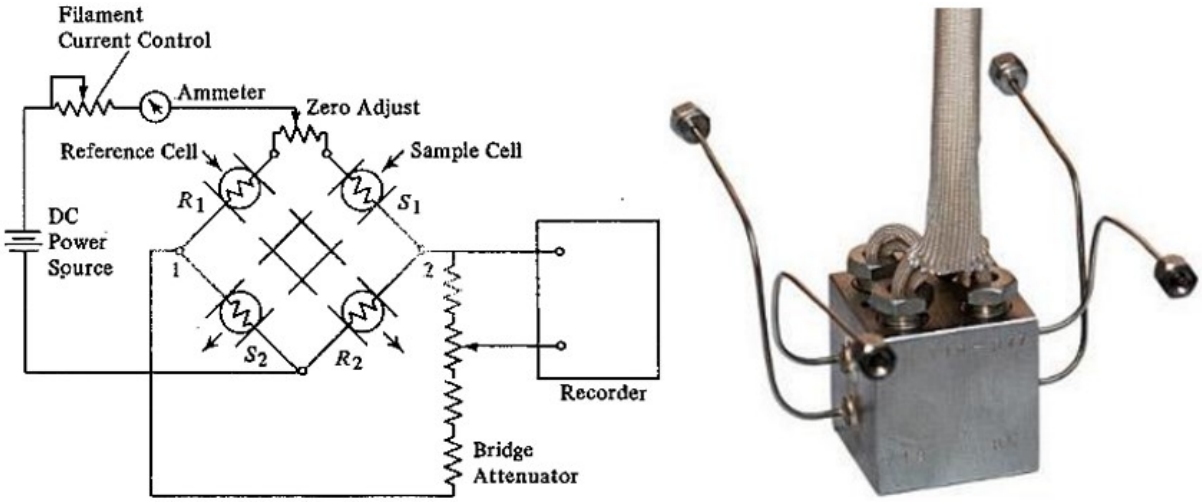



Figure 5. Left – Schematic of the measurement principle of TCD (Christian & O'Reilly, 1986); Right – A typical TCD (AGC Instruments [*Online*])

### 2.1.4 Flame Ionisation Detectors

The most commonly used detectors in GC are flame ionisation detectors (FID) (Cazes, 2004; Christian, 1994; Christian & O'Reilly, 1986). The schematic of the measurement principle for this type of instruments is shown in Figure 6. Typically, an FID consists of a hydrogen-air flame and is used in the case that the sample component in the effluent gas flowing out of the chromatographic column is ionisable in the flame whilst the carrier gas is not. As the effluent gas passes into the flame, the sample component is ignited and ionised, and the ions generated are collected with the use of a pair of oppositely charged electrodes. An electric current is thus produced of which the intensity is proportional to the number of ions generated from the sample

component and thus proportional to its concentration in the effluent. FID is primarily used for the detection of organic compounds which can be oxidised in the flame and produce ions. It responds strongly to C-C and C-H but less strongly to oxygenated carbons such as -(C=O)- and -COOH. The response is usually considerably weak to certain functional groups of organic compounds such as amine, halogen and hydroxyl, and this technique does not respond to permanent gases such as argon, carbon dioxide, water vapour, helium and nitrogen. Typically, the response is proportional to the number of carbon atoms in the organic compounds. In some cases, air is substituted by oxygen in order to achieve a higher flame temperature which makes the ionisation of many inorganic compounds possible. Due to the measurement principle, this technique is destructive, but sample collection is possible by splitting the effluent gas into two streams, one of which is for the FID analysis while the other is used for collection. Fortunately, FID only requires a small portion of the effluent for analysis, thus most of it can be collected for further use.

FID has excellent sensitivity which is much higher than that of TCD. Therefore, this technique is well suitable for the analysis of trace amount of organic components in a mixture even down to ppb levels. FID can also be used independently for on-line composition measurement of binary gas mixtures in which one gas component is ionisable in the flame while the other is not. It is not applicable if the two gas components are both non-ionisable, while if they are both ionisable, theoretically FID might also be applicable as long as its responses to them are different. As mentioned above, although this technique is destructive, gas collection can be achieved if the gas mixture is split into two streams before being tested. FID is reliable, but due to the use of hydrogen and a combustion-supporting gas for the flame, this technique always has safety and logistical issues. In addition, this technique is generally not low cost. And similar to GC-TCD, GC-FID is also not usually used for on-line measurements due to the very limited applicability, intermediate cost and complexity.

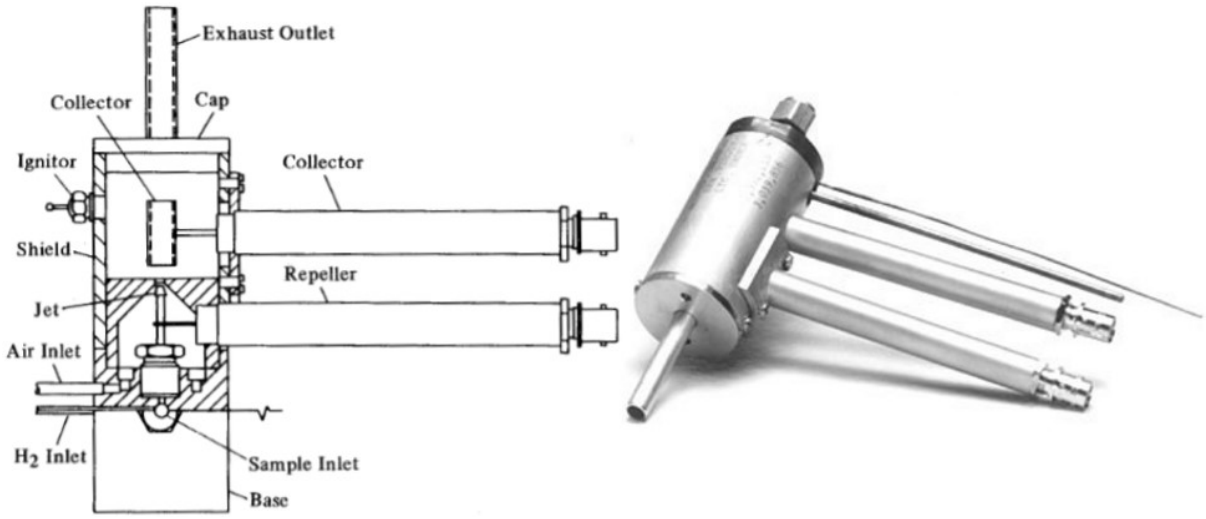



Figure 6. Left – Schematic of the measurement principle of FID (Christian & O'Reilly, 1986); Right – A typical FID (GOW-MAC Instrument Co. [*Online*])

### 2.1.5 Fourier Transform Infrared Spectrometers

The most important applications of Fourier transform infrared (FT-IR) spectrometers are in identification and structure analysis of organic substances, but they can also be employed for the quantitative analysis of mixtures (Cazes, 2004; Christian, 1994; Christian & O'Reilly, 1986). Typically, an FT-IR instrument uses a Michelson interferometer for spectrum generation, which basically consists of a beam splitter, a fixed mirror and a movable mirror (see Figure 7). The infrared source is polychromatic light source in the mid-infrared (MIR) region (4000 to 400 $cm^{-1}$). Current convention uses the term IR, rather than MIR. With the use of the beam splitter, ideally 50% of the incoming radiation from the source at all frequencies is transmitted towards the fixed mirror at a right angle while the other 50% is refracted towards the movable mirror at a right angle. The two beams are reflected back to the splitter by the two mirrors respectively and interference will occur when they are recombined. In practice, the movable mirror is continuously translated at a linear velocity in the direction parallel to the incoming beam, thus the optical path difference (OPD) between the two beams keeps changing, and so does the interference pattern in the recombined beam which is focused on the sample in the sample cell. As the radiation passes through the sample, absorption takes place at frequencies which match the vibrational frequencies of chemical bonds in the sample molecules. The transmitted radiation through the sample cell is measured by a detector, from which a spectrum in time domain (intensity of signal versus OPD), also called the interferogram, can be obtained. The interferogram is computationally converted into the conventional frequency-domain

absorption or transmission spectrum (percent of absorbance or transmittance versus wavenumber) via a mathematical operation called Fourier transformation. It is worth mentioning that in order to acquire the spectrum specific for the sample or certain sample component of interest, a proper background spectrum needs to be generated in advance and then subtracted from the spectrum obtained from the sample of interest. Since the wavenumbers of the peaks in a frequency-domain absorption or transmission spectrum are characteristic of specific types of bonds or functional groups, they in theory can be used to identify or analyse the structure of the molecules in a sample of either pure substance or mixture. Moreover, theoretically the intensity of a peak which is specific for a certain component in a sample of mixture can be correlated to its concentration according to Beer-Lambert Law, but which in practice always requires complicated and careful calibrations. In common with many spectroscopic techniques which use the Beer-Lambert Law, the measurement range would not usually exceed 1000 from maximum to minimum concentration.

In comparison with the traditional dispersive infrared spectrometers which use monochromatic radiation, FT-IR measures all frequencies simultaneously and thus generally is faster and has higher resolution and signal-to-noise ratio. However, in terms of on-line composition measurement of gas mixtures, although due to the measurement principle this technique theoretically can be applied to mixtures with more than two components directly, it is generally slow, complicated and expensive.

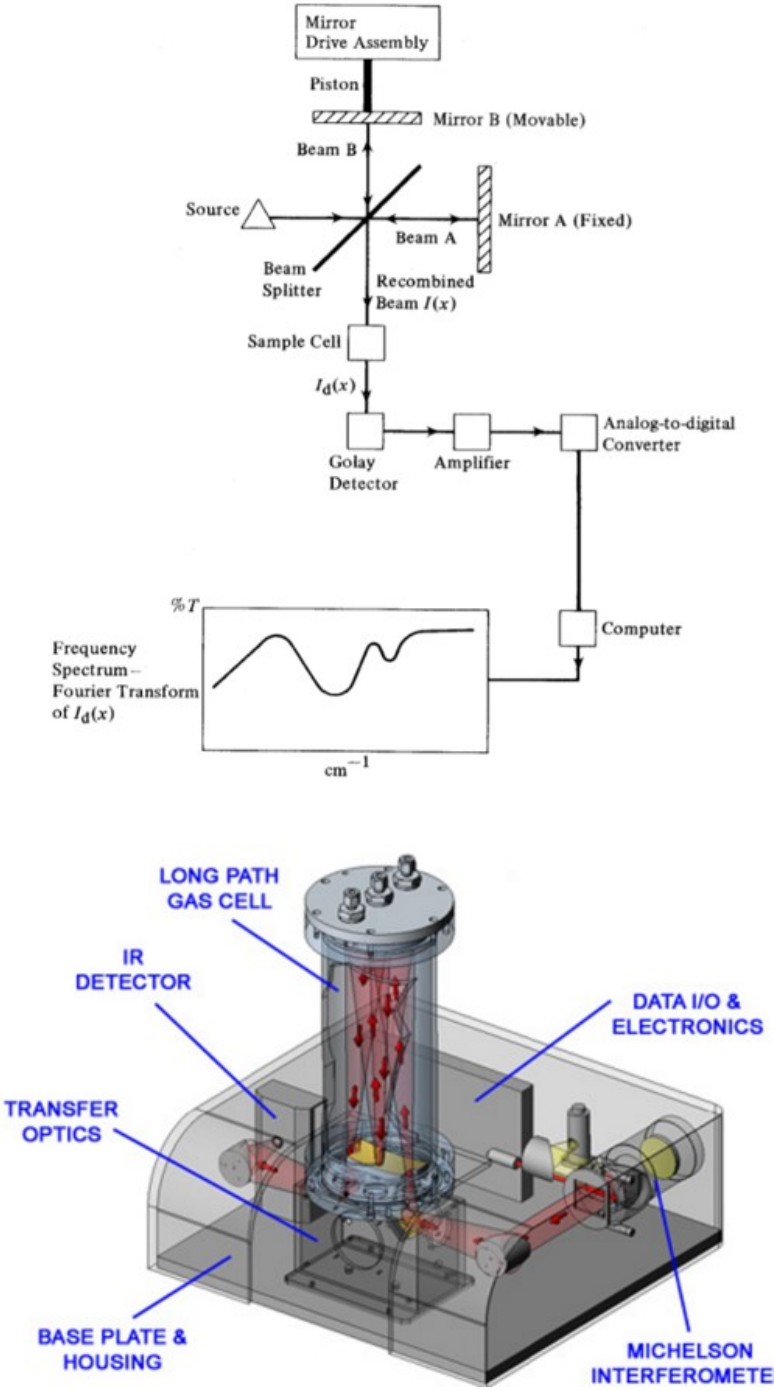



Figure 7. Above – Schematic of Michelson interferometer and associated electronics (Christian & O'Reilly, 1986); Below – Schematic of an FT-IR spectrometer for gas analysis (Gemini Scientific Instruments [*Online*])

### 2.1.6 Near-Infrared Spectrometers

The characteristic absorption of electromagnetic radiation by substances in the IR region (4000 to 400 $cm^{-1}$) is generally due to the fundamental molecular vibrations, while those in the near-infrared (NIR) region (13300 to 3000 $cm^{-1}$) typically results from overtones and combinations

of fundamental vibrations. Although the absorption bands in the NIR region are weak and rather featureless, they are very useful for quantitative analysis (Cazes, 2004; Christian, 1994). Because of the availability of high intensity light sources, high light throughput and sensitive detectors in NIR spectrometers, the signal-to-noise ratio for a spectrum in this region is high. NIR spectroscopy is a fast and non-destructive technique, and also enables real-time analysis of industrial gases for example. Remote sampling can be facilitated by using fiber-optic probes. However, the calibration processes for NIR spectrometers are also not simple. The methods for analysing NIR spectra are more complex than that for the IR range due to the less fundamental spectral characteristics.

Instrumentation for NIR and IR spectroscopies are basically the same in configuration. Fourier transform instruments for spectroscopy such as for NIR have been introduced in the previous section in FT-IR. Here the operating principle of a simple type of dispersive instrument, which can be used for IR or NIR, is illustrated in Figure 8. Polychromatic radiation emitted from the source passes through an entrance slit and is diffracted on a grating. The diffraction is dependent upon the wavelength, the incident angle and the spacing of the periodic structure on the grating surface. In the reflected beam, the wavelengths composing the incident beam are distinguishable spatially from one another. An exit slit is used to allow a monochromatic light to pass through and irradiate the sample to be analysed. The scanning of different wavelengths is enabled by rotating the monochromator grating by mean of a motor. In this way, the absorption/transmission spectrum of the sample can be generated.

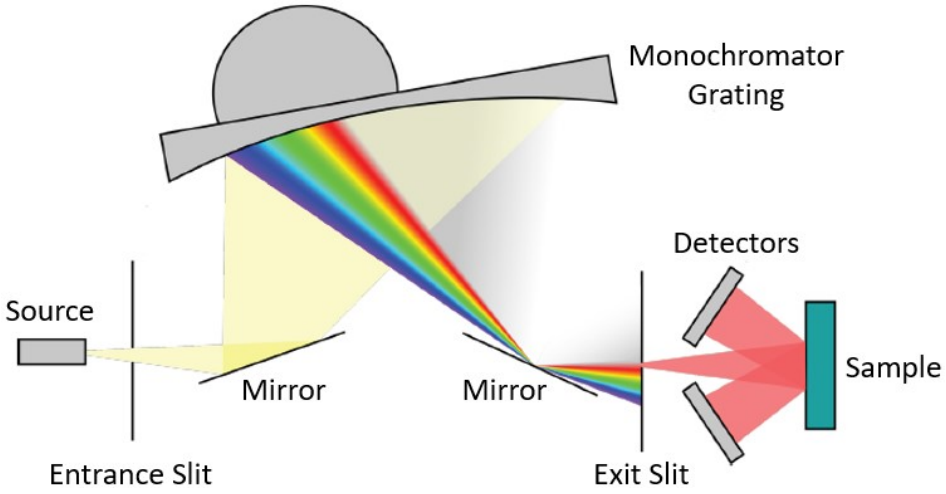



Figure 8. Schematic of a simple dispersive NIR spectrometer (Metrohm AG [*Online*])

### 2.1.7 Summary of the Typical Characteristics of Different On-Line Gas Composition Measurement Techniques

The typical characteristics of using DPA, TCD, FID, FT-IR, NIR and SoS-ToF (the technique employed in this research project) for on-line gas composition measurement are summarised in Table 1. Capacitive technique as mentioned in Section 2.1.1 is excluded because it is specifically designed for humidity measurement. In order to achieve the best measurement accuracy for a particular type of gas mixture, except DPA which generally only requires temperature calibration, all of the other techniques require careful calibration using reference samples of the same type of mixture with known compositions. In this table, the term calibration transferability indicates whether or not the gas mixture calibration results obtained from one instrument are transferable to the others of the same design without the need to repeat the same calibration. It is worth mentioning that some other techniques can also be used for on-line gas composition measurement, however, they typically have one or more of the following disadvantages – insensitive, complicated, expensive or having limited applicability, and are thus not contained in this table.

Table 1. General summary of the typical characteristics of different on-line gas composition measurement techniques

| Techniques | Application | Sensitivity Range | Temperature Dependence | Measurement Time | Price | Calibration Transferability | Comments |
|---|---|---|---|---|---|---|---|
| DPA | Binary gas mixtures in which one component is condensable while the other is not (primarily for humidity measurement) | $10^{-3}$ | Strong | 0.5 to 3 min | \$2 to 5K | N/A | Requires a higher level of maintenance; limited application to organic-vapour-contained binary mixtures; not applicable to permanent gas mixtures |
| TCD | Binary gas mixtures in which the two components have distinguishable thermal conductivities | $10^{-4}$ to $10^{-3}$ | Strong | < 10 s | \$2 to 4K | No | Requires an additional gas stream for the reference cell; generally much less sensitive for binary mixtures containing no hydrogen or helium component |
| FID | Binary gas mixtures in which one component is ionisable (usually an organic compound) while the other is not or they are both ionisable but with distinguishable instrumental responses | $10^{-8}$ to $10^{-6}$ | Low | < 1 s | \$5 to 30K | No | Safety and logistical issues; destructive; generally not applicable to permanent gas mixtures; linear dynamic range exceeds $10^6$ |
| FT-IR NIR | Binary or multi-component gas mixtures in which the components have distinguishable infrared or near-infrared absorption properties | $10^{-3}$ | Low | 10 s to 3 min | \$20 to 50K | No | The applicability to multi-component mixtures is the biggest advantage; requires relatively long method development times |
| SoS-ToF | Binary gas mixtures in which the two components have distinguishable speed of sound | $10^{-6}$ | Strong | < 1 s | < \$2K | Yes | Easy to achieve highly accurate measurement of time; requires much less effort to calibrate manufactured instruments |

## 2.2 Equations of State (EoSs) for Gases

### 2.2.1 Ideal Gas Law (Ideal Gas EoS)

The thermodynamic state of an ideal gas is governed by the ideal gas law:

$$PV = RT \tag{1}$$

or

$$P = \rho RT \tag{2}$$

where $P$ indicates the pressure, $R$ = 8.314510 J/(mol·K) the universal gas constant, $T$ the temperature, $V$ the volume (molar) and $\rho$ the density (molar).

### 2.2.2 Virial EoS

The thermodynamic state of a real gas can be represented by the virial EoS:

$$\frac{PV}{RT} = 1 + \frac{\mathcal{B}}{V} + \frac{\mathcal{C}}{V^2} + \cdots \tag{3}$$

or

$$\frac{PV}{RT} = 1 + \mathcal{B}_{\mathcal{P}}P + \mathcal{C}_{\mathcal{P}}P^2 + \cdots \tag{4}$$

where $\mathcal{B}$ and $\mathcal{C}$ denote the second and third virial coefficients corresponding to the interactions between pairs and triplets of molecules, respectively; $\mathcal{B}_{\mathcal{P}}$ and $\mathcal{C}_{\mathcal{P}}$ are called the virial pressure coefficients. In practice, the higher level terms in the power series expansion which are those not shown in the above equations are usually discarded. $\mathcal{B}_{\mathcal{P}}$ and $\mathcal{C}_{\mathcal{P}}$ are related to $\mathcal{B}$ and $\mathcal{C}$ by:

$$\mathcal{B}_{\mathcal{P}} = \frac{\mathcal{B}}{RT} \tag{5}$$

$$C_{\mathcal{P}} = \frac{\mathcal{C} - \mathcal{B}^2}{(RT)^2}. \tag{6}$$

It is worth mentioning that for pure gases the virial coefficients are considered to be only dependent upon temperature. When the pressure is extremely high, the thermodynamic state cannot be represented by a power series expansion, thus Equations (3) and (4) will lose their utility.

### 2.2.3 Van Der Waals EoS

The Van der Waals EoS is the simplest cubic equation of state which was developed to represent the thermodynamic state of real gases:

$$\left(P + \frac{a}{V^2}\right)(V - b) = RT \tag{7}$$

where the term $a/V^2$ provides a correction for intermolecular attractive force and the parameter $b$ is a correction for finite molecular size which takes into account the intermolecular repulsive force. The parameters $a$ and $b$ for a pure gas are given by:

$$a = \frac{27R^2{T_c}^2}{64P_c} \tag{8}$$

$$b = \frac{RT_c}{8P_c} \tag{9}$$

where $T_c$ and $P_c$ are the critical temperature and the critical pressure. Generally, the Van der Waals EoS is suitable for uncompressed non-polar or weak polar gases.

### 2.2.4 Basic Mixing Rules

The properties of a gas mixture can be determined from available experimental data specific for the mixture itself, or have to be determined from known values of the corresponding properties of its individual components and appropriate mixing rules.

In a gas mixture of $N$ components, it must be true that:

$$\sum_{i=1}^{N} x_i = 1 \tag{10}$$

where $x_i$ indicates the mole fraction of the $i$th component.

The linear mixing rule can be represented as:

$$Y = \sum_{i=1}^{N} x_i Y_i \tag{11}$$

where $Y$ denotes the mixture property and $Y_i$ the pure-gas property of the $i$th component. This is the simplest mixing rule.

The quadratic and cubic mixing rules are written as follows:

$$Y = \sum_{i=1}^{N} \sum_{j=1}^{N} x_i x_j Y_{ij} \tag{12}$$

$$Y = \sum_{i=1}^{N} \sum_{j=1}^{N} \sum_{k=1}^{N} x_i x_j x_k Y_{ijk} \tag{13}$$

where $Y_{ij}$ and $Y_{ijk}$ are pure-gas properties if $i = j$ and $i = j = k$, respectively; otherwise, they are called the unlike-interaction properties. For the latter, $Y_{ij}$ corresponds to the interaction between a pair of molecules of different species, $Y_{ijk}$ corresponds to the interaction between a triplet of molecules of not all identical species, and the order of the subscripts has no physical meaning.

It should be noted that the representations of mixing rules in polynomial forms are not exclusive, they can be more complex for some properties.

The molecular weight $M$ of a gas mixture follows the linear mixing rule, and the molar density and molar volume can be written as:

$$\rho_{(molar)} = \frac{\rho_{(mass)}}{M} = \rho_{(mass)} \left( \sum_{i=1}^{N} x_i M_i \right)^{-1} = \frac{1}{V}. \tag{14}$$

By substituting this equation into Equation (1) or (2), the ideal gas law can be expressed in a composition dependent form.

For the virial EoS, the second and third virial coefficients, $\mathcal{B}$ and $\mathcal{C}$, obey the quadratic and cubic mixing rules, respectively. It is worth mentioning that the availability of the unlike-interaction virial coefficients is generally limited, especially for the unlike-interaction third virial coefficients.

The quadratic mixing rule applies to both $a$ and $b$ in the Van der Waals EoS. The unlike-interaction properties $a_{ij}$ and $b_{ij}$ $(i \neq j)$ are related to pure-gas properties by:

$$a_{ij} = \left(1 - k_{ij}\right)\sqrt{a_{ii} a_{jj}} \tag{15}$$

$$b_{ij} = \frac{b_{ii} + b_{jj}}{2} \tag{16}$$

where $k_{ij}$ is called the coupling factor. Similar to the case of unlike-interaction virial coefficients, the available $k_{ij}$ data for gas mixtures are not sufficient either.

### 2.2.5 H-EoSs for Pure Gases

The equations of state which are fundamental equations explicit in the Helmholtz energy or the reduced Helmholtz energy will be referred to as H-EoSs in this thesis. The general form of the fundamental equation for a pure gas in real gas state explicit in the Helmholtz energy can be written as:

$$\mathcal{H}(T, \rho) = \mathcal{H}^o(T, \rho) + \mathcal{H}^r(T, \rho) \tag{17}$$

where $\mathcal{H}(T, \rho)$ represents the pure-gas Helmholtz energy, $\mathcal{H}^o(T, \rho)$ the ideal gas contribution to $\mathcal{H}$, and $\mathcal{H}^r(T, \rho)$ the residual Helmholtz energy resulting from the non-ideality of the gas (intermolecular forces). The independent variables in the functions $\mathcal{H}$, $\mathcal{H}^o$ and $\mathcal{H}^r$ are the temperature $T$ and the density $\rho$. In practical applications, the reduced or dimensionless

Helmholtz energy $\hbar(\eta,\zeta)$, $\hbar^o(\eta,\zeta)$ and $\hbar^r(\eta,\zeta)$ with independent variables of the inverse reduced temperature $\eta$ $(= T_c/T)$ and the reduced density $\zeta$ $(= \rho/\rho_c$, $\rho_c$ is the critical density) are usually used ($\hbar = \mathcal{H}/RT$, $\hbar^o = \mathcal{H}^o/RT$, $\hbar^r = \mathcal{H}^r/RT$). Equation (17) then becomes:

$$\hbar(\eta,\zeta) = \hbar^o(\eta,\zeta) + \hbar^r(\eta,\zeta) \tag{18}$$

which is explicit in the reduced Helmholtz energy. All thermodynamic properties of the gas can be determined by combining derivatives of this equation as long as two independent thermodynamic parameters are specified (not have to be $T$ and $\rho$, can be $T$ and the pressure $P$, etc.). The ideal gas term can be obtained if the ideal gas isobaric heat capacity $C_P^o$ is known. For a particular pure substance, $C_P^o$ is a function of temperature only and can be determined by statistical mechanics or by correlating experimental data. The residual term is basically obtained by fitting an equation of a multi-parameter mathematical structure to the available relevant experimental data in an empirical way coupling with a particular structural-optimisation method. Since the application of H-EoSs in this research project is achieved by using the NIST REFPROP software, the detailed methods to determine the above two terms are not discussed in this thesis. An H-EoS is much more sophisticated than the EoSs mentioned in the previous sections, which typically contains upwards of 20 substance specific parameters. However, it generally can provide the best accuracy for the description of the thermodynamic state of a gas and thus for the prediction of its thermodynamic properties over wide ranges of temperature and pressure.

The pure gases of interest in this research project (including the pure gas components in gas mixtures) for which H-EoSs are available in commercial software (i.e. the thermodynamic data are available in the software environment) and are involved in the data analysis are given in Table 2, together with the literature values where the H-EoS specific for each pure gas can be found. It is worth mentioning that the experimental temperatures and pressures are within the applicable ranges of these H-EoSs.

Table 2. Pure gases with available thermodynamic data in the NIST REFPROP software

| No. | Pure Gases | Literatures |
|---|---|---|
| 1 | Nitrogen | Span et al., 2000 |
| 2 | Oxygen | Schmidt & Wagner, 1985 |
| 3 | Argon | Tegeler et al., 1999 |

| | | |
|---|---|---|
| 4 | Carbon Dioxide | Span & Wagner, 1996 |
| 5 | Helium | Ortiz Vega, 2013 |
| 6 | n-Hexane | Span & Wagner, 2003 |
| 7 | n-Heptane | |
| 8 | n-Octane | |
| 9 | n-Nonane | Lemmon & Span, 2006 |
| 10 | n-Decane | |
| 11 | Toluene | |
| 12 | Cyclohexane | Zhou et al., 2014 |
| 13 | Water | Wagner & Pruß, 2002 |

### 2.2.6 H-EoSs for Gas Mixtures

Similar to Equation (18), the general form of the H-EoS for a gas mixture in real gas state can be written as:

$$\hbar(\eta, \zeta, \bar{x}) = \hbar^o(T, \rho, \bar{x}) + \hbar^r(\eta, \zeta, \bar{x}) \tag{19}$$

where $\hbar(\eta, \zeta, \bar{x})$ indicates the reduced mixture Helmholtz energy, $\hbar^o(T, \rho, \bar{x})$ the ideal gas contribution to $\hbar$, and $\hbar^r(\eta, \zeta, \bar{x})$ the residual reduced Helmholtz energy which takes into account the non-ideal mixture behavior. The functions $\hbar$ and $\hbar^r$ have the inverse reduced mixture temperature $\eta$, the reduced mixture density $\zeta$ and $\bar{x}$ which is a vector of molar composition as the independent variables, while the function $\hbar^o$ has the mixture temperature $T$, the mixture density $\rho$ and $\bar{x}$ as the independent variables. If the composition of the mixture is known and two independent thermodynamic parameters are specified ($T$ and $\rho$, or $T$ and $P$, etc.), all thermodynamic properties of the mixture can be obtained by combining various derivatives of this equation. $\eta$ and $\zeta$ are calculated from:

$$\eta = \frac{T_r(\bar{x})}{T} = \frac{1}{T}\left[\sum_{i=1}^{N} {x_i}^2 T_{ci} + \sum_{i=1}^{N-1}\sum_{j=i+1}^{N} 2x_i x_j \beta_{T\,ij}\gamma_{T\,ij}\frac{x_i + x_j}{{\beta_{T\,ij}}^2 x_i + x_j}\sqrt{T_{ci}T_{cj}}\right] \tag{20}$$

$$\zeta = \frac{\rho}{\rho_r(\bar{x})} = \rho \left[ \sum_{i=1}^{N} {x_i}^2 \frac{1}{\rho_{c_i}} + \sum_{i=1}^{N-1} \sum_{j=i+1}^{N} 2x_i x_j \beta_{v_{ij}} \gamma_{v_{ij}} \frac{x_i + x_j}{{\beta_{v_{ij}}}^2 x_i + x_j} \frac{1}{8} \left( \frac{1}{{\rho_{c_i}}^{\frac{1}{3}}} + \frac{1}{{\rho_{c_j}}^{\frac{1}{3}}} \right)^3 \right]. \tag{21}$$

$T_r(\bar{x})$ and $\rho_r(\bar{x})$ indicate the composition-dependent reducing functions for the mixture temperature and density respectively. The binary parameters, $\beta_{T_{ij}}$, $\gamma_{T_{ij}}$, $\beta_{v_{ij}}$ and $\gamma_{v_{ij}}$, are fitted to data for specific binary mixtures if available with reasonably high quality; when there are only poor or even no such experimental data available for a certain binary subsystem in a gas mixture (the binary subsystem in a binary gas mixture actually refers to the mixture itself), the critical properties of the two pure components can be combined according to certain rules such as the Lorentz-Berthelot or the linear combining rules. For the former, it is equivalent to set all of the four binary parameters to unity, while the latter is equivalent to set $\beta_{T_{ij}}$ and $\beta_{v_{ij}}$ to unity and

$$\gamma_{T_{ij}} = \frac{1}{2} \frac{T_{c_i} + T_{c_j}}{\sqrt{T_{c_i} T_{c_j}}} \tag{22}$$

$$\gamma_{v_{ij}} = 4 \frac{\frac{1}{\rho_{c_i}} + \frac{1}{\rho_{c_j}}}{\left( \frac{1}{{\rho_{c_i}}^{\frac{1}{3}}} + \frac{1}{{\rho_{c_j}}^{\frac{1}{3}}} \right)^3}. \tag{23}$$

The ideal gas term in Equation (19) is determined as follows:

$$\hbar^o(T, \rho, \bar{x}) = \sum_{i=1}^{N} [x_i \hbar^o{}_i(T, \rho) + x_i \ln x_i] \tag{24}$$

where $\hbar^o{}_i(T, \rho)$ is the reduced Helmholtz energy in the ideal gas state of the $i$th component and is the same as the pure-gas $\hbar^o(T, \rho)$ function (the $\hbar^o$ in Equation (18) but expressed in the

form with $T$ and $\rho$ as the independent variables) except with the independent variables of the mixture $T$ and the mixture $\rho$; $x_i \ln x_i$ accounts for the entropy of mixing.

The residual term in Equation (19) is given by:

$$\hbar^r(\eta, \zeta, \bar{x}) = \sum_{i=1}^{N} x_i \hbar^r{}_i(\eta, \zeta) + \Delta\hbar^r(\eta, \zeta, \bar{x}) \tag{25}$$

with

$$\Delta\hbar^r(\eta, \zeta, \bar{x}) = \sum_{i=1}^{N-1} \sum_{j=i+1}^{N} \Delta\hbar^r{}_{ij}(\eta, \zeta, \bar{x}) = \sum_{i=1}^{N-1} \sum_{j=i+1}^{N} x_i x_j F_{ij} \hbar^r{}_{ij}(\eta, \zeta) \tag{26}$$

where $\hbar^r{}_i(\eta, \zeta)$ is the residual part of the reduced Helmholtz energy for the $i$th component and is the same as the pure-gas $\hbar^r$ function (see Equation (18)) except with the $\eta$ and $\zeta$ determined from Equations (20) and (21) as the independent variables; $\Delta\hbar^r(\eta, \zeta, \bar{x})$ is the departure function which is the summation over all binary subsystem departure functions $\Delta\hbar^r{}_{ij}(\eta, \zeta, \bar{x})$; the function $\hbar^r{}_{ij}(\eta, \zeta)$ is part of $\Delta\hbar^r{}_{ij}$ and is developed for either a specific binary mixture having binary specific parameters ($\Delta\hbar^r{}_{ij}$ will be a binary specific departure function) or a group of binary mixtures having a uniform structure for all of them ($\Delta\hbar^r{}_{ij}$ will be a generalised departure function). The development of both of these two types of $\hbar^r{}_{ij}$ requires data fitting in connection with a structure-optimisation technique. The adjustable factor $F_{ij}$ is set to unity in a binary specific departure function, or is fitted to binary specific data for each mixture in the group of generalised binary mixtures, or is set to zero (departure function equals zero) if no $\hbar^r{}_{ij}$ is available for a certain binary subsystem.

In general, the H-EoS for a gas mixture is based on the fundamental equations for the pure mixture components together with specific mixing rules. In this research project, ten gas mixtures of interest have available H-EoSs or available thermodynamic data in the NIST REFPROP software (see Table 3). The experimental conditions (temperature, pressure, composition) are within the applicable ranges of these H-EoSs. The fundamental equations for the pure components in those mixtures can be found in the literatures listed in Table 2. The method used to determine the binary parameters in Equations (20) and (21) and the type of departure function employed for each binary subsystem in those mixtures are given in Table 4.

Table 3. Gas mixtures of interest with available thermodynamic data in the NIST REFPROP software

| No. | Gas Mixtures |
|---|---|
| 1 | Dry air |
| 2 | n-Hexane/dry air |
| 3 | n-Heptane/dry air |
| 4 | n-Octane/dry air |
| 5 | n-Nonane/dry air |
| 6 | n-Decane/dry air |
| 7 | Toluene/dry air |
| 8 | Cyclohexane/dry air |
| 9 | Water/dry air |
| 10 | Carbon dioxide/nitrogen |
| Notes<br>In the use of this software to determine the thermodynamic data (densities) of these gas mixtures in this research project, dry air was simplified to a gas mixture only comprising nitrogen, oxygen, argon and carbon dioxide. The other gas components in dry air are not taken into account. | |

Table 4. Binary subsystems in the gas mixtures of interest with available thermodynamic data in the NIST REFPROP software

| | Nitrogen | Oxygen | Argon | Carbon Dioxide |
|---|---|---|---|---|
| n-Hexane | | | | |
| n-Heptane | | | | |
| n-Octane | | | | |
| n-Nonane | | | | |
| n-Decane | | | | |
| Toluene | | | | |
| Cyclohexane | | | | |
| Water | | | | |
| Carbon Dioxide | | | | |
| Argon | | | | |
| Oxygen | | | | |

Notes

Yellow – binary parameters from fitting to experimental data, binary specific departure function

Orange – binary parameters from fitting to experimental data, departure function equal to zero

Green – binary parameters from Lorentz-Berthelot combining rules, departure function equal to zero

Red – binary parameters from unspecified method (fitting or combining rules), generalised departure function available

Blue – binary parameters from unspecified method (fitting or combining rules), departure function equal to zero

Black – binary parameters from unspecified combining rules, departure function equal to zero

Purple – binary parameters estimated from toluene/oxygen, departure function equal to zero

In using the software, for these binary subsystems, the binary parameters and $F_{ij}$ are all available and visible, while the functions $\mathcal{R}^{r}{}_{ij}$, if exist, are all available but invisible. The literatures where these information can be traced to for the binary subsystems containing toluene or cyclohexane are not known, while for all the other binary subsystems, the information can be found from Kunz & Wagner (2012) and Kunz et al. (2007).

## 2.3 Fundamental Theory of Speed of Sound

### 2.3.1 The Linearised Propagation of Plane Sound Waves in Non-Dissipative Fluids

Sound is a longitudinal mechanical wave (or pulse) that is created by a vibrating object and can propagate in a transmission medium via the motions of the particles in it. Unlike electromagnetic waves, sound cannot travel in vacuum. It is noteworthy that this research project is only interested in the sound propagation in fluids, to be more specific, in gases (pure gases or gas mixtures), thus the propagation in solids will not be discussed. Typically, in a fluid where sound propagates, there are regions where the fluid matter are compressed and other regions where the fluid matter are spread out. These two types of regions are called compressions and rarefactions, respectively. On a microscopic scale, an element of fluid (fixed in space, the same hereinafter) experiences alternate compression and expansion cycles while sound passes through, thus the local pressure and density experience periodic fluctuations which are generally accompanied with fluctuations in local temperature (Trusler, 1991).

For the derivation of the isentropic SoS of a fluid as will be given below, the effects of mechanisms which could cause dissipation of acoustic energy whilst sound waves propagate in the fluid are neglected. Therefore, this derivation is strictly applicable only to a fluid in which viscosity and heat conduction are negligible, and local thermodynamic equilibrium can be achieved instantaneously. If the fluid is a mixture then it is further assumed that the fluid composition remains completely homogeneous; both diffusion and chemical reactions are neglected. Such a fluid is called non-dissipative. The acoustic cycles associated with passage of sound in a non-dissipative fluid take place isentropically (adiabatically and reversibly), i.e. the local fluctuations in pressure, density and temperature follow an isentropic path. It is worth mentioning that boundary effects are also not taken into account in this derivation.

The state of a non-dissipative fluid in motion can be phenomenologically specified by assigning a flow velocity $v(\mathbf{X}, t)$ at each point fixed in space and at all times $t$, and by any two independent thermodynamic parameters, say the pressure $P(\mathbf{X}, t)$ and the mass density $\rho(\mathbf{X}, t)$

(Bhatia, 1985). The components of $v(\mathbf{X}, t)$ and the coordinates of the point $\mathbf{X}$ in space along the three Cartesian coordinate axes are represented by $v_i(\mathbf{X}, t)$ and $X_i$ respectively, where $i$ = 1, 2 and 3. In a non-dissipative fluid, the force on a surface element only comes from the pressure acting normal to it. Consequently, for a small rectangular parallelepiped element of fluid centered at point $(X_1, X_2, X_3)$ with sides of $dX_1$, $dX_2$ and $dX_3$ in parallel with the three coordinate axes respectively, the force acting on it in the $X_1$ direction can be written as:

$$-\left[P\left(\left(X_1+\frac{1}{2}dX_1, X_2, X_3\right), t\right) - P\left(\left(X_1-\frac{1}{2}dX_1, X_2, X_3\right), t\right)\right] dX_2 dX_3 = -\frac{\partial P}{\partial X_1} d^3\mathbf{X} \tag{27}$$

where the expression in the square brackets refers to the difference between the pressures acting on the two surfaces of the element normal to the $X_1$ direction; $d^3\mathbf{X}$ indicates the volume of the element equal to the product of $dX_1$, $dX_2$ and $dX_3$. The forces in the $X_2$ and the $X_3$ directions can be expressed in a similar way. Since the force in each direction is equal to the product of the mass of the element of fluid and its acceleration in the same direction, one obtains:

$$\rho \frac{dv_i}{dt} = -\frac{\partial P}{\partial X_i} \ (i = 1, 2, 3), \tag{28}$$

which are the Euler's equations of motion. $dv_i$ can be expressed as the total derivative of $v_i$:

$$dv_i = \left(\frac{\partial v_i}{\partial t}\right) dt + \sum_{j=1}^{3} \left(\frac{\partial v_i}{\partial X_j}\right) dX_j. \tag{29}$$

Dividing both sides of this equation by $dt$ yields:

$$\frac{dv_i}{dt} = \frac{\partial v_i}{\partial t} + \sum_{j=1}^{3} v_j \left(\frac{\partial v_i}{\partial X_j}\right). \tag{30}$$

In a time interval $dt$, the variation in the amount of fluid contained in the element should be equivalent to the quantity of fluid flowing into the element from the three pairs of surfaces normal to the three coordinate axes minus that flowing out of the element from those surfaces. This yields the Euler's equation of continuity:

$$\frac{\partial \rho}{\partial t} + \sum_{j=1}^{3} \frac{\partial (\rho v_j)}{\partial X_j} = 0. \tag{31}$$

The derivation below is based on the assumption that the fluid is at rest except for the motion due to sound propagation. Therefore, the flow in the fluid arises from the propagation of sound exclusively. The changes in the pressure and density of the element of fluid due to the flow are designated as $\delta P(\mathbf{X}, t)$ and $\delta \rho(\mathbf{X}, t)$, thus the pressure $P(\mathbf{X}, t)$ and the density $\rho(\mathbf{X}, t)$ of the element can be represented by:

$$P = P_0 + \delta P \tag{32}$$

$$\rho = \rho_0 + \delta \rho \tag{33}$$

where $P_0$ and $\rho_0$ denote the equilibrium pressure and density of the fluid (in absence of the sound wave) and they can be assumed constant throughout the whole fluid. It should be noted the relationship shown in the above two equations also applies to the temperature variation of the element which is accompanied with the pressure and density variations, i.e. $T = T_0 + \delta T$, where $T(\mathbf{X}, t)$ indicates the temperature of the element, $T_0$ the equilibrium temperature and $\delta T(\mathbf{X}, t)$ the change in temperature arising from the flow. $T_0$ can also be assumed constant at all points in the fluid. With the substitutions of Equations (32) and (33) into Equations (28) and (31), in order to linearise them, the linear acoustic approximation[2] is applied which consists of assuming the amplitude of the local disturbance due to the passage of sound is such small that $\delta P \ll P_0$, $\delta \rho \ll \rho_0$ (also $\delta T \ll T_0$) and the flow velocity $v_i \ll W$ (see below); and therefore neglecting all terms containing double or higher products of any of the quantities $\delta P$, $\delta \rho$ and $v_i$. According to this approximation, one obtains:

$$\rho_0 \frac{\partial v_i}{\partial t} = -\left(\frac{\delta P}{\delta \rho}\right) \frac{\partial \rho}{\partial X_i} \ (i = 1, 2, 3) \tag{34}$$

[2] The linear acoustic approximation can be regarded as valid for all the SoS measurement techniques considered in this thesis.

$$\frac{\partial \rho}{\partial t} = -\rho_0 \sum_{j=1}^{3} \frac{\partial v_j}{\partial X_j}. \tag{35}$$

By differentiating Equation (34) with respect to $t$ and Equation (35) with respect to $X_i$, it can be found that:

$$\frac{\partial^2 v_i}{\partial t^2} = \left(\frac{\delta P}{\delta \rho}\right) \sum_{j=1}^{3} \frac{\partial}{\partial X_i} \left(\frac{\partial v_j}{\partial X_j}\right). \tag{36}$$

For a plane sound wave of angular frequency $\omega$ ($= 2\pi f$, $f$ is the regular frequency in Hz) and wavelength $\lambda$ propagating along the positive $X_1$ direction, $v_2$ and $v_3$ are taken to be zero, and

$$v_1 = v_1^0 e^{\mathbf{i}(\omega t - kX_1)} \tag{37}$$

$$\delta P = P_1^0 e^{\mathbf{i}(\omega t - kX_1)} \tag{38}$$

$$\delta \rho = \rho_1^0 e^{\mathbf{i}(\omega t - kX_1)} \tag{39}$$

where $v_1^0$, $P_1^0$ and $\rho_1^0$ indicate the amplitudes of the variations in flow velocity, pressure and density in the $X_1$ direction, **i** the imaginary unit, and $k$ the wave number equal to $2\pi/\lambda$. With the understanding that the true flow field is represented by the real parts of these complex equations, by substituting Equations (37), (38) and (39) into Equation (36) and for the convenience of later use converting the mass density into molar density, the velocity of the sound wave $W_s$ can be obtained as follows:

$$W_s = \frac{\omega}{k} = \sqrt{\frac{1}{M}\frac{\delta P}{\delta \rho}} = \sqrt{\frac{1}{M}\left(\frac{\partial P}{\partial \rho}\right)_S} \tag{40}$$

where the conversion from $\delta P/\delta \rho$ to $(\partial P/\partial \rho)_S$ is because the periodic fluctuations in the local pressure and density (also the local temperature) of an element of non-dissipative fluid associated with sound propagation are adiabatic and reversible, i.e. isentropic (at constant entropy $S$). Hereinafter, $W_s$ is defined as the isentropic SoS of a fluid. It is a fundamental thermodynamic property of the fluid which can be determined from equation of state analysis

and is a unique value as long as the temperature (if the ideal gas law applies) or any two independent thermodynamic parameters, say the temperature and pressure, are specified.

The derivations below are based on the methods given in Zuckerwar (2002) in order to convert the above equation to a form that can be used more conveniently for the determination of the isentropic speed of sound of a gaseous fluid. According to the rules of partial differentiation, one obtains:

$$\left(\frac{\partial P}{\partial \rho}\right)_S = -\frac{\left(\frac{\partial S}{\partial \rho}\right)_P}{\left(\frac{\partial S}{\partial P}\right)_\rho} = -\frac{\left(\frac{\partial S}{\partial T}\right)_P \left(\frac{\partial T}{\partial \rho}\right)_P}{\left(\frac{\partial S}{\partial T}\right)_\rho \left(\frac{\partial T}{\partial P}\right)_\rho} = \frac{C_P}{C_V}\left(\frac{\partial P}{\partial \rho}\right)_T = \gamma\left(\frac{\partial P}{\partial \rho}\right)_T \tag{41}$$

where $\gamma$ refers to the ratio of isobaric heat capacity $C_P$ to isochoric heat capacity $C_V$; and by definition:

$$C_P = T\left(\frac{\partial S}{\partial T}\right)_P \tag{42}$$

$$C_V = T\left(\frac{\partial S}{\partial T}\right)_V. \tag{43}$$

Substituting Equation (41) into Equation (40) yields:

$$W_s = \sqrt{\frac{\gamma}{M}\left(\frac{\partial P}{\partial \rho}\right)_T}. \tag{44}$$

$\gamma$ can be expressed in terms of thermodynamic state variables, then the above equation becomes:

$$W_s = \sqrt{\frac{1}{M}\left[1 - \frac{T}{C_V^o}\frac{\left(\frac{\partial V}{\partial P}\right)_T \left(\frac{\partial P}{\partial T}\right)_V^{\,2}}{1 + \frac{T}{C_V^o}\int \left(\frac{\partial^2 P}{\partial T^2}\right)_V dV}\right]\left(\frac{\partial P}{\partial \rho}\right)_T} \tag{45}$$

where $C_V^o$ is the ideal gas isochoric heat capacity. The detailed procedures for the conversion from $\gamma$ to the expression in the square brackets are not included in this thesis for simplicity. $C_V^o$ is related to $C_P^o$ which is the ideal gas isobaric heat capacity as follows:

$$C_V^o = C_P^o - R. \tag{46}$$

$C_P^o$ and $C_V^o$ for a particular pure substance are functions of temperature only.

### 2.3.2 Ideal Gas and Lossless Real Gas SoS

The ideal gas SoS of a gas medium $W_o$ is defined as the isentropic SoS while the thermodynamic state is governed by the ideal gas law. It can be calculated from Equation (44) with the replacement of $\gamma$ by the ideal gas heat capacity ratio $\gamma^o$ $(= C_P^o/C_V^o)$ and with the substitution of the partial derivative determined from Equation (2). Thus the ideal gas SoS is written as:

$$W_o = \sqrt{\gamma^o \frac{RT}{M}} = \sqrt{\frac{C_P^o}{C_V^o}\frac{RT}{M}}. \tag{47}$$

The lossless real gas SoS of a gas medium $W_\theta$ refers to the isentropic SoS based on the thermodynamic state of real gas. It could be calculated from Equation (45) with the substitutions of the partial derivatives determined from an EoS for real gas. The calculation given below is based on the virial EoS because it is mathematically convenient for this purpose and also able to provide reasonably high accuracy.

According to Equations (3) to (6) with the terms in the virial expansions being retained only up to $\mathcal{C}/V^2$ and $\mathcal{C}_\mathcal{P}P^2$, one obtains the following expressions for the four partial derivatives in Equation (45):

$$\left(\frac{\partial V}{\partial P}\right)_T = -\frac{RT}{P^2}[1 - \mathcal{C}_\mathcal{P}P^2] = -\frac{RT}{P^2}\left[1 + \frac{\mathcal{B}^2P^2}{(RT)^2} - \frac{\mathcal{C}P^2}{(RT)^2}\right] \tag{48}$$

$$\left(\frac{\partial P}{\partial T}\right)_V = \frac{R}{V}\left(1 + \frac{\mathcal{B}}{V} + \frac{\mathcal{C}}{V^2} + \frac{T}{V}\frac{d\mathcal{B}}{dT} + \frac{T}{V^2}\frac{d\mathcal{C}}{dT}\right) \tag{49}$$

$$\int \left(\frac{\partial^2 P}{\partial T^2}\right)_V dV = -\frac{R}{V}\left(2\frac{d\mathcal{B}}{dT} + \frac{1}{V}\frac{d\mathcal{C}}{dT} + T\frac{d^2\mathcal{B}}{dT^2} + \frac{T}{2V}\frac{d^2\mathcal{C}}{dT^2}\right) \tag{50}$$

$$\left(\frac{\partial P}{\partial \rho}\right)_T = \left(\frac{\partial P}{\partial V}\right)_T \left(\frac{\partial V}{\partial \rho}\right)_T = -RT\left(\frac{1}{V^2} + \frac{2\mathcal{B}}{V^3} + \frac{3\mathcal{C}}{V^4}\right)(-V^2) \tag{51}$$
$$= RT\left(1 + \frac{2\mathcal{B}}{V} + \frac{3\mathcal{C}}{V^2}\right).$$

Substituting these four equations into Equation (45) yields:

$$W_\theta = \sqrt{\frac{\gamma^o RT}{M}\left(1 + \frac{\mathcal{K}}{V} + \frac{\mathcal{L}}{V^2}\right)} \tag{52}$$

where $\mathcal{K}$ and $\mathcal{L}$ indicate the second and third acoustic virial coefficients and are related to $\mathcal{B}$ and $\mathcal{C}$ by:

$$\mathcal{K} = 2\mathcal{B} + 2(\gamma^o - 1)T\frac{d\mathcal{B}}{dT} + \frac{(\gamma^o - 1)^2}{\gamma^o}T^2\frac{d^2\mathcal{B}}{dT^2} \tag{53}$$

$$\mathcal{L} = \left[\mathcal{B} + (2\gamma^o - 1)T\frac{d\mathcal{B}}{dT} + (\gamma^o - 1)T^2\frac{d^2\mathcal{B}}{dT^2}\right]^2\left(\frac{\gamma^o - 1}{\gamma^o}\right) + \frac{1 + 2\gamma^o}{\gamma^o}\mathcal{C} \tag{54}$$
$$+ \frac{(\gamma^o)^2 - 1}{\gamma^o}T\frac{d\mathcal{C}}{dT} + \frac{(\gamma^o - 1)^2}{2\gamma^o}T^2\frac{d^2\mathcal{C}}{dT^2}.$$

In practice, it would be more convenient if $W_\theta$ is expressed in terms of pressure instead of molar volume because the former is usually a directly measured quantity in experiments. Then Equation (52) turns into:

$$W_\theta = \sqrt{\frac{\gamma^o RT}{M}(1 + \mathcal{F}P + \mathcal{G}P^2)} \tag{55}$$

where $\mathcal{F}$ and $\mathcal{G}$ are called the acoustic virial pressure coefficients and can be related to $\mathcal{K}$ and $\mathcal{L}$ by:

$$\mathcal{F} = \frac{\mathcal{K}}{RT} \tag{56}$$

$$\mathcal{G} = \frac{\mathcal{L} - \mathcal{B}\mathcal{K}}{(RT)^2}. \tag{57}$$

Equations (52) and (55) can both be written in the following form by introducing a virial correction factor $K_v$:

$$W_\theta = W_o\sqrt{1 + K_v} \tag{58}$$

where

$$K_v = \frac{\mathcal{K}}{V} + \frac{\mathcal{L}}{V^2} = \mathcal{F}P + \mathcal{G}P^2. \tag{59}$$

While using Equations (47) and (58) for the calculations of $W_o$ and $W_\theta$ for gas mixtures, the property parameters should be determined according to mixing rules. To be more specific, the molecular weight $M$ and the ideal gas heat capacities $C_P^o$ and $C_V^o$ obey the linear mixing rule (see Equation (11)), and the second and third virial coefficients $\mathcal{B}$ and $\mathcal{C}$ respectively comply with quadratic and cubic mixing rules (see Equations (12) and (13)). In the calculation of $W_\theta$, if there is no available data for the interaction virial coefficients, then they can be set to zero and the error in SoS resulting from neglecting these coefficients should be considered in the uncertainty analysis. The NIST REFPROP software can also be used for the determinations of $W_o$ and $W_\theta$ for pure gases and gas mixtures as long as the H-EoSs are available in it and are valid at the conditions of interest ($W_o$ is obtained if the pressure or density input is set to zero).

### 2.3.3 Relaxation Phenomena and Real Gas SoS

In the derivation of the isentropic SoS $W_s$ it is assumed that the fluid is non-dissipative, thus there is no dissipation of acoustic energy or absorption of sound taking place while sound waves propagating through. However, in reality, no fluid is truly non-dissipative, and acoustic dissipative processes could give rise to acoustic dispersion or frequency dependence of SoS. For a gas medium, $W_s$ is frequency independent, while the real gas SoS $W$ accounts for the frequency dependence of speed of sound. It needs to be emphasised that both $W_s$ and $W$ are free-field SoS, i.e. the boundary effects are not taken into account. $W$ can be considered as a gas fundamental property at a particular frequency, and is related to the lossless real gas SoS $W_\theta$ and the ideal gas SoS $W_o$ by:

$$W = W_\theta \sqrt{1 + K_d} = W_o \sqrt{(1 + K_v)(1 + K_d)} \tag{60}$$

where $K_d$ indicates the correction factor for acoustic dispersion. The dissipative processes associated with free-field propagation of sound include vibrational, rotational, chemical, structural, and translational relaxation. Relaxation refers to the process by which a perturbed system returns toward equilibrium. Detailed discussion regarding the effects of relaxation processes on the absorption and dispersion of sound can be found from Bhatia (1985), Trusler (1991) and Zuckerwar (2002); dispersion is of more interest and relevance to this research project.

#### 2.3.3.1 Vibrational and Rotational Relaxation

The total energy of a polyatomic gas[3] is distributed partially among the translational (external) degrees of freedom (DoFs) of the molecules and partially among their vibrational and rotational (internal) DoFs. Acoustic energy is only related to the translational energy modes. A sound wave may disturb the equilibrium energy distribution between the external and internal DoFs, and since the relaxation process requires a finite time, there is instantaneously a lack of thermal equilibrium between the two sets of DoFs. The consequent irreversible exchange of energy between the external and internal energy modes leads to the dissipation of acoustic energy. In general, the relaxation of vibrational modes is much slower than the relaxation of rotational modes. These two types of relaxation processes do not exist in a monatomic gas[4]. For a polyatomic gas at constant temperature and pressure, the dispersion effect on the real gas SoS of a vibrational or rotational relaxation process which can be characterised by a single relaxation time $\tau_r$ (relaxation frequency $f_r = (2\pi\tau_r)^{-1}$) is illustrated in Figure 9 (neglecting all the other mechanisms which could cause dispersion). When $\omega\tau_r \ll 1$, there is no or insignificant dispersion taking place and $W$ can be considered equal to the lossless real gas SoS $W_\theta$. Therefore, the latter can also be called the low-frequency-limit SoS. As $\omega$ increases, significant dispersion starts to occur when $\omega$ is of comparable magnitude to $1/\tau_r$ ($\omega\tau_r \approx 1$); then the curve of $W^2$ passes through a 'halfway' point, and levels off reaching $W_\infty^2$ at higher frequencies ($\omega\tau_r \gg 1$). $W_\infty$ indicates the high-frequency-limit SoS. $W_\theta$ and $W_\infty$ can be related by:

[3] A pure polyatomic gas, or a mixture containing at least one polyatomic component.
[4] A pure gas or mixture consisting of only monatomic molecules.

$$W_\infty = \frac{W_\theta}{\sqrt{1-\varepsilon_r}} \tag{61}$$

where $\varepsilon_r$ represents the relaxation strength. At the frequency $\omega = 1/\tau_r$,

$$W^2 = \frac{1}{2}\left(W_\theta^2 + W_\infty^2\right), \tag{62}$$

and this can be called the 'halfway' point. Typically, vibrational $\tau_r$ is much greater than rotational $\tau_r$; the latter is very small (of the order of the collision time between molecules $\tau_c$), thus significant dispersion due to rotational relaxation can only occur at considerably high frequencies. In usual experiments such high frequencies are not reached.

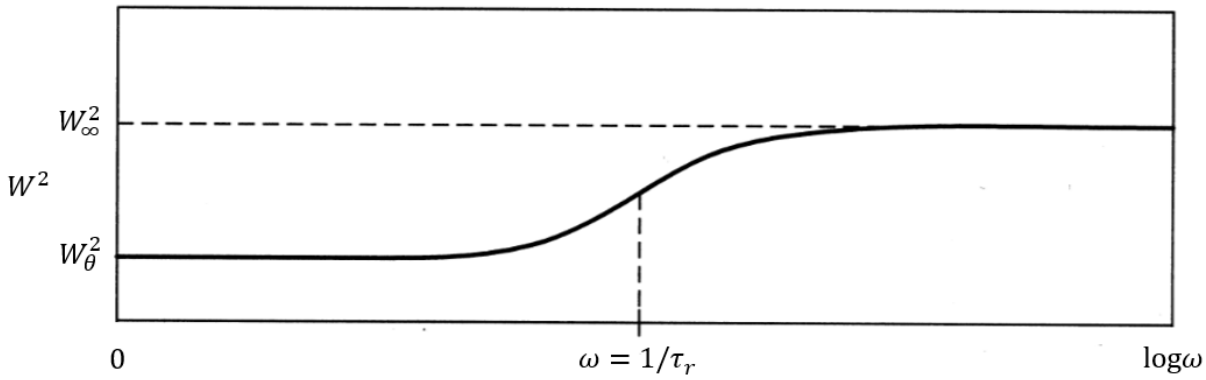



Figure 9. Dispersion effect on $W$ of a vibrational or rotational relaxation process characterised by a single $\tau_r$ (x-axis – logarithm of angular frequency; y-axis – square of real gas SoS)

### 2.3.3.2 Chemical and Structural Relaxation

The extent to which one or more chemical reactions in a gas may be displaced by sound, can as an effect result in the system no longer be a fluid phase of fixed composition. The finite reaction rate may result in the reaction extent lagging behind that which would be attained provided local equilibrium were maintained, and this can lead to acoustic energy dissipation. If the associated relaxation process is characterised by a single $\tau_r$, the accompanied dispersion has much the same kind of behaviour as illustrated above in Figure 9. Relaxations associated with structural rearrangements can be treated within the framework of chemical effects. This phenomenon is exhibited by dense fluids (typically not in gas phase) and especially by those with specific molecular interactions such as hydrogen bonding.

#### 2.3.3.3 Translational Relaxation

As a true fluid possesses viscosity, viscous damping occurs during the propagation of sound and results in acoustic energy losses. Sound propagation can give rise to temperature fluctuations and formation of temperature gradients. Consequently, there is irreversible heat flow to regions of lower temperature from those of higher temperature, and this leads to the thermodynamic path of acoustic cycle deviating from an isentropic one. The dissipation resulting from these mechanisms occurs in the relaxation processes which are associated with transport of momentum and heat, and are related to translational energy transfer between molecules. The propagation of sound in either a polyatomic or monatomic gas is always accompanied by such relaxation process. The time for the redistribution of energy amongst translational degrees of freedom is of the order of $\tau_c$, and is generally very short. In usual experiments the condition $f \ll f_c$ (the molecular collision frequency $f_c = 1/\tau_c$) is satisfied, and in this time regime significant dispersion due to the effects of momentum transport and heat transfer cannot occur. The magnitude of these effects is controlled by the transport coefficients – viscosity and heat conductivity, respectively.

As a sound wave passes through a gas mixture the components will tend to undergo partial fractionation, but diffusion which is an entropy-producing process will take place to diminish the gradients in concentration thereby generated. The relaxation associated with this phenomenon is solely related to the translational motions of molecules. In fact, there are insufficient studies on this relaxation mechanism reported, especially regarding the effect on dispersion. However, according to Bhatia (1985), Kohler (1950) and Trusler (1991), for the calculation of the real gas SoS of dry air at the experimental conditions as in this research project, it may be inferred that the dispersion due to this mechanism is negligible.

### 2.3.4 Summary

For a gas medium, the ideal gas SoS $W_o$, lossless real gas SoS $W_\theta$ and real gas SoS $W$ can be determined as long as the temperature $T$, pressure $P$, frequency $f$ and/or composition $\bar{x}$ are given. The functional relationships between $W_o/K_v/W_\theta/K_d/W$ and $T/P/f/\bar{x}$ are summarised in Table 5. In some cases, e.g. a monatomic gas at low enough frequencies (no chemical reactions occur), the dispersion effect is insignificant, and thus $W$ can be considered equal to $W_\theta$ ($K_d = 0$). In the case of a binary gas mixture, provided that the species of the two gas components, $T$, $P$ and $f$ are known, $W$ should be in one-to-one correspondence with the mole fraction of either

gas component. This is the theoretical fundamental principle of the SoS technique for the composition measurement of binary gas mixtures.

Table 5. Summary of temperature/pressure/frequency/composition dependences of SoSs and correction factors

| | Pure Gases | | | Gas Mixtures | | | |
|---|---|---|---|---|---|---|---|
| | $T$ | $P$ | $f$ | $T$ | $P$ | $f$ | $\bar{x}$ |
| $W_o$ | ● | ○ | ○ | ● | ○ | ○ | ● |
| $K_v$ | ● | ● | ○ | ● | ● | ○ | ● |
| $W_\theta$ | ● | ● | ○ | ● | ● | ○ | ● |
| $K_d$ | ● | ● | ● | ● | ● | ● | ● |
| $W$ | ● | ● | ● | ● | ● | ● | ● |
| ● – dependent; ○ – independent | | | | | | | |

In this research project, the values of $W$ for Ar, He, $N_2$ and dry air at certain experimental temperatures and pressures and at the operating frequency of the SoS sensor need to be known. The methods for their determination will be given in Appendix A1, together with the uncertainties of the determined values. The effects of chemical reactions, structural rearrangement and diffusion are neglected.

## 2.4 SoS Measurement Methods

Time of flight (ToF), acoustic resonance and interferometry methods are the most commonly used for the measurement of SoS in gases. In this section, their basic principles of measurement and the typical measuring apparatus are introduced.

### 2.4.1 ToF Method

#### 2.4.1.1 Ultrasonic Transducers

In this thesis, an ultrasonic transducer refers to a device with which electrical energy can be converted to mechanical energy in the form of ultrasound, and vice versa. Consequently, it can act as an ultrasound transmitter (electrical to mechanical energy), a receiver (mechanical to electrical energy), or both. The best operating frequency of an ultrasonic transducer usually refers to its resonance frequency at which it can give the maximum response. The bandwidth is defined as the frequency range over which such a device can give at least half of the maximum response. The spreading of the ultrasound beam sent out from a transducer (transmitter) is characterised by the beam width. The angle between two directions for which the ultrasound intensity is half of the maximum at center axis is called the -3 dB beam width.

The most commonly used type of ultrasonic transducers are piezoelectric transducers (NDT Resource Center [*Online*]). The typical cross-sectional structure of this type of transducer is shown in Figure 10. The piezoelectric element with electrodes attached to two of its opposite faces can deform under an electric field. An AC voltage can make it oscillate and produce acoustic waves. On the other hand, the positive and negative charge centers in the element can be shifted under mechanical stress, thus voltage can be generated when acoustic waves are applied to it. This is the basic operating principle of piezoelectric transducers. The energy radiating from the back face of the piezoelectric element is absorbed by the backing layer, which is typically a strongly attenuating material. It can be used to control the bandwidth of the transducer. The matching layer is employed to improve the energy coupling between the piezoelectric element and the external environment.

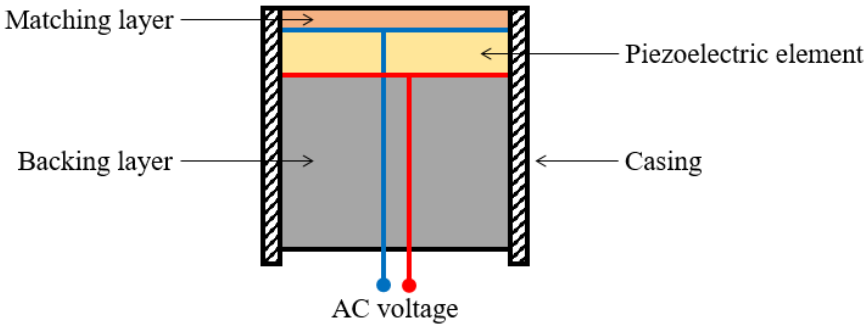



Figure 10. Typical cross-sectional structure of piezoelectric ultrasonic transducers

### 2.4.1.2 Theory for SoS Determination Using ToF Method

Unlike the acoustic resonance and interferometry methods which utilise constant waves, ToF methods use acoustic pulses. The fundamentals of typical ToF or pulse techniques are given in Cantrell & Yost (1998), Papadakis (1976) and Trusler (1991). The review given in this thesis primarily focuses on the technique based on a single pulse (generating one pulse in a single measurement) of constant frequency travelling over a fixed distance (see Sections 2.4.1.2 to 2.4.1.5). This technique is considered to be the most suitable for this project due to the simplicity and the great potential for achieving high precision rapid on-line SoS measurement. The other types of pulse techniques, such as those based on double/multiple pulses, variable frequency/pathlength/pulse repetition rate, or dual reflector measuring systems, are briefly introduced in Section 2.4.1.6.

By measuring the transit time (ToF) of an acoustic pulse propagating through a gas over a known distance, SoS can be determined. This is the basic SoS measurement principle of ToF method, which can be expressed by the following equation:

$$W_m = \frac{L}{t_m} \tag{63}$$

where $W_m$ denotes the measured SoS, $L$ the propagation distance or the pathlength, and $t_m$ the measured transit time or the measured ToF. Ultrasound is defined as the sound of frequency above 20 kHz, and is usually utilised in this method because it typically has narrower beam width, better anti-interference capability and higher resolution for measurement than both the audible sound (20 Hz to 20 kHz) and the infrasound (below 20 Hz).

### 2.4.1.3 SoS Sensors Based on ToF Method

SoS measuring apparatus can be called speed of sound sensors or SoS sensors. Generally, the SoS sensors based on ToF method, or SoS-ToF sensors, can be divided into two different categories according to the number of ultrasonic transducers used, which are:

1) double-transducer sensors – the transmitting and receiving of ultrasound pulses are performed by two individual ultrasonic transducers
2) single-transducer sensors – the two actions are performed alternately by only one single ultrasonic transducer.

The schematics of the typical transducer configurations and propagation paths of the ultrasound pulses in these two types of sensors are illustrated in Figures 11 and 12.

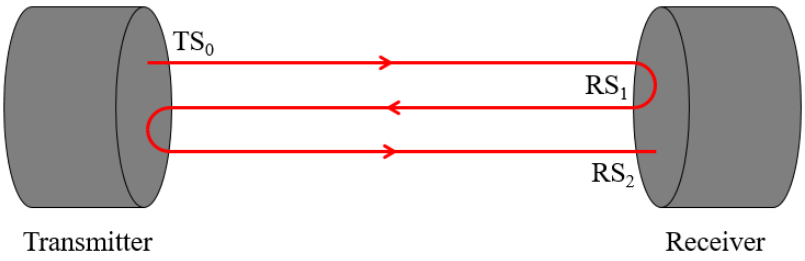



Figure 11. Schematic of transducer configuration and ultrasound propagation path in a typical double-transducer SoS-ToF sensor ($TS_0$ – transmitted signal; $RS_1$ – the 1st received signal; $RS_2$ – the 2nd received signal)

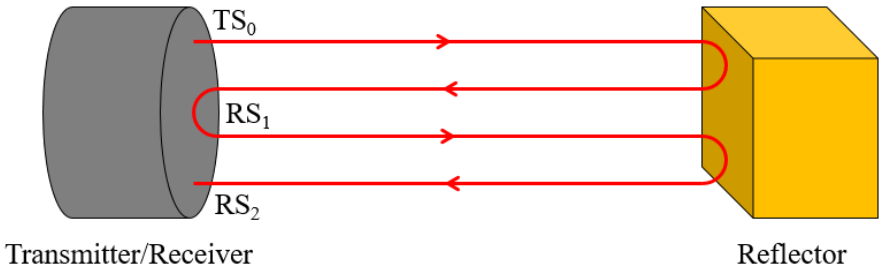



Figure 12. Schematic of transducer configuration and ultrasound propagation path in a typical single-transducer SoS-ToF sensor ($TS_0$ – transmitted signal; $RS_1$ – the 1st received signal; $RS_2$ – the 2nd received signal)

For simplicity, only the ultrasound propagation paths associated with the generation of the first two received signals ($RS_1$ and $RS_2$) are shown in these two figures. It is worth mentioning that

both the transmitted signal ($TS_0$) and the received signals ($RS_1$, $RS_2$, etc.) refer to electrical signals: the former is generated from the transmitter electronics, while the latter come from the ultrasound detected by the receiver. For a double-transducer SoS-ToF sensor with transducer configuration as is shown in Figure 11 if the distance between the ultrasound transmitter and receiver is designated by $L_0$, then $RS_1$ corresponds to the ultrasound pulse sent out from the transmitter travelling a distance of $L_0$; $RS_2$ corresponds to the same pulse but being reflected twice (once at the receiver front face and once at the transmitter front face) and travelling a distance of $3L_0$; and the pulse will continue in transit between the two transducers giving rise to the following received signals until it disappears, i.e. until its energy is completely dissipated. For a single-transducer SoS-ToF sensor with a transducer configuration as illustrated in Figure 12, if $L_0$ represents the distance between the transducer and the reflector, then $RS_1$ corresponds to the transmitted pulse propagating a distance of $2L_0$ with a reflection at the reflector front surface; $RS_2$ corresponds to the same pulse but being reflected two more times (once at the transducer front surface and once at the reflector font surface again) and propagating a total distance of $4L_0$; and similarly, the received signals will continue to appear periodically until the disappearance of the pulse.

In theory, for these two categories of SoS-ToF sensors, the time difference between any two signals (between the transmitted signal and a received signal or between two received signals) can be used as the measured ToF for SoS determination. The corresponding pathlength can be determined from a mechanical measurement or a calibration experiment with the use of a reference gas with known SoS.

#### 2.4.1.4 Signal Analysis Methods for ToF Determination

In practice, a highly accurate measurement of ToF usually cannot be achieved from simply analysing the time difference between the transmitted signal and a received signal. This is because of signal shape distortions and non-zero delay times introduced by the signal processing in the transducer(s) and electronics. However, an accurate ToF determination may be achieved from the time difference between two received signals. The reasons for this include the following factors:

1) the two received signals both come from the ultrasound pulse detected by the receiver and thus the effect of signal shape distortion is minimised

2) the ToF measured using this method has no dependency on any delay associated with the transmitting of the ultrasound pulse
3) theoretically any delays associated with the receiving of the ultrasound pulse are the same for both of the two received signals and thus can be cancelled out.

Four typical types of methods for waveform analysis which are suitable for the automatic on-line measurement of the time difference between two received ultrasonic waveform signals are introduced below. A general summary of the advantages and disadvantages of these methods are given in Table 6.

In order to obtain the time difference between two received signals, the following approaches could be used[5]:

1) Amplitude thresholding method
   - The signal time(s) is determined at which the signal waveform or waveform envelope first exceeds a preset signal amplitude threshold level (see Figure 13).

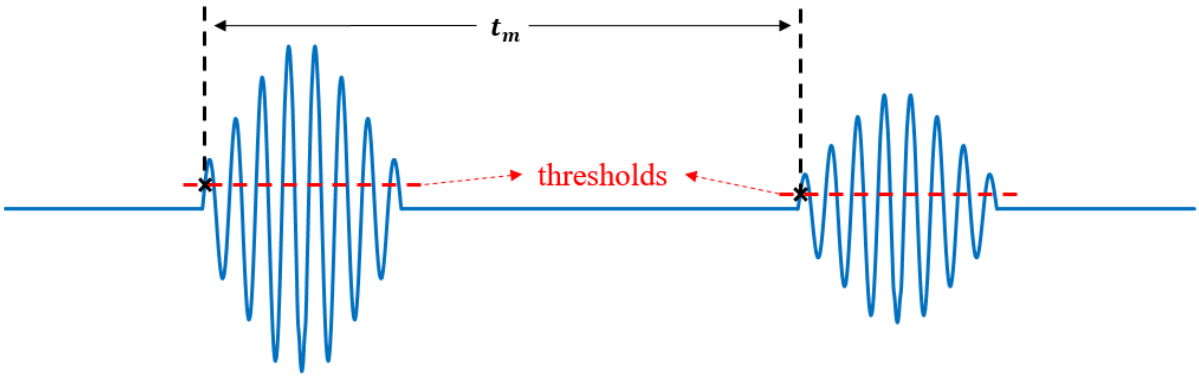



Figure 13. Schematic of a typical amplitude thresholding method with preset signal waveform amplitude thresholds

2) Fitting method
   - The signal time(s) is determined according to a mathematical function fitted to the signal waveform or to the envelope of the signal waveform (see Figure 14).

[5] For the measurement of the time difference between transmitted signal and a received signal, amplitude thresholding, fitting and waveform marker methods could also be employed for determining the received signal time. The transmitted signal time could be determined from the time when the electronics initiates the transmitted signal.

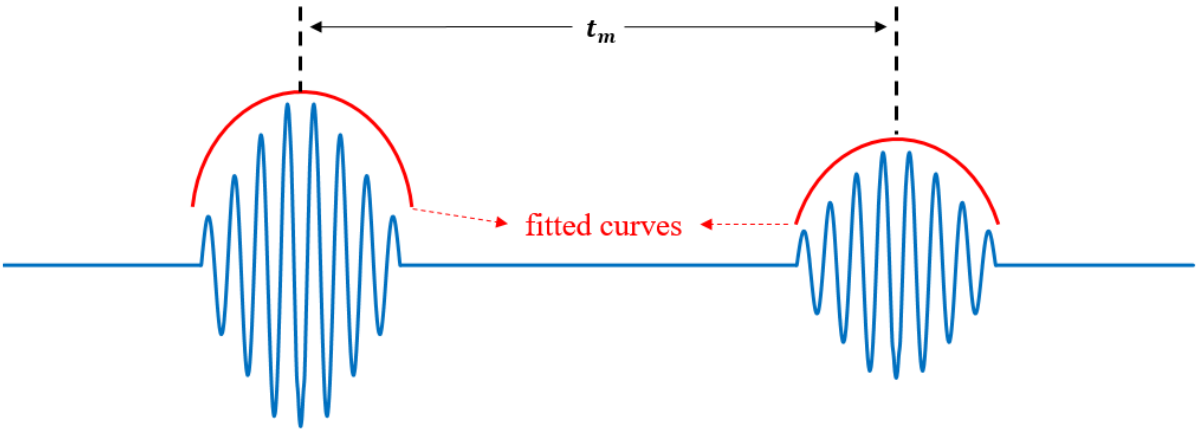



Figure 14. Schematic of a typical fitting method with functions (curves) fitted to waveform envelopes

3) Waveform marker method
   - By introducing a marker or perturbation into the transmitted signal such as a significant phase change (see Figure 15), the presence of this marker (possibly in a different form) in the two received signals can be identified and quantified.

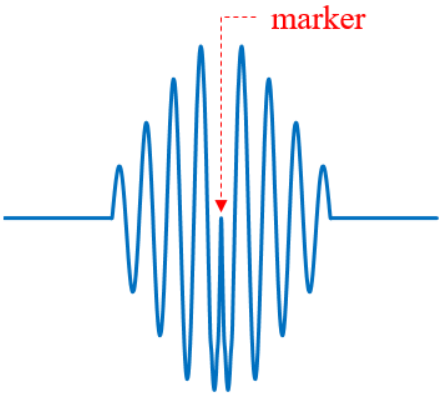



Figure 15. Schematic of a transmitted signal with a phase-reversal marker

4) Auto-correlation method
   - By correlating one received signal waveform with the other at different time points, theoretically the separation between the two signals can be determined due to the similarities between them (Oppenheim, 2010).

Table 6. Advantages and disadvantages of typical methods for ToF determination

| Methods | Advantages | Disadvantages |
|---|---|---|
| Amplitude Thresholding | Simple, straightforward, fast, and easy to implement using analog electronics | Limited accuracy; depends on threshold selection |
| Fitting | Accurate providing the shape of signal remains constant | Complicated; requires longer processing time and more processing power; difficult to compensate for changes in signal shape |
| Waveform Marker | Potentially very accurate and only requires moderate processing power | Requires the use of custom broadband ultrasonic transducers which are usually much more expensive than common narrow-band ones |
| Auto-Correlation | Works well for sharp impulses which are well defined | Complicated; requires longer processing time and more processing power; does not work well for extended pulse trains |

#### 2.4.1.5 SoS Measurement Error Using ToF Method

The error in an SoS measurement is defined as the deviation between $W_m$ and the real gas SoS $W$. For the ToF method, two typical sources of SoS measurement error associated with pulse propagation are the effects of diffraction and boundary layer.

Diffraction occurs during the propagation of acoustic pulse, which can lead to a phase advance of the pulse relative to a plane one traversing the same distance and thus cause the measured ToF to be in error (Trusler, 1991). In order to correct for this, $t_m$ should be increased by an amount $\delta t$. If $t_m$ corresponds to a propagation path of length $L$ starting from the sound source, then the theoretical model as follows may be used for the determination of $\delta t$:

$$A\exp(\mathbf{i}\Phi) = 1 - \frac{1}{\pi}\int_0^{\frac{\pi}{2}} \exp\left\{\mathbf{i}kL\left[1 - \sqrt{1 + \left(\frac{2r_s\cos\theta}{L}\right)^2}\right]\right\}\sin^2\theta\, d\theta \tag{64}$$

$$\delta t = \frac{\tan^{-1}\left(\frac{\mathbf{Im}\langle A\exp(\mathbf{i}\Phi)\rangle}{\mathbf{Re}\langle A\exp(\mathbf{i}\Phi)\rangle}\right)}{\omega} \tag{65}$$

where $A\exp(\mathbf{i}\Phi)$ is a complex function providing a complete description of the free-field diffraction effects for a piston-like source and any parallel receiver of the same radius which

responds to the mean sound pressure over its surface, **Im** and **Re** the imaginary and real parts, $k$ the wavenumber, $r_s$ the radius of the source, and $\omega$ the angular frequency. It is worth mentioning that this free-field diffraction model is also valid for single-transducer system provided that the radius of the parallel reflector is not less than that of the source, in which case, the transducer acts as both the source and the receiver. While if $t_m$ corresponds to a propagation path of length $L$ not starting from the source, say $L = L_1 - L_2$ where $L_1$ denotes the propagation distance from the source to the end point of the path and $L_2$ that from the source to the starting point of the path, then the value of $\delta t$ added to $t_m$ is equal to $\delta t_1$ minus $\delta t_2$ which are the values determined from the above two equations corresponding to $L_1$ and $L_2$ respectively. In real cases, since the assumptions for this theoretical model cannot be fully satisfied and appropriate models are usually too difficult to establish, an accurate diffraction correction $\delta t$ may not be available. Typically, the diffraction effect is reduced at high ultrasonic frequencies; and a nominal plane wave could be achieved if the pulse propagation is guided, in which case the effect of diffraction is also reduced.

For the propagation of sound in a confined enclosure, the boundary layer at the gas-wall interface could result in the propagation velocity deviating from $W$. In the case of plane wave propagation in a cylindrical tube, the analysis of the boundary layer effect on SoS can be based on the Helmholtz-Kirchhoff tube correction formula (Kaye & Sherratt, 1933):

$$W_t = W\left(1 - \frac{c}{2r\sqrt{\pi f}}\right) \tag{66}$$

where $W_t$ refers to the sound propagation velocity in the tube, $r$ the tube radius, $f$ the acoustic frequency; $c$ is the Kirchhoff constant, given by:

$$c = \sqrt{\nu} + (\gamma - 1)\sqrt{\frac{D}{\gamma}} \tag{67}$$

where $\nu$ denotes the kinematic viscosity, $\gamma$ the heat capacity ratio, and $D$ the thermal diffusivity. It can be found that by using a wider space or a higher frequency the boundary layer effect can be reduced. This conclusion also applies to cases which are more complex than this theoretical model. The boundary layer at the interface between gas and the front surface of transducer or reflector could also lead to SoS measurement error. Similar to the diffraction

correction, for a real case, an accurate correction for boundary layer effect may also be difficult to achieve.

Provided that the effects which could cause error in SoS measurement can be quantified or partially quantified with reasonable accuracy, the measured SoS can then be corrected and thus the measurement will be more accurate. If a correction is not made for an effect, which may be because the quantification is too difficult or the correction is not necessary, then the corresponding error should be contained in the overall measurement error. For the SoS measurement in a gaseous fluid with the use of ToF method, the real gas SoS of the fluid can generally be related to the pathlength and the measured ToF by introducing a correction factor $K_c$ as follows:

$$W = \frac{L}{t_m}(1 + K_c). \tag{68}$$

The possible reasons for this correction primarily include the effects of diffraction and boundary layer, as well as the ToF measurement error introduced by signal processing and analysis. In real cases exact pathlength is not known and this is another error source for SoS measurement.

#### 2.4.1.6 Other Typical Pulse Methods

Besides the ToF methods discussed previously, there are also a number of other typical pulse-based techniques which can be utilised for SoS measurement, including the basic pulse-echo, pulse superposition, gated double-pulse superposition, pulse phase-locked loop, echo-overlap, and dual-path methods. The measurement principles of the former five methods are summarised in Cantrell & Yost (1998); and the typical SoS measurement uncertainties that can be achieved using these methods are 1 ppt, 200 ppm, 100 ppm, 100ppm and 20ppm, respectively (Zuckerwar, 2002). The dual-path method is discussed in Ball & Trusler (2001), Dávila & Trusler (2009), Lin & Trusler (2012), Peleties et al., (2010) and Trusler (1991).

1) Basic pulse-echo method

   The method for the determination of SoS based on a single-transducer system (one transducer and one reflector) by using the time difference between corresponding reference points of two received signals generated from reflected pulses as ToF, which is analysed on an oscilloscope, is known as the basic pulse-echo method.

Provided that variable pathlength is employed, by measuring the displacement of the transducer which can delay the reflected pulse by a specified amount of time, SoS can also be obtained. This variable-pathlength pulse-echo method is beneficial for the improvement of measurement accuracy since the consideration of multiple reflections is not needed.

By placing a pair of ultrasonic transducers opposite each other (one as pulse transmitter while the other as receiver), SoS can be determined based upon the sing-around method, which is a variation of the basic pulse-echo method. A continuous succession of pulses can be produced by using received signals to retrigger the pulse generator, then the pulse repetition rate can be utilised for SoS measurement.

2) Pulse superposition method

This method is typically applied to a single-transducer system. A continuous-wave low-frequency oscillator is employed to control and adjust the repetition rate of a series of radio-frequency pulses (tone-bursts) transmitted into the medium under test to correspond to an integer multiple $p$ of the round-trip pulse propagation time $t_r$ ($= 2t_s$, $t_s$ is the single-trip transit time) approximately. By adjusting the oscillator frequency, an in-phase superposition of pulses is achieved as the amplitude of the received signal displayed on an oscilloscope reaches a maximum. Since the reciprocal of the oscillator frequency is equivalent to the measured time delay $t_d$ between two superimposed pulses, $t_d$ is given as follows:

$$t_d = pt_r - \frac{p\varphi}{360f} + \frac{n}{f} \tag{69}$$

where $\varphi$ indicates the phase shift due to pulse reflection, $f$ the acoustic pulse frequency, and $n$ an integer number (+ or -) designating the cyclic mismatch between pulses. The method for the calculation of $\varphi$ can be found in Redwood & Lamb (1956). Then provided $t_d$ corresponding to a given $n$ is known, $t_r$ or $t_s$ which is used for SoS determination can be obtained.

3) Gated double-pulse superposition method

This method is suitable for a double-transducer system (one transmitter and one receiver). The transmitter sends out a tone-burst produced by gating a continuously running oscillator, and then a second which is phase locked and delayed by a time $2t_s$

($t_s$ is the single-trip travel time). Two pulse-echo trains are then generated as the two tone-bursts reflecting between the two transducers. The signals detected by the receiver opposite the transmitter are amplified and displayed on an oscilloscope. By adjusting the delay time, superposition of the echoes from the two pulse-echo trains can be achieved. The oscillator frequency $f = \omega/2\pi$ is adjusted to make the two pulses interfere destructively, and a superimposed signal of zero amplitude may be obtained independently of time provided that the condition as follows is satisfied:

$$\omega t_s - \varphi = (2n + 1)\frac{\pi}{2} \tag{70}$$

where $\varphi$ is the phase shift associated with once reflection, and $n$ an integer number ($\geq$ 0). The pulse propagation time $t_s$ can be obtained if $\varphi$ and $n$ are known, which is then used in the determination of SoS.

4) Pulse phase-locked loop method

   Typically, this method is applied to a single-transducer variable-pathlength measurement system. The transmitted ultrasonic tone-burst is generated by gating a continuous-wave reference oscillator. A phase-sensitive detector is utilised to monitor the relative phase between the continuous-wave reference signal and the received echo signal. A relative phase change may be caused, for example, by a pathlength variation or by an SoS variation. SoS may be determined from the change in phase corresponding to a given pathlength variation. The detector output can be maintained constant by adjusting the frequency of the reference signal. A voltage-controlled oscillator network is employed in this pulse phase-locked loop system. A correction for the variations of the frequency-dependent non-acoustic contributions to the phase change, including those from the propagation paths of electrical signals and phase perturbations associated with electrical components, needs to be made in the SoS calculation.

5) Echo-overlap method

   In a single-transducer system, a series of radio-frequency pulses are transmitted into the medium under test. This method uses a sufficiently slow pulse repetition rate in order to ensure that the echo train dies out before the next burst is applied. Only a pair of echoes are selected to be displayed on an oscilloscope by gating the received signals. For the purpose of determining the time delay between the two echoes, the horizontal axis of the oscilloscope is triggered by using an oscillator the frequency of which is

variable and is adjusted to an integer multiple of the reciprocal of the delay time. This condition gives rise to cycle-for-cycle overlap between the pair of echoes, which can be observed on the oscilloscope. The round-trip pulse propagation time is determined according to Equation (69) with $n = 0$. A steady display can be achieved provided that the receiver gate, pulse repetition and oscilloscope time base are synchronised to the same clock signal. The delay time is derived from the time base frequency. The methodologies for achieving a proper cycle-for-cycle echo overlap and for determining the reflection-associated phase shift are given in McSkimin (1965) and McSkimin & Andreatch Jr (1967).

6) Dual-path method

The schematic of a dual-path ultrasonic cell is shown in Figure 16. A piezoelectric disc transducer is positioned between two identical plane parallel reflectors mounted at different distances, $L_1$ and $L_2$ ($L_1 < L_2$), from the transducer. The medium under test is on both sides of the transducer in the system. In an SoS measurement, by exciting the transducer ultrasonic pulses are emitted into the medium in opposite directions simultaneously. The echoes returning from the two reflectors are detected by the same transducer. Then, SoS can be determined according to the following equation:

$$W_m = \frac{2(L_2 - L_1)}{t_2 - t_1} \tag{71}$$

where $t_1$ and $t_2$ denote the round-trip pulse transit times on the shorter and longer paths, respectively ($t_1 < t_2$). The pathlength difference $2(L_2 - L_1)$ is obtained from a calibration measurement using a reference medium with known SoS. For the purpose of determining the time difference ($t_2 - t_1$), the received echo signals captured by a digital oscilloscope can be analysed in a similar way to the basic pulse-echo method. A numerical analysis for improving the measurement resolution is outlined in Ball & Trusler (2001). The time difference can also be obtained from the time delay between two excitations applied to the transducer when the echo of the second pulse on the shorter path and the echo of the first pulse on the longer path reach the transducer simultaneously and cancel each other completely. The details of this method are given in Kortbeek et al. (1985) and Kortbeek & Schouten (1990). For improving SoS measurement accuracy, the factors such as the diffraction effect which may result in measurement errors should be taken into consideration. With the use of this dual-path

method for SoS determination, signal distortions and phase shifts due to pulse reflections cancel, and the errors associated with electronic delays and diffraction effects may be reduced effectively or even eliminated completely.

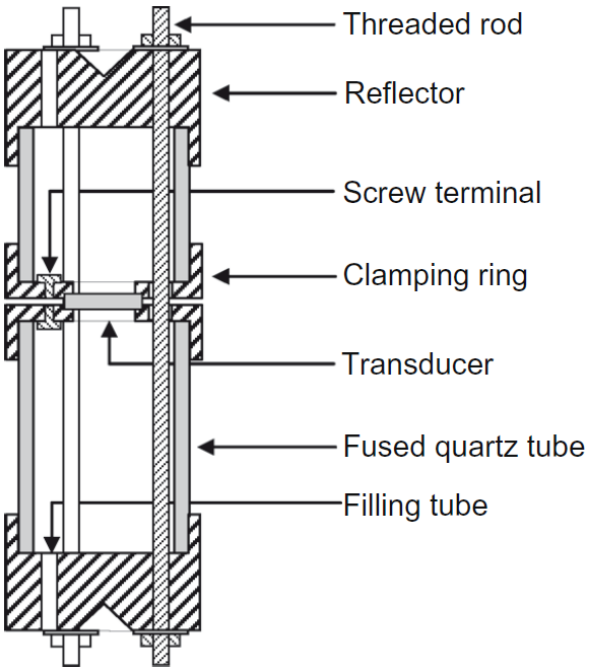



Figure 16. Dual-path ultrasonic cell (Peleties et al., 2010)

### 2.4.2 Acoustic Resonance Method

If sound is produced continuously inside a closed cavity, a steady state can be achieved in which the wave motion is that of a standing wave. Resonance will occur provided the acoustic frequency matches a natural frequency of the system. The resonance frequencies and linewidths can be related to the SoS and also the sound absorption properties of the medium. This is the basic principle of acoustic resonance method for the measurement of those quantities, which typically can be achieved with spherical or cylindrical acoustic resonators (Trusler, 1991). It should be noted that only the measurement of gas SoS is of interest in this review.

#### 2.4.2.1 Spherical Acoustic Resonator

For an excited gas in a spherical resonator having a cavity radius $r$, the resonance frequencies of the system $f_{ln}$ can generally be expressed by (Zuckerwar, 2002):

$$f_{ln} = \frac{W \upsilon_{ln}}{2\pi r} + \sum_i \Delta f_i \tag{72}$$

where $(l, n)$ are two resonance mode indices[6], $W$ the real gas SoS, $\upsilon_{ln}$ the $n$th turning point of the spherical Bessel function of order $l$, and $\Delta f_i$ the $i$th frequency perturbation term. The first term on the right refers to the unperturbed eigenfrequencies which correspond to ideal conditions. The primary perturbation terms are those arising from the thermal boundary layer, gas-structure interaction and non-idealities of the resonator. If a perturbation term is involved to correct for frequency dispersion, then $W$ turns into $W_\theta$ which is the lossless real gas SoS. Since the non-radial resonance modes ($l \neq 0$) suffer significant thermoviscous losses, the radial ones $(0, n)$ (particle motion normal to the cavity walls) are generally used for SoS measurement. The first several $\upsilon_{0n}$ values are given in Table 7. The fundamental radial mode is (0, 2).

Table 7. Turning points of the spherical Bessel function of zero order

| $n$ | $\upsilon_{0n}$ |
|---|---|
| 1 | 0 |
| 2 | 4.493409458 |
| 3 | 7.725251837 |
| 4 | 10.904121659 |
| 5 | 14.066193913 |
| 6 | 17.220755272 |

Spherical resonators are the instruments which are typically the most suitable for highly accurate SoS measurements. The schematic of a spherical resonator is shown in Figure 17, which was used by Moldover et al. (1988) for the redetermination of gas constant $R$ based on the measured SoS in argon gas at 0.01 °C (water triple point) and 25 to 500 kPa. It was fabricated in two hemispherical shells joined at the equator. Two transducers which were

[6] The modes designated $(l, n)$ have $l$ conical nodal surfaces and $n$ spherical nodal surfaces (except for $l = 0$ when there are $n - 1$ spherical nodes) (Trusler, 1991).

commercial capacitance microphones were employed: one as the constant wave source to excite the resonances and the other as the detector. They were mounted at strategic locations in the shell wall for the purpose of minimizing sensitivity to certain non-radial modes. By measurements of the in-phase and quadrature voltages produced by the detector as a function of the frequency of the source transducer, the resonance frequencies of the radial modes (0, 2) to (0, 6) were determined which spanned the range around 2.5 to 9.5 kHz. The volume of the spherical cavity $V_s$ was measured by weighing the mercury required to fill it at 0.01 °C. The mean cavity radius $\bar{r}$ was then determined according to $\bar{r} = \sqrt[3]{3V_s/4\pi}$, which was found to be around 0.0889 m. The methods for the estimation of the perturbation terms are not discussed in this thesis.

Based on this spherical resonator, the authors succeeded in achieving $R$ with an uncertainty of only 1.7 ppm (the uncertainty of the most accurate previous reported value was 8.4 ppm). The SoS was measured with an uncertainty of 0.44 to 2.1 ppm according to the estimation by Zuckerwar (2002), and this is the most accurate gas SoS measurement until now. For a more routine application of spherical acoustic resonator, the cavity radius can be determined by calibration with a reference gas for which the thermodynamic data are known with high accuracy. This still suffices for reasonably accurate measurement of SoS. By using argon as the reference gas, Ewing & Trusler (1989 and 1992) achieved an SoS measurement uncertainty estimated by Zuckerwar (2002) of 17 to 125 ppm for tetrafluromethane and 3 ppm for nitrogen.

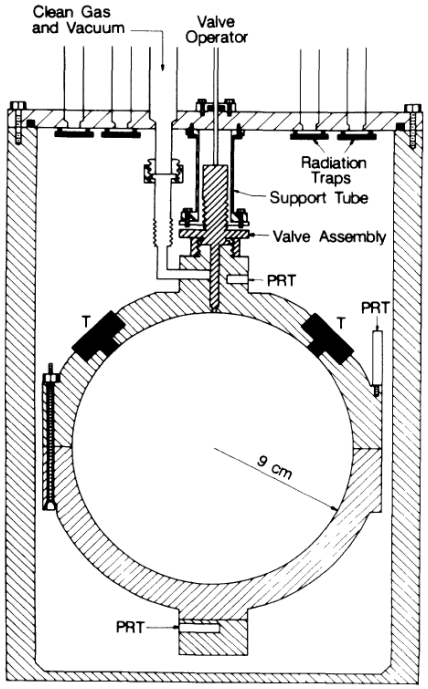



Figure 17. The spherical resonator of Moldover et al. (1988)

#### 2.4.2.2 Cylindrical Acoustic Resonator

The resonance frequencies of an excited gas in a cylindrical resonator $f_{lmn}$ are given by (Zuckerwar, 2002):

$$f_{lmn} = \frac{W}{2\pi}\sqrt{\left(\frac{l\pi}{L}\right)^2 + \left(\frac{\chi_{mn}}{r}\right)^2} + \sum_i \Delta f_i \tag{73}$$

where $(l, m, n)$ are mode indices[7], $L$ and $r$ the cavity length and radius, $\chi_{mn}$ the $n$th turning point of the cylindrical Bessel function of order $m$. Similar to Equation (72), the first term on the right indicates the unperturbed eigenfrequencies. The principle reasons for frequency perturbation are similar to those in the case of a spherical resonator. The longitudinal modes ($l$, 0, 0) ($\chi_{00} = 0$, sound propagation along the cylinder axis as a plane wave) are generally used for the measurement of SoS. In this case, Equation (73) is simplified to:

$$f_{l00} = \frac{Wl}{2L} + \sum_i \Delta f_i. \tag{74}$$

Typically, the cavity dimensions can be obtained from a calibration measurement with a reference gas or a mechanical measurement.

Figure 18 illustrates the schematic of the cylindrical acoustic resonator with the electronics used by Younglove & McCarty (1980) for the measurement of SoS in nitrogen at temperatures from 80 to 350 K and pressures from 0.3 to 15 atm. The diameter and length of the cylindrical cavity were 0.01 m and 0.067 m. Two electrostatic transducers were used as the constant wave source and the detector respectively. The tube was closed at each end with the active surface (aluminised polymer film) of a transducer. This configuration can facilitate both the excitation and detection of longitudinal modes (Trusler, 1991). The source frequency was controlled by the oscillator. By adjusting the frequency of the oscillator until the amplitude of the received signal which was observed on the oscilloscope reached a maximum, the oscillator frequency at that time was recorded as the resonance frequency of a longitudinal mode. In their

[7] The modes designated $(l, m, n)$ have $l$ nodal planes perpendicular to the cylindrical axis, $|m|$ plane radial nodal surfaces and $n$ cylindrical nodal surfaces concentric with the axis (Zhang et al., 2010). The resonance frequencies of the $(l, m, n)$ and $(l, -m, n)$ modes are exactly the same.

measurements on nitrogen the resonance frequencies ranged from 16 to 19 kHz, and the SoS measurement uncertainty was 0.03%.

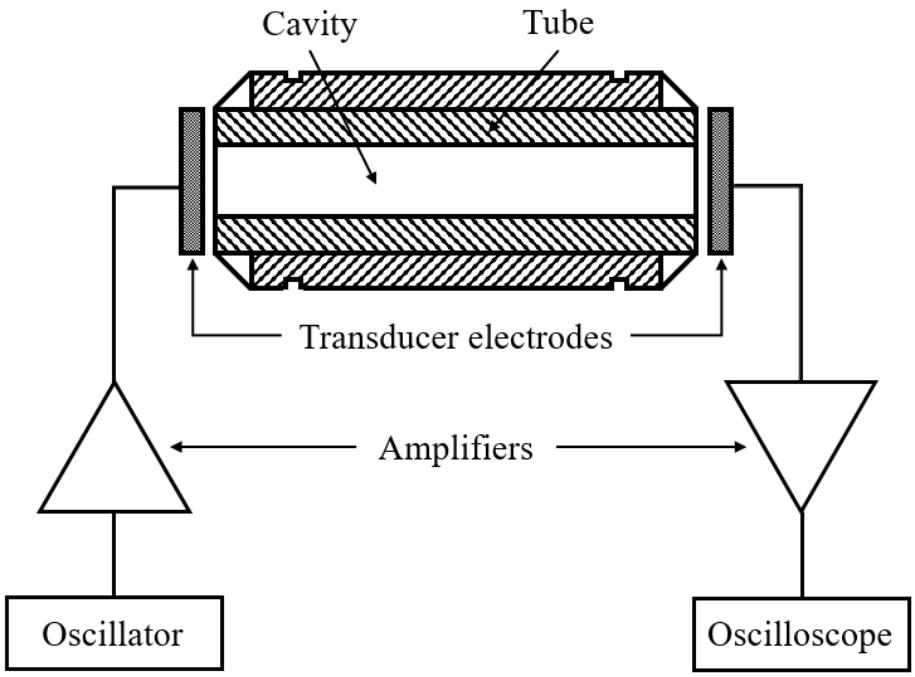



Figure 18. Cylindrical resonator with electronics as used by Younglove & McCarty (1980)

### 2.4.3 Interferometry Method

Similar to the acoustic resonance method, the interferometry method also involves the use of a constant acoustic wave source and the formation of standing waves (Trusler, 1991). For the former method, the frequency of source is variable and is adjusted to match a natural frequency of the system, but the volume of acoustic cavity is fixed; while for the latter method, on the contrary, typically the source is operated at a fixed frequency but the cavity volume is variable. An instrument which is based on the interferometry method for SoS measurement is called acoustic interferometer. In essence, a typical interferometer consists of a tube closed at one end by the active surface of the source transducer and fitted with a movable piston as reflector. The source generates what are assumed to be continuous plane waves, and by moving the piston successive longitudinal resonances of the cavity can be achieved. According to Equation (74), $L$ is altered, then resonance occurs when a longitudinal frequency $f_{l00}$ matches the source frequency. Assuming total reflections take place at both ends of the cavity (reflection coefficients equal to unity), the displacement of the piston between two resonances is an integer multiple of half wavelength $\lambda/2$. There are two ways for the detection of resonances. First, as the piston is moved, the mechanical or electrical impedance of the source transducer may be

monitored and used to infer the input mechanical impedance of the fluid under test in the cavity. Alternatively, the piston may be fitted with another transducer which is employed to measure the acoustic pressure there as a function of the piston's displacement.

Previous to the work of Moldover et al. (1988) as discussed in Section 2.4.2.1, Colclough et al. (1979) had determined the gas constant $R$ with an uncertainty of 25 ppm. It was a sequel to a prior work (Quinn et al., 1976). The determination of $R$ was based on the SoS of argon measured using an acoustic interferometer (see Figure 19) at approximately the triple-point temperature of water over a pressure range from around 0.03 to 1.3 MPa. It was a single transducers system. A low frequency (5.6 kHz) and a narrow cavity (15 mm in radius) were chosen so that the apparatus could be operated below the cut-off frequency of the first radial resonance mode thus avoiding the problems associated with radial resonances. The piston could be moved over a distance of around 15 cm and the movement was controlled by a motorised lead screw assembly. The piston's displacement was monitored optically and could be measured with an uncertainty of 3 ppm. The transducer was a moving-coil-driven metal diaphragm, fitted with a piezoelectric accelerometer on its rear face. The latter served as an indicator of the mechanical impedance of the transducer from which successive resonances could be detected. Then, the wavelength $\lambda$ was determined from the displacement of the piston between two resonances. With the wavelength and the acoustic frequency, SoS could be obtained. The greatest correction the authors made in the determination of SoS was the boundary layer correction. The uncertainty of the SoS measurement was estimated to be 9 ppm by Zuckerwar (2002).

For an acoustic interferometer, the piston movement can be controlled with a micrometer lead screw and the positions of the piston can be determined from the screw's readings. Generally, this method is relatively less accurate than an optical technique for the measurement of the displacement of piston or the absolute length of cavity. It is worth mentioning that the absolute length can also be used for SoS determination, which although may require additional correction terms (Trusler, 1991). A typical single-transducer interferometer operated at high frequency can be found in Henderson & Peselnick (1957), and a typical double-transducer high-frequency interferometer can be found in Gammon & Douslin (1976).

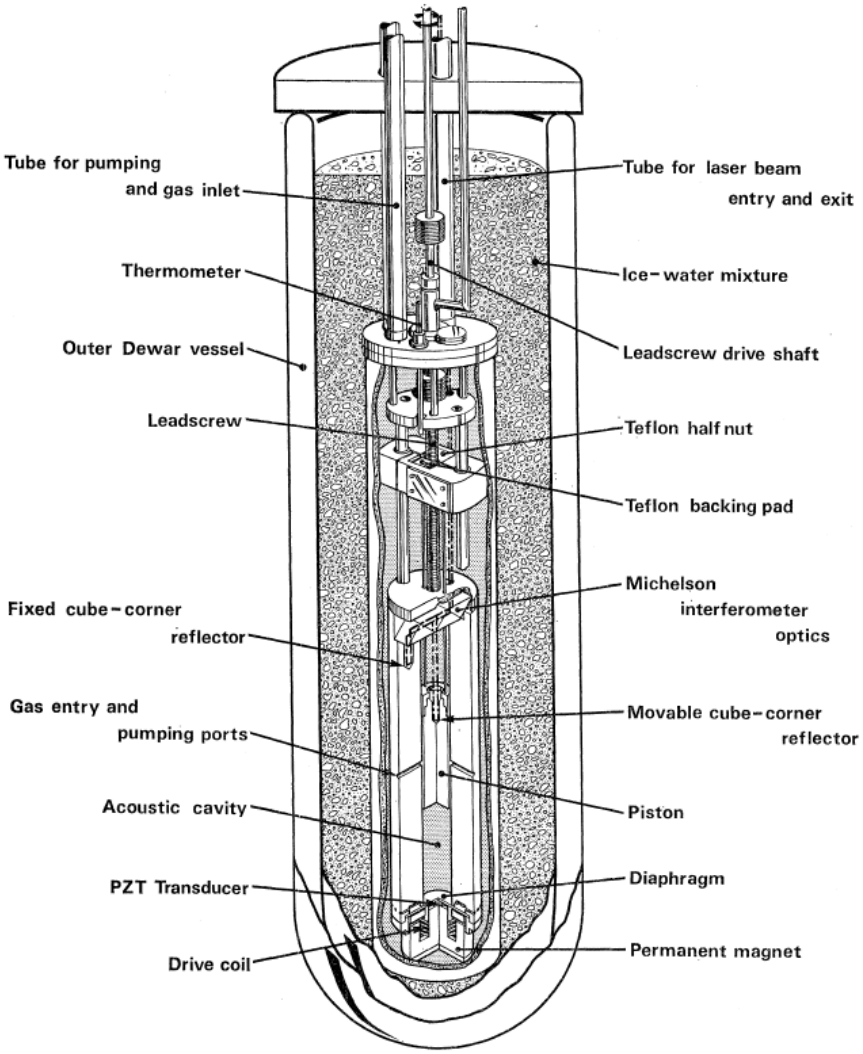



Figure 19. The acoustic interferometer (Colclough et al., 1979; Quinn et al., 1976)

## 2.5 Review of SoS Measurements for Pure Gases

A review of the reported SoS measurements for pure gases is given in Table 8, including the experimental temperatures and pressures, the measurement uncertainties and methods. The uncertainties of these measurements are summarised in Zuckerwar (2002).

Table 8. Reported SoS Measurements for Pure Gases

| No. | Gases | Temperatures (K) | Pressures (atm) | Uncertainties | Methods | References |
|---|---|---|---|---|---|---|
| 1 | Ar | 298.15 | 997 to 12582 | 1% | Pulse (double-transducer, single-pulse) | Nishitake & Hanayama, 1975 |
| 2 | He | 298.15 | 1355 to 14518 | | | |
| 3 | $N_2$ | 298.15 | 1200 to 14518 | | | |
| 4 | Ar | 148.15 to 298.15 | 987 to 9869 | 0.02% | Pulse (dual-path) | Kortbeek et al., 1985 |
| 5 | He | 298.15 | 99 to 1974 | 0.2% | Pulse (double-transducer, single-pulse) | Kimura et al., 1987 |
| 6 | Kr | 293.15 | 99 to 8211 | | | |
| 7 | Ne | 295.15 | 1934 to 34493 | | | |
| 8 | Para-$H_2$ | 15 to 100 | 3.5 to 319 | 0.05% | Pulse (double-transducer, pulse-overlap) | Younglove, 1965 |
| 9 | $O_2$ | 70 to 300 | 27 to 342 | 0.05% | Pulse (double-transducer, pulse-overlap) | Straty & Younglove, 1973 |
| 10 | Ethylene | 285.15 to 362.15 | 1 | 0.1% | Pulse (mostly mechanical system, coiled path) | Dixon & Greenwood, 1924 |
| 11 | Ar | 273.15, 373.15 | 1 | 0.07% | Spherical resonator | Bancroft, 1956 |

| | | | | | | |
|---|---|---|---|---|---|---|
| 12 | Ar | 273.16 | 0.25 to 5.0 | 0.44 to 2.1 ppm | Spherical resonator | Moldover et al., 1988 |
| 13 | Ar | 99.97 to 303.88 | 0.13 to 4.9 | 9 to 48 ppm | Spherical resonator | [2]Ewing et al., 1989 |
| 14 | Ar | 90.06 to 373.15 | 0.05 to 5.4 | 3 to 18 ppm | Spherical resonator | Ewing & Trusler, 1992 |
| 15 | $N_2$ | 80.05 to 373.16 | 0.05 to 5.8 | 3 ppm | | |
| 16 | Ar | 255 to 300 | 0.60 to 69 | 0.85 to 65 ppm | Spherical resonator | [1]Ewing & Goodwin, 1992 |
| 17 | Ar | 110 to 450 | 0.07 to 190 | 10 to 70 ppm | Spherical resonator | Estrada-Alexanders & Trusler, 1995 |
| 18 | $CF_4$ (R14) | 174.78 to 300.45 | 0.79 to 9.9 | 17 to 125 ppm | Spherical resonator | Ewing & Trusler, 1989 |
| 19 | $CH_2F_2$ (R32) | 273.16 to 343.15 | 0.19 to 2.5 | 0.01% | Spherical resonator | Hozumi et al., 1994 |
| 20 | $CH_2F_2$ (R32) | 308.19 to 343.14 | 0.20 to 5.1 | 61 ppm | Spherical resonator | Hozumi et al., 1996 |
| 21 | $CHCl_2$-$CF_3$ (R123) | 260 to 335 | 0.02 to 0.76 | 75 to 239 ppm | Spherical resonator | Goodwin & Moldover, 1991 |
| 22 | Ethylene | 273.15 to 373.15 | 1.0 to 10 | 0.02% | Spherical resonator | Mehl & Moldover, 1981 |
| 23 | Methanol | 280 to 360 | 0.01 to 0.79 | 157 to 1246 ppm | Spherical resonator | Boyes et al., 1992 |
| 24 | Methane | 275 to 375 | 3.8 to 100 | 18 ppm | Spherical resonator | Trusler & Zarari, 1992 |
| 25 | Methane | 255 to 300 | 1.7 to 70 | 10 ppm | Spherical resonator | [2]Ewing & Goodwin, 1992 |
| 26 | Ethane | 220 to 450 | 0.14 to 103 | 0.01% | Spherical resonator | Estrada-Alexanders & Trusler, 1997 |
| 27 | Propane | 225 to 375 | 0.10 to 8.4 | 0.01% | Spherical resonator | Trusler & Zarari, 1996 |
| 28 | n-Butane | 250 to 320 | 0.05 to 1.1 | 173 to 673 ppm | Spherical resonator | Ewing et al., 1988 |
| 29 | Isopentane | 260 to 320 | 0.03 to 0.80 | 0.019 to 0.64% | Spherical resonator | [3]Ewing & Goodwin, 1992 |
| 30 | Neopentane | 250 to 323.15 | 0.04 to 1.1 | 16 to 760 ppm | Spherical resonator | Ewing et al., 1987 |
| 31 | n-Pentane | 270 to 330 | 0.02 to 0.87 | 200 to 1683 ppm | Spherical resonator | [1]Ewing et al., 1989 |
| 32 | Ar | 302.4 to 539.8 | 0.98 | 0.03% | Cylindrical resonator | Goring, 1971 |
| 33 | Ar | 251.16 to 329.91 | 0.18 to 1.0 | 30 to 125 ppm | Cylindrical resonator | Ewing et al., 1985 |
| 34 | Kr | 285.02 to 320.10 | 0.19 to 1.1 | 60 to 150 ppm | | |

| | | | | | | |
|---|---|---|---|---|---|---|
| 35 | Ar | 298.15 | 0.97 to 0.98 | 0.15% | Cylindrical resonator | Giacobbe, 1993 |
| 36 | He | 298.15 | 0.98 to 0.99 | | | |
| 37 | Ne | 297.55, 297.95 | 0.98 | | | |
| 38 | Normal-$H_2$ | 298.15 | 0.97 to 0.98 | | | |
| 39 | $N_2$ | 298.15 | 0.98 | | | |
| 40 | $O_2$ | 298.15 | 0.99 | | | |
| 41 | $CO_2$ | 298.15 | 0.98 | | | |
| 42 | $N_2O$ | 298.15 | 0.97 | | | |
| 43 | Methane | 298.15 | 0.98 | | | |
| 44 | He | 273.15 | 1 | 0.011% | Cylindrical resonator | McIntyre et al., 1972 |
| 45 | He | 225 to 400 | 1.5 to 15 | 0.01% | Cylindrical resonator | Hurly et al., 1997 |
| 46 | Xe | 209.97 to 399.97 | 0.40 to 14 | 50 ppm | | |
| 47 | $N_2$ | 303.15 | 1 | 28 ppm | Cylindrical resonator | Smith & Harlow, 1963 |
| 48 | $N_2$ | 80 to 350 | 0.28 to 15 | 0.03% | Cylindrical resonator | Younglove & McCarty, 1980 |
| 49 | Neopentane | 251.23 to 340.17 | 0.07 to 1.0 | 0.46 to 13% | Cylindrical resonator | Ewing et al., 1986 |
| 50 | Ar | 273.16 | 0.30 to 13 | 9 ppm | Interferometer | Colclough et al., 1979 |
| 51 | He | 98.15 to 423.15 | 10 to 150 | 82 ppm | Interferometer | Gammon, 1976 |
| 52 | Para-$H_2$ | 292.15 | 1 | 0.1% | Interferometer | Van Itterbeek & Thys, 1938 |
| 53 | $D_2$ | 238.35 to 292.75 | 0.82 to 0.89 | | | |
| 54 | $D_2$ | 20.36 | 0.13, 0.30 | 0.1% | Interferometer | Van Itterbeek & Van Paemel, 1938 |
| 55 | CO | 1273.15 to 2073.15 | 1 | 1.2% | Interferometer | Sherratt & Griffiths, 1934 |
| 56 | $N_2$ | 227.77 to 298.72 | 1.2 to 59 | 50 ppm | Interferometer | Van Itterbeek et al., 1957 |
| 57 | $O_2$ | 313.75 | 0.005 to 1.1 | 0.2 to 4% | Interferometer | Connor, 1958 |
| 58 | $O_2$ | 231.8 to 302.9 | 0.97 to 69 | 50 ppm | Interferometer | Van Itterbeek & Zink, 1958 |

| | | | | | | |
|---|---|---|---|---|---|---|
| 59 | $CO_2$ | 273.15 to 1273.15 | 1 | 0.57% | Interferometer | Sherratt & Griffiths, 1936 |
| 60 | $CO_2$ | 298.15 to 798.15 | 1.0 | 0.23 to 0.35% | Interferometer | Overbeck & Kendall, 1941 |
| 61 | $CO_2$ | 371.15 | 0.97 | 0.1% | Interferometer | Pielemeier & Byers, 1943 |
| 62 | $H_2O$ | 373.15 to 1273.15 | 1 | 0.16% | Interferometer | Shilling, 1927 |
| 63 | $N_2O$ | 287.65 to 873.15 | 1 | | | |
| 64 | $H_2O$ | 593.15 to 672.59 | 14 to 68 | 0.15% | Interferometer | Woodburn, 1964 |
| 65 | $SO_2$ | 273.15 to 421.75 | 0.99 | 0.36% | Interferometer | Warner, 1937 |
| 66 | $CCl_2F_2$ (R12) | 278.15 to 381.95 | 3.6 to 39 | 1.4% | Interferometer | Komarov et al., 1967 |
| 67 | $CCl_3F$ (R11) | 293.15 to 433.15 | 0.90 to 25 | | | |
| 68 | $CCl_4$ (R10) | 350.15 | 1.0 | 0.5 to 2.5% | Interferometer | Railston, 1939 |
| 69 | $CH_2Cl_2$ (R30) | 316.15 | 1.1 | | | |
| 70 | Methanol | 340.15 | 1.1 | | | |
| 71 | Diethyl ether | 308.15 | 1.0 | | | |
| 72 | Benzene | 363.15 | 1.4 | | | |
| 73 | Acetone | 331.15 | 1.0 | | | |
| 74 | $CCl_4$ (R10) | 303.15 | 0.09 | 0.8% | Interferometer | Sette et al., 1955 |
| 75 | $CH_2Cl_2$ (R30) | 303.15 | 0.02 to 0.37 | | | |
| 76 | $CH_3Cl$ (R40) | 303.15 | 0.35 | | | |
| 77 | $CF_4$ (R14) | 295.15 | 0.28 to 2.9 | 0.022 to 0.27% | Interferometer | Byers, 1943 |
| 78 | $CH_2F_2$ (R32) | 273.16 to 333.15 | 0.48 to 3.8 | 0.1% | Interferometer | Sun et al., 1997 |
| 79 | Methanol | 305.40 | 0.01 to 0.21 | 0.05 to 0.5% | Interferometer | Ener et al., 1955 |

| | | | | | | |
|---|---|---|---|---|---|---|
| 80 | Methane | 314.15 | 0.03 to 0.69 | 0.04 to 0.12% | Interferometer | Kelly, 1957 |
| 81 | n-Hexane | 308.30 | 0.01 to 0.16 | 0.1% | Interferometer | Klose, 1958 |
| 82 | Sulfur hexafluoride | 309.25 | 0.06 to 0.66 | 0.2% | Interferometer | Leonard O'Connor, 1954 |

## 2.6 Review of SoS Measurements for Binary Gas Mixtures

### 2.6.1 ToF Method

The ultrasonic gas analysis system used by Hallewell et al. (1988) for the measurement of SoS in binary gas mixtures ethane/methane ($C_2H_6/CH_4$), isobutane/methane ($C_4H_{10}/CH_4$), isobutane/nitrogen ($C_4H_{10}/N_2$) and perfluoro-n-pentane/nitrogen ($C_5H_{12}/N_2$) at various compositions is illustrated in Figure 20. SoS measurements were performed in an aluminum tube (called sonar tube by the authors) of around 8 cm in diameter and 90 cm in length, which was immersed in a recirculating temperature control bath and contained a pair of electrostatic ultrasonic transducers facing each other as the transmitter and receiver. The distance between the active surfaces of the two transducers (designated as 'd' in the figure) was measured to an accuracy of ± 1 mm. The transmitted signal was a 45 kHz 8-cycle pulse train, and the SoS was determined from the distance 'd' and the time delay between the transmitted signal and the first received signal. The temperature measurement error of the two platinum resistance thermometers was ≤ 0.3 °C. The sonar tube was operated at atmospheric pressure. For $C_2H_6/CH_4$, $C_4H_{10}/CH_4$, $C_4H_{10}/N_2$, SoS measurements were performed at 30 °C, and mixtures of different compositions were achieved with the use of the mass flow controllers (MFCs). For $C_5H_{12}/N_2$, SoS measurements were conducted at 41 °C, and the sonar tube could be evacuated by means of a high precision sub-atmospheric pressure gauge to allow the two gas components to be mixed in situ. A gas chromatograph was employed to independently monitor the input or exhaust gas to verify the mixture in the sonar tube. These authors estimated the systematic error in composition for all of the mixtures to be ± 1%. The systematic error in SoS measurement was estimated to be ± 0.3%. The confining effects of the sonar tube on SoS were investigated based on the Helmholtz-Kirchhoff model and found to be negligible; however, any consideration of the effects of diffraction was not given in the paper. For $C_2H_6/CH_4$, the SoS predictions from a 'linear density weighting' formula (assuming SoS in a mixture linearly proportional to the concentration of the components by weight) and a simple EoS analysis are compared with the experimental measured SoSs as a function of gas composition in Figure 21. The authors stated that for any binary gas mixture concentration determinations might be achieved with high precision by using the sonar device independently in an on-line mode, without the need for any knowledge of the EoS, from a numerical fit to SoS measurements taken at known temperature and various known compositions.

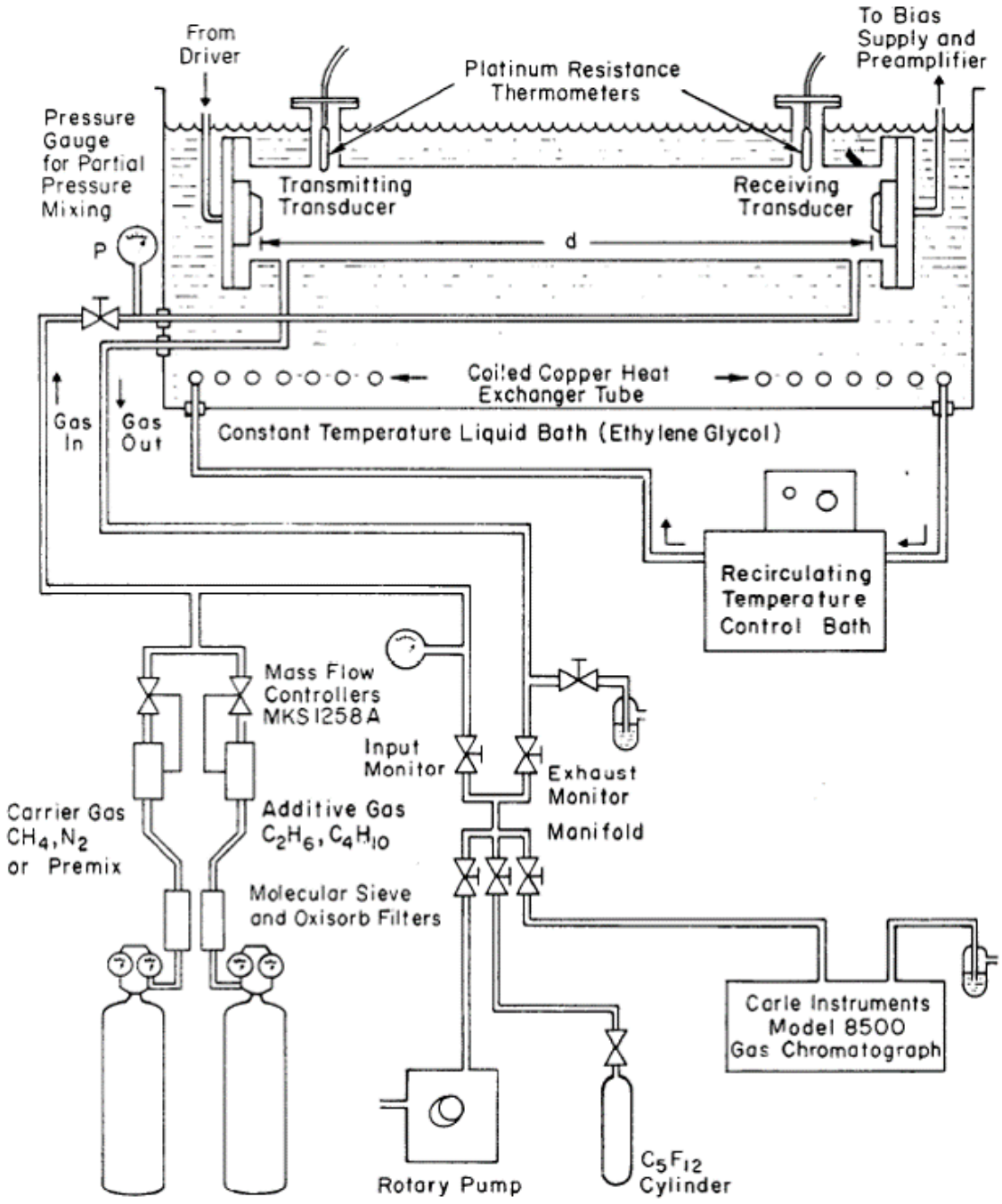



Figure 20. The ultrasonic gas analysis system (Hallewell et al., 1988)

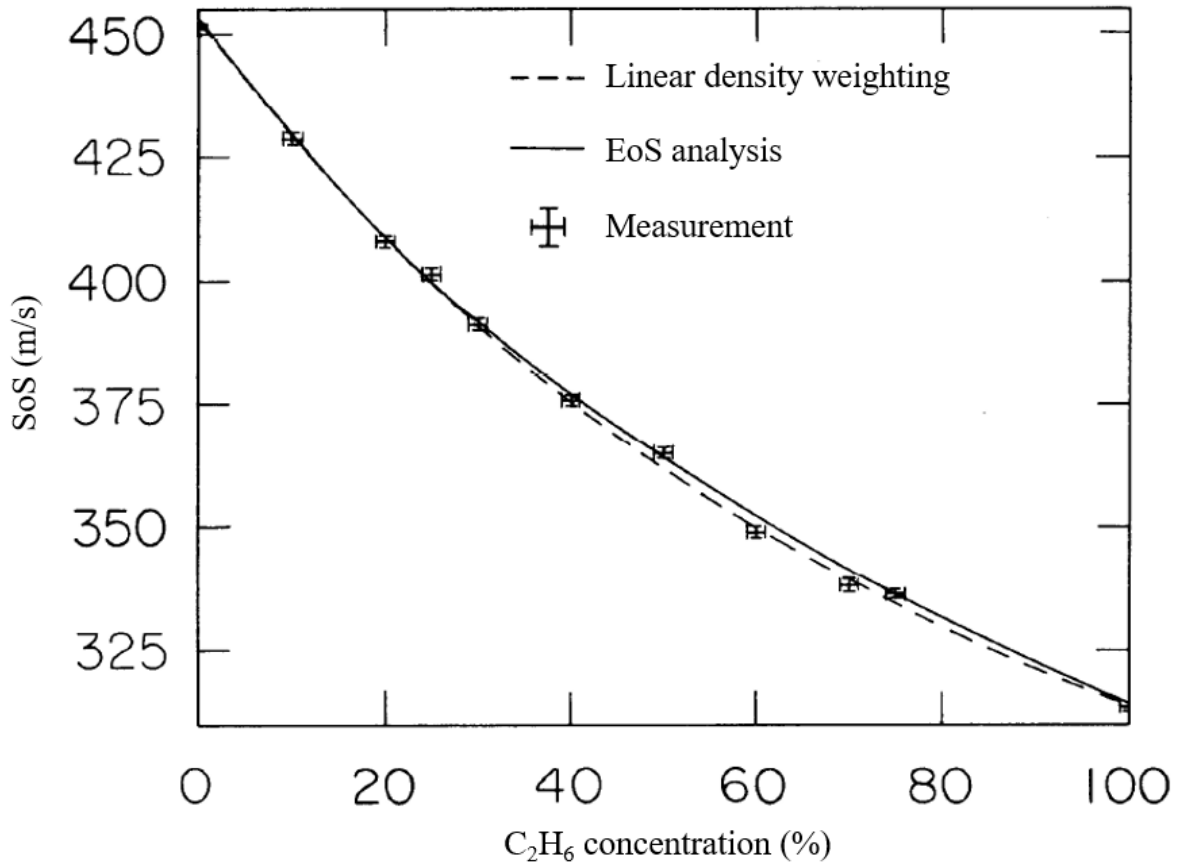



Figure 21. SoS versus $C_2H_6$ concentration in $CH_4$ at 30 °C (Hallewell et al., 1988)

An SoS measurement on perfluoroethane ($C_2F_6$) and perfluoropropane ($C_3F_8$) binary gas mixtures of three different compositions over a temperature range of -15 to 50 °C and a pressure range of 0.2 to 0.3 MPa was performed by Vacek et al. (2013). The method for the SoS determination was very similar to that used by Hallewell et al. (1988) as discussed above. However, in order to achieve a high measurement accuracy, the inter-transducer distance (around 50 cm) was determined by calibration using reference gases, nitrogen and xenon, the SoS's of which were obtained from the NIST REFPROP software. The uncertainty of the measured SoS was estimated to be around 0.03% (confidence level not specified by the authors), which consisted of the uncertainties of the calibrated pathlength and the measured ToF; the authors did not mention in the paper that the effects of diffraction and boundary layer were taken into account. The preparation of the gas mixtures was achieved by using needle valves for precise setting of the gas partial pressure in the measuring system without any further verification. The measured SoS were compared with the SoS data provided by the NIST REFPROP software, and the average difference between them was found to be 0.15%, 0.2% and 0.3% for the mixture with 0.048, 0.110 and 0.146 $C_2H_6$ mole fraction, respectively. The

authors believed that the SoS measuring system can be employed to provide a reasonable on-line monitoring of mixture compositions.

Löfqvist et al. (2003) used an ultrasonic gas flow meter equipped with a pair of 800 kHz silicon based transducers for the measurement of SoS in argon/nitrogen, oxygen/nitrogen and carbon dioxide/air binary gas mixtures at room temperature and atmospheric pressure. The flow meter was mounted in a custom made chamber in which the pressure could be kept constant. A small fan in the chamber was used to create gas flow through the meter. The chamber was initially filled with nitrogen or air (the so called background gas by the authors). During the experiment, the composition of the gas in the chamber was changed slowly by means of continuously adding argon, oxygen or carbon dioxide into the system at a very low flow rate. The two transducers of the flow meter were both able to act as ultrasound transmitter and receiver, and both the up- and down-stream propagation times of ultrasound pulses were measured. The SoS was determined using both of these two times, therefore, the effect of the gas flow on SoS measurement was negated. A gas chromatograph was employed to analyse gas samples taken from the chamber. The flow meter and the gas chromatograph recorded concurrent measurements of both SoS and gas composition. The SoS measurement uncertainty was estimated to be around 0.08%; the diffraction and boundary layer effects on the measurement were probably not considered. Figure 22 shows the measured SoS as a function of the argon mole fraction in nitrogen, in which the solid line represents the SoS predictions according to the ideal gas law. The authors concluded that the ultrasonic gas flow meter could be used for determining the composition of flowing binary gas mixtures by simultaneous measurements of SoS and temperature.

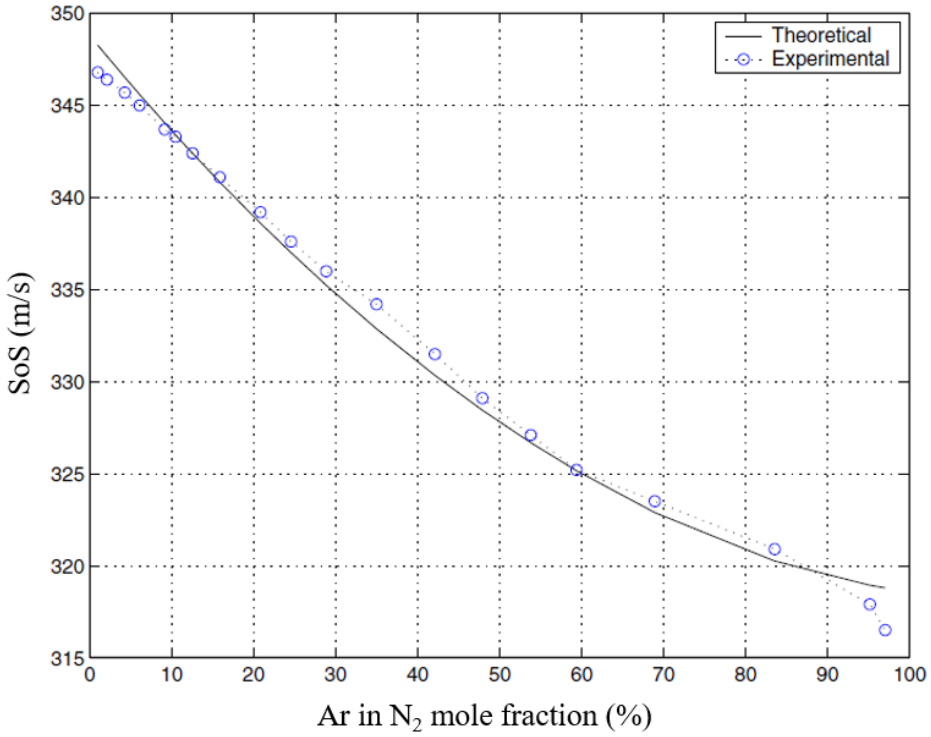



Figure 22. SoS versus Ar mole fraction in $N_2$ (Löfqvist et al., 2003)

Some other reported studies on binary gas mixtures using ToF method can be found from Hallewell et al. (2010) and Vacek et al. (2001) for $C_3F_8/C_4F_{10}$ from -20 to 30 °C and 0.01 to 0.4 MPa; Bates et al. (2012) for $C_2F_6/C_3F_8$, Joos et al. (1993) for $CO_2$/air, He/air and Ar/$SF_6$, Valdes & Cadet (1991) for He/Ar and $H_2/AsH_3$, and Vyas et al. (2006) for $H_2$/air, He/air and $CO_2$/air at around room temperature and ambient pressure; Schaik et al. (2010) for moisture in air from 20 to 90 °C and ambient pressure.

### 2.6.2 Acoustic Resonance Method and Interferometry Method

With the use of a spherical resonator, the SoS in difluoromethane ($CH_2F_2$) and 1,1,1,2-tetrafluroethane ($CF_3CH_2F$) binary gas mixtures were measured by Hozumi et al. (1997) over temperature, pressure and $CH_2F_2$ mole fraction ranges of 303 to 343 K, 30 to 240 kPa and 0.16 to 0.90. The cavity radius (around 50 mm) was determined as a function of temperature by calibration with argon. Details of the calibration process can be found in Hozumi et al. (1993). Radial modes were used for SoS determination. The two gas components were premixed, then the sample mixture of a specified composition was introduced into the measuring system which was at thermodynamic equilibrium. A series of measurements were then taken at constant

temperature but different pressures. The temperature and pressure measurement uncertainties were 4.0 mK and 0.05 kPa, respectively. Since the composition was only known approximately and the frequency shift correction is composition dependent, SoS could not be directly obtained with a high accuracy. The authors applied an iterative method (see Figure 23) to solve this problem, and then the SoS and gas composition could be determined with an uncertainty of 36 ppm and 0.03%, respectively.

More published studies on binary gas mixtures based on acoustic resonance method can be found from the work of He & Liu (2002) for $CH_3CHF_2$ (1,1-difluoroethane)/$CHClF_2$ (chlorodifluoromethane) at 293 to 323 °C and 200 to 405 kPa (spherical resonator); Colgate et al. (1990) for n-heptane/Ar at around 298.15 °C and 0.1 MPa (spherical resonator); Younglove & Frederick (1990), and Younglove & McCarty (1993) for $CH_4/C_2H_6$, $CH_4/C_3H_8$, $CH_4/N_2$, $CH_4/CO_2$ and $N_2/CO_2$ at temperatures from 250 to 350 K and pressures up to around 10 MPa (cylindrical resonator).

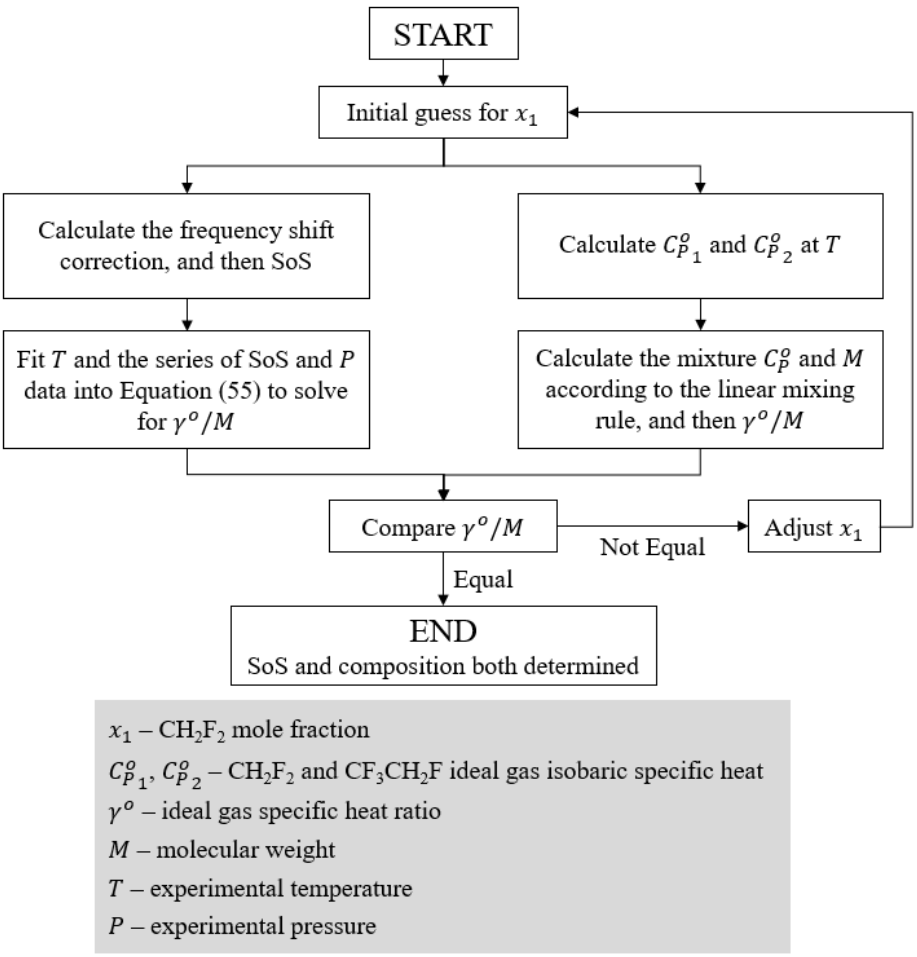



Figure 23. Iterative method for SoS and gas composition determination (Hozumi et al., 1997)

Previous studies on the use of interferometry for SoS measurements are far fewer than those reported using ToF and acoustic resonance. With the use of an acoustic interferometer, Van Itterbeek & Van Doninck (1946) measured the SoS in Ar/He, Ar/$H_2$, $H_2$/He and Ar/$D_2$ binary gas mixtures. Their experiments on a mixture of a certain composition was carried out at several different pressures below 1 atm and a fixed temperature near 20 K or 90 K which was achieved using liquid hydrogen or oxygen respectively. The acoustic frequency used was 524 kHz, and the interferometer had a micrometer for monitoring the position of the movable piston. A detailed description of the apparatus was given in Van Itterbeek & Keesom (1930). From these measurements, the interaction between different gas components in the mixtures was studied according to the EoS of Kamerlingh Onnes.

## 2.7 Comparisons of Different SoS Measurement Methods

Table 9 summarises the typical characteristics of ToF, acoustic resonance and interferometry methods for the measurement of gas SoS. For achieving high measurement accuracy, the environmental conditions need to be kept stable and measured accurately; accurate information regarding the dimension(s) or the dimension change(s) of the acoustic cavity wherein measurement is performed is also required; and the effects which could lead to errors need to be appropriately managed. Although spherical resonators are difficult to machine and assemble, they are generally the most suitable apparatus for super-high accuracy (ppm level uncertainty). Interferometers contain movable parts which can increase the structures mechanical complexity. Using an optical technique to measure the displacement of piston is beneficial for the improvement of the accuracy of interferometry method, however, this will further increase the instrument complexity and significantly increase the cost of measuring system. Due to the requirement for piston movement during measurement, this method is considered not well suited for operating in on-line mode for fast SoS determination. Published studies can be found on using interferometers and cylindrical resonators to measure SoS of gases with uncertainties from around 10 ppm to several tens of ppm. Amongst these three different types of methods, only ToF method operates in pulse mode. This method may also be impacted more significantly by the effects of sound wave diffraction, signal attenuation and distortion. The typical uncertainties of gas SoS measurement using ToF method in reported studies range from several hundreds of ppm to several ppt.

Applications of spherical resonators in on-line mode are difficult to find. A process analytical instrument, *BGA244 Binary Gas Analyzer*, which can be employed to determine the composition of binary gas mixtures based on the measurement of SoS using a cylindrical resonator has been recently developed and commercialised (Stanford Research Systems Inc. [*Online*]). The operating temperature range is from -20 to 70 °C, and the temperature can be measured with an accuracy of ± 0.1 °C. For Ar gas at 1 atm with a flow rate of 200 sccm, the SoS measurement accuracy is claimed to be ± 0.05%. The accuracy of gas composition determination is species dependent and is typically around ± 0.1%. The measurement rate is 4.4 Hz, and the price starts from around $4K which is 3 to 4 times higher than the anticipated price of the SoS sensor developed in this research project. Acoustic resonance method requires frequency sweeps and nonlinear curve fitting algorithms to determine resonance frequencies. These could make this type of SoS measurement technique less simple and more processing power consuming in comparison with the ToF technique adopted in this project. Consequently, the ToF approach is preferred to fulfill the project requirements.

Table 9. Typical characteristics of different SoS measurement methods

| Methods | ToF | Acoustic Resonance | | Interferometry |
|---|---|---|---|---|
| | | Spherical | Cylindrical | |
| Ease of Apparatus Fabrication | High | Low | High | Low |
| Suitability for Rapid On-Line Measurement | High | Unsure | High | Low |
| Requirement for Frequency Variations | No | Yes | Yes | No |
| Requirement for Cavity Dimension Changes | No | No | No | Yes |
| Pulse or Constant Wave (CW) Mode | Pulse | CW | | |

# CHAPTER 3. Experimental Methods

## 3.1 Mechanical Design for the SoS Sensor

The SoS sensor design[8] is based on the double-transducer configuration (see Figures 24 and 25). A pair of Airmar ATK120 piezoelectric ultrasonic transducers (Airmar Technology Corporation, NH, USA) which have a chemically resistant PVDF housing and an optimal operating frequency of 125 ± 5 kHz with a full-angle beam width at -3 dB of 10 ± 2° are used as the ultrasound transmitter and receiver transducers. They are cylindrical in shape; the diameter and height are both approximately 25 mm. Each transducer is fixed firmly and tightly in a transducer holder with three clamping grub screws at an angle of 120° to each other and perpendicular to the transducer sidewall, and the two transducer holders are screwed to the main body to ensure a coaxial and symmetrical arrangement between the two transducers and a separation of approximately 60 mm between their front surfaces. The inner diameter of the main body is about 36 mm and both the transducer holders and the main body are made of 316 stainless steel. Since the ultrasound beam spreads during propagation, for the purpose of reducing the noise level in received signals, a cylindrical piece of woven fiberglass mesh is mounted on the inner surface of the main body as an ultrasound absorbing liner to minimise the effects of reflections from the inner wall. Fiberglass material is inert to all the gas systems tested in this research project under the experimental conditions, thus the liner will not cause contamination to the measuring environment during experiments. A calibrated PT100 platinum resistance thermometer is placed in a recess in the outer wall of the main body and entirely buried in high thermal conductive diamond paste to achieve good thermal contact with the metal. The recess is covered by a piece of heat resistant adhesive tape so that the PT100 is isolated from the external environment. The grooved spiral channel whose length exceeds 1 m inside the wall of the main body was designed to ensure the incoming gas can reach thermal equilibrium with the metal before entering the measuring chamber through the inlet hole. The outer sleeve and the grooved tube of the main body are welded together for sealing purposes, and the other joints between different parts of the sensor which could leak are all sealed by the use of O-rings. After being completely assembled, the sensor has a total length and an outer

[8] The mechanical structure of the SoS sensor was designed by Mr. Paul Collins (Surface Measurement Systems Ltd.). The use of the woven fiberglass mesh as ultrasound absorbing liner came from the candidate's original idea.

diameter of around 176 and 50 mm respectively. A photo of the SoS sensor can be found in Appendix A2.

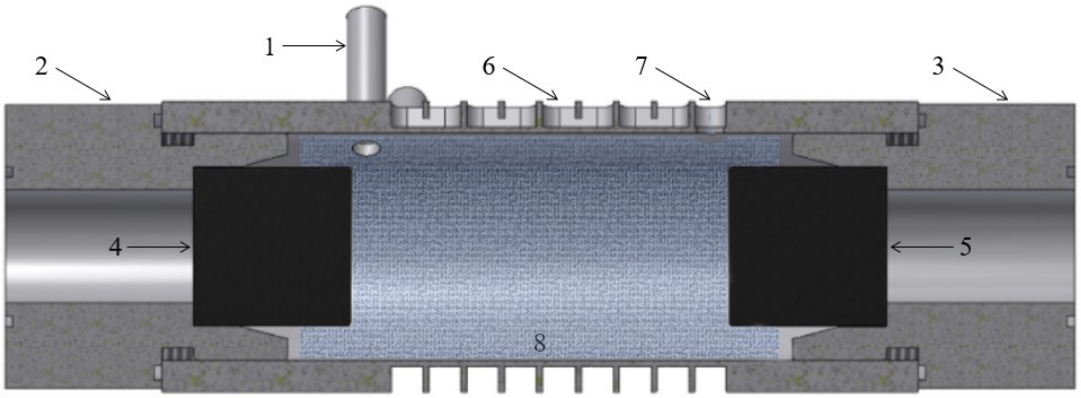



Figure 24. Cross-section view of the SoS sensor: 1 – outlet tube; 2, 3 – transducer holders; 4, 5 – ATK120 transducers; 6 – spiral grooved channel; 7 – inlet hole; 8 – woven fiberglass mesh (blue area)

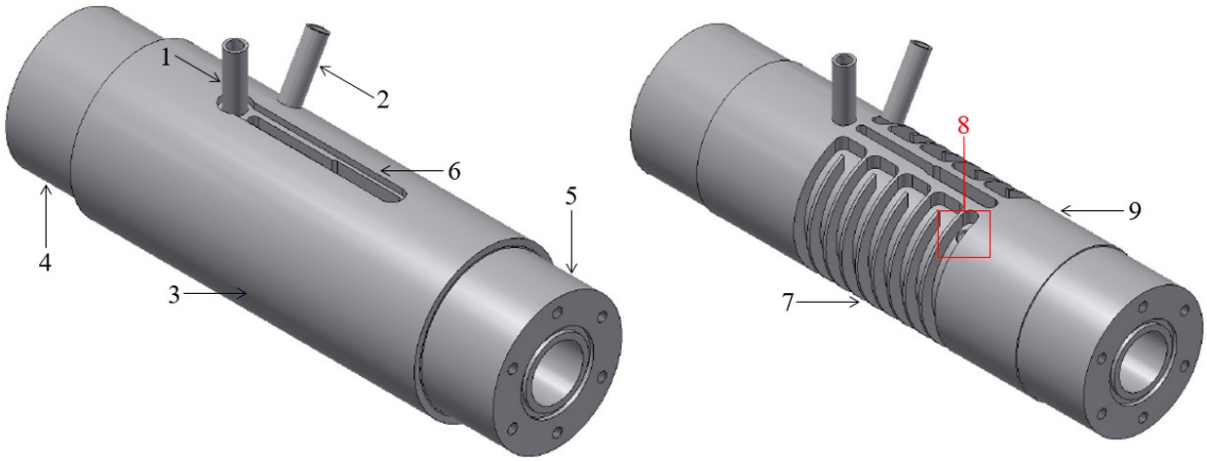



Figure 25. 3-D views of the SoS sensor: 1 – outlet tube; 2 – inlet tube; 3 – main body (outer sleeve shown); 4, 5 – transducer holders; 6 – recess for PT100; 7 – spiral grooved channel; 8 – inlet hole; 9 – grooved tube (main body, outer sleeve not shown)

## 3.2 Electronics Design for the SoS Sensor

A custom sensor electronics board[9] (see Figure 26) interfaces with the two ultrasonic transducers. The transmitter electronics generate the transmitted pulse train from a lookup table which is converted into a voltage via the microcontroller unit's (MCU) digital to analog

[9] The electronics and firmware of the SoS sensor were developed by Mr. Dirk Bruere (Surface Measurement Systems Ltd.).

converter (DAC). This pulse is then smoothed and amplified to a signal of a theoretical maximum peak to peak voltage of 60 V (60 $V_{pp}$) which feeds through a matching resistor to the transmitter transducer. The matching resistor is chosen to optimise the response of the transducer and minimise resonances which could distort the signal. The overall strength of the transmitted signal is controlled by modifying the numbers in the lookup table. The receiver transducer has a similar matching resistor, this time in parallel, whose value is chosen to minimise resonances. The signal from this transducer is fed to an amplifier, then a narrow band filter centered on the peak transducer response frequency, then another amplifier. The output from the latter amplifier can be controlled by a potentiometer to match the overall signal strength to the MCU's analog to digital converter (ADC) which has an input voltage range of 0 to 3 V. To allow for variations in transducer efficiency under different experimental conditions, this potentiometer is set to 70% of the allowed maximum output of the ADC. Typical values in practice are 20 $V_{pp}$ on the transmitter transducer terminals, with a theoretical maximum of that 60 $V_{pp}$ if no matching resistors are used. An automatic amplitude control is implemented in firmware by changing the numbers in the DAC lookup table to keep the ADC input amplitude optimised. This electronics board is a 4-layer printed circuit board (PCB), and is connected to a personal computer (PC) through a USB interface for both power supply and data transfer. A temperature compensated crystal oscillator (TCXO, Pletronics THD3004-16.384MHz) in this electronics board is used for timing. The SoS sensor's temperature probe is connected to the electronics package for temperature measurement, and a barometric sensor (Measurement Specialties MS5607-02BA03) is included in this electronics board which can measure atmospheric pressure with an uncertainty of 0.75 mbar (0.01 mbar resolution).

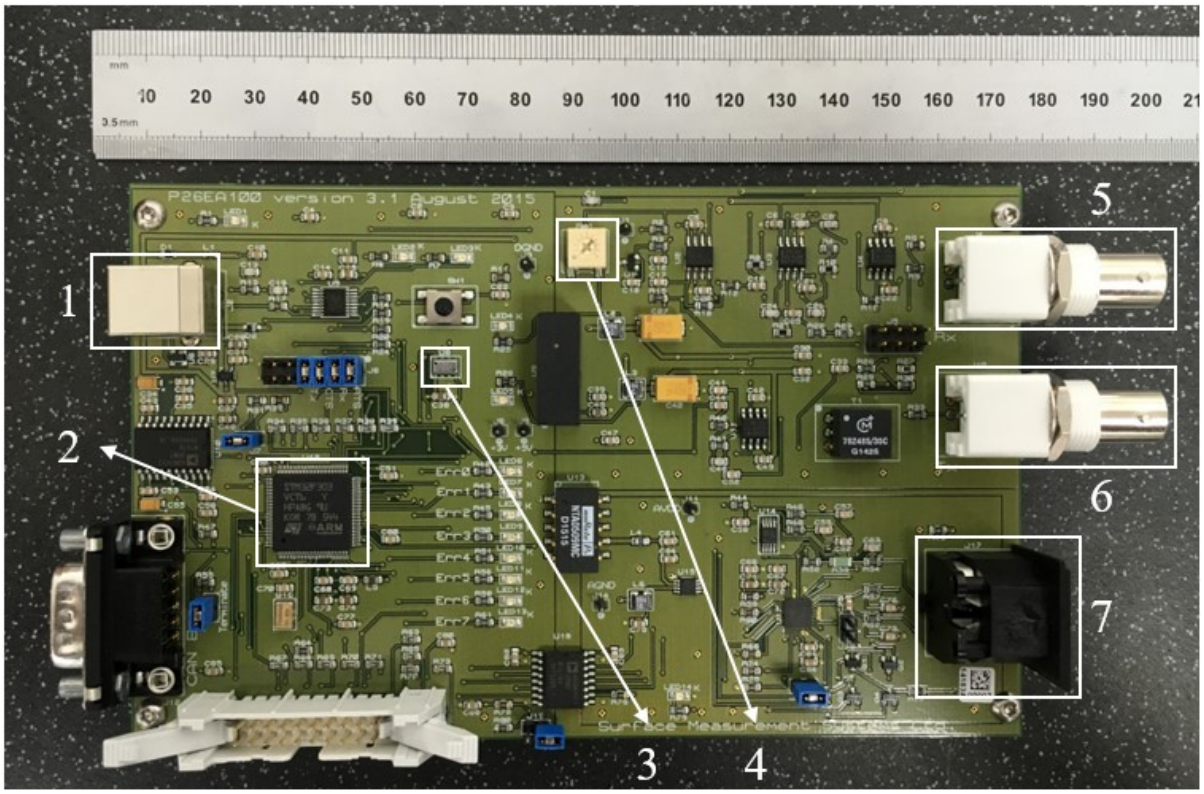



Figure 26. SoS sensor electronics board: 1 – USB interface; 2 – MCU; 3 – barometric sensor; 4 – potentiometer; 5 – receiver transducer connector; 6 – transmitter transducer connector; 7 – PT100 connector

## 3.3 ToF Signal Analysis Algorithm

Following the discussion in Section 2.4.1.4, this SoS sensor uses the time difference between two received signals as the measured ToF for SoS determination. The two received signals selected for the ToF measurement are the first and second received signals ($RS_1$ and $RS_2$ as shown in Figure 11) because their intensities are greater than those of the subsequent ones and their higher signal to noise levels can help improve ToF measurement precision and accuracy. Considering that the ATK120 ultrasonic transducers used in the SoS sensor have a narrow bandwidth and this research project requires fast SoS measurement, the fitting method, waveform marker method and auto-correlation method are not well suited for the measurement of ToF. Actually, a novel variation of the amplitude thresholding method is employed here in order to both fulfill the fast measurement requirement and achieve the required precision and accuracy.

The transmitted signal train is contained in an ellipsoidal-shaped 9-cycle pulse envelope with a frequency of 121362 Hz. A typical received signal waveform is shown in Figure 27, where

the first and second pulses correspond to the first and second received signals respectively, i.e. $RS_1$ and $RS_2$. This original waveform is created from samples taken from the ADC sampling at approximately 40 times the fundamental signal frequency, thus each cycle is made up of approximately 40 data points. A typical ratio of the amplitudes of the two pulses is around 1.7 : 1 for dry air at 25 °C and atmospheric pressure. Due to the fact that both transducers exhibit signal distortion characteristics, most notably 'ringing', the sequentially received signals have only a passing resemblance to the original transmitted pulse train. Comparing both received signals, it is observed that most of the wave distortions occur on the trailing edges of the pulses, while the leading edges are nearly undistorted and identical. Therefore, the time difference measurements reported here are only performed on the forward nearly non-distorted parts of the two pulses. It should be noted that the second pulse is found to be 180° out of phase from the first pulse.

The measurement algorithm[10] is as described below:

1) Find all the cycle maxima and minima in each pulse.
2) Use this to locate the maximum and minimum of each pulse (the maximum and minimum of the pulse envelope).
3) Find the position of the nearest cycle maximum to the upper half-height level in the first pulse and the position of the nearest cycle minimum to the lower half-height level in the second pulse (illustrated by $P_1$ and $P_2$ in Figure 27). These two cycle extrema can be considered as corresponding points in the two pulses, and that they lie on edges of opposite polarities (one on leading rising edge and the other on leading falling edge) is due to the phase reversal between the two pulses.
4) Normalise the amplitude of the second received pulse to the amplitude of the first.
5) From $P_1$ search for the first forward and backward zero crossing points of the waveform, $Z_1$ and $Z_2$. These are located by indexing forward or backward through the ADC samples in pairs starting from $P_1$ until one sample lies on or above the zero line which is at approximate amplitude of 1985 in Figure 27, and the other on or below it. The zero crossing point is then interpolated using these two samples.
6) Use a similar process to find the first forward and backward zero crossing points $Z_1'$ and $Z_2'$ relative to $P_2$. $Z_1'$ and $Z_2'$ correspond to $Z_1$ and $Z_2$, respectively.

[10] The design of the ToF measurement algorithm was an original work of Mr. Dirk Bruere (Surface Measurement Systems Ltd.) and the candidate.

7) Calculate the average time difference between corresponding zero crossing points as the results of one single measurement.

In theory, the nearest cycle minimum to the lower half-height level in the first pulse and the nearest cycle maximum to the upper half-height level in the second pulse are also corresponding points; however, usually the latter cannot be determined consistently because the half-height level lies approximately right in the middle between the amplitudes of two adjacent cycle maxima. The 'thresholds' are set at half-height levels where the difference in amplitude between adjacent cycle extrema are more significant than those at too high or too low levels, thus theoretically the probability of locating a wrong cycle extrema (usually one-cycle off) caused by background noise can be minimised. The time difference between $P_1$ and $P_2$ may be used as the measurement result, but due to digital timing error the time difference is only consistent within a couple of samples out of approximately 40 samples per cycle. Zero-crossing points determined from interpolation are used in this algorithm in order to refine the precision and accuracy of the results further.

This algorithm can handle small amplitude pulses down to 0.5 V. The measurement described above is repeated 100 times per second and the average of a selection of the 100 single measurement results by a median filter is outputted with a resolution of 1 ns. The output frequency can be controlled up to 1 Hz. When temperature and pressure are stable, ToF (SoS) can be measured with a typical precision of better than 1 part in half million[11].

[11] A discussion of the measurement precision of the SoS sensor can be found in Appendix A3, which was provided by Mr. Dirk Bruere (Surface Measurement Systems Ltd.).

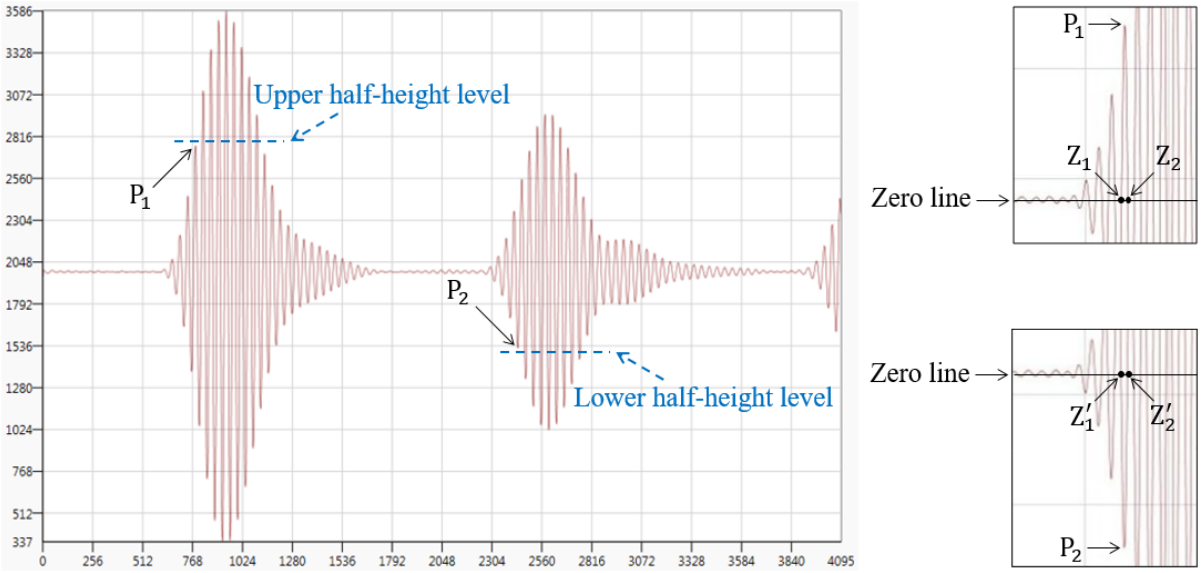



Figure 27. A typical received signal waveform and detailed views of the zero crossing points (x-axis – time with a unit of 200 ns; y-axis – amplitude with a unit of 3/4095 V)[12]

## 3.4 Experimental Setup

A Dynamic Vapour Sorption (DVS) Advantage instrument (Surface Measurement Systems Limited, Alperton, London) was used to generate binary gas mixtures and was configured to allow gas composition measurement using gas density[13]. Several photos of the experimental system are given in Appendix A2. A schematic of the experimental setup for the measurements on binary gas mixtures other than $CO_2/N_2$ (e.g. n-heptane/dry air) is shown in Figure 28. The inlets of the two mass flow controllers, MFC-1 and MFC-2, are both connected to the same carrier gas supply. The outlet gas from MFC-1 ($f_1$) is bubbled through the liquid (nominally pure) in the reservoir so that the vapour phase should be 100% saturated with the liquid. According to the Dalton's law, the vapour mole fraction $x$ in the gas phase inside the reservoir and in the outlet gas flow ($f_3$) can both be represented as:

$$x = x_{SAT} = \frac{P_{SAT}}{P} \tag{75}$$

[12] The waveform was generated using a PC interface software for the SoS sensor developed by Mr. Christopher Cawe (Surface Measurement Systems Ltd.).

[13] The DVS Advantage instrument was manufactured by Surface Measurement Systems Ltd., and the configuration of the instrument for fulfilling the purpose of this research project was an original work of Dr. Daryl Williams (Imperial College London) and the candidate.

where $x_{SAT}$ refers to the saturated vapour mole fraction, $P_{SAT}$ the saturated vapour pressure, and $P$ the total gas pressure. The pure carrier gas component with flow $f_2$ mixes with $f_3$ in a manifold then the resultant flow $f_4$ of binary gas mixture passes through the SoS sensor.

The volumetric flow rates of $f_1$ and $f_2$ are designated by $u_1$ and $u_2$, respectively; $u$ denotes their total flow rate which can be controlled by the two MFCs up to 200 sccm. The two MFCs are operated in an antagonistic manner, and by using them to control $u_1$ and $u_2$ the vapour mole fraction in $f_4$ can be adjusted from 0 to 1. The upper and lower limits of the vapour pressure in $f_4$ are the saturated vapour pressure (100% saturated) and zero (0% saturated) respectively, which can be achieved by keeping one MFC fully closed and running all the carrier gas through the other. %SAT indicates percentage of saturated vapour mole fraction, or percentage of the maximum achievable vapour mole fraction which corresponds to 100% saturation at the experimental temperature and pressure. For convenience, the target mole fraction of the vapour component in $f_4$, $x_T$, is expressed in %SAT and is given by:

$$x_T = \frac{100u_1}{u_1 + u_2} = \frac{100u_1}{u} \text{ (\%SAT).} \tag{76}$$

$x_T$ is determined simply from the flow rates, and is considered as a theoretical estimate of the true mole fraction. The upper and lower limits of $x_T$ are 100%SAT and 0%SAT respectively. If $u$ is equal to 100 sccm, then 75 sccm $u_1$ and 25 sccm $u_2$ correspond to 75%SAT $x_T$; 25 sccm $u_1$ and 75 sccm $u_2$ correspond to 25%SAT $x_T$.

For the measurements on $CO_2/N_2$, the mixture generation module of the DVS instrument needs to be modified: the two MFCs are connected to different gas sources; and no liquid is present in the reservoir. Similarly, different target gas composition in $f_4$ can be achieved by using the MFCs to control $u_1$ and $u_2$. If the target mole fraction in $f_4$ of the pure gas component flowing though MFC-1 is denoted by $x_T$, then the relationship between $x_T$ and the volumetric flow rates can be found from:

$$x_T = \frac{u_1}{u_1 + u_2} = \frac{u_1}{u}. \tag{77}$$

The SoS measurement is performed in the SoS sensor, then the outlet flow $f_5$ will enter the test chamber of the DVS instrument for gas composition measurement using the Archimedes' Principle. This DVS system has a symmetrical recording microbalance with a closed hollow

glass sphere suspended on one side and a counterweight of similar mass but with a much smaller volume suspended on the other side. The resolution of this microbalance is 1 μg. When the gas density is $\rho^I$, the apparent mass difference between the two sides $m_d^I$ (mass reading $m_{read}^I$) can be represented by:

$$m_d^I = (m_1 - \rho^I V_1) - (m_2 - \rho^I V_2) \tag{78}$$

where $m_1$ and $V_1$ are the mass and volume of the glass sphere, $m_2$ and $V_2$ the mass and volume of the counterweight, $\rho^I V_1$ and $\rho^I V_2$ the apparent mass reductions due to buoyancy effects according to Archimedes' Principle. If the gas density changes to $\rho^{II}$, then the apparent mass difference $m_d^{II}$ (mass reading $m_{read}^{II}$) will become:

$$m_d^{II} = (m_1 - \rho^{II} V_1) - (m_2 - \rho^{II} V_2) \tag{79}$$

and the change in the mass readings of the microbalance $\Delta m_{read}$ can be expressed by:

$$\begin{aligned} \Delta m_{read} = m_{read}^{II} - m_{read}^I = m_d^{II} - m_d^I &= (\rho^I - \rho^{II})(V_1 - V_2) \\ &= (\rho^I - \rho^{II})\Delta V. \end{aligned} \tag{80}$$

It is noteworthy that although practically the apparent mass difference is different from the mass reading at the same gas density, the variation between the two apparent mass differences can be considered equivalent to that between the two mass readings.

The volume difference between the two sides $\Delta V$ was first determined from $\Delta m_{read}$ by running two pure gases both with known densities alternately through the measuring system (see Section 3.7). Then, with this known $\Delta V$, by running a gas with known density $\rho^I$ and a gas with unknown density $\rho^{II}$ successively through the measuring system, $\rho^{II}$ can be determined from $\Delta m_{read}$. In the case of this research project, the gas with known density was the pure carrier gas, while the gas with unknown density was the generated binary gas mixture for SoS measurement. The mixture density determined with this method was then used for the determination of the gas composition according to equation of state (see Section 3.8). It is worth mentioning that, for a binary gas mixture, if the species of the two gas components, temperature and pressure are known, then the mixture density should be in one-to-one correspondence with the mole fraction of any of the two gas components.

The microbalance chamber is purged by inert gas $f_8$ which is then mixed with $f_5$ and exhausted to the atmosphere outside the temperature controlled incubator through $f_6$ and $f_7$. It should be noted that the purge gas will not reach the glass sphere or the counter weight so that it will not affect the gas composition measurement. Considering the reasonably low gas flow rate of $f_4$ (typically not exceeding 250 ml/min) and the dimensions of the flow path between the inlet hole of the SoS sensor (see Figures 24 and 25) and the exhaust outlets at the end of the measuring system, the pressure drop should be negligible, and thus both SoS and gas composition measurements are performed at atmospheric pressure. In fact, the pressures of $f_1$ to $f_4$ and the gas phase inside the liquid reservoir can all be considered equal to the atmospheric pressure. Considering that the gas flow velocity in the cylindrical measuring chamber of the SoS sensor is reasonably low (bulk velocity along the chamber axis below 0.5 cm/s) and that the SoS sensor uses the time difference between the first and second received signals for SoS determination which corresponds to a round trip of the ultrasound pulse (one upstream and one downstream), the effect of gas flow on SoS measurement is effectively negated. The gas flow effect on the measurement of gas density (composition) is also neglected.

The SoS sensor electronics board is located in the local environment, thus the atmospheric pressure can be continuously monitored by the on-board barometric sensor. The DVS's temperature controlled incubator has a long-term stability of ± 0.1 °C and a short-term stability of ± 0.01 °C, and the operating temperature range is 5 to 60 °C. The temperature control of the incubator is based on PID control mechanism. Once the incubator temperature is set, the PID controller continuously monitors the difference between the measured incubator temperature and the set point, and attempts to minimise the difference over time by adjustment of the heating/cooling rate of the incubator. It is worth mentioning that the temperature probe for the measurement of the incubator temperature is neither the DVS temperature probe nor the SoS sensor's temperature probe, but is a separate one (not shown in Figure 28).

The DVS temperature probe is a 3-wire Class-B PT100 and is used to measure the temperature in the DVS test chamber. The temperature measurement resolution was 0.01 °C, and the uncertainty was $0.15 + 0.0025|T|$ °C ($T$ in °C) which was estimated according to the accuracy class of the probe (B). Hereinafter, the temperature measured by this temperature probe will be referred to as the DVS temperature.

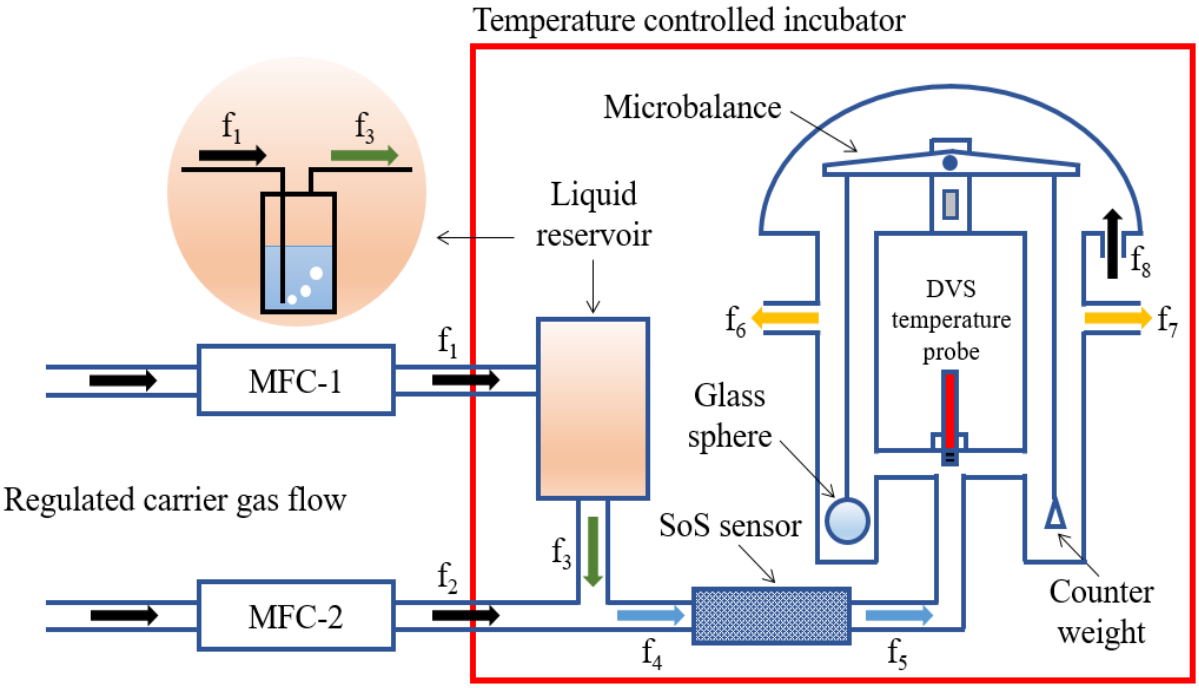



Figure 28. Schematic of DVS based experimental system with SoS sensor

## 3.5 Temperature Calibration

The SoS sensor's temperature probe (called SoS temperature probe) was a 4-wire 1/10 DIN PT100 and was used to determine the temperature in the sensor. Before being mounted to the SoS sensor, it was first calibrated [14] using a Fluke 5699 standard platinum resistance thermometer (SPRT) previously calibrated on the International Temperature Scale of 1990 (ITS-90). A Fluke 1594A super-thermometer together with a Fluke 2590 multiplexer was used to measure the resistance of both the probe under test and the reference SPRT which were placed in the same environment. The calibration was performed at 0.01, 10, 20, 40, 80 and 90 °C. 0.01 °C was achieved by using a Fluke 5901 water triple point cell maintained in a Fluke 9210 maintenance apparatus and the other temperatures were achieved by using either a Fluke 7040 or 6020 temperature calibration bath. The measured resistance values of the probe under test and the temperature values converted from the measured resistance values of the reference SPRT were fitted to the Callendar-Van Dusen equation:

$$R_T = R_0(1 + A_c T + B_c T^2) \quad t \geq 0 \tag{81}$$

[14] Technical assistance in temperature calibration was provided by Dr. Emmanuel Efika (Imperial College London); the calibration instruments were provided by Prof. Martin Trusler (Imperial College London).

where $R_T$ is the resistance in Ω, $T$ the temperature in °C, $R_0$, $A_c$ and $B_c$ the fitting coefficients. Then, in theory, providing the resistance of the SoS temperature probe is known this equation can be used for temperature determination; and the temperature uncertainty resulting from this calibration over the whole temperature range from 0.01 to 90 °C was estimated to be 12.5 m°C. The derivation of this value can be found in Table 10.

Table 10. Uncertainty schedule for the calibration of the SoS temperature probe

| Uncertainty Sources | Type | Uncertainty (m°C) |
|---|---|---|
| Probe Under Test Measurement Precision | A | Negligible |
| Reference SPRT Measurement Precision | A | Negligible |
| Reference SPRT Calibration | B | 1.5 |
| Reference SPRT Drift | B | 2.34 |
| Bath Uniformity | B | 2.31 |
| Bath Stability | B | 1.74 |
| Reference SPRT Readout | B | 0.86 |
| Probe Under Test Readout | B | 0.71 |
| Callendar-Van Dusen Equation Fitting | A | 11.59 |
| Calibration uncertainty (temperature measurement uncertainty resulting from calibration): $\sqrt{1.5^2 + 2.34^2 + 2.31^2 + 1.74^2 + 0.86^2 + 0.71^2 + 11.59^2} \approx 12.5$ m°C | | |

The above calibration was for the PT100 on its own, however, there might be an offset when using the electronics on the sensor board to measure the probe resistance. In order to compensate for this, a 100 Ω standard resistor and a 4-wire short-circuited plug simulating a 0 Ω resistor were connected to the electronics board individually, and a linear correction was applied to Equation (81) according to the difference between the measured and the true resistance values. The model of the standard resistor was Fluke 742A-100 with a true resistance of 100.00008 ± 0.00004 Ω (68% confidence level).

The performance of the SoS temperature probe with the electronics on temperature measurement was tested when all the experiments in this research project had been completed. The test was performed at the same six temperatures as in the calibration, and the instrument setup was the same as well except using the electronics on the sensor board to measure the resistance of the SoS temperature probe which was then converted to temperature readings according to Equation (81) with the linear correction. It was found that the difference between

the temperature from the SoS temperature probe and that from the reference SPRT was approximately linear with respect to temperature and over the experimental temperature range from 5 to 55 °C the difference was within the calibration uncertainty of the former. Therefore, the drift of the SoS temperature probe with the electronics can be ignored, and for all the experiments in this research project the measured temperature data from this probe should be valid. The uncertainty of the measured temperature data over the whole experimental temperature range was 12.5 m°C (0.1 m°C measurement resolution). Hereinafter, the temperature measured by this temperature probe will be called the SoS temperature.

It should be note that due to the effects of non-uniform temperature distribution, at different positions within the DVS's incubator the temperatures can be slightly different. At the same time the SoS temperature can be slightly different from the DVS temperature, and both can be different from the incubator set temperature and the measured incubator temperature as well.

## 3.6 Microbalance Calibration and Stability Check

The microbalance needed to be calibrated before suspending the glass sphere and the counterweight. The calibration was performed at the incubator set temperature of 25 °C with dry air flowrate of 100 sccm. The procedure was as follows: suspending one sample pan on each side; taring the balance; placing a calibrated 1 g (nominal mass value) standard weight (Troemner, USA) in the left sample pan; then correcting the mass reading to 1.000000 g. The last step was automatically done with the use of the balance calibration programme in the DVS Advantage control software. Sufficient time was given between each two steps for the system to stabilise. The true mass value of the calibrated standard weight was 1.0000020 ± 0.0000075 g (68% confidence level). The stability of the microbalance over the whole operating temperature range of the incubator was tested after the calibration by keeping the instrument setup and the dry air flowrate the same but changing the incubator set temperature from 5 to 60 °C at an interval of 10 or 15 °C. The incubator was kept at each temperature for at least 300 minutes for the system to reach thermal equilibrium. It was found that neither the inaccuracy of the calibration nor the instability of the microbalance resulted in significant errors in the following mass measurements. The resolution of the microbalance is 1 μg, therefore, assuming a rectangular distribution the uncertainty of the mass readings is estimated to be $1/\sqrt{3}$ μg.

## 3.7 Volume Difference Measurement

The volume difference between the glass sphere and the counterweight on the microbalance can be determined according to Equation (80). Argon and helium were used in this experiment for improving the accuracy of $\Delta V$ measurement because their density data are known with reasonably high accuracy and the difference in density between these two gases are significant. This experiment was performed at the incubator set temperature of 25 °C by running the two different gases alternately through the measuring system in the order of Ar, He, Ar and then He. Each experimental step ran for 60 minutes in order to ensure the measuring system was filled up with the test gas. Since the end of each step had the best stability, the average values of the last 30 seconds data (DVS temperature, pressure, mass reading) in each step were used for $\Delta V$ determination. One $\Delta V$ value can be obtained from the mass reading difference and the density difference between one pair of adjacent stages; there were three such pairs, thus three volume difference values can be gained; the average of these three values was considered as the final result. The instrument setup was the same as that shown in Figure 28. During the experiment, MFC-1 was kept fully closed and thus Ar or He flowed into the measuring system through MFC-2. The flowrate was controlled at around 100 sccm. The density data are available in the NIST REFPROP software.

With the above method, $\Delta V$ was found to be around 13 $cm^3$, and the measurement uncertainty was estimated to be 1250 ppm (see Appendix A4 for details). In this research project, since the DVS-based measuring system was operated at atmospheric pressure, any $\Delta V$ dependence on pressure variation was ignored; by taking into consideration the thermal expansion properties of the glass sphere and the counterweight, the possible change in $\Delta V$ within the whole experimental temperature range from 5 to 55 °C should be much lower than 1250 ppm and thus the dependence of $\Delta V$ on temperature variation was also ignored. Therefore, $\Delta V$ was considered constant in all experiments.

## 3.8 Experimental Procedure

Basic information about the experiments performed in this research project on binary gas mixtures is listed in Table 11. For each type of binary gas mixture, each experiment was performed isothermally (nominally, at constant incubator set temperature), and before starting the incubator was thermally stabilised for 2 hours at the experimental temperature.

Table 11. Basic experimental information

| Type No. | Gas Component 1 (Solute) | Gas Component 2 (Carrier Gas) | Experimental Temperatures (Incubator Setpoint Temperatures) |
|---|---|---|---|
| 1 | n-Hexane | Dry air | 5, 15, 25, 35, 45 °C |
| 2 | n-Heptane | Dry air | 5, 15, 25, 35, 45, 55 °C |
| 3 | n-Octane | Dry air | 5, 15, 25, 35, 45, 55 °C |
| 4 | n-Nonane | Dry air | 15, 25, 35, 45, 55 °C |
| 5 | n-Decane | Dry air | 25, 35, 45, 55 °C |
| 6 | Toluene | Dry air | 5, 15, 25, 35, 45, 55 °C |
| 7 | Cyclohexane | Dry air | 15, 25, 35, 45, 55 °C |
| 8 | Water | Dry air | 25, 35, 45, 55 °C |
| 9 | Acetone | Dry air | 5, 15, 25, 35 °C |
| 10 | Methyl ethyl ketone | Dry air | 5, 15, 25, 35, 45, 55 °C |
| 11 | Ethyl acetate | Dry air | 5, 15, 25, 35, 45, 55 °C |
| 12 | Methanol | Dry air | 5, 15, 25, 35, 45 °C |
| 13 | Ethanol | Dry air | 5, 15, 25, 35, 45, 55 °C |
| 14 | Isopropanol | Dry air | 5, 15, 25, 35, 45, 55 °C |
| 15 | Dichloromethane | Dry air | 5, 15, 25 °C |
| 16 | Chloroform | Dry air | 5, 15, 25, 35 °C |
| 17 | 1,2-Dichloroethane | Dry air | 5, 15, 25, 35, 45, 55 °C |
| 18 | m-Xylene | Dry air | 30, 40, 50 °C |
| 19 | o-Xylene | Dry air | 30, 40, 50 °C |
| 20 | p-Xylene | Dry air | 30, 40, 50 °C |
| 21 | Ethylbenzene | Dry air | 30, 40, 50 °C |
| 22 | n-Butylamine | Dry air | 25, 35, 45 °C |
| 23 | Limonene | Dry air | 25, 35, 45 °C |
| 24 | α-Pinene | Dry air | 25, 35, 45 °C |
| 25 | Carbon dioxide | Nitrogen | 10, 20, 25, 30, 40, 50 °C |

A typical procedure for the isothermal experiments on organic vapour/dry air and $H_2O$ vapour/dry air binary gas mixtures (Type No. 1 to 24 in Table 11) is illustrated in Figure 29, wherein the curve represents the target mole fraction of the vapour component (solute) in the binary gas mixture flow to be tested (i.e. in $f_4$ as shown in Figure 28) $x_T$ (in %SAT) versus time. The method to achieve different levels of $x_T$ can be found in Section 3.4. The experimental procedure starts with a 90%SAT step which is designed as a preliminary step to

examine the performance of the measuring system specifically for the gas mixture to be tested. The second step is set at 0%SAT for purging the vapour generated in the previous step from the measuring system. Then $x_T$ is raised up to 95%SAT at an interval of 10%SAT or 5%SAT (only the change in $x_T$ between the highest two steps is 5%SAT) in an alternate method by resetting to zero after each non-zero step. After the peak step, $x_T$ is returned to zero step by step in the same alternate way. The first zero step lasts for 45 minutes and the following steps typically last for 30 minutes each. In some cases, especially when the saturated vapour pressure is low, the duration of some or all steps needs to be extended in order to ensure the mass reading data and the measured ToF data at the end of these steps can reach stability, i.e. the gas composition in the measuring system becomes stabilised. For some binary gas mixtures, the experimental procedure is only the ascending half of the full procedure as is shown in Figure 29 (from the start of the preliminary step to the end of the 95%SAT step). For some experiments at 25 °C, the experimental procedure contains about twice the number of steps in Figure 29; based on the same alternate method, after the preliminary step, $x_T$ is increased from 0%SAT to 95%SAT and then decreased to 0%SAT step by step at an interval of 5%SAT. The total carrier gas flowrate was 100 sccm, except for the experiments on water/dry air where the total carrier gas flowrate was 200 sccm.

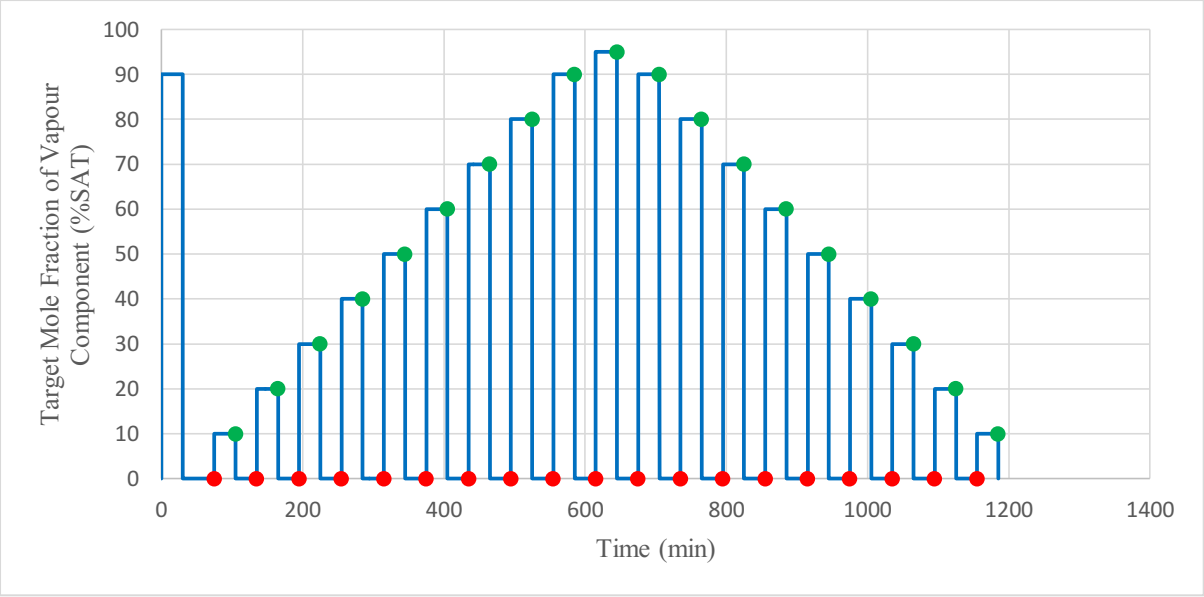



Figure 29. A typical procedure for the isothermal experiments on organic vapour/dry air and water vapour/dry air binary gas mixtures

The procedure for the isothermal experiments on $CO_2/N_2$ mixtures is shown in Figure 30; the y-axis indicates the target mole fraction of $CO_2$ in the mixture flow to be tested (i.e. in $f_4$ as shown in Figure 28) which is denoted by $x_T$ as well; and the x-axis represents the experiment time. The procedure starts from a 0.25 preliminary step, then $x_T$ is reset to zero and then increased to 0.02, 0.03, 0.05, 0.07, 0.09, 0.11, 0.13, 0.15, 0.20, 0.25 and 0.30 in the same alternate manner as in the experiments on the other binary gas mixtures. The duration of the first zero step is 45 minutes and that of the other step is 30 minutes each. The total flowrate of $CO_2$ and $N_2$ was controlled at around 200 sccm. Since $CO_2$ has a high acoustic absorption characteristic under these experimental conditions, when its mole fraction in the test binary mixture exceeds a certain level, the amplitude of the second received signal will become too low, and the consequence will be a significant reduction in the accuracy and precision of the measured ToF data. This is why the upper limit of $x_T$ for $CO_2$ in the experiments was not set too high. However, the experimental mole fraction range of $CO_2$ chosen here should cover most of the potential industrial applications in the field of carbon capture where the $CO_2$ mole fraction of measurement interest is normally below 0.30.

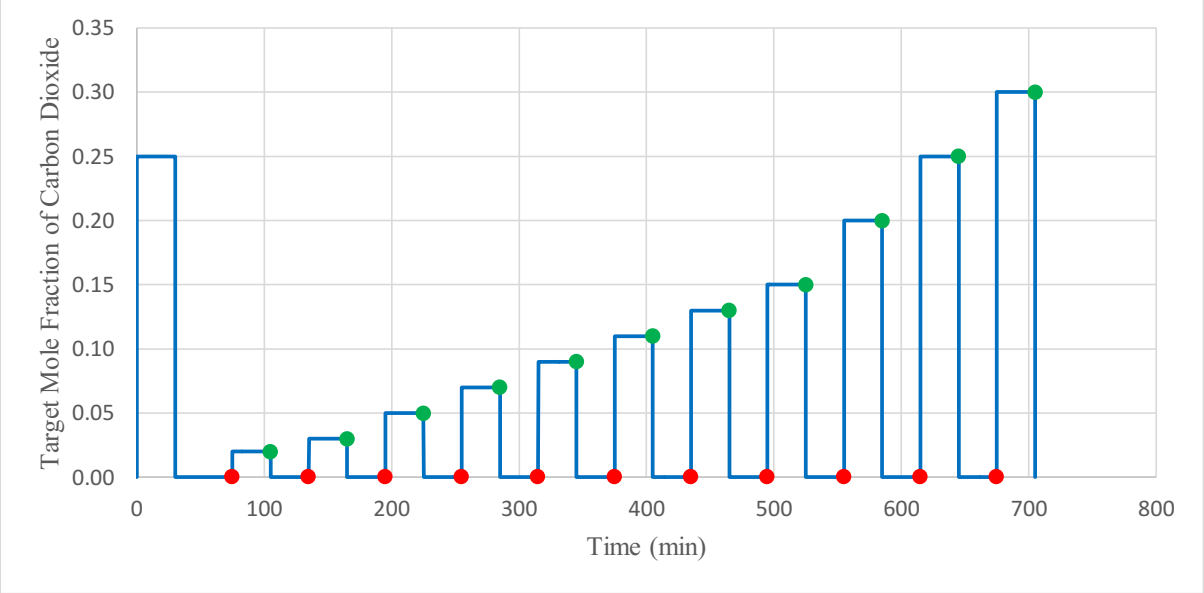



Figure 30. The procedure for the experiments on $CO_2/N_2$ binary gas mixtures

Since at the end of each experimental step the system had its most stable data, the correlation of SoS with gas composition, temperature and pressure (acoustic frequency was constant) was based on the average values of the last 30 seconds data at each step (except the preliminary step). The average data used included the mass reading $m_{read}$, the SoS temperature $T_{SoS}$, the

DVS temperature $T_{DVS}$, the atmospheric pressure $P$ and the measured ToF $t_m$. Each isothermal experiment consisted of zero steps ($x_T = 0$) and non-zero steps ($x_T \neq 0$), and it is noteworthy that the preliminary step will be excluded in the non-zero step(s) mentioned hereinafter.

The $T_{SoS}$, $P$ and $t_m$ corresponding to the first zero step were used for the pathlength calibration of the SoS sensor, and the $t_m$ corresponding to the non-zero steps were used for the SoS measurements at different $x_T$ levels.

The gas composition corresponding to each non-zero step, denoted by $x$ which is the mole fraction of the solute, was determined by using the $m_{read}$, $T_{DVS}$ and $P$ corresponding to both the non-zero step itself and the preceding adjacent zero step. It was obtained from the gas density corresponding to the non-zero step $\rho$ according to equation of state. In order to achieve $\rho$, Equation (80) needs to be used: $\rho = \rho^{II}$; $\rho^0 = \rho^I$ was the carrier gas density at the zero-step $T_{DVS}$ and $P$, and was obtained using equation of state as well; $\Delta m_{read}$ was the difference between the non-zero-step and zero-step $m_{read}$ (the former minus the latter); and $\Delta V$ was known. The binary gas mixtures tested in this research project can be divided into two groups: Group A includes the ones with available thermodynamic data in the NIST REFPROP software; and Group B includes the others, i.e. the ones without available thermodynamic data in the software. The methods used to determine $\rho^0$ and $x$ for the experiments on the binary gas mixtures in Group A and Group B are given in Tables 12 and 13, respectively. For a non-zero step, the measured SoS can be correlated to $T_{SoS}$, $P$, $x$ and the acoustic frequency (constant value).

Only the data from adjacent experimental steps were used together in the gas density calculation as this minimises drift errors associated with the microbalance. The DVS Advantage control software interfaces with the SoS sensor[15], therefore, both the experiments and the data collection processes were performed automatically.

[15] The interface software was developed by Mr. Christopher Cawe (Surface Measurement Systems Ltd.).

Table 12. Methods used to determine $\rho^0$ and $x$ for the experiments on the binary gas mixtures in Group A (the binary gas mixtures with available thermodynamic data in the NIST REFPROP software)

| Carrier Gas | | Dry Air | Nitrogen |
|---|---|---|---|
| Solute | | n-hexane, n-heptane, n-octane, n-nonane, n-decane, toluene, cyclohexane and water | Carbon dioxide |
| Carrier Gas Density $\rho^0$ | EoS used | H-EoS | H-EoS |
| | Method | Set a mixture in the software as dry air comprising $N_2$, $O_2$, Ar and $CO_2$ with mole fractions of 0.780796, 0.209461, 0.009339 and 0.000404 respectively → input the zero-step $T_{DVS}$ and $P$ → output $\rho^0$ | Set pure $N_2$ in the software → input the zero-step $T_{DVS}$ and $P$ → output $\rho^0$ |
| Gas Composition $x$ (Mole Fraction of the Solute) | EoS used | H-EoS | H-EoS |
| | Method | Set a mixture in the software comprising the solute, $N_2$, $O_2$, Ar and $CO_2$ with mole fractions of $y$ (an arbitrary number between 0 and 1), 0.780796(1-$y$), 0.209461(1-$y$), 0.009339(1-$y$) and 0.000404(1-$y$) respectively (i.e. a binary gas mixture comprising the solute and dry air with mole fractions of $y$ and (1-$y$) respectively) → input the non-zero-step $T_{DVS}$ and $P$ → compare the output density with the non-zero-step $\rho$ → change $y$ and repeat the above processes until the output density is equal to $\rho$ (at this time, $y = x$). | Set a mixture in the software comprising $CO_2$ and $N_2$ with mole fractions of $y$ (an arbitrary number between 0 and 1) and (1-$y$) respectively → input the non-zero-step $T_{DVS}$ and $P$ → compare the output density with the non-zero-step $\rho$ → change $y$ and repeat the above processes until the output density is equal to $\rho$ (at this time, $y = x$). |
| Comments | | The method for determining $x$ is equivalent to solving for the composition of a gas mixture comprising the solute and dry air with mole fractions of $x$ and (1-$x$) respectively according to the H-EoS for the gas mixture when the temperature, pressure and density are equal to the non-zero-step $T_{DVS}$, $P$ and $\rho$. | The method for determining $x$ is equivalent to solving for the composition of a gas mixture comprising $CO_2$ and $N_2$ with mole fractions of $x$ and (1-$x$) respectively according to the H-EoS for the gas mixture when the temperature, pressure and density are equal to the non-zero-step $T_{DVS}$, $P$ and $\rho$. |

Table 13. Methods used to determine $\rho^0$ and $x$ for the experiments on the binary gas mixtures in Group B (the binary gas mixtures without available thermodynamic data in the NIST REFPROP software)

| Carrier Gas | | Dry Air |
|---|---|---|
| Solute | | Acetone, methyl ethyl ketone, ethyl acetate, methanol, ethanol, isopropanol, dichloromethane, chloroform, 1,2-dichloromethane, m-xylene, o-xylene, p-xylene, ethylbenzene, n-butylamine, limonene and α-pinene. |
| Carrier Gas Density $\rho^0$ | EoS used | Van der Waals EoS |
| | Method | Use the Van der Waals EoS to determine the density ($\rho^0$) at the zero-step $T_{DVS}$ and $P$ of a gas mixture (regarded as dry air) comprising $N_2$, $O_2$, Ar and $CO_2$ with mole fractions of 0.780796, 0.209461, 0.009339 and 0.000404 respectively (coupling factors all assumed to be zero, see Section 2.2.2.2). |

| | | |
|---|---|---|
| Gas Composition $x$ (Mole Fraction of the Solute) | EoS used | Van der Waals EoS |
| | Method | Solve for the composition of a gas mixture comprising the solute, $N_2$, $O_2$, Ar and $CO_2$ with mole fractions of $x$, 0.780796(1-$x$), 0.209461(1-$x$), 0.009339(1-$x$) and 0.000404(1-$x$) respectively (i.e. a binary gas mixture comprising the solute and dry air with mole fractions of $x$ and (1-$x$) respectively) according to the Van der Waals EoS when the temperature, pressure and density are equal to the non-zero-step $T_{DVS}$, $P$ and $\rho$ (coupling factors all assumed to be zero). |
| Comments | | The Van der Waals EoS is utilised for mathematical convenience and ease of obtaining model parameters. The data for critical temperature $T_c$ and critical pressure $P_c$ used to determine the model parameters $a$ and $b$ are given in the appendix (see Table 61). |

## 3.9 Materials

The suppliers and purities of the materials used in this research project (except dry air) are given in Table 14.

For distinguishing the dry air used in this research project from the standard dry air (U.S. Standard Atmosphere, 1976), the former can be called the experimental dry air which was obtained from dehydrating the atmosphere air and had a dew point < -50 °C (nominal 0% relative humidity, residual water content negligible). The difference in composition between the standard and experimental dry air primarily resulted from the variation of $CO_2$ mole fraction.

In the standard dry air the mole fraction of $CO_2$ is 314 ppm, whilst for the experimental dry air the number was considered to be 404 ppm according to the data reported by the Earth System Research Laboratory corresponding to the period of this research project (Ed Dlugokencky & Pieter Tans, NOAA/ESRL [*Online*]). The method for the calculation of the real gas SoS of the standard dry air can be found in Zuckerwar (2002), and the real gas SoS of the experimental dry air which was used for the pathlength calibration of the SoS sensor was determined based on this method but with a correction for the difference in $CO_2$ mole fraction.

For the experiments on binary gas mixtures with the experimental dry air as the carrier gas component, in the calculation of the carrier gas density and the mixture composition using equation of state analysis, for simplicity the experimental dry air was treated as a gas mixture only comprising $N_2$, $O_2$, Ar and $CO_2$ with respective mole fractions of 0.780796, 0.209461, 0.009339 and 0.000404. There is no need to take into account the other constituents of dry air because of their low mole fractions. It is noteworthy that the mole fraction ratios between $N_2$ and $O_2$, $N_2$ and Ar, $O_2$ and Ar are the same as those in the standard dry air; and since these ratios in the experimental dry air should reasonably approximate those in the standard dry air,

the simplified experimental dry air should be a valid simulation of the true experimental dry air.

The presence of impurities in the materials used, the difference between the true mole fraction of $CO_2$ in the experimental dry air and the estimated number, and the simplification of the experimental dry air in the calculation of gas density and composition could all introduce errors into the experimental results. However, in comparison with the reported uncertainties of the results, these errors were considered to be insignificant and thus negligible.

Table 14. Suppliers and purities of materials

| | Materials | Suppliers | Purities |
|---|---|---|---|
| Liquids | n-Hexane | Sigma-Aldrich | ≥ 99% |
| | n-Heptane | Sigma-Aldrich | ≥ 99% |
| | n-Octane | Sigma-Aldrich | ≥ 99.0% |
| | n-Nonane | Sigma-Aldrich | ≥ 99% |
| | n-Decane | Sigma-Aldrich | ≥ 99% |
| | Toluene | Sigma-Aldrich | ≥ 99.9% |
| | Cyclohexane | Fisher Chemical | ≥ 99.99% |
| | Water | Fisher Chemical | HPLC fluorescence grade |
| | Acetone | Sigma-Aldrich | ≥ 99.8% |
| | Methyl ethyl ketone | Sigma-Aldrich | ≥ 99.5% |
| | Ethyl acetate | Sigma-Aldrich | ≥ 99.7% |
| | Methanol | Sigma-Aldrich | ≥ 99.9% |
| | Ethanol | Sigma-Aldrich | ≥ 99.8% |
| | Isopropanol | Sigma-Aldrich | ≥ 99.9% |
| | Dichloromethane | Sigma-Aldrich | ≥ 99.8% |
| | Chloroform | Sigma-Aldrich | ≥ 99.8% |
| | 1,2-Dichloroethane | Sigma-Aldrich | ≥ 99.8% |
| | m-Xylene | Sigma-Aldrich | ≥ 99.0% |
| | o-Xylene | Acros Organics | ≥ 99% |
| | p-Xylene | Sigma-Aldrich | ≥ 99% |
| | Ethylbenzene | Sigma-Aldrich | ≥ 99.8% |
| | n-Butylamine | Sigma-Aldrich | ≥ 99.5% |
| | Limonene | Fluka Chemika | ≥ 99.0% |
| | α-Pinene | Sigma-Aldrich | ≥ 98% |

| | | | |
|---|---|---|---|
| Gases | Nitrogen | BOC | ≥ 99.998% |
| | Carbon dioxide | BOC | ≥ 99.995% |
| | Argon | Ryval Gas | ≥ 99.998% |
| | Helium | BOC | ≥ 99.999% |
| Notes<br>The saturated vapour pressure of the liquids can be found from Table 62 in the appendix. | | | |

## 3.10 Pathlength Calibration

Precise pathlength calibration is needed before using the SoS sensor. During the first zero step of each experiment a pure carrier gas (dry air or $N_2$) with known real gas SoS was used, therefore, in theory the pathlength could be determined from the corresponding measured ToF and correction factor according to Equation (68). However, it was found in practice that to determine the correction factor accurately was extremely difficult, hence, for simplicity, in both the pathlength calibration and the following SoS measurements the correction factors were equated to zero. The equation used to calibrate the pathlength becomes:

$$L' = W^0 \times t_m^0 \tag{82}$$

where $L'$ represents the calibrated pathlength, $W^0$ the carrier gas real gas SoS at the operating acoustic frequency of the SoS sensor $f$ (121362 Hz) and at the first-zero-step $T_{SoS}$ and $P$, and $t_m^0$ the first-zero-step measured ToF. Then, with $L'$, the measured SoS $W_m$ corresponding to each non-zero step can be obtained from:

$$W_m = \frac{L'}{t_m}. \tag{83}$$

The pathlength was calibrated and assumed constant in each experiment on binary gas mixtures which was performed under atmospheric pressure and at nominally isothermal conditions. The effect of atmospheric pressure variation on pathlength should be negligible. Besides, the effect of temperature variation on pathlength can also be ignored and this was demonstrated by experiments as discussed in Section 5.1. Therefore, the assumption of a constant pathlength in each of the experiments is valid.

# CHAPTER 4. Results

## 4.1 Typical Raw Experimental Data for Mass Readings and Measured ToF

A typical set of raw experimental data for mass readings and measured ToF in the experiments on the binary gas mixtures other than $CO_2/N_2$ are shown in Figure 31. Since the density of the vapour (n-heptane) is higher than that of the carrier gas (dry air), as $x_T$ (target mole fraction of vapour component) increases, the density of the gas system should increase. According to Equation (80), $\rho^{II} > \rho^{I}$, thus $m_{read}^{II} < m_{read}^{I}$, i.e. the mass reading should decrease. It can also be found that in this experiment the measured ToF increases with the increasing $x_T$ level, which means as the mole fraction of the vapour component increases the measured SoS in the gas system decreases. This figure also shows for higher $x_T$ steps the mass reading increased slowly and the measured ToF decreased slowly with time, or both of the two series of data tend towards lower $x_T$ level. This is mainly because during the period of a higher $x_T$ step the evaporation rate of the liquid in the reservoir is higher and the heat transfer rate from the surrounding environment to the reservoir is lower than the heat absorption rate of the evaporation process, thus the temperature in the reservoir decreases slowly leading to a reduction in the saturated vapour pressure, i.e. although $x_T$ remains the same the mole fraction of the vapour component in the gas system reduces. This phenomenon is generally more significant if the liquid in the reservoir is more volatile (higher experimental temperatures; more volatile species).

A typical set of raw experimental data for mass readings and measured ToF in the experiments for $CO_2/N_2$ are displayed in Figure 32. Similar to Figure 31, the mass reading also decreases with the increasing $x_T$ level due to the higher density of $CO_2$ than that of $N_2$ which is the carrier gas; and the measured ToF (SoS) increases (decreases) with the increasing $x_T$ level as well. These experiments were not associated with any evaporation effects.

A drift in the mass reading baseline ($x_T = 0$) can be observed in each of the above two figures and this is predominantly caused by the variation of atmospheric pressure. ± 1 mbar change in pressure could result in a mass reading baseline drift of approximately ± 15 μg. Typically, the variation of atmospheric pressure during the period of one experiment did not exceed 11 mbar.

If the gas composition remains constant, SoS (ToF) should be much more sensitive to the temperature variation (typically within ± 0.1 °C) than to the pressure variation in one experiment.

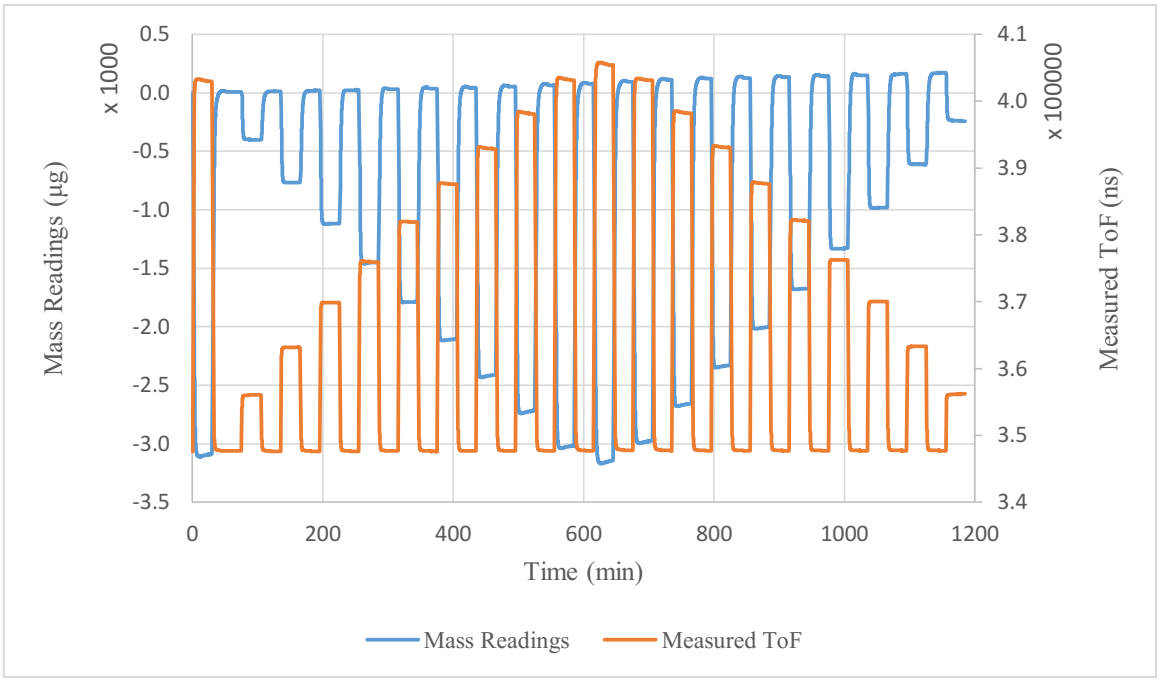



Figure 31. Raw experimental data for mass readings and measured ToF (n-heptane/dry air at 35 °C)

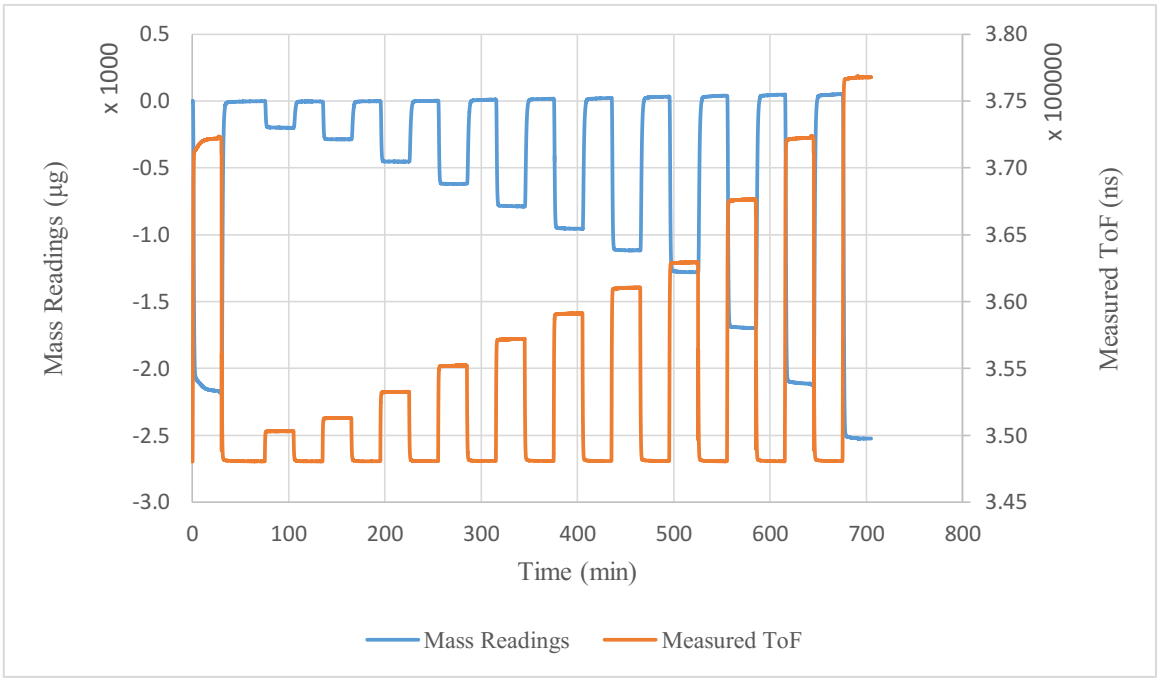



Figure 32. Raw experimental data for mass readings and measured ToF (carbon dioxide/nitrogen at 25 °C)

## 4.2 Representation of the Experimental Results

The results for an experiment on binary gas mixtures given in this thesis include the DVS temperature $T_{DVS}$ (°C), SoS temperature $T_{SoS}$ (°C), pressure $P$ (mbar), measured ToF $t_m$ (ns), gas density $\rho$ (kg/m$^3$), gas composition $x$ (dimensionless, the mole fraction of the non-carrier gas component or the solute) and measured SoS $W_m$ (m/s) corresponding to each non-zero step (under 'Non-Zero Step' in the result tables); the $T_{DVS}$ (°C), $P$ (mbar) and gas density $\rho^0$ (kg/m$^3$) corresponding to the adjacent zero step preceding each non-zero step (under 'Zero Step' in the result tables); and the difference in mass reading between the non-zero step and the preceding adjacent zero step $\Delta m_{read}$ (μg). The data corresponding to the first zero step used for pathlength calibration are given at the bottom of each result table including the $T_{SoS}$ (°C), $P$ (mbar, the same as the $P$ in the first row of data under 'Zero Step'), measured ToF $t_m^0$ (ns) and carrier gas real gas SoS $W^0$ (m/s). For an experiment with procedure consisting of an ascending half and a descending half as shown in Figure 29, if the non-zero step belongs in the former then the row of data in the result table is labelled with 'A'; while if the non-zero step belongs in the latter then the row of data is labelled with 'D' (the row corresponding to the peak step is not labelled). The data of $T_{DVS}$, $T_{SoS}$, $P$ and $t_m$ ($t_m^0$) in the result tables are all displayed up to the limits of their respective measurement resolutions. The data of $\Delta m_{read}$ are displayed up to the limit of the resolution of the DVS microbalance.

## 4.3 Experimental Results

The results for the experiments on n-heptane/dry air and $CO_2/N_2$ at different experimental temperatures are shown in Tables 15 to 20 and Tables 21 to 26, respectively. The experimental results for the other binary gas mixtures can be found in Appendix A6. Since the SoS sensor has a fixed acoustic frequency, the real gas SoS for a binary gas mixture under test should only vary with temperature, pressure and gas composition. During each experiment, the change in gas composition was the predominant reason for the measured SoS variation between different $x_T$ levels. The plots of $W_m$ versus $x$ for the experiments on each type of binary gas mixture at different isotherms, including the pathlength calibration points ($W_m = W^0, x = 0$), are given in Figures 33 to 57. It can be found that for these binary gas mixtures at atmospheric pressure and acoustic frequency of 121362 Hz, the SoS should increase as the temperature increases at constant composition; and except for the water/dry air binary gas mixture, the SoS should

decrease as the mole fraction of the non-carrier gas component increases at constant temperature (water/dry air has the opposite trend). It can also be seen from the figures for the binary gas mixtures other than $CO_2/N_2$ the molar composition variation range at a higher temperature is wider than that at a lower temperature. This is because at different experimental temperatures but the same $x_T$ level the mole fraction of the vapour component in the binary gas mixture under test increases with increasing saturated vapour pressure which is higher at higher temperatures.

Table 15. n-Heptane/dry air results (5 °C isotherm)

| $x_T$/%SAT | | Zero Step | | | $\Delta m_{read}$/µg | Non-Zero Step | | | | | | |
|---|---|---|---|---|---|---|---|---|---|---|---|---|
| | | $T_{DVS}$/°C | $P$/mbar | $\rho^0$/(kg/m$^3$) | | $T_{DVS}$/°C | $T_{SoS}$/°C | $P$/mbar | $t_m$/ns | $\rho$/(kg/m$^3$) | $x$ | $W_m$/(m/s) |
| 10 | A | 4.42 | 1018.36 | 1.2788 | 100 | 4.44 | 4.1556 | 1019.12 | 368230 | 1.2865 | 0.0021 | 332.61 |
| | D | 4.52 | 1024.97 | 1.2867 | 82 | 4.54 | 4.2756 | 1024.82 | 368145 | 1.2929 | 0.0021 | 332.68 |
| 20 | A | 4.49 | 1019.29 | 1.2797 | 173 | 4.45 | 4.1834 | 1019.58 | 369694 | 1.2930 | 0.0040 | 331.29 |
| | D | 4.50 | 1025.02 | 1.2868 | 165 | 4.52 | 4.2513 | 1024.94 | 369647 | 1.2995 | 0.0040 | 331.33 |
| 30 | A | 4.42 | 1019.78 | 1.2806 | 249 | 4.43 | 4.1537 | 1020.07 | 371162 | 1.2997 | 0.0059 | 329.98 |
| | D | 4.45 | 1025.08 | 1.2871 | 243 | 4.51 | 4.2286 | 1025.01 | 371116 | 1.3057 | 0.0060 | 330.02 |
| 40 | A | 4.41 | 1020.19 | 1.2811 | 326 | 4.43 | 4.1514 | 1020.42 | 372569 | 1.3061 | 0.0078 | 328.73 |
| | D | 4.43 | 1024.74 | 1.2868 | 324 | 4.43 | 4.1681 | 1024.92 | 372543 | 1.3116 | 0.0077 | 328.76 |
| 50 | A | 4.42 | 1020.94 | 1.2821 | 406 | 4.43 | 4.1578 | 1021.36 | 373948 | 1.3132 | 0.0097 | 327.52 |
| | D | 4.45 | 1024.47 | 1.2864 | 398 | 4.46 | 4.2017 | 1024.54 | 373918 | 1.3169 | 0.0096 | 327.55 |
| 60 | A | 4.43 | 1021.98 | 1.2833 | 479 | 4.44 | 4.1657 | 1022.41 | 375302 | 1.3201 | 0.0114 | 326.34 |
| | D | 4.42 | 1024.12 | 1.2861 | 475 | 4.50 | 4.2080 | 1024.31 | 375300 | 1.3224 | 0.0115 | 326.34 |
| 70 | A | 4.43 | 1022.60 | 1.2841 | 556 | 4.43 | 4.1630 | 1022.89 | 376655 | 1.3267 | 0.0133 | 325.17 |
| | D | 4.46 | 1023.80 | 1.2855 | 555 | 4.44 | 4.1774 | 1024.04 | 376645 | 1.3280 | 0.0133 | 325.18 |
| 80 | A | 4.43 | 1022.97 | 1.2846 | 629 | 4.44 | 4.1708 | 1023.13 | 377999 | 1.3328 | 0.0151 | 324.01 |
| | D | 4.42 | 1023.80 | 1.2857 | 624 | 4.43 | 4.1642 | 1023.78 | 377993 | 1.3335 | 0.0151 | 324.02 |
| 90 | A | 4.42 | 1023.28 | 1.2850 | 702 | 4.43 | 4.1642 | 1023.33 | 379344 | 1.3388 | 0.0169 | 322.86 |
| | D | 4.50 | 1023.60 | 1.2851 | 706 | 4.45 | 4.2053 | 1023.73 | 379334 | 1.3392 | 0.0169 | 322.87 |
| 95 | | 4.45 | 1023.45 | 1.2851 | 741 | 4.51 | 4.2207 | 1023.53 | 379987 | 1.3419 | 0.0179 | 322.32 |
| Data used for pathlength calibration (the first zero step): $T_{SoS}$ = 4.1372 °C, $P$ = 1018.36 mbar, $t_m^0$ = 366645 ns, $W^0$ = 334.04 m/s. | | | | | | | | | | | | |

Table 16. n-Heptane/dry air results (15 °C isotherm)

| $x_T$/%SAT | | Zero Step | | | $\Delta m_{read}$/µg | Non-Zero Step | | | | | | |
|---|---|---|---|---|---|---|---|---|---|---|---|---|
| | | $T_{DVS}$/°C | $P$/mbar | $\rho^0$/(kg/m$^3$) | | $T_{DVS}$/°C | $T_{SoS}$/°C | $P$/mbar | $t_m$/ns | $\rho$/(kg/m$^3$) | $x$ | $W_m$/(m/s) |
| 10 | A | 14.43 | 1006.28 | 1.2195 | 152 | 14.41 | 14.0690 | 1006.49 | 362921 | 1.2312 | 0.0038 | 337.26 |
| | D | 14.42 | 1015.82 | 1.2311 | 153 | 14.43 | 14.0752 | 1016.17 | 362866 | 1.2429 | 0.0037 | 337.31 |
| 20 | A | 14.40 | 1006.14 | 1.2195 | 277 | 14.43 | 14.0591 | 1006.02 | 365575 | 1.2407 | 0.0071 | 334.81 |
| | D | 14.43 | 1015.06 | 1.2302 | 293 | 14.44 | 14.0867 | 1015.49 | 365497 | 1.2526 | 0.0072 | 334.88 |
| 30 | A | 14.39 | 1006.30 | 1.2197 | 437 | 14.41 | 14.0478 | 1007.28 | 368115 | 1.2532 | 0.0107 | 332.50 |
| | D | 14.44 | 1014.52 | 1.2295 | 427 | 14.43 | 14.0806 | 1014.80 | 368037 | 1.2622 | 0.0106 | 332.57 |
| 40 | A | 14.40 | 1007.06 | 1.2206 | 554 | 14.41 | 14.0539 | 1007.10 | 370560 | 1.2631 | 0.0141 | 330.31 |
| | D | 14.37 | 1014.05 | 1.2292 | 556 | 14.44 | 14.0685 | 1014.32 | 370496 | 1.2718 | 0.0140 | 330.36 |
| 50 | A | 14.40 | 1007.20 | 1.2208 | 686 | 14.41 | 14.0559 | 1007.47 | 372949 | 1.2733 | 0.0173 | 328.19 |
| | D | 14.38 | 1013.33 | 1.2283 | 686 | 14.37 | 14.0220 | 1013.76 | 372863 | 1.2809 | 0.0171 | 328.27 |
| 60 | A | 14.40 | 1007.70 | 1.2214 | 815 | 14.40 | 14.0456 | 1007.83 | 375265 | 1.2838 | 0.0206 | 326.16 |
| | D | 14.44 | 1012.74 | 1.2273 | 819 | 14.45 | 14.0954 | 1013.06 | 375216 | 1.2901 | 0.0206 | 326.21 |
| 70 | A | 14.37 | 1008.11 | 1.2220 | 944 | 14.40 | 14.0382 | 1008.55 | 377555 | 1.2943 | 0.0238 | 324.19 |
| | D | 14.43 | 1012.27 | 1.2268 | 945 | 14.40 | 14.0597 | 1012.61 | 377505 | 1.2992 | 0.0237 | 324.23 |
| 80 | A | 14.38 | 1009.14 | 1.2232 | 1075 | 14.39 | 14.0336 | 1009.61 | 379815 | 1.3056 | 0.0271 | 322.26 |
| | D | 14.44 | 1011.85 | 1.2262 | 1075 | 14.43 | 14.0632 | 1012.20 | 379793 | 1.3086 | 0.0270 | 322.27 |
| 90 | A | 14.39 | 1010.16 | 1.2244 | 1201 | 14.39 | 14.0354 | 1010.58 | 382047 | 1.3165 | 0.0302 | 320.37 |
| | D | 14.42 | 1011.21 | 1.2256 | 1199 | 14.38 | 14.0445 | 1011.53 | 382028 | 1.3175 | 0.0301 | 320.39 |
| 95 | | 14.44 | 1010.76 | 1.2249 | 1262 | 14.44 | 14.0854 | 1010.90 | 383157 | 1.3216 | 0.0319 | 319.45 |
| Data used for pathlength calibration (the first zero step): $T_{SoS}$ = 14.0746 °C, $P$ = 1006.28 mbar, $t_m^0$ = 360002 ns, $W^0$ = 339.99 m/s. | | | | | | | | | | | | |

Table 17. n-Heptane/dry air results (25 °C isotherm)

| $x_T$/%SAT | | Zero Step | | | $\Delta m_{read}$/µg | Non-Zero Step | | | | | | |
|---|---|---|---|---|---|---|---|---|---|---|---|---|
| | | $T_{DVS}$/°C | $P$/mbar | $\rho^0$/(kg/m$^3$) | | $T_{DVS}$/°C | $T_{SoS}$/°C | $P$/mbar | $t_m$/ns | $\rho$/(kg/m$^3$) | $x$ | $W_m$/(m/s) |
| 5 | A | 24.94 | 1025.25 | 1.1986 | 136 | 24.95 | 24.5803 | 1025.04 | 356587 | 1.2090 | 0.0036 | 343.52 |
| | D | 24.83 | 1024.47 | 1.1981 | 130 | 24.83 | 24.4151 | 1024.24 | 356633 | 1.2081 | 0.0035 | 343.48 |
| 10 | A | 24.95 | 1024.91 | 1.1982 | 258 | 24.93 | 24.5772 | 1024.87 | 358949 | 1.2180 | 0.0067 | 341.26 |
| | D | 24.85 | 1024.89 | 1.1986 | 251 | 24.84 | 24.4297 | 1024.65 | 358959 | 1.2178 | 0.0066 | 341.25 |
| 15 | A | 24.84 | 1024.72 | 1.1984 | 369 | 24.82 | 24.4708 | 1024.66 | 361222 | 1.2267 | 0.0096 | 339.12 |
| | D | 24.85 | 1025.11 | 1.1988 | 367 | 24.85 | 24.4410 | 1025.04 | 361199 | 1.2269 | 0.0095 | 339.14 |
| 20 | A | 24.80 | 1024.88 | 1.1987 | 491 | 24.81 | 24.4431 | 1025.32 | 363419 | 1.2364 | 0.0125 | 337.07 |
| | D | 24.86 | 1025.14 | 1.1988 | 483 | 24.85 | 24.4544 | 1025.12 | 363377 | 1.2358 | 0.0125 | 337.10 |
| 25 | A | 24.90 | 1025.65 | 1.1992 | 611 | 24.96 | 24.5609 | 1025.89 | 365552 | 1.2460 | 0.0158 | 335.10 |
| | D | 24.89 | 1025.09 | 1.1986 | 602 | 24.89 | 24.4875 | 1025.14 | 365507 | 1.2447 | 0.0156 | 335.14 |
| 30 | A | 24.95 | 1026.13 | 1.1996 | 719 | 24.96 | 24.5836 | 1026.30 | 367607 | 1.2547 | 0.0185 | 333.23 |
| | D | 24.91 | 1024.96 | 1.1984 | 714 | 24.91 | 24.5071 | 1024.99 | 367599 | 1.2531 | 0.0185 | 333.23 |
| 35 | A | 24.93 | 1026.39 | 1.2000 | 826 | 24.93 | 24.5594 | 1026.45 | 369600 | 1.2633 | 0.0213 | 331.43 |
| | D | 24.93 | 1024.78 | 1.1981 | 823 | 24.92 | 24.5235 | 1024.85 | 369628 | 1.2612 | 0.0213 | 331.40 |
| 40 | A | 24.91 | 1026.44 | 1.2001 | 936 | 24.91 | 24.5381 | 1026.67 | 371568 | 1.2718 | 0.0241 | 329.67 |
| | D | 24.84 | 1024.52 | 1.1982 | 934 | 24.94 | 24.5114 | 1024.61 | 371640 | 1.2697 | 0.0243 | 329.61 |
| 45 | A | 24.92 | 1026.77 | 1.2004 | 1043 | 24.93 | 24.5502 | 1026.84 | 373530 | 1.2804 | 0.0269 | 327.94 |
| | D | 24.92 | 1024.26 | 1.1975 | 1040 | 24.85 | 24.4823 | 1024.33 | 373539 | 1.2772 | 0.0268 | 327.93 |
| 50 | A | 24.84 | 1027.10 | 1.2012 | 1141 | 24.83 | 24.4670 | 1027.10 | 375390 | 1.2886 | 0.0294 | 326.32 |
| | D | 24.96 | 1024.46 | 1.1976 | 1154 | 24.95 | 24.5590 | 1024.26 | 375516 | 1.2860 | 0.0299 | 326.21 |
| 55 | A | 24.81 | 1027.17 | 1.2014 | 1249 | 24.80 | 24.4316 | 1027.09 | 377248 | 1.2971 | 0.0323 | 324.71 |
| | D | 24.86 | 1024.88 | 1.1985 | 1250 | 24.92 | 24.5054 | 1024.75 | 377365 | 1.2943 | 0.0325 | 324.61 |
| 60 | A | 24.79 | 1027.00 | 1.2013 | 1352 | 24.80 | 24.4197 | 1026.87 | 379094 | 1.3049 | 0.0350 | 323.13 |
| | D | 24.97 | 1025.32 | 1.1986 | 1360 | 24.92 | 24.5555 | 1025.10 | 379182 | 1.3027 | 0.0352 | 323.05 |

| | | | | | | | | | | | | |
|---|---|---|---|---|---|---|---|---|---|---|---|---|
| 65 | A | 24.80 | 1026.70 | 1.2009 | 1457 | 24.80 | 24.4123 | 1026.70 | 380902 | 1.3125 | 0.0376 | 321.59 |
| | D | 24.96 | 1025.92 | 1.1993 | 1463 | 24.97 | 24.5769 | 1025.59 | 381026 | 1.3114 | 0.0380 | 321.49 |
| 70 | A | 24.86 | 1026.64 | 1.2006 | 1572 | 24.90 | 24.4890 | 1026.71 | 382815 | 1.3210 | 0.0406 | 319.99 |
| | D | 24.97 | 1026.44 | 1.1999 | 1569 | 24.97 | 24.5816 | 1026.24 | 382831 | 1.3201 | 0.0406 | 319.97 |
| 75 | A | 24.90 | 1026.70 | 1.2004 | 1679 | 24.91 | 24.5211 | 1026.84 | 384600 | 1.3291 | 0.0433 | 318.50 |
| | D | 25.01 | 1027.04 | 1.2004 | 1680 | 25.00 | 24.6135 | 1026.76 | 384656 | 1.3291 | 0.0435 | 318.46 |
| 80 | A | 24.91 | 1026.85 | 1.2006 | 1784 | 24.91 | 24.5235 | 1026.87 | 386357 | 1.3373 | 0.0460 | 317.05 |
| | D | 24.96 | 1027.24 | 1.2008 | 1779 | 24.99 | 24.5943 | 1027.16 | 386358 | 1.3372 | 0.0460 | 317.05 |
| 85 | A | 24.90 | 1026.86 | 1.2006 | 1888 | 24.93 | 24.5303 | 1026.95 | 388127 | 1.3453 | 0.0487 | 315.61 |
| | D | 24.94 | 1027.60 | 1.2013 | 1883 | 24.95 | 24.5566 | 1027.42 | 388106 | 1.3456 | 0.0487 | 315.63 |
| 90 | A | 24.92 | 1027.06 | 1.2008 | 1991 | 24.85 | 24.4931 | 1027.27 | 389783 | 1.3534 | 0.0512 | 314.27 |
| | D | 24.91 | 1027.50 | 1.2013 | 1990 | 24.94 | 24.5338 | 1027.59 | 389846 | 1.3538 | 0.0513 | 314.22 |
| 95 | | 24.86 | 1027.34 | 1.2014 | 2093 | 24.91 | 24.5006 | 1027.51 | 391525 | 1.3618 | 0.0540 | 312.87 |
| Data used for pathlength calibration (the first zero step): $T_{SOS}$ = 24.5641 °C, $P$ = 1025.25 mbar, $t_m^0$ = 353871 ns, $W^0$ = 346.16 m/s. | | | | | | | | | | | | |

Table 18. n-Heptane/dry air results (35 °C isotherm)

| $x_T$/%SAT | | Zero Step | | | $\Delta m_{read}$/µg | Non-Zero Step | | | | | | |
|---|---|---|---|---|---|---|---|---|---|---|---|---|
| | | $T_{DVS}$/°C | $P$/mbar | $\rho^0$/(kg/m$^3$) | | $T_{DVS}$/°C | $T_{SoS}$/°C | $P$/mbar | $t_m$/ns | $\rho$/(kg/m$^3$) | $x$ | $W_m$/(m/s) |
| 10 | A | 34.61 | 1010.33 | 1.1440 | 410 | 34.65 | 34.2570 | 1010.19 | 356050 | 1.1754 | 0.0113 | 343.44 |
| | D | 34.53 | 999.87 | 1.1324 | 417 | 34.56 | 34.1699 | 999.96 | 356198 | 1.1643 | 0.0114 | 343.30 |
| 20 | A | 34.62 | 1010.06 | 1.1436 | 781 | 34.63 | 34.2464 | 1009.86 | 363182 | 1.2034 | 0.0213 | 336.69 |
| | D | 34.54 | 1000.42 | 1.1330 | 773 | 34.56 | 34.1696 | 1000.10 | 363320 | 1.1922 | 0.0213 | 336.57 |
| 30 | A | 34.64 | 1009.74 | 1.1432 | 1140 | 34.65 | 34.2577 | 1009.55 | 369824 | 1.2305 | 0.0310 | 330.65 |
| | D | 34.54 | 1001.02 | 1.1337 | 1132 | 34.55 | 34.1728 | 1000.79 | 369994 | 1.2204 | 0.0311 | 330.50 |
| 40 | A | 34.62 | 1009.32 | 1.1428 | 1474 | 34.58 | 34.1936 | 1009.17 | 375916 | 1.2557 | 0.0400 | 325.29 |
| | D | 34.55 | 1001.53 | 1.1342 | 1472 | 34.56 | 34.1894 | 1001.16 | 376206 | 1.2470 | 0.0404 | 325.04 |
| 50 | A | 34.61 | 1009.14 | 1.1426 | 1814 | 34.65 | 34.2523 | 1008.85 | 381916 | 1.2816 | 0.0494 | 320.18 |
| | D | 34.54 | 1002.08 | 1.1348 | 1809 | 34.56 | 34.1974 | 1001.82 | 382089 | 1.2734 | 0.0496 | 320.03 |
| 60 | A | 34.65 | 1008.56 | 1.1418 | 2143 | 34.70 | 34.3014 | 1008.20 | 387574 | 1.3060 | 0.0584 | 315.50 |
| | D | 34.56 | 1002.55 | 1.1353 | 2132 | 34.55 | 34.1912 | 1002.30 | 387631 | 1.2987 | 0.0583 | 315.46 |
| 70 | A | 34.61 | 1008.08 | 1.1414 | 2457 | 34.61 | 34.2370 | 1007.71 | 392863 | 1.3297 | 0.0669 | 311.26 |
| | D | 34.56 | 1002.94 | 1.1358 | 2452 | 34.57 | 34.2040 | 1002.56 | 393036 | 1.3237 | 0.0671 | 311.12 |
| 80 | A | 34.59 | 1007.48 | 1.1408 | 2768 | 34.62 | 34.2320 | 1006.87 | 398064 | 1.3529 | 0.0755 | 307.19 |
| | D | 34.55 | 1003.68 | 1.1366 | 2769 | 34.56 | 34.1977 | 1003.42 | 398175 | 1.3488 | 0.0756 | 307.10 |
| 90 | A | 34.61 | 1006.58 | 1.1397 | 3084 | 34.63 | 34.2437 | 1006.10 | 403143 | 1.3760 | 0.0841 | 303.32 |
| | D | 34.50 | 1004.68 | 1.1379 | 3070 | 34.55 | 34.1802 | 1004.10 | 403122 | 1.3732 | 0.0839 | 303.34 |
| 95 | | 34.60 | 1005.69 | 1.1387 | 3221 | 34.54 | 34.1785 | 1005.28 | 405332 | 1.3855 | 0.0877 | 301.68 |
| Data used for pathlength calibration (the first zero step): $T_{SoS}$ = 34.2200 °C, $P$ = 1010.33 mbar, $t_m^0$ = 347650 ns, $W^0$ = 351.74 m/s. | | | | | | | | | | | | |

Table 19. n-Heptane/dry air results (45 °C isotherm)

| $x_T$/%SAT | | Zero Step | | | $\Delta m_{read}$/µg | Non-Zero Step | | | | | | |
|---|---|---|---|---|---|---|---|---|---|---|---|---|
| | | $T_{DVS}$/°C | $P$/mbar | $\rho^0$/(kg/m³) | | $T_{DVS}$/°C | $T_{SoS}$/°C | $P$/mbar | $t_m$/ns | $\rho$/(kg/m³) | $x$ | $W_m$/(m/s) |
| 10 | A | 43.97 | 1012.31 | 1.1123 | 641 | 43.98 | 43.6313 | 1012.22 | 355368 | 1.1614 | 0.0179 | 343.85 |
| | D | N/A | N/A | N/A | N/A | N/A | N/A | N/A | N/A | N/A | N/A | N/A |
| 20 | A | 43.94 | 1012.34 | 1.1124 | 1210 | 43.94 | 43.6163 | 1012.31 | 366113 | 1.2051 | 0.0338 | 333.76 |
| | D | N/A | N/A | N/A | N/A | N/A | N/A | N/A | N/A | N/A | N/A | N/A |
| 30 | A | 43.96 | 1012.37 | 1.1124 | 1748 | 43.91 | 43.6000 | 1012.52 | 375807 | 1.2464 | 0.0486 | 325.15 |
| | D | N/A | N/A | N/A | N/A | N/A | N/A | N/A | N/A | N/A | N/A | N/A |
| 40 | A | 43.91 | 1012.82 | 1.1131 | 2256 | 43.91 | 43.5567 | 1013.07 | 384618 | 1.2860 | 0.0627 | 317.70 |
| | D | 43.99 | 1013.12 | 1.1131 | 2264 | 43.97 | 43.6527 | 1013.27 | 384646 | 1.2866 | 0.0630 | 317.68 |
| 50 | A | 43.96 | 1013.43 | 1.1135 | 2759 | 44.04 | 43.6275 | 1013.75 | 392956 | 1.3250 | 0.0768 | 310.96 |
| | D | 43.92 | 1012.91 | 1.1131 | 2755 | 44.00 | 43.6479 | 1012.93 | 392934 | 1.3242 | 0.0768 | 310.98 |
| 60 | A | 44.05 | 1013.78 | 1.1136 | 3237 | 44.02 | 43.6667 | 1013.88 | 400604 | 1.3617 | 0.0900 | 305.02 |
| | D | 43.95 | 1013.12 | 1.1132 | 3219 | 43.95 | 43.6263 | 1012.99 | 400515 | 1.3599 | 0.0897 | 305.09 |
| 70 | A | 43.99 | 1014.02 | 1.1141 | 3694 | 44.05 | 43.6665 | 1013.83 | 407877 | 1.3971 | 0.1029 | 299.58 |
| | D | 43.96 | 1012.90 | 1.1130 | 3685 | 43.96 | 43.6255 | 1013.06 | 407725 | 1.3954 | 0.1025 | 299.69 |
| 80 | A | 44.05 | 1013.91 | 1.1137 | 4150 | 43.99 | 43.6541 | 1013.90 | 414719 | 1.4318 | 0.1153 | 294.64 |
| | D | 43.99 | 1013.04 | 1.1130 | 4137 | 43.96 | 43.6334 | 1012.95 | 414680 | 1.4300 | 0.1151 | 294.67 |
| 90 | A | 44.03 | 1013.70 | 1.1136 | 4592 | 43.98 | 43.6455 | 1013.56 | 421290 | 1.4655 | 0.1276 | 290.04 |
| | D | 43.98 | 1013.37 | 1.1134 | 4594 | 44.03 | 43.6820 | 1013.07 | 421420 | 1.4654 | 0.1279 | 289.95 |
| 95 | | 43.96 | 1013.43 | 1.1135 | 4802 | 43.97 | 43.6213 | 1013.45 | 424387 | 1.4815 | 0.1334 | 287.93 |
| Data used for pathlength calibration (the first zero step): $T_{SoS}$ = 43.6231 °C, $P$ = 1012.31 mbar, $t_m^0$ = 342196 ns, $W^0$ = 357.08 m/s. | | | | | | | | | | | | |

Table 20. n-Heptane/dry air results (55 °C isotherm)

| $x_T$/%SAT | | Zero Step | | | $\Delta m_{read}$/µg | Non-Zero Step | | | | | | |
|---|---|---|---|---|---|---|---|---|---|---|---|---|
| | | $T_{DVS}$/°C | $P$/mbar | $\rho^0$/(kg/m$^3$) | | $T_{DVS}$/°C | $T_{SoS}$/°C | $P$/mbar | $t_m$/ns | $\rho$/(kg/m$^3$) | $x$ | $W_m$/(m/s) |
| 10 | A | 53.77 | 993.43 | 1.0587 | 1022 | 53.78 | 53.4511 | 993.41 | 358124 | 1.1371 | 0.0300 | 340.97 |
| | D | 53.75 | 997.34 | 1.0630 | 1021 | 53.77 | 53.4374 | 997.39 | 357974 | 1.1412 | 0.0298 | 341.11 |
| 20 | A | 53.77 | 993.62 | 1.0589 | 1898 | 53.78 | 53.4473 | 993.71 | 374429 | 1.2043 | 0.0556 | 326.12 |
| | D | 53.73 | 997.45 | 1.0632 | 1887 | 53.76 | 53.4381 | 997.46 | 374144 | 1.2078 | 0.0551 | 326.37 |
| 30 | A | 53.76 | 994.09 | 1.0595 | 2701 | 53.74 | 53.4119 | 994.27 | 388391 | 1.2665 | 0.0789 | 314.39 |
| | D | 53.75 | 997.24 | 1.0629 | 2693 | 53.76 | 53.4438 | 997.35 | 388095 | 1.2692 | 0.0785 | 314.63 |
| 40 | A | 53.75 | 994.51 | 1.0600 | 3465 | 53.78 | 53.4647 | 994.68 | 400821 | 1.3255 | 0.1013 | 304.65 |
| | D | 53.76 | 996.98 | 1.0625 | 3445 | 53.75 | 53.4470 | 997.02 | 400401 | 1.3265 | 0.1004 | 304.96 |
| 50 | A | 53.77 | 994.87 | 1.0603 | 4176 | 53.77 | 53.4578 | 995.22 | 411928 | 1.3803 | 0.1218 | 296.43 |
| | D | 53.73 | 996.54 | 1.0622 | 4137 | 53.75 | 53.4300 | 996.84 | 411431 | 1.3792 | 0.1205 | 296.79 |
| 60 | A | 53.76 | 995.52 | 1.0610 | 4838 | 53.73 | 53.4346 | 995.88 | 421884 | 1.4317 | 0.1409 | 289.44 |
| | D | 53.77 | 996.22 | 1.0617 | 4814 | 53.74 | 53.4209 | 996.46 | 421562 | 1.4306 | 0.1402 | 289.66 |
| 70 | A | 53.73 | 996.10 | 1.0617 | 5475 | 53.75 | 53.4255 | 996.12 | 431229 | 1.4813 | 0.1596 | 283.16 |
| | D | 53.80 | 995.91 | 1.0613 | 5468 | 53.79 | 53.4733 | 996.08 | 431094 | 1.4803 | 0.1593 | 283.25 |
| 80 | A | 53.75 | 996.21 | 1.0618 | 6094 | 53.75 | 53.4206 | 996.18 | 439986 | 1.5288 | 0.1775 | 277.53 |
| | D | 53.78 | 996.02 | 1.0615 | 6085 | 53.79 | 53.4773 | 995.98 | 439880 | 1.5278 | 0.1773 | 277.59 |
| 90 | A | 53.73 | 996.31 | 1.0619 | 6657 | 53.71 | 53.3800 | 996.27 | 447819 | 1.5721 | 0.1937 | 272.67 |
| | D | 53.79 | 996.20 | 1.0616 | 6681 | 53.78 | 53.4772 | 996.19 | 448071 | 1.5736 | 0.1944 | 272.52 |
| 95 | | 53.77 | 996.21 | 1.0617 | 6969 | 53.78 | 53.4673 | 996.18 | 451970 | 1.5958 | 0.2028 | 270.17 |
| Data used for pathlength calibration (the first zero step): $T_{SoS}$ = 53.4591 °C, $P$ = 993.43 mbar, $t_m^0$ = 336768 ns, $W^0$ = 362.59 m/s. | | | | | | | | | | | | |

Table 21. Carbon dioxide/nitrogen results (10 °C isotherm)

| $x_T$ | Zero Step | | | $\Delta m_{read}$/µg | Non-Zero Step | | | | | | |
|---|---|---|---|---|---|---|---|---|---|---|---|
| | $T_{DVS}$/°C | $P$/mbar | $\rho^0$/(kg/m$^3$) | | $T_{DVS}$/°C | $T_{SoS}$/°C | $P$/mbar | $t_m$/ns | $\rho$/(kg/m$^3$) | $x$ | $W_m$/(m/s) |
| 0.02 | 9.33 | 1010.82 | 1.20606 | 206 | 9.34 | 8.9964 | 1010.85 | 359773 | 1.2218 | 0.0228 | 340.28 |
| 0.03 | 9.37 | 1011.08 | 1.20619 | 298 | 9.36 | 9.0211 | 1011.15 | 360718 | 1.2290 | 0.0327 | 339.39 |
| 0.05 | 9.33 | 1011.37 | 1.20670 | 484 | 9.34 | 8.9966 | 1011.70 | 362783 | 1.2438 | 0.0529 | 337.46 |
| 0.07 | 9.33 | 1011.82 | 1.20725 | 659 | 9.33 | 8.9868 | 1011.86 | 364796 | 1.2577 | 0.0726 | 335.59 |
| 0.09 | 9.33 | 1011.83 | 1.20726 | 843 | 9.33 | 8.9925 | 1011.78 | 366840 | 1.2719 | 0.0932 | 333.72 |
| 0.11 | 9.31 | 1011.89 | 1.20742 | 1023 | 9.31 | 8.9722 | 1011.89 | 368822 | 1.2858 | 0.1129 | 331.93 |
| 0.13 | 9.37 | 1011.90 | 1.20717 | 1204 | 9.41 | 9.0510 | 1011.81 | 370737 | 1.2994 | 0.1333 | 330.22 |
| 0.15 | 9.40 | 1011.81 | 1.20693 | 1389 | 9.40 | 9.0620 | 1011.93 | 372710 | 1.3134 | 0.1531 | 328.47 |
| 0.20 | 9.37 | 1011.79 | 1.20703 | 1834 | 9.33 | 9.0102 | 1011.66 | 377582 | 1.3476 | 0.2023 | 324.23 |
| 0.25 | 9.35 | 1011.62 | 1.20691 | 2279 | 9.38 | 9.0329 | 1011.61 | 382291 | 1.3816 | 0.2516 | 320.24 |
| 0.30 | 9.35 | 1011.62 | 1.20693 | 2719 | 9.39 | 9.0509 | 1011.67 | 386898 | 1.4153 | 0.3000 | 316.42 |
| Data used for pathlength calibration (the first zero step): $T_{SoS}$ = 9.0126 °C, $P$ = 1010.82 mbar, $t_m^0$ = 357428 ns, $W^0$ = 342.51 m/s. | | | | | | | | | | | |

Table 22. Carbon dioxide/nitrogen results (20 °C isotherm)

| $x_T$ | Zero Step | | | $\Delta m_{read}$/µg | Non-Zero Step | | | | | | |
|---|---|---|---|---|---|---|---|---|---|---|---|
| | $T_{DVS}$/°C | $P$/mbar | $\rho^0$/(kg/m$^3$) | | $T_{DVS}$/°C | $T_{SoS}$/°C | $P$/mbar | $t_m$/ns | $\rho$/(kg/m$^3$) | $x$ | $W_m$/(m/s) |
| 0.02 | 19.34 | 1008.20 | 1.16164 | 200 | 19.36 | 18.9675 | 1008.23 | 353319 | 1.1770 | 0.0230 | 346.28 |
| 0.03 | 19.34 | 1008.22 | 1.16165 | 286 | 19.34 | 18.9537 | 1008.25 | 354336 | 1.1836 | 0.0328 | 345.29 |
| 0.05 | 19.34 | 1008.13 | 1.16157 | 461 | 19.35 | 18.9487 | 1008.20 | 356291 | 1.1969 | 0.0529 | 343.39 |
| 0.07 | 19.35 | 1007.98 | 1.16136 | 635 | 19.34 | 18.9472 | 1007.89 | 358267 | 1.2100 | 0.0730 | 341.50 |
| 0.09 | 19.33 | 1007.96 | 1.16139 | 809 | 19.34 | 18.9466 | 1007.81 | 360273 | 1.2234 | 0.0932 | 339.60 |
| 0.11 | 19.34 | 1007.67 | 1.16104 | 985 | 19.35 | 18.9468 | 1007.64 | 362211 | 1.2365 | 0.1132 | 337.78 |
| 0.13 | 19.33 | 1007.55 | 1.16093 | 1158 | 19.34 | 18.9435 | 1007.53 | 364157 | 1.2497 | 0.1331 | 335.98 |
| 0.15 | 19.33 | 1007.38 | 1.16074 | 1330 | 19.33 | 18.9394 | 1007.41 | 366077 | 1.2626 | 0.1527 | 334.21 |
| 0.20 | 19.31 | 1006.99 | 1.16036 | 1760 | 19.32 | 18.9244 | 1007.00 | 370832 | 1.2953 | 0.2022 | 329.93 |
| 0.25 | 19.32 | 1006.98 | 1.16031 | 2190 | 19.32 | 18.9224 | 1006.92 | 375476 | 1.3281 | 0.2515 | 325.85 |
| 0.30 | 19.32 | 1007.08 | 1.16043 | 2609 | 19.33 | 18.9226 | 1007.01 | 380044 | 1.3604 | 0.2996 | 321.93 |
| Data used for pathlength calibration (the first zero step): $T_{SoS}$ = 18.9559 °C, $P$ = 1008.20 mbar, $t_m^0$ = 351062 ns, $W^0$ = 348.51 m/s. | | | | | | | | | | | |

Table 23. Carbon dioxide/nitrogen results (25 °C isotherm)

| $x_T$ | Zero Step | | | $\Delta m_{read}$/µg | Non-Zero Step | | | | | | |
|---|---|---|---|---|---|---|---|---|---|---|---|
| | $T_{DVS}$/°C | $P$/mbar | $\rho^0$/(kg/m$^3$) | | $T_{DVS}$/°C | $T_{SoS}$/°C | $P$/mbar | $t_m$/ns | $\rho$/(kg/m$^3$) | $x$ | $W_m$/(m/s) |
| 0.02 | 24.30 | 1015.72 | 1.15073 | 199 | 24.31 | 23.8376 | 1015.81 | 350302 | 1.1660 | 0.0230 | 349.15 |
| 0.03 | 24.30 | 1015.93 | 1.15099 | 282 | 24.30 | 23.8279 | 1015.85 | 351295 | 1.1726 | 0.0329 | 348.17 |
| 0.05 | 24.28 | 1015.73 | 1.15084 | 452 | 24.28 | 23.8144 | 1015.52 | 353246 | 1.1855 | 0.0528 | 346.24 |
| 0.07 | 24.26 | 1015.45 | 1.15060 | 622 | 24.26 | 23.7945 | 1015.13 | 355212 | 1.1983 | 0.0727 | 344.33 |
| 0.09 | 24.26 | 1014.89 | 1.14996 | 801 | 24.26 | 23.7903 | 1014.73 | 357206 | 1.2113 | 0.0932 | 342.40 |
| 0.11 | 24.27 | 1014.56 | 1.14955 | 973 | 24.27 | 23.8022 | 1014.41 | 359119 | 1.2241 | 0.1131 | 340.58 |
| 0.13 | 24.27 | 1014.10 | 1.14903 | 1140 | 24.27 | 23.7949 | 1013.69 | 361047 | 1.2364 | 0.1330 | 338.76 |
| 0.15 | 24.28 | 1013.42 | 1.14822 | 1314 | 24.31 | 23.8331 | 1013.21 | 362937 | 1.2489 | 0.1532 | 337.00 |
| 0.20 | 24.31 | 1012.83 | 1.14743 | 1737 | 24.33 | 23.8489 | 1012.45 | 367635 | 1.2805 | 0.2026 | 332.69 |
| 0.25 | 24.31 | 1012.23 | 1.14675 | 2172 | 24.31 | 23.8374 | 1012.10 | 372286 | 1.3132 | 0.2526 | 328.53 |
| 0.30 | 24.30 | 1011.90 | 1.14642 | 2577 | 24.31 | 23.8298 | 1011.63 | 376782 | 1.3439 | 0.3001 | 324.61 |
| Data used for pathlength calibration (the first zero step): $T_{SoS}$ = 23.8359 °C, $P$ = 1015.72 mbar, $t_m^0$ = 348047 ns, $W^0$ = 351.41 m/s. | | | | | | | | | | | |

Table 24. Carbon dioxide/nitrogen results (30 °C isotherm)

| $x_T$ | Zero Step | | | $\Delta m_{read}$/µg | Non-Zero Step | | | | | | |
|---|---|---|---|---|---|---|---|---|---|---|---|
| | $T_{DVS}$/°C | $P$/mbar | $\rho^0$/(kg/m$^3$) | | $T_{DVS}$/°C | $T_{SoS}$/°C | $P$/mbar | $t_m$/ns | $\rho$/(kg/m$^3$) | $x$ | $W_m$/(m/s) |
| 0.02 | 29.38 | 1007.03 | 1.12169 | 197 | 29.39 | 28.9409 | 1007.30 | 347228 | 1.1368 | 0.0231 | 352.14 |
| 0.03 | 29.38 | 1007.55 | 1.12226 | 283 | 29.38 | 28.9418 | 1007.95 | 348184 | 1.1439 | 0.0329 | 351.18 |
| 0.05 | 29.39 | 1008.10 | 1.12286 | 449 | 29.35 | 28.8909 | 1008.29 | 350177 | 1.1573 | 0.0528 | 349.18 |
| 0.07 | 29.35 | 1008.63 | 1.12360 | 613 | 29.36 | 28.8998 | 1008.58 | 352099 | 1.1706 | 0.0730 | 347.27 |
| 0.09 | 29.39 | 1008.68 | 1.12348 | 790 | 29.38 | 28.9395 | 1008.67 | 354055 | 1.1840 | 0.0938 | 345.35 |
| 0.11 | 29.38 | 1008.65 | 1.12349 | 954 | 29.38 | 28.9426 | 1008.64 | 355951 | 1.1966 | 0.1133 | 343.51 |
| 0.13 | 29.39 | 1008.73 | 1.12356 | 1123 | 29.36 | 28.9209 | 1008.73 | 357879 | 1.2097 | 0.1332 | 341.66 |
| 0.15 | 29.37 | 1008.85 | 1.12378 | 1289 | 29.35 | 28.8948 | 1008.71 | 359802 | 1.2226 | 0.1531 | 339.84 |
| 0.20 | 29.35 | 1008.93 | 1.12393 | 1710 | 29.33 | 28.8791 | 1008.89 | 364479 | 1.2550 | 0.2029 | 335.48 |
| 0.25 | 29.34 | 1008.97 | 1.12401 | 2123 | 29.35 | 28.9001 | 1008.98 | 369015 | 1.2867 | 0.2518 | 331.35 |
| 0.30 | 29.37 | 1008.95 | 1.12387 | 2549 | 29.37 | 28.9256 | 1009.27 | 373630 | 1.3192 | 0.3016 | 327.26 |
| Data used for pathlength calibration (the first zero step): $T_{SoS}$ = 28.9297 °C, $P$ = 1007.03 mbar, $t_m^0$ = 344998 ns, $W^0$ = 354.42 m/s. | | | | | | | | | | | |

Table 25. Carbon dioxide/nitrogen results (40 °C isotherm)

| $x_T$ | Zero Step | | | $\Delta m_{read}$/µg | Non-Zero Step | | | | | | |
|---|---|---|---|---|---|---|---|---|---|---|---|
| | $T_{DVS}$/°C | $P$/mbar | $\rho^0$/(kg/m$^3$) | | $T_{DVS}$/°C | $T_{SoS}$/°C | $P$/mbar | $t_m$/ns | $\rho$/(kg/m$^3$) | $x$ | $W_m$/(m/s) |
| 0.02 | 39.07 | 1009.95 | 1.08997 | 191 | 38.96 | 38.6589 | 1009.92 | 341565 | 1.1046 | 0.0228 | 357.76 |
| 0.03 | 39.03 | 1009.89 | 1.09005 | 272 | 38.99 | 38.6960 | 1009.85 | 342501 | 1.1109 | 0.0331 | 356.78 |
| 0.05 | 39.04 | 1009.81 | 1.08992 | 438 | 38.96 | 38.6674 | 1009.95 | 344429 | 1.1235 | 0.0530 | 354.78 |
| 0.07 | 38.99 | 1009.94 | 1.09024 | 598 | 38.96 | 38.6482 | 1009.96 | 346343 | 1.1360 | 0.0730 | 352.82 |
| 0.09 | 38.99 | 1009.95 | 1.09025 | 761 | 39.02 | 38.6833 | 1009.82 | 348256 | 1.1486 | 0.0936 | 350.88 |
| 0.11 | 39.05 | 1009.93 | 1.09000 | 928 | 38.98 | 38.6700 | 1009.96 | 350119 | 1.1611 | 0.1132 | 349.02 |
| 0.13 | 39.00 | 1010.15 | 1.09042 | 1090 | 38.97 | 38.6498 | 1010.19 | 352002 | 1.1739 | 0.1331 | 347.15 |
| 0.15 | 39.01 | 1010.55 | 1.09082 | 1257 | 38.96 | 38.6473 | 1010.95 | 353856 | 1.1871 | 0.1527 | 345.33 |
| 0.20 | 39.13 | 1006.12 | 1.08562 | 1654 | 39.11 | 38.7517 | 1006.10 | 358491 | 1.2124 | 0.2032 | 340.90 |
| 0.25 | 39.15 | 1006.11 | 1.08552 | 2056 | 39.07 | 38.7512 | 1006.29 | 362953 | 1.2431 | 0.2517 | 336.71 |
| 0.30 | 39.06 | 1006.26 | 1.08602 | 2451 | 39.04 | 38.7159 | 1006.35 | 367414 | 1.2738 | 0.3006 | 332.62 |
| Data used for pathlength calibration (the first zero step): $T_{SoS}$ = 38.7353 °C, $P$ = 1009.95 mbar, $t_m^0$ = 339308 ns, $W^0$ = 360.14 m/s. | | | | | | | | | | | |

Table 26. Carbon dioxide/nitrogen results (50 °C isotherm)

| $x_T$ | Zero Step | | | $\Delta m_{read}$/µg | Non-Zero Step | | | | | | |
|---|---|---|---|---|---|---|---|---|---|---|---|
| | $T_{DVS}$/°C | $P$/mbar | $\rho^0$/(kg/m$^3$) | | $T_{DVS}$/°C | $T_{SoS}$/°C | $P$/mbar | $t_m$/ns | $\rho$/(kg/m$^3$) | $x$ | $W_m$/(m/s) |
| 0.02 | 48.85 | 1004.13 | 1.05069 | 181 | 48.86 | 48.4798 | 1003.90 | 336109 | 1.0645 | 0.0234 | 363.34 |
| 0.03 | 48.88 | 1003.89 | 1.05035 | 261 | 48.88 | 48.5111 | 1004.03 | 337015 | 1.0703 | 0.0329 | 362.36 |
| 0.05 | 48.89 | 1003.94 | 1.05037 | 426 | 48.81 | 48.4412 | 1004.36 | 338953 | 1.0830 | 0.0529 | 360.29 |
| 0.07 | 48.86 | 1004.31 | 1.05084 | 583 | 48.87 | 48.4992 | 1004.48 | 340801 | 1.0955 | 0.0739 | 358.34 |
| 0.09 | 48.87 | 1004.73 | 1.05125 | 737 | 48.84 | 48.4684 | 1004.67 | 342713 | 1.1077 | 0.0936 | 356.34 |
| 0.11 | 48.85 | 1004.56 | 1.05113 | 894 | 48.89 | 48.4954 | 1004.60 | 344565 | 1.1196 | 0.1137 | 354.42 |
| 0.13 | 48.90 | 1004.47 | 1.05088 | 1051 | 48.87 | 48.4855 | 1004.52 | 346381 | 1.1314 | 0.1333 | 352.56 |
| 0.15 | 48.85 | 1004.33 | 1.05090 | 1211 | 48.76 | 48.4064 | 1004.18 | 348330 | 1.1437 | 0.1536 | 350.59 |
| 0.20 | 48.77 | 1004.08 | 1.05090 | 1601 | 48.75 | 48.3778 | 1003.82 | 352863 | 1.1736 | 0.2038 | 346.09 |
| 0.25 | 48.75 | 1003.65 | 1.05051 | 1990 | 48.73 | 48.3508 | 1003.57 | 357314 | 1.2030 | 0.2528 | 341.78 |
| 0.30 | 48.72 | 1003.38 | 1.05033 | 2374 | 48.70 | 48.3032 | 1003.20 | 361687 | 1.2323 | 0.3017 | 337.64 |
| Data used for pathlength calibration (the first zero step): $T_{SoS}$ = 48.4636 °C, $P$ = 1004.13 mbar, $t_m^0$ = 333922 ns, $W^0$ = 365.72 m/s. | | | | | | | | | | | |

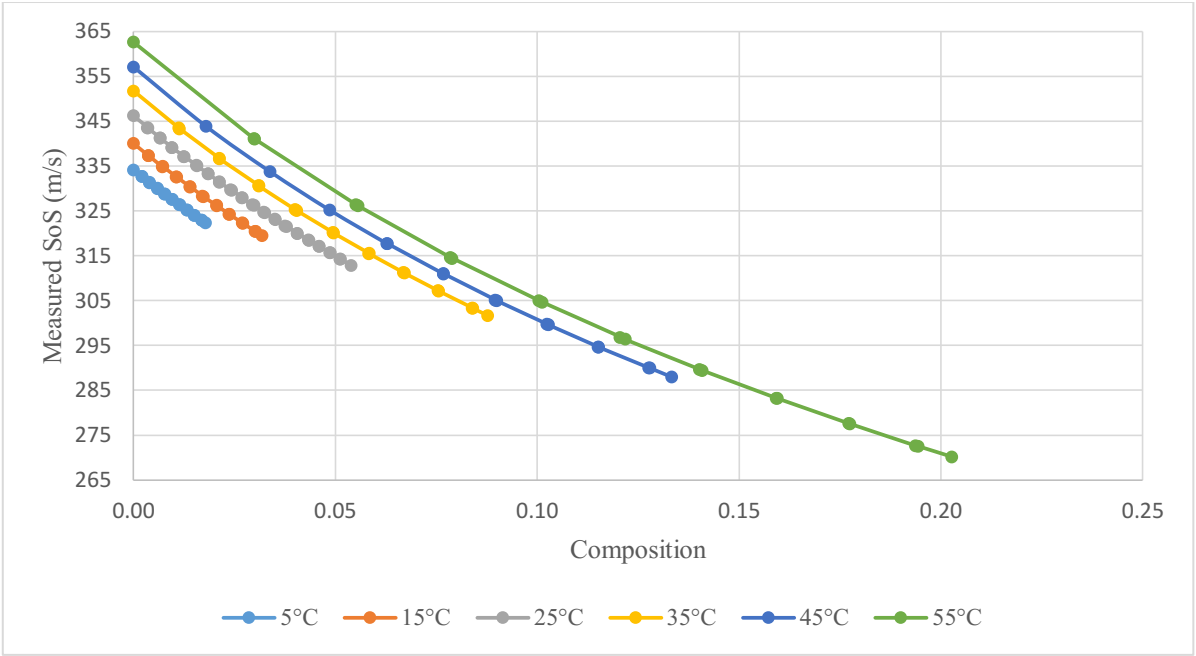



Figure 33. Measured SoS versus composition for n-heptane/dry air binary gas mixture

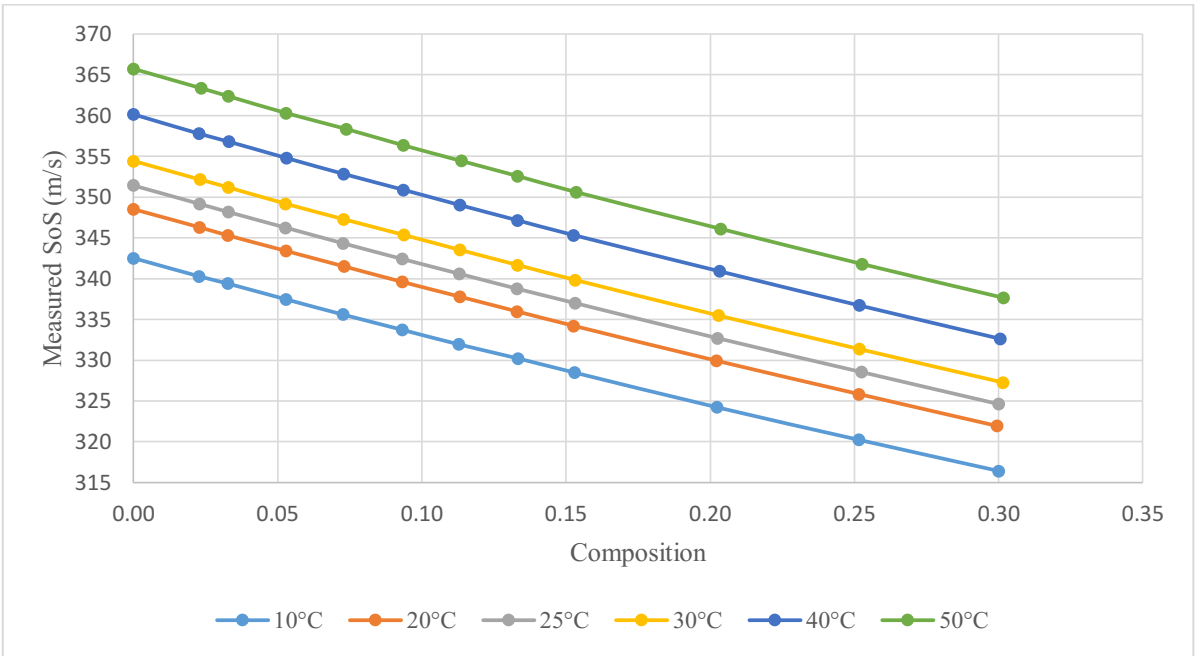



Figure 34. Measured SoS versus composition for carbon dioxide/nitrogen binary gas mixture

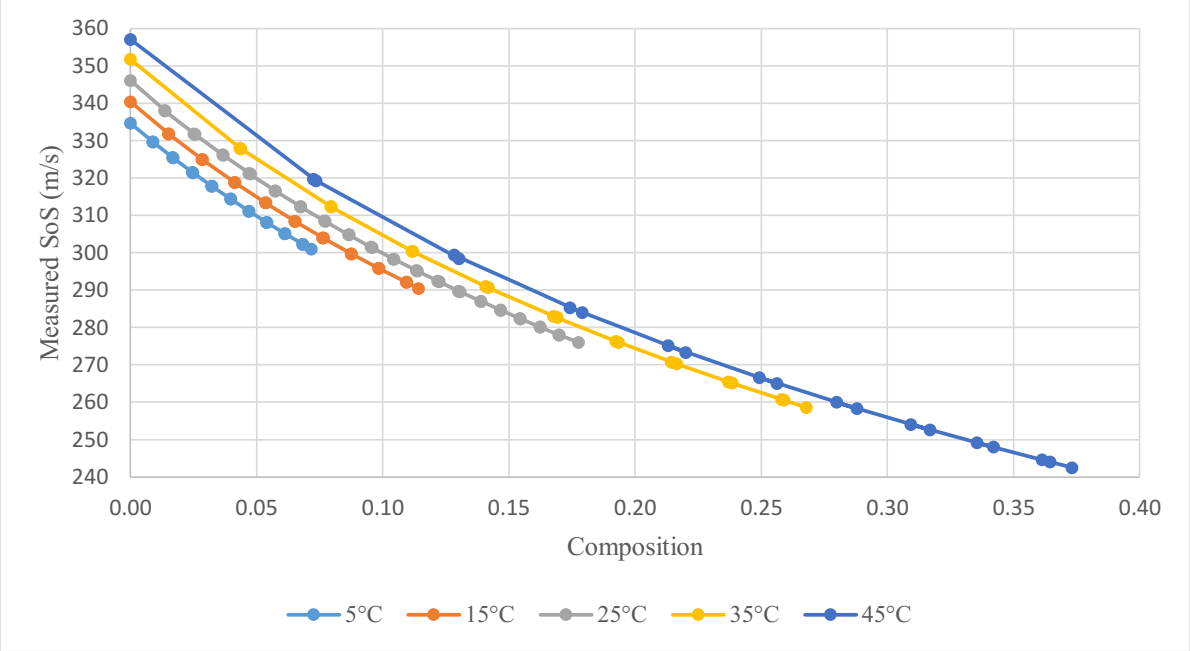



Figure 35. Measured SoS versus composition for n-hexane/dry air binary gas mixture

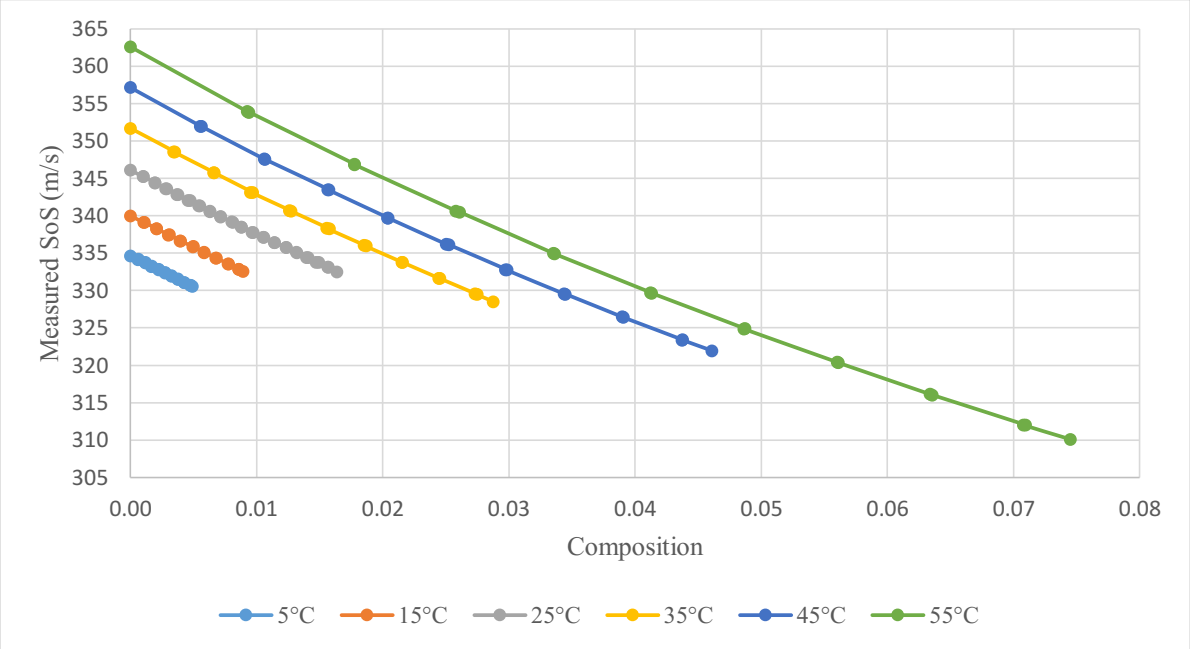



Figure 36. Measured SoS versus composition for n-octane/dry air binary gas mixture

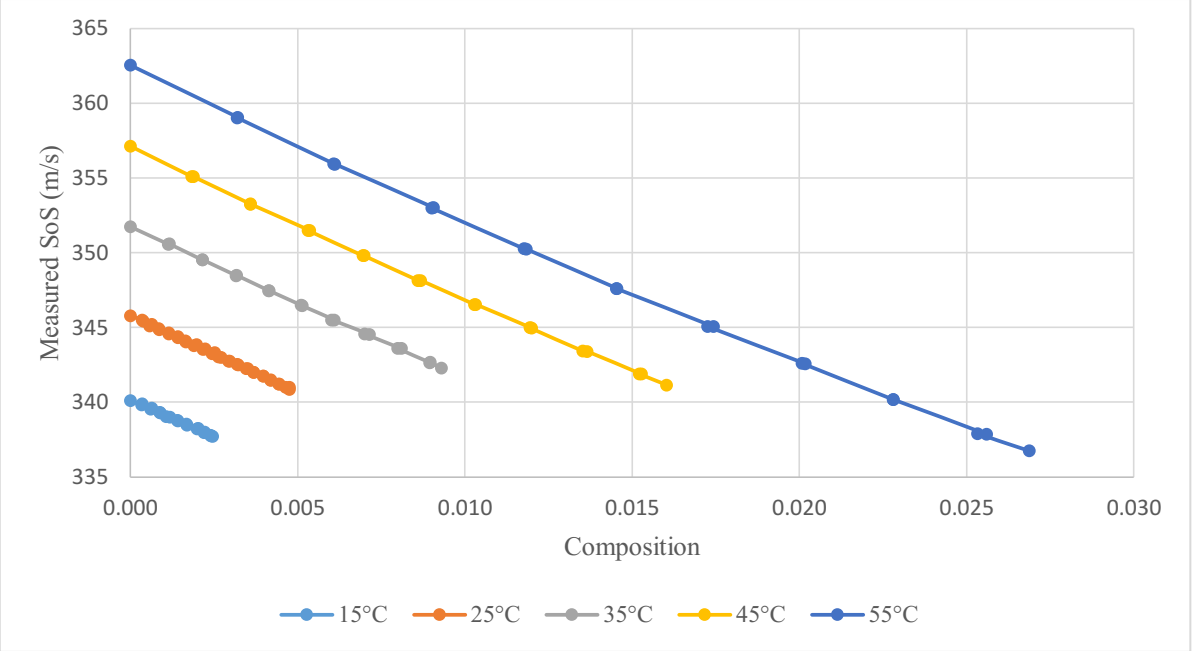



Figure 37. Measured SoS versus composition for n-nonane/dry air binary gas mixture

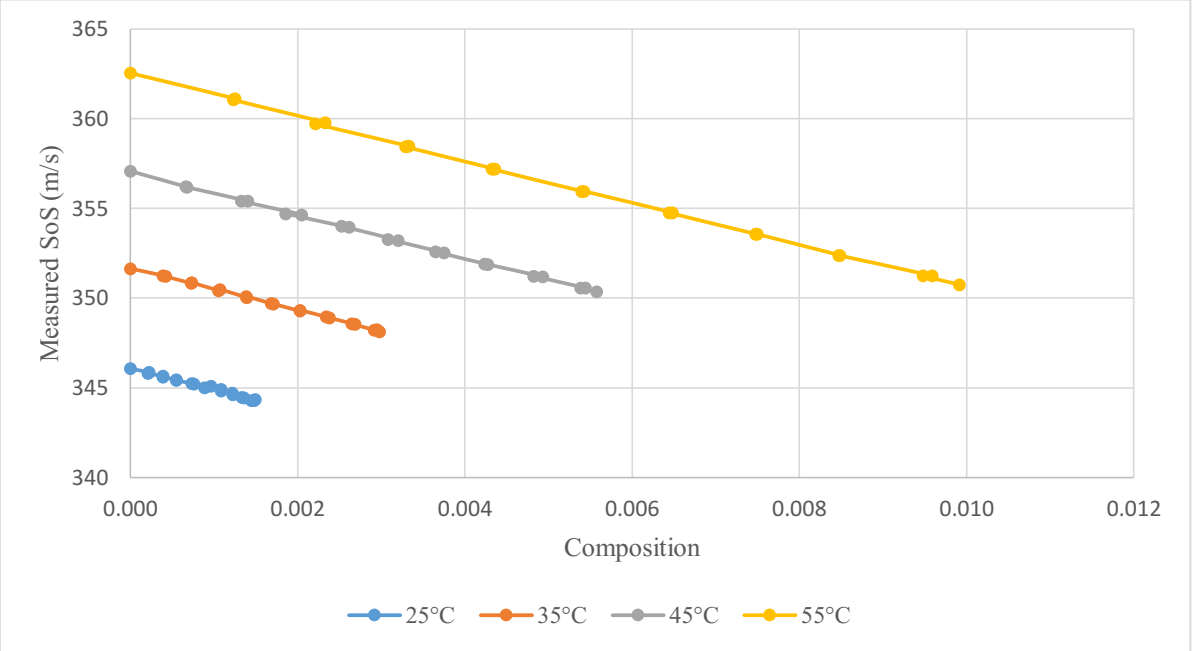



Figure 38. Measured SoS versus composition for n-decane/dry air binary gas mixture

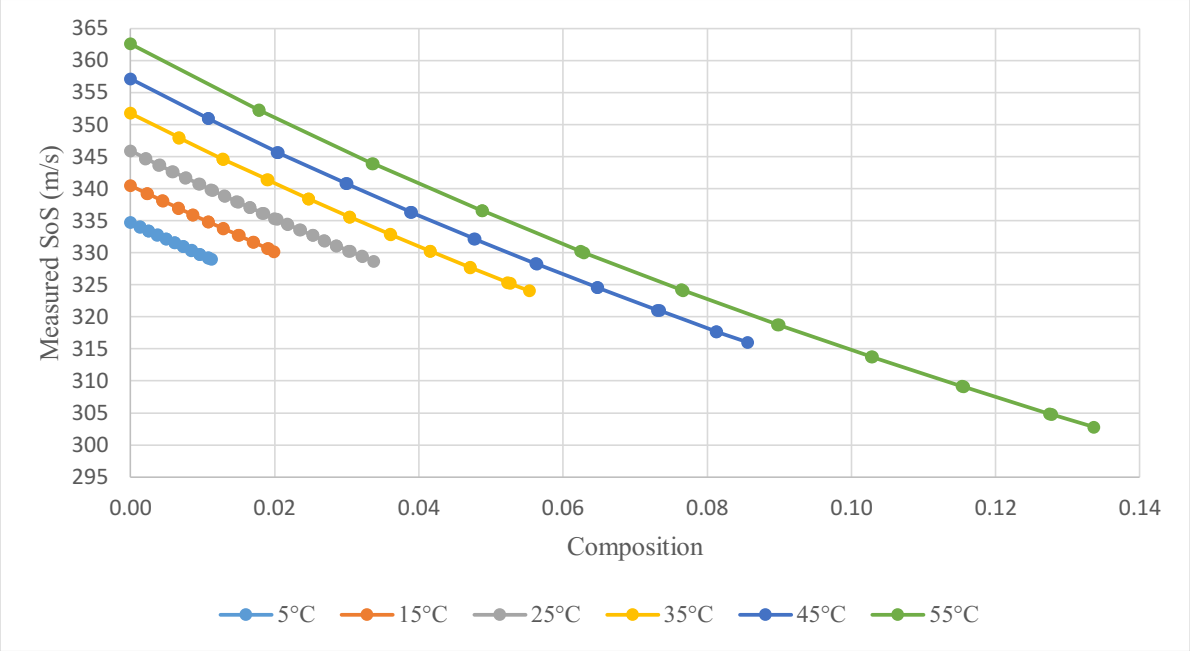



Figure 39. Measured SoS versus composition for toluene/dry air binary gas mixture

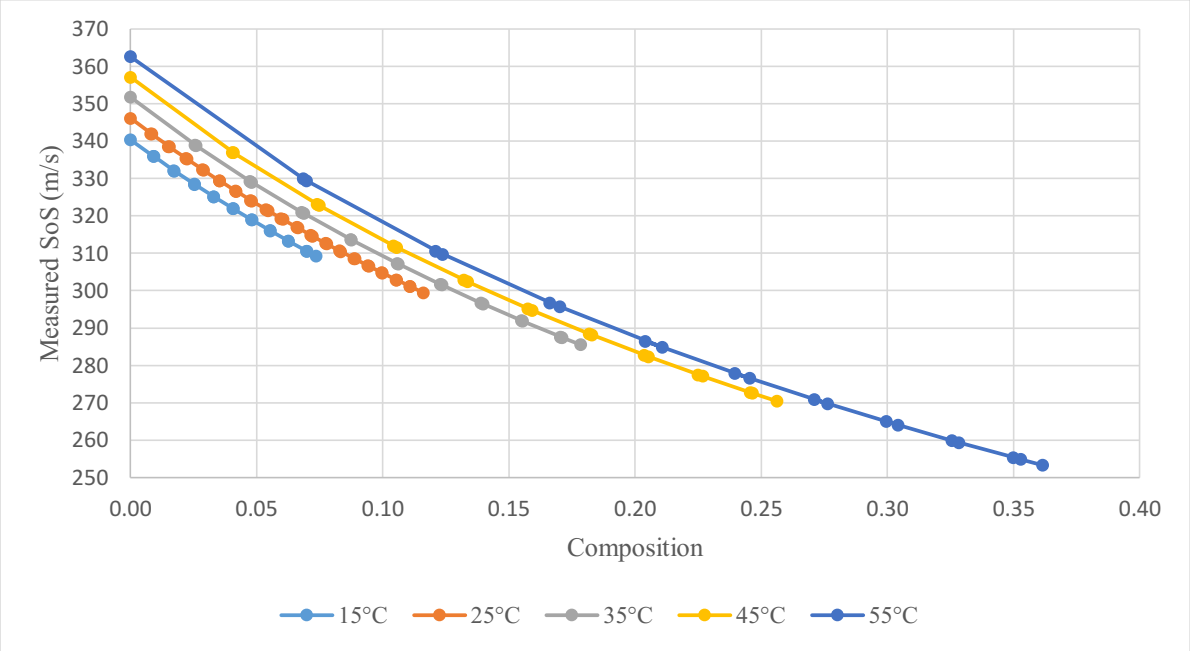



Figure 40. Measured SoS versus composition for cyclohexane/dry air binary gas mixture

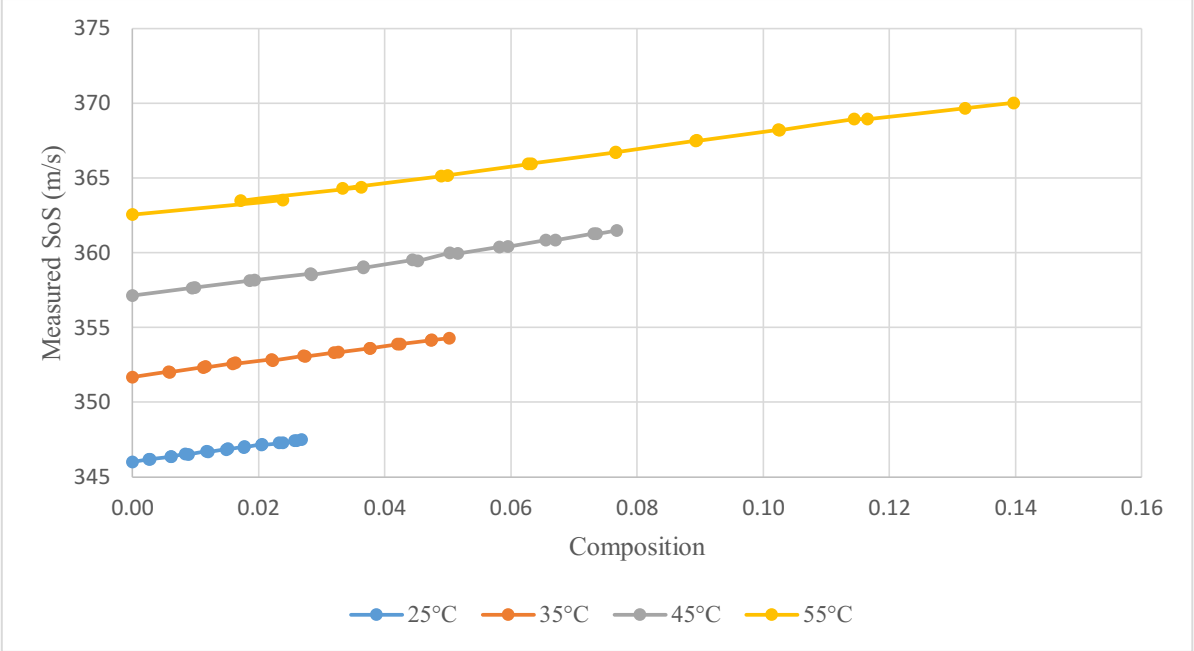



Figure 41. Measured SoS versus composition for water/dry air binary gas mixture

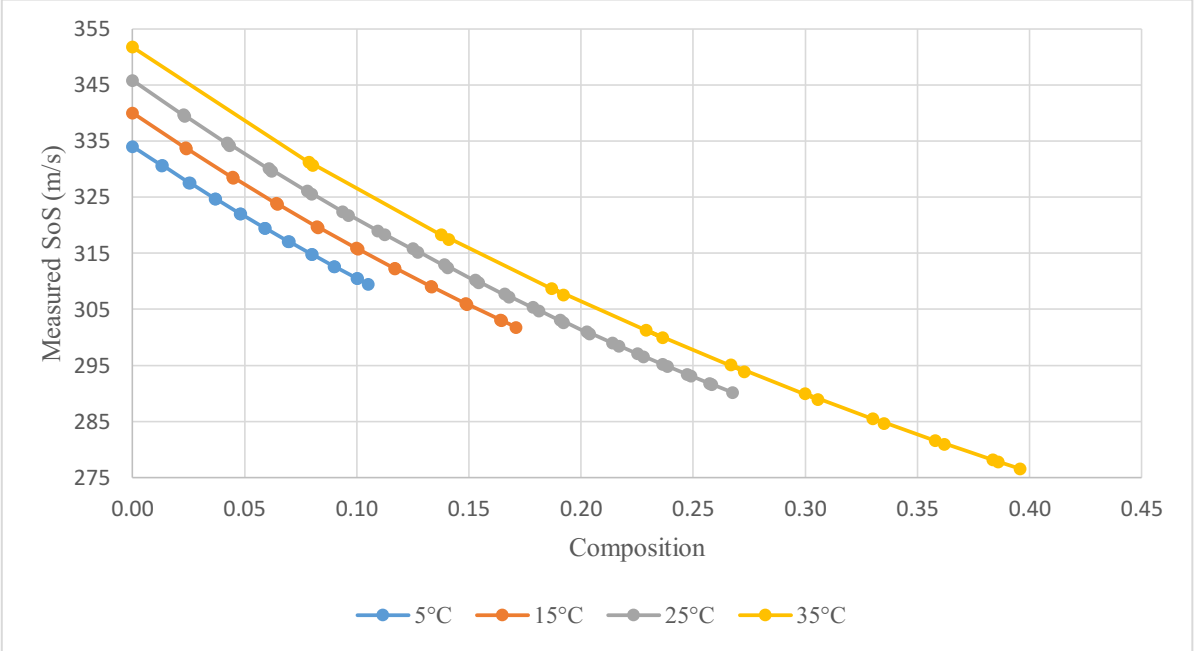



Figure 42. Measured SoS versus composition for acetone/dry air binary gas mixture

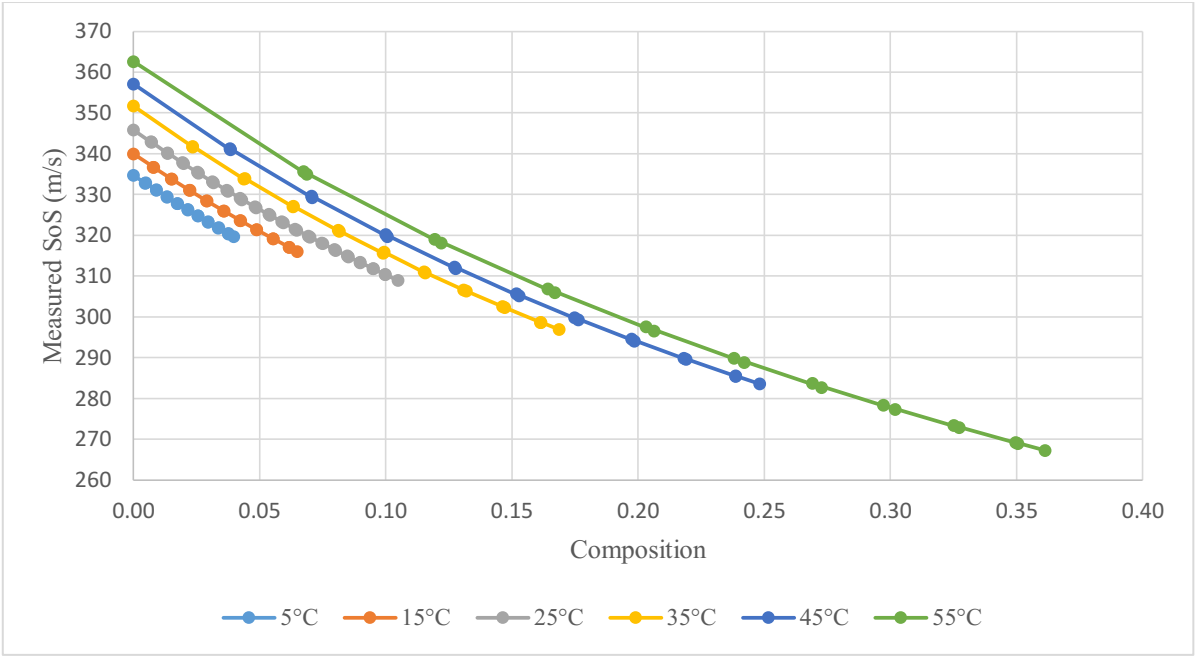



Figure 43. Measured SoS versus composition for methyl ethyl ketone/dry air binary gas mixture

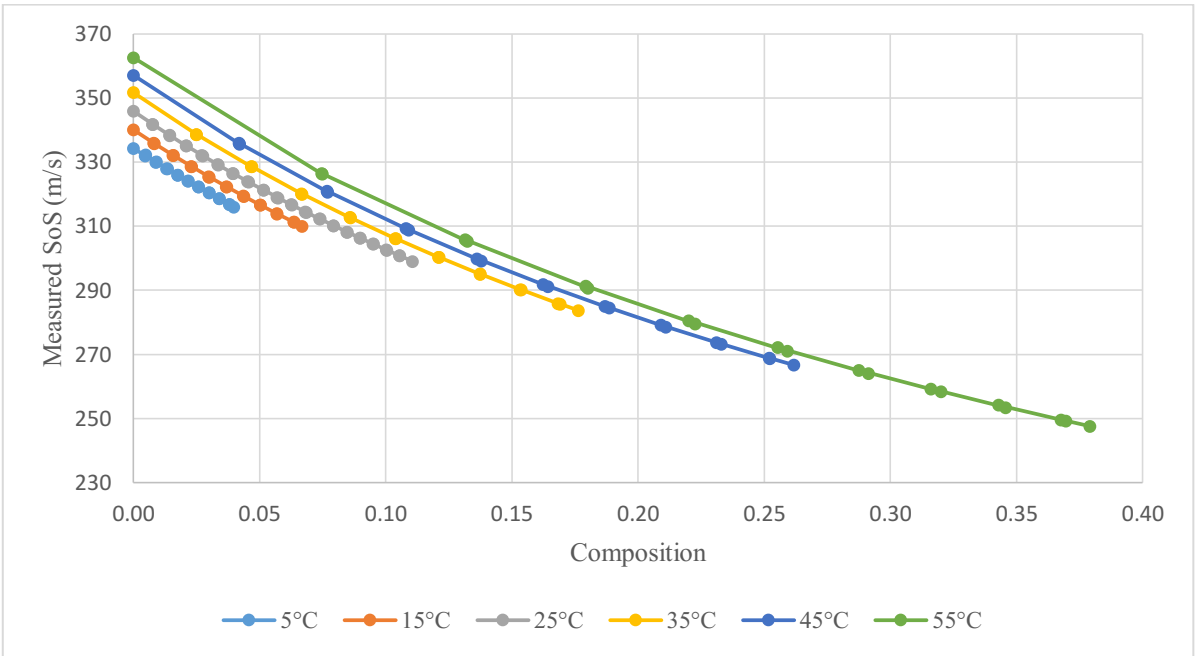



Figure 44. Measured SoS versus composition for ethyl acetate/dry air binary gas mixture

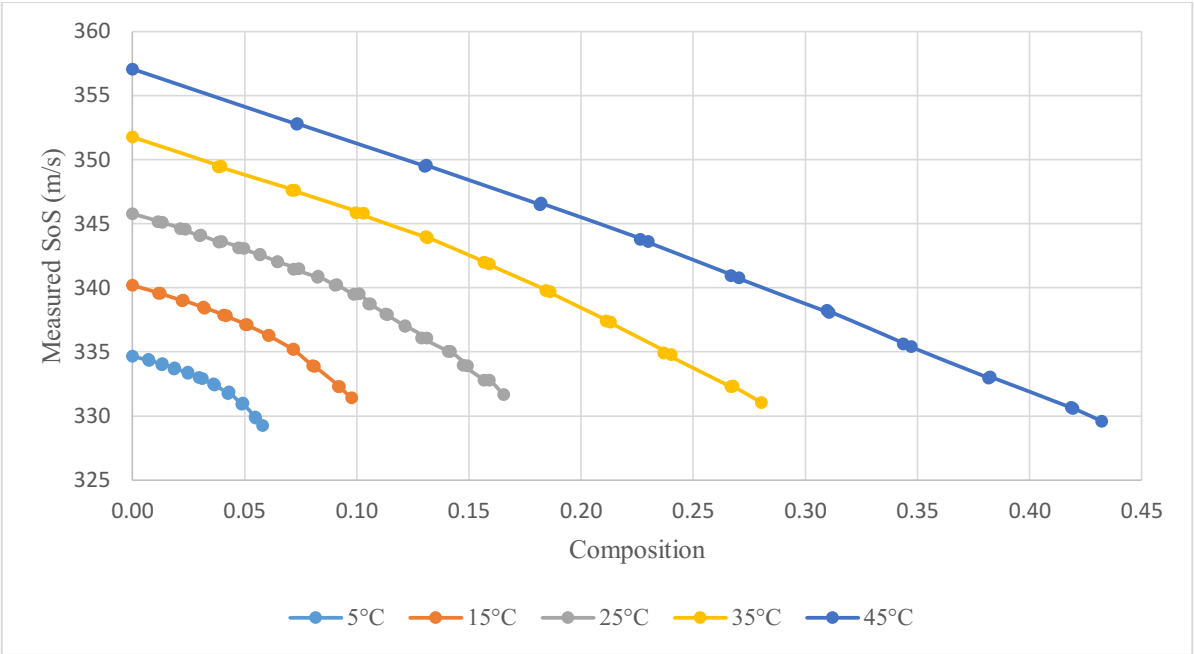



Figure 45. Measured SoS versus composition for methanol/dry air binary gas mixture

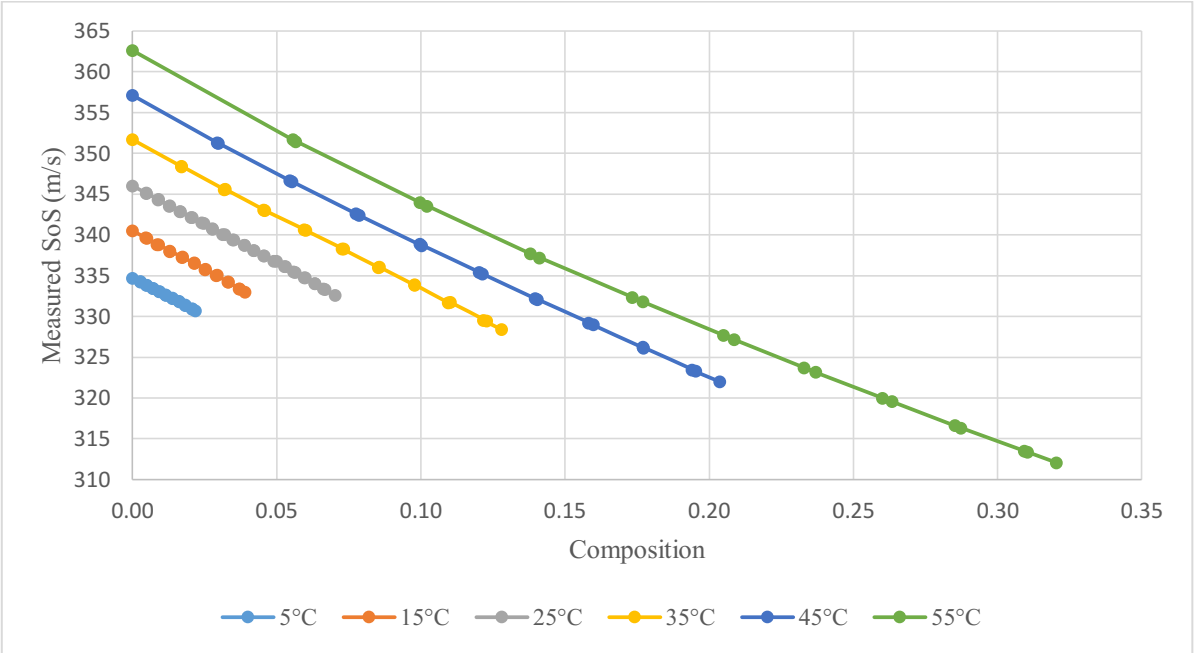



Figure 46. Measured SoS versus composition for ethanol/dry air binary gas mixture

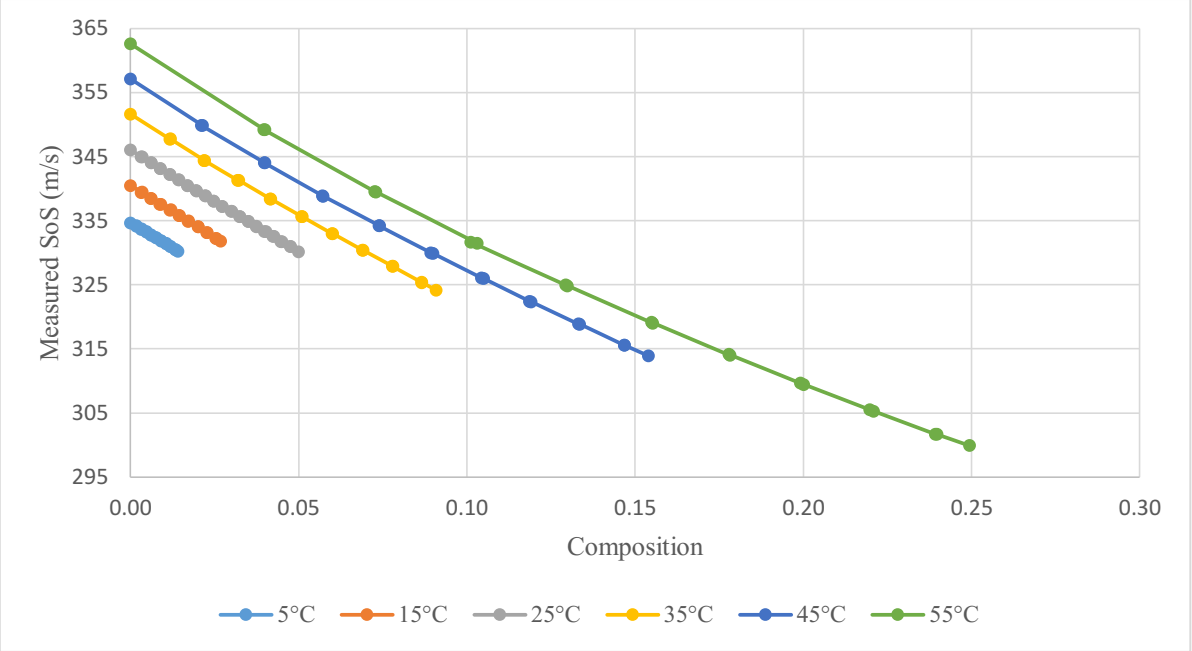



Figure 47. Measured SoS versus composition for isopropanol/dry air binary gas mixture

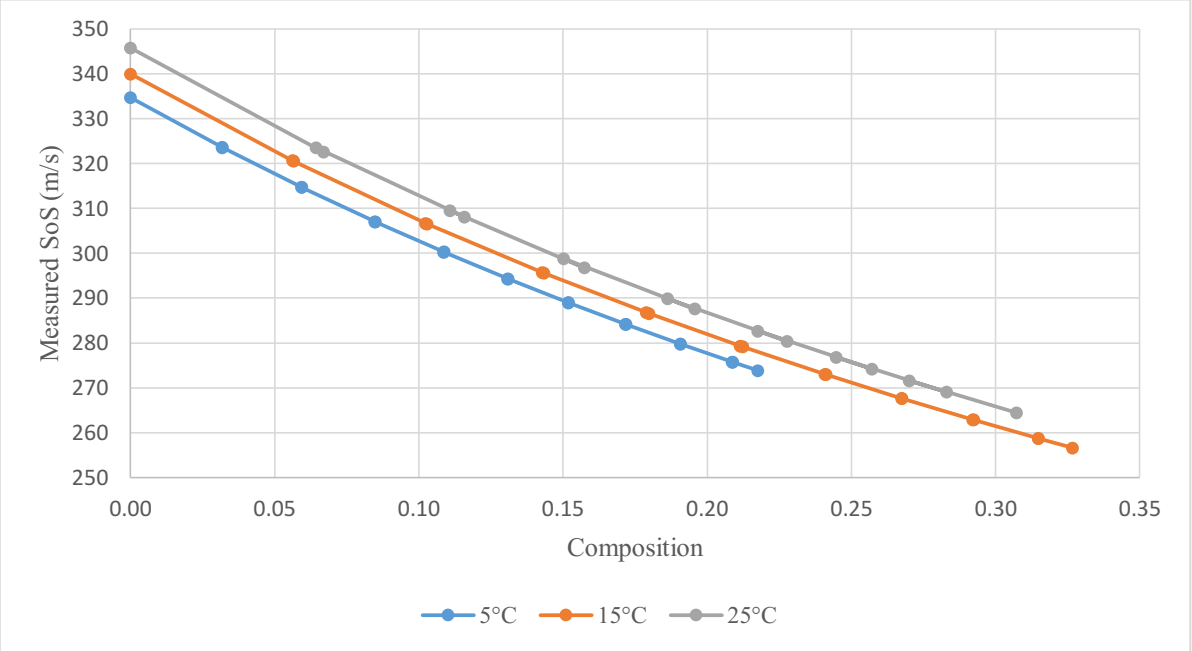



Figure 48. Measured SoS versus composition for dichloromethane/dry air binary gas mixture

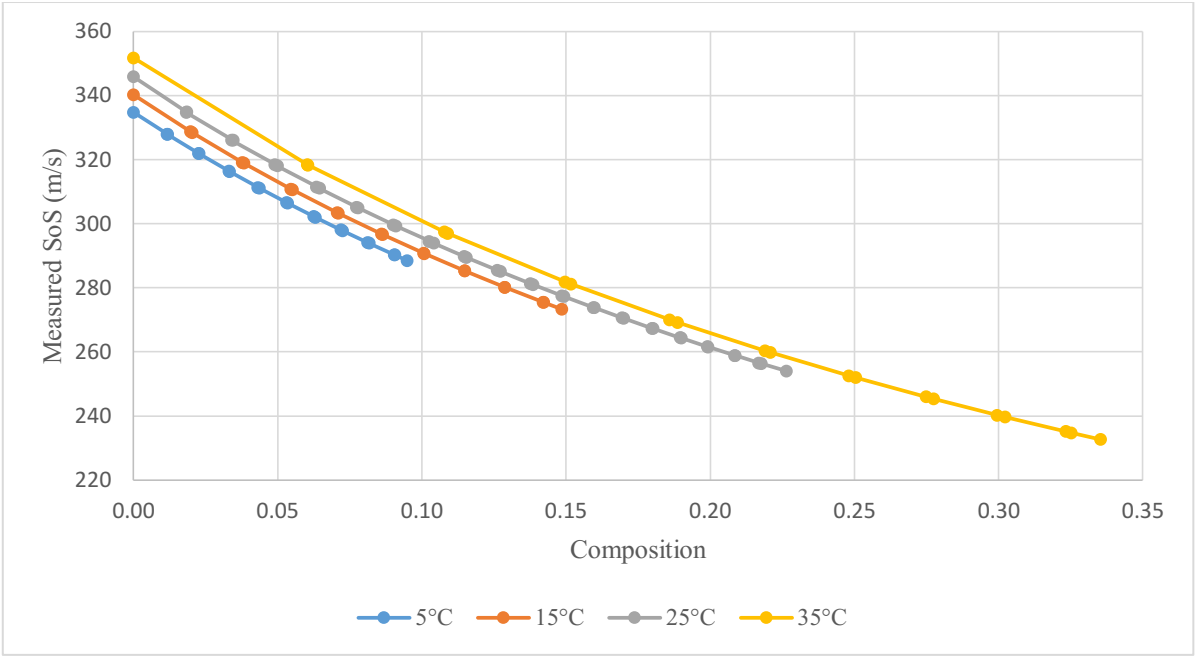



Figure 49. Measured SoS versus composition for chloroform/dry air binary gas mixture

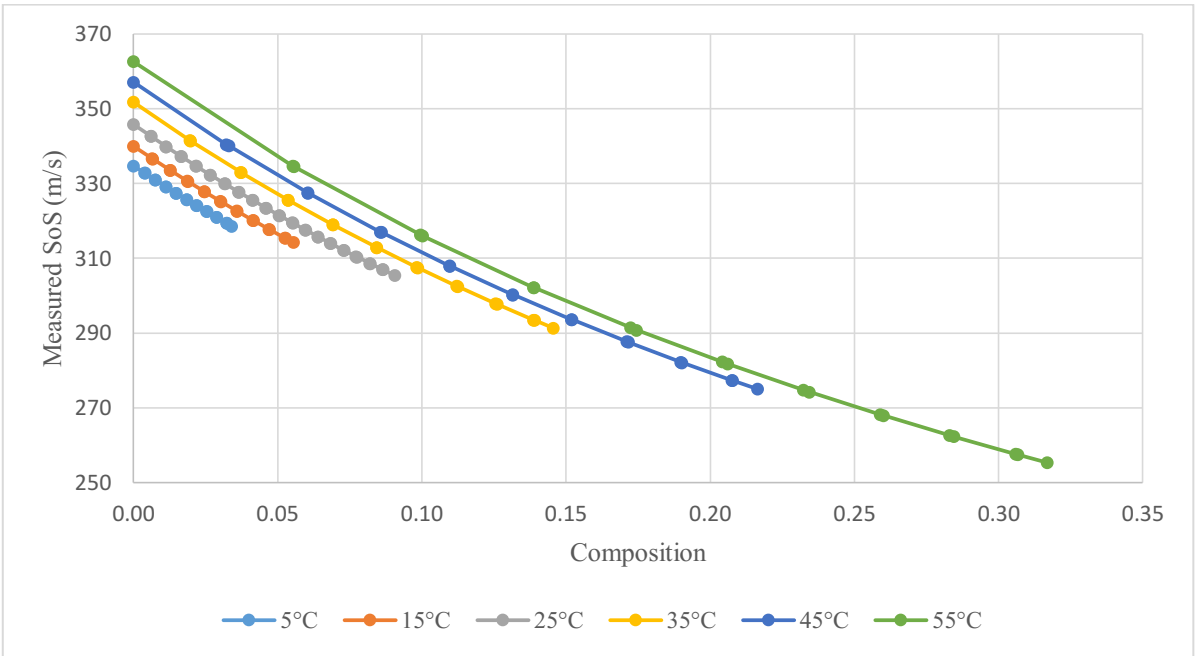



Figure 50. Measured SoS versus composition for 1,2-dichloroethane/dry air binary gas mixture

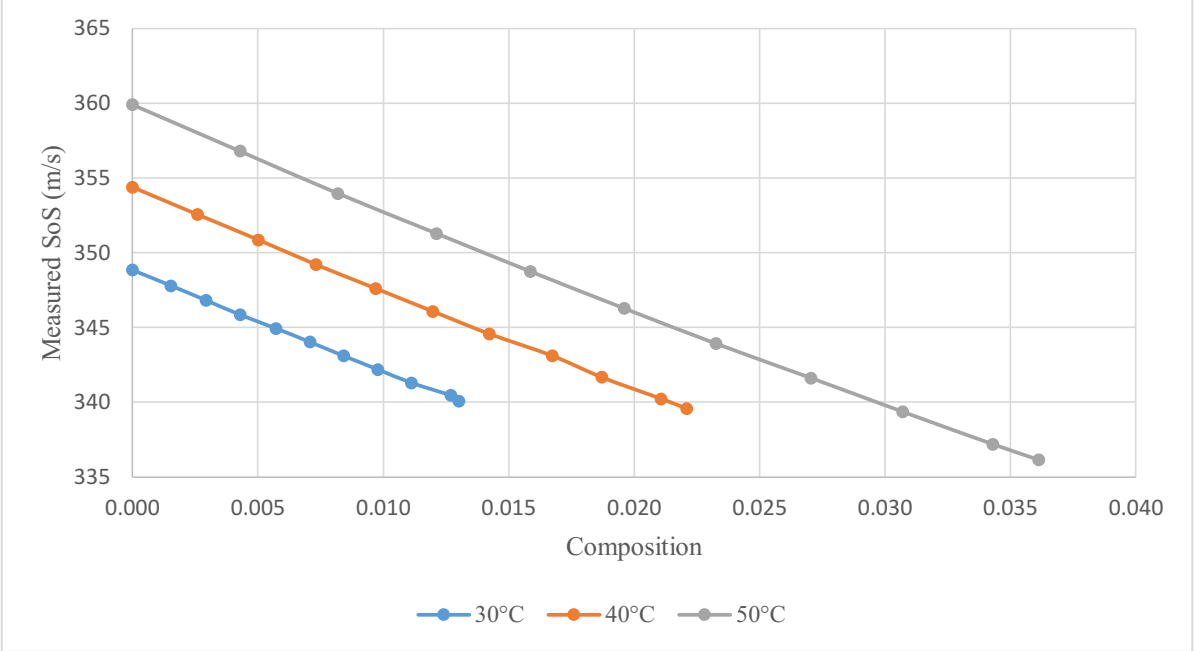



Figure 51. Measured SoS versus composition for m-xylene/dry air binary gas mixture

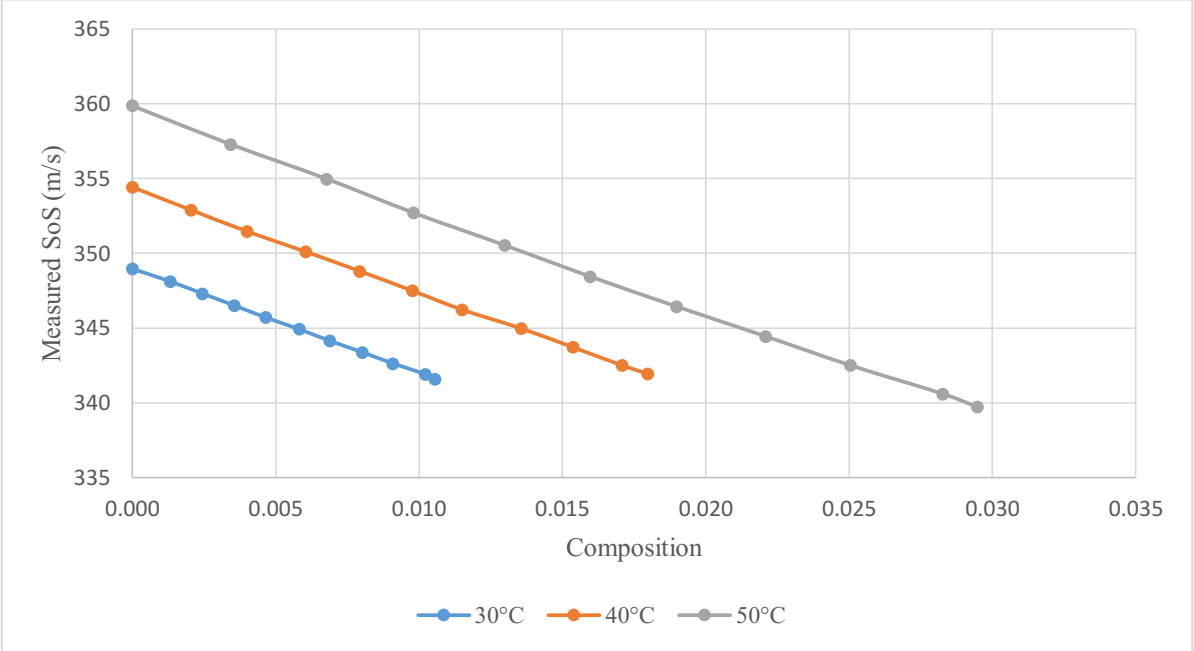



Figure 52. Measured SoS versus composition for o-xylene/dry air binary gas mixture

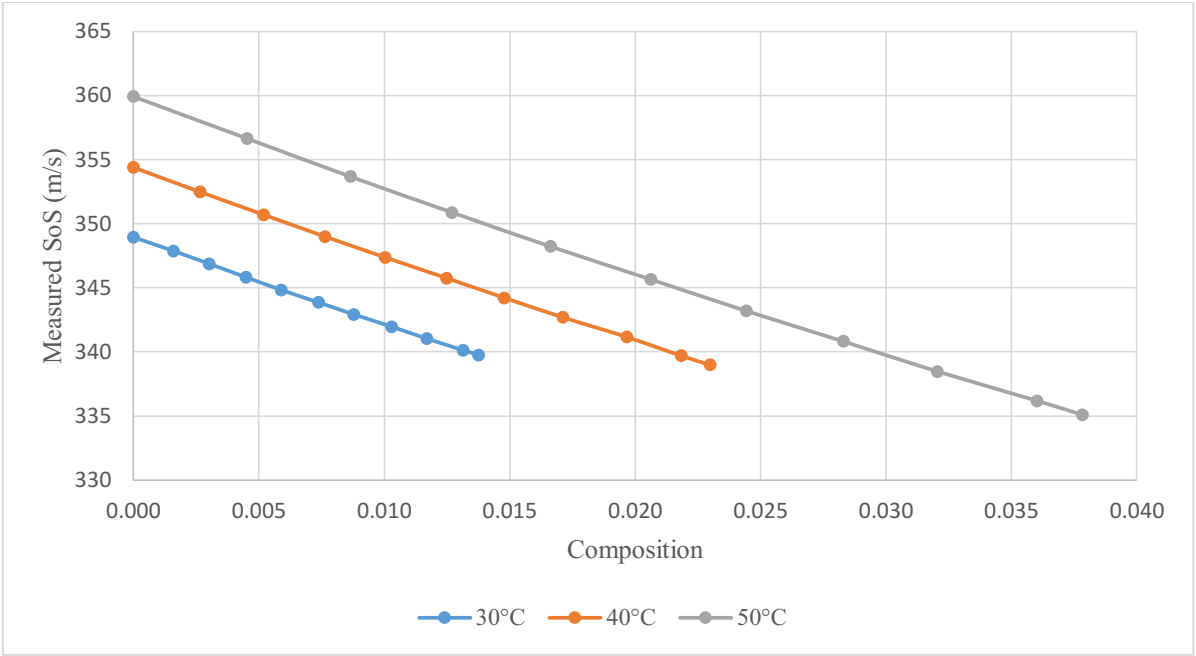



Figure 53. Measured SoS versus composition for p-xylene/dry air binary gas mixture

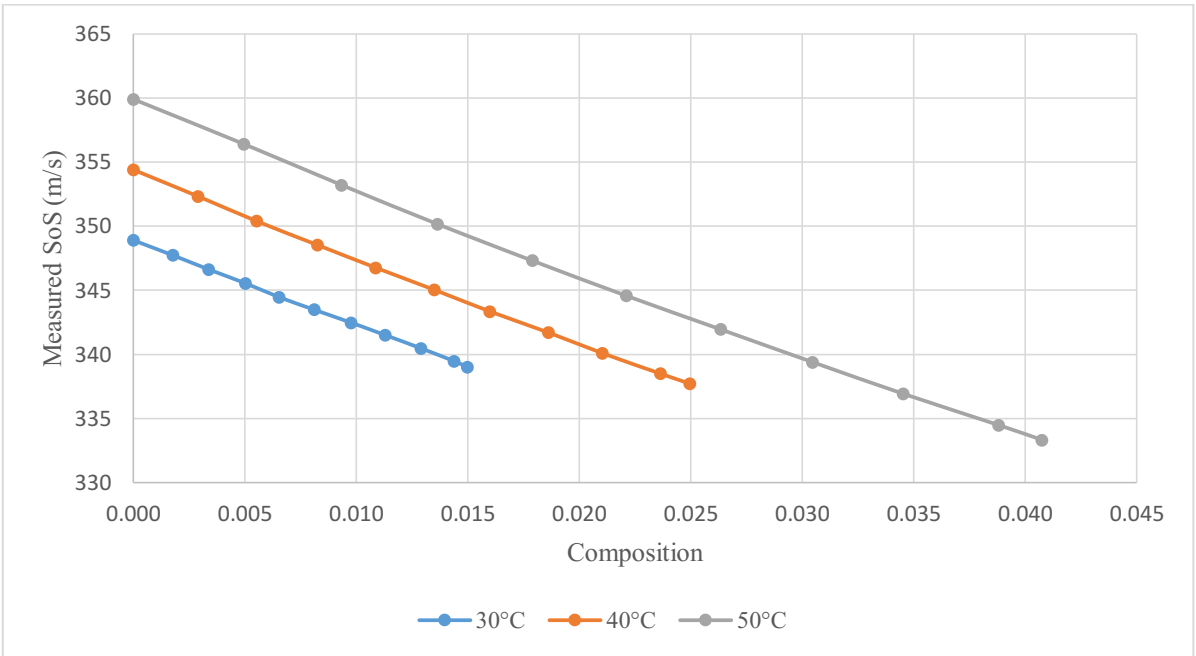



Figure 54. Measured SoS versus composition for ethylbenzene/dry air binary gas mixture

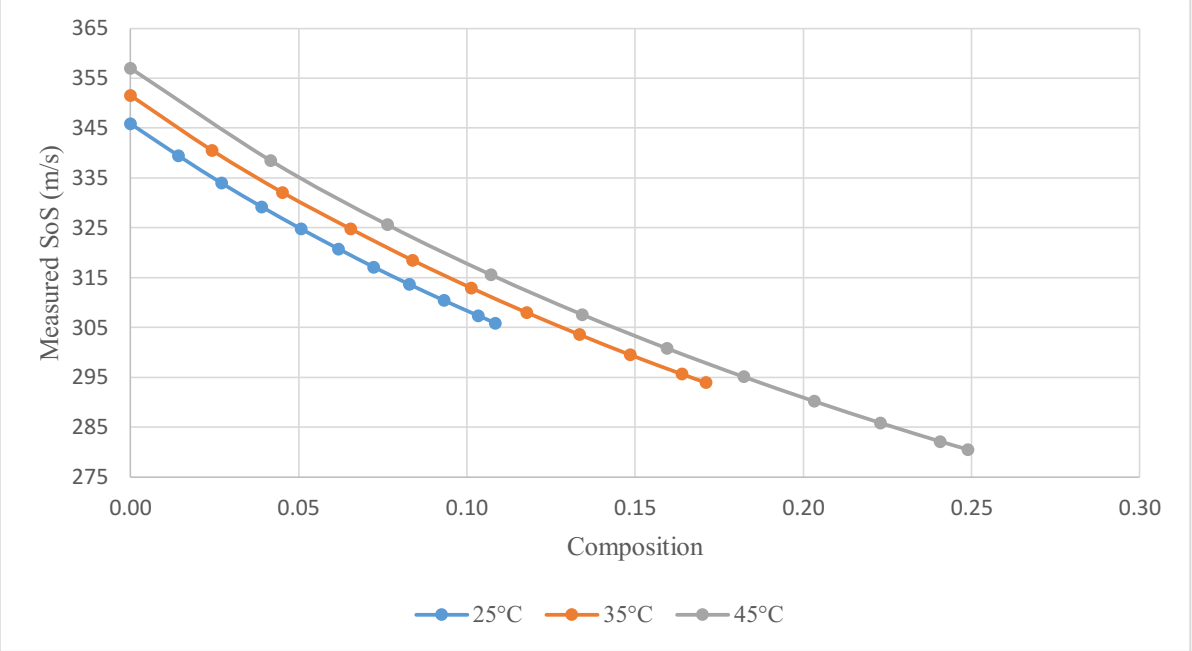



Figure 55. Measured SoS versus composition for n-butylamine/dry air binary gas mixture

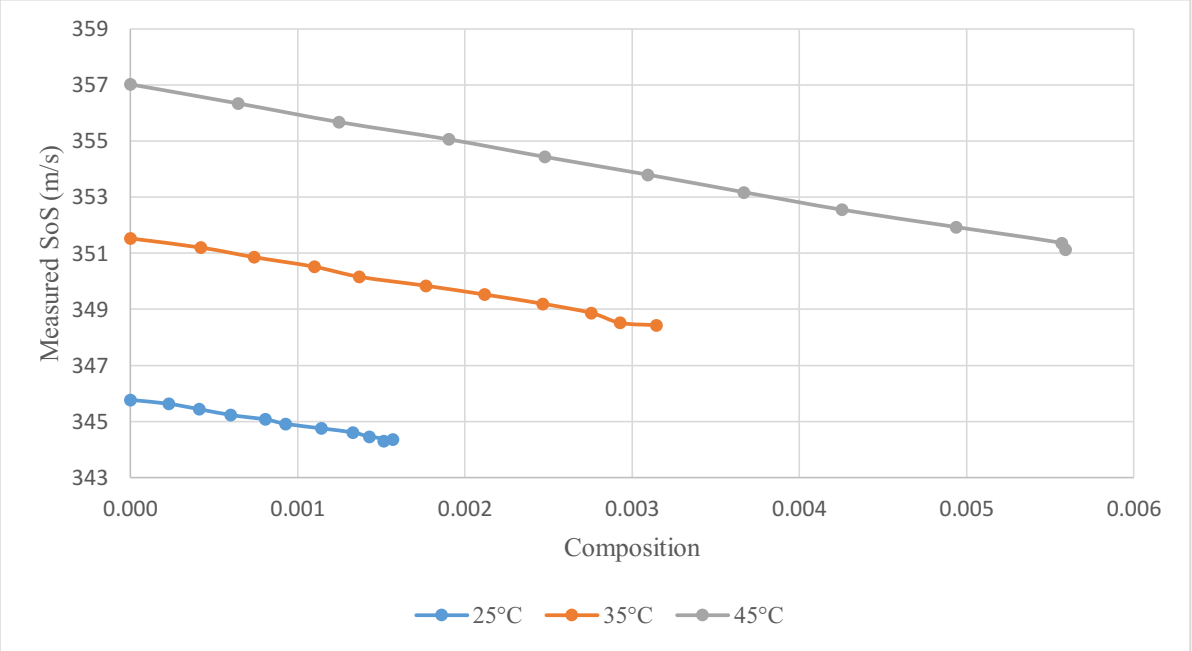



Figure 56. Measured SoS versus composition for limonene/dry air binary gas mixture

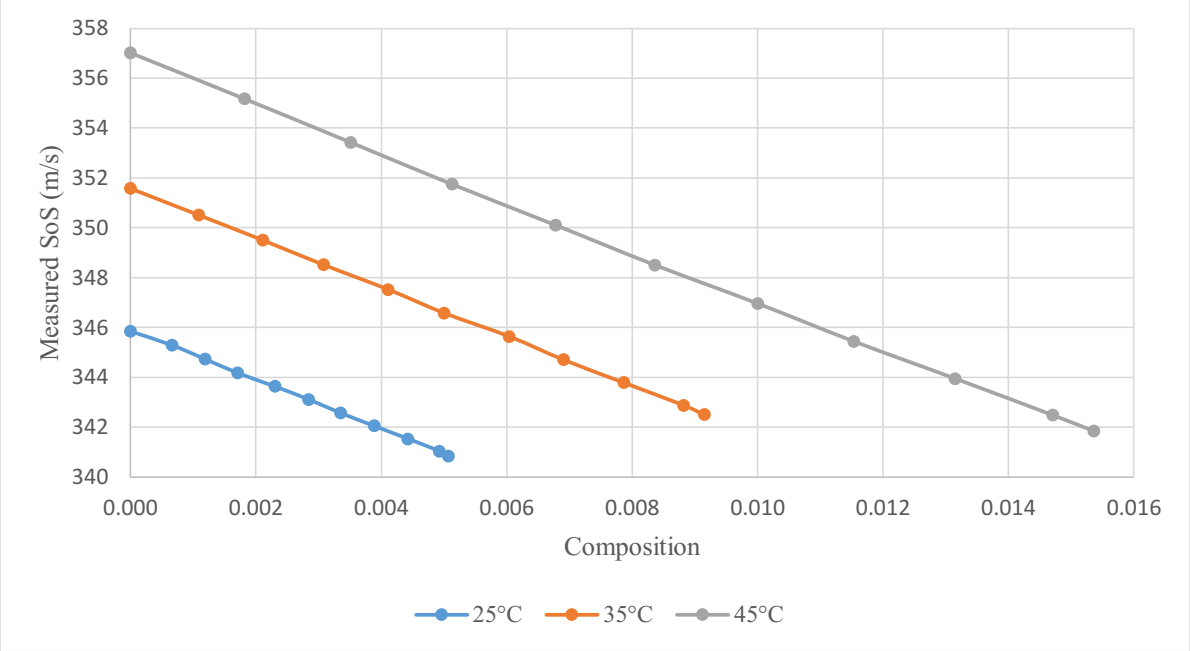



Figure 57. Measured SoS versus composition for α-pinene/dry air binary gas mixture

# CHAPTER 5. Discussion

## 5.1 SoS Measurement Uncertainty and Rate of Change in Pathlength with Temperature

The uncertainty in the SoS measurement characterises the possible variation between the measured SoS $W_m$ in a particular gas system using the SoS sensor and the real gas SoS $W$ of the gas system at the measured temperature $T_{SoS}$, the measured pressure $P$ and the operating acoustic frequency 121362 Hz. Ar, He and $N_2$ for which the $W$ data are known with reasonably high accuracy were used in the experiment for investigating the SoS measurement uncertainty using the SoS sensor in order to minimise the effect of data inaccuracy on the reliability of this uncertainty analysis.

The instrument setup was the same as that for the volume difference measurement, and before starting the incubator was thermally stabilised at the experimental temperature. $N_2$ and Ar were run through the measuring system successively and each step was given enough time for the pure gas to fill up the measuring system. The average values of the last 30 seconds data ($T_{SoS}$, $P$ and $t_m$) at both steps were used in the calculations. Firstly, $W$ for $N_2$ and Ar at $T_{SoS}$ and $P$ corresponding to the respective steps and 121362 Hz were determined; then, the pathlength of the SoS sensor was determined according to Equation (82) using the $N_2$-step $W$ and $t_m$ as $W^0$ and $t_m^0$; finally, with the calibrated pathlength $L'$ and the Ar-step $t_m$, the measured SoS in Ar $W_m$ was obtained according to Equation (83). This experiment was performed from 5 to 55 °C in 5 °C increments.

The relative errors between $W_m$ and $W$, $\Delta_{RE}$ $(= (W_m - W)/W \times 100)$, for Ar over the whole temperature range were around 0.08 to 0.1% (see Figure 58). In the above experiment, at the same experimental temperature, the $W$ values for Ar were lower than those for $N_2$. In order to investigate the SoS measurement uncertainty in a gas system with higher SoS than $N_2$, another experiment was performed at 25 °C with $N_2$ and He being measured successively. Similarly, the incubator was thermally stabilised before starting and each step was given reasonably long time for the pure gas to fill up the measuring system. According to the same data analysis method, $\Delta_{RE}$ for He was also found around 0.1% (see Figure 58). The uncertainties of $W$ for $N_2$, Ar and He are all much lower than 0.1%.

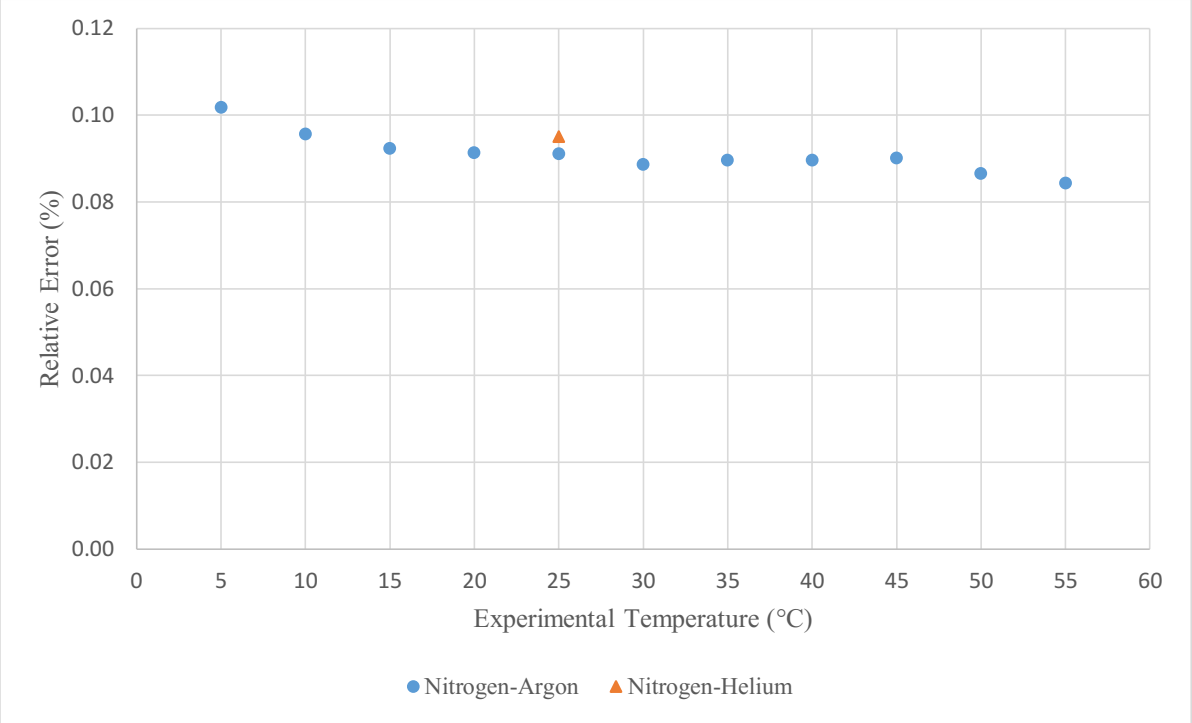



Figure 58. Relative error between $W_m$ and $W$ versus experimental temperature

With the calibrated pathlength values determined from the $N_2$-step $W$ and $t_m$ at different temperatures from 5 to 55 °C, the rate of change in pathlength with respect to temperature was estimated to be around 70 ppm/°C. The typical temperature variation in each nominally isothermal experiment was ± 0.1 °C and this could only lead to about ± 7 ppm change in pathlength and in turn about ± 7 ppm inaccuracy in $W_m$ which was insignificant and negligible.

For the experiments on binary gas mixtures with $N_2$ as the carrier gas ($CO_2/N_2$), 0.1% is considered to be the SoS measurement uncertainty, i.e. the $W_m$ results are within the range of [1 - 0.1%, 1 + 0.1%] of the $W$ values at the same temperature $T_{SoS}$, pressure $P$, composition $x$ and acoustic frequency $f$ with a confidence level of 68%. For the experiments on binary gas mixtures with dry air as the carrier gas, an additional source of SoS measurement uncertainty needs to be taken into account resulting from the difference between the uncertainties of the $W$ data for dry air and for $N_2$. The $W$ data for dry air under the experimental conditions also have an uncertainty of around 0.1%, thus $\sqrt{[(0.1\%)^2 + (0.1\%)^2]} \approx 0.14\%$ can be regarded as the SoS measurement uncertainty. As will be discussed in Section 5.4, the effect of SoS measurement error on the accuracy of gas composition determination using this SoS technique is negligible.

## 5.2 SoS Comparisons

Reported SoS literature data for the tested binary gas mixtures close to the experimental conditions used in this project were not found. Significant amounts of reported data are for high pressures and high temperatures. However, it might be useful to compare the measured SoS $W_m$ (here the calculated carrier gas real gas SoS corresponding to the first zero step for pathlength calibration, $W^0$, is taken to be $W_m$ as well) with the lossless real gas SoS $W_\theta$ predicted from using the NIST REFPROP software. It is noteworthy that $W_m$ corresponds to the SoS at frequency of 121362 Hz, while $W_\theta$ is frequency independent. These SoS comparisons are only performed on the binary gas mixtures with available thermodynamic data in the software (Group A). The methods for determining $W_\theta$ using the software are given in Table 27. $x$ denotes the measured mole fraction of the solute component.

Table 27. Methods for the determination of $W_\theta$ using the NIST REFPROP software

| Carrier Gas | | Dry Air | Nitrogen |
|---|---|---|---|
| Solute | | n-hexane, n-heptane, n-octane, n-nonane, n-decane, toluene, cyclohexane and water | Carbon dioxide |
| $W_\theta$ for the first zero step | EoS used | H-EoS | H-EoS |
| | Method | Set a mixture in the software as dry air comprising $N_2$, $O_2$, Ar and $CO_2$ with mole fractions of 0.780796, 0.209461, 0.009339 and 0.000404 respectively → input the first-zero-step $T_{SoS}$ and $P$ → output $W_\theta$ | Set pure $N_2$ in the software → input the first-zero-step $T_{SoS}$ and $P$ → output $W_\theta$ |
| $W_\theta$ for the non-zero steps | EoS used | H-EoS | H-EoS |
| | Method | Set a mixture in the software comprising the solute, $N_2$, $O_2$, Ar and $CO_2$ with mole fractions of $x$, 0.780796(1-$x$), 0.209461(1-$x$), 0.009339(1-$x$) and 0.000404(1-$x$) respectively (i.e. a binary gas mixture comprising the solute and dry air with mole fractions of $x$ and (1-$x$) respectively) → input the non-zero-step $T_{SoS}$ and $P$ → output $W_\theta$ | Set a mixture in the software comprising $CO_2$ and $N_2$ with mole fractions of $x$ and (1-$x$) respectively → input the non-zero-step $T_{SoS}$ and $P$ → output $W_\theta$ |

Figures 59 to 76 illustrate the differences $\Delta_D$ $(= W_m - W_\theta)$ and the relative differences $\Delta_{RD}$ $(= (W_m - W_\theta)/W_\theta \times 100)$ between $W_m$ and $W_\theta$ for the nine different types of binary gas mixtures at different experimental temperatures. The x-axis refers to the target mole fraction

of the solute component (i.e. $x_T$), and the y-axis represents $\Delta_D$ or $\Delta_{RD}$. It can be found that $\Delta_D$ and $\Delta_{RD}$ are generally greater than zero (except several points for water/dry air at 55 °C), which means $W_m > W_\theta$. Therefore, it may be concluded that in these cases the real gas SoS $W$ is greater than $W_\theta$, i.e. $K_d > 0$. The exceptions might be due to experimental errors. The figures for n-hexane, n-heptane, toluene, cyclohexane/dry air and $CO_2/N_2$ clearly indicate that at the same temperature $\Delta_D$ and $\Delta_{RD}$ increase as the solute mole fraction increases, which is probably because the dispersion effect on the solute component is more significant than that on the carrier gas component; in addition, at the same target solute mole fraction $\Delta_D$ and $\Delta_{RD}$ are higher at higher temperatures. These characteristics generally cannot be observed in the figures for n-octane (at lower temperatures), n-nonane, n-decane and water/dry air. This might be attributed to the fact that the solute mole fractions in these binary gas mixtures are much lower (the variation of $x_T$ cannot result in significant SoS change) and those characteristics are hidden in the experimental errors. It is also found that the values of $\Delta_{RD}$ for the mixtures except $CO_2/N_2$ are reasonably small; the absolute values of $\Delta_{RD}$ are all less than 0.5%. The relative difference between $W_m$ and $W_\theta$ for $CO_2/N_2$ is large because of the significant dispersion effect on the solute component $CO_2$; the maximum $\Delta_{RD}$ is 1.8% approximately.

The SoS comparisons for the binary gas mixtures without available thermodynamic data in the NIST REFPROP software (Group B) are not contained in this thesis. The other types of EoSs, such as the ideal gas law, the Van der Waals EoS and the virial EoS could be employed for the calculation of $W_\theta$ in this case.

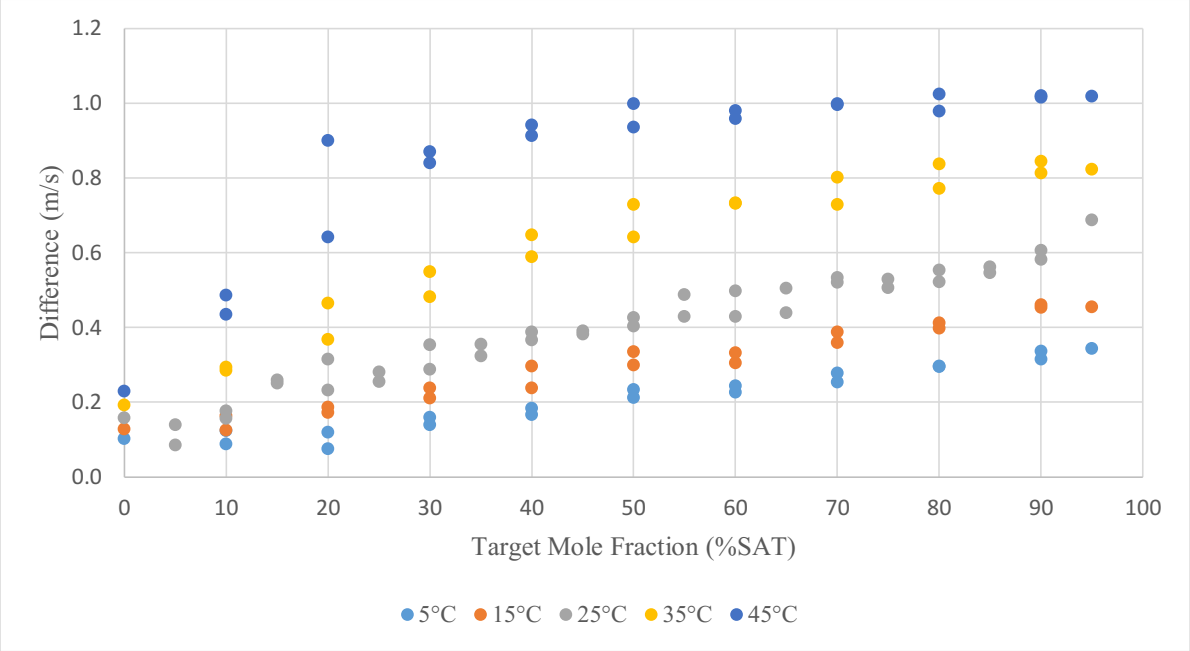



Figure 59. Difference between $W_m$ and $W_\theta$ ($\Delta_D$) for n-hexane/dry air

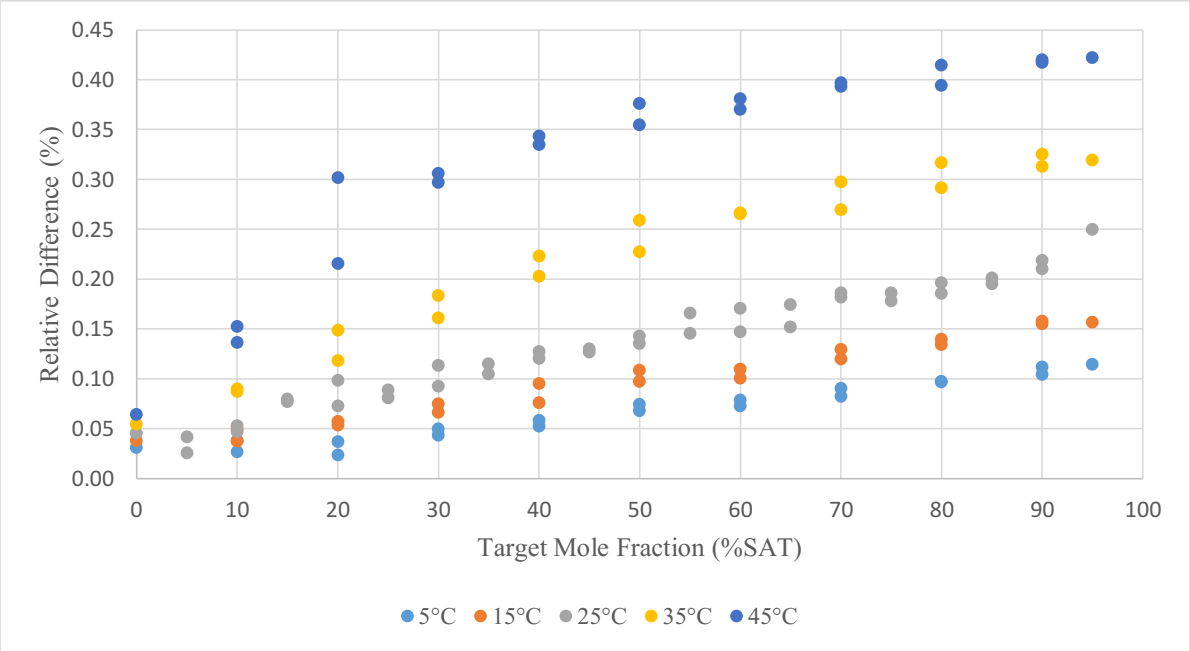



Figure 60. Relative difference between $W_m$ and $W_\theta$ ($\Delta_{RD}$) for n-hexane/dry air

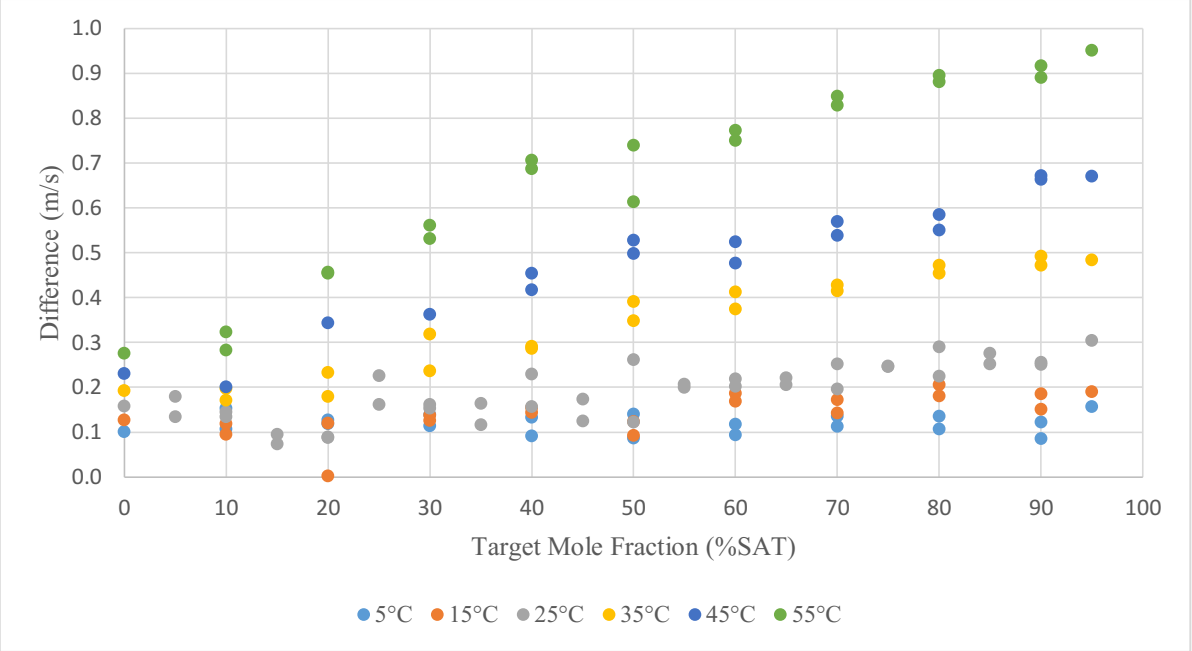



Figure 61. Difference between $W_m$ and $W_\theta$ ($\Delta_D$) for n-heptane/dry air

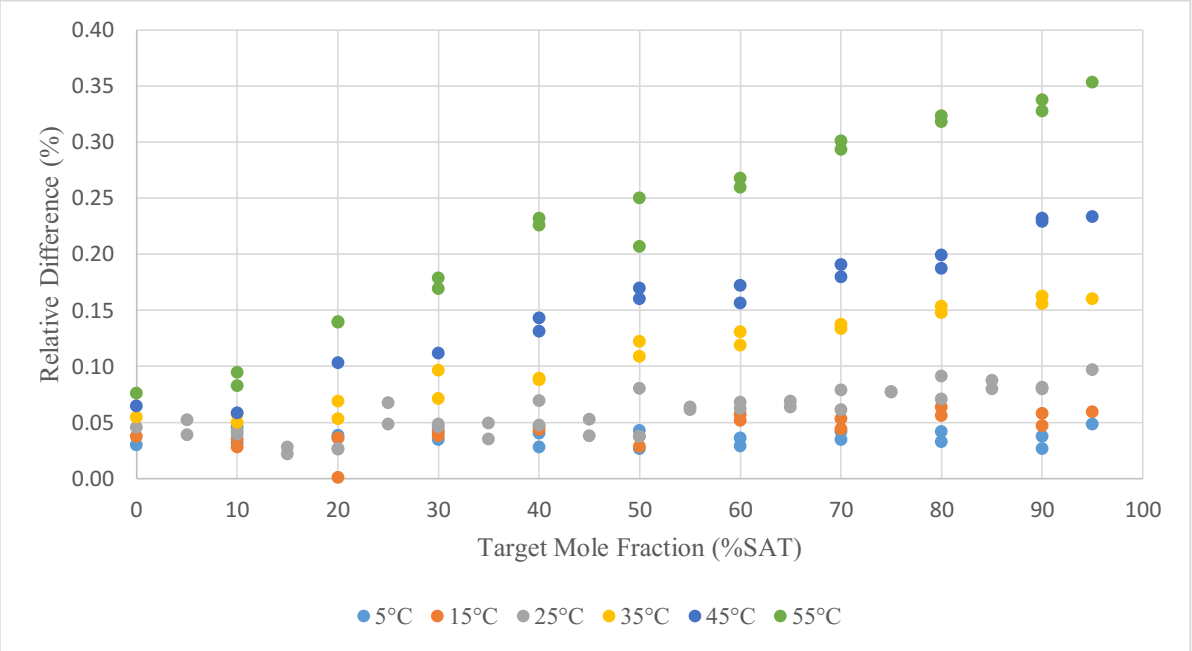



Figure 62. Relative difference between $W_m$ and $W_\theta$ ($\Delta_{RD}$) for n-heptane/dry air

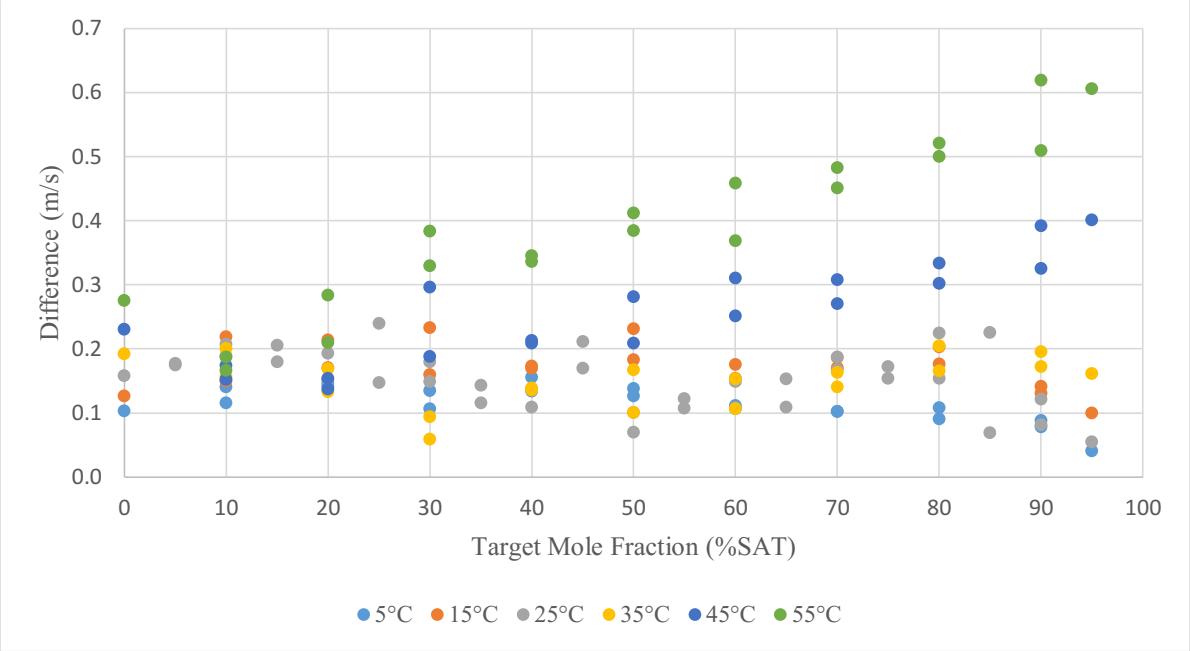



Figure 63. Difference between $W_m$ and $W_\theta$ ($\Delta_D$) for n-octane/dry air

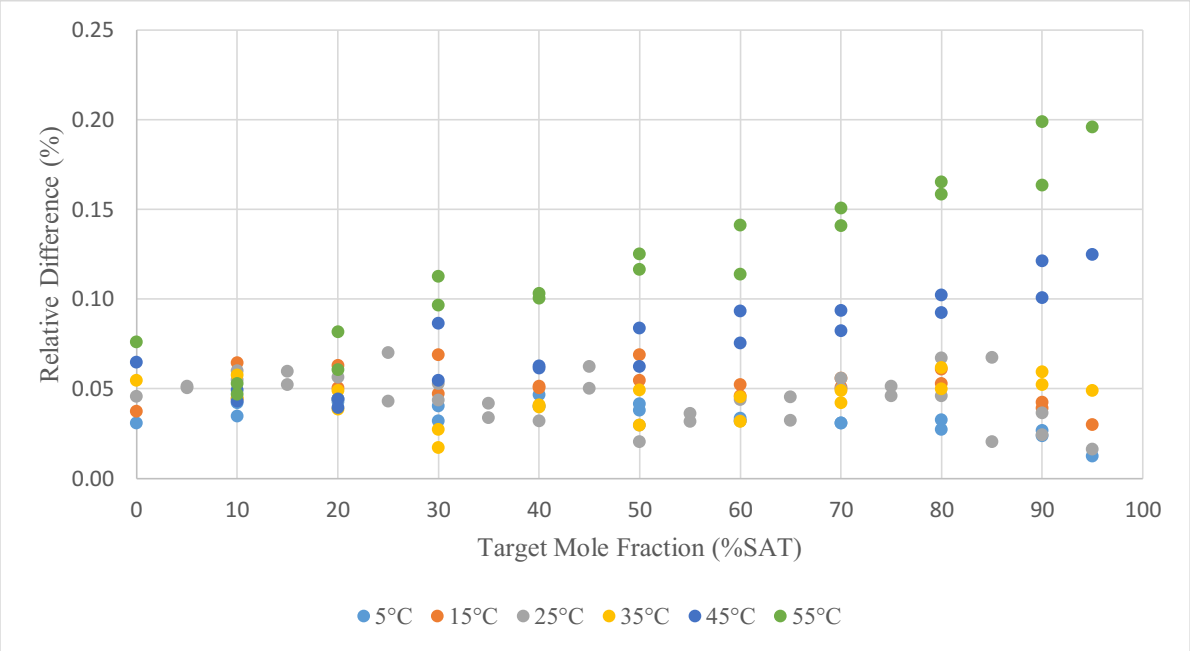



Figure 64. Relative difference between $W_m$ and $W_\theta$ ($\Delta_{RD}$) for n-octane/dry air

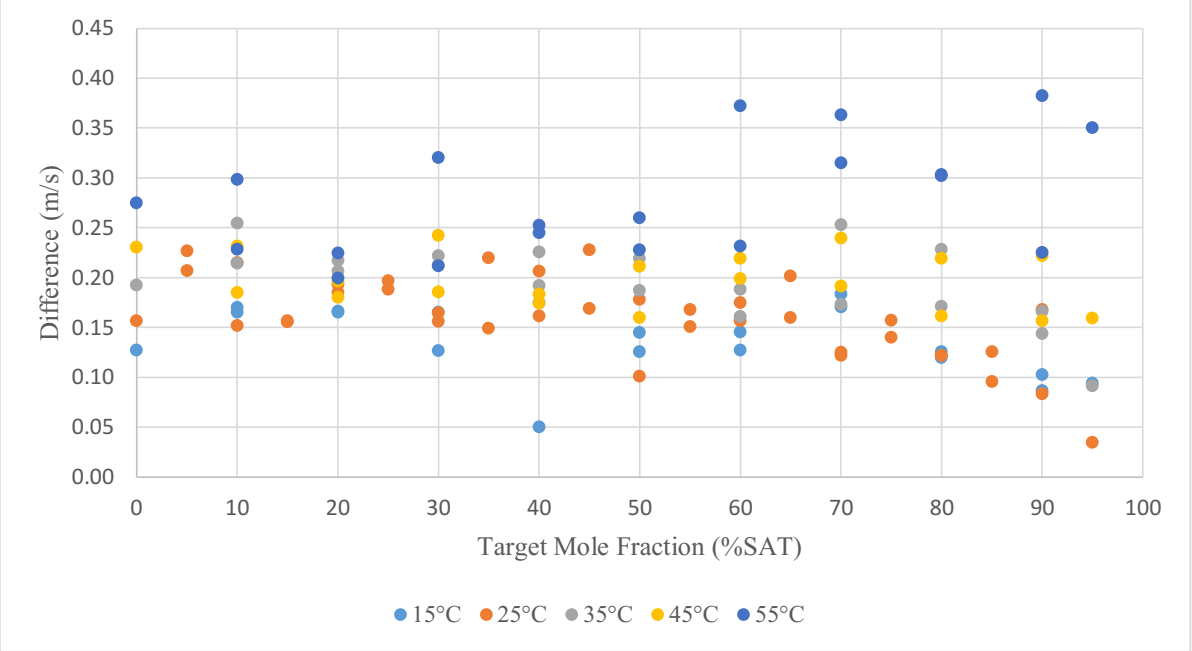



Figure 65. Difference between $W_m$ and $W_\theta$ ($\Delta_D$) for n-nonane/dry air

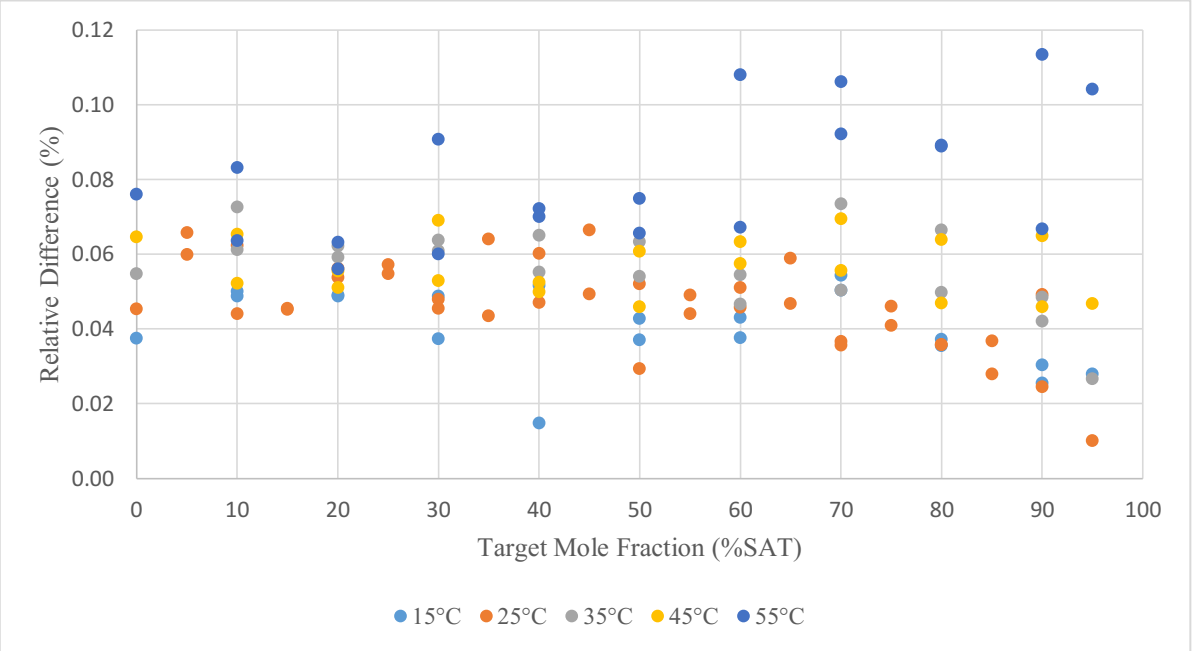



Figure 66. Relative difference between $W_m$ and $W_\theta$ ($\Delta_{RD}$) for n-nonane/dry air

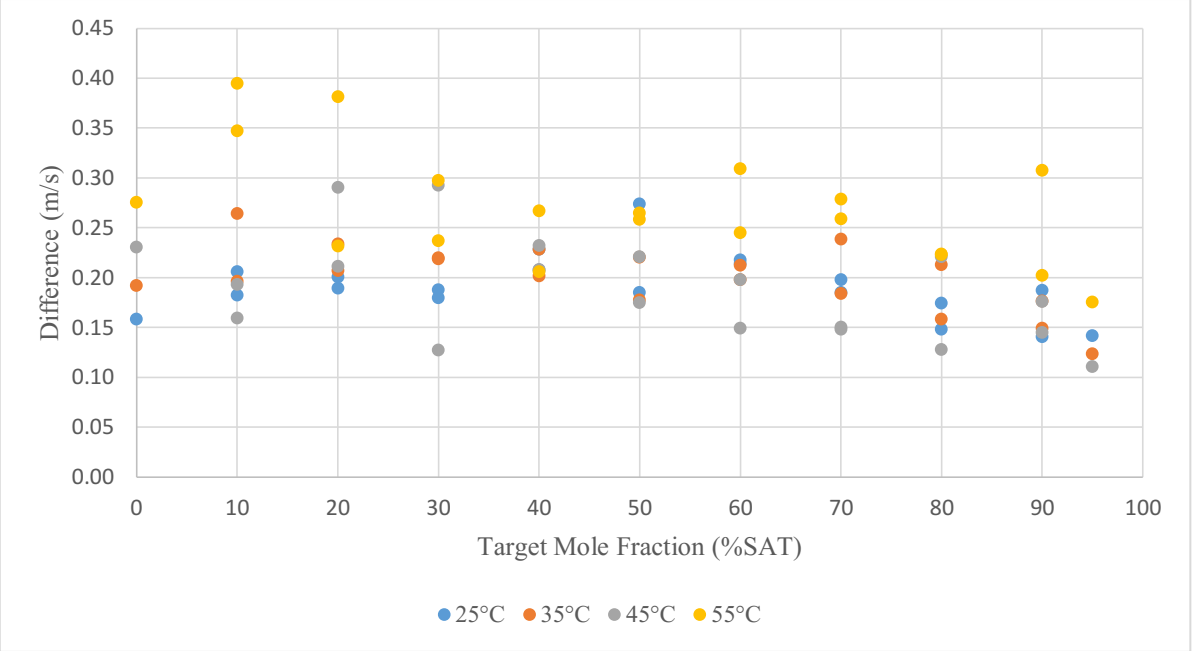



Figure 67. Difference between $W_m$ and $W_\theta$ ($\Delta_D$) for n-decane/dry air

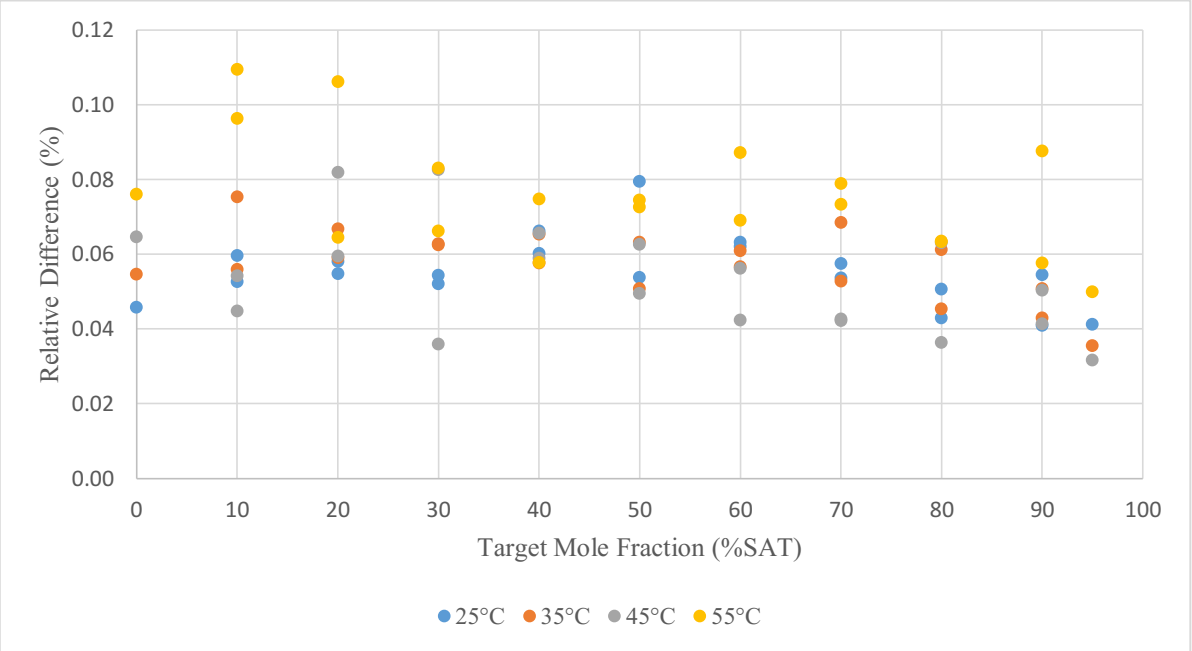



Figure 68. Relative difference between $W_m$ and $W_\theta$ ($\Delta_{RD}$) for n-decane/dry air

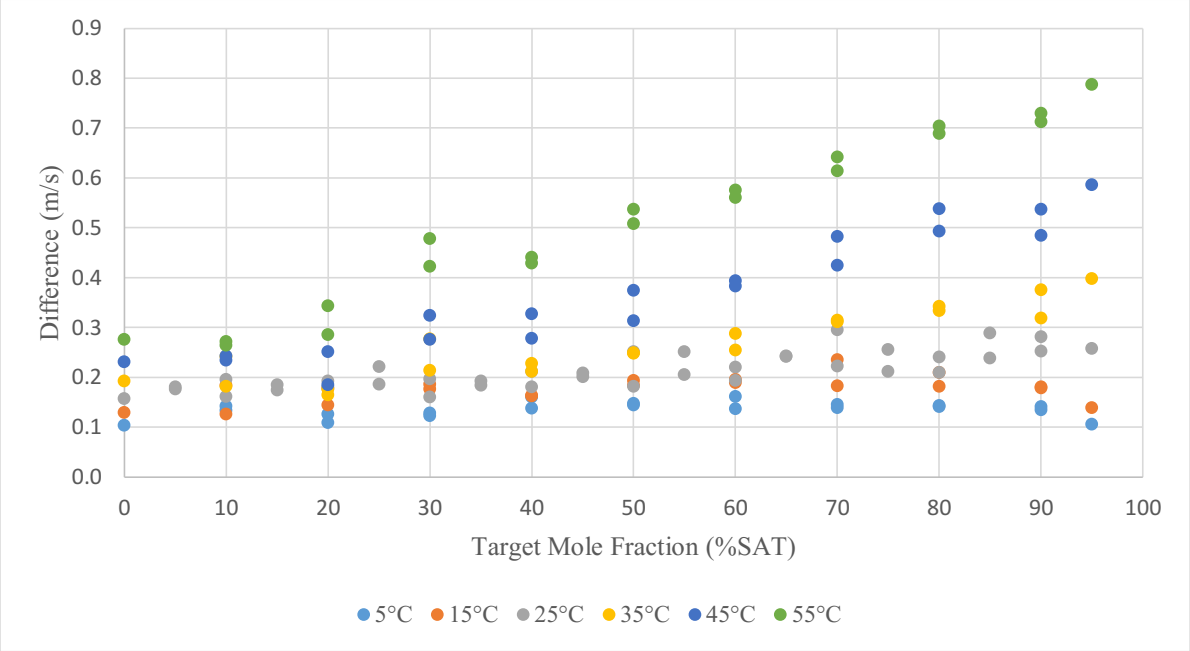



Figure 69. Difference between $W_m$ and $W_\theta$ ($\Delta_D$) for toluene/dry air

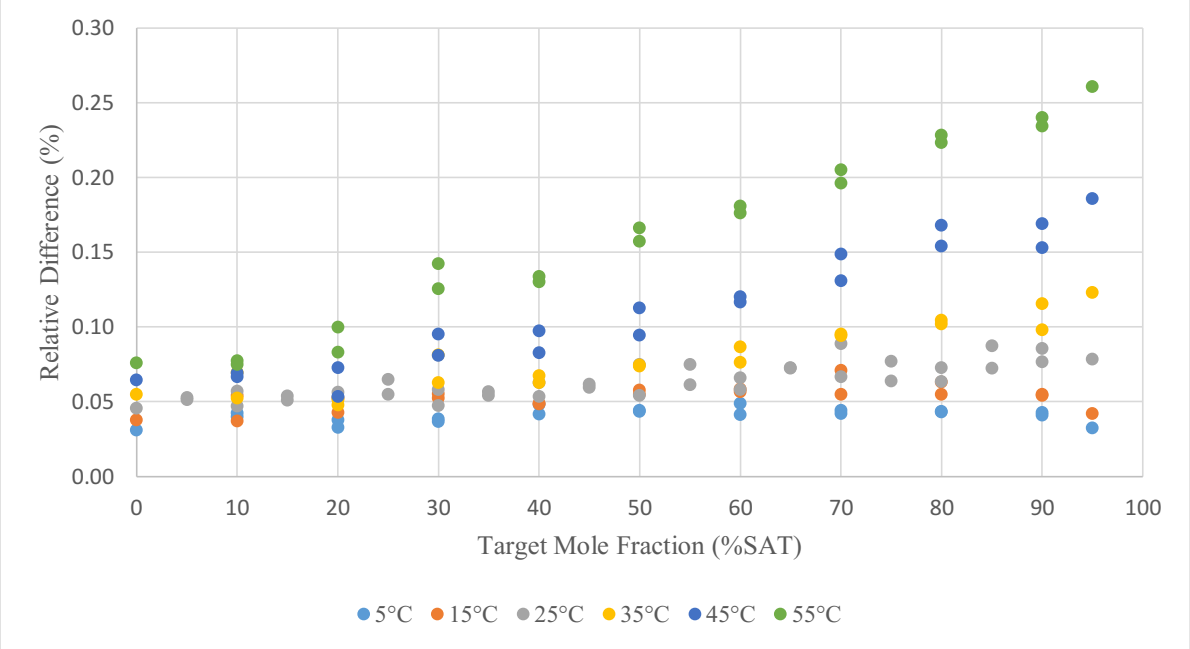



Figure 70. Relative difference between $W_m$ and $W_\theta$ ($\Delta_{RD}$) for toluene/dry air

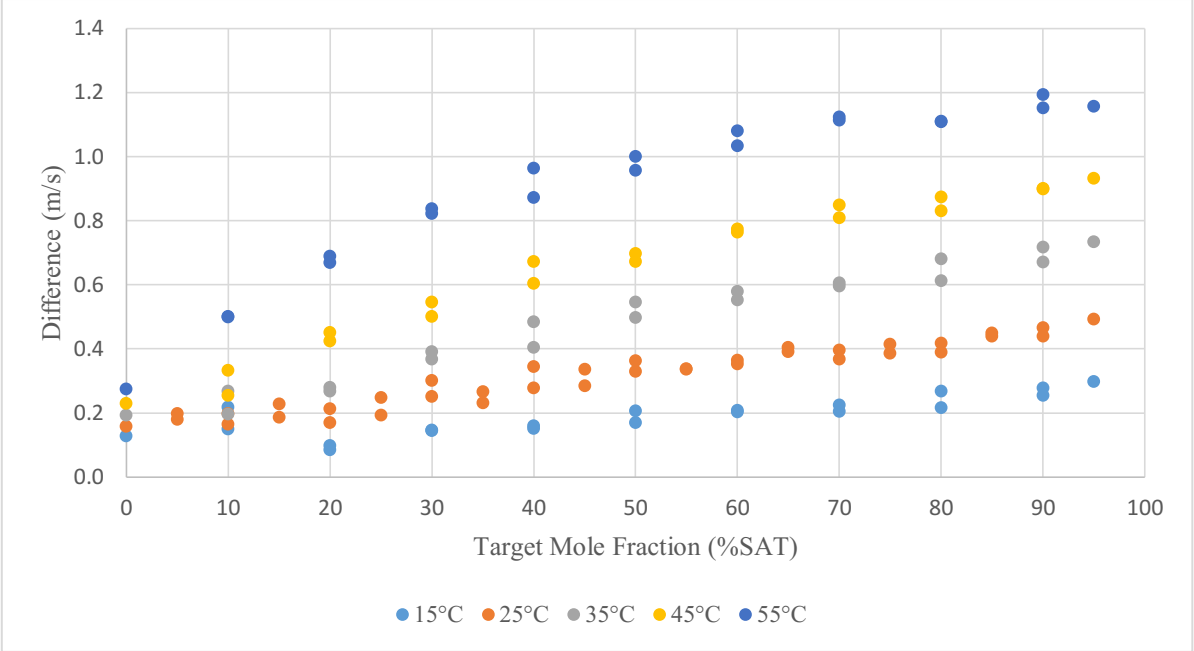



Figure 71. Difference between $W_m$ and $W_\theta$ ($\Delta_D$) for cyclohexane/dry air

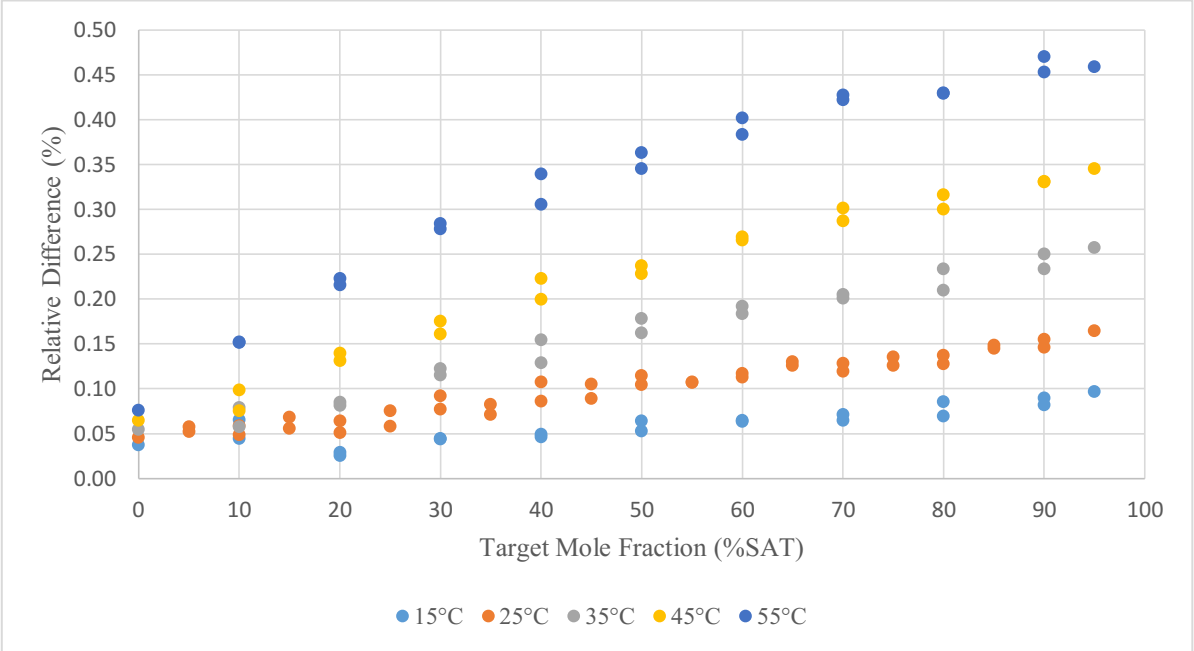



Figure 72. Relative difference between $W_m$ and $W_\theta$ ($\Delta_{RD}$) for cyclohexane/dry air

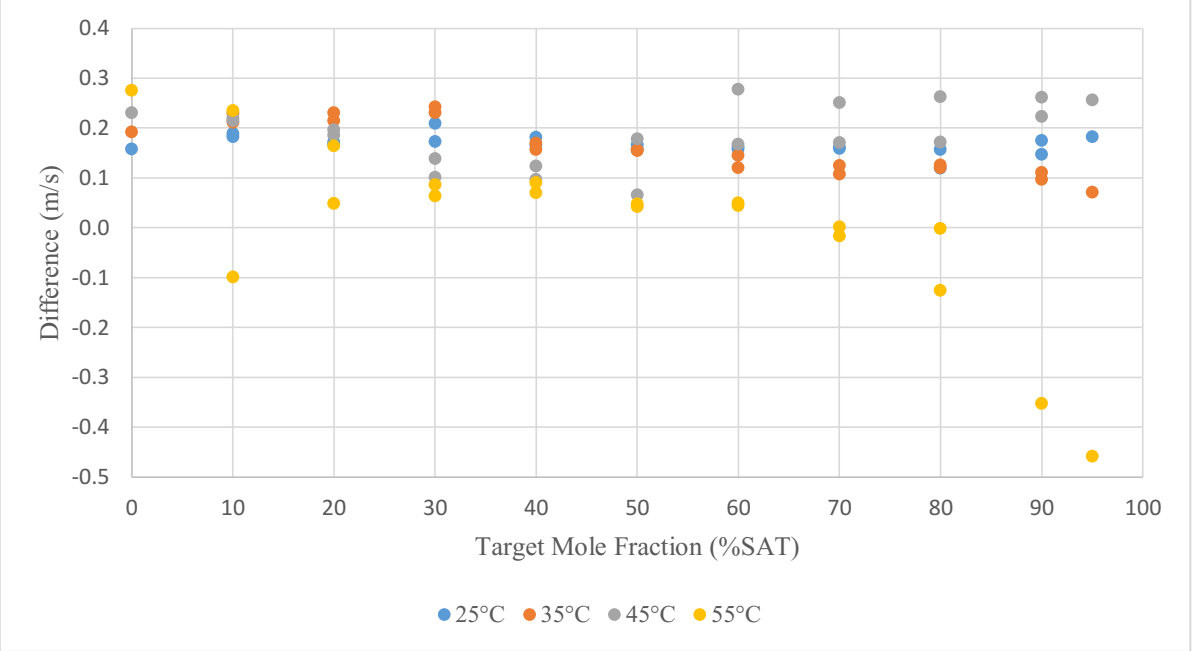



Figure 73. Difference between $W_m$ and $W_\theta$ ($\Delta_D$) for water/dry air

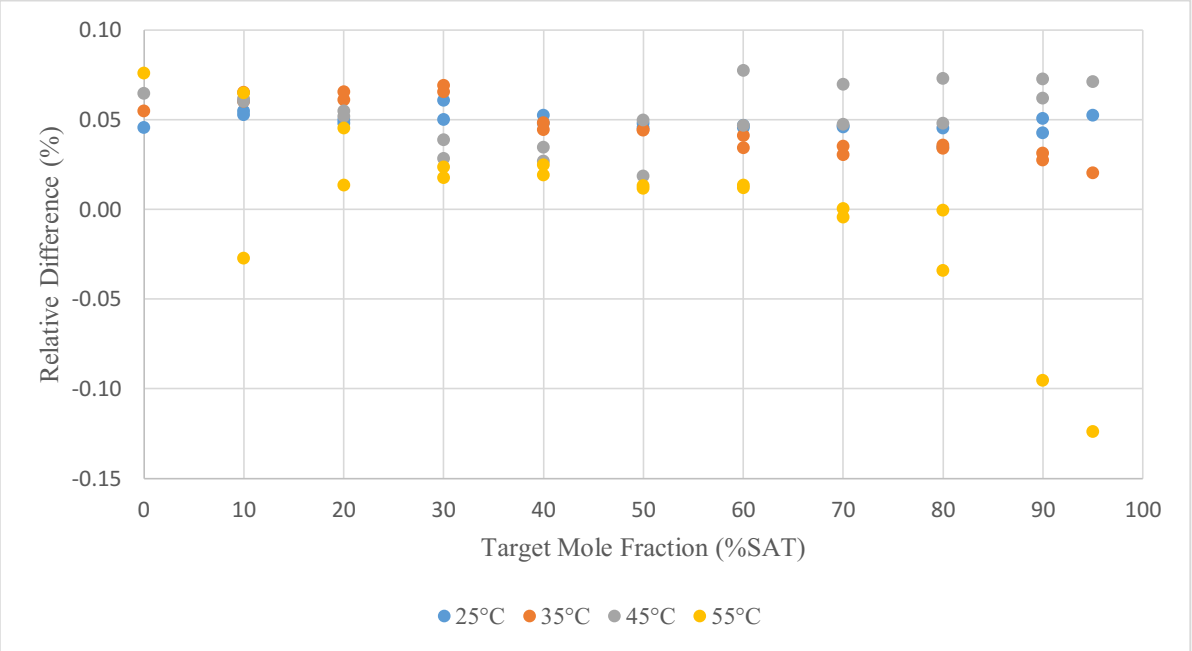



Figure 74. Relative difference between $W_m$ and $W_\theta$ ($\Delta_{RD}$) for water/dry air

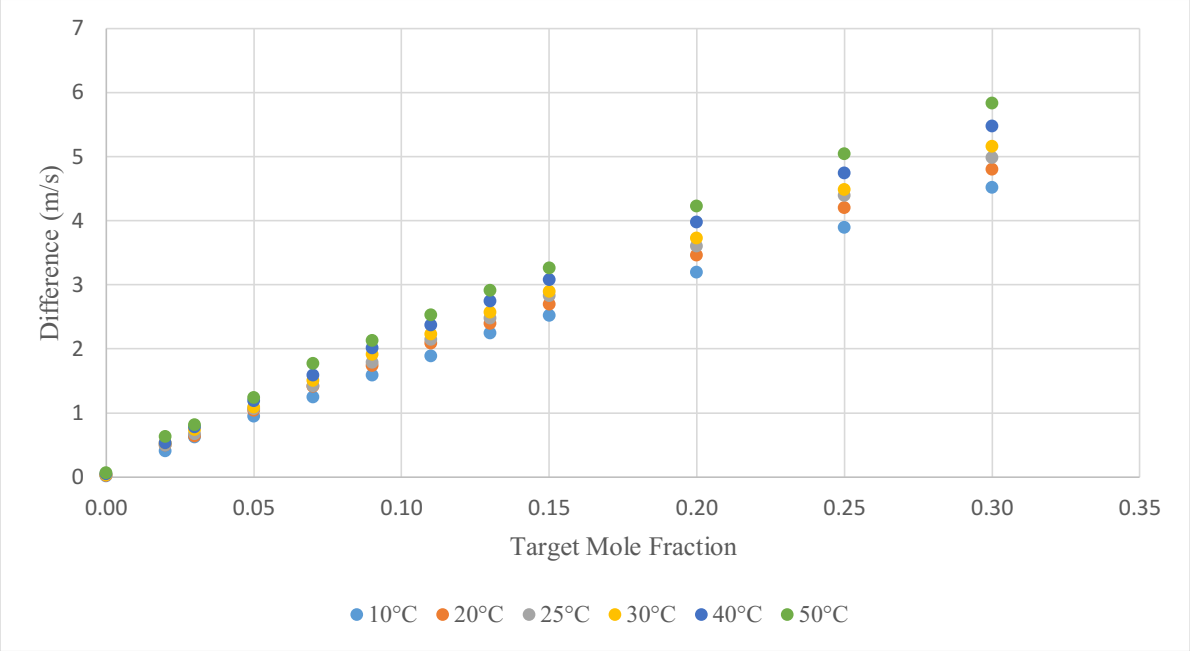



Figure 75. Difference between $W_m$ and $W_\theta$ ($\Delta_D$) for $CO_2/N_2$

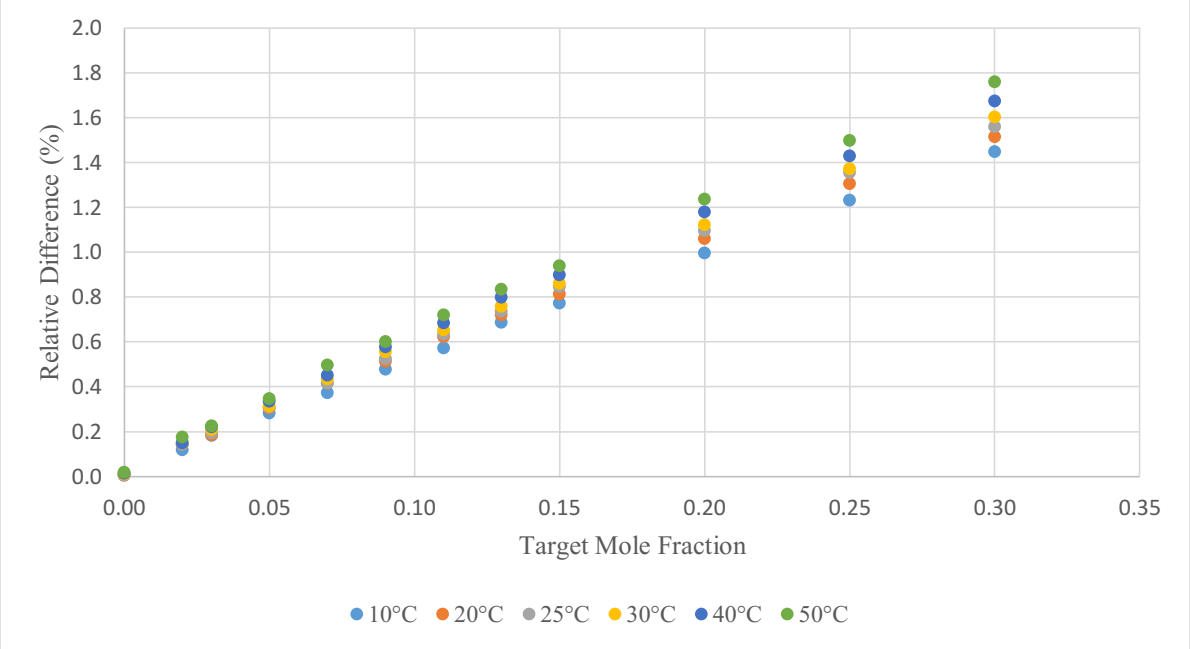



Figure 76. Relative difference between $W_m$ and $W_\theta$ ($\Delta_{RD}$) for $CO_2/N_2$

As is shown in Appendix A1.3, in the calculation of dry air (experimental dry air) $W$ for pathlength calibration, $W_\theta$ is determined according to the method given in Zuckerwar (2002) (called Zuckerwar's method). Therefore, a comparison of $W_\theta$ for dry air determined using the Zuckerwar's method (denoted by $W_{\theta_Z}$) and the NIST REFPROP software (denoted by $W_{\theta_N}$) needs to be made (see Table 28). This comparison is performed at 1 atm and from 0 to 55 °C in 5 °C increments. The differences $\Delta'_D$ $(= W_{\theta_Z} - W_{\theta_N})$ and relative differences $\Delta'_{RD}$ $(= (W_{\theta_Z} - W_{\theta_N})/W_{\theta_N} \times 100)$ between $W_{\theta_Z}$ and $W_{\theta_N}$ are all positive, and as the temperature increases $\Delta'_D$ and $\Delta'_{RD}$ both decrease. It is found that the dry air $W_\theta$ calculated using the Zuckerwar's method and the software are not significantly different. And since $\Delta'_D$ is much smaller than $\Delta_D$ for dry air, the effect of the simplification of dry air composition in the use of the software on the determination of $W_\theta$ for the binary gas mixtures with dry air as the carrier gas component should be negligible.

Table 28. Comparison between $W_{\theta_Z}$ and $W_{\theta_N}$ at 1 atm

| Temperature/°C | $W_{\theta_Z}$/(m/s) | $W_{\theta_N}$/(m/s) | $\Delta'_D$/(m/s) | $\Delta'_{RD}$/% |
|---|---|---|---|---|
| 0 | 331.451 | 331.443 | 0.008 | 0.0022 |
| 5 | 334.469 | 334.461 | 0.008 | 0.0022 |
| 10 | 337.458 | 337.451 | 0.007 | 0.0022 |
| 15 | 340.419 | 340.412 | 0.007 | 0.0021 |
| 20 | 343.352 | 343.345 | 0.007 | 0.0020 |
| 25 | 346.258 | 346.252 | 0.006 | 0.0018 |
| 30 | 349.138 | 349.133 | 0.005 | 0.0016 |
| 35 | 351.992 | 351.988 | 0.004 | 0.0013 |
| 40 | 354.821 | 354.818 | 0.003 | 0.0011 |
| 45 | 357.626 | 357.623 | 0.003 | 0.0008 |
| 50 | 360.406 | 360.404 | 0.002 | 0.0005 |
| 55 | 363.163 | 363.162 | 0.001 | 0.0002 |

## 5.3 Uncertainty Analysis of Gas Density and Composition Experimental Results

### 5.3.1 Binary Gas Mixtures in Group A

These binary gas mixtures refer to the ones with available thermodynamic data in the NIST REFPROP software, including n-hexane, n-heptane, n-octane, n-nonane, n-decane, toluene, cyclohexane, water/dry air and carbon dioxide/nitrogen. For these binary gas mixtures, the gas composition at the non-zero steps in each experiment was determined by equation of state analysis of the corresponding measured gas density with the use of the NIST REFPROP software, and the density was obtained from Equation (80). And the carrier gas density data $\rho^0$ come from the software as well. According to the given information, for $N_2$ in the range from 270 to 350 K at pressures less than 12 MPa the density uncertainty is 0.005% (Span et al., 2000). Based on comparisons with data with known uncertainty, within the experimental temperature and pressure range the density uncertainty for dry air is conservatively estimated to be 0.05% (Lemmon et al., 2000).

Uncertainty is denoted by $U$. The sources of the uncertainty of the measured gas density $U(\rho)$ can be divided into three categories: 1) the uncertainties of $\Delta m_{read}$, $\Delta V$ and the $\rho^0$ data at the zero-step $T_{DVS}$ and $P$; 2) the uncertainty of the zero-step $T_{DVS}$; and 3) the uncertainty of the zero-step $P$. The contribution to $U(\rho)$ from the first category, represented by $U(\rho)_1$, can be calculated as follows:

$$U(\rho)_1{}^2 = U(\rho^0)^2 + U\left(\frac{\Delta m_{read}}{\Delta V}\right)^2 \tag{84}$$

$$U\left(\frac{\Delta m_{read}}{\Delta V}\right)^2 = \left(\frac{\Delta m_{read}}{\Delta V}\right)^2 \left\{\left[\frac{U(\Delta m_{read})}{\Delta m_{read}}\right]^2 + \left[\frac{U(\Delta V)}{\Delta V}\right]^2\right\} \tag{85}$$

$$U(\Delta m_{read})^2 = U(m_{read}^{II} - m_{read}^{I})^2 = U(m_{read}^{II})^2 + U(m_{read}^{I})^2. \tag{86}$$

$U(\rho^0)$ is taken to be $0.005\%\rho^0$ for $N_2$ and $0.05\%\rho^0$ for dry air; $U(m_{read}^{II})$ and $U(m_{read}^{I})$ are equal to $1/\sqrt{3}$ μg (see Section 3.6); $\Delta V$ and $U(\Delta V)/\Delta V$ can be found in Appendix A4. The

contributions from the second and third categories, $U(\rho)_2$ and $U(\rho)_3$, can be estimated according to the changes in $\rho$ by altering $T_{DVS}$ by $\pm\, U(T_{DVS})$ and $P$ by $\pm\, U(P)$, respectively ($\rho^0$ is redetermined). $U(\rho)$ is equated to the square root of the sum of squares of $U(\rho)_1$, $U(\rho)_2$ and $U(\rho)_3$. Based on this analysis, $U(\rho)$ for all of these binary gas mixtures is found to be around 0.0015 kg/m$^3$.

For carbon dioxide/nitrogen, the H-EoS for nitrogen according to which $\rho^0$ is determined is also used in the establishment of the H-EoS for the mixture according to which $x$ is determined from $\rho$. Hence, the error in $x$ resulting from the inaccuracy of the mixture H-EoS is minimised. For the other binary gas mixtures (the ones with dry air as the carrier gas), the H-EoS for the carrier gas according to which $\rho^0$ is determined is based on the H-EoSs for the considered pure components of dry air with the mixing rules, and these are also used in the establishment of the mixture H-EoS. Consequently, the effect of the mixture H-EoS's inaccuracy on $x$ is also minimised. The temperature and pressure variations in each experiment were actually both very small, therefore the errors of the measured temperature and pressure values during the period of an experiment are respectively relatively constant.

The method for the estimation of the gas composition uncertainty $U(x)$ is basically as follows:

1) Keep the non-zero-step $T_{DVS}$ and $P$ the same but increase (or decrease) $\rho$ by $U(\rho)_1$; redetermine $x$; calculate the difference between the redetermined and the original $x$ as $\Delta x_\rho$.
2) Keep $\Delta m_{read}$, $\Delta V$ and both the zero- and non-zero-step $P$ the same but increase (or decrease) both the zero- and non-zero-step $T_{DVS}$ by $U(T_{DVS})$; redetermine $\rho^0$, $\rho$ then $x$; calculate the difference between the redetermined and the original $x$ as $\Delta x_{T_{DVS}}$.
3) Keep $\Delta m_{read}$, $\Delta V$ and both the zero- and non-zero-step $T_{DVS}$ the same but increase (or decrease) both the zero- and non-zero-step $P$ by $U(P)$; redetermine $\rho^0$, $\rho$ then $x$; calculate the difference between the redetermined and the original $x$ as $\Delta x_P$.
4) $U(x)$ is equated to the square root of the sum of squares of $\Delta x_\rho$, $\Delta x_{T_{DVS}}$ and $\Delta x_P$.

### 5.3.2 Binary Gas Mixtures in Group B

The carrier gas component in these binary gas mixtures is invariably dry air, and the non-carrier gas component is a vapour including acetone, methyl ethyl ketone, ethyl acetate, methanol, ethanol, isopropanol, dichloromethane, chloroform, 1,2-dichloroethane, m-/o-/p-xylene,

ethylbenzene, n-butylamine, limonene and α-pinene. The determination of the carrier gas density $\rho^0$ and the determination of the gas composition $x$ from the measured density $\rho$ are both based on the Van der Waals EoS. Using the same type of EoS for both $\rho^0$ and $x$ calculations is beneficial to the minimization of the error of $x$, in spite of the fact that using the NIST RERPROP software to determine $\rho^0$ can improve the accuracy of both $\rho^0$ and $\rho$.

In order to analyse the effect of using the Van der Waals EoS in the data analysis on the uncertainties of the experimental gas density and composition results, $U(\rho)$ and $U(x)$, for the binary gas mixtures in Group A except carbon dioxide/nitrogen, $\rho^0$ (dry air density), $\rho$ and $x$ were redetermined by using the same method as that for the binary gas mixtures in Group B, i.e. based on the Van der Waals EoS. By means of comparisons with the values determined based on the H-EoSs with the use of the software, the redetermined $\rho$ is found to be around 0.0005 kg/m$^3$ higher (the redetermined dry air density $\rho^0$ is also around 0.0005 kg/m$^3$ higher) and the discrepancy in $x$ is typically much less than 0.3% (the largest discrepancy is approximately 0.3%) for all the considered binary gas mixtures at different experimental temperatures and $x_T$ levels. Therefore, for the binary gas mixtures in Group B, $U(\rho)$ can be considered the same as that reported in the previous section, i.e. 0.0015 kg/m$^3$ (the discrepancy in $\rho$ is well within this range); the estimation of $U(x)$ should take the 0.3%$x$ discrepancy into account and the estimation method is given below.

Firstly, based on the method for the binary gas mixtures in Group A, a gas composition uncertainty can be obtained. It is noteworthy that $U(\rho^0)/\rho^0$ is assumed to be the same for the calculation of $U(\rho)_1$, i.e. 500 ppm for dry air. This uncertainty can be represented by $U(x)_A$ and is expressed in %SAT. A 0.3%$x$ discrepancy corresponds to a gas composition error of $0.3x/x_{SAT}$ %SAT where $x_{SAT}$ refers to the saturated mole fraction of the vapour component. The maximum value of $x/x_{SAT}$ is around 0.95 at the highest $x_T$ level, consequently the maximum value of the error is around 0.3%SAT. This is added to $U(x)_A$, and the sum is considered to be the uncertainty of the gas composition experimental results $U(x)$ for the binary gas mixtures in Group B. For example, if $U(x)_A$ is 1%SAT, then $U(x)$ is estimated to be 1.3%SAT.

## 5.4 Gas Composition Measurement with an SoS Sensor

The experimental results $T_{SoS}$, $W_m$ and $x$ for a binary gas mixture at different experimental temperatures including the data at the pathlength calibration points ($T_{SoS}$, $W_m = W^0$ and $x = 0$) are fitted to one of the following 3-D polynomial equations:

$$Z = P_{00} + P_{10}X + P_{01}Y + P_{20}X^2 + P_{11}XY + P_{02}Y^2 \tag{87}$$

$$Z = P_{00} + P_{10}X + P_{01}Y + P_{20}X^2 + P_{11}XY + P_{02}Y^2 + P_{30}X^3 + P_{21}X^2Y + P_{12}XY^2 + P_{03}Y^3 \tag{88}$$

$$Z = P_{00} + P_{10}X + P_{01}Y + P_{20}X^2 + P_{11}XY + P_{02}Y^2 + P_{30}X^3 + P_{21}X^2Y + P_{12}XY^2 + P_{03}Y^3 + P_{40}X^4 + P_{31}X^3Y + P_{22}X^2Y^2 + P_{13}XY^3 + P_{04}Y^4 \tag{89}$$

where $X$, $Y$ and $Z$ represent temperature in °C, SoS in m/s and gas composition (dimensionless); $P_{00}$, $P_{10}$, $P_{01}$, $P_{20}$, $P_{11}$, $P_{02}$, $P_{30}$, $P_{21}$, $P_{12}$, $P_{03}$, $P_{40}$, $P_{31}$, $P_{22}$, $P_{13}$ and $P_{04}$ are the polynomial coefficients.

The SoS sensor can be used for the measurement of gas composition under atmospheric pressure by substituting the temperature measured by the SoS temperature probe and the measured SoS into the polynomial equation which is specific for the binary gas mixture under test. The temperature should be within the experimental temperature range in this research project. The applicable gas composition range of the polynomial equation is also considered to be the same as the experimental range. For the carbon dioxide/nitrogen binary mixture, the carbon dioxide mole fraction should be below around 0.3; for the other binary gas mixtures, the non-carrier gas component (vapour) should typically be less than 95% saturated. It is worth mentioning that at different temperatures the saturated vapour mole fraction is different. The validity of the extrapolation of the polynomial equation beyond these temperature and composition ranges is not discussed in this thesis. The establishment of the equation is based on the dependence of SoS on temperature and gas composition. The pressure dependence is ignored because the sensitivity of SoS to the atmospheric pressure variations is much less significant than to the temperature and gas composition variations.

The pathlength is calibrated according to Equation (82) by multiplying the real gas SoS of dry air (if the to-be-tested binary gas mixture is dry air contained) or nitrogen (if the to-be-tested mixture is carbon dioxide/nitrogen) by the corresponding measured ToF. With the calibrated pathlength, Equation (83) is then used for SoS measurement. These are the same as the pathlength calibration and SoS determination methods used in this research project. The difference in temperature between the calibration point and the measurement point should not give rise to significant change in pathlength. And provided that the measurement is going to be performed at a significantly different temperature, the pathlength needs to be recalibrated.

The uncertainty in gas composition measurement using the SoS sensor $U(x)_{SoS}$ based on the above methods is mainly attributed to the uncertainty of the gas composition experimental results $U(x)$ which are used in the polynomial equation fitting and also the error of the fitting. The latter can be estimated according to the fitting residuals which are the discrepancies between the gas composition experimental results and the corresponding predicted values from the equation. It is found that the effect of the fitting error is less significant (in most cases much less significant) than the effect of $U(x)$ on $U(x)_{SoS}$. $U(x)$ is not given in this thesis, but it can be considered the same as $U(x)_{SoS}$ despite the fact that the latter is slightly higher.

The form of the polynomial equation together with the coefficients, and the estimated $U(x)_{SoS}$ at the experimental temperatures in this research project for each binary gas mixture are given in Tables 29 to 53. The statistics for characterising the goodness of fit including sum of squares due to error (SSE), R-square ($R^2$) and root mean squared error (RMSE) (MathWorks [*Online*]) are also shown in these tables.

For the organic vapour/dry air and water vapour/dry air binary gas mixtures, $U(x)_{SoS}$ is expressed in %SAT, which means, e.g. for n-heptane/dry air at 25 °C, the gas composition can be measured with an uncertainty of 0.4% of the saturated vapour mole fraction at 25 °C and atmospheric pressure; for $H_2O$/dry air at 45 °C, the gas composition can be measured with an uncertainty of 1.8% of the saturated vapour mole fraction at 45 °C and atmospheric pressure. If the measurement is performed at a temperature between two adjacent listed temperatures $T_1$ and $T_2$ in the tables ($T_1 < T_2$), then the $U(x)_{SoS}$ in %SAT can be considered equal to that corresponding to $T_1$. For instance, the $U(x)_{SoS}$ for a measurement on n-heptane/dry air at 50 °C between the two adjacent listed temperatures 45 and 55 °C is estimated to be 0.2%SAT (0.2% of the saturated vapour mole fraction at 50 °C and atmospheric pressure), which is the same as the uncertainty in %SAT corresponding to the temperature of 45 °C. For carbon

dioxide/nitrogen, the $U(x)_{SoS}$ at any temperature within the range from 10 to 50 °C is estimated to be 0.0006. The 3-D polynomial surfaces plotted from the fitted polynomial equation for each binary gas mixture are given in Figures 77 to 101.

The SoS sensor used in this research project is a prototype. Its manufacture based on the same or reasonably similar mechanical and electronics designs, with the same type of ultrasonic transducers operated at the same fixed acoustic frequency, and with the PT100s calibrated to approximately the same temperature measurement accuracy should generate SoS data equivalent to that reported in this thesis. Since the fitted polynomial equations used for gas composition determination are not pressure dependent and the effect of atmospheric pressure variations on SoS is not significant, the barometric sensor in theory is no longer needed (for the calculation of the real gas SoS of dry air or nitrogen in pathlength calibration the pressure can be assumed equal to the standard atmospheric pressure 1013.25 mbar). However, considering the barometric sensor unit is actually very simple and inexpensive, it is still recommended to keep the unit in the manufactured SoS sensors' electronics in case some potential applications of the SoS sensors may require tracking the atmospheric pressure. It is noteworthy that for the experiments performed in this research project an accurate pressure measurement was necessary because the measurement of gas density for composition determination required accurate pressure data.

Based on the same methods for pathlength calibration and SoS determination, the difference in the measured gas composition results for a binary gas mixture according to the same polynomial equation between using the prototype SoS sensor and a manufactured one is considered to be primarily attributed to the inconsistencies in temperature and SoS measurements. The temperature measurement inconsistency refers to the deviation between the temperatures measured by the prototype's temperature probe ($T_{SoS}$) and by a manufactured SoS sensor's temperature probe ($T'_{SoS}$) at the same true temperature. Based on the assumption that $T'_{SoS}$ has the same uncertainty as $T_{SoS}$ (12.5 m°C), the uncertainty of the deviation, $U(T_{SoS} - T'_{SoS})$ is estimated to be around 17.7 m°C according to $U(T_{SoS} - T'_{SoS}) = \sqrt{U(T_{SoS})^2 + U(T'_{SoS})^2} = \sqrt{12.5^2 + 12.5^2}$. The SoS measurement inconsistency refers to the deviation between the SoS measured by the prototype and a second manufactured SoS sensor at the same true SoS. The primary reason for this is the temperature measurement inconsistency in pathlength calibration which has an estimated uncertainty of 17.7 m°C as derived above and this could typically lead to about 0.01 m/s SoS measurement inconsistency.

In comparisons with the $U(x)_{SoS}$ reported in this thesis, the discrepancy in measured gas composition between using the prototype and a second manufactured SoS sensor resulting from the temperature and SoS measurement inconsistencies is not significant. Therefore, the gas composition measurement uncertainty by using a manufactured SoS sensor can be considered the same as that by using the prototype, and thus can be estimated according to the reported $U(x)_{SoS}$ as well. It should be noted the SoS measurement uncertainty of a manufactured SoS sensor should also be approximately the same as that of the prototype, i.e. 0.1% or 0.14% (see Section 5.1), however, the SoS measurement inconsistency is only about 0.003% typically.

Table 29. Fitted 3-D polynomial equation and estimated $U(x)_{SoS}$ (n-hexane/dry air)

| | | | | | |
|---|---|---|---|---|---|
| $P_{00}$ | 4.13230E+00 | $P_{11}$ | -5.06238E-05 | $P_{12}$ | 6.88894E-08 |
| $P_{10}$ | 1.03274E-02 | $P_{02}$ | 7.92581E-05 | $P_{03}$ | -7.10336E-08 |
| $P_{01}$ | -3.09343E-02 | $P_{30}$ | 3.01265E-08 | | |
| $P_{20}$ | 6.60008E-06 | $P_{21}$ | -2.68455E-08 | | |
| Goodness of fit | | | | | |
| SSE | 3.0E-06 | $R^2$ | 0.999997 | RMSE | 1.7E-04 |
| Polynomial equation used for fitting: Equation (88) | | | | | |

| Temperature/°C | 5 | 15 | 25 | 35 | 45 |
|---|---|---|---|---|---|
| $U(x)_{SoS}$/%SAT | 0.41 | 0.27 | 0.20 | 0.17 | 0.15 |

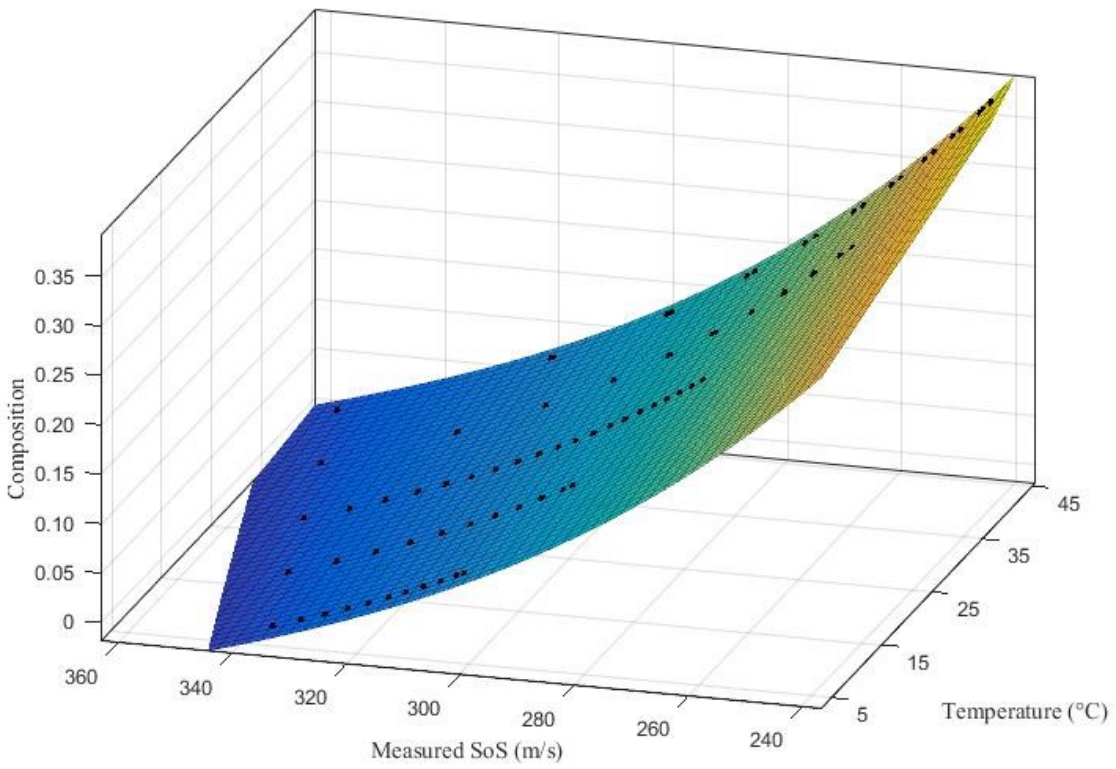



Figure 77. 3-D polynomial surface for n-hexane/dry air

Table 30. Fitted 3-D polynomial equation and estimated $U(x)_{SoS}$ (n-heptane/dry air)

| | | | | | |
|---|---|---|---|---|---|
| $P_{00}$ | 3.07363E+00 | $P_{11}$ | -3.75862E-05 | $P_{12}$ | 4.88688E-08 |
| $P_{10}$ | 7.95572E-03 | $P_{02}$ | 5.56450E-05 | $P_{03}$ | -4.83109E-08 |
| $P_{01}$ | -2.24090E-02 | $P_{30}$ | -1.14009E-09 | | |
| $P_{20}$ | 2.95518E-06 | $P_{21}$ | -9.30566E-09 | | |
| Goodness of fit | | | | | |
| SSE | 8.3E-07 | $R^2$ | 0.999997 | RMSE | 8.2E-05 |
| Polynomial equation used for fitting: Equation (88) | | | | | |

| Temperature/°C | 5 | 15 | 25 | 35 | 45 | 55 |
|---|---|---|---|---|---|---|
| $U(x)_{SoS}$/%SAT | 1.2 | 0.65 | 0.40 | 0.27 | 0.20 | 0.16 |

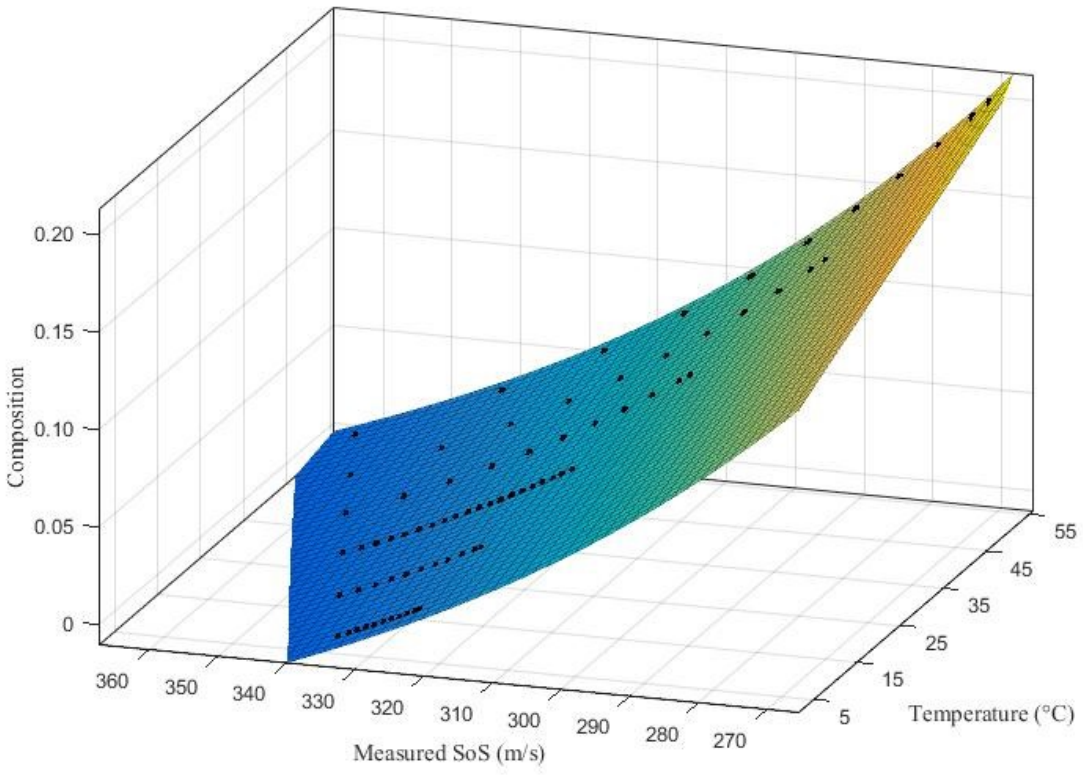



Figure 78. 3-D polynomial surface for n-heptane/dry air

Table 31. Fitted 3-D polynomial equation and estimated $U(x)_{SoS}$ (n-octane/dry air)

| | | | | | |
|---|---|---|---|---|---|
| $P_{00}$ | 2.33105E+00 | $P_{11}$ | -1.68552E-05 | $P_{12}$ | 1.65292E-08 |
| $P_{10}$ | 4.50940E-03 | $P_{02}$ | 3.76062E-05 | $P_{03}$ | -3.01333E-08 |
| $P_{01}$ | -1.61867E-02 | $P_{30}$ | 6.11885E-09 | | |
| $P_{20}$ | -3.39594E-06 | $P_{21}$ | 8.31820E-09 | | |
| Goodness of fit | | | | | |
| SSE | 3.3E-07 | $R^2$ | 0.999991 | RMSE | 5.1E-05 |
| Polynomial equation used for fitting: Equation (88) | | | | | |

| Temperature/°C | 5 | 15 | 25 | 35 | 45 | 55 |
|---|---|---|---|---|---|---|
| $U(x)_{SoS}$/%SAT | 3.3 | 1.8 | 1.0 | 0.59 | 0.39 | 0.26 |

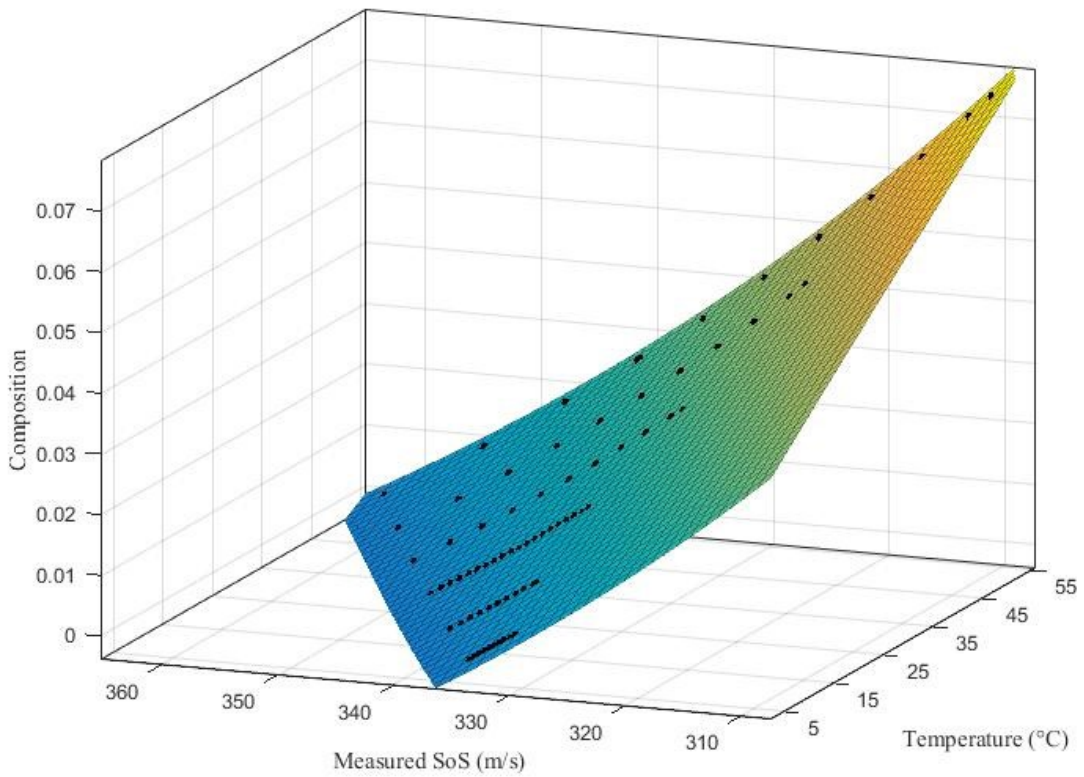



Figure 79. 3-D polynomial surface for n-octane/dry air

Table 32. Fitted 3-D polynomial equation and estimated $U(x)_{SoS}$ (n-nonane/dry air)

| | | | | | |
|---|---|---|---|---|---|
| $P_{00}$ | 9.83577E-01 | $P_{01}$ | -4.91310E-03 | $P_{11}$ | -4.37583E-06 |
| $P_{10}$ | 2.07029E-03 | $P_{20}$ | 3.31581E-08 | $P_{02}$ | 5.87116E-06 |
| Goodness of fit | | | | | |
| SSE | 1.6E-07 | $R^2$ | 0.999964 | RMSE | 3.8E-05 |
| Polynomial equation used for fitting: Equation (87) | | | | | |

| Temperature/°C | 15 | 25 | 35 | 45 | 55 |
|---|---|---|---|---|---|
| $U(x)_{SoS}$/%SAT | 5.3 | 2.9 | 1.5 | 0.88 | 0.54 |

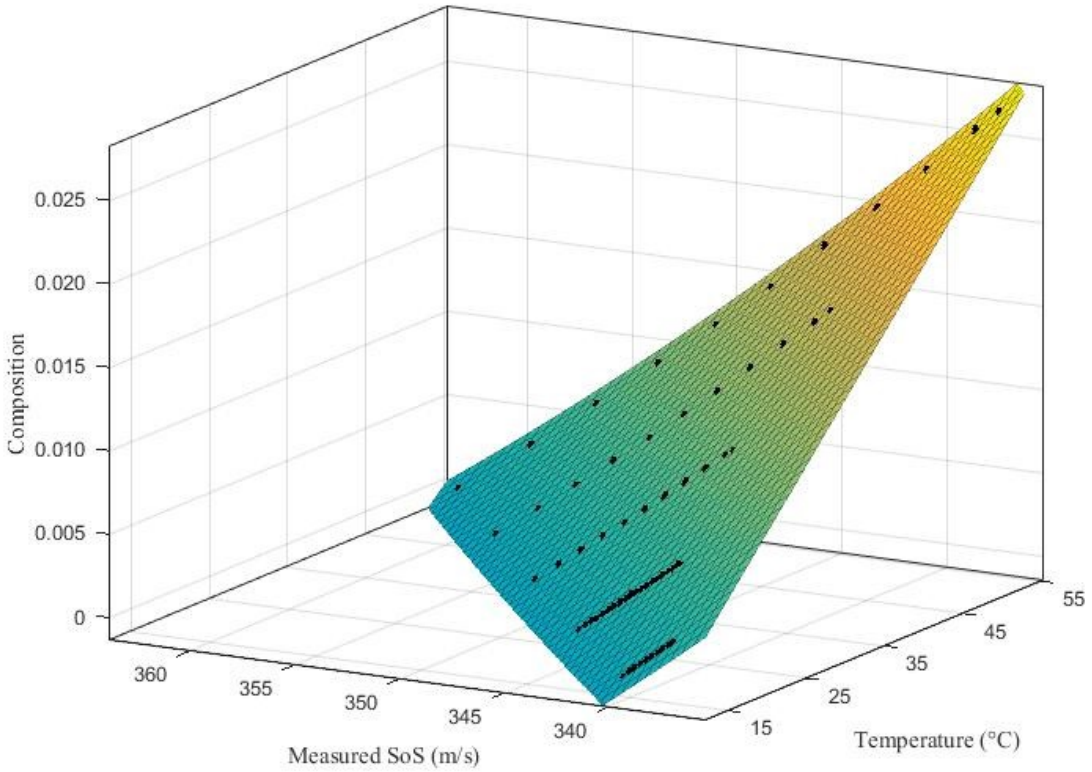



Figure 80. 3-D polynomial surface for n-nonane/dry air

Table 33. Fitted 3-D polynomial equation and estimated $U(x)_{SoS}$ (n-decane/dry air)

| | | | | | |
|---|---|---|---|---|---|
| $P_{00}$ | -2.97798E+00 | $P_{11}$ | -1.79169E-04 | $P_{12}$ | 2.87576E-07 |
| $P_{10}$ | 2.83442E-02 | $P_{02}$ | -6.02068E-05 | $P_{03}$ | 4.63327E-08 |
| $P_{01}$ | 2.38485E-02 | $P_{30}$ | 7.97190E-08 | | |
| $P_{20}$ | 8.94634E-05 | $P_{21}$ | -2.83453E-07 | | |
| Goodness of fit | | | | | |
| SSE | 7.6E-08 | $R^2$ | 0.999845 | RMSE | 3.3E-05 |
| Polynomial equation used for fitting: Equation (88) | | | | | |

| Temperature/°C | 25 | 35 | 45 | 55 |
|---|---|---|---|---|
| $U(x)_{SoS}$/%SAT | 7.5 | 4 | 2.2 | 1.3 |

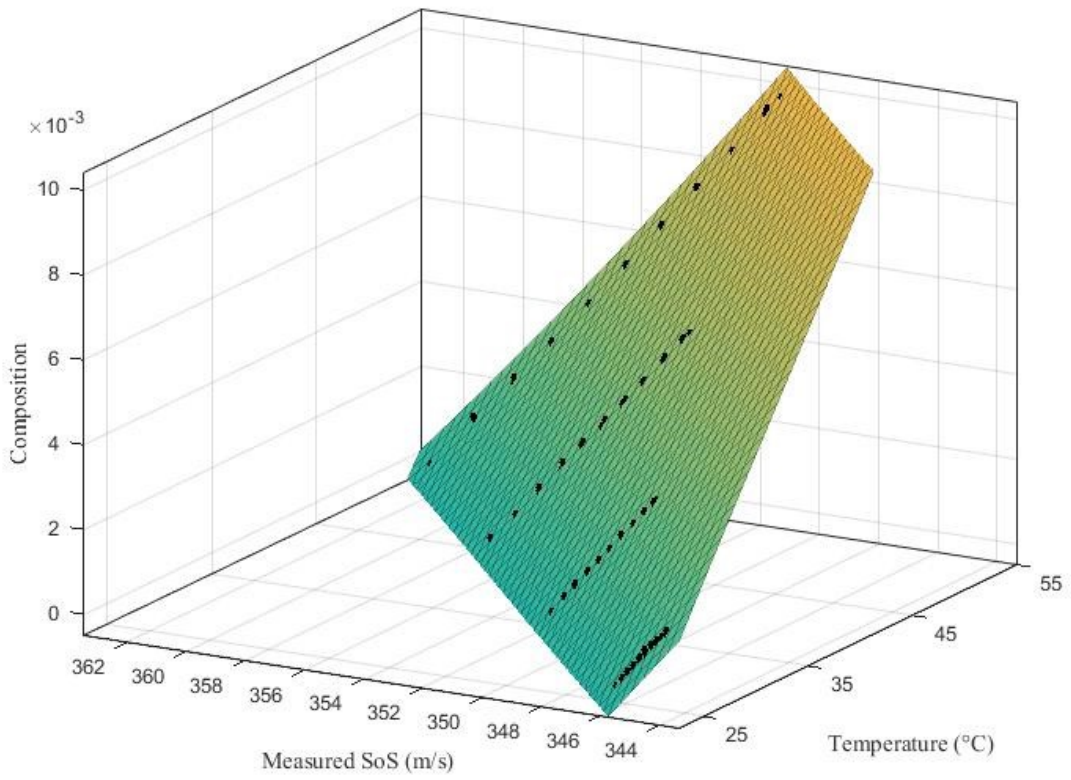



Figure 81. 3-D polynomial surface for n-decane/dry air

Table 34. Fitted 3-D polynomial equation and estimated $U(x)_{SoS}$ (toluene/dry air)

| | | | | | |
|---|---|---|---|---|---|
| $P_{00}$ | 3.17490E+00 | $P_{11}$ | -2.32552E-05 | $P_{12}$ | 2.74028E-08 |
| $P_{10}$ | 5.89017E-03 | $P_{02}$ | 4.97851E-05 | $P_{03}$ | -4.03698E-08 |
| $P_{01}$ | -2.16445E-02 | $P_{30}$ | 9.15476E-09 | | |
| $P_{20}$ | -1.31460E-06 | $P_{21}$ | -1.98725E-09 | | |
| Goodness of fit | | | | | |
| SSE | 3.5E-07 | $R^2$ | 0.999997 | RMSE | 5.3E-05 |
| Polynomial equation used for fitting: Equation (88) | | | | | |

| Temperature/°C | 5 | 15 | 25 | 35 | 45 | 55 |
|---|---|---|---|---|---|---|
| $U(x)_{SoS}$/%SAT | 2.0 | 1.1 | 0.66 | 0.42 | 0.29 | 0.21 |

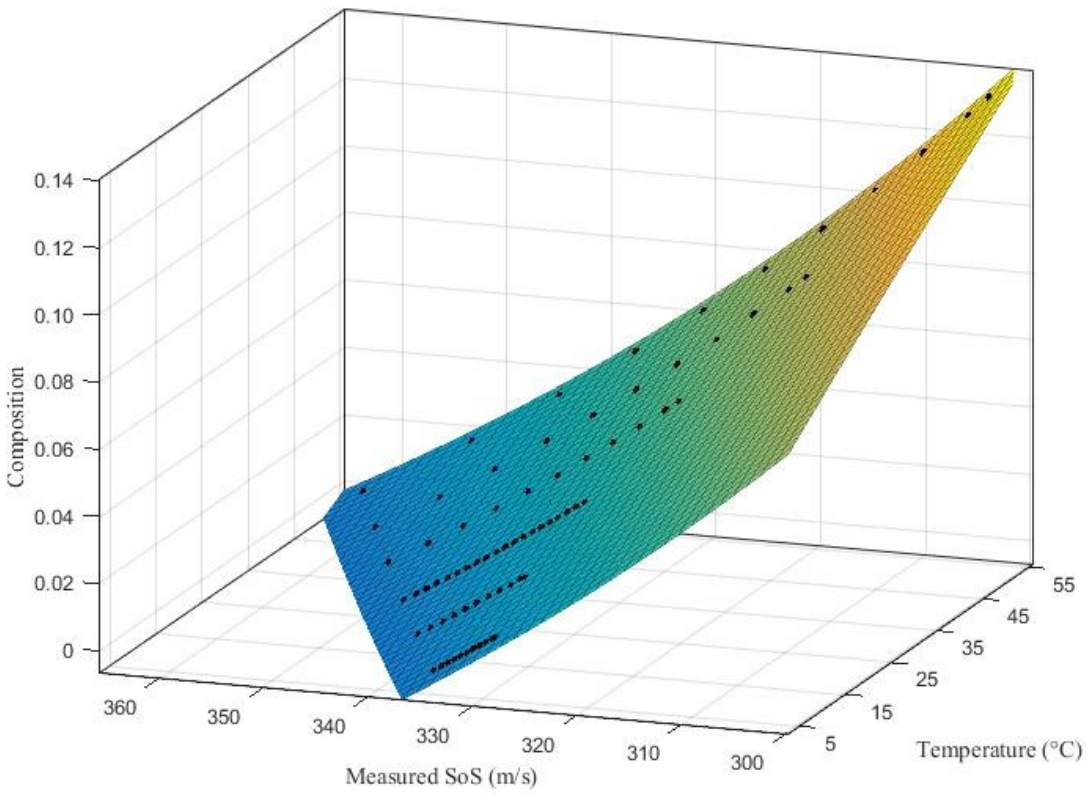



Figure 82. 3-D polynomial surface for toluene/dry air

Table 35. Fitted 3-D polynomial equation and estimated $U(x)_{SoS}$ (cyclohexane/dry air)

| | | | | | |
|---|---|---|---|---|---|
| $P_{00}$ | 4.15398E+00 | $P_{11}$ | -4.69697E-05 | $P_{12}$ | 6.57608E-08 |
| $P_{10}$ | 9.73478E-03 | $P_{02}$ | 7.59188E-05 | $P_{03}$ | -6.73023E-08 |
| $P_{01}$ | -3.03044E-02 | $P_{30}$ | 3.70416E-08 | | |
| $P_{20}$ | 2.47438E-06 | $P_{21}$ | -2.27968E-08 | | |
| Goodness of fit | | | | | |
| SSE | 2.2E-06 | $R^2$ | 0.999998 | RMSE | 1.4E-04 |
| Polynomial equation used for fitting: Equation (88) | | | | | |

| Temperature/°C | 15 | 25 | 35 | 45 | 55 |
|---|---|---|---|---|---|
| $U(x)_{SoS}$/%SAT | 0.39 | 0.27 | 0.20 | 0.17 | 0.16 |

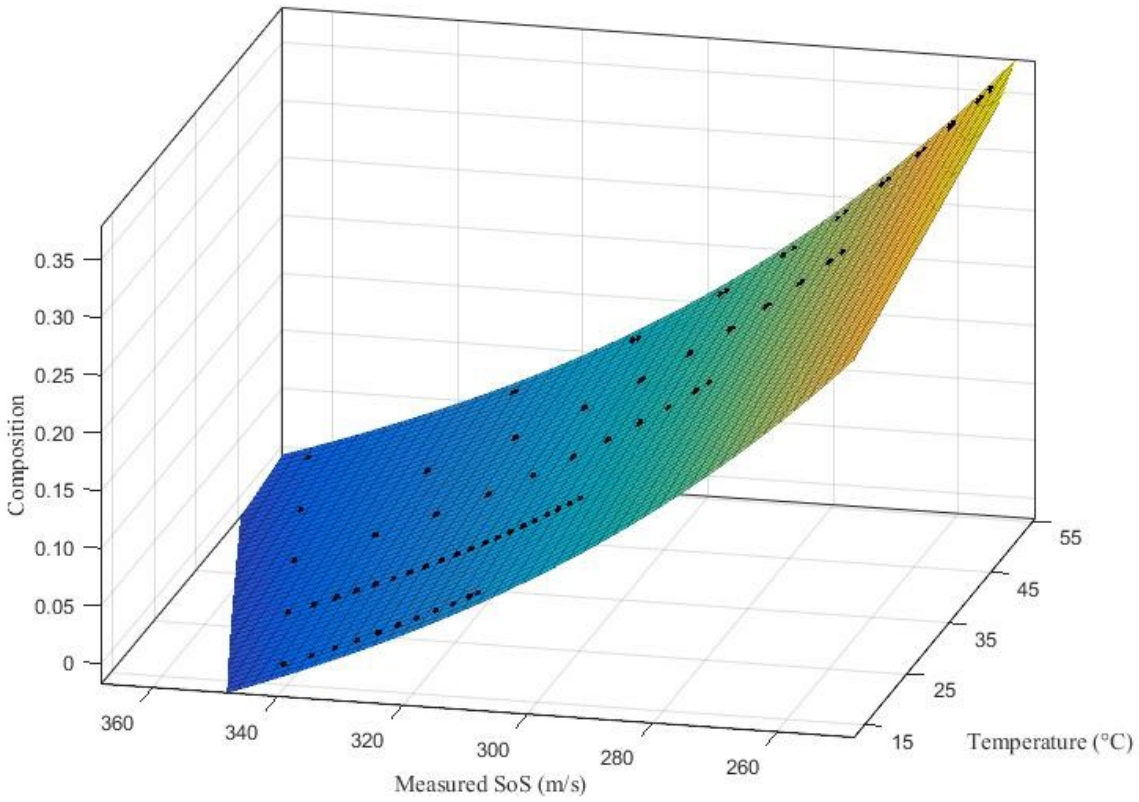



Figure 83. 3-D polynomial surface for cyclohexane/dry air

Table 36. Fitted 3-D polynomial equation and estimated $U(x)_{SoS}$ (water/dry air)

| | | | | | |
|---|---|---|---|---|---|
| $P_{00}$ | -4.9554263E+03 | $P_{11}$ | 1.5857248E-01 | $P_{12}$ | -2.3747004E-04 |
| $P_{10}$ | -2.6483154E+01 | $P_{02}$ | -1.3293214E-01 | $P_{03}$ | 1.3259475E-04 |
| $P_{01}$ | 4.4444293E+01 | $P_{30}$ | -2.8522409E-05 | | |
| $P_{20}$ | -4.7746696E-02 | $P_{21}$ | 1.4302422E-04 | | |
| Goodness of fit | | | | | |
| SSE | 5.8E-05 | $R^2$ | 0.999284 | RMSE | 9.2E-04 |
| Polynomial equation used for fitting: Equation (88) | | | | | |

| Temperature/°C | 25 | 35 | 45 | 55 |
|---|---|---|---|---|
| $U(x)_{SoS}$/%SAT | 5.2 | 2.9 | 1.8 | 1.1 |

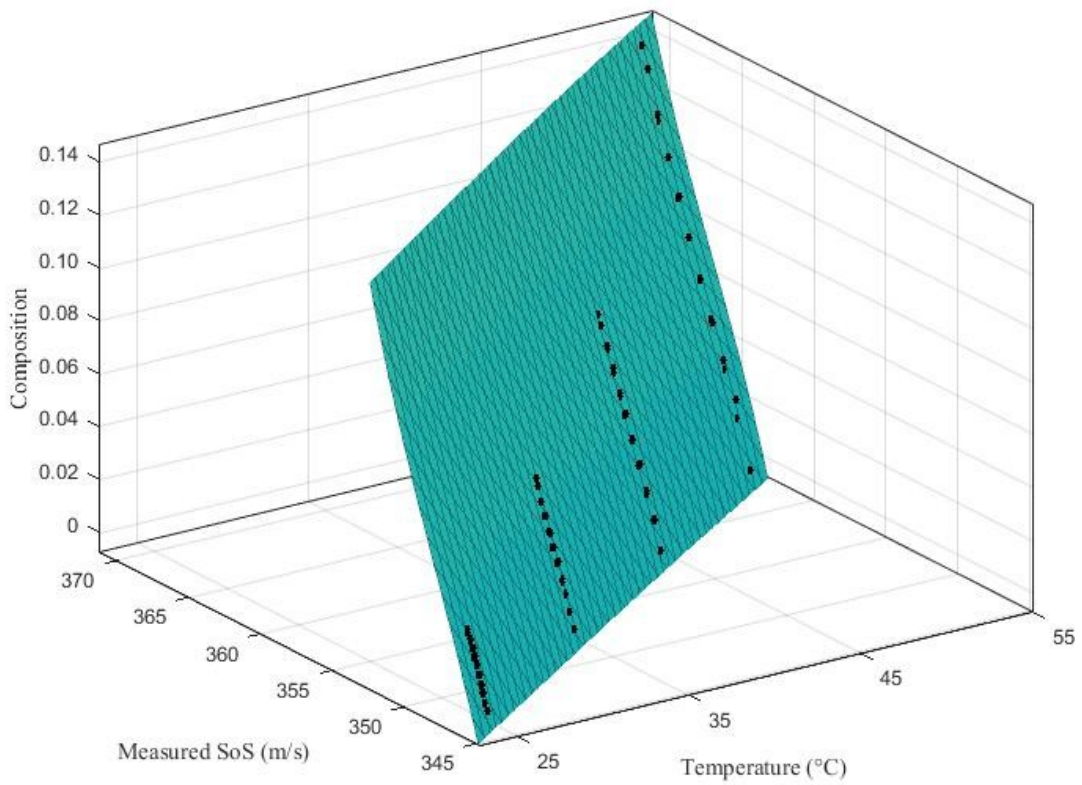



Figure 84. 3-D polynomial surface for water/dry air

Table 37. Fitted 3-D polynomial equation and estimated $U(x)_{SoS}$ (acetone/dry air)

| | | | | | |
|---|---|---|---|---|---|
| $P_{00}$ | 7.58568E+00 | $P_{11}$ | -8.86514E-05 | $P_{12}$ | 1.17938E-07 |
| $P_{10}$ | 1.87508E-02 | $P_{02}$ | 1.36952E-04 | $P_{03}$ | -1.19818E-07 |
| $P_{01}$ | -5.51152E-02 | $P_{30}$ | 1.63207E-08 | | |
| $P_{20}$ | 1.35162E-05 | $P_{21}$ | -4.75188E-08 | | |
| Goodness of fit | | | | | |
| SSE | 1.4E-05 | $R^2$ | 0.999986 | RMSE | 4.0E-04 |
| Polynomial equation used for fitting: Equation (88) | | | | | |

| Temperature/°C | 5 | 15 | 25 | 35 |
|---|---|---|---|---|
| $U(x)_{SoS}$/%SAT | 0.82 | 0.63 | 0.53 | 0.48 |

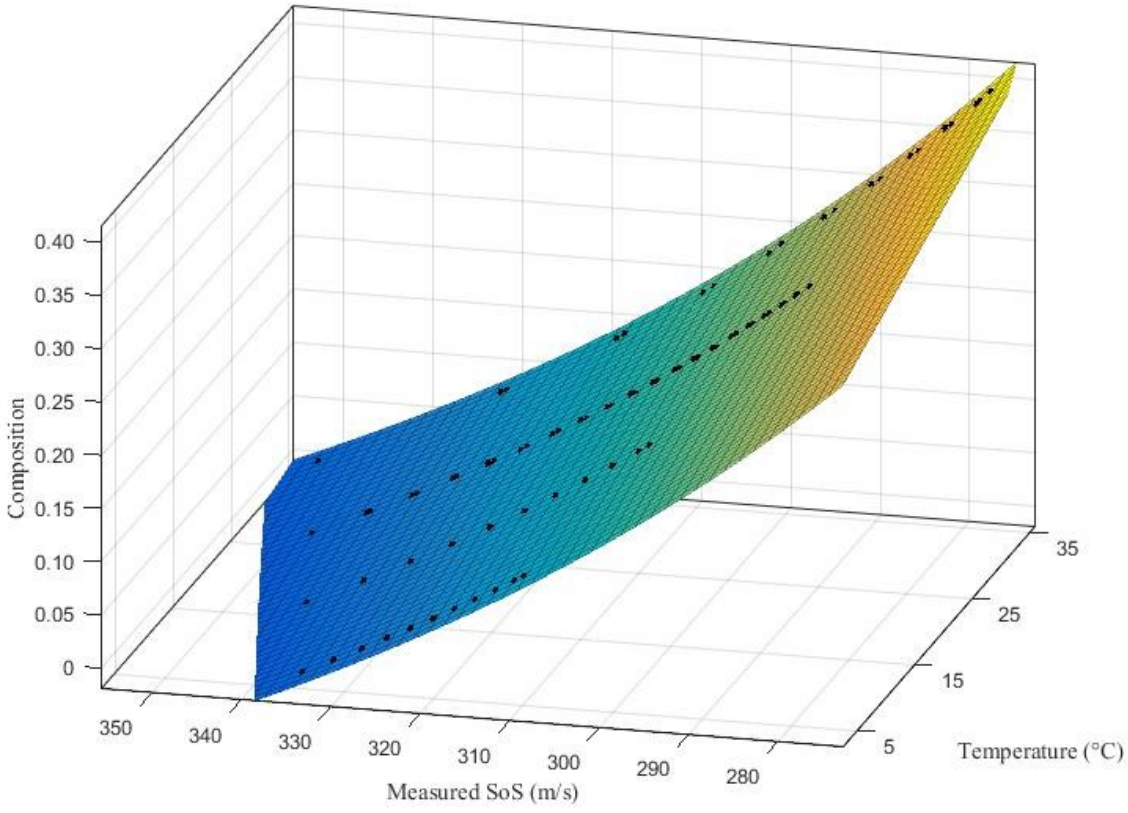



Figure 85. 3-D polynomial surface for acetone/dry air

Table 38. Fitted 3-D polynomial equation and estimated $U(x)_{SoS}$ (methyl ethyl ketone/dry air)

| | | | | | |
|---|---|---|---|---|---|
| $P_{00}$ | 5.27106E+00 | $P_{11}$ | -5.92284E-05 | $P_{12}$ | 7.61026E-08 |
| $P_{10}$ | 1.27688E-02 | $P_{02}$ | 9.65759E-05 | $P_{03}$ | -8.45768E-08 |
| $P_{01}$ | -3.86209E-02 | $P_{30}$ | 4.03755E-09 | | |
| $P_{20}$ | 3.39944E-06 | $P_{21}$ | -1.20180E-08 | | |
| Goodness of fit | | | | | |
| SSE | 1.0E-05 | $R^2$ | 0.999990 | RMSE | 2.8E-04 |
| Polynomial equation used for fitting: Equation (88) | | | | | |

| Temperature/°C | 5 | 15 | 25 | 35 | 45 | 55 |
|---|---|---|---|---|---|---|
| $U(x)_{SoS}$/%SAT | 1.3 | 0.87 | 0.66 | 0.54 | 0.49 | 0.46 |

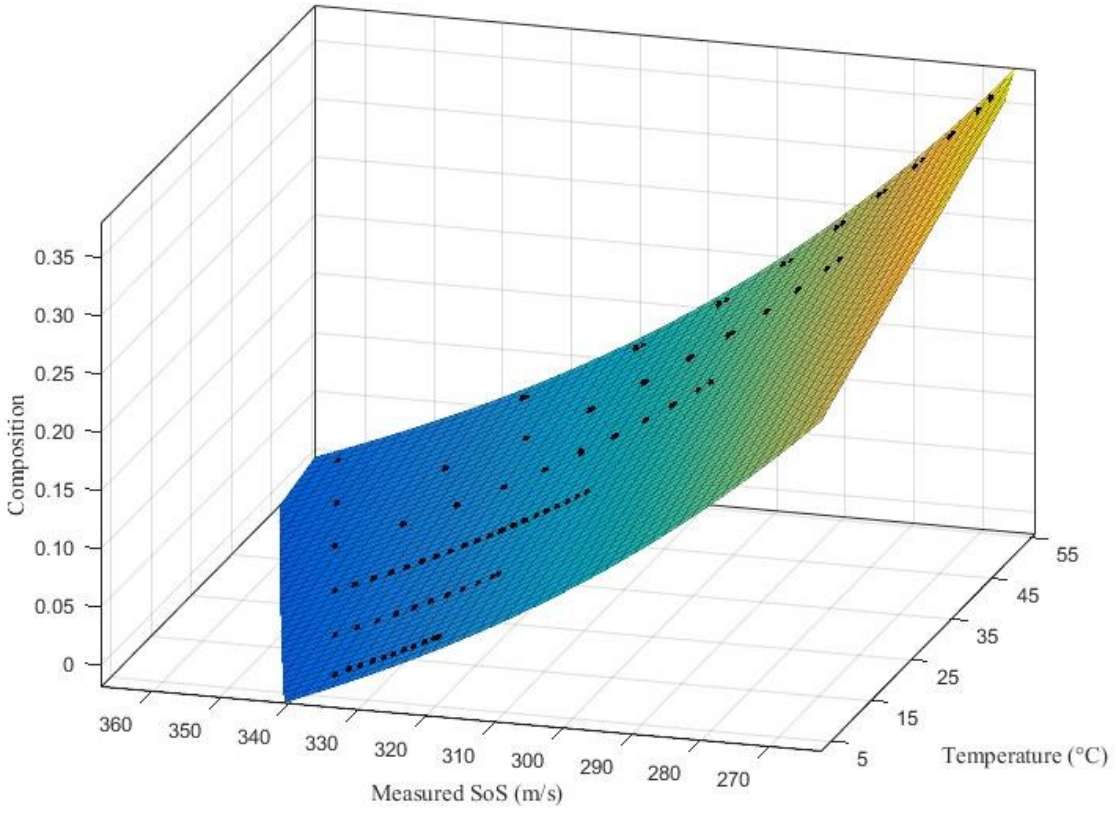



Figure 86. 3-D polynomial surface for methyl ethyl ketone/dry air

Table 39. Fitted 3-D polynomial equation and estimated $U(x)_{SoS}$ (ethyl acetate/dry air)

| | | | | | |
|---|---|---|---|---|---|
| $P_{00}$ | 4.11218E+00 | $P_{11}$ | -4.65270E-05 | $P_{12}$ | 6.29683E-08 |
| $P_{10}$ | 9.70988E-03 | $P_{02}$ | 7.78153E-05 | $P_{03}$ | -7.01031E-08 |
| $P_{01}$ | -3.04966E-02 | $P_{30}$ | 2.64892E-09 | | |
| $P_{20}$ | 3.52610E-06 | $P_{21}$ | -1.28965E-08 | | |
| Goodness of fit | | | | | |
| SSE | 7.9E-06 | $R^2$ | 0.999993 | RMSE | 2.5E-04 |
| Polynomial equation used for fitting: Equation (88) | | | | | |

| Temperature/°C | 5 | 15 | 25 | 35 | 45 | 55 |
|---|---|---|---|---|---|---|
| $U(x)_{SoS}$/%SAT | 1.1 | 0.75 | 0.58 | 0.50 | 0.47 | 0.45 |

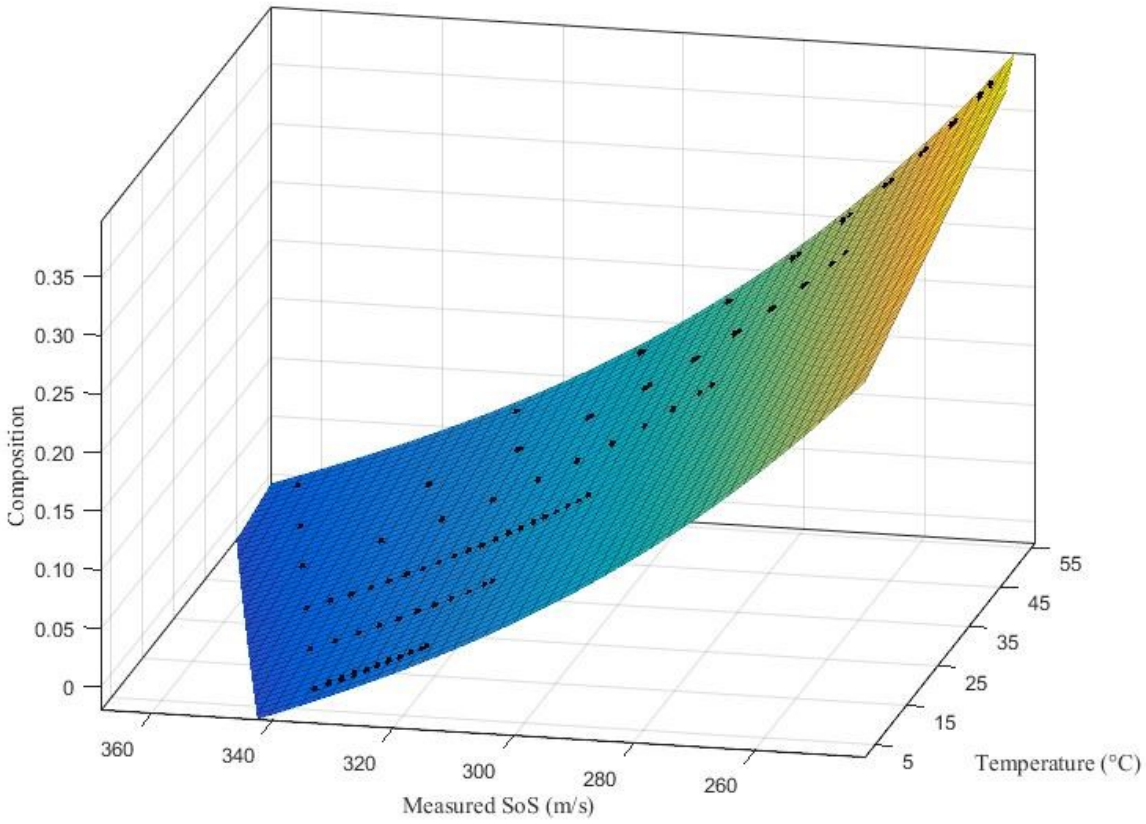



Figure 87. 3-D polynomial surface for ethyl acetate/dry air

Table 40. Fitted 3-D polynomial equation and estimated $U(x)_{SoS}$ (methanol/dry air)

| | | | | | |
|---|---|---|---|---|---|
| $P_{00}$ | 7.2924519E+03 | $P_{02}$ | 3.6877245E-01 | $P_{40}$ | -1.1725650E-07 |
| $P_{10}$ | -2.6793556E-01 | $P_{30}$ | -2.3104681E-04 | $P_{31}$ | 7.3424352E-07 |
| $P_{01}$ | -8.4911568E+01 | $P_{21}$ | 7.0840830E-04 | $P_{22}$ | -1.1717126E-06 |
| $P_{20}$ | -1.0637038E-01 | $P_{12}$ | -1.8378588E-04 | $P_{13}$ | 2.8067036E-07 |
| $P_{11}$ | 3.0914383E-02 | $P_{03}$ | -7.0741360E-04 | $P_{04}$ | 5.0521043E-07 |
| Goodness of fit | | | | | |
| SSE | 1.6E-04 | $R^2$ | 0.999873 | RMSE | 1.2E-03 |
| Polynomial equation used for fitting: Equation (89) | | | | | |

| Temperature/°C | 5 | 15 | 25 | 35 | 45 |
|---|---|---|---|---|---|
| $U(x)_{SoS}$/%SAT | 9.2 | 5.5 | 3.4 | 2.2 | 1.5 |

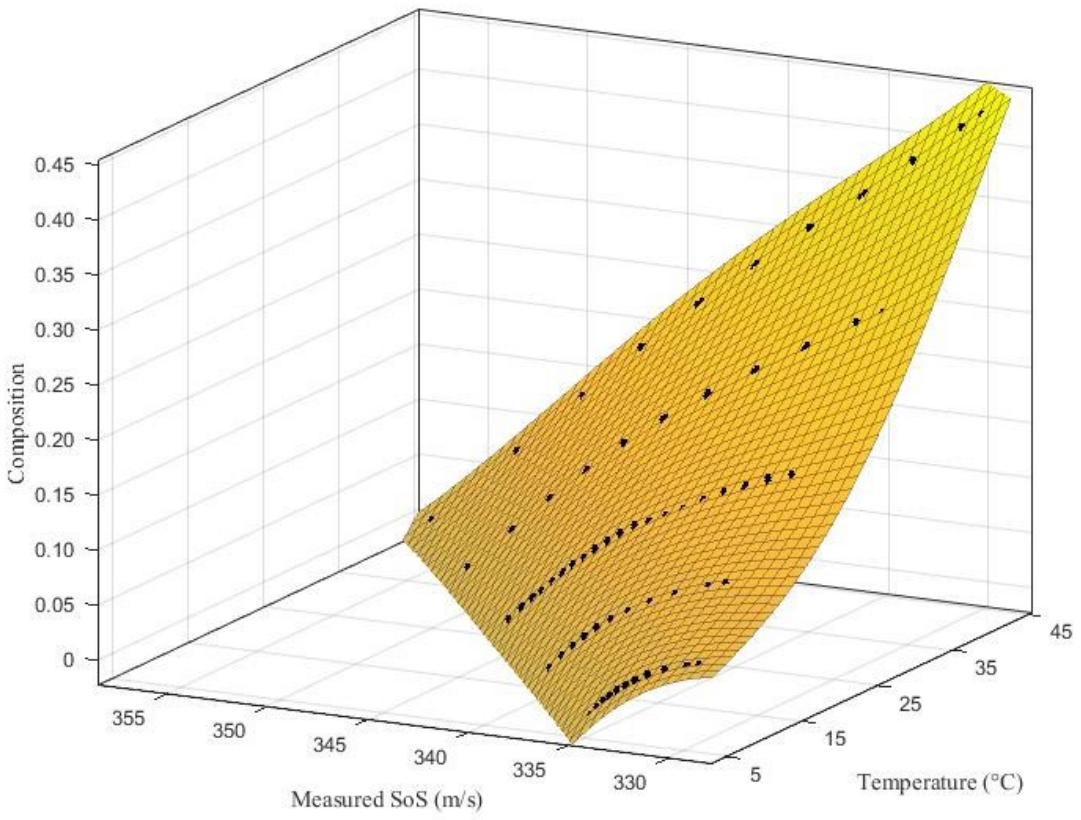



Figure 88. 3-D polynomial surface for methanol/dry air

Table 41. Fitted 3-D polynomial equation and estimated $U(x)_{SoS}$ (ethanol/dry air)

| | | | | | |
|---|---|---|---|---|---|
| $P_{00}$ | -8.008600E+01 | $P_{02}$ | -1.769268E-03 | $P_{40}$ | -7.931313E-09 |
| $P_{10}$ | 1.742438E+00 | $P_{30}$ | -1.027564E-05 | $P_{31}$ | 3.333955E-08 |
| $P_{01}$ | 6.741619E-01 | $P_{21}$ | -2.702212E-06 | $P_{22}$ | -1.997283E-09 |
| $P_{20}$ | 1.099717E-03 | $P_{12}$ | 4.364758E-05 | $P_{13}$ | -4.151602E-08 |
| $P_{11}$ | -1.515364E-02 | $P_{03}$ | 1.114203E-06 | $P_{04}$ | 8.646683E-10 |
| Goodness of fit | | | | | |
| SSE | 1.2E-05 | $R^2$ | 0.999985 | RMSE | 3.1E-04 |
| Polynomial equation used for fitting: Equation (89) | | | | | |

| Temperature/°C | 5 | 15 | 25 | 35 | 45 | 55 |
|---|---|---|---|---|---|---|
| $U(x)_{SoS}$/%SAT | 4.3 | 2.4 | 1.5 | 0.98 | 0.73 | 0.59 |

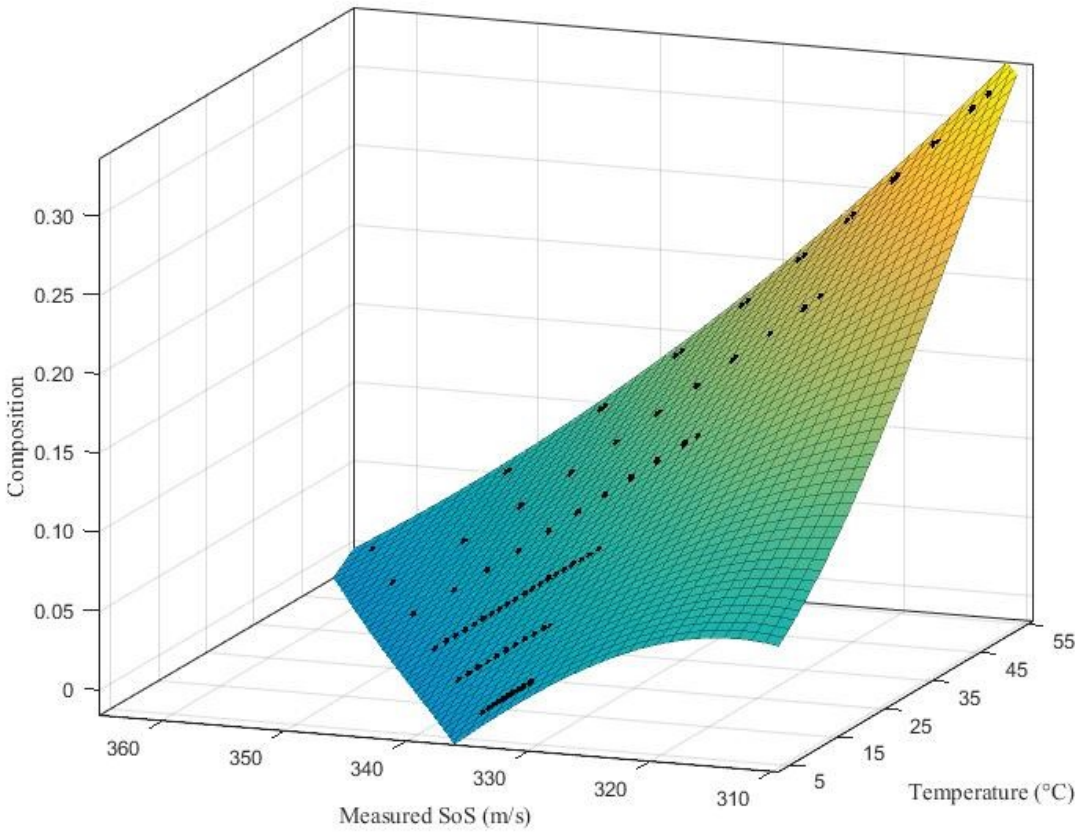



Figure 89. 3-D polynomial surface for ethanol/dry air

Table 42. Fitted 3-D polynomial equation and estimated $U(x)_{SoS}$ (isopropanol/dry air)

| | | | | | |
|---|---|---|---|---|---|
| $P_{00}$ | -3.036420E+01 | $P_{02}$ | -9.953701E-04 | $P_{40}$ | -2.734998E-09 |
| $P_{10}$ | 5.591372E-01 | $P_{30}$ | -4.524593E-06 | $P_{31}$ | 1.441889E-08 |
| $P_{01}$ | 2.936004E-01 | $P_{21}$ | 2.645226E-06 | $P_{22}$ | -6.356366E-09 |
| $P_{20}$ | -1.836150E-04 | $P_{12}$ | 1.303084E-05 | $P_{13}$ | -1.187076E-08 |
| $P_{11}$ | -4.696247E-03 | $P_{03}$ | 1.353643E-06 | $P_{04}$ | -5.707442E-10 |
| Goodness of fit | | | | | |
| SSE | 2.7E-06 | $R^2$ | 0.999994 | RMSE | 1.5E-04 |
| Polynomial equation used for fitting: Equation (89) | | | | | |

| Temperature/°C | 5 | 15 | 25 | 35 | 45 | 55 |
|---|---|---|---|---|---|---|
| $U(x)_{SoS}$/%SAT | 3.3 | 1.9 | 1.2 | 0.79 | 0.61 | 0.51 |

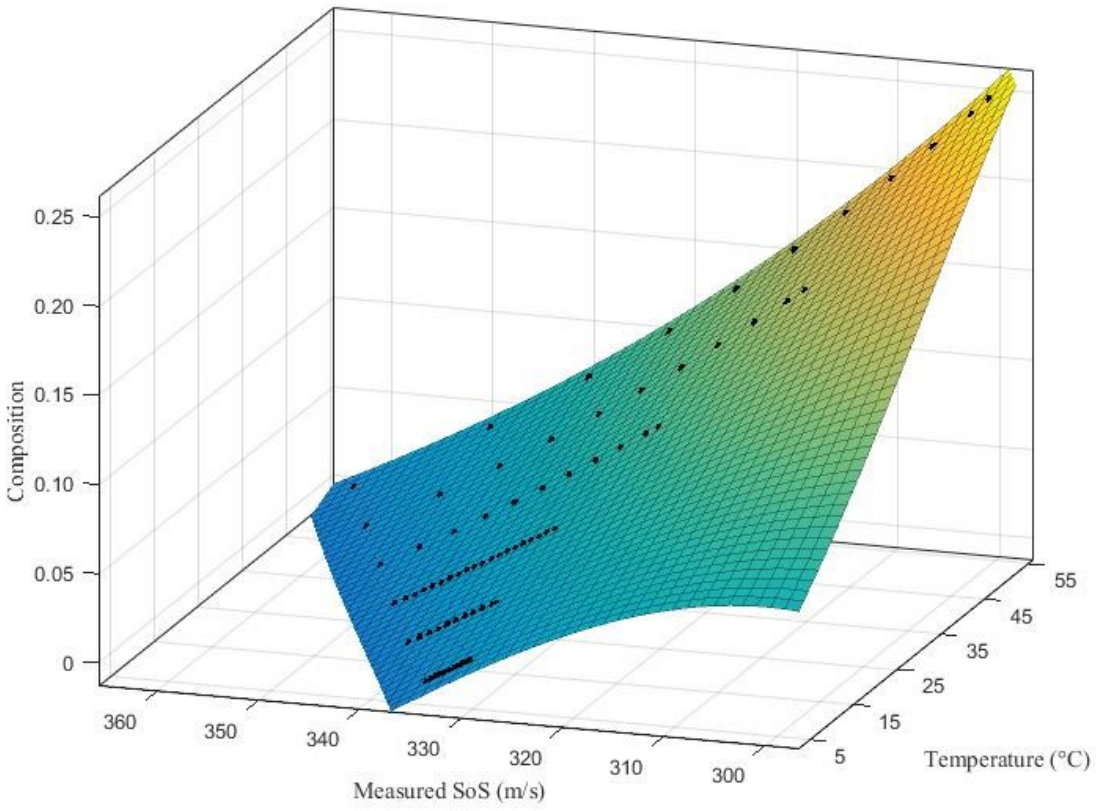



Figure 90. 3-D polynomial surface for isopropanol/dry air

Table 43. Fitted 3-D polynomial equation and estimated $U(x)_{SoS}$ (dichloromethane/dry air)

| | | | | | |
|---|---|---|---|---|---|
| $P_{00}$ | 2.75728E+00 | $P_{01}$ | -1.40745E-02 | $P_{11}$ | -1.14040E-05 |
| $P_{10}$ | 5.45247E-03 | $P_{20}$ | -3.71787E-06 | $P_{02}$ | 1.73752E-05 |
| Goodness of fit | | | | | |
| SSE | 5.0E-05 | $R^2$ | 0.999885 | RMSE | 1.0E-03 |
| Polynomial equation used for fitting: Equation (87) | | | | | |

| Temperature/°C | 5 | 15 | 25 |
|---|---|---|---|
| $U(x)_{SoS}$/%SAT | 0.61 | 0.51 | 0.45 |

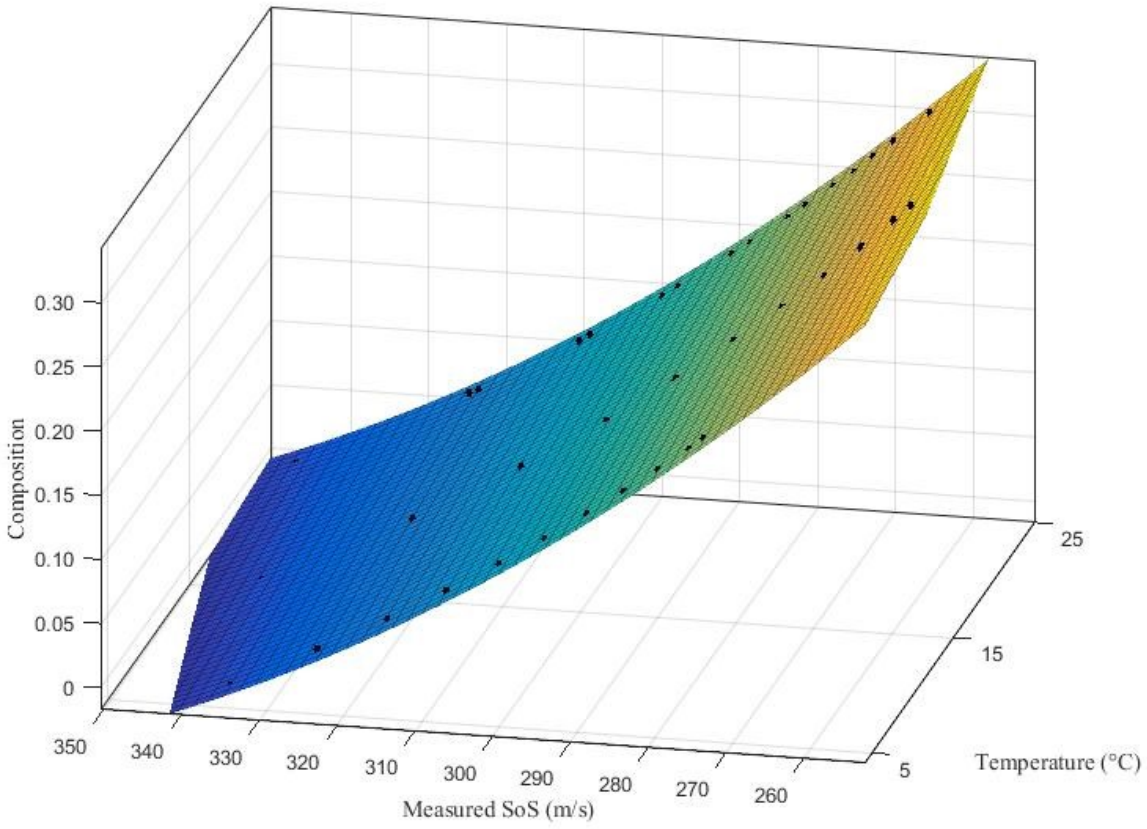



Figure 91. 3-D polynomial surface for dichloromethane/dry air

Table 44. Fitted 3-D polynomial equation and estimated $U(x)_{SoS}$ (chloroform/dry air)

| | | | | | |
|---|---|---|---|---|---|
| $P_{00}$ | 3.15738E+00 | $P_{11}$ | -3.57861E-05 | $P_{12}$ | 5.02812E-08 |
| $P_{10}$ | 7.52643E-03 | $P_{02}$ | 6.10201E-05 | $P_{03}$ | -5.66576E-08 |
| $P_{01}$ | -2.35290E-02 | $P_{30}$ | 1.47537E-07 | | |
| $P_{20}$ | -6.61184E-06 | $P_{21}$ | -7.50061E-09 | | |
| Goodness of fit | | | | | |
| SSE | 4.3E-06 | $R^2$ | 0.999994 | RMSE | 2.2E-04 |
| Polynomial equation used for fitting: Equation (88) | | | | | |

| Temperature/°C | 5 | 15 | 25 | 35 |
|---|---|---|---|---|
| $U(x)_{SoS}$/%SAT | 0.54 | 0.48 | 0.45 | 0.44 |

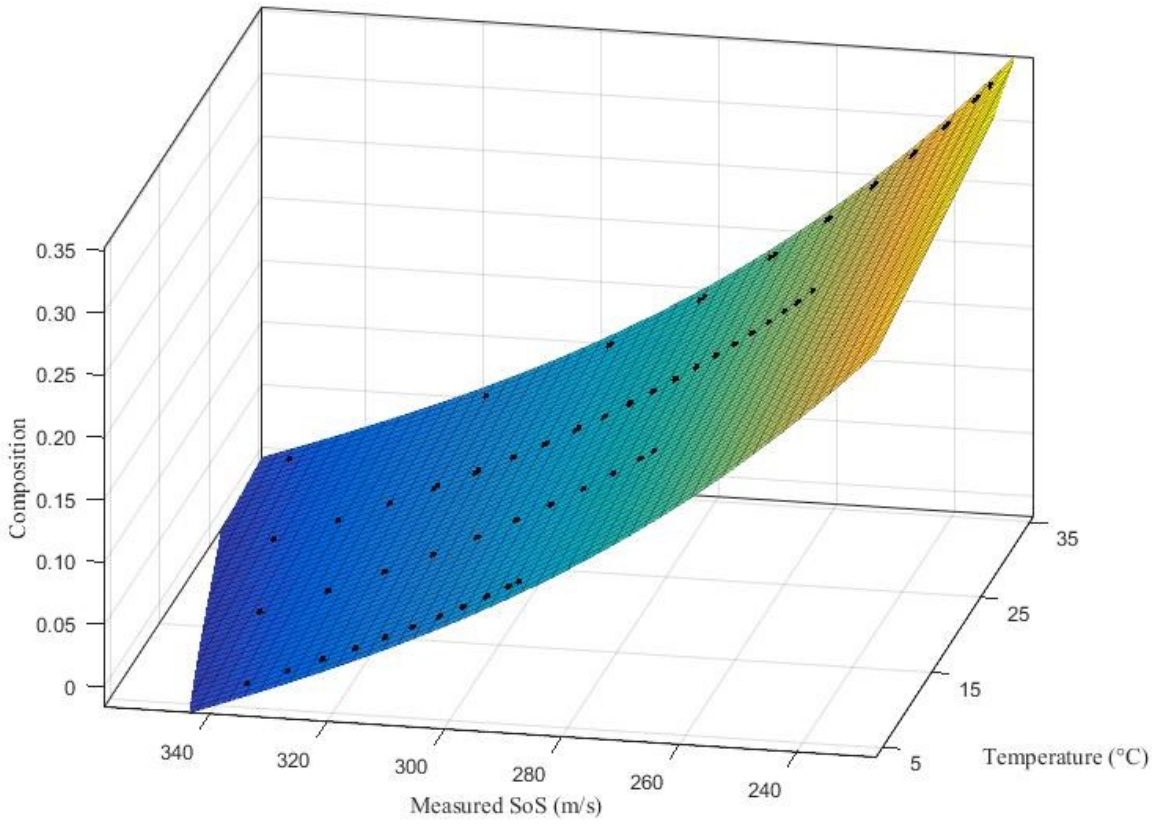



Figure 92. 3-D polynomial surface for chloroform/dry air

Table 45. Fitted 3-D polynomial equation and estimated $U(x)_{SoS}$ (1,2-dichloroethane/dry air)

| | | | | | |
|---|---|---|---|---|---|
| $P_{00}$ | 3.58097E+00 | $P_{11}$ | -3.12243E-05 | $P_{12}$ | 4.00464E-08 |
| $P_{10}$ | 7.14721E-03 | $P_{02}$ | 6.44477E-05 | $P_{03}$ | -5.71639E-08 |
| $P_{01}$ | -2.58844E-02 | $P_{30}$ | -2.62285E-09 | | |
| $P_{20}$ | 6.88617E-07 | $P_{21}$ | -3.41831E-09 | | |
| Goodness of fit | | | | | |
| SSE | 1.5E-06 | $R^2$ | 0.999998 | RMSE | 1.1E-04 |
| Polynomial equation used for fitting: Equation (88) | | | | | |

| Temperature/°C | 5 | 15 | 25 | 35 | 45 | 55 |
|---|---|---|---|---|---|---|
| $U(x)_{SoS}$/%SAT | 0.89 | 0.67 | 0.55 | 0.48 | 0.45 | 0.44 |

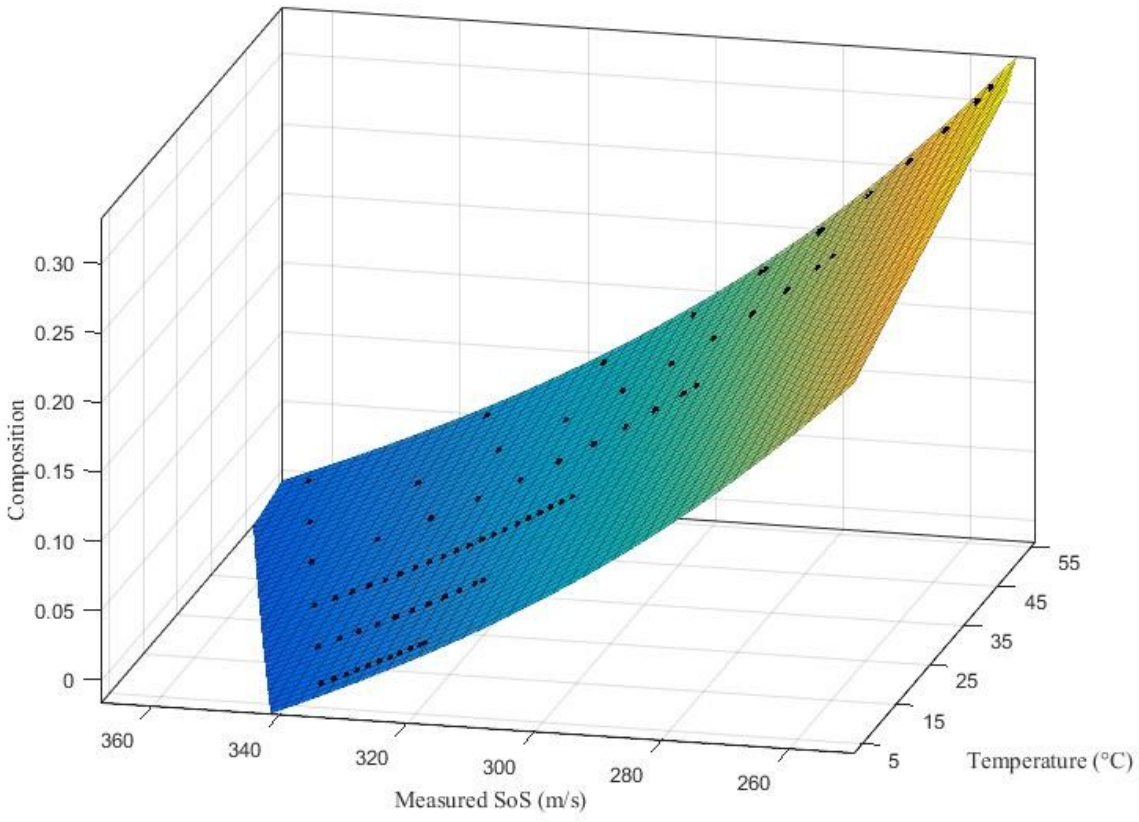



Figure 93. 3-D polynomial surface for 1,2-dichloroethane/dry air

Table 46. Fitted 3-D polynomial equation and estimated $U(x)_{SoS}$ (m-xylene/dry air)

| | | | | | |
|---|---|---|---|---|---|
| $P_{00}$ | 1.36998E+00 | $P_{01}$ | -6.70399E-03 | $P_{11}$ | -4.34679E-06 |
| $P_{10}$ | 2.39575E-03 | $P_{20}$ | -9.43263E-07 | $P_{02}$ | 7.75588E-06 |
| Goodness of fit | | | | | |
| SSE | 6.5E-08 | $R^2$ | 0.999979 | RMSE | 4.9E-05 |
| Polynomial equation used for fitting: Equation (87) | | | | | |
| Temperature/°C | 30 | | 40 | | 50 |
| $U(x)_{SoS}$/%SAT | 1.7 | | 1.2 | | 0.81 |

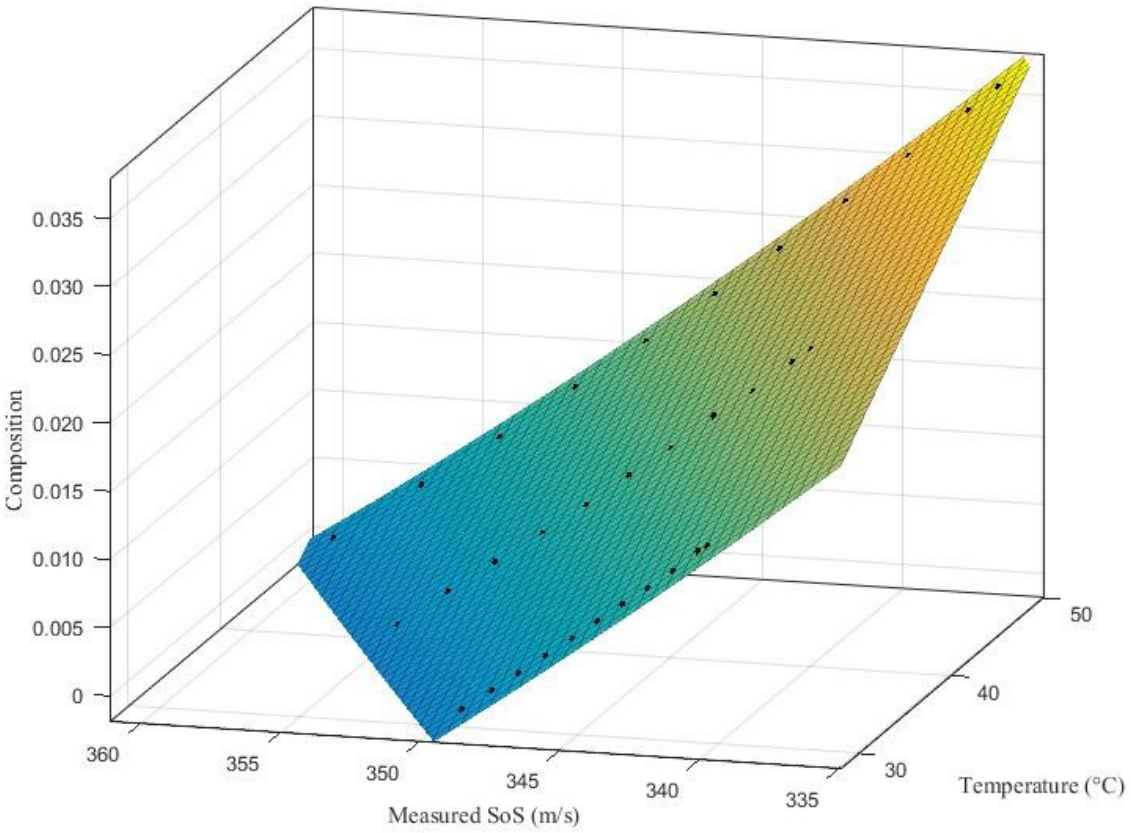



Figure 94. 3-D polynomial surface for m-xylene/dry air

Table 47. Fitted 3-D polynomial equation and estimated $U(x)_{SoS}$ (o-xylene/dry air)

| | | | | | |
|---|---|---|---|---|---|
| $P_{00}$ | 1.30883E+00 | $P_{01}$ | -6.36763E-03 | $P_{11}$ | -4.16993E-06 |
| $P_{10}$ | 2.30063E-03 | $P_{20}$ | -7.03954E-07 | $P_{02}$ | 7.30068E-06 |
| Goodness of fit | | | | | |
| SSE | 8.1E-08 | $R^2$ | 0.999961 | RMSE | 5.5E-05 |
| Polynomial equation used for fitting: Equation (87) | | | | | |

| Temperature/°C | 30 | 40 | 50 |
|---|---|---|---|
| $U(x)_{SoS}$/%SAT | 2.0 | 1.3 | 0.93 |

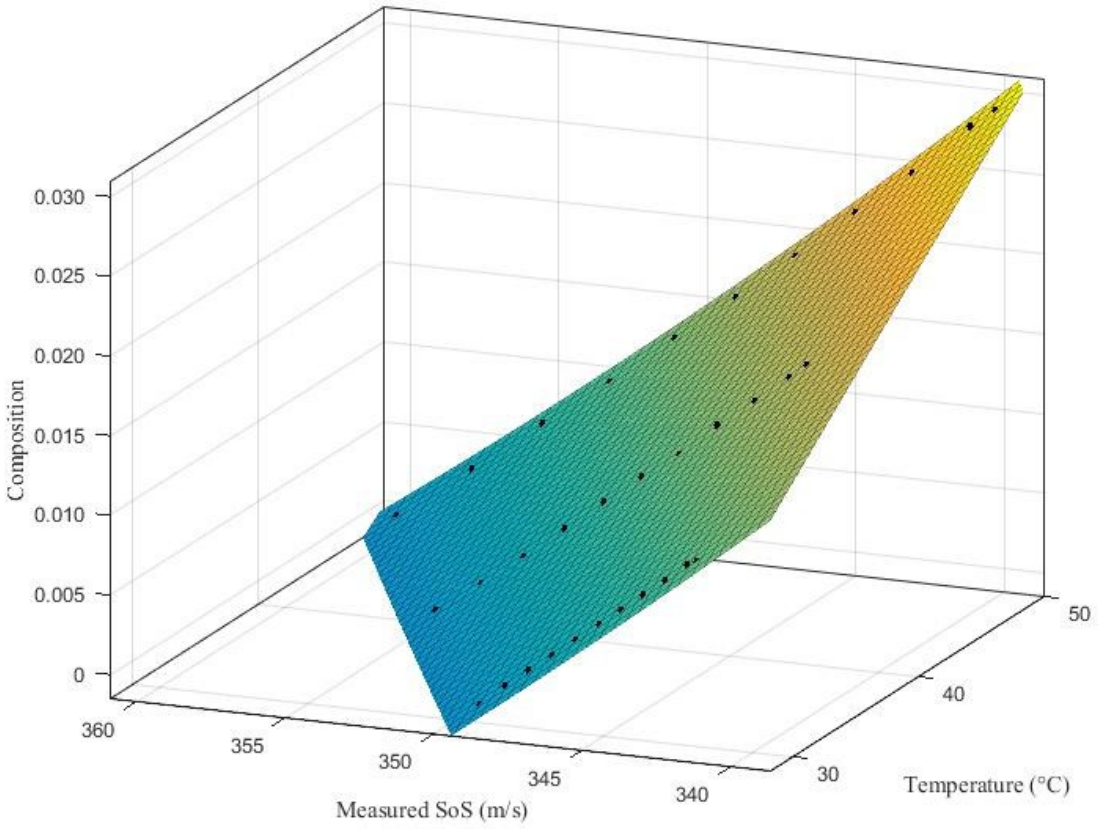



Figure 95. 3-D polynomial surface for o-xylene/dry air

Table 48. Fitted 3-D polynomial equation and estimated $U(x)_{SoS}$ (p-xylene/dry air)

| | | | | | |
|---|---|---|---|---|---|
| $P_{00}$ | 1.38222E+00 | $P_{01}$ | -6.75698E-03 | $P_{11}$ | -3.97373E-06 |
| $P_{10}$ | 2.24407E-03 | $P_{20}$ | -6.63984E-07 | $P_{02}$ | 7.81029E-06 |
| Goodness of fit | | | | | |
| SSE | 2.9E-08 | $R^2$ | 0.999991 | RMSE | 3.3E-05 |
| Polynomial equation used for fitting: Equation (87) | | | | | |
| Temperature/°C | 30 | | 40 | | 50 |
| $U(x)_{SoS}$/%SAT | 1.6 | | 1.1 | | 0.79 |

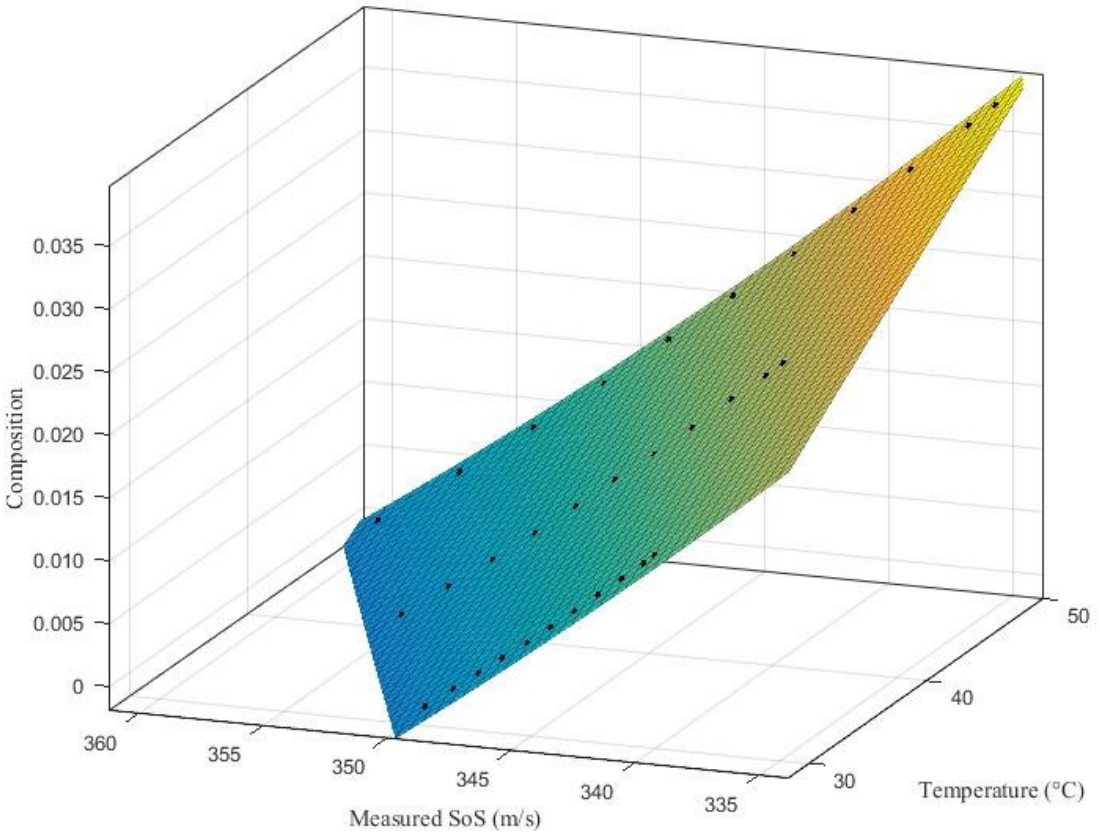



Figure 96. 3-D polynomial surface for p-xylene/dry air

Table 49. Fitted 3-D polynomial equation and estimated $U(x)_{SoS}$ (ethylbenzene/dry air)

| | | | | | |
|---|---|---|---|---|---|
| $P_{00}$ | 1.41344E+00 | $P_{01}$ | -6.88606E-03 | $P_{11}$ | -2.82919E-06 |
| $P_{10}$ | 1.78672E-03 | $P_{20}$ | -1.53302E-08 | $P_{02}$ | 7.93363E-06 |
| Goodness of fit | | | | | |
| SSE | 1.4E-07 | $R^2$ | 0.999964 | RMSE | 7.2E-05 |
| Polynomial equation used for fitting: Equation (87) | | | | | |
| Temperature/°C | 30 | | 40 | | 50 |
| $U(x)_{SoS}$/%SAT | 1.6 | | 1.1 | | 0.77 |

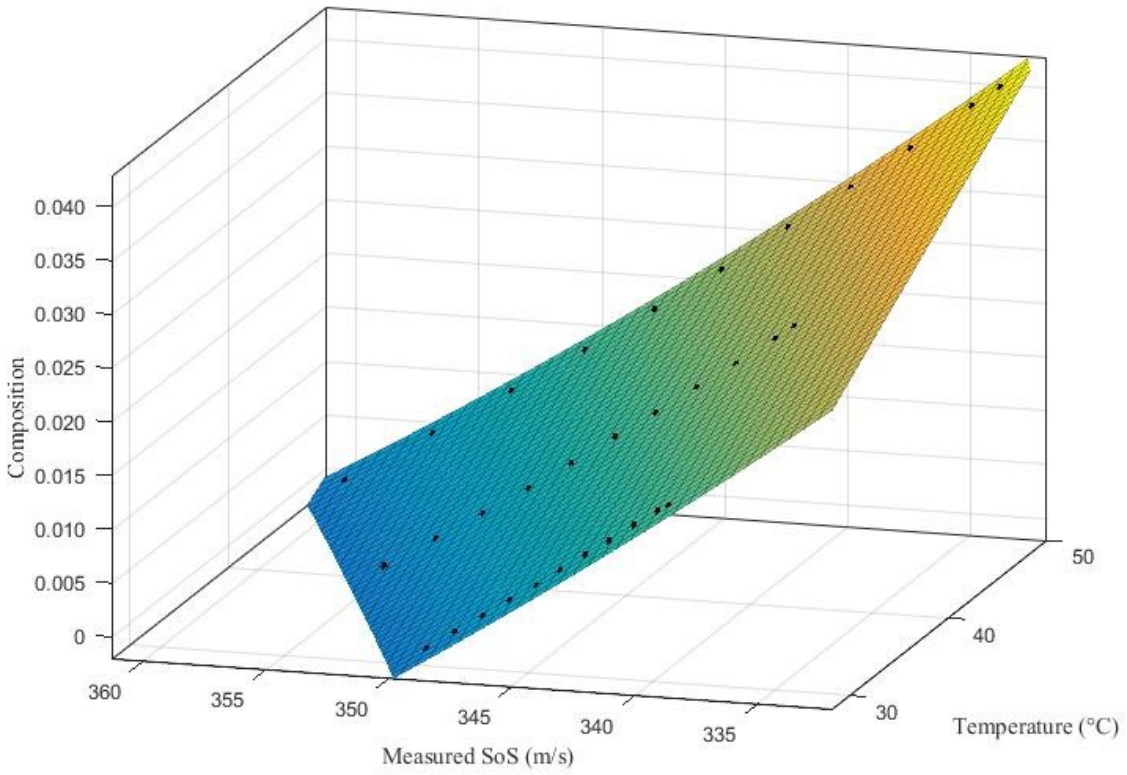



Figure 97. 3-D polynomial surface for ethylbenzene/dry air

Table 50. Fitted 3-D polynomial equation and estimated $U(x)_{SoS}$ (n-butylamine/dry air)

| | | | | | |
|---|---|---|---|---|---|
| $P_{00}$ | 2.75994E+00 | $P_{01}$ | -1.45032E-02 | $P_{11}$ | -1.35649E-05 |
| $P_{10}$ | 6.00157E-03 | $P_{20}$ | -2.54681E-06 | $P_{02}$ | 1.86165E-05 |
| Goodness of fit | | | | | |
| SSE | 1.4E-05 | $R^2$ | 0.999909 | RMSE | 7.3E-04 |
| Polynomial equation used for fitting: Equation (87) | | | | | |
| Temperature/°C | 25 | | 35 | | 45 |
| $U(x)_{SoS}$/%SAT | 0.83 | | 0.63 | | 0.53 |

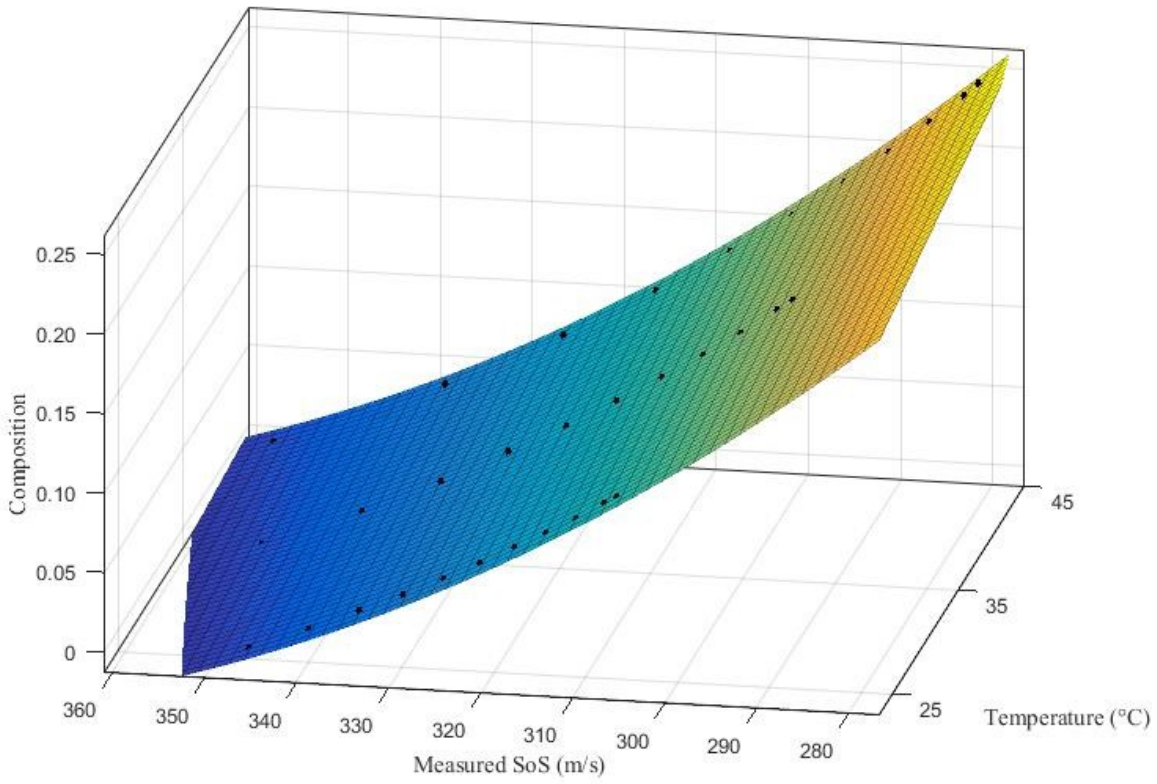



Figure 98. 3-D polynomial surface for n-butylamine/dry air

Table 51. Fitted 3-D polynomial equation and estimated $U(x)_{SoS}$ (limonene/dry air)

| | | | | | |
|---|---|---|---|---|---|
| $P_{00}$ | 9.63338E-01 | $P_{01}$ | -4.67629E-03 | $P_{11}$ | -1.61606E-06 |
| $P_{10}$ | 1.19569E-03 | $P_{20}$ | -1.07017E-06 | $P_{02}$ | 5.34511E-06 |
| Goodness of fit | | | | | |
| SSE | 5.5E-08 | $R^2$ | 0.999301 | RMSE | 4.5E-05 |
| Polynomial equation used for fitting: Equation (87) | | | | | |
| Temperature/°C | 25 | | 35 | | 45 |
| $U(x)_{SoS}$/%SAT | 5.9 | | 3.4 | | 2.1 |

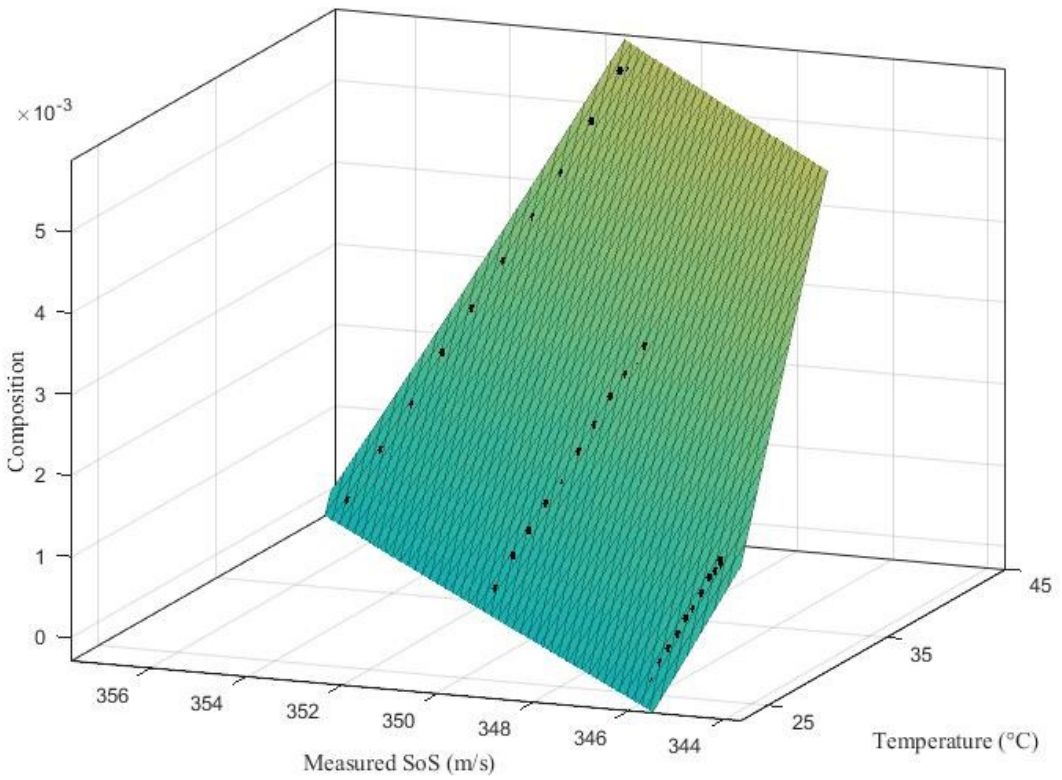



Figure 99. 3-D polynomial surface for limonene/dry air

Table 52. Fitted 3-D polynomial equation and estimated $U(x)_{SoS}$ (α-pinene/dry air)

| | | | | | |
|---|---|---|---|---|---|
| $P_{00}$ | 8.17559E-01 | $P_{01}$ | -3.87550E-03 | $P_{11}$ | -2.48413E-06 |
| $P_{10}$ | 1.45817E-03 | $P_{20}$ | -4.42296E-07 | $P_{02}$ | 4.25280E-06 |
| Goodness of fit | | | | | |
| SSE | 2.3E-08 | $R^2$ | 0.999960 | RMSE | 2.9E-05 |
| Polynomial equation used for fitting: Equation (87) | | | | | |
| Temperature/°C | 25 | | 35 | | 45 |
| $U(x)_{SoS}$/%SAT | 2.5 | | 1.6 | | 1.1 |

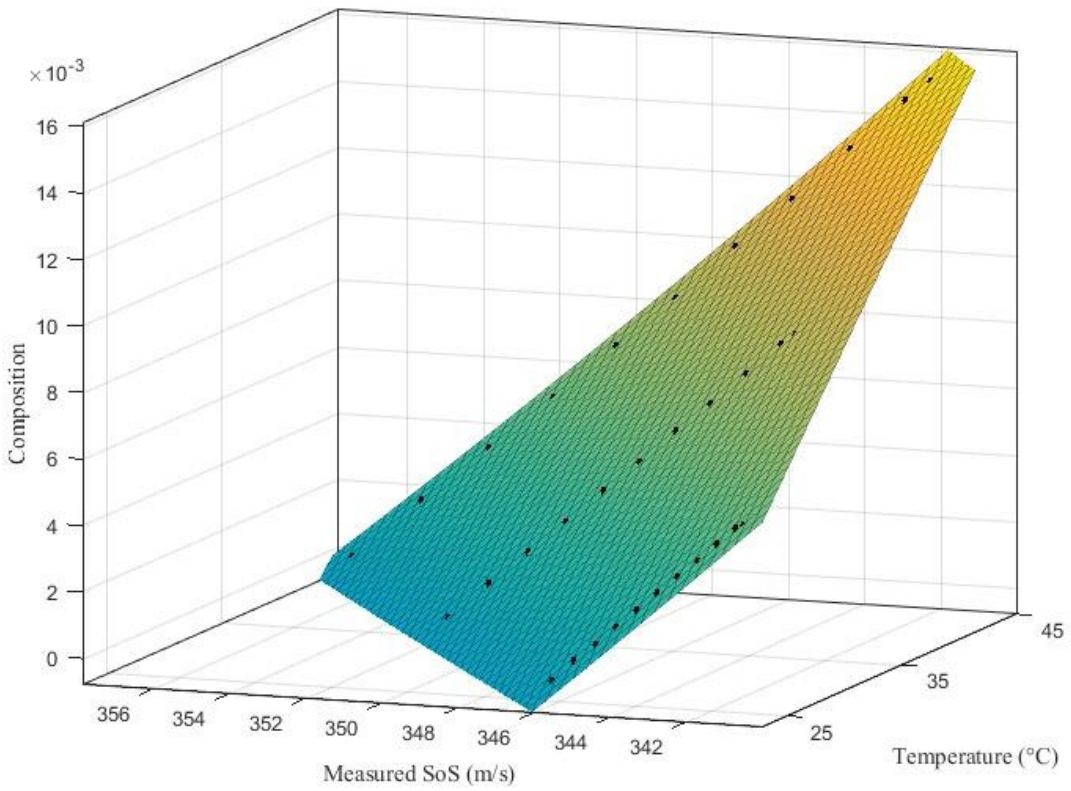



Figure 100. 3-D polynomial surface for α-pinene/dry air

Table 53. Fitted 3-D polynomial equation and estimated $U(x)_{SoS}$ (carbon dioxide/nitrogen)

| | | | | | |
|---|---|---|---|---|---|
| $P_{00}$ | 8.76926E+00 | $P_{01}$ | -4.15778E-02 | $P_{11}$ | -3.41799E-05 |
| $P_{10}$ | 1.79869E-02 | $P_{20}$ | -1.08753E-06 | $P_{02}$ | 4.61573E-05 |
| Goodness of fit | | | | | |
| SSE | 4.8E-06 | $R^2$ | 0.999992 | RMSE | 2.7E-04 |
| Polynomial equation used for fitting: Equation (87) | | | | | |

| Temperature/°C | 10 | 20 | 25 | 30 | 40 | 50 |
|---|---|---|---|---|---|---|
| $U(x)_{SoS}$ | 0.0006 | 0.0006 | 0.0006 | 0.0006 | 0.0006 | 0.0006 |

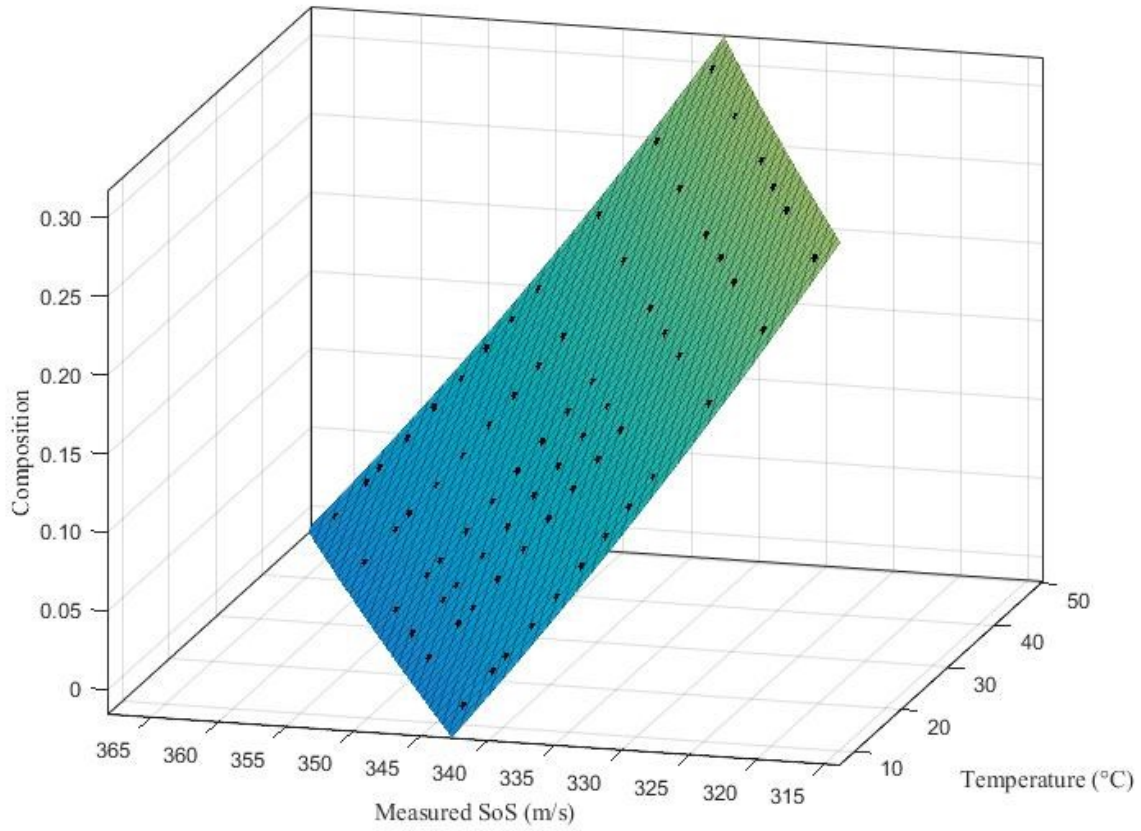



Figure 101. 3-D polynomial surface for carbon dioxide/nitrogen

# CHAPTER 6. Conclusions

A novel SoS sensor operated at a fixed acoustic frequency of 121362 Hz has been deployed in this project which can achieve SoS measurement based on ToF method. The SoS sensor is a double-transducer system with fixed path: one piezoelectric transducer is employed as the ultrasound pulse transmitter while the other as the receiver. In a single measurement only one pulse is generated. SoS is determined from the time delay between the first and the second (after twice reflections) received signals together with the corresponding pulse propagation pathlength. The first two received signals are used because of the higher signal-to-noise level, less distortion effect, and in theory the independence of the measured ToF on any delay associated with the transmitting and receiving of acoustic pulses. This technique is considered the most suitable for fulfilling the requirements of this project due to the simplicity and the great potential for achieving precise and fast on-line measurement of SoS, in comparison with the acoustic resonance, interferometry and the other type of pulse methods. An ultrasound absorbing liner was introduced to reduce the noises in the signals caused by the reflections from the sidewall of the acoustic cavity. The grooved spiral channel inside the wall of the main body of the SoS sensor was designed for achieving reliable and accurate temperature determination. Temperature was determined with an uncertainty of 12.5 m°C using the calibrated SoS sensor's temperature probe, and the uncertainty in atmospheric pressure measurement using the barometric sensor in the electronics board was 0.75 mbar.

Time of fight is measured with 1 ns resolution, and speed of sound can be resolved typically to better than 1 part in half million and determined quickly at a data output rate of 1 Hz. Careful selection of algorithms for waveform analysis is critical to the achievement of rapid and precise measurement. A novel wave interpolation algorithm was employed for the SoS sensor: firstly the corresponding points in the two signals are determined from half-height cycle extrema; then

zero-crossing points are located by interpolation and used to refine the measurement precision and accuracy; ToF is obtained from the time difference between corresponding zero-crossing points; by repeating the measurement 100 times per second and averaging the results, the precision and resolution can be further improved.

Real gas SoS is a function of temperature, pressure, frequency and gas composition, and according to which the SoS sensor is able to be used for composition measurement of binary gas mixtures.

The SoS measurements were performed on $CO_2/N_2$, $H_2O$ vapour/dry air and a wide range of organic vapour (n-hexane, n-heptane, n-octane, n-nonane, n-decane, toluene, cyclohexane, acetone, methyl ethyl ketone, ethyl acetate, methanol, ethanol, isopropanol, dichloromethane, chloroform, 1,2-dichloroethane, m-/o-/p-xylene, ethylbenzene, n-butylamine, limonene and α-pinene)/dry air binary gas mixtures under atmospheric pressure. The experimental temperature range is within 5 to 55 °C. For $CO_2/N_2$, experiments were conducted with the mole fraction of $CO_2$ up to 0.3. While for the other mixtures, the experimental composition range of the vapour component was from 0 to 95%SAT. The pathlength of the SoS sensor was calibrated by using the carrier gas as the reference gas in each isothermal experiment. Ar, He and $N_2$ were used in the investigation of SoS measurement uncertainty since the speed of sound data for these gases have been reported in literature with reasonably high accuracy. The uncertainty of SoS measurement was estimated to be 0.1% for $CO_2/N_2$ and 0.14% for the others.

For the gas mixtures with available thermodynamic data in the NIST REFPROP software including n-hexane, n-heptane, n-octane, n-nonane, n-decane, toluene, cyclohexane and water/dry air and $CO_2/N_2$ (Group A), comparisons were made between the measured SoS $W_m$ at frequency of 121362 Hz and the frequency-independent lossless real gas SoS $W_\theta$ calculated using the software (dry air is simplified to a gas mixture consisting of $N_2$, $O_2$, Ar and $CO_2$ in

the use of the software). For the investigated mixtures except $CO_2/N_2$, the deviations between $W_m$ and $W_\theta$ are reasonably small (< 0.5%). The deviation for $CO_2/N_2$ is large (the maximum deviation is around 1.8%) due to the significant dispersion effect on $CO_2$.

Gas composition was determined simultaneously with the SoS measurement, which was achieved using a novel gas density measurement based upon Archimedes' Principle. The mixture density was obtained from the known carrier gas density, the volume difference between the two sides of the DVS microbalance, and the change in the microbalance mass readings. The volume difference was determined experimentally using Ar and He for which accurate density data are available. The significant density difference between these two pure gases is beneficial for the improvement of measurement accuracy. For all the tested binary mixtures, the uncertainty in density measurement is estimated to be 0.0015 kg/m$^3$.

Equation of state analysis was used to convert density to composition. For the gas mixtures in Group A, the EoS analysis was performed with the use of the software based on the Helmholtz equations of state. For the other gas mixtures (Group B) the Van der Waals equation was used due to the mathematical convenience and the ease of access to model parameters. The carrier gas density and composition for a binary gas mixture were determined according to the same type of EoS (either the Helmholtz or the Van der Waals EoS) for the purpose of minimising the composition error due to EoS inaccuracy. It is found that for each tested gas mixture at constant composition the SoS increases with rising temperature; and at constant temperature as the solute mole fraction increases, the SoS in water vapour/dry air increases as well, while the SoS decreases for all the other mixtures.

By using the 3-D polynomial equations fitted to the experimental results (measured SoS, temperature and composition), gas composition determinations for the tested binary gas mixtures within the respective experimental temperature and composition ranges and under

atmospheric pressure can be achieved using the SoS sensor. For example, within the temperature ranges of 5 to 15, 15 to 25, 25 to 35, 35 to 45 and 45 to 55 °C, the composition measurement uncertainties for n-heptane/dry air are estimated to be 1.2, 0.65, 0.40, 0.27 and 0.20%SAT, respectively; while the uncertainties for ethanol/dry air are 4.3, 2.4, 1.5, 0.98 and 0.73%SAT, respectively. For $CO_2/N_2$ at temperatures from 10 to 50 °C, the uncertainty is 0.0006. In this composition uncertainty analysis, the error in the measurement of temperature and pressure, the error in the measured density resulting from the inaccuracies of the carrier gas density data, mass reading and volume difference, and the fitting error were taken into account. For the mixtures in Group B, an error associated with using the Van der Waals equation in the data analysis was considered additionally (also considered in the analysis of density uncertainty) by means of a comparison of the results obtained using the Helmholtz EoS and the Van der Waals EoS for the mixtures in Group A.

This prototype SoS sensor can be manufactured and the uncertainty in composition determination using a manufactured sensor is considered to be the same as the prototype. It is noteworthy that the accuracy of this technique is predominantly dependent upon the accuracy of the gas composition data in the establishment of the 3-D polynomial equations and the consistency in SoS (0.003%) and temperature (17.7 m°C) measurements between a manufactured sensor and the prototype. In comparison with the traditional measurement techniques, this technique is not only robust but also has the potential to be faster, simpler, more cost-effective, more precise and even more accurate, and is well suited for being used in analytical or process instrumentation for on-line binary gas composition measurement.

# CHAPTER 7. Future Work

1) Since the temperature differences along and across the SoS sensor need to be equalised as fast as possible, metal material which is more thermally conductive than stainless steel is better to be used to make the sensor. Additionally, the grooved channel inside the wall of the sensor's main body might be unnecessarily too long. If it can be shortened, the production of the sensors will become simpler, and the response to the variation of input gas composition will be quicker. The new generation of the SoS sensor has been designed and built by Surface Measurement Systems Limited. Brass is selected as the material for the transducer holders and the main body due to its high thermal conductivity and excellent chemical resistance; the channel is shortened to only one circle; and the PT100 probe is placed in a hole drilled in the main body in order to achieve better thermal contact with the metal.
2) The uncertainty in gas composition measurement using the SoS sensor was determined from theoretical derivations. Consequently, it would be useful to use both a traditional technique and the SoS sensor to measure the composition of the same gas mixture and compare the results. In this way, I was able to confirm the validity and reliability of the theoretical uncertainty analysis and the method employed in this project for the determination of gas composition from density measurement coupled with EoS analysis. Besides, the performances of the SoS and the traditional techniques in terms of, for example, measurement time and precision, can also be compared. For achieving the above purposes, I could apply the SoS sensor to the carbon capture pilot plant in the Department of Chemical Engineering at Imperial College London, which is designed to capture $CO_2$ from a gas mixture of $CO_2$ and $N_2$ using monoethanolamine or MEA solutions. Over 250 ABB's process instruments are used for the real-time monitoring

of the system, and $CO_2$ concentration is monitored using a thermal conductivity gas analyser.

3) The SoS comparisons ($W_m$ versus $W_\theta$) for the binary gas mixtures in Group B can be made by using the ideal gas law, the Van der Waals EoS or the virial EoS to determine $W_\theta$.
4) The current experimental and data analysis methods can be used to establish the 3-D polynomial equations (composition versus SoS and temperature) for more different types of binary gas mixtures. For example, by changing the carrier gas from dry air to $N_2$, a series of organic vapour/$N_2$ binary gas mixtures can be generated and tested.
5) It is of interest to investigate the potential applications of the SoS sensor in other fields such as gas flow rate measurement.

# References


AGC Instruments [*Online*] http://www.agc-instruments.com/thermal-conductivity-detectors-tcd

Atmosphere, U. S. (1976) NOAA-S/T76-1562. *Washington, DC: US Govternment Printing Office.*

Ball, S. & Trusler, J. (2001) Speed of Sound of n-Hexane and n-Hexadecane at Temperatures Between 298 and 373 K and Pressures up to 100 MPa. *International Journal of Thermophysics.* 22 (2), 427-443.

Bancroft, D. (1956) Measurement of velocity of sound in gases. *American Journal of Physics.* 24 (5), 355-358.

Bates, R., Battistin, M., Berry, S., Bitadze, A., Bonneau, P., Bousson, N., Boyd, G., Botelho-Direito, J., DiGirolamo, B. & Doubek, M. (2012) An on-line acoustic fluorocarbon coolant mixture analyzer for the ATLAS silicon tracker. *IEEE Transactions on Nuclear Science.* 59 (5), 2367-2374.

BBC GCSE Bitesize Science [*Online*] http://www.bbc.co.uk/schools/gcsebitesize/science/triple_ocr_21c/further_chemistry/chromatography/revision/5/

Bhatia, A. B. (1985) *Ultrasonic absorption: an introduction to the theory of sound absorption and dispersion in gases, liquids, and solids.* , Courier Corporation.

Boyes, S., Ewing, M. & Goodwin, A. (1992) Heat capacities and second virial coefficients for gaseous methanol determined from speed-of-sound measurements at temperatures between 280 K and 360 K and pressures from 1.03 kPa to 80.5 kPa. *The Journal of Chemical Thermodynamics.* 24 (11), 1151-1166.

Byers, W. H. (1943) Specific Heats of Carbon Tetrafluoride from Supersonic Measurements. *The Journal of Chemical Physics.* 11 (8), 348-350.

Cantrell, J. H. & Yost, W. T. (1998) Ultrasonic velocity. *Encyclopedia of Acoustics, Volume Two.* 629-639.

CARDOZO-FILHO, L., WOLFF, F. & MEIRELES, M. A. A. (1997) High pressure phase equilibrium: prediction of essential oil solubility. *Food Science and Technology (Campinas).* 17 (4), 485-488.

Cazes, J. (2004) *Analytical instrumentation handbook.* , CRC Press.

Christian, G. D. (1994) *Analytical chemistry.* New York, Wiley & Sons.

Christian, G. D. & O'Reilly, J. E. (1986) *Instrumental analysis.* Boston, Allen & Bacon.

Colclough, A., Quinn, T. & Chandler, T. (1979) An acoustic redetermination of the gas constant. *Proceedings of the Royal Society of London A: Mathematical, Physical and Engineering Sciences.* , The Royal Society. pp.125-139.

Colgate, S. O., Sona, C. F., Reed, K. R. & Sivaraman, A. (1990) Experimental ideal gas reference state heat capacities of gases and vapors. *Journal of Chemical and Engineering Data.* 35 (1), 1-5.

Connor, J. V. (1958) Ultrasonic dispersion in oxygen. *The Journal of the Acoustical Society of America.* 30 (4), 297-300.

Davies, M., Snell, D., Trollope, L. & Moses, A. (1998) A chilled mirror dew point measurement system for assessment of decarburisation furnace atmosphere. *Le Journal De Physique IV.* 8 (PR2), Pr2-701-Pr2-704.

Dávila, M. J. & Trusler, J. M. (2009) Thermodynamic properties of mixtures of N-methyl-2-pyrrolidinone and methanol at temperatures between 298.15 K and 343.15 K and pressures up to 60MPa. *The Journal of Chemical Thermodynamics.* 41 (1), 35-45.

Dixon, H. B. & Greenwood, G. (1924) On the Velocity of Sound in Gases and Vapours, and the Ratio of the Specific Heats. *Proceedings of the Royal Society of London.Series A, Containing Papers of a Mathematical and Physical Character.* 105 (730), 199-220.

Ed Dlugokencky & Pieter Tans, NOAA/ESRL [*Online*] www.esrl.noaa.gov/gmd/ccgg/trends/

Ejakov, S. G., Phillips, S., Dain, Y., Lueptow, R. M. & Visser, J. H. (2003) Acoustic attenuation in gas mixtures with nitrogen: Experimental data and calculations. *The Journal of the Acoustical Society of America.* 113 (4), 1871-1879.

Ener, C., Busala, A. & Hubbard, J. (1955) Ultrasonic Dispersion in Methyl Alcohol Vapor. *The Journal of Chemical Physics.* 23 (1), 155-158.

Estrada-Alexanders, A. & Trusler, J. (1997) The speed of sound and derived thermodynamic properties of ethane at temperatures between 220 K and 450 K and pressures up to 10.5 MPa. *The Journal of Chemical Thermodynamics.* 29 (9), 991-1015.

Estrada-Alexanders, A. & Trusler, J. (1995) The speed of sound in gaseous argon at temperatures between 110 K and 450 K and at pressures up to 19 MPa. *The Journal of Chemical Thermodynamics.* 27 (10), 1075-1089.

[1]Ewing, M. & Goodwin, A. (1992) An apparatus based on a spherical resonator for measuring the speed of sound in gases at high pressures. Results for argon at temperatures between 255 K and 300 K and at pressures up to 7 MPa. *The Journal of Chemical Thermodynamics.* 24 (5), 531-547.

[2]Ewing, M. & Goodwin, A. (1992) Speeds of sound, perfect-gas heat capacities, and acoustic virial coefficients for methane determined using a spherical resonator at temperatures between 255 K and 300 K and pressures in the range 171 kPa to 7.1 MPa. *The Journal of Chemical Thermodynamics.* 24 (12), 1257-1274.

[3]Ewing, M. & Goodwin, A. (1992) Thermophysical properties of alkanes from speeds of sound determined using a spherical resonator 5. 2-Methylbutane at temperatures in the range 260 K to 320 K and pressures in the range 2.8 kPa to 80.9 kPa. *The Journal of Chemical Thermodynamics.* 24 (3), 301-315.

Ewing, M., Goodwin, A., McGlashan, M. & Trusler, J. (1988) Thermophysical properties of alkanes from speeds of sound determined using a spherical resonator 2. n-Butane. *The Journal of Chemical Thermodynamics.* 20 (2), 243-256.

Ewing, M., Goodwin, A., McGlashan, M. & Trusler, J. (1987) Thermophysical properties of alkanes from speeds of sound determined using a spherical resonator I. Apparatus, acoustic model, and results for dimethylpropane. *The Journal of Chemical Thermodynamics.* 19 (7), 721-739.

[1]Ewing, M., Goodwin, A. & Trusler, J. (1989) Thermophysical properties of alkanes from speeds of sound determined using a spherical resonator 3. n-Pentane. *The Journal of Chemical Thermodynamics.* 21 (8), 867-877.

Ewing, M., McGlashan, M. & Trusler, J. (1986) The speed of sound in gases II. Acoustic virial coefficients and perfect-gas heat capacities for 2, 2-dimethylpropane obtained using a cylindrical interferometer. *The Journal of Chemical Thermodynamics.* 18 (6), 511-517.

Ewing, M., McGlashan, M. & Trusler, J. (1985) The speed of sound in gases I. A cylindrical interferometer and the speed of sound in argon and in krypton. *The Journal of Chemical Thermodynamics.* 17 (6), 549-559.

[2]Ewing, M., Owusu, A. & Trusler, J. (1989) Second acoustic virial coefficients of argon between 100 and 304 K. *Physica A: Statistical Mechanics and its Applications.* 156 (3), 899-908.

Ewing, M. & Trusler, J. (1992) Second acoustic virial coefficients of nitrogen between 80 and 373 K. *Physica A: Statistical Mechanics and its Applications.* 184 (3-4), 415-436.

Ewing, M. & Trusler, J. (1989) Speeds of sound in CF4 between 175 and 300 K measured with a spherical resonator. *The Journal of Chemical Physics.* 90 (2), 1106-1115.

Gammon, B. (1976) The velocity of sound with derived state properties in helium at− 175 to 150° C with pressure to 150 atm. *The Journal of Chemical Physics.* 64 (6), 2556-2568.

Gammon, B. & Douslin, D. (1976) The velocity of sound and heat capacity in methane from near-critical to subcritical conditions and equation-of-state implications. *The Journal of Chemical Physics.* 64 (1), 203-218.

Gemini Scientific Instruments [*Online*] http://www.gascell.com/htmls/direct3a.htm

General Chemistry [*Online*]
http://antoine.frostburg.edu/chem/senese/101/matter/chromatography.shtml

General Electric Company [*Online*] https://www.gemeasurement.com/moisture-and-humidity-measurement

Giacobbe, F. (1993) Precision measurement of acoustic velocities in pure gases and gas mixtures. *The Journal of the Acoustical Society of America.* 94 (3), 1200-1210.

Gomes, M. C. & Trusler, J. M. (1998) The speed of sound in nitrogen at temperatures betweenT= 250 K andT= 350 K and at pressures up to 30 MPa. *The Journal of Chemical Thermodynamics.* 30 (5), 527-534.

Goodwin, A. & Moldover, M. (1991) Thermophysical properties of gaseous refrigerants from speed-of-sound measurements. III. Results for 1, 1-dichloro-2, 2, 2-trifluoroethane (CHCl2-CF3) and 1, 2-dichloro-1, 2, 2-trifluoroethane (CHClF-CClF2). *The Journal of Chemical Physics.* 95 (7), 5236-5242.

Goring, G. (1971) Velocity of Sound in Argon at Atmospheric Pressure in the Temperature Range 300–540° K. *The Journal of Chemical Physics.* 54 (10), 4514-4515.

GOW-MAC Instrument Co. [*Online*] http://www.gow-mac.com/Products/GCDetectorsandFilaments/FlameIonizationDetectorFIDModel12800.aspx

Hallewell, G., Crawford, G., McShurley, D., Oxoby, G. & Reif, R. (1988) A sonar-based technique for the ratiometric determination of binary gas mixtures. *Nuclear Instruments and Methods in Physics Research Section A: Accelerators, Spectrometers, Detectors and Associated Equipment.* 264 (2-3), 219-234.

Hallewell, G., Vacek, V. & Vinš, V. (2010) Properties of saturated fluorocarbons: Experimental data and modeling using perturbed-chain-SAFT. *Fluid Phase Equilibria.* 292 (1), 64-70.

He, M. & Liu, Z. (2002) Speed of sound measurements in gaseous binary mixtures of difluoroethane (HFC152a) difluoromethane (HCFC22) with a spherical resonator. *Fluid Phase Equilibria.* 198 (2), 185-193.

Henderson, M. & Peselnick, L. (1957) Ultrasonic Velocity and Thermal Relaxation in Dry CO 2 at Moderate Pressures. *The Journal of the Acoustical Society of America.* 29 (10), 1074-1080.

Hozumi, T., Koga, T., Sato, H. & Watanabe, K. (1993) Sound-velocity measurements for HFC-134a and HFC-152a with a spherical resonator. *International Journal of Thermophysics.* 14 (4), 739-762.

Hozumi, T., Sato, H. & Watanabe, K. (1996) Speed-of-sound measurements and ideal-gas heat capacity for 1, 1, 1, 2-tetrafluoroethane and difluoromethane. *Journal of Chemical & Engineering Data.* 41 (5), 1187-1190.

Hozumi, T., Sato, H. & Watanabe, K. (1997) Speed-of-sound measurements in gaseous binary refrigerant mixtures of difluoromethane (R-32) 1, 1, 1, 2-tetrafluoroethane (R-134a). *Journal of Chemical & Engineering Data.* 42 (3), 541-547.

Hozumi, T., Sato, H. & Watanabe, K. (1994) Speed of sound in gaseous difluoromethane. *Journal of Chemical and Engineering Data.* 39 (3), 493-495.

Hurly, J. J., Schmidt, J. W., Boyes, S. & Moldover, M. R. (1997) Virial equation of state of helium, xenon, and helium-xenon mixtures from speed-of-sound and burnett P ρ T measurements. *International Journal of Thermophysics.* 18 (3), 579-634.

Innovative Sensor Technology [*Online*] http://www.ist-usadivision.com/sensors/humidity/

Joos, M., Müller, H. & Lindner, G. (1993) An ultrasonic sensor for the analysis of binary gas mixtures. *Sensors and Actuators B: Chemical.* 16 (1-3), 413-419.

Kaye, G. & Sherratt, G. (1933) The velocity of sound in gases in tubes. *Proceedings of the Royal Society of London.Series A, Containing Papers of a Mathematical and Physical Character.* 141 (843), 123-143.

Kelly, B. T. (1957) Ultrasonic velocity, absorption, and rotational dispersion in methane. *The Journal of the Acoustical Society of America.* 29 (9), 1005-1008.

Kimura, M., Hanayama, Y. & Nishitake, T. (1987) Measurement of ultrasound velocity in gases under high pressures up to 3.5 GPa. *Japanese Journal of Applied Physics.* 26 (8R), 1366.

Klose, J. Z. (1958) Ultrasonic Dispersion and Absorption in n-Hexane Vapor. *The Journal of the Acoustical Society of America.* 30 (7), 605-609.

Kohler, M. (1950) Schallabsorption in binären Gasmischungen. *Zeitschrift Für Physik A Hadrons and Nuclei.* 127 (1), 41-48.

Komarov, S., Solov'ev, A. & Sheludyakov, E. (1967) Speed of sound in freons on the saturation line. *Journal of Applied Mechanics and Technical Physics.* 8 (5), 74-76.

Korean Thermophysical Properties Data Bank (KDB) [*Online*] https://www.cheric.org/research/kdb/hcprop/cmpsrch.php

Kortbeek, P., Muringer, M., Trappeniers, N. & Biswas, S. (1985) Apparatus for sound velocity measurements in gases up to 10 kbar: Experimental data for argon. *Review of Scientific Instruments.* 56 (6), 1269-1273.

Kortbeek, P. & Schouten, J. (1990) Measurements of the compressibility and sound velocity in methane up to 1 GPa, revisited. *International Journal of Thermophysics.* 11 (3), 455-466.

Kunz, O., Klimeck, R., Wagner, W. & Jaeschke, M. (2007) The GERG-2004 wide-range equation of state for natural gases and other mixtures, Fortschr. *Ber.VDI, VDI-Verlag, Düsseldorf.*

Kunz, O. & Wagner, W. (2012) The GERG-2008 wide-range equation of state for natural gases and other mixtures: an expansion of GERG-2004. *Journal of Chemical & Engineering Data.* 57 (11), 3032-3091.

Lemmon, E. W., Jacobsen, R. T., Penoncello, S. G. & Friend, D. G. (2000) Thermodynamic properties of air and mixtures of nitrogen, argon, and oxygen from 60 to 2000 K at pressures to 2000 MPa. *Journal of Physical and Chemical Reference Data.* 29 (3), 331-385.

Lemmon, E. W. & Span, R. (2006) Short fundamental equations of state for 20 industrial fluids. *Journal of Chemical & Engineering Data.* 51 (3), 785-850.

Leonard O'Connor, C. (1954) Thermal relaxation of vibrational states in sulfur hexafluoride. *The Journal of the Acoustical Society of America.* 26 (3), 361-364.

Lin, C. & Trusler, J. (2012) The speed of sound and derived thermodynamic properties of pure water at temperatures between (253 and 473) K and at pressures up to 400 MPa. *The Journal of Chemical Physics.* 136 (9), 094511.

Löfqvist, T., Delsing, J. & Sokas, K. (2003) *Speed of sound measurements in gas- mixtures at varying composition using an ultrasonic gas flow meter with silicon based transducers.*

Lordi, J. A. & Mates, R. E. (1970) Rotational relaxation in nonpolar diatomic gases. *The Physics of Fluids.* 13 (2), 291-308.

MathWorks [*Online*] http://uk.mathworks.com/help/curvefit/evaluating-goodness-of-fit.html?requestedDomain=uk.mathworks.com&requestedDomain=uk.mathworks.com

McIntyre, R. G., Barnes, T. G. & Chew, E. W. (1972) Precision Measurement of the Low-Frequency Velocity of Sound in Helium under Standard Conditions by a Resonance Tube Method. *The Journal of the Acoustical Society of America.* 51 (5A), 1394-1399.

McSkimin, H. (1965) Variations of the Ultrasonic Pulse-Superposition Method for Increasing the Sensitivity of Delay-Time Measurements. *The Journal of the Acoustical Society of America.* 37 (5), 864-871.

McSkimin, H. & Andreatch Jr, P. (1967) Measurement of very small changes in the velocity of ultrasonic waves in solids. *The Journal of the Acoustical Society of America.* 41 (4B), 1052-1057.

Mehl, J. B. & Moldover, M. R. (1981) Precision acoustic measurements with a spherical resonator: Ar and C2H4. *The Journal of Chemical Physics.* 74 (7), 4062-4077.

Metrohm AG [*Online*] https://www.metrohm.com/en-gb/applications/%7B732556B5-E952-4862-A11A-2577F9597E31%7D?fromApplicationFinder=true

Michell Instruments [*Online*] http://www.michell.com/us/category/chilled-mirror-instruments.htm

Miller, D. R. & Andres, R. (1967) Rotational relaxation of molecular nitrogen. *The Journal of Chemical Physics.* 46 (9), 3418-3423.

Moldover, M., Trusler, J. P., Edwards, T. & Mehl, J. (1988) Measurement of the Universal Gas Constant R Using a Spherical Acoustic Resonator. *Journal of Research of the National Bureau of Standards.* 93 (2), .

NDT Resource Center [*Online*] https://www.nde-ed.org/EducationResources/CommunityCollege/Ultrasonics/cc_ut_index.htm

Nishitake, T. & Hanayama, Y. (1975) Velocity of Ultrasound Wave in Helium, Argon, and Nitrogen Gases at High Pressure. *Journal of the Physical Society of Japan.* 39 (4), 1065-1067.

Oppenheim, A. V., 1937-. (2010) *Discrete-time signal processing.* 3rd, International edition. Upper Saddle River, N.J. ; London, Pearson.

Overbeck, C. & Kendall, H. (1941) The Temperature and Frequency Effects on Ultrasonic Velocities in Carbon Dioxide. *The Journal of the Acoustical Society of America.* 13 (1), 26-32.

Papadakis, E. P. (1976) Ultrasonic velocity and attenuation: Measurement methods with scientific and industrial applications. *Physical Acoustics.* 12 277-374.

Parker, J. (1959) Rotational and vibrational relaxation in diatomic gases. *The Physics of Fluids.* 2 (4), 449-462.

Peleties, F., Segovia, J., Trusler, J. & Vega-Maza, D. (2010) Thermodynamic properties and equation of state of liquid di-isodecyl phthalate at temperature between (273 and 423) K and at pressures up to 140MPa. *The Journal of Chemical Thermodynamics.* 42 (5), 631-639.

Perry, R. H., 1924-1978., Green, D. W. & Maloney, J. O. (1997) *Perry's chemical engineers' handbook.* 7th edition. New York ; London, McGraw-Hill.

Pielemeier, W. & Byers, W. (1943) Supersonic measurements in CO 2 and H 2 O at 98° C. *The Journal of the Acoustical Society of America.* 15 (1), 17-21.

Quinn, T., Colclough, A. & Chandler, T. (1976) A new determination of the gas constant by an acoustical method. *Philosophical Transactions of the Royal Society of London A: Mathematical, Physical and Engineering Sciences.* 283 (1314), 367-420.

Railston, W. (1939) Supersonic dispersion in vapors. *The Journal of the Acoustical Society of America.* 11 (1), 107-112.

Redwood, M. & Lamb, J. (1956) On the measurement of attenuation in ultrasonic delay lines. *Proceedings of the IEE-Part B: Radio and Electronic Engineering.* 103 (12), 773-780.

Rotronic Instrument Corporation [*Online*] https://www.rotronic.com/en-us/humidity-measurement-feuchtemessung-temperaturmessung/humidity-measurement-feuchte-messung.html

Roveti, D. (2001) Choosing a Humidity Sensor: A Review of Three Technologies [*Online*] http://www.sensorsmag.com/sensors/humidity-moisture/choosing-a-humidity-sensor-a-review-three-technologies-840

Schaik, W. v., Grooten, M., Wernaart, T. & Geld, C. v. d. (2010) High Accuracy Acoustic Relative Humidity Measurement inDuct Flow with Air. *Sensors.* 10 (8), 7421-7433.

Schmidt, R. & Wagner, W. (1985) A new form of the equation of state for pure substances and its application to oxygen. *Fluid Phase Equilibria.* 19 (3), 175-200.

Sette, D., Busala, A. & Hubbard, J. (1955) Energy transfer by collisions in vapors of chlorinated methanes. *The Journal of Chemical Physics.* 23 (5), 787-793.

Sherratt, G. & Griffiths, E. (1936) The Determination of the Specific Heat of Gases at High Temperatures by the Sound Velocity Method. II. Carbon Dioxide. *Proceedings of the Royal Society of London.Series A, Mathematical and Physical Sciences.* 156 (889), 504-517.

Sherratt, G. & Griffiths, E. (1934) The Determination of the Specific Heat of Gases at High Temperatures by the Sound Velocity Method. I. Carbon Monoxide. *Proceedings of the Royal Society of London.Series A, Mathematical and Physical Sciences.* 147 (861), 292-308.

Shilling, W. (1927) XXIX. Measurements of the velocity of sound in steam, nitrous oxide, and carbon dioxide, with, special reference to the temperature coefficient of the molecular heats. *The London, Edinburgh, and Dublin Philosophical Magazine and Journal of Science.* 3 (14), 273-301.

Smith, D. & Harlow, R. (1963) The velocity of sound in air, nitrogen and argon. *British Journal of Applied Physics.* 14 (2), 102.

Span, R. & Wagner, W. (2003) Equations of state for technical applications. II. Results for nonpolar fluids. *International Journal of Thermophysics.* 24 (1), 41-109.

Span, R., Lemmon, E. W., Jacobsen, R. T., Wagner, W. & Yokozeki, A. (2000) A reference equation of state for the thermodynamic properties of nitrogen for temperatures from 63.151 to 1000 K and pressures to 2200 MPa. *Journal of Physical and Chemical Reference Data.* 29 (6), 1361-1433.

Span, R. & Wagner, W. (1996) A new equation of state for carbon dioxide covering the fluid region from the triple-point temperature to 1100 K at pressures up to 800 MPa. *Journal of Physical and Chemical Reference Data.* 25 (6), 1509-1596.

Stanford Research Systems Inc. (*BGA244 Binary Gas Analyzer*) [*Online*] http://www.thinksrs.com/products/BGA244.htm

Straty, G. & Younglove, B. (1973) Velocity of sound in saturated and compressed fluid oxygen. *The Journal of Chemical Thermodynamics.* 5 (3), 305-312.

Sun, L., Duan, Y., Shi, L., Zhu, M. & Han, L. (1997) Speed of sound and ideal-gas heat capacity at constant pressure of gaseous difluoromethane. *Journal of Chemical & Engineering Data.* 42 (4), 795-799.

Tegeler, C., Span, R. & Wagner, W. (1999) A new equation of state for argon covering the fluid region for temperatures from the melting line to 700 K at pressures up to 1000 MPa. *Journal of Physical and Chemical Reference Data.* 28 (3), 779-850.

Trusler, J. P. M. (1991) *Physical acoustics and metrology of fluids.* Bristol, Adam Hilger.

Trusler, J. & Zarari, M. (1992) The speed of sound and derived thermodynamic properties of methane at temperatures between 275 K and 375 K and pressures up to 10 MPa. *The Journal of Chemical Thermodynamics.* 24 (9), 973-991.

Trusler, J. & Zarari, M. (1996) The Speed of Sound in Gaseous Propane at Temperatures between 225 K and 375 K and at Pressures up to 0.8 MPa. *The Journal of Chemical Thermodynamics.* 28 (3), 329-335.

Vacek, V., Hallewell, G. & Lindsay, S. (2001) Velocity of sound measurements in gaseous per-fluorocarbons and their mixtures. *Fluid Phase Equilibria.* 185 (1), 305-314.

Vacek, V., Vítek, M. & Doubek, M. (2013) Velocity of sound in Perfluoropropane (C 3 F 8), Perfluoroethane (C 2 F 6) and their mixtures. *Fluid Phase Equilibria.* 351 53-60.

Valdes, J. L. & Cadet, G. (1991) Ultrasonic time-of-flight method for on-line quantitation of in situ generated arsine. *Analytical Chemistry.* 63 (4), 366-369.

Van Itterbeek, A., De Rop, W. & Forrez, G. (1957) Measurements on the velocity of sound in nitrogen under high pressure. *Applied Scientific Research.* 6 (5), 421-432.

Van Itterbeek, A. & Keesom, W. H. (1930) Determination of the ratio of the specific heats (cp/cv) of helium gas at the boiling point of oxygen, by means of the velocity of sound. *Communication from the Physical Laboratory at Leiden.* 209a.

Van Itterbeek, A. & Thys, L. (1938) Measurements on the absorption and the velocity of sound in hydrogen-, deuterium-, helium-and neon gas. *Physica.* 5 (9), 889-897.

Van Itterbeek, A. & Van Doninck, W. (1946) Velocity of sound in mixtures of argon, helium and hydrogen at low temperatures. *Proceedings of the Physical Society.* 58 (5), 615.

Van Itterbeek, A. & Van Paemel, O. (1938) Measurements on the velocity of sound in gaseous argon and deuterium respectively at liquid oxygen and hydrogen temperatures. Calculation and discussion, of the second virial coefficient of argon. *Physica.* 5 (9), 845-854.

Van Itterbeek, A. & Zink, J. (1958) Measurements on the velocity of sound in oxygen gas under high pressure. *Applied Scientific Research, Section A.* 7 (5), 375-385.

Ortiz Vega, D. (2013) *A new wide range equation of state for helium- 4.*

Vyas, J., Katti, V., Gupta, S. & Yakhmi, J. (2006) A non-invasive ultrasonic gas sensor for binary gas mixtures. *Sensors and Actuators B: Chemical.* 115 (1), 28-32.

Wagner, W. & Pruß, A. (2002) The IAPWS formulation 1995 for the thermodynamic properties of ordinary water substance for general and scientific use. *Journal of Physical and Chemical Reference Data.* 31 (2), 387-535.

Warner, G. W. (1937) A Study of the Effect of Frequency and Temperature on the Velocity of Ultrasonic Waves in Gases. *The Journal of the Acoustical Society of America.* 9 (1), 30-36.

Woodburn, J. (1964) Velocity of Sound Measurements in High-Pressure Steam. *The Journal of the Acoustical Society of America.* 36 (10), 1918-1921.

Younglove, B. (1965) Speed of sound in fluid parahydrogen. *The Journal of the Acoustical Society of America.* 38 (3), 433-438.

Younglove, B. & Frederick, N. (1990) Sound speed measurements on gas mixtures of natural gas components using a cylindrical resonator. *International Journal of Thermophysics.* 11 (5), 897-910.

Younglove, B. & McCarty, R. (1993) Speed of Sound Data and Related Models for Mixtures ofNatural Gas Constituents.

Younglove, B. A. & McCarty, R. D. (1980) Speed-of-sound measurements for nitrogen gas at temperatures from 80 to 350 K and pressures to 1.5 MPa. *The Journal of Chemical Thermodynamics.* 12 (12), 1121-1128.

Zhang, J., Lin, H., Sun, J., Feng, X., Gillis, K. & Moldover, M. (2010) Cylindrical acoustic resonator for the re-determination of the Boltzmann constant. *International Journal of Thermophysics.* 31 (7), 1273-1293.

Zhou, Y., Liu, J., Penoncello, S. G. & Lemmon, E. W. (2014) An equation of state for the thermodynamic properties of cyclohexane. *Journal of Physical and Chemical Reference Data.* 43 (4), 043105.

Zuckerwar, A. J. (2002) *Handbook of the speed of sound in real gases.* , Academic Press.

# Appendix

## A1. Determination of Real Gas SoS

In this research project, the real gas SoS $W$ of argon, helium, nitrogen and dry air at the experimental conditions are required to be known. The conditions are as follows: $P \approx 1$ atm; $f$ = 121362 Hz; $T \approx 5$ to 55 °C for Ar, $N_2$, dry air, and $T \approx 25$ °C for He.

### A1.1 Real Gas SoS of Argon and Helium

In order to determine $W$ for Ar and He, firstly the NIST REFPROP software is utilised to generate the lossless real gas SoS $W_\theta$. For these two pure monatomic gases, only the dispersion effect of translational relaxation needs to be accounted for. The effect is estimated based on the method given in Zuckerwar (2002).

The magnitude of dispersion could be estimated as follows:

$$\frac{W}{W_\theta} \approx \sqrt{1 + \omega^2 \tau_{r_tr}^2} \tag{90}$$

where $\omega$ refers to the angular frequency and $\tau_{r_tr}$ the translational relaxation time. This equation should be accurate up to $\omega\tau_{r_tr} = 1$. $\tau_{r_tr}$ is given by:

$$\tau_{r_tr} = \frac{1}{\rho W_\theta^2}\left(\frac{4}{3}\mu + \frac{\kappa M}{C_P}\right) \tag{91}$$

where $\rho$ denotes the mass density, $\mu$ the dynamic viscosity, $\kappa$ the thermal conductivity, $M$ the molecular weight, and $C_P$ the isobaric heat capacity (real gas). For estimation purposes, $C_P$ can be assumed equivalent to the ideal gas isobaric heat capacity $C_P^o$.

It is found that for both Ar and He under the experimental conditions the ratios of $W/W_\theta$ are not significantly different from unity (see Table 54 for example). As a consequence, I conclude that the dispersion effect is negligible and thus $W = W_\theta$. In this case, the uncertainties of $W$ and $W_\theta$, i.e. $U(W)$ and $U(W_\theta)$, are also equivalent. According to the information given in the software $U$ is estimated to be 50 ppm for He (Ortiz Vega, 2013). For Ar, by comparison with

reported experimentally measured Ar SoS data (Ewing & Trusler, 1992; Moldover et al., 1988), $U$ is estimated to be within 10 ppm. The experimental data were organised in *Handbook of Speed of Sound in Real Gases* (Zuckerwar, 2002), and under the conditions of these experiments the translational dispersion was also negligible.

Table 54. Estimation of dispersion effect for Ar and He

| Gas | Ar | He |
|---|---|---|
| $T$ (K) | 298.15 | |
| $P$ (Pa) | 101325 | |
| $f$ (Hz) | 121362 | |
| $\rho$ (kg/m$^3$)* | 1.6339 | 0.16352 |
| $W_\theta$ (m/s)* | 321.67 | 1016.4 |
| $\mu$ (Pa·s)* | $2.2624 \times 10^{-5}$ | $1.9846 \times 10^{-5}$ |
| $\kappa$ (J/(m·s·K))* | $1.7746 \times 10^{-2}$ | $1.5531 \times 10^{-1}$ |
| $M$ (g/mol)* | 39.948 | 4.002602 |
| $C_P^o$ (J/(mol·K))* | 20.786 | 20.786 |
| $\tau_{r_tr}$ (s) | $3.8 \times 10^{-10}$ | $3.3 \times 10^{-10}$ |
| $W/W_\theta$ | 1.00000004 | 1.00000003 |
| *Data source: NIST REFPROP software | | |

## A1.2 Real Gas SoS of Nitrogen

For the determination of $W$ for $N_2$, similar to the case for Ar and He, the first step is to obtain $W_\theta$ from the NIST REFPROP software. $N_2$ is a diatomic gas, thus the molecules have both internal and external degrees of freedom, and dispersion phenomenon may be caused by translational, rotational and vibrational relaxations.

The method used to estimate the translational dispersion for $N_2$ is similar to that given in Section A1.1, while Equation (90) turns into:

$$\frac{W_{tr}}{W_\theta} \approx \sqrt{1 + \omega^2 \tau_{r_tr}^2} \tag{92}$$

where $W_{tr}$ represents the real gas SoS under the assumption that dispersion could only result from translational relaxation. $\tau_{r_tr}$ can still be calculated from Equation (91). Under the

experimental conditions, the ratios of $W_{tr}/W_{\theta}$ are extremely close to unity (see Table 55 for example), thus the dispersion due to this relaxation mechanism is negligible.

Table 55. Estimation of translational dispersion effect for $N_2$

| | |
|---|---|
| $T$ (K) | 298.15 |
| $P$ (Pa) | 101325 |
| $f$ (Hz) | 121362 |
| $\rho$ (kg/m$^3$)* | 1.1452 |
| $W_{\theta}$ (m/s)* | 352.07 |
| $\mu$ (Pa·s)* | $1.7805 \times 10^{-5}$ |
| $\kappa$ (J/(m·s·K))* | $2.5835 \times 10^{-2}$ |
| $M$ (g/mol)* | 28.01348 |
| $C_P^o$ (J/(mol·K))* | 29.125 |
| $\tau_{r_tr}$ (s) | $3.4 \times 10^{-10}$ |
| $W_{tr}/W_{\theta}$ | 1.00000003 |
| *Data source: NIST REFPROP software | |

The rotational relaxation time $\tau_{r_ro}$ can be estimated according to (Miller & Andres, 1967):

$$\tau_{r_ro} = Z_{ro}\frac{\pi\mu}{4P} \tag{93}$$

where $Z_{ro}$ indicates the rotational collision number. $Z_{ro}$ is temperature dependent, and is around 3 to 6 for $N_2$ within the experimental temperature range (Lordi & Mates, 1970; Parker, 1959). At around 5 to 55 °C and 1 atm, $\tau_{r_ro}$ is about 0.4 to 0.9 ns and of the same order of magnitude as that of $\tau_{r_tr}$ (see Table 56 for example). $\omega\tau_{r_ro} \ll 1$ is satisfied, therefore, at the experimental conditions the dispersion caused by rotational relaxation can be neglected.

Table 56. Estimation of rotational relaxation time for $N_2$

| | |
|---|---|
| $T$ (K) | 298.15 |
| $P$ (Pa) | 101325 |
| $Z_{ro}$ | 4.5 |
| $\mu$ (Pa·s)* | $1.7805 \times 10^{-5}$ |

| $\tau_{r_ro}$ (s) | $6.2 \times 10^{-10}$ |
|---|---|
| *Data source: NIST REFPROP software | |

For $N_2$ under the experimental conditions, only vibrational relaxation can give rise to significant dispersion. Since $f/P \gg 30$ Hz·MPa$^{-1}$ in the experiments, $W$ of $N_2$ can be considered equivalent to the vibrational relaxation high-frequency-limit SoS $W_{\infty_vb}$ (Gomes & Trusler, 1998). In this case the dispersion correction factor $K_d$ is related to the vibrational relaxation strength $\varepsilon_{r_vb}$ by:

$$K_d = \frac{\varepsilon_{r_vb}}{1 - \varepsilon_{r_vb}} \tag{94}$$

and

$$\varepsilon_{r_vb} = \frac{RC_{vb}}{(C_P^o - C_{vb})(C_P^o - R)} \tag{95}$$

$$\frac{C_{vb}}{R} = \left(\frac{\theta_{vb}}{T}\right)^2 \frac{\exp\left(-\frac{\theta_{vb}}{T}\right)}{\left[1 - \exp\left(-\frac{\theta_{vb}}{T}\right)\right]^2} \tag{96}$$

where $C_{vb}$ is the contribution of the molecular vibrational mode to heat capacity, and $\theta_{vb}$ the characteristic vibrational temperature equal to 3352.0 K for $N_2$ (Zuckerwar, 2002). The data for $C_P^o$ can be found from the NIST REFPROP software. If $T$ = 25 °C, then $K_d \approx 190$ ppm. At the experimental conditions, $U(W)$ is estimated to be within 10 ppm by comparison between reported experimental data for $N_2$ (Ewing & Trusler, 1992) and the corresponding real gas SoS determined using the above method. The data can be found in Zuckerwar's handbook, and under the conditions of their experiment, similarly, significant dispersion can only arise from vibrational relaxation and $f/P \gg 30$ Hz·MPa$^{-1}$.

## A1.3 Real Gas SoS of Dry Air

The method used by Zuckerwar (2002) for the determination of the real gas SoS of standard dry air (U.S. Standard Atmosphere, 1976) including the uncertainty analysis is given in

Sections A1.3.1 to A1.3.4. The correction for the composition variation between the standard and the experimental dry air can be found in Section A1.3.5.

### A1.3.1 Ideal Gas SoS of Standard Dry Air

The leading constituents of standard dry air and their molecular weights $M_i$ and mole factions $x_i$ are given in Table 57. The molecular weight of standard dry air $M$ is determined using the values of $M_i$ and $x_i$ of only the listed constituents according to the linear mixing rule.

Table 57. Leading constituents of standard dry air

| Constituents | Molecular Weights, $M_i$ (g/mol) | Mole Fractions, $x_i$ |
|---|---|---|
| $N_2$ | 28.01348 | 0.78084 |
| $O_2$ | 31.9988 | 0.209476 |
| Ar | 39.948 | 0.00934 |
| $CO_2$ | 44.0095 | 0.000314 |
| Ne | 20.1797 | $1.818 \times 10^{-5}$ |
| He | 4.002602 | $5.24 \times 10^{-6}$ |
| Kr | 83.8 | $1.14 \times 10^{-6}$ |
| $CH_4$ | 16.04246 | $2 \times 10^{-6}$ |
| $H_2$ | 2.01588 | $5 \times 10^{-7}$ |
| Xe | 131.29 | $8.7 \times 10^{-8}$ |
| $N_2O$ | 44.01288 | $2.7 \times 10^{-7}$ |
| CO | 28.011 | $1.9 \times 10^{-7}$ |
| Molecular Weight of Standard Dry Air, $M$ = 28.9645 g/mol | | |

$C_P^o$ for standard dry air can be obtained according to the linear mixing rule as well. However, it is more convenient to use the following polynomial equation:

$$\frac{C_P^o}{R} = a_0 + a_1 T + a_2 T^2 + a_3 T^3 \tag{97}$$

$$a_0 = 3.5623$$

$$a_1 = -6.128 \times 10^{-4}\ \text{K}^{-1}$$

$$a_2 = 1.401 \times 10^{-6}\ \text{K}^{-2}$$

$$a_3 = -1.696 \times 10^{-10}\ \text{K}^{-3}$$

where $a_0$ to $a_3$ represent the equation coefficients. It should be noted that this equation is valid for temperatures between 250 and 600 K. $C_V^o$ is then obtained from Equation (46). $W_o$ can then be determined according to Equation (47).

### A1.3.2 Virial Correction Factor and Lossless Real Gas SoS of Standard Dry Air

In theory, the quadratic and cubic mixing rules can be employed for the calculation of the second and third viral coefficients of standard dry air $\mathcal{B}$ and $\mathcal{C}$, respectively. However, in practice, the following two equations are always used for convenience:

$$\mathcal{B} = a_v - b_v \exp(\frac{c_v}{T}) \tag{98}$$

$$a_v = 152.2\ \text{cm}^3/\text{mol}$$

$$b_v = 111.3\ \text{cm}^3/\text{mol}$$

$$c_v = 108.1\ \text{K}$$

$$\mathcal{C} = \left[d_v - e_v \exp(\frac{f_v}{T})\right] \exp(-g_v T) + C_\infty \tag{99}$$

$$d_v = 3871.0\ (\text{cm}^3/\text{mol})^2$$

$$e_v = 1237.0\ (\text{cm}^3/\text{mol})^2$$

$$f_v = 171.1\ \text{K}$$

$$g_v = 0.0058\ \text{K}^{-1}$$

$$C_\infty = 1000\ (\text{cm}^3/\text{mol})^2$$

where $a_v$ to $g_v$ and $C_\infty$ indicate the equation coefficients. These two equations are valid over the temperature range from 230 to 650 K, and differentiating or double differentiating them with respect to temperature will yield $d\mathcal{B}/dT$, $d\mathcal{C}/dT$, $d^2\mathcal{B}/dT^2$ and $d^2\mathcal{C}/dT^2$. Equations

(53), (54), (56) and (57) are utilised for the computation of the second and third acoustic virial coefficients $\mathcal{K}$ and $\mathcal{L}$, and the second and third acoustic virial pressure coefficients $\mathcal{F}$ and $\mathcal{G}$. Then, the virial correction factor $K_v$ is obtained from Equation (59). With $W_o$ and $K_v$, $W_\theta$ can be determined from Equation (58).

### A1.3.3 Dispersion Correction Factor and Real Gas SoS of Standard Dry Air

In order to obtain $W$ for standard dry air, the dispersion effects need to be analysed. According to Equation (92), it can be found that under the experimental conditions translational dispersion is insignificant (see Table 58 for example).

Table 58. Estimation of translational dispersion effect for standard dry air

| | |
|---|---|
| $T$ (K) | 298.15 |
| $P$ (Pa) | 101325 |
| $f$ (Hz) | 121362 |
| $\rho$ (kg/m$^3$)* | 1.1843 |
| $W_\theta$ (m/s) | 346.268 |
| $\mu$ (Pa·s)* | $1.8490 \times 10^{-5}$ |
| $\kappa$ (J/(m·s·K))* | $2.5850 \times 10^{-2}$ |
| $M$ (g/mol) | 28.9645 |
| $C_P^o$ (J/(mol·K)) | 29.098 |
| $\tau_{r_tr}$ (s) | $3.5 \times 10^{-10}$ |
| $W_{tr}/W_\theta$ | 1.00000004 |
| *Data are obtained using the NIST REFPROP software by simplifying the standard dry air to be a mixture comprising only $N_2$, $O_2$, Ar and $CO_2$ with mole fractions of 0.780864, 0.209482, 0.00934 and 0.000314, respectively. This composition is determined by setting the mole fractions of all the other constituents in standard dry air to zero and then multiplying the mole fractions of those four constituents by a same factor to normalise the sum of them to unity. | |

The rotational relaxation frequency $f_{r_ro}$ can be estimated as follows:

$$\frac{f_{r_ro}}{P} = 458.1 \frac{\exp\left(16.8T^{-1/3}\right)}{\mu} \tag{100}$$

At the experimental conditions $f \ll f_{r_ro}$ (see Table 59 for example), hence, rotational dispersion is negligible.

Table 59. Estimation of rotational relaxation frequency

| | |
|---|---|
| $T$ (K) | 298.15 |
| $P$ (atm) | 1 |
| $\mu$ (Pa·s)* | $1.8490 \times 10^{-5}$ |
| $f_{r_ro}$ (Hz) | $3.06 \times 10^{8}$ |
| *Data source: NIST REFPROP software | |

Only vibrational dispersion is significant at the experimental conditions. The vibrational relaxation frequencies of $N_2$ and $O_2$, $f_{r_vb}^{\mathrm{N}}$ and $f_{r_vb}^{\mathrm{O}}$ (Hz), are given by:

$$f_{r_vb}^{\mathrm{N}} = \frac{P}{P^*}\left(\frac{T^*}{T}\right)^{1/2}\left[6.614 \times 10^4 \exp\left(-58.90 T^{-1/3}\right)\right] \tag{101}$$

$$f_{r_vb}^{\mathrm{O}} = \frac{P}{P^*}\left[2.131 \times 10^5 \exp\left(-60.40 T^{-1/3}\right)\right] \tag{102}$$

where $P^*$ refers to the reference pressure of 1 atm and $T^*$ the reference temperature of 293.15 K. The vibrational relaxation strengths, $\varepsilon_{r_vb}^{\mathrm{N}}$ and $\varepsilon_{r_vb}^{\mathrm{O}}$, are written:

$$\varepsilon_{r_vb}^{\mathrm{N}} = \frac{x_{\mathrm{N}} R C_{vb}^{\mathrm{N}}}{\left(C_P^o - x_{\mathrm{N}} C_{vb}^{\mathrm{N}} - x_{\mathrm{X}} C_{vb}^{\mathrm{O}}\right)\left(C_P^o - R\right)} \tag{103}$$

$$\varepsilon_{r_vb}^{\mathrm{O}} = \frac{x_{\mathrm{X}} R C_{vb}^{\mathrm{O}}}{\left(C_P^o - x_{\mathrm{N}} C_{vb}^{\mathrm{N}} - x_{\mathrm{X}} C_{vb}^{\mathrm{O}}\right)\left(C_P^o - R\right)} \tag{104}$$

where $x_{\mathrm{N}}$ and $x_{\mathrm{O}}$ indicate $N_2$ and $O_2$ mole fractions; $C_{vb}^{\mathrm{N}}$ and $C_{vb}^{\mathrm{O}}$ the vibrational heat capacities which are calculated using Equation (96) with $\theta_{vb}^{\mathrm{N}}$ = 3352.0 K and $\theta_{vb}^{\mathrm{O}}$ = 2239.1 K. The dispersion correction factor is obtained as follows:

$$K_d = \frac{\varepsilon_{r_vb}^{\mathrm{N}}}{1-\varepsilon_{r_vb}^{\mathrm{N}}}\left[\frac{\left(f/f_{r_vb}^{\mathrm{N}}\right)^2}{1+\left(f/f_{r_vb}^{\mathrm{N}}\right)^2}\right] + \frac{\varepsilon_{r_vb}^{\mathrm{O}}}{1-\varepsilon_{r_vb}^{\mathrm{O}}}\left[\frac{\left(f/f_{r_vb}^{\mathrm{O}}\right)^2}{1+\left(f/f_{r_vb}^{\mathrm{O}}\right)^2}\right]. \tag{105}$$

Then, by substituting $W_\theta$ and $K_d$ into Equation (60), $W$ for standard dry air can be determined.

At around 5 to 55 °C and 1 atm $f_{r_vb}^{\mathrm{N}}$ and $f_{r_vb}^{\mathrm{O}}$ are below 35 Hz, thus $W$ under the experimental conditions can be considered equivalent to $W_{\infty_vb}$ (vibrational relaxation high-frequency-limit SoS)[16], in which case $K_d$ can simply be obtained from:

$$K_d = \frac{\varepsilon_{r_vb}^{\mathrm{N}}}{1-\varepsilon_{r_vb}^{\mathrm{N}}} + \frac{\varepsilon_{r_vb}^{\mathrm{O}}}{1-\varepsilon_{r_vb}^{\mathrm{O}}}. \tag{106}$$

### A1.3.4 Uncertainty Analysis for Real Gas SoS of Standard Dry Air

The uncertainty of $W$ is estimated according to[17]:

$$\frac{U(W)}{W} = \frac{1}{2}\left(\left|\frac{U(\gamma^o)}{\gamma^o}\right| + \left|\frac{U(K_v)}{1+K_v}\right| + \left|\frac{U(K_d)}{1+K_d}\right|\right). \tag{107}$$

The first term in the brackets on the right hand side is given by:

$$\frac{U(\gamma^o)}{\gamma^o} = -\frac{U(C_P^o)}{C_P^o}(\gamma^o - 1) \tag{108}$$

where $U(C_P^o) = 0.005C_P^o$; the second term:

$$\frac{U(K_v)}{1+K_v} = \frac{[\psi(1-\psi\mathcal{B})q_{v1} - \psi^2\mathcal{K} + \psi^2 q_{v2}]U(\mathcal{B}) + \psi^2 q_{v3}U(\mathcal{C})}{1+K_v} \tag{109}$$

where

$$\psi = \frac{P}{RT} \tag{110}$$

[16] Also applies to the case of the experimental dry air under the same conditions.
[17] The uncertainties of the universal gas constant and molecular weight are considered negligible.

$$q_{v1} = 2 - 2(\gamma^o - 1)\frac{c_v}{T} + \frac{(\gamma^o - 1)^2}{\gamma^o}\frac{c_v}{T}\left(2 + \frac{c_v}{T}\right) \tag{111}$$

$$q_{v2} = \frac{2(\gamma^o - 1)}{\gamma^o}\left[\mathcal{B} + \left(1 - \frac{c_v\gamma^o}{T} + \frac{c_v}{T}\right)\frac{b_v c_v}{T}\exp\left(\frac{c_v}{T}\right)\right]\left[1 - \frac{c_v}{T}\left(1 - \frac{c_v\gamma^o}{T} + \frac{c_v}{T}\right)\right] \tag{112}$$

$$q_{v3} = \frac{1 + 2\gamma^o}{\gamma^o} - \frac{f_v}{T}\frac{[(\gamma^o)^2 - 1]}{\gamma^o} + \frac{f_v}{T}\left(2 + \frac{f_v}{T}\right)\frac{(\gamma^o - 1)^2}{2\gamma^o} \tag{113}$$

with $U(\mathcal{B}) = 0.2 + 0.035|\mathcal{B}|$ in cm$^3$/mol and $U(\mathcal{C}) = 200$ (cm$^3$/mol)$^2$; and the third term:

$$\frac{U(K_d)}{1 + K_d} = \frac{-2f^2}{1 + K_d}\left[\frac{\varepsilon^{\mathrm{N}}_{r_vb}}{1 - \varepsilon^{\mathrm{N}}_{r_vb}}\frac{f^{\mathrm{N}}_{r_vb}}{\left[\left(f^{\mathrm{N}}_{r_vb}\right)^2 + f^2\right]^2}U\left(f^{\mathrm{N}}_{r_vb}\right) + \frac{\varepsilon^{\mathrm{O}}_{r_vb}}{1 - \varepsilon^{\mathrm{O}}_{r_vb}}\frac{f^{\mathrm{O}}_{r_vb}}{\left[\left(f^{\mathrm{O}}_{r_vb}\right)^2 + f^2\right]^2}U\left(f^{\mathrm{O}}_{r_vb}\right)\right] \tag{114}$$

where $U\left(f^{\mathrm{N}}_{r_vb}\right) = 0.15f^{\mathrm{N}}_{r_vb}$ ($f^{\mathrm{N}}_{r_vb} \geq 200$ Hz) or $0.25f^{\mathrm{N}}_{r_vb}$ ($f^{\mathrm{N}}_{r_vb} < 200$ Hz), $U\left(f^{\mathrm{O}}_{r_vb}\right) = 0.1f^{\mathrm{O}}_{r_vb}$ ($f^{\mathrm{O}}_{r_vb} \geq 30$ Hz) or $0.5f^{\mathrm{O}}_{r_vb}$ ($f^{\mathrm{O}}_{r_vb} < 30$ Hz). Under the experimental conditions $W$ uncertainty is around 0.1%.

### A1.3.5 Real Gas SoS of Experimental Dry Air

For convenience, standard dry air and experimental dry air will be referred to as 'SA' and 'EA', respectively. SA can be regarded as a binary mixture of $CO_2$ and a $CO_2$-free part; the latter will be referred to as 'CFS' ($CO_2$-free standard dry air). EA can also be treated in this way, and the $CO_2$-free part is denoted by 'CFE' ($CO_2$-free experimental dry air). The $CO_2$ mole fractions in SA and EA are represented by $x_{\mathrm{C}}$ (314 ppm) and $x'_{\mathrm{C}}$ (404 ppm), respectively. The correction for the composition variation in the determination of $W$ for EA is also based upon the methodology given in Zuckerwar (2002). Similar to the case for SA, translational and rotational dispersion effects for EA are considered to be negligible.

The molecular weight and ideal gas isobaric heat capacity of CFS and CFE can be expressed by:

$$M(CFE) = M(CFS) = \frac{M(SA) - x_{\mathrm{C}} M(CO_2)}{1 - x_{\mathrm{C}}} \tag{115}$$

$$C_P^o(CFE) = C_P^o(CFS) = \frac{C_P^o(SA) - x_{\mathrm{C}} C_P^o(CO_2)}{1 - x_{\mathrm{C}}}. \tag{116}$$

For EA,

$$M(EA) = (1 - x'_{\mathrm{C}}) M(CFS) + x'_{\mathrm{C}} M(CO_2) \tag{117}$$

$$C_P^o(EA) = (1 - x'_{\mathrm{C}}) C_P^o(CFS) + x'_{\mathrm{C}} C_P^o(CO_2). \tag{118}$$

$C_P^o(\mathrm{CO_2})$ can be determined according to Equation (97) with $a_0 = 2.3457$, $a_1 = 8.9374 \times 10^{-3}$ K$^{-1}$ , $a_2 = -6.7157 \times 10^{-6}$ K$^{-2}$ and $a_3 = 1.8369 \times 10^{-9}$ K$^{-3}$. The second and third virial coefficients $\mathcal{B}$ and $\mathcal{C}$ for EA are considered equivalent to those for SA because the contribution of $CO_2$ is negligible. The mole fractions of $N_2$ and $O_2$ in EA, $x'_{\mathrm{N}}$ and $x'_{\mathrm{O}}$, are written:

$$x'_{\mathrm{N}} = x_{\mathrm{N}} \frac{1 - x'_{\mathrm{C}}}{1 - x_{\mathrm{C}}} \tag{119}$$

$$x'_{\mathrm{O}} = x_{\mathrm{O}} \frac{1 - x'_{\mathrm{C}}}{1 - x_{\mathrm{C}}}. \tag{120}$$

$K_d$ is calculated according to Equation (106). Based on the above corrections, $W$ for EA can be determined, and the uncertainty is taken to be the same as that for SA under the experimental conditions.

## A2. Photos of Experimental System and SoS sensor

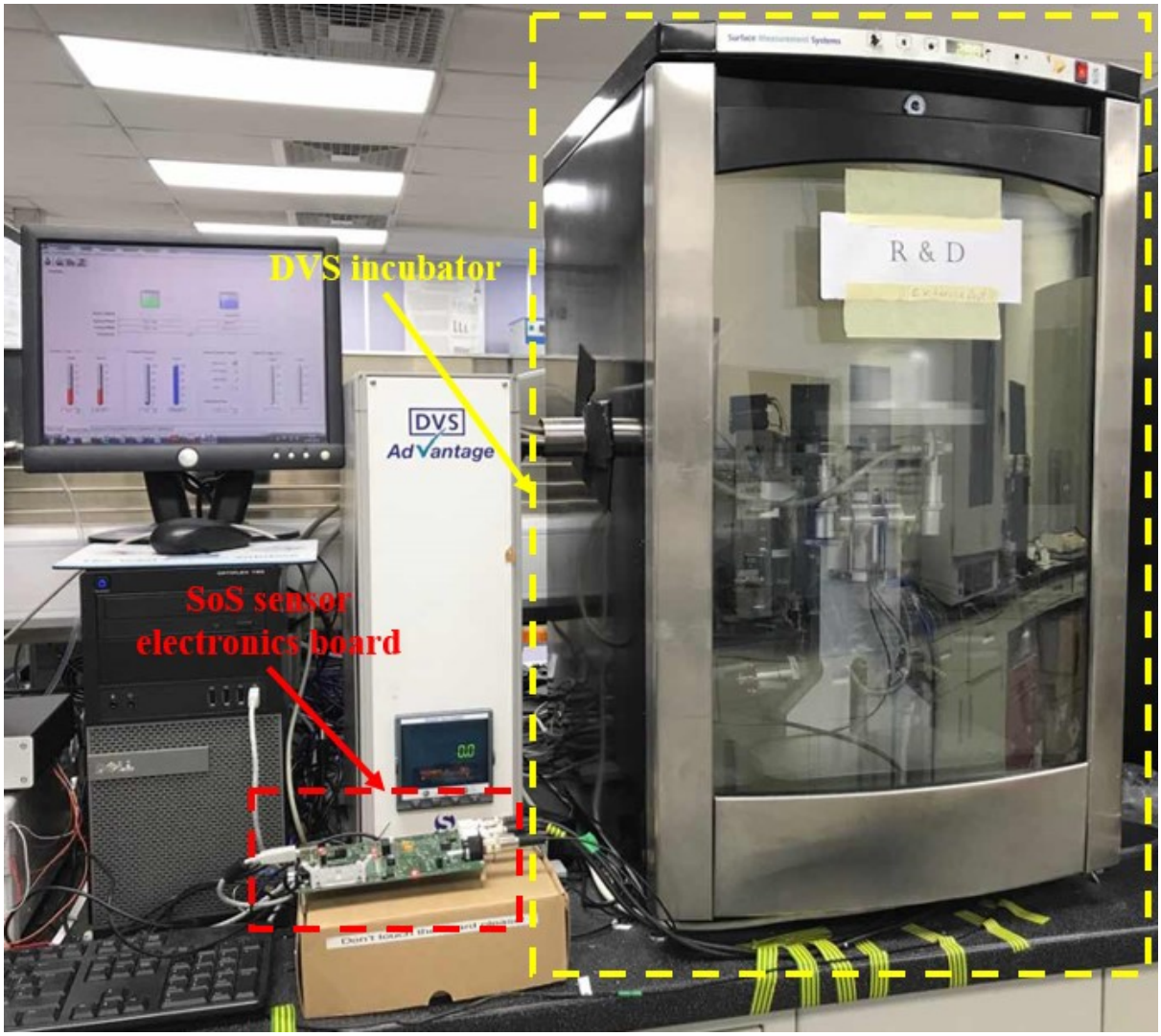



Figure 102. DVS based experimental system

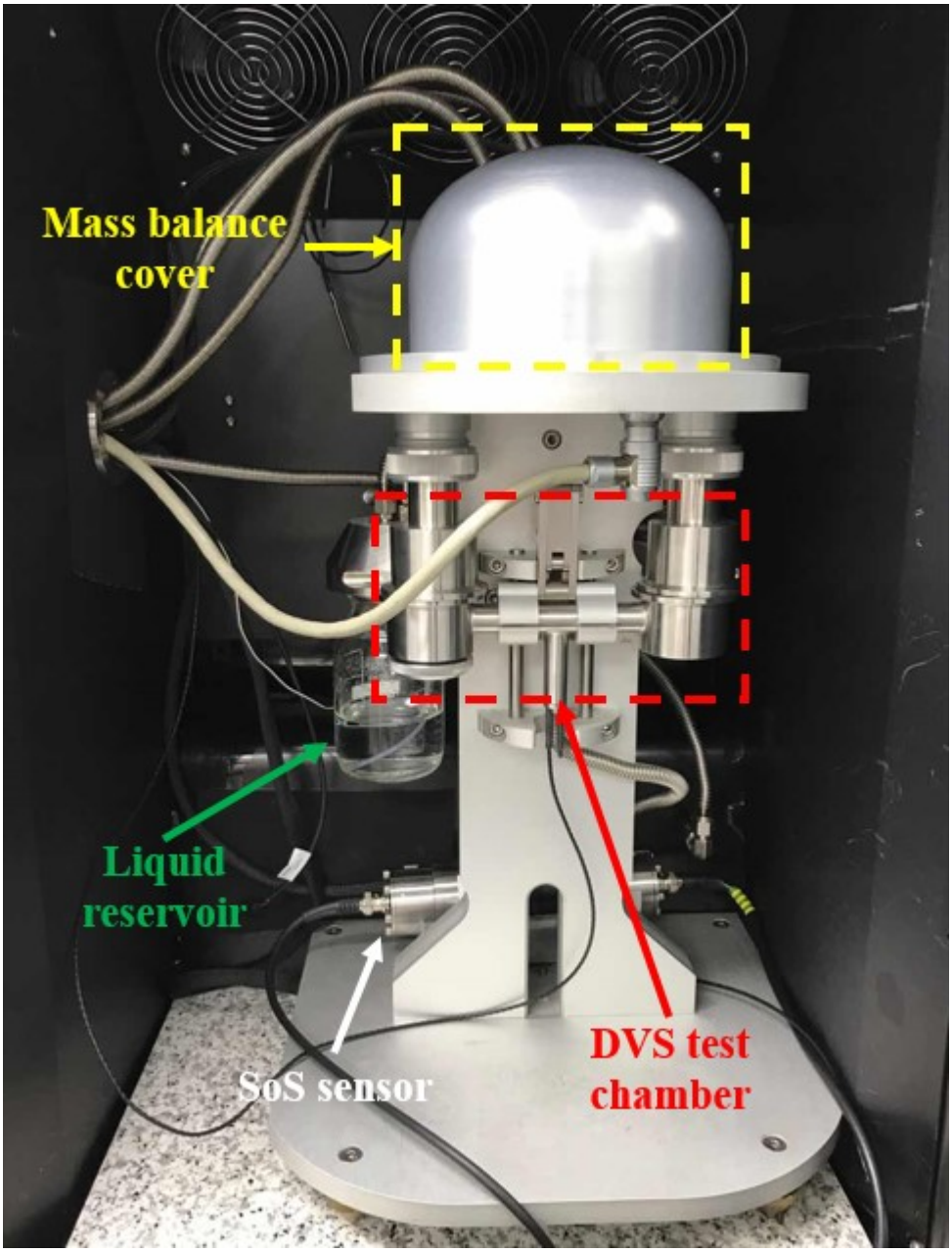



Figure 103. Interior of DVS incubator

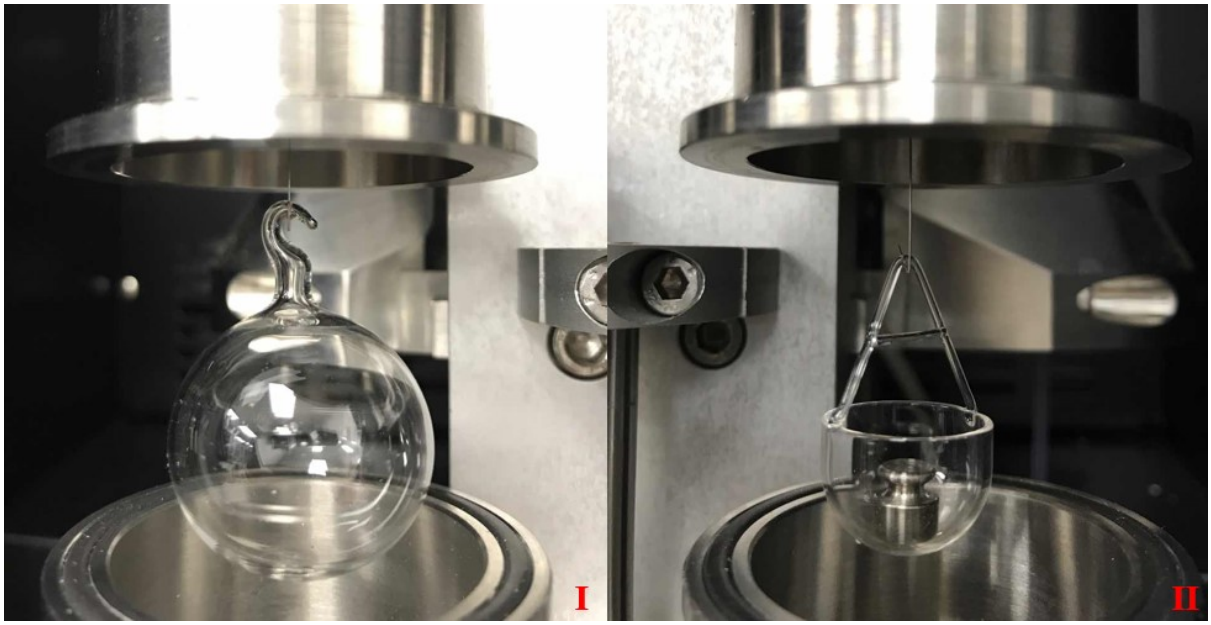



Figure 104. I – glass sphere; II – counterweight




Figure 105. SoS sensor

# A3. Measurement Precision of SoS Sensor

**Speed of Sound Sensor Precision**

Author: Dirk Bruere

Date: 7 December 2017

Version: 1.1

Company: Surface Measurement Systems Ltd.

**Overview**

This document discusses the precision of the measurements delivered by the Speed of Sound (SoS) sensor, and covers data acquisition, statistical processing and observed precision under constant temperature conditions. The electronic design, firmware and onboard data processing was created the author.

The original remit was to determine the speed of sound in a gas to a precision of one part in 50,000, or 1:30,000 worst case.

**Data Acquisition**

The firmware for data acquisition and onboard processing runs under a 10 ms interrupt. That is, the whole chain of events from the transmission of the ultrasonic pulse, its reception and the data processing resulting in a number representing time of flight (ToF) happens 100 times per second.

In the electronics, the peak to peak amplitude of the first received ultrasonic signal is approximately 2100 mV, with peak to peak noise of 71 mV and RMS noise of 1.4 mV, which is typical. The effect of noise on the overall precision of the system appears to have very little effect, although it has not been quantified. The analog to digital (ADC) converter used was part of the STM32F303 MCU, resolution 12 bits. Hence circuit noise was comparable to ADC resolution. The time resolution was approximately 200 ns for 5 msps ADC limit. At 125 kHz there are approximately 40 samples per received cycle of which between 5 and 8 cycles per pulse train are used in the current algorithm.

**Statistical Processing**

Note that no deep theoretical statistical analysis was done on the limitations imposed by electronics noise or the sampling limitations. From an engineering perspective it was simpler just to build to best practice and test for results after "back of envelope" calculations indicated the correct ballpark values.

From a post hoc point of view one can argue that with the current algorithm we employ a minimum of 4 data points (actually more in practice, SMS Ltd. proprietary information) to determine zero crossings. Hence it reduces time uncertainty from 200 ns to 100 ns, and sampling at a rate of 100 per second will reduce it to 10ns providing a total expected resolution of 1:30,000 given a 300,000 ns ToF. Naturally, this assumption is only valid for a signal having a certain amount of jitter or uncertainty between sets of readings, which we assume is present due to temperature fluctuations, variations in signal propagation in the analog electronics and variations in the precise timing of the transmitted signal. The latter is partially due to different code execution paths and timings (even though ultimately coming from the same oscillator).

These assumptions appear to be borne out by the fact we can see changes in ToF of less than 1 ns as temperature varies by a fraction of a milliKelvin (we can resolve down to 200 μK).

A total of 100 results are processed every second to provide an averaged number plus a crude statistical indication of precision. The processing is done in two stages.

Results are collected in batches of 10 which are then subjected to a median filtering process whereby they are sorted in numerical order and then a certain number of the extrema are discarded. The number discarded can be set by external command, but typically the default is used, which discards the two highest and two lowest values. The remaining 6 values are averaged.

After one second we have a set of 10 such averaged values. We then determine the mean and standard deviations (SD) for each set of 10 which is delivered to the PC software approximately every second. The standard deviation includes a small sample correction. This involves increasing SD by $\sqrt{[N/(N-1)]}$ which is a precalculated value in the firmware of 1.054.

The resulting relative standard deviation (RSD) is delivered as a ratio of 1:N, or more precisely, the value N is delivered every second along with the mean value of the results.

Another limitation of the statistical calculation is that ToF is delivered in integer nanoseconds, which means that at close to constant temperature we get "jumps" between two values one nanosecond apart rather than seeing a more accurate value. This was done for a number of reasons, not least because 1 ns is "good enough" for engineering purposes. It means that given a ToF of typically around 300,000 ns any RSD beyond 1:300,000 is likely unreliable, although from the results below one can quite easily see that RSD may well be higher than that in practice if averaging is done over a longer period than one second.

In the PC software Test Tool developed for the SoS sensor we provide a real-time graphical representation of the quality of the results. See picture below.

**Results**

A plot of temperature, ToF and RSD is shown below. This was captured in the Lab at Surface Measurement Systems Ltd. 10:30, 5 December 2017 in a temperature stable (0.1 °C) DVS incubator over a period of 10 minutes.

It shows results over a temperature variation of 10 mK during that time.

Typically, ToF varies by 5 ns over that range, and the RSD averages (by eye) approximately $1{:}10^6$.

The timing limitation on the SoS board is determined by the crystal oscillator THD3004-16 by Pletronics with a stability of 0.28 ppm and a 15 year stability of 3.4 ppm. For all practical purposes, again it is the short term stability in an air conditioned constant temperature (2 °C) laboratory that matters for the electronics and measurements. Note that the electronics lies outside the DVS incubator.

Full screen capture is included, hopefully of sufficient detail. If necessary, raw data can be captured and added later. Overall, we get a remarkably consistent set of results which are numerically robust under repeated temperature excursions of a few degrees.

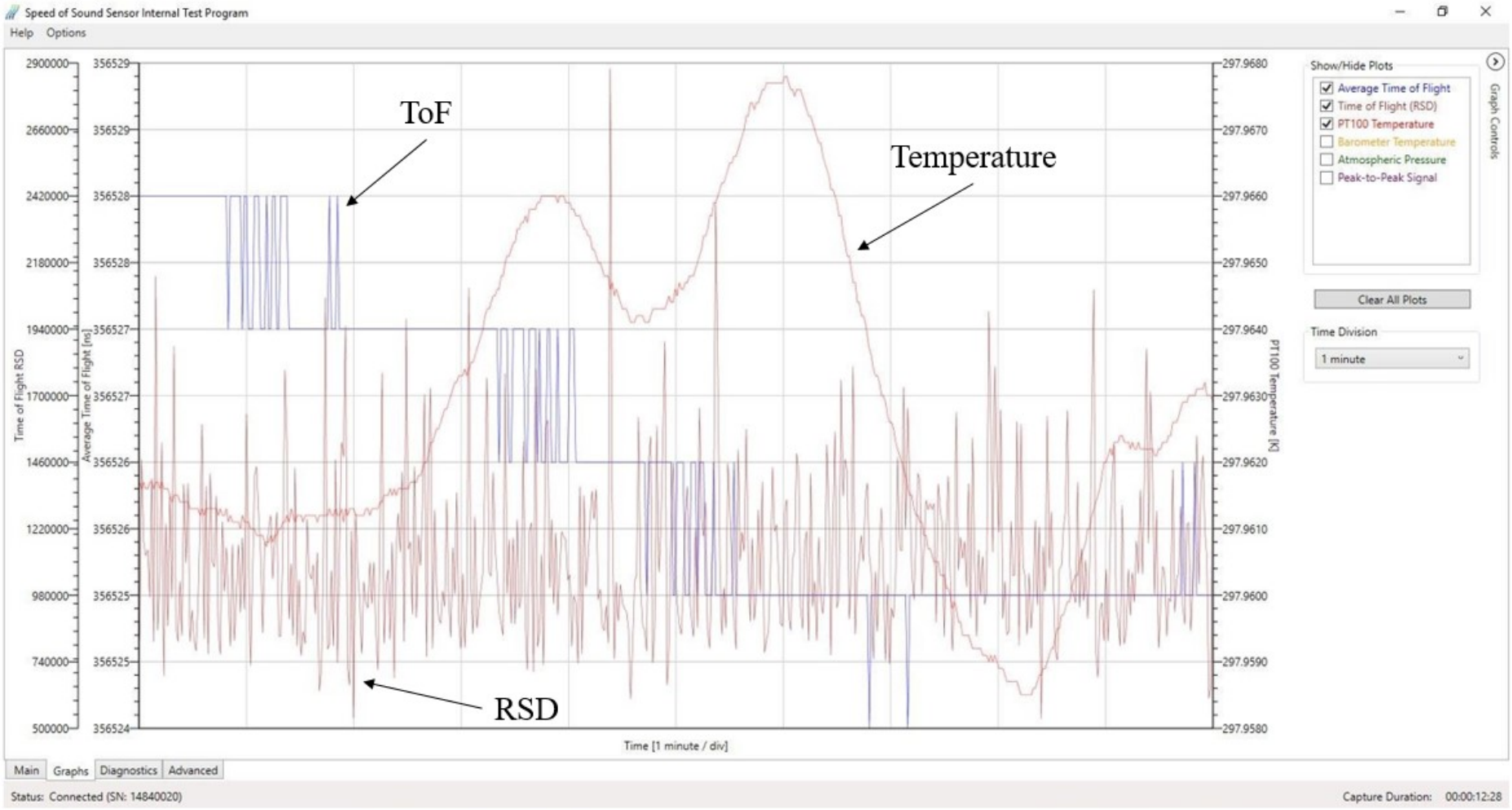



Figure 106. A captured plot of temperature, ToF and RSD in the SoS Sensor Internal Test Program

## A4. Determination of Volume Difference

For convenience, the four consecutive experimental steps are numbered from 1 to 4 which represent the 1st Ar step, the 1st He step, the 2nd Ar step and the 2nd He step, respectively. The three pairs of adjacent steps are denoted by (1, 2), (2, 3) and (3, 4). The experimental data and results are given in the table below. More decimal places are kept to minimise rounding error.

Table 60. Details of $\Delta V$ measurement experiment

| Steps | $T_{DVS}$/°C | $P$/mbar | $\rho$/(kg/m$^3$)* |
|---|---|---|---|
| 1 | 24.527 | 1030.0 | 1.663538 |
| 2 | 24.584 | 1029.0 | 0.166296 |
| 3 | 24.640 | 1028.0 | 1.659673 |
| 4 | 24.671 | 1027.0 | 0.165924 |
| Pairs | $\Delta m_{read}$/μg | | $\Delta V'$/cm$^3$ |
| (1, 2) | 19532.0 | | 13.04532 |
| (2, 3) | 19492.6 | | 13.05270 |
| (3, 4) | 19493.6 | | 13.05012 |
| Final result: $\Delta V = \frac{1}{3}\sum \Delta V'$ = 13.04938 cm$^3$ | | | |
| *Data source: NIST REFPROP software | | | |

The uncertainty (designate by $U$) of the density data, $U(\rho)$, are conservatively estimated to be $0.01\%\rho$ for Ar and $0.015\%\rho$ for He, respectively[18]. Besides $U(\rho)$, $U(T_{DVS})$, $U(\Delta m_{read})$ and $U(P)$ can also result in $\Delta V$ measurement inaccuracy. $U(T_{DVS})$ can be found from Section 3.4 (around 0.21 °C), and $U(\Delta m_{read})$ is given in Equation (86) (around 0.82 μg). In this experiment, the resolution of the output pressure data was 1 mbar (0.01 mbar for the experiments on binary gas mixtures). This is higher than 0.75 mbar which is the pressure measurement uncertainty of the barometric sensor claimed by the manufacture (see Section

[18] According to the information given in the NIST REFPROP software, for pressures up to 12 MPa and temperatures up to 340 K with the exception of the critical region $U(\rho)$ for Ar is less than 0.01% (Tegeler et al., 1999); and at temperatures higher than 200 K and up to pressures of 20 MPa $U(\rho)$ for He is 0.015% (Ortiz Vega, 2013).

3.2). In the uncertainty analysis for $\Delta V$, $U(P)$ is considered to be 1 mbar. The method for the estimation of $U(\Delta V)/\Delta V$ is shown in Figure 107.

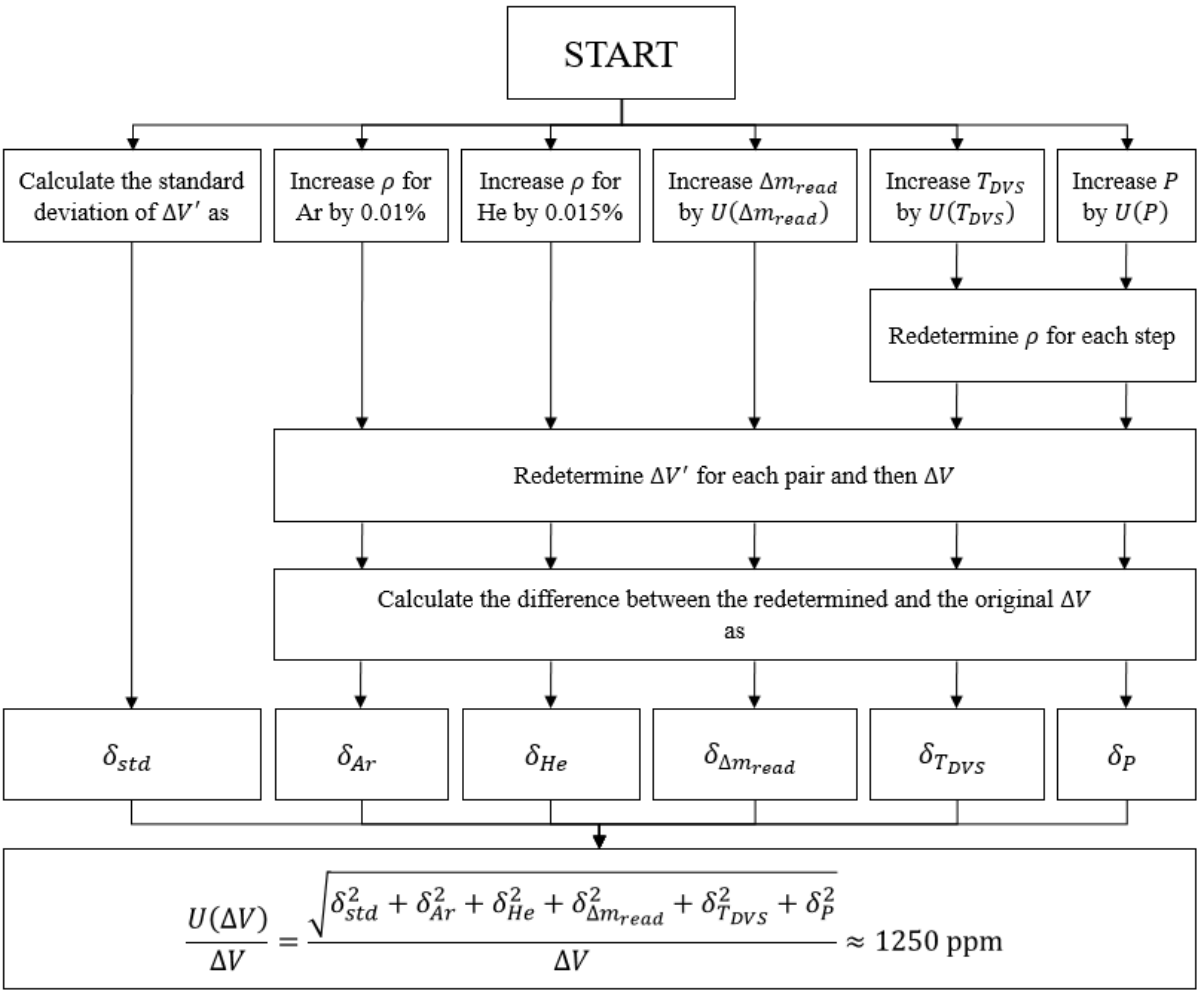



Figure 107. Estimation of $\Delta V$ measurement uncertainty

# A5. Property Parameters

Table 61. Molecular weights and critical constants

| Name | Chemical Formula | Molecular Weights, $M$ (g/mol) | Critical Temperature, $T_c$ (K) | Critical Pressure, $P_c$ (MPa) |
|---|---|---|---|---|
| Nitrogen | $N_2$ | 28.0135 | 126.2 | 3.39 |
| Oxygen | $O_2$ | 31.9988 | 154.58 | 5.02 |
| Argon | Ar | 39.9478 | 150.86 | 4.90 |
| Carbon Dioxide | $CO_2$ | 44.0095 | 304.21 | 7.39 |
| n-Hexane | $C_6H_{14}$ | 86.1754 | 507.6 | 3.04 |
| n-Heptane | $C_7H_{16}$ | 100.2019 | 540.2 | 2.72 |
| n-Octane | $C_8H_{18}$ | 114.2285 | 568.7 | 2.47 |
| n-Nonane | $C_9H_{20}$ | 128.2551 | 594.6 | 2.31 |
| n-Decane | $C_{10}H_{22}$ | 142.2817 | 617.7 | 2.09 |
| Toluene | $C_7H_8$ | 92.1384 | 591.8 | 4.1 |
| Cyclohexane | $C_6H_{12}$ | 84.1595 | 553.58 | 4.1 |
| Water | $H_2O$ | 18.0153 | 647.13 | 21.94 |
| Acetone | $C_3H_6O$ | 58.0791 | 508.2 | 4.71 |
| Methyl Ethyl Ketone | $C_4H_8O$ | 72.1057 | 535.5 | 4.12 |
| Ethyl Acetate | $C_4H_8O_2$ | 88.1051 | 523.3 | 3.85 |
| Methanol | $CH_4O$ | 32.0419 | 512.64 | 8.14 |
| Ethanol | $C_2H_6O$ | 46.0684 | 513.92 | 6.12 |
| Isopropanol | $C_3H_8O$ | 60.0950 | 508.3 | 4.79 |
| Dichloromethane | $CH_2Cl_2$ | 84.9320 | 510 | 6.1 |
| Chloroform | $CHCl_3$ | 119.3767 | 536.4 | 5.55 |
| 1,2-Dichloroethane | $C_2H_4Cl_2$ | 98.9586 | 561 | 5.4 |
| m-Xylene | $C_8H_{10}$ | 106.1650 | 617.05 | 3.53 |
| o-Xylene | $C_8H_{10}$ | 106.1650 | 630.33 | 3.74 |
| p-Xylene | $C_8H_{10}$ | 106.1650 | 616.23 | 3.5 |
| Ethylbenzene | $C_8H_{10}$ | 106.1650 | 617.2 | 3.6 |
| n-Butylamine | $C_4H_{11}N$ | 73.1369 | 531.9 | 4.25 |
| Limonene | $C_{10}H_{16}$ | 136.2340 | 661.11 | 2.756 |
| α-Pinene | $C_{10}H_{16}$ | 136.2340 | 630.87 | 2.89 |

Data sources:

Yellow – calculated based on the atomic masses given in Zuckerwar (2002)

Orange – Korean Thermophysical Properties Data Bank (KDB) [*Online*]

Green – Cardozo-Filho et al., 1997

Blue – Perry et al., 1997

Table 62. Vapour pressure of liquids

| Name | Parameters | | | | | Operational Temperature Range | |
|---|---|---|---|---|---|---|---|
| | $C_1$ | $C_2$ | $C_3$ | $C_4$ | $C_5$ | $T_{min}$ (K) | $T_{max}$ (K) |
| n-Hexane | 104.65 | -6995.5 | -12.702 | 1.2381E-05 | 2 | 177.83 | 507.6 |
| n-Heptane | 87.829 | -6996.4 | -9.8802 | 7.2099E-06 | 2 | 182.57 | 540.2 |
| n-Octane | 96.084 | -7900.2 | -11.003 | 7.1802E-06 | 2 | 216.38 | 568.7 |
| n-Nonane | 109.35 | -9030.4 | -12.882 | 7.8544E-06 | 2 | 219.66 | 594.6 |
| n-Decane | 112.73 | -9749.6 | -13.245 | 7.1266E-06 | 2 | 243.51 | 617.7 |
| Toluene | 80.877 | -6902.4 | -8.7761 | 5.8034E-06 | 2 | 178.18 | 591.8 |
| Cyclohexane | 116.51 | -7103.3 | -15.49 | 1.6959E-02 | 1 | 279.69 | 553.58 |
| Water | 73.649 | -7258.2 | -7.3037 | 4.1653E-06 | 2 | 273.16 | 647.13 |
| Acetone | 69.006 | -5599.6 | -7.0985 | 6.2237E-06 | 2 | 178.45 | 508.2 |
| Methyl Ethyl Ketone | 72.698 | -6143.6 | -7.5779 | 5.6476E-06 | 2 | 186.48 | 535.5 |
| Ethyl Acetate | 66.824 | -6227.6 | -6.41 | 1.7914E-17 | 6 | 189.6 | 523.3 |
| Methanol | 81.768 | -6876 | -8.7078 | 7.1926E-06 | 2 | 175.47 | 512.64 |
| Ethanol | 74.475 | -7164.3 | -7.327 | 3.1340E-06 | 2 | 159.05 | 513.92 |
| Isopropanol | 76.964 | -7623.8 | -7.4924 | 5.9436E-18 | 6 | 185.28 | 508.3 |
| Dichloromethane | 87.786 | -6030.6 | -10.086 | 9.8125E-06 | 2 | 178.01 | 510.00 |
| Chloroform | 146.43 | -7792.3 | -20.614 | 2.4578E-02 | 1 | 207.15 | 536.4 |
| 1,2-Dichloroethane | 90.876 | -6904.9 | -10.382 | 8.3681E-06 | 2 | 237.49 | 561.00 |
| m-Xylene | 84.782 | -7598.3 | -9.2612 | 5.5445E-06 | 2 | 225.3 | 617.05 |
| o-Xylene | 90.356 | -7948.7 | -10.081 | 5.9756E-06 | 2 | 247.98 | 630.33 |
| p-Xylene | 85.475 | -7595.8 | -9.378 | 5.6875E-06 | 2 | 286.41 | 616.23 |
| Ethylbenzene | 88.09 | -7688.3 | -9.7708 | 5.8844E-06 | 2 | 178.15 | 617.2 |
| n-Butylamine | 65.361 | -6041.9 | -6.3048 | 2.9039E-06 | 2 | 224.05 | 531.90 |
| Limonene | 59.360 | -7089.8 | -5.2636 | 0 | 0 | 287.15 | 367.75 |
| α-Pinene | 59.248 | -6686.1 | -5.3185 | 0 | 0 | 272.15 | 349.95 |

Equation for determining saturated vapour pressure ($T$ in K; $P_{SAT}$ in Pa):

$P_{SAT} = \exp[C_1 + C_2/T + C_3 \times \ln(T) + C_4 \times T^{C_5}]$.

Data sources:

Yellow – directly given in Perry et al. (1997)

Orange – Korean Thermophysical Properties Data Bank (KDB) [*Online*]

Green – $C_1$ to $C_5$ determined from fitting to the discrete data given in Perry et al., (1997); $T_{min}$ and $T_{max}$ the temperature range those data correspond to

## A6. Results

## A6.1 n-Hexane/dry air

Table 63. n-Hexane/dry air results (5 °C isotherm)

| $x_T$/%SAT | | Zero Step | | | $\Delta m_{read}$/µg | Non-Zero Step | | | | | | |
|---|---|---|---|---|---|---|---|---|---|---|---|---|
| | | $T_{DVS}$/°C | $P$/mbar | $\rho^0$/(kg/m$^3$) | | $T_{DVS}$/°C | $T_{SoS}$/°C | $P$/mbar | $t_m$/ns | $\rho$/(kg/m$^3$) | $x$ | $W_m$/(m/s) |
| 10 | A | 5.19 | 1014.63 | 1.2706 | 288 | 5.19 | 5.0785 | 1014.49 | 370967 | 1.2927 | 0.0088 | 329.68 |
| | D | 5.20 | 1013.08 | 1.2686 | 284 | 5.22 | 5.0969 | 1012.67 | 371042 | 1.2904 | 0.0089 | 329.62 |
| 20 | A | 5.17 | 1014.69 | 1.2708 | 554 | 5.17 | 5.0571 | 1014.74 | 375829 | 1.3132 | 0.0168 | 325.42 |
| | D | 5.16 | 1013.37 | 1.2692 | 548 | 5.21 | 5.0817 | 1013.13 | 375924 | 1.3112 | 0.0169 | 325.34 |
| 30 | A | 5.15 | 1014.78 | 1.2710 | 811 | 5.17 | 5.0462 | 1014.75 | 380467 | 1.3331 | 0.0246 | 321.45 |
| | D | 5.14 | 1014.02 | 1.2701 | 810 | 5.17 | 5.0491 | 1013.88 | 380529 | 1.3321 | 0.0247 | 321.40 |
| 40 | A | 5.18 | 1014.73 | 1.2708 | 1065 | 5.20 | 5.0719 | 1014.88 | 384860 | 1.3524 | 0.0323 | 317.78 |
| | D | 5.15 | 1014.63 | 1.2708 | 1055 | 5.16 | 5.0419 | 1014.29 | 384876 | 1.3517 | 0.0322 | 317.77 |
| 50 | A | 5.19 | 1015.05 | 1.2711 | 1314 | 5.21 | 5.0838 | 1015.27 | 389082 | 1.3718 | 0.0398 | 314.33 |
| | D | 5.15 | 1014.84 | 1.2710 | 1307 | 5.16 | 5.0451 | 1014.79 | 389079 | 1.3712 | 0.0397 | 314.34 |
| 60 | A | 5.19 | 1015.26 | 1.2714 | 1552 | 5.21 | 5.0853 | 1015.47 | 393115 | 1.3904 | 0.0470 | 311.11 |
| | D | 5.15 | 1014.93 | 1.2712 | 1545 | 5.17 | 5.0488 | 1014.88 | 393109 | 1.3896 | 0.0469 | 311.11 |
| 70 | A | 5.21 | 1015.96 | 1.2722 | 1786 | 5.22 | 5.0895 | 1015.97 | 397005 | 1.4091 | 0.0541 | 308.06 |
| | D | 5.16 | 1014.99 | 1.2712 | 1782 | 5.17 | 5.0498 | 1015.02 | 397001 | 1.4077 | 0.0540 | 308.06 |
| 80 | A | 5.19 | 1015.98 | 1.2723 | 2020 | 5.19 | 5.0738 | 1015.94 | 400838 | 1.4271 | 0.0612 | 305.12 |
| | D | 5.17 | 1015.14 | 1.2713 | 2019 | 5.19 | 5.0653 | 1015.07 | 400880 | 1.4261 | 0.0612 | 305.08 |
| 90 | A | 5.19 | 1015.97 | 1.2723 | 2259 | 5.20 | 5.0751 | 1016.20 | 404582 | 1.4454 | 0.0683 | 302.29 |
| | D | 5.17 | 1015.51 | 1.2718 | 2248 | 5.18 | 5.0618 | 1015.27 | 404597 | 1.4441 | 0.0682 | 302.28 |
| 95 | | 5.18 | 1016.15 | 1.2725 | 2361 | 5.19 | 5.0709 | 1015.68 | 406407 | 1.4535 | 0.0717 | 300.93 |
| Data used for pathlength calibration (the first zero step): $T_{SoS}$ = 5.0755 °C, $P$ = 1014.63 mbar, $t_m^0$ = 365505 ns, $W^0$ = 334.61 m/s. | | | | | | | | | | | | |

Table 64. n-Hexane/dry air results (15 °C isotherm)

| $x_T$/%SAT | | Zero Step | | | $\Delta m_{read}$/µg | Non-Zero Step | | | | | | |
|---|---|---|---|---|---|---|---|---|---|---|---|---|
| | | $T_{DVS}$/°C | $P$/mbar | $\rho^0$/(kg/m³) | | $T_{DVS}$/°C | $T_{SoS}$/°C | $P$/mbar | $t_m$/ns | $\rho$/(kg/m³) | $x$ | $W_m$/(m/s) |
| 10 | A | 14.97 | 1012.81 | 1.2252 | 483 | 14.97 | 14.6790 | 1012.82 | 369475 | 1.2622 | 0.0152 | 331.77 |
| | D | 14.99 | 1010.62 | 1.2224 | 480 | 14.92 | 14.6440 | 1010.56 | 369447 | 1.2592 | 0.0151 | 331.79 |
| 20 | A | 14.97 | 1012.83 | 1.2252 | 910 | 14.97 | 14.6802 | 1012.90 | 377350 | 1.2949 | 0.0286 | 324.84 |
| | D | 14.91 | 1010.73 | 1.2229 | 897 | 14.94 | 14.6346 | 1010.56 | 377292 | 1.2916 | 0.0284 | 324.89 |
| 30 | A | 14.97 | 1012.63 | 1.2249 | 1315 | 14.98 | 14.6820 | 1012.54 | 384607 | 1.3257 | 0.0415 | 318.71 |
| | D | 14.92 | 1010.68 | 1.2228 | 1311 | 14.92 | 14.6334 | 1010.89 | 384543 | 1.3232 | 0.0412 | 318.77 |
| 40 | A | 14.96 | 1012.70 | 1.2250 | 1702 | 14.98 | 14.6826 | 1012.56 | 391268 | 1.3555 | 0.0537 | 313.29 |
| | D | 14.92 | 1010.30 | 1.2223 | 1694 | 14.92 | 14.6322 | 1010.33 | 391229 | 1.3521 | 0.0534 | 313.32 |
| 50 | A | 14.95 | 1012.49 | 1.2248 | 2079 | 14.97 | 14.6752 | 1012.51 | 397540 | 1.3841 | 0.0654 | 308.34 |
| | D | 14.91 | 1010.51 | 1.2226 | 2067 | 14.93 | 14.6244 | 1010.52 | 397484 | 1.3810 | 0.0652 | 308.39 |
| 60 | A | 14.94 | 1012.45 | 1.2248 | 2436 | 14.94 | 14.6544 | 1012.59 | 403385 | 1.4115 | 0.0766 | 303.88 |
| | D | 14.90 | 1010.88 | 1.2231 | 2421 | 14.87 | 14.5916 | 1010.82 | 403299 | 1.4086 | 0.0762 | 303.94 |
| 70 | A | 14.91 | 1012.20 | 1.2246 | 2790 | 14.92 | 14.6330 | 1012.47 | 408990 | 1.4384 | 0.0876 | 299.71 |
| | D | 14.91 | 1011.17 | 1.2234 | 2778 | 14.90 | 14.6310 | 1010.97 | 409004 | 1.4363 | 0.0876 | 299.70 |
| 80 | A | 14.94 | 1012.32 | 1.2247 | 3132 | 14.92 | 14.6368 | 1012.40 | 414368 | 1.4647 | 0.0984 | 295.82 |
| | D | 14.94 | 1011.94 | 1.2242 | 3126 | 14.96 | 14.6613 | 1011.71 | 414422 | 1.4638 | 0.0985 | 295.78 |
| 90 | A | 14.92 | 1012.15 | 1.2246 | 3478 | 14.98 | 14.6749 | 1012.13 | 419718 | 1.4911 | 0.1094 | 292.05 |
| | D | 14.90 | 1012.05 | 1.2245 | 3471 | 14.95 | 14.6540 | 1011.97 | 419647 | 1.4905 | 0.1092 | 292.10 |
| 95 | | 14.90 | 1011.89 | 1.2243 | 3637 | 14.93 | 14.6487 | 1012.04 | 422105 | 1.5031 | 0.1143 | 290.40 |
| Data used for pathlength calibration (the first zero step): $T_{SoS}$ = 14.6725 °C, $P$ = 1012.81 mbar, $t_m^0$ = 360159 ns, $W^0$ = 340.35 m/s. | | | | | | | | | | | | |

Table 65. n-Hexane/dry air results (25 °C isotherm)

| $x_T$/%SAT | | Zero Step | | | $\Delta m_{read}$/µg | Non-Zero Step | | | | | | |
|---|---|---|---|---|---|---|---|---|---|---|---|---|
| | | $T_{DVS}$/°C | $P$/mbar | $\rho^0$/(kg/m³) | | $T_{DVS}$/°C | $T_{SoS}$/°C | $P$/mbar | $t_m$/ns | $\rho$/(kg/m³) | $x$ | $W_m$/(m/s) |
| 5 | A | 24.73 | 1018.08 | 1.1910 | 422 | 24.74 | 24.3790 | 1017.89 | 362498 | 1.2234 | 0.0138 | 337.96 |
| | D | 24.56 | 1012.70 | 1.1854 | 412 | 24.56 | 24.1879 | 1012.63 | 362473 | 1.2170 | 0.0135 | 337.98 |
| 10 | A | 24.73 | 1017.73 | 1.1906 | 787 | 24.75 | 24.3876 | 1017.68 | 369397 | 1.2510 | 0.0256 | 331.65 |
| | D | 24.70 | 1012.84 | 1.1850 | 778 | 24.64 | 24.2895 | 1012.86 | 369275 | 1.2447 | 0.0252 | 331.76 |
| 15 | A | 24.75 | 1017.74 | 1.1906 | 1135 | 24.76 | 24.4004 | 1017.71 | 375707 | 1.2775 | 0.0368 | 326.08 |
| | D | 24.64 | 1012.90 | 1.1853 | 1120 | 24.69 | 24.2898 | 1012.84 | 375646 | 1.2712 | 0.0366 | 326.13 |
| 20 | A | 24.76 | 1017.94 | 1.1908 | 1469 | 24.76 | 24.4047 | 1018.05 | 381574 | 1.3033 | 0.0475 | 321.06 |
| | D | 24.58 | 1013.12 | 1.1858 | 1441 | 24.58 | 24.2041 | 1013.00 | 381464 | 1.2963 | 0.0469 | 321.16 |
| 25 | A | 24.66 | 1017.85 | 1.1911 | 1773 | 24.64 | 24.3003 | 1017.74 | 387025 | 1.3269 | 0.0574 | 316.54 |
| | D | 24.59 | 1012.85 | 1.1855 | 1763 | 24.59 | 24.2159 | 1012.97 | 387033 | 1.3206 | 0.0573 | 316.53 |
| 30 | A | 24.63 | 1017.70 | 1.1910 | 2085 | 24.61 | 24.2610 | 1017.82 | 392215 | 1.3508 | 0.0674 | 312.35 |
| | D | 24.60 | 1012.86 | 1.1855 | 2070 | 24.60 | 24.2317 | 1012.74 | 392318 | 1.3441 | 0.0674 | 312.27 |
| 35 | A | 24.58 | 1017.68 | 1.1912 | 2378 | 24.59 | 24.2392 | 1017.74 | 397161 | 1.3734 | 0.0769 | 308.46 |
| | D | 24.62 | 1012.75 | 1.1853 | 2371 | 24.62 | 24.2431 | 1012.74 | 397290 | 1.3670 | 0.0771 | 308.36 |
| 40 | A | 24.58 | 1017.55 | 1.1910 | 2668 | 24.59 | 24.2327 | 1017.46 | 401913 | 1.3955 | 0.0864 | 304.82 |
| | D | 24.62 | 1012.51 | 1.1850 | 2665 | 24.63 | 24.2516 | 1012.64 | 402027 | 1.3891 | 0.0866 | 304.73 |
| 45 | A | 24.57 | 1017.32 | 1.1908 | 2948 | 24.57 | 24.2157 | 1017.31 | 406411 | 1.4167 | 0.0954 | 301.44 |
| | D | 24.61 | 1012.37 | 1.1848 | 2944 | 24.62 | 24.2458 | 1012.42 | 406543 | 1.4105 | 0.0957 | 301.34 |
| 50 | A | 24.57 | 1017.13 | 1.1906 | 3221 | 24.56 | 24.2005 | 1016.83 | 410737 | 1.4374 | 0.1043 | 298.27 |
| | D | 24.60 | 1012.16 | 1.1846 | 3213 | 24.61 | 24.2339 | 1012.26 | 410792 | 1.4309 | 0.1044 | 298.23 |
| 55 | A | 24.64 | 1016.82 | 1.1899 | 3509 | 24.67 | 24.2876 | 1016.55 | 415138 | 1.4588 | 0.1138 | 295.11 |
| | D | 24.63 | 1012.13 | 1.1845 | 3481 | 24.63 | 24.2411 | 1011.99 | 414992 | 1.4512 | 0.1132 | 295.21 |
| 60 | A | 24.67 | 1016.30 | 1.1892 | 3780 | 24.68 | 24.3103 | 1016.22 | 419221 | 1.4789 | 0.1225 | 292.23 |
| | D | 24.63 | 1012.31 | 1.1847 | 3745 | 24.64 | 24.2600 | 1012.15 | 419052 | 1.4717 | 0.1218 | 292.35 |

| | | | | | | | | | | | | |
|---|---|---|---|---|---|---|---|---|---|---|---|---|
| 65 | A | 24.64 | 1015.94 | 1.1889 | 4034 | 24.65 | 24.2799 | 1015.91 | 423045 | 1.4980 | 0.1306 | 289.59 |
| | D | 24.74 | 1012.71 | 1.1847 | 4006 | 24.65 | 24.3059 | 1012.47 | 422877 | 1.4917 | 0.1301 | 289.70 |
| 70 | A | 24.63 | 1015.78 | 1.1887 | 4289 | 24.64 | 24.2715 | 1015.64 | 426870 | 1.5174 | 0.1389 | 287.00 |
| | D | 24.72 | 1013.19 | 1.1854 | 4277 | 24.74 | 24.3597 | 1012.95 | 426827 | 1.5131 | 0.1390 | 287.02 |
| 75 | A | 24.63 | 1015.48 | 1.1884 | 4536 | 24.63 | 24.2597 | 1015.45 | 430464 | 1.5360 | 0.1468 | 284.60 |
| | D | 24.70 | 1013.90 | 1.1863 | 4521 | 24.72 | 24.3382 | 1013.61 | 430446 | 1.5327 | 0.1468 | 284.61 |
| 80 | A | 24.60 | 1015.47 | 1.1885 | 4778 | 24.61 | 24.2424 | 1015.51 | 433938 | 1.5546 | 0.1546 | 282.32 |
| | D | 24.67 | 1014.30 | 1.1869 | 4763 | 24.68 | 24.3068 | 1014.18 | 433878 | 1.5519 | 0.1544 | 282.36 |
| 85 | A | 24.60 | 1015.44 | 1.1885 | 5018 | 24.61 | 24.2336 | 1015.36 | 437412 | 1.5730 | 0.1624 | 280.08 |
| | D | 24.65 | 1014.63 | 1.1873 | 5010 | 24.68 | 24.2960 | 1014.53 | 437380 | 1.5713 | 0.1624 | 280.10 |
| 90 | A | 24.60 | 1015.34 | 1.1883 | 5249 | 24.60 | 24.2229 | 1015.20 | 440673 | 1.5906 | 0.1698 | 278.01 |
| | D | 24.62 | 1015.09 | 1.1880 | 5252 | 24.63 | 24.2567 | 1014.95 | 440706 | 1.5905 | 0.1700 | 277.98 |
| 95 | | 24.58 | 1015.18 | 1.1882 | 5488 | 24.61 | 24.2303 | 1014.99 | 443916 | 1.6088 | 0.1776 | 275.97 |
| Data used for pathlength calibration (the first zero step): $T_{SOS}$ = 24.3716 °C, $P$ = 1018.08 mbar, $t_m^0$ = 354026 ns, $W^0$ = 346.05 m/s. | | | | | | | | | | | | |

Table 66. n-Hexane/dry air results (35 °C isotherm)

| $x_T$/%SAT | | Zero Step | | | $\Delta m_{read}$/µg | Non-Zero Step | | | | | | |
|---|---|---|---|---|---|---|---|---|---|---|---|---|
| | | $T_{DVS}$/°C | $P$/mbar | $\rho^0$/(kg/m³) | | $T_{DVS}$/°C | $T_{SoS}$/°C | $P$/mbar | $t_m$/ns | $\rho$/(kg/m³) | $x$ | $W_m$/(m/s) |
| 10 | A | 34.54 | 1004.68 | 1.1378 | 1277 | 34.53 | 34.1323 | 1004.44 | 372805 | 1.2356 | 0.0434 | 327.94 |
| | D | 34.54 | 1003.05 | 1.1359 | 1283 | 34.55 | 34.1528 | 1002.82 | 372957 | 1.2342 | 0.0437 | 327.80 |
| 20 | A | 34.52 | 1004.34 | 1.1375 | 2345 | 34.51 | 34.1063 | 1004.38 | 391450 | 1.3172 | 0.0795 | 312.32 |
| | D | 34.51 | 1003.14 | 1.1362 | 2342 | 34.53 | 34.1360 | 1003.16 | 391589 | 1.3156 | 0.0795 | 312.21 |
| 30 | A | 34.48 | 1004.11 | 1.1374 | 3301 | 34.50 | 34.0934 | 1004.23 | 407071 | 1.3903 | 0.1118 | 300.33 |
| | D | 34.54 | 1003.00 | 1.1359 | 3293 | 34.55 | 34.1549 | 1003.17 | 407040 | 1.3883 | 0.1117 | 300.35 |
| 40 | A | 34.54 | 1004.00 | 1.1370 | 4188 | 34.58 | 34.1535 | 1004.06 | 420704 | 1.4580 | 0.1419 | 290.60 |
| | D | 34.54 | 1003.46 | 1.1364 | 4150 | 34.54 | 34.1494 | 1003.30 | 420277 | 1.4544 | 0.1407 | 290.89 |
| 50 | A | 34.60 | 1004.54 | 1.1374 | 4999 | 34.57 | 34.1802 | 1004.34 | 432573 | 1.5205 | 0.1692 | 282.63 |
| | D | 34.59 | 1003.95 | 1.1368 | 4951 | 34.56 | 34.1789 | 1003.72 | 432052 | 1.5162 | 0.1676 | 282.97 |
| 60 | A | 34.51 | 1004.43 | 1.1376 | 5725 | 34.53 | 34.1091 | 1004.58 | 442896 | 1.5763 | 0.1934 | 276.04 |
| | D | 34.52 | 1004.33 | 1.1375 | 5689 | 34.59 | 34.1770 | 1004.17 | 442491 | 1.5734 | 0.1925 | 276.29 |
| 70 | A | 34.53 | 1004.87 | 1.1381 | 6417 | 34.50 | 34.0968 | 1004.97 | 452316 | 1.6298 | 0.2164 | 270.29 |
| | D | 34.48 | 1004.71 | 1.1381 | 6349 | 34.49 | 34.0843 | 1004.56 | 451620 | 1.6246 | 0.2144 | 270.71 |
| 80 | A | 34.46 | 1005.10 | 1.1386 | 7067 | 34.54 | 34.1062 | 1005.01 | 461109 | 1.6801 | 0.2384 | 265.14 |
| | D | 34.52 | 1005.06 | 1.1383 | 7027 | 34.50 | 34.0958 | 1004.84 | 460654 | 1.6768 | 0.2370 | 265.40 |
| 90 | A | 34.59 | 1005.26 | 1.1383 | 7698 | 34.55 | 34.1558 | 1005.49 | 469166 | 1.7282 | 0.2590 | 260.58 |
| | D | 34.52 | 1005.33 | 1.1386 | 7659 | 34.52 | 34.1171 | 1005.11 | 468893 | 1.7256 | 0.2581 | 260.73 |
| 95 | | 34.52 | 1005.35 | 1.1386 | 7963 | 34.51 | 34.1082 | 1005.36 | 472734 | 1.7488 | 0.2680 | 258.62 |
| Data used for pathlength calibration (the first zero step): $T_{SoS}$ = 34.1381 °C, $P$ = 1004.68 mbar, $t_m^0$ = 347627 ns, $W^0$ = 351.69 m/s. | | | | | | | | | | | | |

Table 67. n-Hexane/dry air results (45 °C isotherm)

| $x_T$/%SAT | | Zero Step | | | $\Delta m_{read}$/µg | Non-Zero Step | | | | | | |
|---|---|---|---|---|---|---|---|---|---|---|---|---|
| | | $T_{DVS}$/°C | $P$/mbar | $\rho^0$/(kg/m³) | | $T_{DVS}$/°C | $T_{SoS}$/°C | $P$/mbar | $t_m$/ns | $\rho$/(kg/m³) | $x$ | $W_m$/(m/s) |
| 10 | A | 43.92 | 1013.16 | 1.1134 | 2121 | 43.93 | 43.5743 | 1013.13 | 382883 | 1.2759 | 0.0736 | 319.24 |
| | D | 43.97 | 1012.89 | 1.1129 | 2092 | 43.95 | 43.6089 | 1012.81 | 382418 | 1.2732 | 0.0726 | 319.63 |
| 20 | A | 43.94 | 1013.09 | 1.1132 | 3765 | 43.94 | 43.5909 | 1013.07 | 409635 | 1.4017 | 0.1303 | 298.39 |
| | D | 43.97 | 1012.89 | 1.1129 | 3707 | 43.97 | 43.6184 | 1012.93 | 408359 | 1.3969 | 0.1283 | 299.32 |
| 30 | A | 44.00 | 1013.10 | 1.1131 | 5182 | 44.00 | 43.6471 | 1013.09 | 430523 | 1.5101 | 0.1792 | 283.91 |
| | D | 43.93 | 1013.22 | 1.1134 | 5037 | 43.98 | 43.5977 | 1013.18 | 428434 | 1.4994 | 0.1743 | 285.30 |
| 40 | A | 43.97 | 1013.16 | 1.1132 | 6377 | 44.02 | 43.6157 | 1013.24 | 447194 | 1.6019 | 0.2202 | 273.33 |
| | D | 43.96 | 1013.29 | 1.1134 | 6175 | 43.92 | 43.5571 | 1013.33 | 444331 | 1.5866 | 0.2131 | 275.09 |
| 50 | A | 43.97 | 1013.29 | 1.1133 | 7437 | 44.00 | 43.6018 | 1013.41 | 461317 | 1.6833 | 0.2564 | 264.96 |
| | D | 44.00 | 1013.18 | 1.1131 | 7229 | 44.01 | 43.6126 | 1013.30 | 458458 | 1.6671 | 0.2492 | 266.61 |
| 60 | A | 44.00 | 1013.36 | 1.1133 | 8362 | 43.98 | 43.5938 | 1013.15 | 473245 | 1.7541 | 0.2880 | 258.28 |
| | D | 44.00 | 1013.13 | 1.1131 | 8127 | 43.95 | 43.5756 | 1013.10 | 470233 | 1.7358 | 0.2799 | 259.94 |
| 70 | A | 44.00 | 1013.13 | 1.1131 | 9206 | 44.03 | 43.6242 | 1012.98 | 483824 | 1.8186 | 0.3168 | 252.64 |
| | D | 43.92 | 1012.88 | 1.1131 | 8986 | 44.01 | 43.5887 | 1013.04 | 481085 | 1.8017 | 0.3093 | 254.07 |
| 80 | A | 43.99 | 1012.88 | 1.1128 | 9956 | 43.98 | 43.6157 | 1012.88 | 492907 | 1.8758 | 0.3421 | 247.98 |
| | D | 43.99 | 1012.76 | 1.1127 | 9764 | 43.94 | 43.6015 | 1012.82 | 490623 | 1.8609 | 0.3354 | 249.13 |
| 90 | A | 43.96 | 1012.77 | 1.1128 | 10616 | 43.97 | 43.5964 | 1012.73 | 500879 | 1.9263 | 0.3644 | 244.03 |
| | D | 43.98 | 1012.71 | 1.1127 | 10528 | 44.00 | 43.6298 | 1012.79 | 499801 | 1.9195 | 0.3614 | 244.56 |
| 95 | | 43.97 | 1012.69 | 1.1127 | 10883 | 43.93 | 43.5816 | 1012.74 | 504003 | 1.9467 | 0.3733 | 242.52 |
| Data used for pathlength calibration (the first zero step): $T_{SoS}$ = 43.5519 °C, $P$ = 1013.16 mbar, $t_m^0$ = 342342 ns, $W^0$ = 357.04 m/s. | | | | | | | | | | | | |

## A6.2 n-Octane/dry air

Table 68. n-Octane/dry air results (5 °C isotherm)

| $x_T$/%SAT | | Zero Step | | | $\Delta m_{read}$/µg | Non-Zero Step | | | | | | |
|---|---|---|---|---|---|---|---|---|---|---|---|---|
| | | $T_{DVS}$/°C | $P$/mbar | $\rho^0$/(kg/m$^3$) | | $T_{DVS}$/°C | $T_{SoS}$/°C | $P$/mbar | $t_m$/ns | $\rho$/(kg/m$^3$) | $x$ | $W_m$/(m/s) |
| 10 | A | 5.25 | 1013.34 | 1.2687 | 31 | 5.23 | 5.0717 | 1013.37 | 366010 | 1.2711 | 0.00060 | 334.12 |
| | D | 5.33 | 1013.71 | 1.2688 | 28 | 5.33 | 5.1897 | 1013.54 | 365934 | 1.2710 | 0.00063 | 334.19 |
| 20 | A | 5.22 | 1013.38 | 1.2689 | 55 | 5.23 | 5.0650 | 1013.28 | 366506 | 1.2731 | 0.00117 | 333.67 |
| | D | 5.35 | 1013.70 | 1.2687 | 60 | 5.35 | 5.2101 | 1013.84 | 366417 | 1.2733 | 0.00118 | 333.75 |
| 30 | A | 5.24 | 1013.24 | 1.2686 | 79 | 5.25 | 5.0803 | 1013.10 | 366986 | 1.2747 | 0.00166 | 333.23 |
| | D | 5.35 | 1013.27 | 1.2682 | 86 | 5.37 | 5.2162 | 1013.49 | 366911 | 1.2748 | 0.00171 | 333.30 |
| 40 | A | 5.23 | 1013.08 | 1.2685 | 111 | 5.25 | 5.0828 | 1013.22 | 367462 | 1.2770 | 0.00225 | 332.80 |
| | D | 5.30 | 1013.08 | 1.2682 | 108 | 5.33 | 5.1729 | 1013.12 | 367415 | 1.2765 | 0.00224 | 332.84 |
| 50 | A | 5.25 | 1013.31 | 1.2687 | 137 | 5.25 | 5.0905 | 1013.47 | 367936 | 1.2792 | 0.00274 | 332.37 |
| | D | 5.28 | 1013.34 | 1.2686 | 131 | 5.27 | 5.1262 | 1013.08 | 367922 | 1.2787 | 0.00277 | 332.38 |
| 60 | A | 5.25 | 1013.75 | 1.2692 | 160 | 5.24 | 5.0852 | 1013.78 | 368409 | 1.2815 | 0.00324 | 331.94 |
| | D | 5.26 | 1013.46 | 1.2688 | 157 | 5.27 | 5.1243 | 1013.37 | 368398 | 1.2808 | 0.00325 | 331.95 |
| 70 | A | 5.24 | 1013.70 | 1.2692 | 185 | 5.25 | 5.0858 | 1013.81 | 368881 | 1.2834 | 0.00375 | 331.52 |
| | D | 5.26 | 1013.44 | 1.2688 | 183 | 5.26 | 5.1134 | 1013.35 | 368876 | 1.2828 | 0.00377 | 331.52 |
| 80 | A | 5.22 | 1014.04 | 1.2697 | 210 | 5.25 | 5.0813 | 1014.13 | 369358 | 1.2858 | 0.00429 | 331.09 |
| | D | 5.23 | 1013.75 | 1.2693 | 207 | 5.26 | 5.1046 | 1013.70 | 369358 | 1.2852 | 0.00428 | 331.09 |
| 90 | A | 5.22 | 1014.29 | 1.2700 | 232 | 5.24 | 5.0854 | 1014.29 | 369806 | 1.2878 | 0.00475 | 330.69 |
| | D | 5.24 | 1014.33 | 1.2700 | 229 | 5.25 | 5.0940 | 1014.06 | 369808 | 1.2875 | 0.00477 | 330.69 |
| 95 | | 5.23 | 1014.30 | 1.2700 | 241 | 5.24 | 5.0829 | 1014.38 | 369980 | 1.2885 | 0.00490 | 330.53 |
| Data used for pathlength calibration (the first zero step): $T_{SoS}$ = 5.0667 °C, $P$ = 1013.34 mbar, $t_m^0$ = 365480 ns, $W^0$ = 334.60 m/s. | | | | | | | | | | | | |

Table 69. n-Octane/dry air results (15 °C isotherm)

| $x_T$/%SAT | | Zero Step | | | $\Delta m_{read}$/µg | Non-Zero Step | | | | | | |
|---|---|---|---|---|---|---|---|---|---|---|---|---|
| | | $T_{DVS}$/°C | $P$/mbar | $\rho^0$/(kg/m$^3$) | | $T_{DVS}$/°C | $T_{SoS}$/°C | $P$/mbar | $t_m$/ns | $\rho$/(kg/m$^3$) | $x$ | $W_m$/(m/s) |
| 10 | A | 14.43 | 1009.79 | 1.2238 | 44 | 14.45 | 14.0674 | 1009.47 | 361021 | 1.2272 | 0.00107 | 339.10 |
| | D | 14.40 | 1005.68 | 1.2189 | 52 | 14.40 | 14.0228 | 1005.75 | 360993 | 1.2229 | 0.00108 | 339.12 |
| 20 | A | 14.46 | 1009.18 | 1.2229 | 92 | 14.47 | 14.0854 | 1008.86 | 361898 | 1.2300 | 0.00207 | 338.28 |
| | D | 14.40 | 1005.48 | 1.2187 | 98 | 14.42 | 14.0347 | 1005.61 | 361875 | 1.2262 | 0.00206 | 338.30 |
| 30 | A | 14.40 | 1008.50 | 1.2224 | 137 | 14.41 | 14.0304 | 1008.20 | 362801 | 1.2329 | 0.00302 | 337.43 |
| | D | 14.40 | 1005.32 | 1.2185 | 143 | 14.42 | 14.0398 | 1005.29 | 362766 | 1.2294 | 0.00307 | 337.47 |
| 40 | A | 14.43 | 1008.14 | 1.2218 | 185 | 14.40 | 14.0283 | 1007.88 | 363658 | 1.2360 | 0.00398 | 336.64 |
| | D | 14.37 | 1005.20 | 1.2184 | 185 | 14.39 | 13.9984 | 1005.20 | 363644 | 1.2326 | 0.00395 | 336.65 |
| 50 | A | 14.40 | 1007.66 | 1.2213 | 229 | 14.43 | 14.0394 | 1007.49 | 364499 | 1.2389 | 0.00495 | 335.86 |
| | D | 14.39 | 1004.90 | 1.2180 | 235 | 14.43 | 14.0421 | 1005.07 | 364481 | 1.2360 | 0.00499 | 335.88 |
| 60 | A | 14.38 | 1006.97 | 1.2206 | 272 | 14.39 | 14.0118 | 1006.81 | 365342 | 1.2414 | 0.00584 | 335.09 |
| | D | 14.42 | 1004.89 | 1.2179 | 279 | 14.37 | 14.0169 | 1004.96 | 365330 | 1.2393 | 0.00585 | 335.10 |
| 70 | A | 14.39 | 1006.55 | 1.2200 | 317 | 14.38 | 14.0115 | 1006.25 | 366179 | 1.2443 | 0.00682 | 334.32 |
| | D | 14.35 | 1004.94 | 1.2182 | 318 | 14.36 | 13.9879 | 1004.87 | 366183 | 1.2426 | 0.00679 | 334.32 |
| 80 | A | 14.39 | 1006.15 | 1.2196 | 362 | 14.41 | 14.0310 | 1005.95 | 367004 | 1.2473 | 0.00779 | 333.57 |
| | D | 14.42 | 1004.97 | 1.2180 | 368 | 14.38 | 14.0239 | 1005.12 | 367000 | 1.2462 | 0.00774 | 333.57 |
| 90 | A | 14.36 | 1005.94 | 1.2194 | 401 | 14.38 | 13.9978 | 1005.73 | 367813 | 1.2501 | 0.00860 | 332.84 |
| | D | 14.38 | 1005.35 | 1.2186 | 400 | 14.37 | 13.9987 | 1005.06 | 367815 | 1.2493 | 0.00859 | 332.83 |
| 95 | | 14.40 | 1005.48 | 1.2187 | 413 | 14.40 | 14.0187 | 1005.06 | 368137 | 1.2504 | 0.00894 | 332.54 |
| Data used for pathlength calibration (the first zero step): $T_{SoS}$ = 14.0429 °C, $P$ = 1009.79 mbar, $t_m^0$ = 360090 ns, $W^0$ = 339.97 m/s. | | | | | | | | | | | | |

Table 70. n-Octane/dry air results (25 °C isotherm)

| $x_T$/%SAT | | Zero Step | | | $\Delta m_{read}$/µg | Non-Zero Step | | | | | | |
|---|---|---|---|---|---|---|---|---|---|---|---|---|
| | | $T_{DVS}$/°C | $P$/mbar | $\rho^0$/(kg/m$^3$) | | $T_{DVS}$/°C | $T_{SoS}$/°C | $P$/mbar | $t_m$/ns | $\rho$/(kg/m$^3$) | $x$ | $W_m$/(m/s) |
| 5 | A | 24.66 | 1027.55 | 1.2024 | 49 | 24.65 | 24.4404 | 1027.71 | 354834 | 1.2062 | 0.0010 | 345.22 |
| | D | 24.86 | 1025.90 | 1.1997 | 50 | 24.87 | 24.5049 | 1026.07 | 354829 | 1.2035 | 0.0010 | 345.22 |
| 10 | A | 24.65 | 1027.61 | 1.2025 | 91 | 24.64 | 24.4251 | 1027.64 | 355656 | 1.2095 | 0.0019 | 344.42 |
| | D | 24.85 | 1025.45 | 1.1992 | 94 | 24.85 | 24.4842 | 1025.66 | 355663 | 1.2064 | 0.0020 | 344.41 |
| 15 | A | 24.62 | 1027.84 | 1.2029 | 130 | 24.63 | 24.4104 | 1027.82 | 356478 | 1.2129 | 0.0028 | 343.63 |
| | D | 24.83 | 1025.17 | 1.1989 | 134 | 24.85 | 24.4864 | 1025.24 | 356480 | 1.2092 | 0.0029 | 343.62 |
| 20 | A | 24.60 | 1027.74 | 1.2029 | 169 | 24.60 | 24.3832 | 1027.63 | 357293 | 1.2158 | 0.0037 | 342.84 |
| | D | 24.83 | 1025.04 | 1.1988 | 176 | 24.84 | 24.4794 | 1025.15 | 357291 | 1.2123 | 0.0038 | 342.85 |
| 25 | A | 24.60 | 1027.68 | 1.2028 | 211 | 24.59 | 24.3647 | 1027.65 | 358093 | 1.2190 | 0.0046 | 342.08 |
| | D | 24.78 | 1024.95 | 1.1989 | 216 | 24.83 | 24.4542 | 1024.96 | 358100 | 1.2154 | 0.0047 | 342.07 |
| 30 | A | 24.58 | 1027.49 | 1.2027 | 250 | 24.57 | 24.3532 | 1027.33 | 358880 | 1.2218 | 0.0054 | 341.33 |
| | D | 24.69 | 1024.98 | 1.1993 | 253 | 24.71 | 24.3645 | 1024.93 | 358911 | 1.2187 | 0.0055 | 341.30 |
| 35 | A | 24.56 | 1027.21 | 1.2024 | 288 | 24.56 | 24.3386 | 1026.97 | 359651 | 1.2245 | 0.0063 | 340.59 |
| | D | 24.68 | 1025.08 | 1.1994 | 290 | 24.70 | 24.3570 | 1025.07 | 359677 | 1.2217 | 0.0063 | 340.57 |
| 40 | A | 24.54 | 1026.82 | 1.2020 | 328 | 24.56 | 24.3296 | 1026.67 | 360415 | 1.2272 | 0.0071 | 339.87 |
| | D | 24.70 | 1025.20 | 1.1995 | 330 | 24.71 | 24.3711 | 1025.20 | 360431 | 1.2248 | 0.0072 | 339.86 |
| 45 | A | 24.54 | 1026.66 | 1.2019 | 372 | 24.54 | 24.3202 | 1026.66 | 361164 | 1.2304 | 0.0080 | 339.17 |
| | D | 24.67 | 1025.71 | 1.2002 | 371 | 24.69 | 24.3560 | 1025.47 | 361183 | 1.2287 | 0.0081 | 339.15 |
| 50 | A | 24.52 | 1026.62 | 1.2019 | 409 | 24.53 | 24.3030 | 1026.77 | 361913 | 1.2332 | 0.0088 | 338.47 |
| | D | 24.66 | 1025.65 | 1.2002 | 408 | 24.68 | 24.3524 | 1025.78 | 361918 | 1.2314 | 0.0088 | 338.46 |
| 55 | A | 24.47 | 1026.80 | 1.2023 | 445 | 24.52 | 24.2896 | 1026.86 | 362654 | 1.2364 | 0.0096 | 337.77 |
| | D | 24.78 | 1025.71 | 1.1998 | 454 | 24.71 | 24.4165 | 1025.72 | 362637 | 1.2346 | 0.0097 | 337.79 |
| 60 | A | 24.51 | 1026.66 | 1.2020 | 489 | 24.51 | 24.2865 | 1026.72 | 363380 | 1.2394 | 0.0105 | 337.10 |
| | D | 24.76 | 1025.60 | 1.1997 | 491 | 24.78 | 24.4645 | 1025.76 | 363378 | 1.2374 | 0.0106 | 337.10 |

| | | | | | | | | | | | | |
|---|---|---|---|---|---|---|---|---|---|---|---|---|
| 65 | A | 24.51 | 1026.86 | 1.2022 | 525 | 24.60 | 24.3517 | 1026.94 | 364108 | 1.2425 | 0.0114 | 336.43 |
| | D | 24.76 | 1025.71 | 1.1999 | 526 | 24.77 | 24.4684 | 1025.56 | 364110 | 1.2402 | 0.0114 | 336.42 |
| 70 | A | 24.65 | 1027.12 | 1.2020 | 571 | 24.66 | 24.4257 | 1027.07 | 364834 | 1.2457 | 0.0123 | 335.76 |
| | D | 24.77 | 1025.59 | 1.1997 | 574 | 24.77 | 24.4813 | 1025.70 | 364841 | 1.2437 | 0.0124 | 335.75 |
| 75 | A | 24.66 | 1027.12 | 1.2019 | 606 | 24.66 | 24.4347 | 1026.94 | 365549 | 1.2484 | 0.0131 | 335.10 |
| | D | 24.73 | 1025.49 | 1.1997 | 612 | 24.77 | 24.4674 | 1025.67 | 365571 | 1.2466 | 0.0132 | 335.08 |
| 80 | A | 24.66 | 1026.95 | 1.2017 | 647 | 24.69 | 24.4452 | 1026.75 | 366265 | 1.2513 | 0.0141 | 334.44 |
| | D | 24.68 | 1025.37 | 1.1998 | 647 | 24.68 | 24.4123 | 1025.39 | 366280 | 1.2494 | 0.0140 | 334.43 |
| 85 | A | 24.69 | 1026.60 | 1.2012 | 688 | 24.71 | 24.4628 | 1026.40 | 366996 | 1.2539 | 0.0149 | 333.78 |
| | D | 24.68 | 1025.35 | 1.1998 | 683 | 24.69 | 24.4230 | 1025.43 | 367015 | 1.2521 | 0.0147 | 333.76 |
| 90 | A | 24.72 | 1026.09 | 1.2005 | 723 | 24.73 | 24.4821 | 1025.98 | 367722 | 1.2559 | 0.0157 | 333.12 |
| | D | 24.75 | 1025.47 | 1.1996 | 725 | 24.76 | 24.5058 | 1025.49 | 367745 | 1.2552 | 0.0157 | 333.10 |
| 95 | | 24.74 | 1025.97 | 1.2003 | 752 | 24.75 | 24.4966 | 1025.63 | 368383 | 1.2579 | 0.0164 | 332.52 |
| Data used for pathlength calibration (the first zero step): $T_{SOS}$ = 24.4441 °C, $P$ = 1027.55 mbar, $t_m^0$ = 353940 ns, $W^0$ = 346.09 m/s. | | | | | | | | | | | | |

Table 71. n-Octane/dry air results (35 °C isotherm)

| $x_T$/%SAT | | Zero Step | | | $\Delta m_{read}$/µg | Non-Zero Step | | | | | | |
|---|---|---|---|---|---|---|---|---|---|---|---|---|
| | | $T_{DVS}$/°C | $P$/mbar | $\rho^0$/(kg/m³) | | $T_{DVS}$/°C | $T_{SoS}$/°C | $P$/mbar | $t_m$/ns | $\rho$/(kg/m³) | $x$ | $W_m$/(m/s) |
| 10 | A | 34.53 | 988.92 | 1.1200 | 152 | 34.55 | 34.1598 | 988.99 | 351212 | 1.1316 | 0.0035 | 348.56 |
| | D | 34.45 | 999.30 | 1.1320 | 151 | 34.47 | 34.0684 | 999.51 | 351226 | 1.1436 | 0.0034 | 348.55 |
| 20 | A | 34.55 | 989.11 | 1.1201 | 302 | 34.56 | 34.1822 | 990.12 | 354054 | 1.1433 | 0.0067 | 345.77 |
| | D | 34.44 | 998.59 | 1.1313 | 292 | 34.46 | 34.0435 | 998.96 | 354036 | 1.1537 | 0.0066 | 345.78 |
| 30 | A | 34.47 | 989.94 | 1.1214 | 423 | 34.48 | 34.0973 | 990.19 | 356796 | 1.1538 | 0.0097 | 343.11 |
| | D | 34.35 | 998.25 | 1.1312 | 419 | 34.35 | 33.9599 | 998.50 | 356752 | 1.1633 | 0.0095 | 343.15 |
| 40 | A | 34.47 | 990.53 | 1.1220 | 556 | 34.46 | 34.0830 | 990.82 | 359374 | 1.1646 | 0.0127 | 340.65 |
| | D | 34.37 | 997.67 | 1.1305 | 556 | 34.36 | 33.9762 | 998.01 | 359323 | 1.1731 | 0.0126 | 340.70 |
| 50 | A | 34.45 | 990.99 | 1.1226 | 689 | 34.47 | 34.0743 | 991.37 | 361936 | 1.1754 | 0.0158 | 338.24 |
| | D | 34.37 | 996.89 | 1.1296 | 682 | 34.36 | 33.9764 | 997.17 | 361858 | 1.1819 | 0.0156 | 338.31 |
| 60 | A | 34.44 | 991.81 | 1.1236 | 817 | 34.44 | 34.0542 | 992.32 | 364377 | 1.1862 | 0.0187 | 335.97 |
| | D | 34.38 | 996.31 | 1.1289 | 811 | 34.39 | 33.9984 | 996.67 | 364320 | 1.1911 | 0.0185 | 336.02 |
| 70 | A | 34.43 | 992.71 | 1.1247 | 942 | 34.44 | 34.0494 | 993.18 | 366777 | 1.1968 | 0.0216 | 333.77 |
| | D | 34.39 | 995.76 | 1.1283 | 941 | 34.39 | 34.0026 | 995.99 | 366769 | 1.2004 | 0.0215 | 333.78 |
| 80 | A | 34.43 | 993.40 | 1.1254 | 1068 | 34.43 | 34.0438 | 993.67 | 369176 | 1.2073 | 0.0245 | 331.60 |
| | D | 34.38 | 995.38 | 1.1279 | 1065 | 34.38 | 33.9903 | 995.50 | 369105 | 1.2095 | 0.0244 | 331.67 |
| 90 | A | 34.41 | 993.93 | 1.1261 | 1199 | 34.43 | 34.0355 | 994.31 | 371556 | 1.2180 | 0.0275 | 329.48 |
| | D | 34.38 | 994.91 | 1.1273 | 1192 | 34.39 | 34.0005 | 995.16 | 371478 | 1.2187 | 0.0273 | 329.55 |
| 95 | | 34.40 | 994.48 | 1.1268 | 1254 | 34.39 | 34.0089 | 994.64 | 372642 | 1.2228 | 0.0288 | 328.52 |
| Data used for pathlength calibration (the first zero step): $T_{SoS}$ = 34.1465 °C, $P$ = 988.92 mbar, $t_m^0$ = 348088 ns, $W^0$ = 351.69 m/s. | | | | | | | | | | | | |

Table 72. n-Octane/dry air results (45 °C isotherm)

| $x_T$/%SAT | | Zero Step | | | $\Delta m_{read}$/µg | Non-Zero Step | | | | | | |
|---|---|---|---|---|---|---|---|---|---|---|---|---|
| | | $T_{DVS}$/°C | $P$/mbar | $\rho^0$/(kg/m$^3$) | | $T_{DVS}$/°C | $T_{SoS}$/°C | $P$/mbar | $t_m$/ns | $\rho$/(kg/m$^3$) | $x$ | $W_m$/(m/s) |
| 10 | A | 44.02 | 1019.95 | 1.1205 | 235 | 44.02 | 43.7077 | 1019.64 | 346947 | 1.1385 | 0.0055 | 351.99 |
| | D | 44.01 | 1019.14 | 1.1197 | 238 | 44.03 | 43.6887 | 1018.89 | 347010 | 1.1379 | 0.0056 | 351.93 |
| 20 | A | 43.93 | 1019.56 | 1.1204 | 456 | 43.94 | 43.6379 | 1019.45 | 351357 | 1.1553 | 0.0106 | 347.58 |
| | D | 44.05 | 1019.45 | 1.1198 | 460 | 44.01 | 43.6954 | 1019.30 | 351395 | 1.1551 | 0.0107 | 347.54 |
| 30 | A | 43.96 | 1019.39 | 1.1201 | 675 | 44.04 | 43.6838 | 1019.37 | 355520 | 1.1718 | 0.0157 | 343.51 |
| | D | 44.05 | 1019.79 | 1.1202 | 674 | 44.05 | 43.7132 | 1019.68 | 355550 | 1.1719 | 0.0156 | 343.48 |
| 40 | A | 44.03 | 1019.54 | 1.1200 | 886 | 44.01 | 43.7005 | 1019.75 | 359480 | 1.1879 | 0.0204 | 339.72 |
| | D | 43.94 | 1019.90 | 1.1207 | 879 | 43.98 | 43.6495 | 1019.90 | 359494 | 1.1881 | 0.0204 | 339.71 |
| 50 | A | 43.96 | 1020.12 | 1.1209 | 1088 | 43.95 | 43.6523 | 1020.42 | 363277 | 1.2043 | 0.0251 | 336.17 |
| | D | 43.98 | 1020.02 | 1.1207 | 1089 | 43.98 | 43.6700 | 1019.89 | 363336 | 1.2042 | 0.0252 | 336.12 |
| 60 | A | 43.92 | 1020.53 | 1.1215 | 1290 | 43.99 | 43.6687 | 1020.66 | 366991 | 1.2203 | 0.0299 | 332.77 |
| | D | 43.94 | 1020.05 | 1.1209 | 1285 | 43.94 | 43.6326 | 1020.01 | 366980 | 1.2194 | 0.0297 | 332.78 |
| 70 | A | 43.97 | 1020.68 | 1.1215 | 1487 | 43.96 | 43.6590 | 1020.64 | 370575 | 1.2354 | 0.0344 | 329.55 |
| | D | 43.95 | 1020.08 | 1.1209 | 1489 | 44.00 | 43.6740 | 1020.12 | 370606 | 1.2350 | 0.0345 | 329.52 |
| 80 | A | 43.94 | 1020.73 | 1.1216 | 1689 | 43.91 | 43.6199 | 1020.77 | 374076 | 1.2511 | 0.0390 | 326.47 |
| | D | 43.97 | 1020.08 | 1.1208 | 1690 | 43.98 | 43.6723 | 1020.16 | 374143 | 1.2503 | 0.0391 | 326.41 |
| 90 | A | 43.96 | 1020.75 | 1.1216 | 1892 | 43.97 | 43.6621 | 1020.66 | 377602 | 1.2665 | 0.0438 | 323.42 |
| | D | 44.03 | 1020.27 | 1.1208 | 1889 | 44.01 | 43.7018 | 1020.05 | 377641 | 1.2655 | 0.0437 | 323.38 |
| 95 | | 43.99 | 1020.41 | 1.1211 | 1987 | 44.05 | 43.7081 | 1020.22 | 379309 | 1.2734 | 0.0461 | 321.96 |
| Data used for pathlength calibration (the first zero step): $T_{SoS}$ = 43.7052 °C, $P$ = 1019.95 mbar, $t_m^0$ = 341956 ns, $W^0$ = 357.13 m/s. | | | | | | | | | | | | |

Table 73. n-Octane/dry air results (55 °C isotherm)

| $x_T$/%SAT | | Zero Step | | | $\Delta m_{read}$/µg | Non-Zero Step | | | | | | |
|---|---|---|---|---|---|---|---|---|---|---|---|---|
| | | $T_{DVS}$/°C | $P$/mbar | $\rho^0$/(kg/m³) | | $T_{DVS}$/°C | $T_{SoS}$/°C | $P$/mbar | $t_m$/ns | $\rho$/(kg/m³) | $x$ | $W_m$/(m/s) |
| 10 | A | 53.78 | 997.56 | 1.0631 | 381 | 53.75 | 53.4046 | 997.60 | 344933 | 1.0923 | 0.0092 | 353.94 |
| | D | 53.76 | 992.85 | 1.0582 | 382 | 53.76 | 53.4419 | 992.74 | 345024 | 1.0874 | 0.0094 | 353.85 |
| 20 | A | 53.78 | 997.56 | 1.0631 | 728 | 53.80 | 53.4671 | 997.63 | 351917 | 1.1189 | 0.0178 | 346.92 |
| | D | 53.77 | 993.06 | 1.0583 | 722 | 53.77 | 53.4433 | 992.83 | 352032 | 1.1137 | 0.0178 | 346.81 |
| 30 | A | 53.77 | 997.69 | 1.0633 | 1057 | 53.74 | 53.4384 | 997.58 | 358394 | 1.1443 | 0.0258 | 340.65 |
| | D | 53.80 | 993.35 | 1.0586 | 1063 | 53.79 | 53.4665 | 993.20 | 358554 | 1.1400 | 0.0261 | 340.50 |
| 40 | A | 53.71 | 997.54 | 1.0633 | 1373 | 53.73 | 53.4079 | 997.48 | 364466 | 1.1685 | 0.0335 | 334.97 |
| | D | 53.67 | 993.43 | 1.0591 | 1371 | 53.68 | 53.3451 | 993.40 | 364544 | 1.1641 | 0.0336 | 334.90 |
| 50 | A | 53.71 | 997.46 | 1.0632 | 1691 | 53.72 | 53.3899 | 997.48 | 370256 | 1.1928 | 0.0412 | 329.74 |
| | D | 53.68 | 993.78 | 1.0594 | 1685 | 53.70 | 53.3605 | 993.59 | 370369 | 1.1885 | 0.0413 | 329.63 |
| 60 | A | 53.70 | 997.23 | 1.0630 | 1992 | 53.71 | 53.3585 | 996.97 | 375756 | 1.2157 | 0.0487 | 324.91 |
| | D | 53.66 | 994.02 | 1.0597 | 1985 | 53.66 | 53.3131 | 993.94 | 375813 | 1.2119 | 0.0486 | 324.86 |
| 70 | A | 53.69 | 996.80 | 1.0626 | 2296 | 53.71 | 53.3481 | 996.84 | 381028 | 1.2385 | 0.0560 | 320.41 |
| | D | 53.69 | 994.52 | 1.0601 | 2290 | 53.69 | 53.3549 | 994.23 | 381122 | 1.2356 | 0.0561 | 320.33 |
| 80 | A | 53.70 | 996.73 | 1.0625 | 2598 | 53.71 | 53.3401 | 996.77 | 386186 | 1.2616 | 0.0634 | 316.13 |
| | D | 53.71 | 994.91 | 1.0605 | 2598 | 53.71 | 53.3931 | 994.70 | 386321 | 1.2596 | 0.0636 | 316.02 |
| 90 | A | 53.67 | 996.56 | 1.0624 | 2900 | 53.74 | 53.4078 | 996.27 | 391268 | 1.2846 | 0.0709 | 312.03 |
| | D | 53.72 | 995.36 | 1.0610 | 2895 | 53.72 | 53.4025 | 995.15 | 391303 | 1.2828 | 0.0708 | 312.00 |
| 95 | | 53.72 | 995.97 | 1.0616 | 3048 | 53.74 | 53.4232 | 995.75 | 393703 | 1.2952 | 0.0745 | 310.10 |
| Data used for pathlength calibration (the first zero step): $T_{SoS}$ = 53.4423 °C, $P$ = 997.56 mbar, $t_m^0$ = 336717 ns, $W^0$ = 362.58 m/s. | | | | | | | | | | | | |

## A6.3 n-Nonane/dry air

Table 74. n-Nonane/dry air results (15 °C isotherm)

| $x_T$/%SAT | | Zero Step | | | $\Delta m_{read}$/µg | Non-Zero Step | | | | | | |
|---|---|---|---|---|---|---|---|---|---|---|---|---|
| | | $T_{DVS}$/°C | $P$/mbar | $\rho^0$/(kg/m$^3$) | | $T_{DVS}$/°C | $T_{SoS}$/°C | $P$/mbar | $t_m$/ns | $\rho$/(kg/m$^3$) | $x$ | $W_m$/(m/s) |
| 10 | A | 14.55 | 1022.63 | 1.2388 | 17 | 14.55 | 14.2745 | 1022.56 | 360021 | 1.2402 | 0.00033 | 339.82 |
| | D | 14.67 | 1022.34 | 1.2380 | 14 | 14.67 | 14.4321 | 1021.97 | 359943 | 1.2390 | 0.00036 | 339.89 |
| 20 | A | 14.54 | 1022.71 | 1.2390 | 34 | 14.56 | 14.2808 | 1022.79 | 360311 | 1.2416 | 0.00061 | 339.55 |
| | D | 14.64 | 1022.64 | 1.2385 | 31 | 14.67 | 14.4171 | 1022.50 | 360252 | 1.2409 | 0.00064 | 339.60 |
| 30 | A | 14.57 | 1023.07 | 1.2393 | 53 | 14.56 | 14.2948 | 1023.28 | 360592 | 1.2433 | 0.00089 | 339.28 |
| | D | 14.64 | 1022.92 | 1.2388 | 47 | 14.63 | 14.3845 | 1022.78 | 360559 | 1.2424 | 0.00087 | 339.31 |
| 40 | A | 14.55 | 1023.55 | 1.2400 | 67 | 14.56 | 14.2870 | 1023.70 | 360888 | 1.2451 | 0.00118 | 339.00 |
| | D | 14.66 | 1023.32 | 1.2392 | 59 | 14.64 | 14.3933 | 1023.22 | 360840 | 1.2437 | 0.00107 | 339.05 |
| 50 | A | 14.55 | 1023.74 | 1.2402 | 81 | 14.57 | 14.2947 | 1023.95 | 361173 | 1.2464 | 0.00142 | 338.74 |
| | D | 14.68 | 1023.50 | 1.2393 | 79 | 14.63 | 14.3861 | 1023.36 | 361126 | 1.2454 | 0.00141 | 338.78 |
| 60 | A | 14.56 | 1024.04 | 1.2405 | 99 | 14.56 | 14.2960 | 1024.33 | 361455 | 1.2481 | 0.00169 | 338.47 |
| | D | 14.65 | 1023.78 | 1.2398 | 92 | 14.65 | 14.3969 | 1023.67 | 361398 | 1.2468 | 0.00168 | 338.52 |
| 70 | A | 14.56 | 1024.24 | 1.2407 | 108 | 14.58 | 14.3118 | 1024.11 | 361729 | 1.2490 | 0.00199 | 338.21 |
| | D | 14.62 | 1023.82 | 1.2400 | 111 | 14.63 | 14.3887 | 1023.75 | 361697 | 1.2485 | 0.00202 | 338.24 |
| 80 | A | 14.55 | 1024.07 | 1.2406 | 120 | 14.57 | 14.3034 | 1023.97 | 362006 | 1.2498 | 0.00220 | 337.96 |
| | D | 14.61 | 1024.02 | 1.2402 | 122 | 14.62 | 14.3777 | 1023.97 | 361968 | 1.2496 | 0.00221 | 337.99 |
| 90 | A | 14.57 | 1024.10 | 1.2405 | 133 | 14.58 | 14.3211 | 1024.04 | 362225 | 1.2507 | 0.00240 | 337.75 |
| | D | 14.61 | 1023.89 | 1.2401 | 133 | 14.62 | 14.3602 | 1023.90 | 362203 | 1.2503 | 0.00239 | 337.77 |
| 95 | | 14.64 | 1024.01 | 1.2401 | 138 | 14.61 | 14.3632 | 1023.94 | 362265 | 1.2507 | 0.00246 | 337.71 |
| Data used for pathlength calibration (the first zero step): $T_{SoS}$ = 14.2606 °C, $P$ = 1022.63 mbar, $t_m^0$ = 359720 ns, $W^0$ = 340.10 m/s. | | | | | | | | | | | | |

Table 75. n-Nonane/dry air results (25 °C isotherm)

| $x_T$/%SAT | | Zero Step | | | $\Delta m_{read}$/µg | Non-Zero Step | | | | | | |
|---|---|---|---|---|---|---|---|---|---|---|---|---|
| | | $T_{DVS}$/°C | $P$/mbar | $\rho^0$/(kg/m$^3$) | | $T_{DVS}$/°C | $T_{SoS}$/°C | $P$/mbar | $t_m$/ns | $\rho$/(kg/m$^3$) | $x$ | $W_m$/(m/s) |
| 5 | A | 24.35 | 1018.40 | 1.1930 | 20 | 24.38 | 23.9525 | 1018.57 | 354146 | 1.1944 | 0.00035 | 345.50 |
| | D | 24.31 | 1027.35 | 1.2036 | 21 | 24.32 | 23.8808 | 1027.39 | 354210 | 1.2052 | 0.00039 | 345.43 |
| 10 | A | 24.36 | 1018.60 | 1.1931 | 30 | 24.39 | 23.9492 | 1018.40 | 354445 | 1.1954 | 0.00064 | 345.21 |
| | D | 24.21 | 1027.25 | 1.2039 | 30 | 24.23 | 23.7914 | 1027.18 | 354542 | 1.2061 | 0.00058 | 345.11 |
| 15 | A | 24.37 | 1018.26 | 1.1927 | 46 | 24.37 | 23.9374 | 1018.33 | 354723 | 1.1962 | 0.00084 | 344.94 |
| | D | 24.24 | 1027.40 | 1.2040 | 46 | 24.24 | 23.8068 | 1027.39 | 354813 | 1.2075 | 0.00086 | 344.85 |
| 20 | A | 24.34 | 1018.15 | 1.1927 | 61 | 24.36 | 23.9185 | 1018.20 | 355018 | 1.1974 | 0.00114 | 344.65 |
| | D | 24.23 | 1027.06 | 1.2036 | 65 | 24.24 | 23.8095 | 1027.27 | 355087 | 1.2086 | 0.00116 | 344.58 |
| 25 | A | 24.34 | 1018.07 | 1.1926 | 80 | 24.36 | 23.9243 | 1018.39 | 355299 | 1.1987 | 0.00142 | 344.38 |
| | D | 24.23 | 1026.91 | 1.2034 | 77 | 24.24 | 23.8014 | 1026.95 | 355372 | 1.2093 | 0.00143 | 344.31 |
| 30 | A | 24.34 | 1018.46 | 1.1931 | 92 | 24.34 | 23.9042 | 1018.73 | 355583 | 1.2001 | 0.00165 | 344.10 |
| | D | 24.22 | 1027.27 | 1.2039 | 84 | 24.24 | 23.7989 | 1026.98 | 355644 | 1.2103 | 0.00166 | 344.04 |
| 35 | A | 24.34 | 1018.80 | 1.1935 | 112 | 24.37 | 23.9307 | 1019.28 | 355851 | 1.2020 | 0.00198 | 343.84 |
| | D | 24.23 | 1027.45 | 1.2040 | 103 | 24.24 | 23.8052 | 1027.49 | 355910 | 1.2119 | 0.00190 | 343.78 |
| 40 | A | 24.37 | 1019.50 | 1.1942 | 127 | 24.38 | 23.9430 | 1019.99 | 356120 | 1.2039 | 0.00224 | 343.58 |
| | D | 24.23 | 1027.32 | 1.2039 | 118 | 24.25 | 23.8111 | 1027.40 | 356182 | 1.2129 | 0.00218 | 343.52 |
| 45 | A | 24.37 | 1020.23 | 1.1950 | 139 | 24.39 | 23.9484 | 1020.51 | 356396 | 1.2057 | 0.00253 | 343.32 |
| | D | 24.24 | 1026.69 | 1.2031 | 137 | 24.24 | 23.8027 | 1027.04 | 356453 | 1.2136 | 0.00244 | 343.26 |
| 50 | A | 24.36 | 1020.72 | 1.1956 | 150 | 24.29 | 23.8807 | 1020.99 | 356684 | 1.2071 | 0.00264 | 343.04 |
| | D | 24.24 | 1025.64 | 1.2019 | 156 | 24.26 | 23.8116 | 1026.31 | 356723 | 1.2138 | 0.00272 | 343.00 |
| 55 | A | 24.26 | 1021.34 | 1.1968 | 162 | 24.26 | 23.8246 | 1021.59 | 356971 | 1.2092 | 0.00294 | 342.76 |
| | D | 24.24 | 1024.55 | 1.2006 | 167 | 24.25 | 23.8078 | 1025.06 | 356989 | 1.2134 | 0.00296 | 342.75 |
| 60 | A | 24.25 | 1021.71 | 1.1972 | 174 | 24.26 | 23.8228 | 1021.79 | 357243 | 1.2106 | 0.00322 | 342.50 |
| | D | 24.24 | 1024.36 | 1.2004 | 172 | 24.26 | 23.8175 | 1024.48 | 357226 | 1.2136 | 0.00319 | 342.52 |

| | | | | | | | | | | | | |
|---|---|---|---|---|---|---|---|---|---|---|---|---|
| 65 | A | 24.23 | 1021.87 | 1.1975 | 189 | 24.25 | 23.8124 | 1022.09 | 357515 | 1.2120 | 0.00347 | 342.24 |
| | D | 24.24 | 1024.43 | 1.2004 | 186 | 24.27 | 23.8264 | 1024.31 | 357501 | 1.2147 | 0.00350 | 342.25 |
| 70 | A | 24.24 | 1022.09 | 1.1977 | 202 | 24.26 | 23.8196 | 1022.36 | 357783 | 1.2132 | 0.00369 | 341.99 |
| | D | 24.24 | 1024.65 | 1.2007 | 194 | 24.27 | 23.8153 | 1024.45 | 357775 | 1.2156 | 0.00368 | 341.99 |
| 75 | A | 24.25 | 1022.33 | 1.1980 | 213 | 24.25 | 23.8181 | 1022.34 | 358049 | 1.2143 | 0.00397 | 341.73 |
| | D | 24.23 | 1024.88 | 1.2010 | 212 | 24.25 | 23.8080 | 1024.83 | 358039 | 1.2173 | 0.00397 | 341.74 |
| 80 | A | 24.24 | 1022.48 | 1.1982 | 230 | 24.23 | 23.7986 | 1022.70 | 358320 | 1.2158 | 0.00420 | 341.47 |
| | D | 24.23 | 1024.86 | 1.2010 | 226 | 24.24 | 23.8009 | 1024.89 | 358311 | 1.2183 | 0.00420 | 341.48 |
| 85 | A | 24.20 | 1022.97 | 1.1989 | 244 | 24.22 | 23.7809 | 1023.30 | 358591 | 1.2176 | 0.00446 | 341.21 |
| | D | 24.22 | 1024.98 | 1.2012 | 235 | 24.25 | 23.8045 | 1024.83 | 358577 | 1.2192 | 0.00443 | 341.23 |
| 90 | A | 24.22 | 1023.68 | 1.1997 | 258 | 24.28 | 23.8395 | 1024.02 | 358811 | 1.2194 | 0.00475 | 341.01 |
| | D | 24.21 | 1024.49 | 1.2006 | 255 | 24.24 | 23.7923 | 1024.87 | 358820 | 1.2202 | 0.00465 | 341.00 |
| 95 | | 24.22 | 1024.19 | 1.2003 | 260 | 24.22 | 23.7878 | 1024.44 | 358982 | 1.2202 | 0.00475 | 340.84 |
| Data used for pathlength calibration (the first zero step): $T_{SOS}$ = 23.9215 °C, $P$ = 1018.40 mbar, $t_m^0$ = 353851 ns, $W^0$ = 345.78 m/s. | | | | | | | | | | | | |

Table 76. n-Nonane/dry air results (35 °C isotherm)

| $x_T$/%SAT | | Zero Step | | | $\Delta m_{read}$/µg | Non-Zero Step | | | | | | |
|---|---|---|---|---|---|---|---|---|---|---|---|---|
| | | $T_{DVS}$/°C | $P$/mbar | $\rho^0$/(kg/m³) | | $T_{DVS}$/°C | $T_{SoS}$/°C | $P$/mbar | $t_m$/ns | $\rho$/(kg/m³) | $x$ | $W_m$/(m/s) |
| 10 | A | 34.60 | 998.92 | 1.1310 | 57 | 34.60 | 34.2135 | 998.90 | 348803 | 1.1354 | 0.00113 | 350.57 |
| | D | 34.63 | 1009.69 | 1.1431 | 62 | 34.59 | 34.2277 | 1009.71 | 348790 | 1.1479 | 0.00117 | 350.58 |
| 20 | A | 34.59 | 998.88 | 1.1310 | 109 | 34.61 | 34.2270 | 998.91 | 349859 | 1.1394 | 0.00215 | 349.51 |
| | D | 34.62 | 1009.43 | 1.1429 | 114 | 34.62 | 34.2426 | 1009.66 | 349845 | 1.1516 | 0.00216 | 349.52 |
| 30 | A | 34.58 | 999.26 | 1.1315 | 162 | 34.59 | 34.2059 | 999.37 | 350911 | 1.1439 | 0.00317 | 348.46 |
| | D | 34.59 | 1009.23 | 1.1428 | 164 | 34.62 | 34.2376 | 1009.44 | 350885 | 1.1554 | 0.00317 | 348.49 |
| 40 | A | 34.58 | 999.55 | 1.1319 | 217 | 34.59 | 34.2118 | 1000.03 | 351927 | 1.1485 | 0.00415 | 347.46 |
| | D | 34.47 | 1008.84 | 1.1428 | 212 | 34.56 | 34.1524 | 1009.09 | 351921 | 1.1590 | 0.00414 | 347.46 |
| 50 | A | 34.58 | 1000.50 | 1.1329 | 266 | 34.60 | 34.2111 | 1000.90 | 352935 | 1.1533 | 0.00513 | 346.46 |
| | D | 34.50 | 1007.91 | 1.1416 | 268 | 34.51 | 34.1234 | 1008.37 | 352925 | 1.1621 | 0.00510 | 346.47 |
| 60 | A | 34.61 | 1001.14 | 1.1335 | 316 | 34.57 | 34.2143 | 1001.38 | 353917 | 1.1578 | 0.00610 | 345.50 |
| | D | 34.52 | 1007.08 | 1.1406 | 319 | 34.51 | 34.1241 | 1007.75 | 353910 | 1.1650 | 0.00602 | 345.51 |
| 70 | A | 34.52 | 1001.68 | 1.1345 | 366 | 34.59 | 34.2056 | 1002.04 | 354906 | 1.1625 | 0.00715 | 344.54 |
| | D | 34.52 | 1006.38 | 1.1398 | 365 | 34.52 | 34.1397 | 1006.79 | 354891 | 1.1678 | 0.00701 | 344.55 |
| 80 | A | 34.59 | 1002.19 | 1.1348 | 419 | 34.56 | 34.2044 | 1002.49 | 355892 | 1.1669 | 0.00810 | 343.58 |
| | D | 34.54 | 1004.87 | 1.1380 | 422 | 34.51 | 34.1352 | 1005.67 | 355879 | 1.1704 | 0.00799 | 343.60 |
| 90 | A | 34.53 | 1002.61 | 1.1355 | 462 | 34.54 | 34.1560 | 1003.01 | 356857 | 1.1709 | 0.00896 | 342.66 |
| | D | 34.53 | 1004.19 | 1.1373 | 461 | 34.55 | 34.1599 | 1004.43 | 356851 | 1.1726 | 0.00897 | 342.66 |
| 95 | | 34.54 | 1003.40 | 1.1364 | 482 | 34.55 | 34.1637 | 1003.93 | 357252 | 1.1733 | 0.00930 | 342.28 |
| Data used for pathlength calibration (the first zero step): $T_{SoS}$ = 34.2117 °C, $P$ = 998.92 mbar, $t_m^0$ = 347650 ns, $W^0$ = 351.73 m/s. | | | | | | | | | | | | |

Table 77. n-Nonane/dry air results (45 °C isotherm)

| $x_T$/%SAT | | Zero Step | | | $\Delta m_{read}$/µg | Non-Zero Step | | | | | | |
|---|---|---|---|---|---|---|---|---|---|---|---|---|
| | | $T_{DVS}$/°C | $P$/mbar | $\rho^0$/(kg/m$^3$) | | $T_{DVS}$/°C | $T_{SoS}$/°C | $P$/mbar | $t_m$/ns | $\rho$/(kg/m$^3$) | $x$ | $W_m$/(m/s) |
| 10 | A | 43.96 | 1017.87 | 1.1184 | 93 | 43.93 | 43.6516 | 1017.84 | 344117 | 1.1255 | 0.0018 | 355.09 |
| | D | 43.95 | 1018.38 | 1.1190 | 96 | 43.93 | 43.6413 | 1018.40 | 344129 | 1.1264 | 0.0019 | 355.08 |
| 20 | A | 43.96 | 1017.96 | 1.1185 | 181 | 43.94 | 43.6456 | 1017.95 | 345912 | 1.1324 | 0.0036 | 353.25 |
| | D | 43.98 | 1018.31 | 1.1188 | 181 | 43.96 | 43.6642 | 1018.31 | 345910 | 1.1327 | 0.0036 | 353.25 |
| 30 | A | 43.96 | 1017.93 | 1.1185 | 267 | 43.95 | 43.6718 | 1017.78 | 347644 | 1.1390 | 0.0054 | 351.49 |
| | D | 43.99 | 1018.31 | 1.1188 | 267 | 43.97 | 43.6698 | 1018.31 | 347650 | 1.1393 | 0.0053 | 351.48 |
| 40 | A | 43.95 | 1017.81 | 1.1184 | 349 | 43.91 | 43.6394 | 1017.67 | 349331 | 1.1451 | 0.0070 | 349.79 |
| | D | 43.98 | 1018.47 | 1.1190 | 349 | 44.00 | 43.6792 | 1018.42 | 349329 | 1.1458 | 0.0070 | 349.79 |
| 50 | A | 43.99 | 1017.64 | 1.1181 | 430 | 43.95 | 43.6364 | 1017.41 | 350989 | 1.1510 | 0.0086 | 348.14 |
| | D | 43.99 | 1018.74 | 1.1193 | 434 | 44.04 | 43.6912 | 1018.75 | 350983 | 1.1525 | 0.0087 | 348.14 |
| 60 | A | 43.95 | 1017.27 | 1.1178 | 511 | 43.94 | 43.6347 | 1016.88 | 352608 | 1.1569 | 0.0103 | 346.54 |
| | D | 43.94 | 1019.00 | 1.1197 | 514 | 43.98 | 43.6787 | 1018.77 | 352605 | 1.1591 | 0.0103 | 346.54 |
| 70 | A | 43.98 | 1016.78 | 1.1171 | 600 | 43.96 | 43.6710 | 1016.59 | 354220 | 1.1631 | 0.0120 | 344.96 |
| | D | 43.96 | 1018.84 | 1.1195 | 600 | 44.00 | 43.6991 | 1018.98 | 354207 | 1.1655 | 0.0119 | 344.97 |
| 80 | A | 43.96 | 1016.63 | 1.1171 | 680 | 43.96 | 43.6365 | 1016.74 | 355806 | 1.1691 | 0.0135 | 343.42 |
| | D | 43.98 | 1018.35 | 1.1189 | 689 | 44.00 | 43.7096 | 1018.62 | 355828 | 1.1717 | 0.0137 | 343.40 |
| 90 | A | 44.02 | 1016.81 | 1.1171 | 768 | 44.00 | 43.6722 | 1016.91 | 357412 | 1.1759 | 0.0153 | 341.88 |
| | D | 44.02 | 1017.43 | 1.1177 | 771 | 43.98 | 43.7029 | 1017.83 | 357404 | 1.1768 | 0.0152 | 341.89 |
| 95 | | 44.01 | 1016.92 | 1.1172 | 805 | 44.06 | 43.7287 | 1017.13 | 358171 | 1.1789 | 0.0160 | 341.16 |
| Data used for pathlength calibration (the first zero step): $T_{SoS}$ = 43.6828 °C, $P$ = 1017.87 mbar, $t_m^0$ = 342163 ns, $W^0$ = 357.12 m/s. | | | | | | | | | | | | |

Table 78. n-Nonane/dry air results (55 °C isotherm)

| $x_T$/%SAT | | Zero Step | | | $\Delta m_{read}$/µg | Non-Zero Step | | | | | | |
|---|---|---|---|---|---|---|---|---|---|---|---|---|
| | | $T_{DVS}$/°C | $P$/mbar | $\rho^0$/(kg/m$^3$) | | $T_{DVS}$/°C | $T_{SoS}$/°C | $P$/mbar | $t_m$/ns | $\rho$/(kg/m$^3$) | $x$ | $W_m$/(m/s) |
| 10 | A | 53.69 | 1013.52 | 1.0804 | 155 | 53.71 | 53.3584 | 1013.51 | 340049 | 1.0923 | 0.0032 | 359.05 |
| | D | 53.72 | 1013.85 | 1.0807 | 155 | 53.73 | 53.3866 | 1013.90 | 340070 | 1.0925 | 0.0032 | 359.02 |
| 20 | A | 53.70 | 1013.42 | 1.0803 | 296 | 53.70 | 53.3450 | 1013.49 | 343013 | 1.1030 | 0.0061 | 355.94 |
| | D | 53.73 | 1013.79 | 1.0806 | 298 | 53.74 | 53.4137 | 1013.91 | 343038 | 1.1034 | 0.0061 | 355.92 |
| 30 | A | 53.65 | 1013.49 | 1.0805 | 437 | 53.71 | 53.3718 | 1013.50 | 345865 | 1.1140 | 0.0091 | 353.01 |
| | D | 53.69 | 1013.84 | 1.0807 | 434 | 53.73 | 53.4109 | 1013.73 | 345897 | 1.1140 | 0.0090 | 352.98 |
| 40 | A | 53.70 | 1013.49 | 1.0804 | 570 | 53.71 | 53.3670 | 1013.47 | 348585 | 1.1240 | 0.0118 | 350.25 |
| | D | 53.73 | 1013.94 | 1.0807 | 574 | 53.73 | 53.4204 | 1013.95 | 348602 | 1.1247 | 0.0118 | 350.24 |
| 50 | A | 53.73 | 1013.29 | 1.0801 | 707 | 53.70 | 53.3665 | 1013.32 | 351237 | 1.1342 | 0.0146 | 347.61 |
| | D | 53.73 | 1013.88 | 1.0807 | 707 | 53.69 | 53.3603 | 1013.96 | 351250 | 1.1349 | 0.0145 | 347.60 |
| 60 | A | 53.66 | 1013.25 | 1.0802 | 840 | 53.74 | 53.4093 | 1013.16 | 353836 | 1.1446 | 0.0174 | 345.06 |
| | D | 53.72 | 1013.90 | 1.0807 | 837 | 53.73 | 53.3831 | 1013.90 | 353832 | 1.1449 | 0.0173 | 345.06 |
| 70 | A | 53.74 | 1012.96 | 1.0797 | 977 | 53.75 | 53.4421 | 1012.93 | 356403 | 1.1545 | 0.0202 | 342.57 |
| | D | 53.71 | 1013.89 | 1.0807 | 974 | 53.73 | 53.4024 | 1013.92 | 356384 | 1.1554 | 0.0201 | 342.59 |
| 80 | A | 53.75 | 1013.11 | 1.0798 | 1106 | 53.72 | 53.4048 | 1013.08 | 358912 | 1.1646 | 0.0228 | 340.18 |
| | D | 53.72 | 1013.87 | 1.0807 | 1105 | 53.73 | 53.4077 | 1013.80 | 358906 | 1.1654 | 0.0228 | 340.18 |
| 90 | A | 53.70 | 1013.23 | 1.0801 | 1244 | 53.70 | 53.3969 | 1013.42 | 361378 | 1.1754 | 0.0256 | 337.86 |
| | D | 53.69 | 1013.90 | 1.0808 | 1227 | 53.69 | 53.3548 | 1013.78 | 361328 | 1.1749 | 0.0253 | 337.90 |
| 95 | | 53.70 | 1013.60 | 1.0805 | 1304 | 53.71 | 53.3880 | 1013.67 | 362572 | 1.1804 | 0.0269 | 336.74 |
| Data used for pathlength calibration (the first zero step): $T_{SoS}$ = 53.3432 °C, $P$ = 1013.52 mbar, $t_m^0$ = 336785 ns, $W^0$ = 362.53 m/s. | | | | | | | | | | | | |

## A6.4 n-Decane/dry air

Table 79. n-Decane/dry air results (25 °C isotherm)

| $x_T$/%SAT | | Zero Step | | | $\Delta m_{read}$/µg | Non-Zero Step | | | | | | |
|---|---|---|---|---|---|---|---|---|---|---|---|---|
| | | $T_{DVS}$/°C | $P$/mbar | $\rho^0$/(kg/m$^3$) | | $T_{DVS}$/°C | $T_{SoS}$/°C | $P$/mbar | $t_m$/ns | $\rho$/(kg/m$^3$) | $x$ | $W_m$/(m/s) |
| 10 | A | 24.65 | 1012.32 | 1.1846 | 16 | 24.66 | 24.4097 | 1012.53 | 353776 | 1.1859 | 0.00022 | 345.86 |
| | D | 24.65 | 1010.57 | 1.1826 | 15 | 24.67 | 24.3264 | 1010.78 | 353836 | 1.1837 | 0.00021 | 345.80 |
| 20 | A | 24.66 | 1012.67 | 1.1850 | 25 | 24.66 | 24.4110 | 1012.72 | 353980 | 1.1869 | 0.00039 | 345.66 |
| | D | 24.66 | 1010.46 | 1.1824 | 16 | 24.67 | 24.3280 | 1010.02 | 354039 | 1.1837 | 0.00039 | 345.60 |
| 30 | A | 24.64 | 1012.87 | 1.1853 | 33 | 24.64 | 24.3865 | 1012.84 | 354199 | 1.1878 | 0.00055 | 345.45 |
| | D | 24.67 | 1010.99 | 1.1830 | 29 | 24.69 | 24.3425 | 1010.77 | 354234 | 1.1852 | 0.00055 | 345.41 |
| 40 | A | 24.62 | 1012.68 | 1.1852 | 43 | 24.63 | 24.3677 | 1012.61 | 354409 | 1.1885 | 0.00074 | 345.24 |
| | D | 24.64 | 1010.86 | 1.1830 | 45 | 24.68 | 24.3283 | 1010.93 | 354442 | 1.1864 | 0.00076 | 345.21 |
| 50 | A | 24.71 | 1012.49 | 1.1846 | 58 | 24.75 | 24.4596 | 1012.59 | 354560 | 1.1890 | 0.00097 | 345.09 |
| | D | 24.64 | 1011.44 | 1.1837 | 48 | 24.65 | 24.3043 | 1011.08 | 354653 | 1.1873 | 0.00089 | 345.00 |
| 60 | A | 24.73 | 1012.63 | 1.1847 | 59 | 24.75 | 24.4692 | 1012.25 | 354753 | 1.1892 | 0.00108 | 344.91 |
| | D | 24.62 | 1011.52 | 1.1838 | 59 | 24.64 | 24.3075 | 1011.17 | 354845 | 1.1883 | 0.00108 | 344.82 |
| 70 | A | 24.72 | 1012.07 | 1.1841 | 73 | 24.72 | 24.4365 | 1012.02 | 354962 | 1.1896 | 0.00122 | 344.70 |
| | D | 24.60 | 1012.24 | 1.1848 | 71 | 24.64 | 24.2960 | 1012.17 | 355045 | 1.1902 | 0.00123 | 344.62 |
| 80 | A | 24.61 | 1011.74 | 1.1841 | 78 | 24.61 | 24.3170 | 1011.50 | 355210 | 1.1900 | 0.00134 | 344.46 |
| | D | 24.61 | 1012.10 | 1.1845 | 83 | 24.63 | 24.2916 | 1012.20 | 355227 | 1.1909 | 0.00136 | 344.45 |
| 90 | A | 24.66 | 1011.49 | 1.1836 | 96 | 24.64 | 24.3492 | 1011.75 | 355337 | 1.1909 | 0.00149 | 344.34 |
| | D | 24.59 | 1012.19 | 1.1847 | 90 | 24.60 | 24.2804 | 1012.33 | 355373 | 1.1916 | 0.00145 | 344.30 |
| 95 | | 24.59 | 1012.13 | 1.1846 | 92 | 24.62 | 24.3009 | 1012.33 | 355398 | 1.1917 | 0.00148 | 344.28 |
| Data used for pathlength calibration (the first zero step): $T_{SoS}$ = 24.4055 °C, $P$ = 1012.32 mbar, $t_m^0$ = 353564 ns, $W^0$ = 346.07 m/s. | | | | | | | | | | | | |

Table 80. n-Decane/dry air results (35 °C isotherm)

| $x_T$/%SAT | | Zero Step | | | $\Delta m_{read}$/µg | Non-Zero Step | | | | | | |
|---|---|---|---|---|---|---|---|---|---|---|---|---|
| | | $T_{DVS}$/°C | $P$/mbar | $\rho^0$/(kg/m$^3$) | | $T_{DVS}$/°C | $T_{SoS}$/°C | $P$/mbar | $t_m$/ns | $\rho$/(kg/m$^3$) | $x$ | $W_m$/(m/s) |
| 10 | A | 34.36 | 1003.69 | 1.1373 | 25 | 34.39 | 34.0798 | 1003.82 | 348031 | 1.1393 | 0.00042 | 351.23 |
| | D | 34.52 | 1013.14 | 1.1475 | 27 | 34.52 | 34.1773 | 1013.42 | 348007 | 1.1495 | 0.00039 | 351.25 |
| 20 | A | 34.36 | 1003.82 | 1.1375 | 35 | 34.38 | 34.0695 | 1003.36 | 348431 | 1.1401 | 0.00073 | 350.82 |
| | D | 34.54 | 1012.55 | 1.1467 | 47 | 34.55 | 34.2003 | 1012.83 | 348388 | 1.1503 | 0.00073 | 350.87 |
| 30 | A | 34.37 | 1003.72 | 1.1373 | 66 | 34.38 | 34.0668 | 1004.09 | 348826 | 1.1424 | 0.00105 | 350.43 |
| | D | 34.55 | 1011.86 | 1.1459 | 68 | 34.56 | 34.2141 | 1012.23 | 348770 | 1.1511 | 0.00107 | 350.48 |
| 40 | A | 34.37 | 1003.72 | 1.1373 | 79 | 34.39 | 34.0672 | 1003.67 | 349215 | 1.1434 | 0.00139 | 350.04 |
| | D | 34.55 | 1011.06 | 1.1450 | 88 | 34.56 | 34.2176 | 1011.55 | 349151 | 1.1517 | 0.00139 | 350.10 |
| 50 | A | 34.39 | 1003.76 | 1.1373 | 104 | 34.40 | 34.0764 | 1004.11 | 349592 | 1.1453 | 0.00171 | 349.66 |
| | D | 34.51 | 1010.36 | 1.1444 | 103 | 34.52 | 34.1892 | 1010.68 | 349546 | 1.1522 | 0.00169 | 349.71 |
| 60 | A | 34.40 | 1004.20 | 1.1378 | 122 | 34.40 | 34.0778 | 1004.46 | 349974 | 1.1471 | 0.00203 | 349.28 |
| | D | 34.52 | 1009.46 | 1.1433 | 124 | 34.54 | 34.1912 | 1009.85 | 349926 | 1.1528 | 0.00203 | 349.33 |
| 70 | A | 34.40 | 1004.60 | 1.1382 | 145 | 34.42 | 34.0865 | 1005.08 | 350349 | 1.1493 | 0.00238 | 348.90 |
| | D | 34.51 | 1008.84 | 1.1426 | 143 | 34.52 | 34.1853 | 1009.29 | 350305 | 1.1536 | 0.00234 | 348.95 |
| 80 | A | 34.42 | 1005.37 | 1.1390 | 163 | 34.45 | 34.1144 | 1005.91 | 350716 | 1.1515 | 0.00268 | 348.54 |
| | D | 34.51 | 1008.77 | 1.1425 | 155 | 34.53 | 34.2001 | 1008.85 | 350678 | 1.1544 | 0.00265 | 348.58 |
| 90 | A | 34.46 | 1006.11 | 1.1397 | 177 | 34.47 | 34.1412 | 1006.59 | 351034 | 1.1533 | 0.00292 | 348.22 |
| | D | 34.50 | 1007.80 | 1.1415 | 177 | 34.52 | 34.1891 | 1008.20 | 351016 | 1.1551 | 0.00295 | 348.24 |
| 95 | | 34.46 | 1006.92 | 1.1406 | 178 | 34.48 | 34.1504 | 1007.25 | 351133 | 1.1543 | 0.00298 | 348.12 |
| Data used for pathlength calibration (the first zero step): $T_{SoS}$ = 34.0590 °C, $P$ = 1003.69 mbar, $t_m^0$ = 347619 ns, $W^0$ = 351.64 m/s. | | | | | | | | | | | | |

Table 81. n-Decane/dry air results (45 °C isotherm)

| $x_T$/%SAT | | Zero Step | | | $\Delta m_{read}$/µg | Non-Zero Step | | | | | | |
|---|---|---|---|---|---|---|---|---|---|---|---|---|
| | | $T_{DVS}$/°C | $P$/mbar | $\rho^0$/(kg/m$^3$) | | $T_{DVS}$/°C | $T_{SoS}$/°C | $P$/mbar | $t_m$/ns | $\rho$/(kg/m$^3$) | $x$ | $W_m$/(m/s) |
| 10 | A | 43.96 | 1010.44 | 1.1102 | 32 | 43.91 | 43.5692 | 1009.83 | 342867 | 1.1127 | 0.00067 | 356.20 |
| | D | 43.99 | 1002.41 | 1.1013 | 38 | 43.97 | 43.6055 | 1002.34 | 342893 | 1.1043 | 0.00068 | 356.17 |
| 20 | A | 43.91 | 1009.60 | 1.1095 | 74 | 43.92 | 43.5748 | 1009.21 | 343629 | 1.1151 | 0.00140 | 355.41 |
| | D | 43.86 | 1002.68 | 1.1021 | 68 | 43.94 | 43.5461 | 1002.48 | 343633 | 1.1073 | 0.00133 | 355.41 |
| 30 | A | 43.91 | 1008.93 | 1.1088 | 108 | 43.99 | 43.5893 | 1008.61 | 344369 | 1.1170 | 0.00205 | 354.65 |
| | D | 43.93 | 1003.68 | 1.1029 | 99 | 43.92 | 43.5924 | 1003.22 | 344312 | 1.1105 | 0.00186 | 354.70 |
| 40 | A | 44.02 | 1008.43 | 1.1078 | 141 | 44.02 | 43.6439 | 1007.93 | 345059 | 1.1186 | 0.00262 | 353.94 |
| | D | 43.94 | 1004.21 | 1.1035 | 137 | 43.96 | 43.6210 | 1003.89 | 344993 | 1.1140 | 0.00253 | 354.00 |
| 50 | A | 43.97 | 1007.61 | 1.1071 | 177 | 43.99 | 43.6322 | 1007.37 | 345757 | 1.1207 | 0.00320 | 353.22 |
| | D | 43.89 | 1004.57 | 1.1041 | 172 | 43.90 | 43.5568 | 1004.45 | 345701 | 1.1172 | 0.00308 | 353.28 |
| 60 | A | 43.93 | 1006.83 | 1.1064 | 207 | 43.94 | 43.5863 | 1006.49 | 346437 | 1.1223 | 0.00375 | 352.53 |
| | D | 43.88 | 1004.80 | 1.1043 | 203 | 43.91 | 43.5537 | 1004.67 | 346385 | 1.1199 | 0.00365 | 352.58 |
| 70 | A | 43.96 | 1006.62 | 1.1061 | 242 | 43.90 | 43.5818 | 1006.42 | 347089 | 1.1246 | 0.00428 | 351.87 |
| | D | 43.94 | 1004.89 | 1.1042 | 242 | 43.93 | 43.5755 | 1004.98 | 347046 | 1.1227 | 0.00424 | 351.91 |
| 80 | A | 43.93 | 1006.41 | 1.1059 | 277 | 43.99 | 43.5985 | 1006.43 | 347756 | 1.1272 | 0.00493 | 351.19 |
| | D | 44.00 | 1005.62 | 1.1048 | 271 | 43.97 | 43.6036 | 1005.39 | 347722 | 1.1256 | 0.00482 | 351.23 |
| 90 | A | 43.98 | 1006.17 | 1.1055 | 308 | 43.96 | 43.6161 | 1006.07 | 348376 | 1.1291 | 0.00544 | 350.57 |
| | D | 43.91 | 1006.09 | 1.1057 | 296 | 43.96 | 43.5654 | 1005.64 | 348368 | 1.1283 | 0.00539 | 350.57 |
| 95 | | 43.96 | 1006.06 | 1.1054 | 317 | 43.97 | 43.6279 | 1006.18 | 348587 | 1.1297 | 0.00558 | 350.35 |
| Data used for pathlength calibration (the first zero step): $T_{SoS}$ = 43.6064 °C, $P$ = 1010.44 mbar, $t_m^0$ = 342027 ns, $W^0$ = 357.07 m/s. | | | | | | | | | | | | |

Table 82. n-Decane/dry air results (55 °C isotherm)

| $x_T$/%SAT | | Zero Step | | | $\Delta m_{read}$/µg | Non-Zero Step | | | | | | |
|---|---|---|---|---|---|---|---|---|---|---|---|---|
| | | $T_{DVS}$/°C | $P$/mbar | $\rho^0$/(kg/m$^3$) | | $T_{DVS}$/°C | $T_{SoS}$/°C | $P$/mbar | $t_m$/ns | $\rho$/(kg/m$^3$) | $x$ | $W_m$/(m/s) |
| 10 | A | 53.70 | 1009.79 | 1.0764 | 71 | 53.73 | 53.4085 | 1010.04 | 338174 | 1.0818 | 0.00125 | 361.12 |
| | D | 53.65 | 1009.46 | 1.0762 | 68 | 53.67 | 53.3177 | 1009.56 | 338244 | 1.0815 | 0.00123 | 361.04 |
| 20 | A | 53.73 | 1010.04 | 1.0766 | 131 | 53.73 | 53.4088 | 1010.18 | 339438 | 1.0866 | 0.00233 | 359.77 |
| | D | 53.68 | 1009.48 | 1.0761 | 121 | 53.67 | 53.3131 | 1009.37 | 339493 | 1.0854 | 0.00221 | 359.71 |
| 30 | A | 53.70 | 1010.57 | 1.0772 | 186 | 53.72 | 53.3869 | 1010.79 | 340679 | 1.0915 | 0.00333 | 358.46 |
| | D | 53.71 | 1009.87 | 1.0765 | 180 | 53.69 | 53.3442 | 1009.72 | 340713 | 1.0903 | 0.00329 | 358.43 |
| 40 | A | 53.73 | 1010.74 | 1.0773 | 237 | 53.72 | 53.3855 | 1010.46 | 341882 | 1.0955 | 0.00436 | 357.20 |
| | D | 53.75 | 1010.02 | 1.0765 | 237 | 53.74 | 53.4016 | 1009.87 | 341899 | 1.0946 | 0.00433 | 357.18 |
| 50 | A | 53.72 | 1010.66 | 1.0773 | 295 | 53.73 | 53.3734 | 1010.48 | 343076 | 1.0999 | 0.00540 | 355.96 |
| | D | 53.76 | 1010.11 | 1.0766 | 296 | 53.76 | 53.4346 | 1009.86 | 343080 | 1.0992 | 0.00543 | 355.95 |
| 60 | A | 53.72 | 1010.19 | 1.0768 | 358 | 53.75 | 53.4214 | 1010.29 | 344231 | 1.1042 | 0.00648 | 354.76 |
| | D | 53.76 | 1010.12 | 1.0766 | 355 | 53.76 | 53.4378 | 1010.11 | 344239 | 1.1038 | 0.00644 | 354.75 |
| 70 | A | 53.74 | 1009.93 | 1.0764 | 411 | 53.76 | 53.4340 | 1009.91 | 345386 | 1.1079 | 0.00748 | 353.58 |
| | D | 53.72 | 1010.10 | 1.0767 | 410 | 53.75 | 53.4235 | 1009.97 | 345395 | 1.1081 | 0.00750 | 353.57 |
| 80 | A | 53.76 | 1009.85 | 1.0763 | 464 | 53.77 | 53.4242 | 1009.66 | 346551 | 1.1118 | 0.00848 | 352.39 |
| | D | 53.75 | 1009.46 | 1.0759 | 469 | 53.73 | 53.3847 | 1009.59 | 346561 | 1.1119 | 0.00848 | 352.38 |
| 90 | A | 53.75 | 1009.34 | 1.0758 | 525 | 53.79 | 53.4551 | 1009.25 | 347679 | 1.1160 | 0.00959 | 351.24 |
| | D | 53.75 | 1009.28 | 1.0757 | 525 | 53.76 | 53.4159 | 1009.50 | 347685 | 1.1159 | 0.00949 | 351.24 |
| 95 | | 53.79 | 1009.19 | 1.0755 | 547 | 53.78 | 53.4551 | 1009.21 | 348167 | 1.1174 | 0.00992 | 350.75 |
| Data used for pathlength calibration (the first zero step): $T_{SoS}$ = 53.3584 °C, $P$ = 1009.79 mbar, $t_m^0$ = 336851 ns, $W^0$ = 362.53 m/s. | | | | | | | | | | | | |

## A6.5 Toluene/dry air

Table 83. Toluene/dry air results (5 °C isotherm)

| $x_T$/%SAT | | Zero Step | | | $\Delta m_{read}$/µg | Non-Zero Step | | | | | | |
|---|---|---|---|---|---|---|---|---|---|---|---|---|
| | | $T_{DVS}$/°C | $P$/mbar | $\rho^0$/(kg/m$^3$) | | $T_{DVS}$/°C | $T_{SoS}$/°C | $P$/mbar | $t_m$/ns | $\rho$/(kg/m$^3$) | $x$ | $W_m$/(m/s) |
| 10 | A | 5.31 | 1013.88 | 1.2691 | 45 | 5.33 | 5.1978 | 1013.73 | 366127 | 1.2726 | 0.0013 | 334.01 |
| | D | 5.24 | 1013.52 | 1.2690 | 50 | 5.27 | 5.1522 | 1013.69 | 366161 | 1.2729 | 0.0014 | 333.98 |
| 20 | A | 5.33 | 1013.56 | 1.2686 | 94 | 5.34 | 5.2099 | 1013.65 | 366820 | 1.2758 | 0.0026 | 333.38 |
| | D | 5.23 | 1012.99 | 1.2684 | 94 | 5.26 | 5.1493 | 1013.25 | 366855 | 1.2756 | 0.0025 | 333.35 |
| 30 | A | 5.31 | 1013.70 | 1.2689 | 136 | 5.32 | 5.1950 | 1013.66 | 367513 | 1.2793 | 0.0038 | 332.75 |
| | D | 5.24 | 1012.48 | 1.2677 | 138 | 5.26 | 5.1537 | 1012.70 | 367535 | 1.2783 | 0.0037 | 332.73 |
| 40 | A | 5.30 | 1013.71 | 1.2689 | 181 | 5.32 | 5.1978 | 1013.78 | 368187 | 1.2828 | 0.0050 | 332.15 |
| | D | 5.23 | 1011.97 | 1.2671 | 185 | 5.26 | 5.1525 | 1012.28 | 368207 | 1.2813 | 0.0050 | 332.13 |
| 50 | A | 5.29 | 1013.77 | 1.2691 | 225 | 5.32 | 5.1905 | 1013.91 | 368859 | 1.2863 | 0.0062 | 331.54 |
| | D | 5.23 | 1011.77 | 1.2668 | 223 | 5.24 | 5.1373 | 1011.81 | 368886 | 1.2839 | 0.0061 | 331.52 |
| 60 | A | 5.29 | 1013.92 | 1.2693 | 262 | 5.32 | 5.1897 | 1013.67 | 369522 | 1.2893 | 0.0074 | 330.95 |
| | D | 5.24 | 1011.76 | 1.2668 | 263 | 5.25 | 5.1381 | 1011.69 | 369546 | 1.2870 | 0.0073 | 330.92 |
| 70 | A | 5.28 | 1013.61 | 1.2689 | 307 | 5.29 | 5.1692 | 1013.53 | 370187 | 1.2924 | 0.0085 | 330.35 |
| | D | 5.22 | 1011.75 | 1.2668 | 305 | 5.24 | 5.1231 | 1011.67 | 370213 | 1.2902 | 0.0085 | 330.33 |
| 80 | A | 5.28 | 1013.43 | 1.2687 | 349 | 5.27 | 5.1534 | 1013.27 | 370858 | 1.2954 | 0.0097 | 329.75 |
| | D | 5.24 | 1011.87 | 1.2669 | 348 | 5.24 | 5.1250 | 1011.75 | 370877 | 1.2936 | 0.0097 | 329.74 |
| 90 | A | 5.25 | 1013.15 | 1.2685 | 385 | 5.27 | 5.1462 | 1012.79 | 371508 | 1.2980 | 0.0108 | 329.18 |
| | D | 5.25 | 1012.31 | 1.2674 | 387 | 5.26 | 5.1444 | 1012.03 | 371515 | 1.2971 | 0.0108 | 329.17 |
| 95 | | 5.25 | 1012.51 | 1.2677 | 406 | 5.26 | 5.1386 | 1012.46 | 371790 | 1.2988 | 0.0112 | 328.93 |
| Data used for pathlength calibration (the first zero step): $T_{SoS}$ = 5.1779 °C, $P$ = 1013.88 mbar, $t_m^0$ = 365407 ns, $W^0$ = 334.67 m/s. | | | | | | | | | | | | |

Table 84. Toluene/dry air results (15 °C isotherm)

| $x_T$/%SAT | | Zero Step | | | $\Delta m_{read}$/µg | Non-Zero Step | | | | | | |
|---|---|---|---|---|---|---|---|---|---|---|---|---|
| | | $T_{DVS}$/°C | $P$/mbar | $\rho^0$/(kg/m$^3$) | | $T_{DVS}$/°C | $T_{SoS}$/°C | $P$/mbar | $t_m$/ns | $\rho$/(kg/m$^3$) | $x$ | $W_m$/(m/s) |
| 10 | A | 15.05 | 1011.65 | 1.2234 | 86 | 15.03 | 14.8684 | 1011.99 | 361321 | 1.2300 | 0.0023 | 339.24 |
| | D | 14.96 | 1016.67 | 1.2299 | 84 | 14.98 | 14.7998 | 1016.81 | 361353 | 1.2363 | 0.0024 | 339.21 |
| 20 | A | 15.03 | 1012.10 | 1.2240 | 157 | 15.04 | 14.8712 | 1012.27 | 362522 | 1.2361 | 0.0044 | 338.12 |
| | D | 14.93 | 1016.80 | 1.2301 | 154 | 14.95 | 14.7709 | 1016.56 | 362595 | 1.2419 | 0.0045 | 338.05 |
| 30 | A | 15.03 | 1012.25 | 1.2242 | 236 | 15.06 | 14.8926 | 1012.53 | 363735 | 1.2423 | 0.0067 | 336.99 |
| | D | 14.92 | 1016.89 | 1.2303 | 234 | 14.93 | 14.7579 | 1016.85 | 363824 | 1.2482 | 0.0067 | 336.91 |
| 40 | A | 15.04 | 1012.89 | 1.2249 | 308 | 15.03 | 14.8673 | 1013.10 | 364899 | 1.2485 | 0.0087 | 335.91 |
| | D | 14.94 | 1016.76 | 1.2301 | 307 | 14.94 | 14.7694 | 1016.85 | 364972 | 1.2536 | 0.0087 | 335.85 |
| 50 | A | 15.01 | 1013.50 | 1.2258 | 387 | 15.01 | 14.8422 | 1014.00 | 366077 | 1.2554 | 0.0108 | 334.83 |
| | D | 14.96 | 1016.68 | 1.2299 | 382 | 14.95 | 14.7852 | 1016.69 | 366146 | 1.2591 | 0.0108 | 334.77 |
| 60 | A | 15.05 | 1014.66 | 1.2270 | 464 | 15.01 | 14.8545 | 1015.23 | 367239 | 1.2626 | 0.0129 | 333.77 |
| | D | 14.98 | 1016.88 | 1.2300 | 451 | 14.98 | 14.8077 | 1016.73 | 367281 | 1.2646 | 0.0129 | 333.73 |
| 70 | A | 15.04 | 1015.37 | 1.2280 | 530 | 15.05 | 14.8755 | 1015.35 | 368421 | 1.2686 | 0.0151 | 332.70 |
| | D | 14.93 | 1016.87 | 1.2302 | 524 | 14.95 | 14.7854 | 1016.78 | 368441 | 1.2703 | 0.0149 | 332.68 |
| 80 | A | 14.97 | 1015.22 | 1.2280 | 600 | 15.01 | 14.8406 | 1015.29 | 369576 | 1.2740 | 0.0171 | 331.66 |
| | D | 14.99 | 1016.61 | 1.2297 | 603 | 14.98 | 14.8043 | 1016.84 | 369584 | 1.2759 | 0.0170 | 331.65 |
| 90 | A | 15.00 | 1015.26 | 1.2280 | 675 | 15.00 | 14.8419 | 1015.40 | 370747 | 1.2797 | 0.0191 | 330.61 |
| | D | 14.98 | 1016.08 | 1.2290 | 674 | 14.97 | 14.7971 | 1016.34 | 370705 | 1.2807 | 0.0190 | 330.65 |
| 95 | | 14.98 | 1015.56 | 1.2284 | 705 | 14.96 | 14.8111 | 1015.75 | 371243 | 1.2825 | 0.0199 | 330.17 |
| Data used for pathlength calibration (the first zero step): $T_{SoS}$ = 14.8694 °C, $P$ = 1011.65 mbar, $t_m^0$ = 360022 ns, $W^0$ = 340.46 m/s. | | | | | | | | | | | | |

Table 85. Toluene/dry air results (25 °C isotherm)

| $x_T$/%SAT | | Zero Step | | | $\Delta m_{read}$/µg | Non-Zero Step | | | | | | |
|---|---|---|---|---|---|---|---|---|---|---|---|---|
| | | $T_{DVS}$/°C | $P$/mbar | $\rho^0$/(kg/m$^3$) | | $T_{DVS}$/°C | $T_{SoS}$/°C | $P$/mbar | $t_m$/ns | $\rho$/(kg/m$^3$) | $x$ | $W_m$/(m/s) |
| 5 | A | 24.51 | 998.07 | 1.1685 | 73 | 24.50 | 24.0932 | 998.14 | 355367 | 1.1741 | 0.0021 | 344.72 |
| | D | 24.36 | 1005.15 | 1.1774 | 67 | 24.35 | 23.9217 | 1004.86 | 355456 | 1.1825 | 0.0021 | 344.64 |
| 10 | A | 24.48 | 998.03 | 1.1686 | 137 | 24.48 | 24.0661 | 998.09 | 356461 | 1.1791 | 0.0041 | 343.66 |
| | D | 24.37 | 1006.07 | 1.1784 | 125 | 24.37 | 23.9361 | 1005.54 | 356502 | 1.1880 | 0.0039 | 343.63 |
| 15 | A | 24.47 | 998.34 | 1.1690 | 200 | 24.47 | 24.0594 | 998.48 | 357518 | 1.1843 | 0.0059 | 342.65 |
| | D | 24.38 | 1006.16 | 1.1785 | 193 | 24.38 | 23.9596 | 1005.96 | 357531 | 1.1933 | 0.0058 | 342.64 |
| 20 | A | 24.46 | 998.82 | 1.1696 | 264 | 24.47 | 24.0523 | 999.17 | 358539 | 1.1898 | 0.0077 | 341.67 |
| | D | 24.38 | 1006.76 | 1.1792 | 253 | 24.39 | 23.9622 | 1006.47 | 358555 | 1.1986 | 0.0077 | 341.66 |
| 25 | A | 24.46 | 999.45 | 1.1703 | 323 | 24.48 | 24.0594 | 999.59 | 359558 | 1.1951 | 0.0096 | 340.70 |
| | D | 24.38 | 1007.10 | 1.1796 | 316 | 24.40 | 23.9684 | 1006.93 | 359567 | 1.2038 | 0.0095 | 340.70 |
| 30 | A | 24.46 | 999.71 | 1.1706 | 383 | 24.46 | 24.0504 | 999.83 | 360575 | 1.2000 | 0.0114 | 339.74 |
| | D | 24.40 | 1007.16 | 1.1796 | 376 | 24.40 | 23.9707 | 1007.03 | 360559 | 1.2084 | 0.0112 | 339.76 |
| 35 | A | 24.45 | 999.91 | 1.1709 | 444 | 24.47 | 24.0528 | 1000.18 | 361560 | 1.2049 | 0.0131 | 338.82 |
| | D | 24.40 | 1006.98 | 1.1794 | 440 | 24.40 | 23.9676 | 1007.06 | 361541 | 1.2131 | 0.0130 | 338.84 |
| 40 | A | 24.45 | 1000.39 | 1.1715 | 500 | 24.46 | 24.0533 | 1000.36 | 362541 | 1.2098 | 0.0149 | 337.90 |
| | D | 24.41 | 1006.72 | 1.1790 | 501 | 24.41 | 23.9834 | 1006.93 | 362513 | 1.2174 | 0.0148 | 337.93 |
| 45 | A | 24.46 | 1000.43 | 1.1715 | 561 | 24.45 | 24.0472 | 1000.63 | 363476 | 1.2144 | 0.0166 | 337.03 |
| | D | 24.44 | 1006.03 | 1.1781 | 565 | 24.44 | 24.0077 | 1006.43 | 363480 | 1.2214 | 0.0166 | 337.03 |
| 50 | A | 24.45 | 1000.47 | 1.1716 | 619 | 24.45 | 24.0426 | 1000.44 | 364470 | 1.2190 | 0.0185 | 336.11 |
| | D | 24.42 | 1005.46 | 1.1775 | 620 | 24.44 | 24.0030 | 1005.78 | 364441 | 1.2250 | 0.0183 | 336.14 |
| 55 | A | 24.44 | 1000.35 | 1.1714 | 676 | 24.54 | 24.0977 | 1000.29 | 365450 | 1.2232 | 0.0203 | 335.21 |
| | D | 24.43 | 1004.86 | 1.1768 | 677 | 24.44 | 24.0040 | 1005.06 | 365380 | 1.2286 | 0.0200 | 335.28 |
| 60 | A | 24.46 | 1000.35 | 1.1714 | 737 | 24.45 | 24.0495 | 1000.66 | 366360 | 1.2278 | 0.0218 | 334.38 |
| | D | 24.44 | 1004.40 | 1.1762 | 734 | 24.46 | 24.0226 | 1004.55 | 366313 | 1.2324 | 0.0218 | 334.42 |

| | | | | | | | | | | | | |
|---|---|---|---|---|---|---|---|---|---|---|---|---|
| 65 | A | 24.45 | 1000.69 | 1.1718 | 795 | 24.45 | 24.0419 | 1000.82 | 367304 | 1.2327 | 0.0236 | 333.52 |
| | D | 24.43 | 1003.97 | 1.1757 | 794 | 24.44 | 24.0065 | 1004.26 | 367243 | 1.2366 | 0.0235 | 333.57 |
| 70 | A | 24.43 | 1001.08 | 1.1724 | 855 | 24.43 | 24.0250 | 1001.46 | 368239 | 1.2378 | 0.0253 | 332.67 |
| | D | 24.42 | 1003.68 | 1.1754 | 852 | 24.43 | 23.9991 | 1003.71 | 368185 | 1.2407 | 0.0253 | 332.72 |
| 75 | A | 24.42 | 1001.81 | 1.1733 | 908 | 24.41 | 24.0087 | 1001.98 | 369165 | 1.2428 | 0.0270 | 331.84 |
| | D | 24.41 | 1003.53 | 1.1753 | 906 | 24.42 | 23.9876 | 1003.60 | 369103 | 1.2447 | 0.0269 | 331.89 |
| 80 | A | 24.40 | 1002.29 | 1.1739 | 966 | 24.42 | 24.0093 | 1002.66 | 370063 | 1.2479 | 0.0286 | 331.03 |
| | D | 24.40 | 1003.47 | 1.1752 | 959 | 24.43 | 23.9971 | 1003.45 | 370007 | 1.2487 | 0.0285 | 331.08 |
| 85 | A | 24.39 | 1002.78 | 1.1745 | 1024 | 24.50 | 24.0540 | 1002.96 | 370992 | 1.2529 | 0.0305 | 330.20 |
| | D | 24.50 | 1003.62 | 1.1750 | 1020 | 24.44 | 24.0258 | 1003.45 | 370940 | 1.2532 | 0.0303 | 330.25 |
| 90 | A | 24.51 | 1003.17 | 1.1745 | 1084 | 24.54 | 24.1023 | 1003.28 | 371890 | 1.2575 | 0.0322 | 329.41 |
| | D | 24.51 | 1003.69 | 1.1751 | 1078 | 24.52 | 24.0842 | 1003.61 | 371866 | 1.2577 | 0.0321 | 329.43 |
| 95 | | 24.53 | 1003.40 | 1.1747 | 1138 | 24.53 | 24.1013 | 1003.56 | 372739 | 1.2619 | 0.0338 | 328.66 |
| Data used for pathlength calibration (the first zero step): $T_{SoS}$ = 24.1023 °C, $P$ = 998.07 mbar, $t_m^0$ = 354169 ns, $W^0$ = 345.89 m/s. | | | | | | | | | | | | |

Table 86. Toluene/dry air results (35 °C isotherm)

| $x_T$/%SAT | | Zero Step | | | $\Delta m_{read}$/µg | Non-Zero Step | | | | | | |
|---|---|---|---|---|---|---|---|---|---|---|---|---|
| | | $T_{DVS}$/°C | $P$/mbar | $\rho^0$/(kg/m$^3$) | | $T_{DVS}$/°C | $T_{SoS}$/°C | $P$/mbar | $t_m$/ns | $\rho$/(kg/m$^3$) | $x$ | $W_m$/(m/s) |
| 10 | A | 34.60 | 1006.86 | 1.1400 | 221 | 34.61 | 34.2215 | 1006.96 | 351294 | 1.1570 | 0.0068 | 347.97 |
| | D | 34.57 | 1014.95 | 1.1493 | 224 | 34.58 | 34.1874 | 1015.09 | 351380 | 1.1665 | 0.0068 | 347.89 |
| 20 | A | 34.54 | 1007.36 | 1.1408 | 422 | 34.50 | 34.1560 | 1007.52 | 354757 | 1.1732 | 0.0128 | 344.58 |
| | D | 34.59 | 1014.41 | 1.1486 | 428 | 34.59 | 34.2040 | 1014.65 | 354806 | 1.1814 | 0.0129 | 344.53 |
| 30 | A | 34.53 | 1007.65 | 1.1412 | 621 | 34.60 | 34.2278 | 1007.72 | 358084 | 1.1888 | 0.0191 | 341.38 |
| | D | 34.59 | 1014.08 | 1.1483 | 625 | 34.61 | 34.2105 | 1014.25 | 358093 | 1.1962 | 0.0190 | 341.37 |
| 40 | A | 34.51 | 1007.98 | 1.1417 | 811 | 34.51 | 34.1736 | 1008.23 | 361228 | 1.2038 | 0.0247 | 338.40 |
| | D | 34.58 | 1013.80 | 1.1480 | 812 | 34.58 | 34.1984 | 1013.87 | 361222 | 1.2102 | 0.0247 | 338.41 |
| 50 | A | 34.50 | 1008.87 | 1.1427 | 997 | 34.51 | 34.1644 | 1008.99 | 364307 | 1.2191 | 0.0304 | 335.54 |
| | D | 34.57 | 1013.42 | 1.1476 | 1001 | 34.59 | 34.1968 | 1013.54 | 364287 | 1.2243 | 0.0304 | 335.56 |
| 60 | A | 34.51 | 1009.24 | 1.1431 | 1185 | 34.52 | 34.1665 | 1009.50 | 367287 | 1.2339 | 0.0361 | 332.82 |
| | D | 34.56 | 1013.32 | 1.1475 | 1183 | 34.58 | 34.1973 | 1013.41 | 367254 | 1.2382 | 0.0360 | 332.85 |
| 70 | A | 34.49 | 1009.80 | 1.1438 | 1370 | 34.51 | 34.1595 | 1010.29 | 370183 | 1.2487 | 0.0416 | 330.22 |
| | D | 34.55 | 1013.10 | 1.1473 | 1368 | 34.56 | 34.1899 | 1013.22 | 370166 | 1.2521 | 0.0416 | 330.23 |
| 80 | A | 34.49 | 1010.75 | 1.1449 | 1550 | 34.51 | 34.1535 | 1011.04 | 373070 | 1.2636 | 0.0472 | 327.66 |
| | D | 34.53 | 1012.90 | 1.1472 | 1548 | 34.54 | 34.1722 | 1012.97 | 373045 | 1.2658 | 0.0471 | 327.68 |
| 90 | A | 34.51 | 1011.55 | 1.1457 | 1731 | 34.52 | 34.1596 | 1011.82 | 375880 | 1.2784 | 0.0527 | 325.21 |
| | D | 34.52 | 1012.56 | 1.1468 | 1723 | 34.49 | 34.1276 | 1012.70 | 375808 | 1.2788 | 0.0524 | 325.28 |
| 95 | | 34.53 | 1012.20 | 1.1464 | 1821 | 34.54 | 34.1766 | 1012.45 | 377246 | 1.2859 | 0.0554 | 324.04 |
| Data used for pathlength calibration (the first zero step): $T_{SoS}$ = 34.2130 °C, $P$ = 1006.86 mbar, $t_m^0$ = 347541 ns, $W^0$ = 351.73 m/s. | | | | | | | | | | | | |

Table 87. Toluene/dry air results (45 °C isotherm)

| $x_T$/%SAT | | Zero Step | | | $\Delta m_{read}$/µg | Non-Zero Step | | | | | | |
|---|---|---|---|---|---|---|---|---|---|---|---|---|
| | | $T_{DVS}$/°C | $P$/mbar | $\rho^0$/(kg/m$^3$) | | $T_{DVS}$/°C | $T_{SoS}$/°C | $P$/mbar | $t_m$/ns | $\rho$/(kg/m$^3$) | $x$ | $W_m$/(m/s) |
| 10 | A | 44.08 | 1016.98 | 1.1170 | 348 | 44.04 | 43.6775 | 1017.08 | 348193 | 1.1437 | 0.0108 | 350.94 |
| | D | 44.00 | 1018.94 | 1.1195 | 345 | 43.98 | 43.6288 | 1018.85 | 348236 | 1.1459 | 0.0108 | 350.90 |
| 20 | A | 44.04 | 1017.08 | 1.1173 | 660 | 43.99 | 43.6371 | 1017.25 | 353544 | 1.1678 | 0.0205 | 345.63 |
| | D | 44.04 | 1019.01 | 1.1194 | 655 | 43.97 | 43.6402 | 1018.98 | 353541 | 1.1696 | 0.0204 | 345.63 |
| 30 | A | 44.00 | 1017.29 | 1.1177 | 959 | 44.02 | 43.6516 | 1017.33 | 358594 | 1.1911 | 0.0300 | 340.76 |
| | D | 44.04 | 1018.68 | 1.1190 | 959 | 44.03 | 43.6669 | 1018.76 | 358583 | 1.1925 | 0.0299 | 340.77 |
| 40 | A | 44.01 | 1017.39 | 1.1177 | 1247 | 44.02 | 43.6624 | 1017.43 | 363346 | 1.2133 | 0.0390 | 336.30 |
| | D | 44.00 | 1018.56 | 1.1190 | 1243 | 44.01 | 43.6427 | 1018.54 | 363333 | 1.2143 | 0.0388 | 336.32 |
| 50 | A | 44.00 | 1017.56 | 1.1179 | 1532 | 44.00 | 43.6589 | 1017.73 | 367901 | 1.2353 | 0.0478 | 332.14 |
| | D | 44.02 | 1018.71 | 1.1191 | 1526 | 44.02 | 43.6606 | 1018.68 | 367896 | 1.2361 | 0.0477 | 332.15 |
| 60 | A | 44.00 | 1017.79 | 1.1182 | 1803 | 43.98 | 43.6101 | 1017.97 | 372237 | 1.2564 | 0.0562 | 328.27 |
| | D | 44.09 | 1018.97 | 1.1192 | 1806 | 44.07 | 43.6925 | 1018.94 | 372285 | 1.2576 | 0.0564 | 328.23 |
| 70 | A | 44.00 | 1018.17 | 1.1186 | 2081 | 43.98 | 43.6190 | 1018.46 | 376490 | 1.2781 | 0.0648 | 324.56 |
| | D | 44.08 | 1019.13 | 1.1194 | 2076 | 44.05 | 43.6813 | 1018.99 | 376516 | 1.2784 | 0.0648 | 324.54 |
| 80 | A | 43.98 | 1018.69 | 1.1193 | 2347 | 43.99 | 43.6248 | 1018.92 | 380659 | 1.2991 | 0.0731 | 321.01 |
| | D | 43.97 | 1019.22 | 1.1199 | 2347 | 44.10 | 43.6779 | 1019.16 | 380719 | 1.2997 | 0.0734 | 320.96 |
| 90 | A | 43.98 | 1019.12 | 1.1197 | 2610 | 43.98 | 43.6225 | 1019.28 | 384651 | 1.3197 | 0.0813 | 317.68 |
| | D | 44.04 | 1019.46 | 1.1199 | 2609 | 44.00 | 43.6702 | 1019.49 | 384664 | 1.3198 | 0.0813 | 317.67 |
| 95 | | 44.02 | 1019.48 | 1.1200 | 2745 | 44.04 | 43.6802 | 1019.46 | 386664 | 1.3303 | 0.0856 | 316.02 |
| Data used for pathlength calibration (the first zero step): $T_{SoS}$ = 43.6976 °C, $P$ = 1016.98 mbar, $t_m^0$ = 342162 ns, $W^0$ = 357.13 m/s. | | | | | | | | | | | | |

Table 88. Toluene/dry air results (55 °C isotherm)

| $x_T$/%SAT | | Zero Step | | | $\Delta m_{read}$/µg | Non-Zero Step | | | | | | |
|---|---|---|---|---|---|---|---|---|---|---|---|---|
| | | $T_{DVS}$/°C | $P$/mbar | $\rho^0$/(kg/m$^3$) | | $T_{DVS}$/°C | $T_{SoS}$/°C | $P$/mbar | $t_m$/ns | $\rho$/(kg/m$^3$) | $x$ | $W_m$/(m/s) |
| 10 | A | 53.72 | 991.59 | 1.0569 | 534 | 53.75 | 53.4300 | 991.40 | 346675 | 1.0979 | 0.0178 | 352.24 |
| | D | 53.77 | 993.01 | 1.0583 | 542 | 53.76 | 53.4530 | 993.12 | 346693 | 1.0998 | 0.0179 | 352.22 |
| 20 | A | 53.75 | 991.31 | 1.0565 | 1015 | 53.75 | 53.4347 | 991.39 | 355092 | 1.1343 | 0.0335 | 343.89 |
| | D | 53.79 | 992.83 | 1.0580 | 1020 | 53.79 | 53.4758 | 992.84 | 355094 | 1.1362 | 0.0337 | 343.89 |
| 30 | A | 53.82 | 991.43 | 1.0564 | 1475 | 53.80 | 53.4936 | 991.44 | 362857 | 1.1695 | 0.0488 | 336.53 |
| | D | 53.72 | 992.76 | 1.0582 | 1474 | 53.81 | 53.4845 | 992.79 | 362819 | 1.1711 | 0.0488 | 336.56 |
| 40 | A | 53.78 | 991.47 | 1.0566 | 1904 | 53.75 | 53.4584 | 991.52 | 370043 | 1.2025 | 0.0629 | 329.99 |
| | D | 53.72 | 992.60 | 1.0580 | 1893 | 53.71 | 53.3930 | 992.71 | 369840 | 1.2031 | 0.0625 | 330.18 |
| 50 | A | 53.77 | 991.67 | 1.0569 | 2323 | 53.77 | 53.4598 | 991.90 | 376779 | 1.2348 | 0.0767 | 324.09 |
| | D | 53.78 | 992.39 | 1.0576 | 2318 | 53.75 | 53.4574 | 992.51 | 376657 | 1.2353 | 0.0765 | 324.20 |
| 60 | A | 53.81 | 992.02 | 1.0571 | 2724 | 53.79 | 53.4931 | 991.99 | 383167 | 1.2659 | 0.0900 | 318.69 |
| | D | 53.80 | 992.25 | 1.0574 | 2720 | 53.80 | 53.4917 | 992.39 | 383085 | 1.2658 | 0.0898 | 318.76 |
| 70 | A | 53.81 | 992.07 | 1.0572 | 3117 | 53.79 | 53.4923 | 992.12 | 389248 | 1.2961 | 0.1029 | 313.71 |
| | D | 53.84 | 991.90 | 1.0569 | 3116 | 53.81 | 53.5166 | 992.10 | 389210 | 1.2957 | 0.1028 | 313.74 |
| 80 | A | 53.76 | 992.05 | 1.0573 | 3494 | 53.79 | 53.4823 | 992.11 | 395030 | 1.3251 | 0.1154 | 309.12 |
| | D | 53.80 | 991.67 | 1.0568 | 3499 | 53.85 | 53.5337 | 991.80 | 395079 | 1.3249 | 0.1156 | 309.08 |
| 90 | A | 53.78 | 992.05 | 1.0572 | 3864 | 53.77 | 53.4732 | 992.02 | 400600 | 1.3533 | 0.1275 | 304.82 |
| | D | 53.81 | 991.81 | 1.0569 | 3869 | 53.82 | 53.5131 | 991.75 | 400680 | 1.3534 | 0.1278 | 304.76 |
| 95 | | 53.79 | 991.95 | 1.0571 | 4047 | 53.80 | 53.5016 | 991.83 | 403285 | 1.3672 | 0.1337 | 302.79 |
| Data used for pathlength calibration (the first zero step): $T_{SoS}$ = 53.4168 °C, $P$ = 991.59 mbar, $t_m^0$ = 336801 ns, $W^0$ = 362.56 m/s. | | | | | | | | | | | | |

## A6.6 Cyclohexane/dry air

Table 89. Cyclohexane/dry air results (15 °C isotherm)

| $x_T$/%SAT | | Zero Step | | | $\Delta m_{read}$/µg | Non-Zero Step | | | | | | |
|---|---|---|---|---|---|---|---|---|---|---|---|---|
| | | $T_{DVS}$/°C | $P$/mbar | $\rho^0$/(kg/m$^3$) | | $T_{DVS}$/°C | $T_{SoS}$/°C | $P$/mbar | $t_m$/ns | $\rho$/(kg/m$^3$) | $x$ | $W_m$/(m/s) |
| 10 | A | 14.93 | 1008.46 | 1.2200 | 278 | 14.94 | 14.6482 | 1008.31 | 364983 | 1.2413 | 0.0092 | 335.88 |
| | D | 14.95 | 1009.79 | 1.2216 | 286 | 14.96 | 14.6774 | 1009.98 | 364923 | 1.2435 | 0.0093 | 335.93 |
| 20 | A | 14.96 | 1008.25 | 1.2197 | 526 | 14.97 | 14.6676 | 1008.01 | 369233 | 1.2600 | 0.0174 | 332.01 |
| | D | 14.93 | 1008.94 | 1.2206 | 531 | 14.92 | 14.6450 | 1009.16 | 369169 | 1.2613 | 0.0172 | 332.07 |
| 30 | A | 14.95 | 1007.85 | 1.2192 | 774 | 14.97 | 14.6749 | 1007.78 | 373249 | 1.2785 | 0.0254 | 328.44 |
| | D | 14.93 | 1007.95 | 1.2194 | 784 | 14.92 | 14.6383 | 1008.53 | 373221 | 1.2795 | 0.0253 | 328.46 |
| 40 | A | 14.96 | 1007.78 | 1.2191 | 1009 | 14.96 | 14.6703 | 1007.77 | 377053 | 1.2964 | 0.0331 | 325.12 |
| | D | 14.92 | 1006.67 | 1.2179 | 1014 | 14.90 | 14.6296 | 1007.06 | 377057 | 1.2957 | 0.0330 | 325.12 |
| 50 | A | 14.94 | 1007.70 | 1.2191 | 1243 | 14.94 | 14.6539 | 1007.63 | 380815 | 1.3144 | 0.0408 | 321.91 |
| | D | 14.90 | 1005.66 | 1.2168 | 1246 | 14.90 | 14.6291 | 1006.19 | 380791 | 1.3123 | 0.0406 | 321.93 |
| 60 | A | 14.93 | 1007.46 | 1.2188 | 1463 | 14.93 | 14.6434 | 1007.32 | 384355 | 1.3310 | 0.0480 | 318.95 |
| | D | 14.95 | 1005.17 | 1.2160 | 1466 | 14.93 | 14.6664 | 1005.07 | 384419 | 1.3283 | 0.0482 | 318.89 |
| 70 | A | 14.91 | 1007.14 | 1.2185 | 1684 | 14.92 | 14.6359 | 1006.87 | 387878 | 1.3476 | 0.0553 | 316.05 |
| | D | 14.94 | 1005.13 | 1.2160 | 1686 | 14.91 | 14.6356 | 1004.99 | 387913 | 1.3451 | 0.0554 | 316.02 |
| 80 | A | 14.91 | 1006.65 | 1.2179 | 1904 | 14.91 | 14.6292 | 1006.34 | 391289 | 1.3638 | 0.0626 | 313.30 |
| | D | 14.90 | 1005.45 | 1.2165 | 1905 | 14.90 | 14.6248 | 1005.43 | 391317 | 1.3625 | 0.0625 | 313.27 |
| 90 | A | 14.89 | 1006.13 | 1.2174 | 2123 | 14.90 | 14.6173 | 1005.93 | 394675 | 1.3801 | 0.0697 | 310.61 |
| | D | 14.90 | 1005.68 | 1.2168 | 2127 | 14.97 | 14.6715 | 1005.58 | 394771 | 1.3798 | 0.0700 | 310.53 |
| 95 | | 14.91 | 1005.78 | 1.2169 | 2238 | 14.98 | 14.6718 | 1005.73 | 396392 | 1.3883 | 0.0735 | 309.26 |
| Data used for pathlength calibration (the first zero step): $T_{SoS}$ = 14.6278 °C, $P$ = 1008.46 mbar, $t_m^0$ = 360217 ns, $W^0$ = 340.32 m/s. | | | | | | | | | | | | |

Table 90. Cyclohexane/dry air results (25 °C isotherm)

| $x_T$/%SAT | | Zero Step | | | $\Delta m_{read}$/µg | Non-Zero Step | | | | | | |
|---|---|---|---|---|---|---|---|---|---|---|---|---|
| | | $T_{DVS}$/°C | $P$/mbar | $\rho^0$/(kg/m$^3$) | | $T_{DVS}$/°C | $T_{SoS}$/°C | $P$/mbar | $t_m$/ns | $\rho$/(kg/m$^3$) | $x$ | $W_m$/(m/s) |
| 5 | A | 24.82 | 999.90 | 1.1694 | 243 | 24.83 | 24.5425 | 999.78 | 358305 | 1.1881 | 0.0084 | 341.93 |
| | D | 24.62 | 1009.98 | 1.1820 | 242 | 24.63 | 24.3503 | 1010.23 | 358245 | 1.2006 | 0.0081 | 341.99 |
| 10 | A | 24.81 | 999.40 | 1.1689 | 451 | 24.81 | 24.5247 | 999.27 | 361965 | 1.2035 | 0.0155 | 338.48 |
| | D | 24.56 | 1009.67 | 1.1819 | 448 | 24.55 | 24.2960 | 1009.94 | 361871 | 1.2162 | 0.0150 | 338.56 |
| 15 | A | 24.79 | 999.22 | 1.1687 | 663 | 24.79 | 24.5092 | 999.68 | 365461 | 1.2196 | 0.0224 | 335.24 |
| | D | 24.68 | 1009.17 | 1.1808 | 653 | 24.67 | 24.4078 | 1009.39 | 365322 | 1.2308 | 0.0220 | 335.37 |
| 20 | A | 24.76 | 1000.06 | 1.1698 | 854 | 24.76 | 24.4777 | 1000.29 | 368808 | 1.2353 | 0.0290 | 332.20 |
| | D | 24.68 | 1008.58 | 1.1801 | 848 | 24.70 | 24.4235 | 1008.80 | 368682 | 1.2451 | 0.0286 | 332.31 |
| 25 | A | 24.69 | 1000.42 | 1.1705 | 1044 | 24.65 | 24.3833 | 1000.74 | 372031 | 1.2505 | 0.0354 | 329.32 |
| | D | 24.68 | 1008.53 | 1.1801 | 1043 | 24.70 | 24.4197 | 1008.56 | 371921 | 1.2600 | 0.0353 | 329.41 |
| 30 | A | 24.62 | 1001.01 | 1.1715 | 1227 | 24.63 | 24.3480 | 1001.04 | 375161 | 1.2655 | 0.0418 | 326.57 |
| | D | 24.64 | 1008.29 | 1.1799 | 1232 | 24.68 | 24.3949 | 1008.45 | 375019 | 1.2744 | 0.0417 | 326.69 |
| 35 | A | 24.62 | 1000.95 | 1.1714 | 1410 | 24.61 | 24.3329 | 1001.02 | 378165 | 1.2795 | 0.0480 | 323.98 |
| | D | 24.58 | 1008.17 | 1.1801 | 1403 | 24.59 | 24.3217 | 1008.19 | 377951 | 1.2875 | 0.0475 | 324.16 |
| 40 | A | 24.60 | 1000.97 | 1.1715 | 1592 | 24.69 | 24.3735 | 1000.96 | 381143 | 1.2935 | 0.0545 | 321.44 |
| | D | 24.59 | 1007.91 | 1.1797 | 1587 | 24.60 | 24.3377 | 1007.99 | 380870 | 1.3013 | 0.0537 | 321.67 |
| 45 | A | 24.69 | 1001.14 | 1.1714 | 1775 | 24.71 | 24.4140 | 1001.23 | 384015 | 1.3074 | 0.0605 | 319.04 |
| | D | 24.61 | 1007.56 | 1.1792 | 1763 | 24.61 | 24.3520 | 1007.74 | 383688 | 1.3143 | 0.0596 | 319.31 |
| 50 | A | 24.70 | 1001.30 | 1.1715 | 1944 | 24.70 | 24.4133 | 1001.12 | 386790 | 1.3205 | 0.0664 | 316.75 |
| | D | 24.65 | 1007.03 | 1.1785 | 1951 | 24.69 | 24.4169 | 1007.38 | 386568 | 1.3280 | 0.0660 | 316.93 |
| 55 | A | 24.69 | 1001.28 | 1.1715 | 2120 | 24.69 | 24.4040 | 1001.50 | 389472 | 1.3340 | 0.0721 | 314.57 |
| | D | 24.62 | 1006.39 | 1.1778 | 2112 | 24.62 | 24.3579 | 1006.66 | 389183 | 1.3397 | 0.0714 | 314.80 |
| 60 | A | 24.67 | 1001.72 | 1.1721 | 2289 | 24.67 | 24.3824 | 1002.08 | 392064 | 1.3476 | 0.0778 | 312.49 |
| | D | 24.63 | 1005.86 | 1.1772 | 2284 | 24.64 | 24.3774 | 1006.15 | 391879 | 1.3522 | 0.0773 | 312.64 |

| | | | | | | | | | | | | |
|---|---|---|---|---|---|---|---|---|---|---|---|---|
| 65 | A | 24.65 | 1002.32 | 1.1729 | 2454 | 24.66 | 24.3697 | 1002.62 | 394622 | 1.3610 | 0.0834 | 310.47 |
| | D | 24.65 | 1005.34 | 1.1764 | 2450 | 24.66 | 24.3949 | 1005.57 | 394423 | 1.3642 | 0.0830 | 310.62 |
| 70 | A | 24.65 | 1002.98 | 1.1737 | 2623 | 24.65 | 24.3665 | 1003.42 | 397161 | 1.3747 | 0.0889 | 308.48 |
| | D | 24.66 | 1004.95 | 1.1760 | 2613 | 24.66 | 24.4031 | 1005.13 | 397015 | 1.3762 | 0.0886 | 308.59 |
| 75 | A | 24.65 | 1003.62 | 1.1744 | 2787 | 24.66 | 24.3724 | 1004.03 | 399639 | 1.3880 | 0.0945 | 306.57 |
| | D | 24.66 | 1004.83 | 1.1758 | 2774 | 24.67 | 24.4068 | 1004.82 | 399523 | 1.3884 | 0.0942 | 306.66 |
| 80 | A | 24.66 | 1004.24 | 1.1751 | 2943 | 24.70 | 24.4047 | 1004.38 | 402066 | 1.4006 | 0.0999 | 304.72 |
| | D | 24.75 | 1004.95 | 1.1756 | 2935 | 24.67 | 24.4400 | 1004.72 | 401945 | 1.4005 | 0.0996 | 304.81 |
| 85 | A | 24.69 | 1004.68 | 1.1755 | 3107 | 24.71 | 24.4262 | 1004.86 | 404471 | 1.4136 | 0.1054 | 302.91 |
| | D | 24.73 | 1005.18 | 1.1760 | 3105 | 24.76 | 24.4827 | 1004.97 | 404502 | 1.4139 | 0.1055 | 302.88 |
| 90 | A | 24.70 | 1004.92 | 1.1758 | 3266 | 24.71 | 24.4355 | 1004.95 | 406840 | 1.4261 | 0.1108 | 301.14 |
| | D | 24.73 | 1005.13 | 1.1759 | 3269 | 24.74 | 24.4683 | 1005.38 | 406840 | 1.4264 | 0.1108 | 301.14 |
| 95 | | 24.71 | 1004.96 | 1.1758 | 3422 | 24.73 | 24.4514 | 1004.97 | 409123 | 1.4380 | 0.1161 | 299.46 |
| Data used for pathlength calibration (the first zero step): $T_{SOS}$ = 24.5292 °C, $P$ = 999.90 mbar, $t_m^0$ = 353953 ns, $W^0$ = 346.14 m/s. | | | | | | | | | | | | |

Table 91. Cyclohexane/dry air results (35 °C isotherm)

| $x_T$/%SAT | | Zero Step | | | $\Delta m_{read}$/µg | Non-Zero Step | | | | | | |
|---|---|---|---|---|---|---|---|---|---|---|---|---|
| | | $T_{DVS}$/°C | $P$/mbar | $\rho^0$/(kg/m$^3$) | | $T_{DVS}$/°C | $T_{SoS}$/°C | $P$/mbar | $t_m$/ns | $\rho$/(kg/m$^3$) | $x$ | $W_m$/(m/s) |
| 10 | A | 34.62 | 999.25 | 1.1314 | 727 | 34.65 | 34.2383 | 999.34 | 360742 | 1.1870 | 0.0257 | 338.96 |
| | D | 34.64 | 998.22 | 1.1301 | 735 | 34.67 | 34.2767 | 998.18 | 360998 | 1.1864 | 0.0261 | 338.72 |
| 20 | A | 34.64 | 999.27 | 1.1313 | 1350 | 34.55 | 34.1884 | 999.45 | 371435 | 1.2348 | 0.0475 | 329.20 |
| | D | 34.66 | 998.18 | 1.1300 | 1359 | 34.65 | 34.2715 | 998.23 | 371690 | 1.2342 | 0.0481 | 328.98 |
| 30 | A | 34.50 | 999.29 | 1.1318 | 1919 | 34.54 | 34.1344 | 999.08 | 381041 | 1.2789 | 0.0680 | 320.90 |
| | D | 34.68 | 997.94 | 1.1297 | 1944 | 34.68 | 34.2924 | 998.00 | 381340 | 1.2786 | 0.0687 | 320.65 |
| 40 | A | 34.60 | 999.11 | 1.1313 | 2477 | 34.55 | 34.1842 | 999.00 | 389832 | 1.3211 | 0.0874 | 313.67 |
| | D | 34.64 | 998.11 | 1.1300 | 2477 | 34.64 | 34.2486 | 997.96 | 389984 | 1.3198 | 0.0876 | 313.54 |
| 50 | A | 34.53 | 999.07 | 1.1315 | 2990 | 34.54 | 34.1525 | 998.86 | 397893 | 1.3606 | 0.1056 | 307.31 |
| | D | 34.67 | 998.44 | 1.1303 | 3001 | 34.68 | 34.2825 | 998.18 | 398115 | 1.3602 | 0.1062 | 307.14 |
| 60 | A | 34.54 | 998.82 | 1.1312 | 3481 | 34.53 | 34.1469 | 998.72 | 405342 | 1.3979 | 0.1228 | 301.67 |
| | D | 34.66 | 998.79 | 1.1307 | 3491 | 34.67 | 34.2811 | 998.38 | 405575 | 1.3982 | 0.1235 | 301.49 |
| 70 | A | 34.52 | 998.92 | 1.1313 | 3949 | 34.50 | 34.1151 | 999.18 | 412213 | 1.4340 | 0.1390 | 296.64 |
| | D | 34.69 | 999.03 | 1.1308 | 3981 | 34.65 | 34.2784 | 999.78 | 412473 | 1.4359 | 0.1398 | 296.45 |
| 80 | A | 34.50 | 999.04 | 1.1316 | 4413 | 34.54 | 34.1459 | 999.24 | 418956 | 1.4697 | 0.1554 | 291.86 |
| | D | 34.57 | 999.18 | 1.1315 | 4401 | 34.59 | 34.1821 | 999.42 | 418837 | 1.4687 | 0.1549 | 291.95 |
| 90 | A | 34.58 | 999.56 | 1.1318 | 4864 | 34.60 | 34.2139 | 999.75 | 425315 | 1.5046 | 0.1711 | 287.50 |
| | D | 34.59 | 999.63 | 1.1319 | 4838 | 34.55 | 34.1637 | 999.41 | 425095 | 1.5026 | 0.1703 | 287.65 |
| 95 | | 34.58 | 999.80 | 1.1321 | 5070 | 34.61 | 34.2196 | 999.85 | 428238 | 1.5206 | 0.1784 | 285.54 |
| Data used for pathlength calibration (the first zero step): $T_{SoS}$ = 34.2241 °C, $P$ = 999.25 mbar, $t_m^0$ = 347639 ns, $W^0$ = 351.74 m/s. | | | | | | | | | | | | |

Table 92. Cyclohexane/dry air results (45 °C isotherm)

| $x_T$/%SAT | | Zero Step | | | $\Delta m_{read}$/µg | Non-Zero Step | | | | | | |
|---|---|---|---|---|---|---|---|---|---|---|---|---|
| | | $T_{DVS}$/°C | $P$/mbar | $\rho^0$/(kg/m$^3$) | | $T_{DVS}$/°C | $T_{SoS}$/°C | $P$/mbar | $t_m$/ns | $\rho$/(kg/m$^3$) | $x$ | $W_m$/(m/s) |
| 10 | A | 44.02 | 1013.69 | 1.1136 | 1137 | 44.04 | 43.6981 | 1013.81 | 362805 | 1.2008 | 0.0408 | 336.91 |
| | D | 44.01 | 1018.01 | 1.1184 | 1129 | 44.04 | 43.6875 | 1017.89 | 362734 | 1.2049 | 0.0405 | 336.98 |
| 20 | A | 44.03 | 1014.19 | 1.1141 | 2090 | 44.04 | 43.7043 | 1014.42 | 378712 | 1.2743 | 0.0749 | 322.76 |
| | D | 44.03 | 1017.96 | 1.1183 | 2073 | 43.98 | 43.6504 | 1018.02 | 378346 | 1.2771 | 0.0740 | 323.07 |
| 30 | A | 44.01 | 1014.63 | 1.1147 | 2945 | 44.00 | 43.6783 | 1014.76 | 392264 | 1.3404 | 0.1054 | 311.61 |
| | D | 43.93 | 1017.84 | 1.1185 | 2918 | 44.00 | 43.6285 | 1017.90 | 391851 | 1.3421 | 0.1043 | 311.94 |
| 40 | A | 44.02 | 1015.19 | 1.1153 | 3740 | 44.05 | 43.7141 | 1015.52 | 404192 | 1.4019 | 0.1337 | 302.41 |
| | D | 43.93 | 1017.97 | 1.1186 | 3698 | 43.99 | 43.6404 | 1017.87 | 403666 | 1.4020 | 0.1321 | 302.81 |
| 50 | A | 44.06 | 1015.93 | 1.1159 | 4459 | 43.99 | 43.6832 | 1016.03 | 414711 | 1.4576 | 0.1591 | 294.74 |
| | D | 43.96 | 1017.71 | 1.1182 | 4419 | 43.96 | 43.6297 | 1017.75 | 414137 | 1.4569 | 0.1576 | 295.15 |
| 60 | A | 43.98 | 1016.10 | 1.1164 | 5124 | 43.98 | 43.6621 | 1016.09 | 424200 | 1.5091 | 0.1829 | 288.15 |
| | D | 43.96 | 1017.14 | 1.1176 | 5103 | 44.03 | 43.6678 | 1017.36 | 423789 | 1.5086 | 0.1819 | 288.43 |
| 70 | A | 43.96 | 1016.07 | 1.1164 | 5753 | 44.06 | 43.6842 | 1016.05 | 432888 | 1.5573 | 0.2054 | 282.37 |
| | D | 43.97 | 1016.66 | 1.1171 | 5722 | 43.96 | 43.6287 | 1016.96 | 432336 | 1.5555 | 0.2037 | 282.73 |
| 80 | A | 44.11 | 1016.02 | 1.1159 | 6364 | 44.05 | 43.7315 | 1015.92 | 441063 | 1.6036 | 0.2268 | 277.13 |
| | D | 44.03 | 1016.32 | 1.1165 | 6322 | 43.99 | 43.6618 | 1016.48 | 440500 | 1.6010 | 0.2251 | 277.49 |
| 90 | A | 44.01 | 1015.77 | 1.1159 | 6918 | 44.02 | 43.6979 | 1015.74 | 448437 | 1.6460 | 0.2465 | 272.57 |
| | D | 44.00 | 1016.15 | 1.1164 | 6900 | 44.01 | 43.6858 | 1016.19 | 448156 | 1.6451 | 0.2457 | 272.75 |
| 95 | | 44.07 | 1015.86 | 1.1158 | 7196 | 44.08 | 43.7455 | 1015.93 | 451985 | 1.6672 | 0.2562 | 270.43 |
| Data used for pathlength calibration (the first zero step): $T_{SoS}$ = 43.6628 °C, $P$ = 1013.69 mbar, $t_m^0$ = 342286 ns, $W^0$ = 357.11 m/s. | | | | | | | | | | | | |

Table 93. Cyclohexane/dry air results (55 °C isotherm)

| $x_T$/%SAT | | Zero Step | | | $\Delta m_{read}$/µg | Non-Zero Step | | | | | | |
|---|---|---|---|---|---|---|---|---|---|---|---|---|
| | | $T_{DVS}$/°C | $P$/mbar | $\rho^0$/(kg/m$^3$) | | $T_{DVS}$/°C | $T_{SoS}$/°C | $P$/mbar | $t_m$/ns | $\rho$/(kg/m$^3$) | $x$ | $W_m$/(m/s) |
| 10 | A | 53.70 | 1005.38 | 1.0717 | 1871 | 53.70 | 53.4040 | 1005.51 | 370779 | 1.2151 | 0.0698 | 329.32 |
| | D | 53.74 | 1015.04 | 1.0819 | 1857 | 53.74 | 53.4467 | 1015.40 | 370142 | 1.2241 | 0.0684 | 329.89 |
| 20 | A | 53.66 | 1005.83 | 1.0723 | 3329 | 53.67 | 53.3626 | 1006.27 | 394275 | 1.3275 | 0.1238 | 309.70 |
| | D | 53.72 | 1014.60 | 1.0815 | 3281 | 53.73 | 53.4296 | 1014.86 | 393117 | 1.3329 | 0.1211 | 310.61 |
| 30 | A | 53.69 | 1006.63 | 1.0731 | 4583 | 53.71 | 53.4006 | 1007.09 | 413018 | 1.4243 | 0.1701 | 295.64 |
| | D | 53.71 | 1013.73 | 1.0806 | 4511 | 53.72 | 53.4321 | 1014.15 | 411489 | 1.4262 | 0.1663 | 296.74 |
| 40 | A | 53.74 | 1007.41 | 1.0737 | 5685 | 53.74 | 53.4474 | 1007.73 | 428591 | 1.5094 | 0.2107 | 284.90 |
| | D | 53.71 | 1012.99 | 1.0798 | 5540 | 53.65 | 53.3682 | 1013.23 | 426260 | 1.5043 | 0.2041 | 286.46 |
| 50 | A | 53.74 | 1008.02 | 1.0744 | 6629 | 53.73 | 53.4344 | 1008.19 | 441501 | 1.5824 | 0.2454 | 276.57 |
| | D | 53.73 | 1012.28 | 1.0790 | 6505 | 53.71 | 53.4156 | 1012.74 | 439430 | 1.5774 | 0.2395 | 277.87 |
| 60 | A | 53.74 | 1008.44 | 1.0748 | 7487 | 53.74 | 53.4503 | 1009.00 | 452634 | 1.6486 | 0.2764 | 269.77 |
| | D | 53.74 | 1011.92 | 1.0785 | 7359 | 53.75 | 53.4575 | 1012.13 | 450792 | 1.6425 | 0.2711 | 270.87 |
| 70 | A | 53.75 | 1009.26 | 1.0757 | 8259 | 53.76 | 53.4569 | 1010.10 | 462394 | 1.7086 | 0.3042 | 264.07 |
| | D | 53.69 | 1011.43 | 1.0782 | 8133 | 53.76 | 53.4653 | 1011.70 | 460765 | 1.7015 | 0.2995 | 265.01 |
| 80 | A | 53.74 | 1010.04 | 1.0765 | 8921 | 53.70 | 53.4077 | 1010.12 | 470890 | 1.7601 | 0.3285 | 259.31 |
| | D | 53.74 | 1011.00 | 1.0776 | 8850 | 53.73 | 53.4336 | 1011.28 | 469860 | 1.7558 | 0.3255 | 259.88 |
| 90 | A | 53.75 | 1010.34 | 1.0768 | 9594 | 53.77 | 53.4767 | 1010.50 | 479046 | 1.8120 | 0.3529 | 254.89 |
| | D | 53.74 | 1010.91 | 1.0775 | 9519 | 53.74 | 53.4519 | 1010.95 | 478164 | 1.8069 | 0.3500 | 255.36 |
| 95 | | 53.75 | 1010.71 | 1.0772 | 9839 | 53.71 | 53.4271 | 1010.88 | 482040 | 1.8312 | 0.3614 | 253.31 |
| Data used for pathlength calibration (the first zero step): $T_{SoS}$ = 53.4052 °C, $P$ = 1005.38 mbar, $t_m^0$ = 336786 ns, $W^0$ = 362.56 m/s. | | | | | | | | | | | | |

## A6.7 Water/dry air

Table 94. Water/dry air results (25 °C isotherm)

| $x_T$/%SAT | | Zero Step | | | $\Delta m_{read}$/µg | Non-Zero Step | | | | | | |
|---|---|---|---|---|---|---|---|---|---|---|---|---|
| | | $T_{DVS}$/°C | $P$/mbar | $\rho^0$/(kg/m$^3$) | | $T_{DVS}$/°C | $T_{SoS}$/°C | $P$/mbar | $t_m$/ns | $\rho$/(kg/m$^3$) | $x$ | $W_m$/(m/s) |
| 10 | A | 24.58 | 1006.88 | 1.1785 | 15 | 24.60 | 24.3216 | 1006.96 | 353199 | 1.1774 | 0.0027 | 346.19 |
| | D | 24.66 | 1006.85 | 1.1782 | 18 | 24.67 | 24.3327 | 1006.74 | 353193 | 1.1768 | 0.0028 | 346.20 |
| 20 | A | 24.59 | 1007.08 | 1.1787 | 34 | 24.58 | 24.3115 | 1007.14 | 353037 | 1.1762 | 0.0061 | 346.35 |
| | D | 24.65 | 1007.01 | 1.1784 | 38 | 24.66 | 24.3251 | 1006.87 | 353031 | 1.1755 | 0.0061 | 346.36 |
| 30 | A | 24.57 | 1007.24 | 1.1790 | 51 | 24.68 | 24.3762 | 1007.44 | 352835 | 1.1751 | 0.0084 | 346.55 |
| | D | 24.67 | 1007.01 | 1.1784 | 50 | 24.65 | 24.3285 | 1007.04 | 352869 | 1.1745 | 0.0089 | 346.51 |
| 40 | A | 24.70 | 1007.53 | 1.1788 | 68 | 24.73 | 24.4283 | 1007.58 | 352646 | 1.1736 | 0.0118 | 346.73 |
| | D | 24.64 | 1006.94 | 1.1784 | 68 | 24.66 | 24.3304 | 1007.08 | 352704 | 1.1732 | 0.0120 | 346.68 |
| 50 | A | 24.72 | 1007.48 | 1.1787 | 85 | 24.69 | 24.4209 | 1007.48 | 352491 | 1.1722 | 0.0151 | 346.89 |
| | D | 24.65 | 1006.88 | 1.1782 | 85 | 24.66 | 24.3401 | 1006.91 | 352544 | 1.1717 | 0.0149 | 346.83 |
| 60 | A | 24.71 | 1007.44 | 1.1787 | 102 | 24.72 | 24.4272 | 1007.50 | 352339 | 1.1709 | 0.0178 | 347.04 |
| | D | 24.65 | 1006.83 | 1.1782 | 101 | 24.65 | 24.3402 | 1006.87 | 352391 | 1.1705 | 0.0177 | 346.98 |
| 70 | A | 24.72 | 1007.54 | 1.1788 | 118 | 24.75 | 24.4465 | 1007.62 | 352175 | 1.1697 | 0.0205 | 347.20 |
| | D | 24.66 | 1006.86 | 1.1782 | 118 | 24.67 | 24.3487 | 1006.85 | 352236 | 1.1692 | 0.0205 | 347.14 |
| 80 | A | 24.65 | 1007.64 | 1.1791 | 138 | 24.64 | 24.3557 | 1007.56 | 352086 | 1.1686 | 0.0239 | 347.29 |
| | D | 24.65 | 1007.00 | 1.1784 | 136 | 24.68 | 24.3571 | 1006.90 | 352083 | 1.1680 | 0.0232 | 347.29 |
| 90 | A | 24.63 | 1007.45 | 1.1790 | 152 | 24.64 | 24.3393 | 1007.31 | 351950 | 1.1674 | 0.0260 | 347.42 |
| | D | 24.66 | 1007.09 | 1.1784 | 148 | 24.67 | 24.3625 | 1007.10 | 351923 | 1.1671 | 0.0258 | 347.45 |
| 95 | | 24.62 | 1007.20 | 1.1788 | 158 | 24.70 | 24.3579 | 1007.19 | 351861 | 1.1667 | 0.0268 | 347.51 |
| Data used for pathlength calibration (the first zero step): $T_{SoS}$ = 24.3078 °C, $P$ = 1006.88 mbar, $t_m^0$ = 353385 ns, $W^0$ = 346.01 m/s. | | | | | | | | | | | | |

Table 95. Water/dry air results (35 °C isotherm)

| $x_T$/%SAT | | Zero Step | | | $\Delta m_{read}$/µg | Non-Zero Step | | | | | | |
|---|---|---|---|---|---|---|---|---|---|---|---|---|
| | | $T_{DVS}$/°C | $P$/mbar | $\rho^0$/(kg/m³) | | $T_{DVS}$/°C | $T_{SoS}$/°C | $P$/mbar | $t_m$/ns | $\rho$/(kg/m³) | $x$ | $W_m$/(m/s) |
| 10 | A | 34.52 | 995.78 | 1.1278 | 38 | 34.55 | 34.1558 | 995.45 | 347748 | 1.1249 | 0.0058 | 352.05 |
| | D | 34.49 | 982.36 | 1.1127 | 17 | 34.50 | 34.1080 | 983.41 | 347784 | 1.1114 | 0.0059 | 352.01 |
| 20 | A | 34.54 | 995.28 | 1.1271 | 63 | 34.54 | 34.1602 | 995.37 | 347427 | 1.1224 | 0.0116 | 352.37 |
| | D | 34.46 | 979.17 | 1.1092 | 35 | 34.49 | 34.0999 | 981.04 | 347498 | 1.1065 | 0.0113 | 352.30 |
| 30 | A | 34.53 | 995.24 | 1.1271 | 85 | 34.53 | 34.1511 | 995.57 | 347177 | 1.1206 | 0.0163 | 352.63 |
| | D | 34.38 | 973.58 | 1.1031 | 39 | 34.44 | 34.0414 | 976.90 | 347253 | 1.1001 | 0.0159 | 352.55 |
| 40 | A | 34.51 | 995.33 | 1.1273 | 127 | 34.55 | 34.1502 | 995.09 | 346941 | 1.1176 | 0.0221 | 352.87 |
| | D | 34.35 | 971.27 | 1.1006 | 112 | 34.37 | 33.9746 | 971.78 | 347020 | 1.0920 | 0.0222 | 352.79 |
| 50 | A | 34.45 | 994.77 | 1.1269 | 152 | 34.44 | 34.0698 | 994.54 | 346711 | 1.1153 | 0.0271 | 353.10 |
| | D | 34.35 | 970.75 | 1.1001 | 145 | 34.37 | 33.9697 | 970.94 | 346756 | 1.0889 | 0.0274 | 353.06 |
| 60 | A | 34.43 | 994.03 | 1.1261 | 185 | 34.43 | 34.0483 | 993.37 | 346494 | 1.1120 | 0.0320 | 353.32 |
| | D | 34.37 | 973.92 | 1.1036 | 207 | 34.37 | 33.9730 | 971.77 | 346481 | 1.0877 | 0.0326 | 353.34 |
| 70 | A | 34.41 | 992.51 | 1.1245 | 219 | 34.40 | 34.0191 | 991.61 | 346214 | 1.1077 | 0.0377 | 353.61 |
| | D | 34.38 | 977.45 | 1.1075 | 227 | 34.38 | 33.9868 | 975.80 | 346215 | 1.0901 | 0.0377 | 353.61 |
| 80 | A | 34.40 | 990.38 | 1.1221 | 247 | 34.41 | 34.0220 | 989.23 | 345955 | 1.1032 | 0.0421 | 353.87 |
| | D | 34.41 | 979.56 | 1.1098 | 245 | 34.42 | 34.0248 | 978.52 | 345939 | 1.0910 | 0.0424 | 353.89 |
| 90 | A | 34.40 | 987.94 | 1.1193 | 278 | 34.41 | 34.0270 | 986.60 | 345692 | 1.0980 | 0.0473 | 354.14 |
| | D | 34.40 | 982.44 | 1.1131 | 280 | 34.41 | 34.0149 | 980.87 | 345680 | 1.0916 | 0.0474 | 354.15 |
| 95 | | 34.40 | 985.40 | 1.1165 | 301 | 34.42 | 34.0305 | 983.55 | 345554 | 1.0934 | 0.0503 | 354.28 |
| Data used for pathlength calibration (the first zero step): $T_{SoS}$ = 34.1293 °C, $P$ = 995.78 mbar, $t_m^0$ = 348110 ns, $W^0$ = 351.68 m/s. | | | | | | | | | | | | |

Table 96. Water/dry air results (45 °C isotherm)

| $x_T$/%SAT | | Zero Step | | | $\Delta m_{read}$/µg | Non-Zero Step | | | | | | |
|---|---|---|---|---|---|---|---|---|---|---|---|---|
| | | $T_{DVS}$/°C | $P$/mbar | $\rho^0$/(kg/m³) | | $T_{DVS}$/°C | $T_{SoS}$/°C | $P$/mbar | $t_m$/ns | $\rho$/(kg/m³) | $x$ | $W_m$/(m/s) |
| 10 | A | 44.03 | 1018.73 | 1.1191 | 55 | 44.06 | 43.7189 | 1018.76 | 341358 | 1.1149 | 0.0099 | 357.67 |
| | D | 44.03 | 1020.77 | 1.1214 | 53 | 44.04 | 43.7079 | 1020.68 | 341383 | 1.1173 | 0.0095 | 357.65 |
| 20 | A | 44.05 | 1018.89 | 1.1192 | 105 | 44.03 | 43.7210 | 1018.88 | 340885 | 1.1112 | 0.0193 | 358.17 |
| | D | 43.99 | 1020.88 | 1.1216 | 105 | 44.05 | 43.6949 | 1020.83 | 340928 | 1.1136 | 0.0186 | 358.12 |
| 30 | A | 44.01 | 1019.05 | 1.1195 | 149 | 43.95 | 43.6742 | 1019.24 | 340480 | 1.1081 | 0.0282 | 358.59 |
| | D | 43.90 | 1020.80 | 1.1218 | 157 | 43.94 | 43.5793 | 1020.78 | 340558 | 1.1098 | 0.0284 | 358.51 |
| 40 | A | 43.97 | 1019.36 | 1.1200 | 198 | 43.98 | 43.6770 | 1019.53 | 340043 | 1.1048 | 0.0366 | 359.06 |
| | D | 43.89 | 1020.60 | 1.1217 | 200 | 43.92 | 43.6046 | 1020.71 | 340107 | 1.1063 | 0.0367 | 358.99 |
| 50 | A | 43.92 | 1019.71 | 1.1206 | 241 | 43.91 | 43.6039 | 1019.76 | 339616 | 1.1021 | 0.0444 | 359.51 |
| | D | 43.96 | 1020.29 | 1.1211 | 243 | 43.92 | 43.6223 | 1020.43 | 339667 | 1.1025 | 0.0452 | 359.45 |
| 60 | A | 43.97 | 1020.01 | 1.1207 | 272 | 43.98 | 43.6587 | 1020.23 | 339175 | 1.0999 | 0.0503 | 359.97 |
| | D | 43.97 | 1020.10 | 1.1208 | 280 | 43.98 | 43.6662 | 1020.23 | 339206 | 1.0993 | 0.0516 | 359.94 |
| 70 | A | 43.94 | 1020.32 | 1.1212 | 316 | 43.94 | 43.6396 | 1020.45 | 338785 | 1.0970 | 0.0582 | 360.39 |
| | D | 43.97 | 1019.82 | 1.1205 | 324 | 43.98 | 43.6626 | 1019.94 | 338775 | 1.0957 | 0.0595 | 360.40 |
| 80 | A | 43.93 | 1020.68 | 1.1216 | 364 | 44.00 | 43.6654 | 1020.53 | 338364 | 1.0938 | 0.0655 | 360.84 |
| | D | 43.98 | 1019.73 | 1.1204 | 368 | 43.98 | 43.6640 | 1019.60 | 338367 | 1.0922 | 0.0671 | 360.83 |
| 90 | A | 43.97 | 1020.37 | 1.1211 | 400 | 43.99 | 43.6792 | 1020.44 | 337946 | 1.0905 | 0.0731 | 361.28 |
| | D | 43.92 | 1020.12 | 1.1210 | 408 | 44.00 | 43.6522 | 1019.93 | 337973 | 1.0897 | 0.0736 | 361.25 |
| 95 | | 43.96 | 1020.32 | 1.1211 | 422 | 44.00 | 43.6710 | 1020.24 | 337759 | 1.0888 | 0.0768 | 361.48 |
| Data used for pathlength calibration (the first zero step): $T_{SoS}$ = 43.7093 °C, $P$ = 1018.73 mbar, $t_m^0$ = 341874 ns, $W^0$ = 357.13 m/s. | | | | | | | | | | | | |

Table 97. Water/dry air results (55 °C isotherm)

| $x_T$/%SAT | | Zero Step | | | $\Delta m_{read}$/µg | Non-Zero Step | | | | | | |
|---|---|---|---|---|---|---|---|---|---|---|---|---|
| | | $T_{DVS}$/°C | $P$/mbar | $\rho^0$/(kg/m³) | | $T_{DVS}$/°C | $T_{SoS}$/°C | $P$/mbar | $t_m$/ns | $\rho$/(kg/m³) | $x$ | $W_m$/(m/s) |
| 10 | A | 53.70 | 1002.86 | 1.0690 | 132 | 53.71 | 53.3876 | 1002.32 | 335738 | 1.0589 | 0.0239 | 363.52 |
| | D | 53.65 | 999.25 | 1.0653 | 94 | 53.69 | 53.3703 | 999.05 | 335790 | 1.0581 | 0.0172 | 363.47 |
| 20 | A | 53.69 | 1002.08 | 1.0682 | 193 | 53.69 | 53.3738 | 1001.79 | 334957 | 1.0534 | 0.0363 | 364.37 |
| | D | 53.69 | 999.58 | 1.0656 | 175 | 53.67 | 53.3304 | 999.39 | 335028 | 1.0521 | 0.0333 | 364.30 |
| 30 | A | 53.66 | 1001.56 | 1.0678 | 264 | 53.67 | 53.3416 | 1001.32 | 334233 | 1.0475 | 0.0500 | 365.16 |
| | D | 53.68 | 999.96 | 1.0660 | 257 | 53.67 | 53.3280 | 999.74 | 334276 | 1.0463 | 0.0489 | 365.12 |
| 40 | A | 53.69 | 1001.11 | 1.0672 | 331 | 53.70 | 53.3468 | 1001.04 | 333520 | 1.0419 | 0.0633 | 365.94 |
| | D | 53.69 | 1000.00 | 1.0660 | 327 | 53.69 | 53.3566 | 999.96 | 333521 | 1.0409 | 0.0628 | 365.94 |
| 50 | A | 53.68 | 1000.81 | 1.0669 | 399 | 53.70 | 53.3587 | 1000.84 | 332827 | 1.0363 | 0.0766 | 366.70 |
| | D | 53.69 | 1000.05 | 1.0660 | 398 | 53.69 | 53.3630 | 1000.08 | 332817 | 1.0355 | 0.0766 | 366.72 |
| 60 | A | 53.71 | 1000.65 | 1.0666 | 467 | 53.72 | 53.3960 | 1000.55 | 332110 | 1.0308 | 0.0895 | 367.50 |
| | D | 53.66 | 1000.24 | 1.0664 | 467 | 53.70 | 53.3595 | 1000.16 | 332143 | 1.0306 | 0.0893 | 367.46 |
| 70 | A | 53.71 | 1000.52 | 1.0665 | 532 | 53.71 | 53.3807 | 1000.57 | 331462 | 1.0257 | 0.1024 | 368.21 |
| | D | 53.68 | 1000.72 | 1.0668 | 537 | 53.68 | 53.3395 | 1000.48 | 331490 | 1.0256 | 0.1026 | 368.18 |
| 80 | A | 53.72 | 1000.88 | 1.0669 | 594 | 53.72 | 53.3772 | 1000.99 | 330817 | 1.0213 | 0.1144 | 368.93 |
| | D | 53.73 | 1000.78 | 1.0667 | 607 | 53.70 | 53.3614 | 1000.65 | 330821 | 1.0202 | 0.1166 | 368.93 |
| 90 | A | N/A | N/A | N/A | N/A | N/A | N/A | N/A | N/A | N/A | N/A | N/A |
| | D | 53.73 | 1000.76 | 1.0667 | 686 | 53.73 | 53.3915 | 1000.79 | 330168 | 1.0141 | 0.1320 | 369.66 |
| 95 | | 53.67 | 1001.18 | 1.0673 | 731 | 53.72 | 53.3857 | 1001.02 | 329843 | 1.0113 | 0.1397 | 370.02 |
| Data used for pathlength calibration (the first zero step): $T_{SoS}$ = 53.3765 °C, $P$ = 1002.86 mbar, $t_m^0$ = 336647 ns, $W^0$ = 362.54 m/s. | | | | | | | | | | | | |

## A6.8 Acetone/dry air

Table 98. Acetone/dry air results (5 °C isotherm)

| $x_T$/%SAT | | Zero Step | | | $\Delta m_{read}$/µg | Non-Zero Step | | | | | | |
|---|---|---|---|---|---|---|---|---|---|---|---|---|
| | | $T_{DVS}$/°C | $P$/mbar | $\rho^0$/(kg/m$^3$) | | $T_{DVS}$/°C | $T_{SoS}$/°C | $P$/mbar | $t_m$/ns | $\rho$/(kg/m$^3$) | $x$ | $W_m$/(m/s) |
| 10 | A | 4.42 | 1022.71 | 1.2849 | 219 | 4.44 | 4.1705 | 1022.46 | 370449 | 1.3017 | 0.0132 | 330.60 |
| | D | 4.51 | 1017.22 | 1.2776 | 223 | 4.56 | 4.3020 | 1017.15 | 370366 | 1.2946 | 0.0134 | 330.68 |
| 20 | A | 4.43 | 1022.47 | 1.2845 | 431 | 4.45 | 4.1768 | 1022.58 | 373921 | 1.3176 | 0.0253 | 327.53 |
| | D | 4.50 | 1017.58 | 1.2781 | 430 | 4.52 | 4.2692 | 1017.43 | 373886 | 1.3110 | 0.0256 | 327.56 |
| 30 | A | 4.43 | 1022.77 | 1.2849 | 626 | 4.46 | 4.1847 | 1022.65 | 377229 | 1.3329 | 0.0370 | 324.66 |
| | D | 4.49 | 1017.80 | 1.2784 | 628 | 4.50 | 4.2565 | 1017.66 | 377198 | 1.3265 | 0.0372 | 324.69 |
| 40 | A | 4.45 | 1022.61 | 1.2846 | 817 | 4.48 | 4.2019 | 1022.63 | 380333 | 1.3472 | 0.0481 | 322.01 |
| | D | 4.47 | 1018.25 | 1.2790 | 814 | 4.49 | 4.2424 | 1018.02 | 380330 | 1.3414 | 0.0483 | 322.01 |
| 50 | A | 4.45 | 1022.71 | 1.2847 | 1001 | 4.46 | 4.1969 | 1022.60 | 383337 | 1.3614 | 0.0589 | 319.49 |
| | D | 4.48 | 1018.63 | 1.2795 | 1003 | 4.49 | 4.2415 | 1018.58 | 383345 | 1.3563 | 0.0592 | 319.48 |
| 60 | A | 4.46 | 1022.68 | 1.2846 | 1180 | 4.48 | 4.2089 | 1022.58 | 386224 | 1.3751 | 0.0694 | 317.10 |
| | D | 4.47 | 1019.17 | 1.2802 | 1178 | 4.51 | 4.2540 | 1018.87 | 386245 | 1.3705 | 0.0699 | 317.08 |
| 70 | A | 4.45 | 1022.47 | 1.2845 | 1357 | 4.49 | 4.2181 | 1022.40 | 389031 | 1.3884 | 0.0799 | 314.81 |
| | D | 4.48 | 1019.73 | 1.2808 | 1356 | 4.49 | 4.2391 | 1019.41 | 389041 | 1.3847 | 0.0801 | 314.80 |
| 80 | A | 4.48 | 1022.33 | 1.2841 | 1530 | 4.47 | 4.2138 | 1022.10 | 391753 | 1.4014 | 0.0900 | 312.62 |
| | D | 4.48 | 1020.32 | 1.2816 | 1526 | 4.48 | 4.2317 | 1019.90 | 391770 | 1.3986 | 0.0902 | 312.61 |
| 90 | A | 4.47 | 1021.86 | 1.2836 | 1704 | 4.48 | 4.2232 | 1021.72 | 394457 | 1.4142 | 0.1002 | 310.48 |
| | D | 4.46 | 1020.68 | 1.2821 | 1703 | 4.50 | 4.2317 | 1020.61 | 394465 | 1.4127 | 0.1003 | 310.47 |
| 95 | | 4.48 | 1021.48 | 1.2831 | 1783 | 4.47 | 4.2187 | 1021.01 | 395749 | 1.4197 | 0.1052 | 309.47 |
| Data used for pathlength calibration (the first zero step): $T_{SoS}$ = 4.1411 °C, $P$ = 1022.71 mbar, $t_m^0$ = 366627 ns, $W^0$ = 334.05 m/s. | | | | | | | | | | | | |

Table 99. Acetone/dry air results (15 °C isotherm)

| $x_T$/%SAT | | Zero Step | | | $\Delta m_{read}$/µg | Non-Zero Step | | | | | | |
|---|---|---|---|---|---|---|---|---|---|---|---|---|
| | | $T_{DVS}$/°C | $P$/mbar | $\rho^0$/(kg/m$^3$) | | $T_{DVS}$/°C | $T_{SoS}$/°C | $P$/mbar | $t_m$/ns | $\rho$/(kg/m$^3$) | $x$ | $W_m$/(m/s) |
| 10 | A | 14.45 | 1013.80 | 1.2291 | 392 | 14.46 | 14.1561 | 1013.99 | 366744 | 1.2592 | 0.0239 | 333.67 |
| | D | 14.50 | 1022.27 | 1.2392 | 388 | 14.50 | 14.2208 | 1022.13 | 366629 | 1.2689 | 0.0238 | 333.77 |
| 20 | A | 14.48 | 1014.15 | 1.2294 | 736 | 14.45 | 14.1561 | 1014.41 | 372641 | 1.2858 | 0.0449 | 328.39 |
| | D | 14.54 | 1022.10 | 1.2388 | 736 | 14.53 | 14.2538 | 1022.20 | 372439 | 1.2952 | 0.0448 | 328.56 |
| 30 | A | 14.49 | 1014.73 | 1.2301 | 1062 | 14.47 | 14.1765 | 1015.19 | 378034 | 1.3115 | 0.0647 | 323.70 |
| | D | 14.53 | 1022.16 | 1.2389 | 1056 | 14.50 | 14.2262 | 1022.20 | 377793 | 1.3198 | 0.0642 | 323.91 |
| 40 | A | 14.45 | 1015.55 | 1.2312 | 1361 | 14.45 | 14.1572 | 1016.07 | 382966 | 1.3355 | 0.0829 | 319.53 |
| | D | 14.52 | 1022.02 | 1.2388 | 1356 | 14.48 | 14.2039 | 1022.09 | 382701 | 1.3427 | 0.0823 | 319.75 |
| 50 | A | 14.45 | 1016.62 | 1.2325 | 1651 | 14.47 | 14.1689 | 1017.07 | 387614 | 1.3590 | 0.1006 | 315.70 |
| | D | 14.55 | 1021.67 | 1.2382 | 1645 | 14.50 | 14.2326 | 1021.70 | 387375 | 1.3643 | 0.1000 | 315.90 |
| 60 | A | 14.44 | 1017.38 | 1.2335 | 1922 | 14.45 | 14.1491 | 1017.74 | 391935 | 1.3808 | 0.1171 | 312.22 |
| | D | 14.52 | 1021.13 | 1.2377 | 1925 | 14.54 | 14.2405 | 1021.35 | 391759 | 1.3853 | 0.1171 | 312.36 |
| 70 | A | 14.51 | 1017.92 | 1.2339 | 2191 | 14.48 | 14.1972 | 1018.01 | 396082 | 1.4017 | 0.1336 | 308.95 |
| | D | 14.52 | 1020.65 | 1.2371 | 2191 | 14.52 | 14.2278 | 1020.95 | 395896 | 1.4050 | 0.1331 | 309.10 |
| 80 | A | 14.44 | 1018.13 | 1.2344 | 2443 | 14.51 | 14.1882 | 1018.37 | 400034 | 1.4217 | 0.1491 | 305.90 |
| | D | 14.51 | 1019.94 | 1.2363 | 2449 | 14.52 | 14.2264 | 1020.37 | 399862 | 1.4240 | 0.1488 | 306.03 |
| 90 | A | 14.50 | 1018.51 | 1.2346 | 2703 | 14.52 | 14.2251 | 1018.89 | 403809 | 1.4418 | 0.1645 | 303.04 |
| | D | 14.50 | 1019.56 | 1.2359 | 2699 | 14.51 | 14.2122 | 1019.73 | 403709 | 1.4427 | 0.1642 | 303.11 |
| 95 | | 14.47 | 1019.03 | 1.2354 | 2815 | 14.45 | 14.1749 | 1019.43 | 405482 | 1.4511 | 0.1710 | 301.79 |
| Data used for pathlength calibration (the first zero step): $T_{SoS}$ = 14.1384 °C, $P$ = 1013.80 mbar, $t_m^0$ = 359880 ns, $W^0$ = 340.03 m/s. | | | | | | | | | | | | |

Table 100. Acetone/dry air results (25 °C isotherm)

| $x_T$/%SAT | | Zero Step | | | $\Delta m_{read}$/µg | Non-Zero Step | | | | | | |
|---|---|---|---|---|---|---|---|---|---|---|---|---|
| | | $T_{DVS}$/°C | $P$/mbar | $\rho^0$/(kg/m$^3$) | | $T_{DVS}$/°C | $T_{SoS}$/°C | $P$/mbar | $t_m$/ns | $\rho$/(kg/m$^3$) | $x$ | $W_m$/(m/s) |
| 5 | A | 24.45 | 1001.75 | 1.1736 | 369 | 24.47 | 24.0278 | 1002.14 | 360902 | 1.2018 | 0.0234 | 339.39 |
| | D | 24.44 | 1008.72 | 1.1818 | 359 | 24.36 | 23.9422 | 1008.68 | 360572 | 1.2093 | 0.0227 | 339.70 |
| 10 | A | 24.47 | 1001.44 | 1.1731 | 676 | 24.48 | 24.0439 | 1001.68 | 366495 | 1.2249 | 0.0434 | 334.21 |
| | D | 24.44 | 1008.66 | 1.1817 | 665 | 24.46 | 24.0146 | 1008.78 | 366006 | 1.2327 | 0.0425 | 334.65 |
| 15 | A | 24.47 | 1001.95 | 1.1737 | 962 | 24.49 | 24.0488 | 1001.86 | 371541 | 1.2474 | 0.0620 | 329.67 |
| | D | 24.42 | 1008.54 | 1.1816 | 953 | 24.45 | 24.0084 | 1008.66 | 371007 | 1.2546 | 0.0609 | 330.14 |
| 20 | A | 24.48 | 1001.45 | 1.1731 | 1244 | 24.50 | 24.0626 | 1001.74 | 376259 | 1.2684 | 0.0798 | 325.53 |
| | D | 24.33 | 1008.15 | 1.1815 | 1219 | 24.43 | 23.9606 | 1008.34 | 375619 | 1.2750 | 0.0781 | 326.09 |
| 25 | A | 24.49 | 1001.58 | 1.1732 | 1501 | 24.49 | 24.0615 | 1001.79 | 380647 | 1.2882 | 0.0963 | 321.78 |
| | D | 24.35 | 1007.68 | 1.1809 | 1472 | 24.33 | 23.9086 | 1007.91 | 379865 | 1.2937 | 0.0938 | 322.44 |
| 30 | A | 24.49 | 1001.82 | 1.1735 | 1755 | 24.50 | 24.0704 | 1002.18 | 384794 | 1.3079 | 0.1125 | 318.31 |
| | D | 24.39 | 1006.87 | 1.1798 | 1724 | 24.37 | 23.9503 | 1007.57 | 383953 | 1.3119 | 0.1095 | 319.01 |
| 35 | A | 24.48 | 1002.47 | 1.1743 | 1978 | 24.49 | 24.0548 | 1002.42 | 388598 | 1.3259 | 0.1272 | 315.20 |
| | D | 24.46 | 1006.16 | 1.1787 | 1959 | 24.47 | 24.0213 | 1006.45 | 387825 | 1.3288 | 0.1251 | 315.83 |
| 40 | A | 24.47 | 1002.70 | 1.1746 | 2197 | 24.39 | 23.9809 | 1002.74 | 392078 | 1.3430 | 0.1407 | 312.40 |
| | D | 24.46 | 1005.33 | 1.1777 | 2178 | 24.46 | 24.0131 | 1005.52 | 391394 | 1.3446 | 0.1393 | 312.95 |
| 45 | A | 24.38 | 1002.90 | 1.1752 | 2410 | 24.37 | 23.9447 | 1003.14 | 395473 | 1.3599 | 0.1543 | 309.72 |
| | D | 24.44 | 1004.96 | 1.1774 | 2388 | 24.46 | 24.0112 | 1005.01 | 394822 | 1.3603 | 0.1529 | 310.23 |
| 50 | A | 24.35 | 1003.22 | 1.1757 | 2616 | 24.42 | 23.9613 | 1003.24 | 398794 | 1.3762 | 0.1680 | 307.14 |
| | D | 24.45 | 1005.04 | 1.1774 | 2594 | 24.44 | 24.0096 | 1005.06 | 398045 | 1.3762 | 0.1660 | 307.72 |
| 55 | A | 24.45 | 1003.20 | 1.1752 | 2831 | 24.47 | 24.0307 | 1003.47 | 401933 | 1.3922 | 0.1812 | 304.74 |
| | D | 24.43 | 1004.99 | 1.1774 | 2791 | 24.45 | 24.0067 | 1005.01 | 401122 | 1.3913 | 0.1786 | 305.36 |
| 60 | A | 24.41 | 1003.49 | 1.1757 | 3002 | 24.37 | 23.9572 | 1003.31 | 404725 | 1.4058 | 0.1923 | 302.64 |
| | D | 24.44 | 1004.95 | 1.1774 | 2982 | 24.44 | 24.0041 | 1004.92 | 404061 | 1.4059 | 0.1908 | 303.14 |

| | | | | | | | | | | | | |
|---|---|---|---|---|---|---|---|---|---|---|---|---|
| 65 | A | 24.34 | 1003.42 | 1.1759 | 3182 | 24.35 | 23.9202 | 1003.31 | 407491 | 1.4198 | 0.2039 | 300.58 |
| | D | 24.41 | 1004.70 | 1.1772 | 3169 | 24.42 | 23.9877 | 1004.81 | 406896 | 1.4200 | 0.2026 | 301.02 |
| 70 | A | 24.40 | 1003.25 | 1.1755 | 3387 | 24.45 | 24.0025 | 1003.34 | 410429 | 1.4351 | 0.2170 | 298.43 |
| | D | 24.40 | 1004.52 | 1.1770 | 3351 | 24.41 | 23.9782 | 1004.72 | 409657 | 1.4338 | 0.2141 | 299.00 |
| 75 | A | 24.44 | 1003.33 | 1.1754 | 3554 | 24.46 | 24.0211 | 1003.03 | 413009 | 1.4478 | 0.2279 | 296.57 |
| | D | 24.39 | 1004.42 | 1.1769 | 3523 | 24.41 | 23.9680 | 1004.38 | 412326 | 1.4469 | 0.2254 | 297.06 |
| 80 | A | 24.46 | 1003.00 | 1.1750 | 3726 | 24.46 | 24.0315 | 1003.02 | 415478 | 1.4606 | 0.2386 | 294.81 |
| | D | 24.40 | 1004.21 | 1.1766 | 3700 | 24.41 | 23.9758 | 1004.41 | 414907 | 1.4602 | 0.2364 | 295.21 |
| 85 | A | 24.44 | 1003.22 | 1.1753 | 3891 | 24.46 | 24.0272 | 1003.27 | 417864 | 1.4735 | 0.2490 | 293.12 |
| | D | 24.40 | 1004.18 | 1.1766 | 3871 | 24.41 | 23.9773 | 1004.25 | 417468 | 1.4732 | 0.2474 | 293.40 |
| 90 | A | 24.43 | 1003.35 | 1.1755 | 4045 | 24.41 | 23.9865 | 1003.50 | 420059 | 1.4855 | 0.2584 | 291.59 |
| | D | 24.38 | 1003.86 | 1.1763 | 4029 | 24.40 | 23.9609 | 1004.00 | 419780 | 1.4851 | 0.2574 | 291.78 |
| 95 | | 24.40 | 1003.66 | 1.1760 | 4190 | 24.40 | 23.9616 | 1003.77 | 422150 | 1.4971 | 0.2677 | 290.15 |
| Data used for pathlength calibration (the first zero step): $T_{SOS}$ = 24.0111 °C, $P$ = 1001.75 mbar, $t_m^0$ = 354173 ns, $W^0$ = 345.84 m/s. | | | | | | | | | | | | |

Table 101. Acetone/dry air results (35 °C isotherm)

| $x_T$/%SAT | | Zero Step | | | $\Delta m_{read}$/µg | Non-Zero Step | | | | | | |
|---|---|---|---|---|---|---|---|---|---|---|---|---|
| | | $T_{DVS}$/°C | $P$/mbar | $\rho^0$/(kg/m$^3$) | | $T_{DVS}$/°C | $T_{SoS}$/°C | $P$/mbar | $t_m$/ns | $\rho$/(kg/m$^3$) | $x$ | $W_m$/(m/s) |
| 10 | A | 34.63 | 1009.12 | 1.1430 | 1218 | 34.66 | 34.2676 | 1009.19 | 369728 | 1.2363 | 0.0805 | 330.69 |
| | D | 34.49 | 1011.89 | 1.1466 | 1191 | 34.50 | 34.1100 | 1011.73 | 369067 | 1.2379 | 0.0787 | 331.28 |
| 20 | A | 34.63 | 1009.23 | 1.1431 | 2141 | 34.62 | 34.2369 | 1009.38 | 385138 | 1.3072 | 0.1412 | 317.46 |
| | D | 34.48 | 1011.87 | 1.1467 | 2093 | 34.50 | 34.1004 | 1012.01 | 384065 | 1.3070 | 0.1377 | 318.34 |
| 30 | A | 34.60 | 1009.54 | 1.1436 | 2915 | 34.63 | 34.2351 | 1009.57 | 397473 | 1.3669 | 0.1922 | 307.61 |
| | D | 34.47 | 1011.81 | 1.1466 | 2845 | 34.49 | 34.0983 | 1011.85 | 396027 | 1.3646 | 0.1871 | 308.73 |
| 40 | A | 34.64 | 1009.79 | 1.1437 | 3592 | 34.67 | 34.2814 | 1009.96 | 407665 | 1.4190 | 0.2364 | 299.92 |
| | D | 34.48 | 1011.59 | 1.1463 | 3488 | 34.48 | 34.0886 | 1011.68 | 405805 | 1.4136 | 0.2290 | 301.29 |
| 50 | A | 34.58 | 1009.62 | 1.1437 | 4145 | 34.57 | 34.1990 | 1009.40 | 415997 | 1.4614 | 0.2729 | 293.91 |
| | D | 34.51 | 1010.89 | 1.1454 | 4068 | 34.51 | 34.1174 | 1011.16 | 414322 | 1.4571 | 0.2668 | 295.10 |
| 60 | A | 34.56 | 1009.46 | 1.1436 | 4653 | 34.55 | 34.1659 | 1009.53 | 423199 | 1.5002 | 0.3057 | 288.91 |
| | D | 34.52 | 1010.54 | 1.1450 | 4571 | 34.50 | 34.1248 | 1010.61 | 421656 | 1.4953 | 0.2999 | 289.96 |
| 70 | A | 34.56 | 1009.52 | 1.1437 | 5100 | 34.55 | 34.1688 | 1009.36 | 429466 | 1.5345 | 0.3351 | 284.69 |
| | D | 34.51 | 1010.09 | 1.1445 | 5034 | 34.52 | 34.1411 | 1010.21 | 428206 | 1.5303 | 0.3303 | 285.53 |
| 80 | A | 34.54 | 1009.32 | 1.1435 | 5513 | 34.55 | 34.1603 | 1009.16 | 435154 | 1.5660 | 0.3620 | 280.97 |
| | D | 34.53 | 1009.74 | 1.1441 | 5460 | 34.54 | 34.1589 | 1009.85 | 434160 | 1.5625 | 0.3581 | 281.61 |
| 90 | A | 34.53 | 1009.23 | 1.1435 | 5886 | 34.55 | 34.1636 | 1009.27 | 440093 | 1.5945 | 0.3860 | 277.82 |
| | D | 34.50 | 1009.38 | 1.1438 | 5852 | 34.56 | 34.1548 | 1009.58 | 439590 | 1.5922 | 0.3837 | 278.13 |
| 95 | | 34.54 | 1009.25 | 1.1435 | 6042 | 34.53 | 34.1547 | 1009.49 | 442087 | 1.6065 | 0.3958 | 276.56 |
| Data used for pathlength calibration (the first zero step): $T_{SoS}$ = 34.2360 °C, $P$ = 1009.12 mbar, $t_m^0$ = 347595 ns, $W^0$ = 351.75 m/s. | | | | | | | | | | | | |

## A6.9 Methyl ethyl ketone/dry air

Table 102. Methyl ethyl ketone/dry air results (5 °C isotherm)

| $x_T$/%SAT | | Zero Step | | | $\Delta m_{read}$/µg | Non-Zero Step | | | | | | |
|---|---|---|---|---|---|---|---|---|---|---|---|---|
| | | $T_{DVS}$/°C | $P$/mbar | $\rho^0$/(kg/m$^3$) | | $T_{DVS}$/°C | $T_{SoS}$/°C | $P$/mbar | $t_m$/ns | $\rho$/(kg/m$^3$) | $x$ | $W_m$/(m/s) |
| 10 | A | 5.28 | 1005.39 | 1.2592 | 115 | 5.31 | 5.1799 | 1005.40 | 367490 | 1.2680 | 0.0048 | 332.77 |
| | D | 5.46 | 1004.52 | 1.2573 | 113 | 5.48 | 5.3529 | 1004.22 | 367369 | 1.2659 | 0.0049 | 332.88 |
| 20 | A | 5.29 | 1005.48 | 1.2592 | 222 | 5.32 | 5.1930 | 1005.54 | 369415 | 1.2763 | 0.0090 | 331.03 |
| | D | 5.45 | 1005.02 | 1.2579 | 219 | 5.47 | 5.3481 | 1004.78 | 369318 | 1.2747 | 0.0091 | 331.12 |
| 30 | A | 5.32 | 1005.34 | 1.2590 | 323 | 5.32 | 5.1974 | 1005.06 | 371290 | 1.2837 | 0.0133 | 329.36 |
| | D | 5.44 | 1005.04 | 1.2580 | 332 | 5.46 | 5.3343 | 1005.19 | 371207 | 1.2834 | 0.0134 | 329.44 |
| 40 | A | 5.31 | 1005.02 | 1.2586 | 427 | 5.34 | 5.2102 | 1004.91 | 373102 | 1.2913 | 0.0174 | 327.76 |
| | D | 5.45 | 1005.31 | 1.2583 | 428 | 5.47 | 5.3287 | 1005.16 | 373030 | 1.2911 | 0.0175 | 327.83 |
| 50 | A | 5.33 | 1004.82 | 1.2582 | 529 | 5.34 | 5.2182 | 1004.68 | 374884 | 1.2988 | 0.0216 | 326.21 |
| | D | 5.44 | 1005.30 | 1.2583 | 531 | 5.46 | 5.3224 | 1005.35 | 374814 | 1.2990 | 0.0216 | 326.27 |
| 60 | A | 5.33 | 1004.57 | 1.2579 | 630 | 5.34 | 5.2186 | 1004.60 | 376615 | 1.3062 | 0.0256 | 324.71 |
| | D | 5.44 | 1005.40 | 1.2585 | 628 | 5.45 | 5.3173 | 1005.25 | 376556 | 1.3066 | 0.0256 | 324.76 |
| 70 | A | 5.33 | 1004.53 | 1.2579 | 728 | 5.35 | 5.2251 | 1004.56 | 378324 | 1.3137 | 0.0296 | 323.24 |
| | D | 5.44 | 1005.46 | 1.2586 | 728 | 5.46 | 5.3151 | 1005.38 | 378272 | 1.3144 | 0.0297 | 323.28 |
| 80 | A | 5.33 | 1004.64 | 1.2580 | 829 | 5.35 | 5.2272 | 1004.76 | 380033 | 1.3216 | 0.0336 | 321.78 |
| | D | 5.35 | 1005.32 | 1.2588 | 838 | 5.41 | 5.2659 | 1005.60 | 379991 | 1.3230 | 0.0339 | 321.82 |
| 90 | A | 5.33 | 1004.66 | 1.2580 | 929 | 5.36 | 5.2357 | 1004.78 | 381718 | 1.3292 | 0.0377 | 320.37 |
| | D | 5.35 | 1004.93 | 1.2583 | 931 | 5.36 | 5.2386 | 1005.13 | 381695 | 1.3296 | 0.0377 | 320.38 |
| 95 | | 5.34 | 1004.88 | 1.2583 | 977 | 5.36 | 5.2400 | 1004.85 | 382535 | 1.3331 | 0.0397 | 319.68 |
| Data used for pathlength calibration (the first zero step): $T_{SoS}$ = 5.1468 °C, $P$ = 1005.39 mbar, $t_m^0$ = 365421 ns, $W^0$ = 334.65 m/s. | | | | | | | | | | | | |

Table 103. Methyl ethyl ketone/dry air results (15 °C isotherm)

| $x_T$/%SAT | | Zero Step | | | $\Delta m_{read}$/µg | Non-Zero Step | | | | | | |
|---|---|---|---|---|---|---|---|---|---|---|---|---|
| | | $T_{DVS}$/°C | $P$/mbar | $\rho^0$/(kg/m$^3$) | | $T_{DVS}$/°C | $T_{SoS}$/°C | $P$/mbar | $t_m$/ns | $\rho$/(kg/m$^3$) | $x$ | $W_m$/(m/s) |
| 10 | A | 14.42 | 996.39 | 1.2081 | 188 | 14.43 | 14.0691 | 996.28 | 363722 | 1.2225 | 0.0081 | 336.67 |
| | D | 14.38 | 997.64 | 1.2098 | 189 | 14.38 | 14.0365 | 997.77 | 363706 | 1.2243 | 0.0079 | 336.68 |
| 20 | A | 14.43 | 996.04 | 1.2076 | 354 | 14.46 | 14.0896 | 995.73 | 366927 | 1.2348 | 0.0153 | 333.72 |
| | D | 14.39 | 996.82 | 1.2088 | 365 | 14.39 | 14.0475 | 997.26 | 366889 | 1.2367 | 0.0151 | 333.76 |
| 30 | A | 14.44 | 995.32 | 1.2067 | 520 | 14.46 | 14.1012 | 994.90 | 369981 | 1.2466 | 0.0224 | 330.97 |
| | D | 14.40 | 996.45 | 1.2083 | 527 | 14.41 | 14.0649 | 996.69 | 369929 | 1.2486 | 0.0221 | 331.02 |
| 40 | A | 14.44 | 994.61 | 1.2059 | 680 | 14.47 | 14.1050 | 994.25 | 372887 | 1.2580 | 0.0291 | 328.39 |
| | D | 14.41 | 996.20 | 1.2079 | 686 | 14.42 | 14.0746 | 996.39 | 372829 | 1.2605 | 0.0289 | 328.44 |
| 50 | A | 14.45 | 993.91 | 1.2050 | 840 | 14.47 | 14.1112 | 993.46 | 375722 | 1.2693 | 0.0360 | 325.91 |
| | D | 14.41 | 995.90 | 1.2076 | 846 | 14.42 | 14.0731 | 995.92 | 375666 | 1.2724 | 0.0358 | 325.96 |
| 60 | A | 14.45 | 993.31 | 1.2043 | 999 | 14.46 | 14.1088 | 993.17 | 378450 | 1.2808 | 0.0425 | 323.56 |
| | D | 14.41 | 995.43 | 1.2070 | 1003 | 14.43 | 14.0780 | 995.77 | 378373 | 1.2839 | 0.0423 | 323.63 |
| 70 | A | 14.44 | 993.15 | 1.2041 | 1160 | 14.45 | 14.0952 | 993.57 | 381108 | 1.2930 | 0.0489 | 321.31 |
| | D | 14.41 | 995.57 | 1.2072 | 1152 | 14.42 | 14.0738 | 995.48 | 381056 | 1.2955 | 0.0488 | 321.35 |
| 80 | A | 14.44 | 993.79 | 1.2049 | 1317 | 14.44 | 14.0925 | 994.38 | 383708 | 1.3058 | 0.0554 | 319.13 |
| | D | 14.41 | 995.32 | 1.2068 | 1311 | 14.43 | 14.0733 | 995.56 | 383654 | 1.3073 | 0.0553 | 319.18 |
| 90 | A | 14.44 | 994.60 | 1.2059 | 1466 | 14.44 | 14.0908 | 994.88 | 386265 | 1.3182 | 0.0619 | 317.02 |
| | D | 14.42 | 995.38 | 1.2069 | 1459 | 14.42 | 14.0768 | 995.42 | 386245 | 1.3187 | 0.0617 | 317.03 |
| 95 | | 14.42 | 995.13 | 1.2066 | 1538 | 14.43 | 14.0837 | 995.39 | 387483 | 1.3244 | 0.0649 | 316.02 |
| Data used for pathlength calibration (the first zero step): $T_{SoS}$ = 14.0418 °C, $P$ = 996.39 mbar, $t_m^0$ = 360185 ns, $W^0$ = 339.97 m/s. | | | | | | | | | | | | |

Table 104. Methyl ethyl ketone/dry air results (25 °C isotherm)

| $x_T$/%SAT | | Zero Step | | | $\Delta m_{read}$/µg | Non-Zero Step | | | | | | |
|---|---|---|---|---|---|---|---|---|---|---|---|---|
| | | $T_{DVS}$/°C | $P$/mbar | $\rho^0$/(kg/m$^3$) | | $T_{DVS}$/°C | $T_{SoS}$/°C | $P$/mbar | $t_m$/ns | $\rho$/(kg/m$^3$) | $x$ | $W_m$/(m/s) |
| 5 | A | 24.39 | 1002.59 | 1.1748 | 166 | 24.40 | 23.9642 | 1002.73 | 357107 | 1.1875 | 0.0071 | 342.75 |
| | D | 24.38 | 1016.73 | 1.1914 | 165 | 24.39 | 23.9620 | 1016.77 | 356958 | 1.2040 | 0.0071 | 342.89 |
| 10 | A | 24.38 | 1002.71 | 1.1750 | 313 | 24.39 | 23.9592 | 1002.93 | 359915 | 1.1989 | 0.0135 | 340.07 |
| | D | 24.36 | 1016.69 | 1.1914 | 313 | 24.38 | 23.9489 | 1016.72 | 359738 | 1.2154 | 0.0135 | 340.24 |
| 15 | A | 24.38 | 1003.07 | 1.1754 | 460 | 24.39 | 23.9531 | 1003.25 | 362626 | 1.2106 | 0.0199 | 337.53 |
| | D | 24.37 | 1016.56 | 1.1912 | 455 | 24.33 | 23.9195 | 1016.61 | 362363 | 1.2261 | 0.0194 | 337.78 |
| 20 | A | 24.36 | 1003.53 | 1.1760 | 602 | 24.36 | 23.9308 | 1004.04 | 365175 | 1.2221 | 0.0258 | 335.17 |
| | D | 24.29 | 1016.38 | 1.1914 | 587 | 24.37 | 23.9220 | 1016.50 | 364914 | 1.2363 | 0.0253 | 335.41 |
| 25 | A | 24.36 | 1004.35 | 1.1770 | 738 | 24.39 | 23.9507 | 1004.99 | 367641 | 1.2335 | 0.0317 | 332.93 |
| | D | 24.38 | 1016.34 | 1.1910 | 730 | 24.39 | 23.9583 | 1016.35 | 367362 | 1.2469 | 0.0314 | 333.18 |
| 30 | A | 24.38 | 1005.32 | 1.1780 | 867 | 24.40 | 23.9638 | 1005.49 | 370049 | 1.2445 | 0.0375 | 330.76 |
| | D | 24.38 | 1015.92 | 1.1905 | 868 | 24.38 | 23.9459 | 1016.19 | 369734 | 1.2570 | 0.0371 | 331.04 |
| 35 | A | 24.38 | 1005.75 | 1.1785 | 999 | 24.39 | 23.9566 | 1006.18 | 372342 | 1.2551 | 0.0430 | 328.72 |
| | D | 24.31 | 1015.63 | 1.1904 | 987 | 24.33 | 23.8876 | 1015.80 | 372003 | 1.2661 | 0.0423 | 329.02 |
| 40 | A | 24.37 | 1006.75 | 1.1797 | 1129 | 24.39 | 23.9545 | 1007.05 | 374591 | 1.2662 | 0.0487 | 326.75 |
| | D | 24.39 | 1015.27 | 1.1897 | 1123 | 24.41 | 23.9716 | 1015.34 | 374280 | 1.2757 | 0.0482 | 327.02 |
| 45 | A | 24.38 | 1006.90 | 1.1799 | 1249 | 24.38 | 23.9469 | 1006.90 | 376783 | 1.2756 | 0.0541 | 324.85 |
| | D | 24.37 | 1014.59 | 1.1889 | 1257 | 24.40 | 23.9580 | 1015.03 | 376463 | 1.2852 | 0.0537 | 325.12 |
| 50 | A | 24.37 | 1007.16 | 1.1802 | 1375 | 24.37 | 23.9391 | 1007.31 | 378911 | 1.2856 | 0.0594 | 323.02 |
| | D | 24.36 | 1014.23 | 1.1885 | 1371 | 24.37 | 23.9374 | 1014.35 | 378564 | 1.2936 | 0.0589 | 323.32 |
| 55 | A | 24.36 | 1007.41 | 1.1805 | 1500 | 24.37 | 23.9333 | 1007.74 | 381005 | 1.2955 | 0.0647 | 321.25 |
| | D | 24.37 | 1013.82 | 1.1880 | 1496 | 24.38 | 23.9450 | 1014.03 | 380654 | 1.3026 | 0.0642 | 321.54 |
| 60 | A | 24.35 | 1007.96 | 1.1812 | 1621 | 24.37 | 23.9372 | 1008.19 | 383024 | 1.3054 | 0.0699 | 319.55 |
| | D | 24.38 | 1013.63 | 1.1878 | 1616 | 24.39 | 23.9532 | 1013.70 | 382718 | 1.3116 | 0.0695 | 319.81 |

| | | | | | | | | | | | | |
|---|---|---|---|---|---|---|---|---|---|---|---|---|
| 65 | A | 24.36 | 1008.41 | 1.1817 | 1737 | 24.36 | 23.9339 | 1008.51 | 385004 | 1.3149 | 0.0750 | 317.91 |
| | D | 24.37 | 1013.58 | 1.1877 | 1733 | 24.39 | 23.9511 | 1013.43 | 384735 | 1.3205 | 0.0746 | 318.13 |
| 70 | A | 24.35 | 1008.66 | 1.1821 | 1859 | 24.37 | 23.9328 | 1008.98 | 386974 | 1.3245 | 0.0801 | 316.29 |
| | D | 24.37 | 1013.47 | 1.1876 | 1854 | 24.39 | 23.9535 | 1013.44 | 386757 | 1.3297 | 0.0798 | 316.47 |
| 75 | A | 24.35 | 1009.22 | 1.1827 | 1980 | 24.35 | 23.9262 | 1009.64 | 388890 | 1.3344 | 0.0852 | 314.73 |
| | D | 24.37 | 1013.32 | 1.1874 | 1974 | 24.38 | 23.9518 | 1013.44 | 388690 | 1.3387 | 0.0848 | 314.90 |
| 80 | A | 24.34 | 1009.97 | 1.1836 | 2092 | 24.34 | 23.9186 | 1010.36 | 390723 | 1.3439 | 0.0899 | 313.26 |
| | D | 24.37 | 1012.95 | 1.1870 | 2091 | 24.39 | 23.9553 | 1013.07 | 390639 | 1.3472 | 0.0899 | 313.32 |
| 85 | A | 24.34 | 1010.70 | 1.1845 | 2214 | 24.33 | 23.9035 | 1010.98 | 392581 | 1.3542 | 0.0952 | 311.78 |
| | D | 24.37 | 1012.60 | 1.1866 | 2209 | 24.38 | 23.9455 | 1012.71 | 392522 | 1.3559 | 0.0950 | 311.82 |
| 90 | A | 24.31 | 1011.26 | 1.1852 | 2324 | 24.34 | 23.9053 | 1011.61 | 394438 | 1.3633 | 0.0999 | 310.31 |
| | D | 24.35 | 1012.24 | 1.1862 | 2322 | 24.37 | 23.9323 | 1012.43 | 394370 | 1.3642 | 0.0998 | 310.36 |
| 95 | | 24.34 | 1011.83 | 1.1858 | 2439 | 24.37 | 23.9307 | 1012.13 | 396216 | 1.3727 | 0.1048 | 308.91 |
| Data used for pathlength calibration (the first zero step): $T_{SOS}$ = 23.9485 °C, $P$ = 1002.59 mbar, $t_m^0$ = 353955 ns, $W^0$ = 345.80 m/s. | | | | | | | | | | | | |

Table 105. Methyl ethyl ketone/dry air results (35 °C isotherm)

| $x_T$/%SAT | | Zero Step | | | $\Delta m_{read}$/µg | Non-Zero Step | | | | | | |
|---|---|---|---|---|---|---|---|---|---|---|---|---|
| | | $T_{DVS}$/°C | $P$/mbar | $\rho^0$/(kg/m$^3$) | | $T_{DVS}$/°C | $T_{SoS}$/°C | $P$/mbar | $t_m$/ns | $\rho$/(kg/m$^3$) | $x$ | $W_m$/(m/s) |
| 10 | A | 34.52 | 998.18 | 1.1310 | 521 | 34.50 | 34.1347 | 998.15 | 357910 | 1.1709 | 0.0235 | 341.65 |
| | D | 34.54 | 1004.25 | 1.1378 | 527 | 34.55 | 34.1728 | 1004.48 | 357749 | 1.1782 | 0.0235 | 341.80 |
| 20 | A | 34.47 | 998.19 | 1.1312 | 966 | 34.47 | 34.1067 | 998.13 | 366342 | 1.2052 | 0.0437 | 333.78 |
| | D | 34.52 | 1003.77 | 1.1373 | 985 | 34.53 | 34.1670 | 1004.01 | 366172 | 1.2128 | 0.0441 | 333.94 |
| 30 | A | 34.44 | 998.15 | 1.1313 | 1399 | 34.45 | 34.0885 | 998.01 | 374012 | 1.2385 | 0.0633 | 326.94 |
| | D | 34.51 | 1003.16 | 1.1367 | 1413 | 34.54 | 34.1679 | 1003.46 | 373811 | 1.2450 | 0.0634 | 327.11 |
| 40 | A | 34.45 | 998.01 | 1.1311 | 1808 | 34.45 | 34.1018 | 998.08 | 380994 | 1.2696 | 0.0816 | 320.95 |
| | D | 34.49 | 1002.75 | 1.1363 | 1805 | 34.51 | 34.1267 | 1002.87 | 380671 | 1.2746 | 0.0811 | 321.22 |
| 50 | A | 34.45 | 998.20 | 1.1313 | 2192 | 34.45 | 34.1090 | 998.29 | 387452 | 1.2993 | 0.0989 | 315.60 |
| | D | 34.48 | 1002.35 | 1.1358 | 2213 | 34.51 | 34.1344 | 1002.59 | 387132 | 1.3054 | 0.0994 | 315.86 |
| 60 | A | 34.49 | 998.28 | 1.1312 | 2564 | 34.52 | 34.1558 | 998.41 | 393514 | 1.3277 | 0.1157 | 310.74 |
| | D | 34.49 | 1002.24 | 1.1357 | 2564 | 34.51 | 34.1363 | 1002.42 | 393178 | 1.3322 | 0.1151 | 311.00 |
| 70 | A | 34.52 | 998.66 | 1.1315 | 2930 | 34.54 | 34.1876 | 999.03 | 399230 | 1.3561 | 0.1319 | 306.29 |
| | D | 34.50 | 1002.30 | 1.1357 | 2914 | 34.50 | 34.1289 | 1002.25 | 398862 | 1.3590 | 0.1310 | 306.57 |
| 80 | A | 34.56 | 999.34 | 1.1321 | 3275 | 34.53 | 34.1942 | 999.73 | 404517 | 1.3831 | 0.1472 | 302.28 |
| | D | 34.50 | 1001.98 | 1.1354 | 3260 | 34.50 | 34.1413 | 1002.14 | 404230 | 1.3852 | 0.1463 | 302.50 |
| 90 | A | 34.50 | 1000.10 | 1.1332 | 3599 | 34.48 | 34.1404 | 1000.64 | 409462 | 1.4090 | 0.1614 | 298.63 |
| | D | 34.51 | 1001.18 | 1.1344 | 3608 | 34.51 | 34.1552 | 1001.83 | 409440 | 1.4109 | 0.1616 | 298.65 |
| 95 | | 34.53 | 1000.86 | 1.1340 | 3761 | 34.50 | 34.1459 | 1001.07 | 411892 | 1.4222 | 0.1688 | 296.87 |
| Data used for pathlength calibration (the first zero step): $T_{SoS}$ = 34.1402 °C, $P$ = 998.18 mbar, $t_m^0$ = 347689 ns, $W^0$ = 351.69 m/s. | | | | | | | | | | | | |

Table 106. Methyl ethyl ketone/dry air results (45 °C isotherm)

| $x_T$/%SAT | | Zero Step | | | $\Delta m_{read}$/µg | Non-Zero Step | | | | | | |
|---|---|---|---|---|---|---|---|---|---|---|---|---|
| | | $T_{DVS}$/°C | $P$/mbar | $\rho^0$/(kg/m$^3$) | | $T_{DVS}$/°C | $T_{SoS}$/°C | $P$/mbar | $t_m$/ns | $\rho$/(kg/m$^3$) | $x$ | $W_m$/(m/s) |
| 10 | A | 43.98 | 1017.17 | 1.1180 | 840 | 43.98 | 43.6584 | 1017.15 | 358423 | 1.1824 | 0.0385 | 340.92 |
| | D | 43.97 | 1019.50 | 1.1206 | 840 | 43.98 | 43.6663 | 1019.45 | 358129 | 1.1850 | 0.0384 | 341.20 |
| 20 | A | 43.92 | 1017.29 | 1.1184 | 1550 | 43.90 | 43.5949 | 1017.33 | 371136 | 1.2371 | 0.0708 | 329.24 |
| | D | 43.99 | 1019.37 | 1.1204 | 1551 | 43.96 | 43.6543 | 1019.40 | 370776 | 1.2393 | 0.0707 | 329.56 |
| 30 | A | 43.93 | 1017.46 | 1.1185 | 2208 | 43.93 | 43.6278 | 1017.70 | 382211 | 1.2878 | 0.1007 | 319.70 |
| | D | 44.03 | 1019.40 | 1.1203 | 2198 | 43.97 | 43.6675 | 1019.47 | 381688 | 1.2888 | 0.1000 | 320.14 |
| 40 | A | 43.96 | 1017.86 | 1.1189 | 2802 | 43.98 | 43.6355 | 1018.11 | 391822 | 1.3336 | 0.1277 | 311.86 |
| | D | 44.05 | 1019.26 | 1.1201 | 2796 | 44.04 | 43.7052 | 1019.34 | 391379 | 1.3344 | 0.1274 | 312.21 |
| 50 | A | 43.97 | 1018.38 | 1.1194 | 3354 | 43.96 | 43.6448 | 1018.48 | 400473 | 1.3765 | 0.1528 | 305.12 |
| | D | 43.89 | 1019.20 | 1.1206 | 3332 | 44.00 | 43.6311 | 1019.35 | 399844 | 1.3759 | 0.1519 | 305.60 |
| 60 | A | 43.99 | 1018.41 | 1.1194 | 3876 | 43.96 | 43.6598 | 1018.57 | 408307 | 1.4164 | 0.1764 | 299.27 |
| | D | 43.92 | 1018.94 | 1.1202 | 3848 | 43.89 | 43.6098 | 1019.18 | 407585 | 1.4151 | 0.1749 | 299.80 |
| 70 | A | 43.98 | 1018.77 | 1.1198 | 4363 | 43.99 | 43.6703 | 1018.76 | 415496 | 1.4541 | 0.1986 | 294.09 |
| | D | 43.93 | 1018.78 | 1.1200 | 4339 | 43.94 | 43.6408 | 1018.86 | 414936 | 1.4525 | 0.1974 | 294.48 |
| 80 | A | 43.95 | 1018.79 | 1.1199 | 4815 | 43.95 | 43.6408 | 1018.75 | 421982 | 1.4889 | 0.2191 | 289.57 |
| | D | 43.90 | 1018.77 | 1.1201 | 4796 | 43.93 | 43.6371 | 1018.71 | 421591 | 1.4876 | 0.2183 | 289.84 |
| 90 | A | 43.92 | 1018.58 | 1.1198 | 5250 | 43.91 | 43.6178 | 1018.46 | 428093 | 1.5221 | 0.2388 | 285.43 |
| | D | 43.95 | 1018.61 | 1.1197 | 5253 | 43.95 | 43.6571 | 1018.67 | 427998 | 1.5223 | 0.2388 | 285.50 |
| 95 | | 43.90 | 1018.55 | 1.1198 | 5457 | 43.93 | 43.6239 | 1018.51 | 430919 | 1.5381 | 0.2482 | 283.56 |
| Data used for pathlength calibration (the first zero step): $T_{SoS}$ = 43.6580 °C, $P$ = 1017.17 mbar, $t_m^0$ = 342175 ns, $W^0$ = 357.10 m/s. | | | | | | | | | | | | |

Table 107. Methyl ethyl ketone/dry air results (55 °C isotherm)

| $x_T$/%SAT | | Zero Step | | | $\Delta m_{read}$/µg | Non-Zero Step | | | | | | |
|---|---|---|---|---|---|---|---|---|---|---|---|---|
| | | $T_{DVS}$/°C | $P$/mbar | $\rho^0$/(kg/m$^3$) | | $T_{DVS}$/°C | $T_{SoS}$/°C | $P$/mbar | $t_m$/ns | $\rho$/(kg/m$^3$) | $x$ | $W_m$/(m/s) |
| 10 | A | 53.77 | 1008.10 | 1.0748 | 1446 | 53.78 | 53.5024 | 1008.30 | 364178 | 1.1856 | 0.0687 | 334.94 |
| | D | 53.73 | 1013.21 | 1.0804 | 1425 | 53.73 | 53.4433 | 1013.30 | 363453 | 1.1896 | 0.0674 | 335.60 |
| 20 | A | 53.74 | 1008.40 | 1.0752 | 2568 | 53.72 | 53.4577 | 1008.45 | 383481 | 1.2720 | 0.1219 | 318.08 |
| | D | 53.67 | 1012.88 | 1.0802 | 2524 | 53.71 | 53.4171 | 1012.95 | 382340 | 1.2737 | 0.1194 | 319.02 |
| 30 | A | 53.68 | 1008.75 | 1.0758 | 3528 | 53.67 | 53.3995 | 1009.10 | 398749 | 1.3461 | 0.1671 | 305.90 |
| | D | 53.71 | 1012.68 | 1.0799 | 3476 | 53.69 | 53.4184 | 1012.72 | 397475 | 1.3463 | 0.1642 | 306.88 |
| 40 | A | 53.60 | 1009.28 | 1.0766 | 4365 | 53.65 | 53.3895 | 1009.83 | 411386 | 1.4111 | 0.2064 | 296.50 |
| | D | 53.67 | 1012.23 | 1.0796 | 4303 | 53.70 | 53.4281 | 1012.46 | 409951 | 1.4093 | 0.2032 | 297.54 |
| 50 | A | 53.67 | 1010.03 | 1.0772 | 5124 | 53.70 | 53.4191 | 1010.38 | 422313 | 1.4699 | 0.2422 | 288.83 |
| | D | 53.71 | 1012.21 | 1.0794 | 5045 | 53.69 | 53.4274 | 1012.21 | 420747 | 1.4660 | 0.2381 | 289.90 |
| 60 | A | 53.69 | 1010.71 | 1.0779 | 5776 | 53.69 | 53.4143 | 1010.81 | 431463 | 1.5205 | 0.2727 | 282.70 |
| | D | 53.70 | 1012.05 | 1.0793 | 5707 | 53.70 | 53.4369 | 1012.19 | 430032 | 1.5166 | 0.2691 | 283.64 |
| 70 | A | 53.74 | 1011.38 | 1.0784 | 6401 | 53.75 | 53.4688 | 1011.51 | 439846 | 1.5689 | 0.3019 | 277.32 |
| | D | 53.72 | 1011.80 | 1.0789 | 6311 | 53.69 | 53.4206 | 1012.06 | 438291 | 1.5625 | 0.2972 | 278.30 |
| 80 | A | 53.74 | 1011.54 | 1.0786 | 6950 | 53.73 | 53.4503 | 1011.69 | 447091 | 1.6112 | 0.3274 | 272.82 |
| | D | 53.75 | 1011.57 | 1.0786 | 6895 | 53.75 | 53.4803 | 1011.45 | 446216 | 1.6069 | 0.3251 | 273.36 |
| 90 | A | 53.69 | 1011.83 | 1.0791 | 7440 | 53.72 | 53.4424 | 1011.63 | 453514 | 1.6492 | 0.3506 | 268.96 |
| | D | 53.71 | 1011.54 | 1.0787 | 7426 | 53.75 | 53.4805 | 1011.68 | 453111 | 1.6477 | 0.3497 | 269.20 |
| 95 | | 53.73 | 1011.49 | 1.0786 | 7671 | 53.73 | 53.4553 | 1011.32 | 456429 | 1.6664 | 0.3614 | 267.24 |
| Data used for pathlength calibration (the first zero step): $T_{SoS}$ = 53.4808 °C, $P$ = 1008.10 mbar, $t_m^0$ = 336391 ns, $W^0$ = 362.60 m/s. | | | | | | | | | | | | |

## A6.10 Ethyl acetate/dry air

Table 108. Ethyl acetate/dry air results (5 °C isotherm)

| $x_T$/%SAT | | Zero Step | | | $\Delta m_{read}$/µg | Non-Zero Step | | | | | | |
|---|---|---|---|---|---|---|---|---|---|---|---|---|
| | | $T_{DVS}$/°C | $P$/mbar | $\rho^0$/(kg/m$^3$) | | $T_{DVS}$/°C | $T_{SoS}$/°C | $P$/mbar | $t_m$/ns | $\rho$/(kg/m$^3$) | $x$ | $W_m$/(m/s) |
| 10 | A | 4.73 | 1004.41 | 1.2605 | 152 | 4.80 | 4.6011 | 1004.25 | 368803 | 1.2721 | 0.0047 | 332.00 |
| | D | 5.29 | 1002.14 | 1.2551 | 165 | 5.29 | 5.1634 | 1002.41 | 368483 | 1.2677 | 0.0048 | 332.28 |
| 20 | A | 4.80 | 1004.09 | 1.2597 | 298 | 4.81 | 4.6289 | 1003.94 | 371178 | 1.2826 | 0.0089 | 329.87 |
| | D | 5.29 | 1001.90 | 1.2548 | 311 | 5.31 | 5.1657 | 1002.04 | 370930 | 1.2786 | 0.0092 | 330.09 |
| 30 | A | 4.84 | 1003.85 | 1.2593 | 442 | 4.87 | 4.6808 | 1003.78 | 373451 | 1.2931 | 0.0132 | 327.86 |
| | D | 5.28 | 1002.07 | 1.2550 | 453 | 5.29 | 5.1482 | 1002.01 | 373305 | 1.2898 | 0.0135 | 327.99 |
| 40 | A | 4.91 | 1003.61 | 1.2586 | 582 | 4.99 | 4.7918 | 1003.45 | 375669 | 1.3032 | 0.0175 | 325.93 |
| | D | 5.27 | 1002.10 | 1.2551 | 593 | 5.26 | 5.1316 | 1001.99 | 375591 | 1.3005 | 0.0177 | 326.00 |
| 50 | A | 5.04 | 1003.28 | 1.2576 | 725 | 5.08 | 4.8971 | 1003.22 | 377869 | 1.3132 | 0.0216 | 324.03 |
| | D | 5.24 | 1002.56 | 1.2558 | 730 | 5.27 | 5.1242 | 1002.27 | 377829 | 1.3118 | 0.0219 | 324.06 |
| 60 | A | 5.11 | 1003.13 | 1.2571 | 871 | 5.14 | 4.9811 | 1003.26 | 380025 | 1.3239 | 0.0258 | 322.19 |
| | D | 5.24 | 1002.69 | 1.2560 | 869 | 5.23 | 5.0961 | 1002.55 | 379995 | 1.3226 | 0.0259 | 322.22 |
| 70 | A | 5.24 | 1003.27 | 1.2567 | 1013 | 5.25 | 5.0813 | 1003.41 | 382188 | 1.3343 | 0.0300 | 320.37 |
| | D | 5.25 | 1002.82 | 1.2561 | 1006 | 5.27 | 5.1133 | 1002.70 | 382161 | 1.3332 | 0.0300 | 320.39 |
| 80 | A | 5.24 | 1003.50 | 1.2570 | 1148 | 5.23 | 5.0859 | 1003.45 | 384299 | 1.3450 | 0.0341 | 318.61 |
| | D | 5.24 | 1002.92 | 1.2563 | 1148 | 5.27 | 5.1168 | 1002.96 | 384304 | 1.3443 | 0.0341 | 318.60 |
| 90 | A | 5.24 | 1003.44 | 1.2569 | 1286 | 5.26 | 5.1226 | 1003.52 | 386427 | 1.3555 | 0.0382 | 316.85 |
| | D | 5.26 | 1003.33 | 1.2567 | 1276 | 5.26 | 5.1232 | 1003.10 | 386420 | 1.3545 | 0.0380 | 316.86 |
| 95 | | 5.29 | 1003.43 | 1.2567 | 1341 | 5.27 | 5.1343 | 1003.32 | 387454 | 1.3595 | 0.0398 | 316.01 |
| Data used for pathlength calibration (the first zero step): $T_{SoS}$ = 4.5372 °C, $P$ = 1004.41 mbar, $t_m^0$ = 366278 ns, $W^0$ = 334.28 m/s. | | | | | | | | | | | | |

Table 109. Ethyl acetate/dry air results (15 °C isotherm)

| $x_T$/%SAT | | Zero Step | | | $\Delta m_{read}$/µg | Non-Zero Step | | | | | | |
|---|---|---|---|---|---|---|---|---|---|---|---|---|
| | | $T_{DVS}$/°C | $P$/mbar | $\rho^0$/(kg/m$^3$) | | $T_{DVS}$/°C | $T_{SoS}$/°C | $P$/mbar | $t_m$/ns | $\rho$/(kg/m$^3$) | $x$ | $W_m$/(m/s) |
| 10 | A | 14.56 | 1008.24 | 1.2219 | 265 | 14.52 | 14.1841 | 1008.10 | 364608 | 1.2422 | 0.0081 | 335.88 |
| | D | 14.47 | 998.70 | 1.2107 | 261 | 14.55 | 14.1878 | 998.64 | 364670 | 1.2307 | 0.0082 | 335.82 |
| 20 | A | 14.51 | 1007.66 | 1.2214 | 501 | 14.57 | 14.1944 | 1007.24 | 368707 | 1.2598 | 0.0156 | 332.14 |
| | D | 14.52 | 998.42 | 1.2101 | 509 | 14.54 | 14.1921 | 998.27 | 368769 | 1.2492 | 0.0158 | 332.09 |
| 30 | A | 14.52 | 1006.75 | 1.2203 | 743 | 14.54 | 14.1876 | 1006.47 | 372606 | 1.2772 | 0.0229 | 328.67 |
| | D | 14.53 | 999.06 | 1.2109 | 745 | 14.51 | 14.1786 | 998.71 | 372691 | 1.2680 | 0.0231 | 328.59 |
| 40 | A | 14.52 | 1006.17 | 1.2196 | 971 | 14.54 | 14.1860 | 1005.88 | 376320 | 1.2940 | 0.0299 | 325.42 |
| | D | 14.50 | 999.80 | 1.2119 | 969 | 14.49 | 14.1537 | 999.38 | 376404 | 1.2862 | 0.0300 | 325.35 |
| 50 | A | 14.54 | 1005.69 | 1.2189 | 1201 | 14.57 | 14.2086 | 1005.62 | 379937 | 1.3110 | 0.0369 | 322.32 |
| | D | 14.53 | 1000.62 | 1.2128 | 1197 | 14.55 | 14.2054 | 1000.20 | 380025 | 1.3045 | 0.0371 | 322.25 |
| 60 | A | 14.54 | 1005.53 | 1.2187 | 1423 | 14.54 | 14.2007 | 1005.51 | 383413 | 1.3277 | 0.0436 | 319.40 |
| | D | 14.55 | 1001.76 | 1.2141 | 1415 | 14.51 | 14.1708 | 1001.21 | 383475 | 1.3225 | 0.0437 | 319.35 |
| 70 | A | 14.52 | 1005.46 | 1.2187 | 1640 | 14.54 | 14.1924 | 1005.37 | 386823 | 1.3443 | 0.0503 | 316.59 |
| | D | 14.50 | 1002.68 | 1.2154 | 1633 | 14.51 | 14.1659 | 1002.24 | 386879 | 1.3406 | 0.0504 | 316.54 |
| 80 | A | 14.51 | 1005.24 | 1.2185 | 1852 | 14.52 | 14.1730 | 1005.01 | 390136 | 1.3604 | 0.0569 | 313.90 |
| | D | 14.54 | 1003.34 | 1.2160 | 1851 | 14.51 | 14.1729 | 1002.98 | 390188 | 1.3579 | 0.0569 | 313.86 |
| 90 | A | 14.51 | 1004.64 | 1.2177 | 2074 | 14.53 | 14.1846 | 1004.59 | 393475 | 1.3767 | 0.0636 | 311.24 |
| | D | 14.52 | 1004.03 | 1.2170 | 2067 | 14.53 | 14.1816 | 1003.72 | 393487 | 1.3753 | 0.0636 | 311.23 |
| 95 | | 14.56 | 1004.49 | 1.2173 | 2178 | 14.53 | 14.1986 | 1004.18 | 395085 | 1.3843 | 0.0669 | 309.97 |
| Data used for pathlength calibration (the first zero step): $T_{SoS}$ = 14.1886 °C, $P$ = 1008.24 mbar, $t_m^0$ = 360122 ns, $W^0$ = 340.06 m/s. | | | | | | | | | | | | |

Table 110. Ethyl acetate/dry air results (25 °C isotherm)

| $x_T$/%SAT | | Zero Step | | | $\Delta m_{read}$/µg | Non-Zero Step | | | | | | |
|---|---|---|---|---|---|---|---|---|---|---|---|---|
| | | $T_{DVS}$/°C | $P$/mbar | $\rho^0$/(kg/m$^3$) | | $T_{DVS}$/°C | $T_{SoS}$/°C | $P$/mbar | $t_m$/ns | $\rho$/(kg/m$^3$) | $x$ | $W_m$/(m/s) |
| 5 | A | 24.48 | 997.93 | 1.1689 | 241 | 24.50 | 24.0759 | 998.04 | 358119 | 1.1874 | 0.0077 | 341.80 |
| | D | 24.36 | 1001.61 | 1.1737 | 232 | 24.37 | 23.9622 | 1001.28 | 358118 | 1.1916 | 0.0076 | 341.80 |
| 10 | A | 24.49 | 998.01 | 1.1690 | 455 | 24.46 | 24.0590 | 998.16 | 361807 | 1.2039 | 0.0144 | 338.32 |
| | D | 24.35 | 1001.89 | 1.1741 | 447 | 24.37 | 23.9546 | 1001.74 | 361765 | 1.2083 | 0.0143 | 338.36 |
| 15 | A | 24.46 | 998.39 | 1.1696 | 667 | 24.39 | 23.9889 | 998.98 | 365319 | 1.2207 | 0.0209 | 335.06 |
| | D | 24.36 | 1002.69 | 1.1750 | 649 | 24.37 | 23.9588 | 1002.30 | 365248 | 1.2248 | 0.0209 | 335.13 |
| 20 | A | 24.35 | 999.62 | 1.1714 | 862 | 24.46 | 24.0096 | 1000.03 | 368700 | 1.2375 | 0.0275 | 331.99 |
| | D | 24.36 | 1003.47 | 1.1759 | 854 | 24.37 | 23.9604 | 1003.41 | 368551 | 1.2414 | 0.0272 | 332.13 |
| 25 | A | 24.47 | 1000.26 | 1.1717 | 1067 | 24.49 | 24.0565 | 1000.92 | 371938 | 1.2535 | 0.0337 | 329.10 |
| | D | 24.38 | 1003.48 | 1.1759 | 1051 | 24.38 | 23.9743 | 1003.53 | 371785 | 1.2564 | 0.0334 | 329.24 |
| 30 | A | 24.49 | 1001.29 | 1.1729 | 1248 | 24.40 | 24.0054 | 1001.34 | 375034 | 1.2685 | 0.0396 | 326.39 |
| | D | 24.37 | 1003.77 | 1.1762 | 1237 | 24.38 | 23.9708 | 1003.53 | 374920 | 1.2710 | 0.0394 | 326.48 |
| 35 | A | 24.44 | 1001.68 | 1.1735 | 1440 | 24.48 | 24.0431 | 1001.91 | 378096 | 1.2839 | 0.0458 | 323.74 |
| | D | 24.47 | 1003.24 | 1.1752 | 1440 | 24.40 | 24.0060 | 1003.79 | 377922 | 1.2856 | 0.0453 | 323.89 |
| 40 | A | 24.46 | 1002.16 | 1.1740 | 1623 | 24.48 | 24.0554 | 1002.27 | 381041 | 1.2984 | 0.0516 | 321.24 |
| | D | 24.46 | 1002.94 | 1.1749 | 1621 | 24.49 | 24.0651 | 1002.80 | 380968 | 1.2991 | 0.0516 | 321.30 |
| 45 | A | 24.46 | 1002.55 | 1.1744 | 1805 | 24.48 | 24.0551 | 1002.67 | 383894 | 1.3128 | 0.0573 | 318.85 |
| | D | 24.36 | 1002.82 | 1.1752 | 1791 | 24.37 | 23.9559 | 1002.82 | 383716 | 1.3124 | 0.0569 | 319.00 |
| 50 | A | 24.44 | 1002.93 | 1.1750 | 1977 | 24.46 | 24.0398 | 1002.89 | 386675 | 1.3265 | 0.0629 | 316.56 |
| | D | 24.37 | 1003.22 | 1.1756 | 1963 | 24.37 | 23.9643 | 1002.91 | 386499 | 1.3260 | 0.0625 | 316.70 |
| 55 | A | 24.44 | 1003.26 | 1.1754 | 2153 | 24.46 | 24.0340 | 1003.22 | 389389 | 1.3404 | 0.0684 | 314.35 |
| | D | 24.48 | 1002.91 | 1.1748 | 2155 | 24.40 | 24.0143 | 1003.25 | 389228 | 1.3400 | 0.0681 | 314.48 |
| 60 | A | 24.45 | 1003.28 | 1.1754 | 2325 | 24.45 | 24.0312 | 1003.14 | 392046 | 1.3535 | 0.0739 | 312.22 |
| | D | 24.45 | 1002.97 | 1.1750 | 2328 | 24.46 | 24.0504 | 1003.06 | 391970 | 1.3534 | 0.0739 | 312.28 |

| | | | | | | | | | | | | |
|---|---|---|---|---|---|---|---|---|---|---|---|---|
| 65 | A | 24.44 | 1003.28 | 1.1754 | 2501 | 24.45 | 24.0248 | 1003.51 | 394629 | 1.3670 | 0.0793 | 310.18 |
| | D | 24.47 | 1003.22 | 1.1752 | 2491 | 24.47 | 24.0599 | 1002.73 | 394601 | 1.3661 | 0.0794 | 310.20 |
| 70 | A | 24.44 | 1003.83 | 1.1760 | 2669 | 24.44 | 24.0229 | 1003.81 | 397225 | 1.3806 | 0.0847 | 308.15 |
| | D | 24.47 | 1003.69 | 1.1758 | 2666 | 24.48 | 24.0591 | 1003.38 | 397200 | 1.3800 | 0.0848 | 308.17 |
| 75 | A | 24.43 | 1004.01 | 1.1763 | 2838 | 24.43 | 24.0145 | 1004.29 | 399690 | 1.3937 | 0.0898 | 306.25 |
| | D | 24.45 | 1004.16 | 1.1764 | 2830 | 24.46 | 24.0417 | 1003.84 | 399658 | 1.3932 | 0.0899 | 306.28 |
| 80 | A | 24.42 | 1004.65 | 1.1771 | 3003 | 24.42 | 24.0039 | 1004.89 | 402098 | 1.4071 | 0.0950 | 304.42 |
| | D | 24.45 | 1004.32 | 1.1765 | 3002 | 24.46 | 24.0416 | 1004.39 | 402108 | 1.4066 | 0.0951 | 304.41 |
| 85 | A | 24.41 | 1004.83 | 1.1773 | 3168 | 24.42 | 24.0018 | 1004.98 | 404544 | 1.4201 | 0.1003 | 302.58 |
| | D | 24.45 | 1004.37 | 1.1766 | 3163 | 24.46 | 24.0394 | 1004.11 | 404589 | 1.4190 | 0.1004 | 302.54 |
| 90 | A | 24.42 | 1005.13 | 1.1776 | 3327 | 24.43 | 24.0093 | 1004.91 | 406956 | 1.4326 | 0.1055 | 300.78 |
| | D | 24.44 | 1004.70 | 1.1770 | 3325 | 24.45 | 24.0313 | 1004.38 | 406976 | 1.4318 | 0.1056 | 300.77 |
| 95 | | 24.43 | 1004.87 | 1.1773 | 3491 | 24.45 | 24.0242 | 1004.78 | 409313 | 1.4448 | 0.1107 | 299.05 |
| Data used for pathlength calibration (the first zero step): $T_{SoS}$ = 24.0564 °C, $P$ = 997.93 mbar, $t_m^0$ = 353915 ns, $W^0$ = 345.86 m/s. | | | | | | | | | | | | |

Table 111. Ethyl acetate/dry air results (35 °C isotherm)

| $x_T$/%SAT | | Zero Step | | | $\Delta m_{read}$/µg | Non-Zero Step | | | | | | |
|---|---|---|---|---|---|---|---|---|---|---|---|---|
| | | $T_{DVS}$/°C | $P$/mbar | $\rho^0$/(kg/m$^3$) | | $T_{DVS}$/°C | $T_{SoS}$/°C | $P$/mbar | $t_m$/ns | $\rho$/(kg/m$^3$) | $x$ | $W_m$/(m/s) |
| 10 | A | 34.50 | 1003.11 | 1.1367 | 758 | 34.50 | 34.0855 | 1003.00 | 361054 | 1.1947 | 0.0250 | 338.63 |
| | D | 34.59 | 1004.69 | 1.1381 | 765 | 34.51 | 34.1236 | 1004.70 | 361016 | 1.1967 | 0.0250 | 338.66 |
| 20 | A | 34.48 | 1003.03 | 1.1366 | 1419 | 34.44 | 34.0472 | 1002.89 | 372104 | 1.2454 | 0.0467 | 328.57 |
| | D | 34.47 | 1004.51 | 1.1383 | 1427 | 34.55 | 34.1139 | 1004.53 | 372122 | 1.2477 | 0.0470 | 328.55 |
| 30 | A | 34.42 | 1003.01 | 1.1368 | 2033 | 34.43 | 34.0241 | 1002.85 | 382088 | 1.2926 | 0.0669 | 319.98 |
| | D | 34.43 | 1004.25 | 1.1382 | 2035 | 34.42 | 34.0159 | 1004.37 | 381914 | 1.2942 | 0.0667 | 320.13 |
| 40 | A | 34.43 | 1003.00 | 1.1368 | 2617 | 34.44 | 34.0340 | 1002.98 | 391144 | 1.3374 | 0.0860 | 312.58 |
| | D | 34.44 | 1003.93 | 1.1378 | 2617 | 34.44 | 34.0323 | 1004.05 | 390971 | 1.3383 | 0.0858 | 312.71 |
| 50 | A | 34.43 | 1002.81 | 1.1366 | 3167 | 34.42 | 34.0171 | 1002.81 | 399482 | 1.3792 | 0.1039 | 306.05 |
| | D | 34.46 | 1003.74 | 1.1375 | 3171 | 34.46 | 34.0476 | 1003.94 | 399360 | 1.3805 | 0.1039 | 306.15 |
| 60 | A | 34.41 | 1002.94 | 1.1368 | 3692 | 34.41 | 34.0131 | 1003.10 | 407188 | 1.4197 | 0.1210 | 300.26 |
| | D | 34.46 | 1003.60 | 1.1373 | 3692 | 34.47 | 34.0568 | 1003.64 | 407095 | 1.4203 | 0.1211 | 300.33 |
| 70 | A | 34.42 | 1003.29 | 1.1372 | 4192 | 34.40 | 33.9969 | 1003.33 | 414414 | 1.4584 | 0.1374 | 295.02 |
| | D | 34.49 | 1003.60 | 1.1372 | 4195 | 34.47 | 34.0733 | 1003.65 | 414363 | 1.4587 | 0.1375 | 295.06 |
| 80 | A | 34.41 | 1003.35 | 1.1372 | 4678 | 34.42 | 34.0076 | 1003.47 | 421260 | 1.4958 | 0.1533 | 290.23 |
| | D | 34.49 | 1003.88 | 1.1376 | 4686 | 34.50 | 34.0872 | 1003.76 | 421324 | 1.4967 | 0.1537 | 290.19 |
| 90 | A | 34.39 | 1003.68 | 1.1377 | 5141 | 34.40 | 33.9922 | 1003.76 | 427688 | 1.5316 | 0.1683 | 285.87 |
| | D | 34.48 | 1003.96 | 1.1377 | 5162 | 34.49 | 34.0854 | 1003.96 | 427886 | 1.5332 | 0.1691 | 285.74 |
| 95 | | 34.43 | 1003.87 | 1.1378 | 5383 | 34.47 | 34.0586 | 1003.89 | 430932 | 1.5503 | 0.1763 | 283.72 |
| Data used for pathlength calibration (the first zero step): $T_{SoS}$ = 34.0772 °C, $P$ = 1003.11 mbar, $t_m^0$ = 347678 ns, $W^0$ = 351.65 m/s. | | | | | | | | | | | | |

Table 112. Ethyl acetate/dry air results (45 °C isotherm)

| $x_T$/%SAT | | Zero Step | | | $\Delta m_{read}$/µg | Non-Zero Step | | | | | | |
|---|---|---|---|---|---|---|---|---|---|---|---|---|
| | | $T_{DVS}$/°C | $P$/mbar | $\rho^0$/(kg/m$^3$) | | $T_{DVS}$/°C | $T_{SoS}$/°C | $P$/mbar | $t_m$/ns | $\rho$/(kg/m$^3$) | $x$ | $W_m$/(m/s) |
| 10 | A | 43.98 | 1018.11 | 1.1191 | 1259 | 44.02 | 43.6747 | 1018.10 | 364215 | 1.2156 | 0.0421 | 335.61 |
| | D | 44.02 | 1017.34 | 1.1181 | 1259 | 43.96 | 43.6403 | 1017.40 | 363955 | 1.2146 | 0.0419 | 335.85 |
| 20 | A | 44.01 | 1017.92 | 1.1188 | 2311 | 44.02 | 43.6895 | 1018.09 | 381204 | 1.2958 | 0.0770 | 320.65 |
| | D | 43.98 | 1017.26 | 1.1182 | 2296 | 44.01 | 43.6463 | 1017.38 | 380833 | 1.2941 | 0.0767 | 320.97 |
| 30 | A | 44.03 | 1018.11 | 1.1189 | 3263 | 44.10 | 43.7327 | 1018.08 | 395788 | 1.3690 | 0.1090 | 308.84 |
| | D | 44.02 | 1017.63 | 1.1184 | 3232 | 43.99 | 43.6515 | 1017.37 | 395234 | 1.3661 | 0.1080 | 309.27 |
| 40 | A | 44.11 | 1018.07 | 1.1186 | 4137 | 44.10 | 43.7683 | 1018.18 | 408543 | 1.4356 | 0.1379 | 299.20 |
| | D | 43.93 | 1017.72 | 1.1188 | 4078 | 43.98 | 43.6155 | 1017.71 | 407603 | 1.4313 | 0.1361 | 299.89 |
| 50 | A | 44.10 | 1018.46 | 1.1190 | 4933 | 44.09 | 43.7645 | 1018.40 | 419781 | 1.4971 | 0.1644 | 291.19 |
| | D | 43.92 | 1017.48 | 1.1186 | 4873 | 43.93 | 43.6167 | 1017.50 | 418826 | 1.4920 | 0.1624 | 291.85 |
| 60 | A | 44.06 | 1018.64 | 1.1194 | 5666 | 44.05 | 43.7406 | 1018.57 | 429729 | 1.5535 | 0.1886 | 284.45 |
| | D | 43.98 | 1017.32 | 1.1182 | 5615 | 43.96 | 43.6433 | 1017.46 | 428942 | 1.5485 | 0.1870 | 284.97 |
| 70 | A | 44.01 | 1018.62 | 1.1195 | 6339 | 44.01 | 43.6923 | 1018.45 | 438787 | 1.6053 | 0.2110 | 278.57 |
| | D | 43.91 | 1017.43 | 1.1186 | 6280 | 43.92 | 43.5981 | 1017.40 | 437942 | 1.5998 | 0.2091 | 279.11 |
| 80 | A | 44.00 | 1018.40 | 1.1193 | 7004 | 44.05 | 43.7221 | 1018.31 | 447407 | 1.6560 | 0.2331 | 273.21 |
| | D | 43.99 | 1017.73 | 1.1186 | 6946 | 43.94 | 43.6259 | 1017.65 | 446579 | 1.6509 | 0.2311 | 273.71 |
| 90 | A | 43.97 | 1018.16 | 1.1192 | 7582 | 43.95 | 43.6471 | 1017.96 | 454854 | 1.7002 | 0.2522 | 268.73 |
| | D | 44.00 | 1017.75 | 1.1186 | 7574 | 43.99 | 43.6474 | 1017.69 | 454638 | 1.6991 | 0.2520 | 268.86 |
| 95 | | 43.93 | 1018.02 | 1.1192 | 7866 | 43.97 | 43.6318 | 1017.80 | 458356 | 1.7220 | 0.2617 | 266.68 |
| Data used for pathlength calibration (the first zero step): $T_{SoS}$ = 43.6362 °C, $P$ = 1018.11 mbar, $t_m^0$ = 342307 ns, $W^0$ = 357.09 m/s. | | | | | | | | | | | | |

Table 113. Ethyl acetate/dry air results (55 °C isotherm)

| $x_T$/%SAT | | Zero Step | | | $\Delta m_{read}$/µg | Non-Zero Step | | | | | | |
|---|---|---|---|---|---|---|---|---|---|---|---|---|
| | | $T_{DVS}$/°C | $P$/mbar | $\rho^0$/(kg/m$^3$) | | $T_{DVS}$/°C | $T_{SoS}$/°C | $P$/mbar | $t_m$/ns | $\rho$/(kg/m$^3$) | $x$ | $W_m$/(m/s) |
| 10 | A | 53.71 | 1018.48 | 1.0861 | 2169 | 53.72 | 53.4496 | 1018.25 | 374256 | 1.2523 | 0.0748 | 326.24 |
| | D | 53.69 | 1008.91 | 1.0759 | 2141 | 53.66 | 53.3971 | 1008.39 | 374013 | 1.2400 | 0.0746 | 326.45 |
| 20 | A | 53.72 | 1018.09 | 1.0856 | 3846 | 53.70 | 53.4368 | 1017.94 | 399933 | 1.3804 | 0.1323 | 305.29 |
| | D | 53.66 | 1009.37 | 1.0765 | 3794 | 53.70 | 53.4296 | 1009.37 | 399347 | 1.3672 | 0.1316 | 305.74 |
| 30 | A | 53.69 | 1017.66 | 1.0853 | 5245 | 53.66 | 53.3961 | 1017.51 | 419993 | 1.4872 | 0.1803 | 290.71 |
| | D | 53.71 | 1009.86 | 1.0769 | 5178 | 53.70 | 53.4222 | 1009.76 | 419130 | 1.4737 | 0.1793 | 291.31 |
| 40 | A | 53.71 | 1017.38 | 1.0849 | 6481 | 53.71 | 53.4428 | 1017.07 | 436719 | 1.5815 | 0.2227 | 279.58 |
| | D | 53.72 | 1010.37 | 1.0774 | 6362 | 53.72 | 53.4511 | 1010.17 | 435192 | 1.5649 | 0.2201 | 280.56 |
| 50 | A | 53.70 | 1016.83 | 1.0844 | 7548 | 53.70 | 53.4289 | 1016.62 | 450586 | 1.6628 | 0.2592 | 270.97 |
| | D | 53.73 | 1010.43 | 1.0774 | 7387 | 53.69 | 53.4242 | 1010.13 | 448720 | 1.6435 | 0.2554 | 272.10 |
| 60 | A | 53.72 | 1016.44 | 1.0839 | 8490 | 53.72 | 53.4519 | 1016.30 | 462439 | 1.7344 | 0.2914 | 264.03 |
| | D | 53.74 | 1011.39 | 1.0784 | 8327 | 53.74 | 53.4634 | 1011.00 | 460644 | 1.7165 | 0.2875 | 265.06 |
| 70 | A | 53.72 | 1016.03 | 1.0834 | 9330 | 53.73 | 53.4509 | 1016.09 | 472685 | 1.7984 | 0.3201 | 258.31 |
| | D | 53.69 | 1012.13 | 1.0794 | 9166 | 53.73 | 53.4635 | 1011.77 | 470955 | 1.7818 | 0.3161 | 259.25 |
| 80 | A | 53.69 | 1015.64 | 1.0831 | 10068 | 53.72 | 53.4378 | 1015.18 | 481743 | 1.8546 | 0.3457 | 253.45 |
| | D | 53.73 | 1012.98 | 1.0802 | 9961 | 53.73 | 53.4530 | 1012.55 | 480454 | 1.8435 | 0.3429 | 254.13 |
| 90 | A | 53.71 | 1014.90 | 1.0822 | 10765 | 53.72 | 53.4487 | 1014.59 | 489884 | 1.9072 | 0.3695 | 249.24 |
| | D | 53.72 | 1013.34 | 1.0806 | 10691 | 53.73 | 53.4649 | 1012.95 | 489148 | 1.8998 | 0.3677 | 249.61 |
| 95 | | 53.71 | 1014.14 | 1.0815 | 11039 | 53.69 | 53.4254 | 1013.69 | 493163 | 1.9274 | 0.3791 | 247.58 |
| Data used for pathlength calibration (the first zero step): $T_{SoS}$ = 53.4354 °C, $P$ = 1018.48 mbar, $t_m^0$ = 336747 ns, $W^0$ = 362.58 m/s. | | | | | | | | | | | | |

## A6.11 Methanol/dry air

Table 114. Methanol/dry air results (5 °C isotherm)

| $x_T$/%SAT | | Zero Step | | | $\Delta m_{read}$/µg | Non-Zero Step | | | | | | |
|---|---|---|---|---|---|---|---|---|---|---|---|---|
| | | $T_{DVS}$/°C | $P$/mbar | $\rho^0$/(kg/m$^3$) | | $T_{DVS}$/°C | $T_{SoS}$/°C | $P$/mbar | $t_m$/ns | $\rho$/(kg/m$^3$) | $x$ | $W_m$/(m/s) |
| 10 | A | 5.28 | 1003.29 | 1.2565 | 13 | 5.30 | 5.1741 | 1003.28 | 365779 | 1.2575 | 0.0074 | 334.33 |
| | D | 5.40 | 1006.19 | 1.2596 | 9 | 5.41 | 5.2871 | 1006.00 | 365692 | 1.2604 | 0.0071 | 334.41 |
| 20 | A | 5.27 | 1003.42 | 1.2568 | 30 | 5.28 | 5.1688 | 1003.82 | 366134 | 1.2591 | 0.0132 | 334.01 |
| | D | 5.39 | 1005.96 | 1.2594 | 24 | 5.41 | 5.2820 | 1005.96 | 366043 | 1.2612 | 0.0134 | 334.09 |
| 30 | A | 5.26 | 1003.94 | 1.2575 | 35 | 5.28 | 5.1623 | 1004.01 | 366503 | 1.2601 | 0.0187 | 333.67 |
| | D | 5.39 | 1006.05 | 1.2595 | 36 | 5.39 | 5.2720 | 1006.12 | 366404 | 1.2623 | 0.0188 | 333.76 |
| 40 | A | 5.26 | 1004.03 | 1.2576 | 48 | 5.27 | 5.1574 | 1004.19 | 366898 | 1.2613 | 0.0248 | 333.31 |
| | D | 5.37 | 1006.06 | 1.2596 | 45 | 5.39 | 5.2610 | 1006.02 | 366790 | 1.2630 | 0.0248 | 333.41 |
| 50 | A | 5.26 | 1004.15 | 1.2577 | 58 | 5.29 | 5.1703 | 1004.23 | 367353 | 1.2622 | 0.0312 | 332.90 |
| | D | 5.37 | 1005.82 | 1.2593 | 56 | 5.38 | 5.2627 | 1005.90 | 367235 | 1.2636 | 0.0297 | 333.01 |
| 60 | A | 5.27 | 1004.34 | 1.2579 | 68 | 5.28 | 5.1714 | 1004.37 | 367911 | 1.2631 | 0.0366 | 332.40 |
| | D | 5.37 | 1005.56 | 1.2590 | 69 | 5.39 | 5.2657 | 1005.74 | 367782 | 1.2643 | 0.0361 | 332.51 |
| 70 | A | 5.26 | 1004.38 | 1.2580 | 80 | 5.28 | 5.1690 | 1004.47 | 368630 | 1.2641 | 0.0426 | 331.75 |
| | D | 5.36 | 1005.61 | 1.2591 | 78 | 5.38 | 5.2525 | 1005.52 | 368508 | 1.2651 | 0.0431 | 331.86 |
| 80 | A | 5.27 | 1004.48 | 1.2581 | 92 | 5.29 | 5.1763 | 1004.59 | 369565 | 1.2651 | 0.0487 | 330.91 |
| | D | 5.29 | 1005.10 | 1.2588 | 90 | 5.33 | 5.2075 | 1005.13 | 369475 | 1.2657 | 0.0492 | 330.99 |
| 90 | A | 5.26 | 1004.63 | 1.2583 | 102 | 5.28 | 5.1767 | 1004.67 | 370748 | 1.2661 | 0.0549 | 329.85 |
| | D | 5.27 | 1004.94 | 1.2587 | 102 | 5.29 | 5.1772 | 1005.02 | 370677 | 1.2665 | 0.0546 | 329.92 |
| 95 | | 5.28 | 1004.68 | 1.2583 | 109 | 5.29 | 5.1802 | 1004.70 | 371411 | 1.2666 | 0.0582 | 329.26 |
| Data used for pathlength calibration (the first zero step): $T_{SoS}$ = 5.1555 °C, $P$ = 1003.29 mbar, $t_m^0$ = 365425 ns, $W^0$ = 334.66 m/s. | | | | | | | | | | | | |

Table 115. Methanol/dry air results (15 °C isotherm)

| $x_T$/%SAT | | Zero Step | | | $\Delta m_{read}$/µg | Non-Zero Step | | | | | | |
|---|---|---|---|---|---|---|---|---|---|---|---|---|
| | | $T_{DVS}$/°C | $P$/mbar | $\rho^0$/(kg/m$^3$) | | $T_{DVS}$/°C | $T_{SoS}$/°C | $P$/mbar | $t_m$/ns | $\rho$/(kg/m$^3$) | $x$ | $W_m$/(m/s) |
| 10 | A | 14.66 | 1020.19 | 1.2360 | 22 | 14.67 | 14.4258 | 1020.21 | 360295 | 1.2376 | 0.0123 | 339.57 |
| | D | 14.71 | 1015.47 | 1.2300 | 18 | 14.69 | 14.4536 | 1015.16 | 360275 | 1.2314 | 0.0118 | 339.59 |
| 20 | A | 14.67 | 1020.27 | 1.2360 | 44 | 14.68 | 14.4396 | 1020.54 | 360907 | 1.2394 | 0.0222 | 339.00 |
| | D | 14.72 | 1016.24 | 1.2309 | 37 | 14.70 | 14.4638 | 1015.91 | 360874 | 1.2337 | 0.0225 | 339.03 |
| 30 | A | 14.67 | 1020.45 | 1.2362 | 60 | 14.68 | 14.4326 | 1020.53 | 361516 | 1.2408 | 0.0322 | 338.43 |
| | D | 14.77 | 1017.04 | 1.2317 | 55 | 14.71 | 14.4934 | 1016.68 | 361462 | 1.2359 | 0.0316 | 338.47 |
| 40 | A | 14.67 | 1020.37 | 1.2361 | 75 | 14.67 | 14.4313 | 1020.29 | 362165 | 1.2419 | 0.0418 | 337.82 |
| | D | 14.75 | 1017.75 | 1.2326 | 72 | 14.71 | 14.4805 | 1017.49 | 362125 | 1.2381 | 0.0406 | 337.86 |
| 50 | A | 14.68 | 1020.26 | 1.2360 | 92 | 14.67 | 14.4280 | 1020.13 | 362917 | 1.2430 | 0.0511 | 337.12 |
| | D | 14.72 | 1017.78 | 1.2328 | 91 | 14.70 | 14.4620 | 1017.63 | 362902 | 1.2397 | 0.0505 | 337.13 |
| 60 | A | 14.67 | 1019.91 | 1.2356 | 110 | 14.66 | 14.4201 | 1019.78 | 363836 | 1.2440 | 0.0609 | 336.27 |
| | D | 14.67 | 1018.04 | 1.2333 | 106 | 14.68 | 14.4336 | 1017.81 | 363839 | 1.2415 | 0.0608 | 336.26 |
| 70 | A | 14.65 | 1019.49 | 1.2351 | 125 | 14.68 | 14.4344 | 1019.24 | 364988 | 1.2447 | 0.0716 | 335.21 |
| | D | 14.66 | 1018.27 | 1.2336 | 128 | 14.68 | 14.4374 | 1018.17 | 364986 | 1.2434 | 0.0718 | 335.21 |
| 80 | A | 14.70 | 1019.04 | 1.2344 | 145 | 14.67 | 14.4241 | 1018.82 | 366425 | 1.2455 | 0.0804 | 333.89 |
| | D | 14.68 | 1018.31 | 1.2336 | 148 | 14.66 | 14.4201 | 1018.23 | 366425 | 1.2449 | 0.0810 | 333.89 |
| 90 | A | 14.69 | 1018.78 | 1.2341 | 165 | 14.70 | 14.4520 | 1018.60 | 368181 | 1.2468 | 0.0923 | 332.30 |
| | D | 14.72 | 1018.33 | 1.2334 | 170 | 14.67 | 14.4430 | 1018.28 | 368169 | 1.2465 | 0.0919 | 332.31 |
| 95 | | 14.65 | 1018.57 | 1.2340 | 172 | 14.73 | 14.4538 | 1018.41 | 369176 | 1.2472 | 0.0977 | 331.40 |
| Data used for pathlength calibration (the first zero step): $T_{SoS}$ = 14.4027 °C, $P$ = 1020.19 mbar, $t_m^0$ = 359642 ns, $W^0$ = 340.19 m/s. | | | | | | | | | | | | |

Table 116. Methanol/dry air results (25 °C isotherm)

| $x_T$/%SAT | | Zero Step | | | $\Delta m_{read}$/µg | Non-Zero Step | | | | | | |
|---|---|---|---|---|---|---|---|---|---|---|---|---|
| | | $T_{DVS}$/°C | $P$/mbar | $\rho^0$/(kg/m$^3$) | | $T_{DVS}$/°C | $T_{SoS}$/°C | $P$/mbar | $t_m$/ns | $\rho$/(kg/m$^3$) | $x$ | $W_m$/(m/s) |
| 5 | A | 24.35 | 1004.40 | 1.1770 | 25 | 24.36 | 23.9157 | 1004.54 | 354710 | 1.1790 | 0.0134 | 345.10 |
| | D | 24.26 | 1001.56 | 1.1741 | 16 | 24.28 | 23.8293 | 1001.36 | 354646 | 1.1753 | 0.0115 | 345.17 |
| 10 | A | 24.37 | 1004.50 | 1.1771 | 39 | 24.39 | 23.9346 | 1004.45 | 355274 | 1.1801 | 0.0237 | 344.56 |
| | D | 24.27 | 1002.20 | 1.1748 | 31 | 24.27 | 23.8326 | 1001.80 | 355211 | 1.1771 | 0.0213 | 344.62 |
| 15 | A | 24.39 | 1004.48 | 1.1770 | 50 | 24.41 | 23.9597 | 1004.42 | 355797 | 1.1808 | 0.0300 | 344.05 |
| | D | 24.27 | 1002.84 | 1.1755 | 47 | 24.29 | 23.8388 | 1002.56 | 355746 | 1.1792 | 0.0305 | 344.10 |
| 20 | A | 24.40 | 1004.33 | 1.1768 | 67 | 24.39 | 23.9484 | 1004.34 | 356312 | 1.1819 | 0.0387 | 343.55 |
| | D | 24.27 | 1003.16 | 1.1759 | 66 | 24.29 | 23.8398 | 1003.03 | 356266 | 1.1810 | 0.0397 | 343.60 |
| 25 | A | 24.39 | 1004.39 | 1.1769 | 84 | 24.44 | 23.9815 | 1004.41 | 356799 | 1.1833 | 0.0497 | 343.08 |
| | D | 24.28 | 1003.11 | 1.1758 | 83 | 24.29 | 23.8392 | 1003.19 | 356792 | 1.1822 | 0.0474 | 343.09 |
| 30 | A | 24.44 | 1004.43 | 1.1767 | 103 | 24.39 | 23.9746 | 1004.53 | 357316 | 1.1846 | 0.0570 | 342.59 |
| | D | 24.28 | 1003.26 | 1.1760 | 96 | 24.30 | 23.8536 | 1003.17 | 357335 | 1.1833 | 0.0569 | 342.57 |
| 35 | A | 24.33 | 1004.55 | 1.1773 | 114 | 24.35 | 23.9147 | 1004.72 | 357893 | 1.1860 | 0.0646 | 342.03 |
| | D | 24.29 | 1003.48 | 1.1762 | 111 | 24.29 | 23.8517 | 1003.41 | 357919 | 1.1847 | 0.0647 | 342.01 |
| 40 | A | 24.32 | 1004.87 | 1.1777 | 131 | 24.33 | 23.8948 | 1005.06 | 358484 | 1.1878 | 0.0742 | 341.47 |
| | D | 24.30 | 1003.82 | 1.1766 | 120 | 24.32 | 23.8876 | 1003.60 | 358496 | 1.1858 | 0.0719 | 341.46 |
| 45 | A | 24.29 | 1005.42 | 1.1785 | 147 | 24.31 | 23.8687 | 1005.74 | 359154 | 1.1898 | 0.0825 | 340.83 |
| | D | 24.43 | 1004.26 | 1.1766 | 140 | 24.42 | 23.9837 | 1004.02 | 359079 | 1.1873 | 0.0828 | 340.91 |
| 50 | A | 24.29 | 1006.01 | 1.1792 | 162 | 24.30 | 23.8585 | 1006.33 | 359830 | 1.1916 | 0.0904 | 340.19 |
| | D | 24.40 | 1004.90 | 1.1774 | 151 | 24.42 | 23.9668 | 1004.52 | 359784 | 1.1890 | 0.0910 | 340.24 |
| 55 | A | 24.29 | 1006.53 | 1.1798 | 173 | 24.29 | 23.8505 | 1006.60 | 360591 | 1.1930 | 0.0988 | 339.48 |
| | D | 24.33 | 1005.60 | 1.1786 | 168 | 24.39 | 23.9210 | 1005.33 | 360545 | 1.1914 | 0.1010 | 339.52 |
| 60 | A | 24.28 | 1006.66 | 1.1800 | 187 | 24.30 | 23.8509 | 1006.86 | 361387 | 1.1943 | 0.1062 | 338.73 |
| | D | 24.26 | 1006.21 | 1.1795 | 178 | 24.26 | 23.8168 | 1005.86 | 361366 | 1.1932 | 0.1054 | 338.75 |

| | | | | | | | | | | | | |
|---|---|---|---|---|---|---|---|---|---|---|---|---|
| 65 | A | 24.27 | 1006.60 | 1.1800 | 201 | 24.28 | 23.8357 | 1006.81 | 362267 | 1.1954 | 0.1138 | 337.91 |
| | D | 24.27 | 1006.73 | 1.1801 | 193 | 24.26 | 23.8252 | 1006.46 | 362228 | 1.1949 | 0.1129 | 337.94 |
| 70 | A | 24.27 | 1006.87 | 1.1803 | 208 | 24.29 | 23.8450 | 1006.67 | 363229 | 1.1962 | 0.1216 | 337.01 |
| | D | 24.25 | 1007.19 | 1.1807 | 207 | 24.27 | 23.8259 | 1006.93 | 363201 | 1.1966 | 0.1216 | 337.04 |
| 75 | A | 24.28 | 1006.63 | 1.1799 | 229 | 24.29 | 23.8478 | 1006.64 | 364234 | 1.1975 | 0.1312 | 336.08 |
| | D | 24.36 | 1007.38 | 1.1805 | 228 | 24.27 | 23.8406 | 1007.29 | 364226 | 1.1980 | 0.1289 | 336.09 |
| 80 | A | 24.26 | 1006.65 | 1.1800 | 244 | 24.27 | 23.8257 | 1006.56 | 365368 | 1.1987 | 0.1409 | 335.04 |
| | D | 24.31 | 1007.39 | 1.1807 | 244 | 24.35 | 23.8792 | 1007.28 | 365353 | 1.1994 | 0.1418 | 335.05 |
| 85 | A | 24.25 | 1006.66 | 1.1801 | 255 | 24.35 | 23.8849 | 1006.61 | 366583 | 1.1996 | 0.1495 | 333.93 |
| | D | 24.21 | 1006.93 | 1.1806 | 261 | 24.22 | 23.7694 | 1007.19 | 366546 | 1.2006 | 0.1474 | 333.96 |
| 90 | A | 24.28 | 1006.61 | 1.1799 | 274 | 24.25 | 23.8240 | 1006.52 | 367815 | 1.2009 | 0.1568 | 332.81 |
| | D | 24.24 | 1006.57 | 1.1800 | 282 | 24.25 | 23.8035 | 1006.85 | 367823 | 1.2016 | 0.1592 | 332.80 |
| 95 | | 24.22 | 1006.43 | 1.1799 | 289 | 24.24 | 23.7914 | 1006.46 | 369100 | 1.2021 | 0.1656 | 331.65 |
| Data used for pathlength calibration (the first zero step): $T_{SoS}$ = 23.9039 °C, $P$ = 1004.40 mbar, $t_m^0$ = 354024 ns, $W^0$ = 345.77 m/s. | | | | | | | | | | | | |

Table 117. Methanol/dry air results (35 °C isotherm)

| $x_T$/%SAT | | Zero Step | | | $\Delta m_{read}$/µg | Non-Zero Step | | | | | | |
|---|---|---|---|---|---|---|---|---|---|---|---|---|
| | | $T_{DVS}$/°C | $P$/mbar | $\rho^0$/(kg/m$^3$) | | $T_{DVS}$/°C | $T_{SoS}$/°C | $P$/mbar | $t_m$/ns | $\rho$/(kg/m$^3$) | $x$ | $W_m$/(m/s) |
| 10 | A | 34.63 | 1015.06 | 1.1497 | 65 | 34.65 | 34.2699 | 1015.02 | 349813 | 1.1547 | 0.0395 | 349.47 |
| | D | 34.48 | 1018.92 | 1.1547 | 63 | 34.48 | 34.1184 | 1018.79 | 349845 | 1.1595 | 0.0384 | 349.44 |
| 20 | A | 34.64 | 1015.07 | 1.1497 | 119 | 34.67 | 34.2779 | 1014.99 | 351689 | 1.1588 | 0.0723 | 347.61 |
| | D | 34.50 | 1018.98 | 1.1546 | 121 | 34.49 | 34.1407 | 1018.98 | 351694 | 1.1639 | 0.0711 | 347.60 |
| 30 | A | 34.65 | 1015.13 | 1.1497 | 177 | 34.64 | 34.2706 | 1015.30 | 353537 | 1.1633 | 0.1030 | 345.79 |
| | D | 34.54 | 1019.05 | 1.1546 | 170 | 34.51 | 34.1705 | 1018.98 | 353492 | 1.1676 | 0.0998 | 345.84 |
| 40 | A | 34.65 | 1015.43 | 1.1501 | 225 | 34.66 | 34.2724 | 1015.62 | 355487 | 1.1673 | 0.1316 | 343.89 |
| | D | 34.58 | 1018.96 | 1.1543 | 222 | 34.59 | 34.2281 | 1018.97 | 355402 | 1.1713 | 0.1309 | 343.98 |
| 50 | A | 34.65 | 1015.83 | 1.1505 | 278 | 34.63 | 34.2709 | 1016.30 | 357605 | 1.1718 | 0.1591 | 341.86 |
| | D | 34.48 | 1019.04 | 1.1548 | 263 | 34.54 | 34.1566 | 1018.93 | 357496 | 1.1749 | 0.1568 | 341.96 |
| 60 | A | 34.62 | 1016.80 | 1.1517 | 327 | 34.61 | 34.2568 | 1017.41 | 359894 | 1.1768 | 0.1864 | 339.68 |
| | D | 34.52 | 1018.94 | 1.1545 | 313 | 34.54 | 34.1698 | 1018.93 | 359807 | 1.1785 | 0.1843 | 339.77 |
| 70 | A | 34.60 | 1017.84 | 1.1530 | 366 | 34.60 | 34.2486 | 1017.99 | 362417 | 1.1810 | 0.2132 | 337.32 |
| | D | 34.53 | 1018.88 | 1.1544 | 362 | 34.54 | 34.1762 | 1018.99 | 362310 | 1.1821 | 0.2112 | 337.42 |
| 80 | A | 34.59 | 1018.15 | 1.1534 | 411 | 34.62 | 34.2585 | 1018.27 | 365148 | 1.1848 | 0.2403 | 334.80 |
| | D | 34.53 | 1018.74 | 1.1543 | 406 | 34.52 | 34.1760 | 1018.77 | 365035 | 1.1854 | 0.2370 | 334.90 |
| 90 | A | 34.60 | 1018.47 | 1.1537 | 457 | 34.59 | 34.2455 | 1018.46 | 367914 | 1.1887 | 0.2668 | 332.28 |
| | D | 34.62 | 1018.62 | 1.1538 | 463 | 34.61 | 34.2724 | 1018.88 | 367870 | 1.1892 | 0.2677 | 332.32 |
| 95 | | 34.60 | 1018.59 | 1.1538 | 480 | 34.61 | 34.2493 | 1018.61 | 369284 | 1.1906 | 0.2804 | 331.05 |
| Data used for pathlength calibration (the first zero step): $T_{SoS}$ = 34.2493 °C, $P$ = 1015.06 mbar, $t_m^0$ = 347545 ns, $W^0$ = 351.75 m/s. | | | | | | | | | | | | |

Table 118. Methanol/dry air results (45 °C isotherm)

| $x_T$/%SAT | | Zero Step | | | $\Delta m_{read}$/µg | Non-Zero Step | | | | | | |
|---|---|---|---|---|---|---|---|---|---|---|---|---|
| | | $T_{DVS}$/°C | $P$/mbar | $\rho^0$/(kg/m$^3$) | | $T_{DVS}$/°C | $T_{SoS}$/°C | $P$/mbar | $t_m$/ns | $\rho$/(kg/m$^3$) | $x$ | $W_m$/(m/s) |
| 10 | A | 43.88 | 1015.92 | 1.1170 | 114 | 43.93 | 43.6184 | 1015.71 | 346228 | 1.1258 | 0.0732 | 352.76 |
| | D | 44.00 | 1010.99 | 1.1112 | 115 | 43.99 | 43.6559 | 1010.68 | 346192 | 1.1200 | 0.0735 | 352.79 |
| 20 | A | 43.92 | 1015.54 | 1.1165 | 207 | 43.97 | 43.6223 | 1015.27 | 349460 | 1.1323 | 0.1303 | 349.49 |
| | D | 43.98 | 1011.34 | 1.1116 | 210 | 43.99 | 43.6586 | 1011.11 | 349406 | 1.1277 | 0.1310 | 349.55 |
| 30 | A | 44.01 | 1015.13 | 1.1157 | 297 | 43.99 | 43.6554 | 1014.98 | 352489 | 1.1385 | 0.1818 | 346.49 |
| | D | 43.91 | 1011.54 | 1.1121 | 294 | 43.99 | 43.6231 | 1011.49 | 352396 | 1.1346 | 0.1823 | 346.58 |
| 40 | A | 44.03 | 1014.81 | 1.1153 | 380 | 44.01 | 43.7017 | 1014.85 | 355435 | 1.1444 | 0.2301 | 343.62 |
| | D | 43.92 | 1011.72 | 1.1122 | 373 | 43.88 | 43.5982 | 1011.70 | 355278 | 1.1408 | 0.2264 | 343.77 |
| 50 | A | 43.97 | 1014.99 | 1.1157 | 445 | 43.97 | 43.6576 | 1014.93 | 358378 | 1.1498 | 0.2704 | 340.80 |
| | D | 43.89 | 1011.44 | 1.1121 | 439 | 43.90 | 43.5993 | 1011.57 | 358219 | 1.1457 | 0.2668 | 340.95 |
| 60 | A | 43.95 | 1014.86 | 1.1156 | 513 | 43.96 | 43.6515 | 1014.89 | 361285 | 1.1549 | 0.3107 | 338.05 |
| | D | 43.94 | 1011.64 | 1.1121 | 508 | 43.96 | 43.6449 | 1011.55 | 361101 | 1.1510 | 0.3098 | 338.23 |
| 70 | A | 43.95 | 1014.84 | 1.1156 | 572 | 43.95 | 43.6439 | 1014.66 | 364119 | 1.1594 | 0.3472 | 335.42 |
| | D | 43.89 | 1011.69 | 1.1123 | 567 | 43.91 | 43.5950 | 1011.76 | 363898 | 1.1558 | 0.3436 | 335.63 |
| 80 | A | 43.94 | 1014.43 | 1.1152 | 629 | 43.96 | 43.6251 | 1014.21 | 366812 | 1.1634 | 0.3818 | 332.96 |
| | D | 43.97 | 1012.11 | 1.1125 | 629 | 43.98 | 43.6789 | 1011.91 | 366715 | 1.1607 | 0.3825 | 333.05 |
| 90 | A | 44.03 | 1013.98 | 1.1144 | 692 | 44.02 | 43.6962 | 1013.64 | 369444 | 1.1674 | 0.4194 | 330.59 |
| | D | 43.93 | 1012.68 | 1.1133 | 685 | 43.99 | 43.6684 | 1012.26 | 369360 | 1.1658 | 0.4187 | 330.66 |
| 95 | | 43.96 | 1013.27 | 1.1138 | 714 | 43.94 | 43.6411 | 1012.99 | 370554 | 1.1686 | 0.4322 | 329.60 |
| Data used for pathlength calibration (the first zero step): $T_{SoS}$ = 43.5841 °C, $P$ = 1015.92 mbar, $t_m^0$ = 342052 ns, $W^0$ = 357.06 m/s. | | | | | | | | | | | | |

## A6.12 Ethanol/dry air

Table 119. Ethanol/dry air results (5 °C isotherm)

| $x_T$/%SAT | | Zero Step | | | $\Delta m_{read}$/µg | Non-Zero Step | | | | | | |
|---|---|---|---|---|---|---|---|---|---|---|---|---|
| | | $T_{DVS}$/°C | $P$/mbar | $\rho^0$/(kg/m$^3$) | | $T_{DVS}$/°C | $T_{SoS}$/°C | $P$/mbar | $t_m$/ns | $\rho$/(kg/m$^3$) | $x$ | $W_m$/(m/s) |
| 10 | A | 5.33 | 1012.65 | 1.2681 | 25 | 5.35 | 5.2066 | 1012.61 | 365869 | 1.2700 | 0.0027 | 334.24 |
| | D | 5.33 | 1014.43 | 1.2703 | 28 | 5.36 | 5.2331 | 1014.59 | 365845 | 1.2724 | 0.0027 | 334.26 |
| 20 | A | 5.33 | 1012.48 | 1.2679 | 49 | 5.34 | 5.2014 | 1012.50 | 366325 | 1.2716 | 0.0050 | 333.83 |
| | D | 5.37 | 1014.34 | 1.2700 | 49 | 5.34 | 5.2295 | 1014.34 | 366292 | 1.2738 | 0.0048 | 333.86 |
| 30 | A | 5.33 | 1012.37 | 1.2677 | 69 | 5.35 | 5.2074 | 1012.24 | 366774 | 1.2730 | 0.0073 | 333.42 |
| | D | 5.36 | 1014.10 | 1.2697 | 73 | 5.38 | 5.2493 | 1014.34 | 366726 | 1.2753 | 0.0071 | 333.46 |
| 40 | A | 5.37 | 1012.03 | 1.2671 | 95 | 5.37 | 5.2250 | 1012.08 | 367212 | 1.2744 | 0.0095 | 333.02 |
| | D | 5.39 | 1013.82 | 1.2693 | 95 | 5.38 | 5.2624 | 1013.98 | 367161 | 1.2766 | 0.0093 | 333.07 |
| 50 | A | 5.32 | 1012.35 | 1.2677 | 117 | 5.37 | 5.2193 | 1012.58 | 367666 | 1.2767 | 0.0117 | 332.61 |
| | D | 5.38 | 1013.46 | 1.2688 | 118 | 5.39 | 5.2722 | 1013.68 | 367601 | 1.2779 | 0.0116 | 332.67 |
| 60 | A | 5.35 | 1012.51 | 1.2678 | 137 | 5.39 | 5.2473 | 1012.54 | 368103 | 1.2782 | 0.0140 | 332.21 |
| | D | 5.39 | 1013.64 | 1.2690 | 136 | 5.39 | 5.2704 | 1013.60 | 368053 | 1.2795 | 0.0138 | 332.26 |
| 70 | A | 5.37 | 1012.84 | 1.2681 | 164 | 5.39 | 5.2518 | 1013.06 | 368562 | 1.2807 | 0.0163 | 331.80 |
| | D | 5.39 | 1013.75 | 1.2691 | 160 | 5.40 | 5.2742 | 1013.79 | 368515 | 1.2814 | 0.0161 | 331.84 |
| 80 | A | 5.37 | 1013.36 | 1.2687 | 185 | 5.39 | 5.2570 | 1013.58 | 369042 | 1.2829 | 0.0184 | 331.37 |
| | D | 5.39 | 1013.76 | 1.2692 | 181 | 5.38 | 5.2618 | 1013.75 | 369008 | 1.2831 | 0.0183 | 331.40 |
| 90 | A | 5.38 | 1013.60 | 1.2690 | 206 | 5.39 | 5.2610 | 1013.68 | 369545 | 1.2848 | 0.0207 | 330.92 |
| | D | 5.39 | 1013.81 | 1.2692 | 203 | 5.40 | 5.2714 | 1013.71 | 369522 | 1.2848 | 0.0207 | 330.94 |
| 95 | | 5.38 | 1013.79 | 1.2693 | 215 | 5.40 | 5.2683 | 1013.76 | 369794 | 1.2858 | 0.0218 | 330.69 |
| Data used for pathlength calibration (the first zero step): $T_{SoS}$ = 5.1928 °C, $P$ = 1012.65 mbar, $t_m^0$ = 365389 ns, $W^0$ = 334.68 m/s. | | | | | | | | | | | | |

Table 120. Ethanol/dry air results (15 °C isotherm)

| $x_T$/%SAT | | Zero Step | | | $\Delta m_{read}$/µg | Non-Zero Step | | | | | | |
|---|---|---|---|---|---|---|---|---|---|---|---|---|
| | | $T_{DVS}$/°C | $P$/mbar | $\rho^0$/(kg/m$^3$) | | $T_{DVS}$/°C | $T_{SoS}$/°C | $P$/mbar | $t_m$/ns | $\rho$/(kg/m$^3$) | $x$ | $W_m$/(m/s) |
| 10 | A | 15.07 | 1014.39 | 1.2272 | 43 | 15.09 | 14.8977 | 1014.27 | 360886 | 1.2304 | 0.0047 | 339.63 |
| | D | 14.99 | 1010.23 | 1.2225 | 46 | 15.02 | 14.8268 | 1010.26 | 360950 | 1.2260 | 0.0049 | 339.57 |
| 20 | A | 15.04 | 1013.81 | 1.2266 | 79 | 15.03 | 14.8592 | 1013.60 | 361738 | 1.2327 | 0.0086 | 338.83 |
| | D | 14.99 | 1010.36 | 1.2226 | 85 | 15.00 | 14.8144 | 1010.31 | 361784 | 1.2291 | 0.0090 | 338.79 |
| 30 | A | 15.02 | 1013.36 | 1.2261 | 119 | 15.06 | 14.8645 | 1013.22 | 362584 | 1.2353 | 0.0129 | 338.04 |
| | D | 14.97 | 1010.27 | 1.2226 | 123 | 14.96 | 14.7822 | 1010.23 | 362649 | 1.2320 | 0.0129 | 337.98 |
| 40 | A | 15.03 | 1013.21 | 1.2259 | 166 | 15.02 | 14.8512 | 1013.19 | 363371 | 1.2387 | 0.0173 | 337.31 |
| | D | 15.01 | 1010.20 | 1.2224 | 169 | 14.96 | 14.8020 | 1010.34 | 363433 | 1.2353 | 0.0172 | 337.25 |
| 50 | A | 15.00 | 1013.35 | 1.2262 | 205 | 15.02 | 14.8360 | 1013.38 | 364192 | 1.2419 | 0.0215 | 336.55 |
| | D | 14.97 | 1010.31 | 1.2227 | 203 | 15.01 | 14.8168 | 1010.30 | 364238 | 1.2382 | 0.0215 | 336.50 |
| 60 | A | 14.99 | 1013.38 | 1.2263 | 241 | 15.00 | 14.8190 | 1013.32 | 365009 | 1.2448 | 0.0253 | 335.79 |
| | D | 14.99 | 1010.48 | 1.2228 | 241 | 14.95 | 14.7913 | 1010.38 | 365049 | 1.2413 | 0.0252 | 335.76 |
| 70 | A | 15.04 | 1013.27 | 1.2259 | 280 | 15.05 | 14.8660 | 1013.19 | 365830 | 1.2474 | 0.0294 | 335.04 |
| | D | 15.01 | 1010.95 | 1.2233 | 277 | 14.96 | 14.7989 | 1010.75 | 365858 | 1.2445 | 0.0290 | 335.01 |
| 80 | A | 14.98 | 1013.20 | 1.2261 | 313 | 15.03 | 14.8433 | 1013.05 | 366702 | 1.2501 | 0.0333 | 334.24 |
| | D | 14.95 | 1011.48 | 1.2242 | 308 | 15.01 | 14.8075 | 1011.14 | 366722 | 1.2477 | 0.0331 | 334.22 |
| 90 | A | 14.97 | 1012.88 | 1.2258 | 349 | 14.97 | 14.7942 | 1012.61 | 367627 | 1.2526 | 0.0370 | 333.40 |
| | D | 15.01 | 1011.98 | 1.2245 | 352 | 15.03 | 14.8381 | 1011.79 | 367626 | 1.2515 | 0.0372 | 333.40 |
| 95 | | 15.01 | 1012.45 | 1.2251 | 370 | 15.03 | 14.8322 | 1012.24 | 368105 | 1.2534 | 0.0391 | 332.97 |
| Data used for pathlength calibration (the first zero step): $T_{SoS}$ = 14.8814 °C, $P$ = 1014.39 mbar, $t_m^0$ = 359993 ns, $W^0$ = 340.47 m/s. | | | | | | | | | | | | |

Table 121. Ethanol/dry air results (25 °C isotherm)

| $x_T$/%SAT | | Zero Step | | | $\Delta m_{read}$/µg | Non-Zero Step | | | | | | |
|---|---|---|---|---|---|---|---|---|---|---|---|---|
| | | $T_{DVS}$/°C | $P$/mbar | $\rho^0$/(kg/m$^3$) | | $T_{DVS}$/°C | $T_{SoS}$/°C | $P$/mbar | $t_m$/ns | $\rho$/(kg/m$^3$) | $x$ | $W_m$/(m/s) |
| 5 | A | 24.61 | 1005.92 | 1.1778 | 41 | 24.62 | 24.3064 | 1005.78 | 354937 | 1.1809 | 0.0047 | 345.12 |
| | D | 24.63 | 997.65 | 1.1680 | 47 | 24.64 | 24.2556 | 997.85 | 354978 | 1.1716 | 0.0049 | 345.08 |
| 10 | A | 24.60 | 1006.03 | 1.1780 | 81 | 24.62 | 24.3084 | 1005.99 | 355745 | 1.1842 | 0.0090 | 344.33 |
| | D | 24.61 | 997.88 | 1.1684 | 78 | 24.63 | 24.2382 | 997.71 | 355787 | 1.1744 | 0.0089 | 344.29 |
| 15 | A | 24.62 | 1005.82 | 1.1776 | 116 | 24.64 | 24.3271 | 1005.71 | 356527 | 1.1865 | 0.0130 | 343.58 |
| | D | 24.60 | 998.12 | 1.1687 | 114 | 24.61 | 24.2262 | 997.94 | 356577 | 1.1774 | 0.0128 | 343.53 |
| 20 | A | 24.63 | 1005.41 | 1.1771 | 143 | 24.62 | 24.3210 | 1004.89 | 357285 | 1.1881 | 0.0164 | 342.85 |
| | D | 24.60 | 998.49 | 1.1691 | 151 | 24.61 | 24.2696 | 998.40 | 357307 | 1.1807 | 0.0168 | 342.83 |
| 25 | A | 24.61 | 1004.30 | 1.1759 | 180 | 24.63 | 24.3167 | 1003.88 | 358020 | 1.1897 | 0.0204 | 342.14 |
| | D | 24.60 | 998.62 | 1.1693 | 190 | 24.61 | 24.2680 | 998.71 | 358066 | 1.1838 | 0.0207 | 342.10 |
| 30 | A | 24.62 | 1003.62 | 1.1751 | 219 | 24.60 | 24.3118 | 1003.46 | 358750 | 1.1919 | 0.0241 | 341.45 |
| | D | 24.54 | 998.68 | 1.1696 | 228 | 24.60 | 24.2418 | 999.06 | 358809 | 1.1871 | 0.0247 | 341.39 |
| 35 | A | 24.51 | 1003.16 | 1.1750 | 253 | 24.50 | 24.2167 | 1003.08 | 359510 | 1.1944 | 0.0277 | 340.73 |
| | D | 24.51 | 998.70 | 1.1698 | 250 | 24.51 | 24.1681 | 998.43 | 359540 | 1.1889 | 0.0279 | 340.70 |
| 40 | A | 24.49 | 1002.91 | 1.1748 | 282 | 24.49 | 24.1934 | 1002.57 | 360220 | 1.1964 | 0.0314 | 340.05 |
| | D | 24.49 | 998.71 | 1.1698 | 290 | 24.51 | 24.1685 | 998.71 | 360269 | 1.1921 | 0.0319 | 340.01 |
| 45 | A | 24.48 | 1002.35 | 1.1741 | 316 | 24.49 | 24.1877 | 1002.16 | 360921 | 1.1984 | 0.0349 | 339.39 |
| | D | 24.48 | 999.27 | 1.1705 | 317 | 24.51 | 24.1627 | 999.13 | 360936 | 1.1948 | 0.0351 | 339.38 |
| 50 | A | 24.48 | 1001.91 | 1.1736 | 357 | 24.50 | 24.1952 | 1002.03 | 361643 | 1.2010 | 0.0389 | 338.72 |
| | D | 24.48 | 999.45 | 1.1707 | 350 | 24.51 | 24.1563 | 999.20 | 361656 | 1.1975 | 0.0389 | 338.70 |
| 55 | A | 24.49 | 1002.07 | 1.1738 | 387 | 24.50 | 24.2050 | 1002.24 | 362348 | 1.2034 | 0.0420 | 338.06 |
| | D | 24.48 | 999.32 | 1.1706 | 385 | 24.50 | 24.1517 | 999.32 | 362356 | 1.2001 | 0.0422 | 338.05 |
| 60 | A | 24.50 | 1002.28 | 1.1740 | 419 | 24.50 | 24.2047 | 1002.40 | 363048 | 1.2061 | 0.0455 | 337.40 |
| | D | 24.59 | 998.56 | 1.1693 | 431 | 24.54 | 24.2136 | 999.25 | 363019 | 1.2023 | 0.0457 | 337.43 |

| | | | | | | | | | | | | |
|---|---|---|---|---|---|---|---|---|---|---|---|---|
| 65 | A | 24.48 | 1002.65 | 1.1745 | 451 | 24.49 | 24.1965 | 1002.79 | 363755 | 1.2090 | 0.0490 | 336.75 |
| | D | 24.51 | 999.42 | 1.1706 | 445 | 24.59 | 24.2123 | 998.89 | 363761 | 1.2047 | 0.0500 | 336.74 |
| 70 | A | 24.54 | 1003.26 | 1.1749 | 487 | 24.58 | 24.2621 | 1003.38 | 364472 | 1.2123 | 0.0531 | 336.09 |
| | D | 24.45 | 999.91 | 1.1714 | 478 | 24.48 | 24.1241 | 999.73 | 364452 | 1.2080 | 0.0527 | 336.10 |
| 75 | A | 24.58 | 1003.90 | 1.1756 | 515 | 24.58 | 24.2797 | 1003.66 | 365203 | 1.2150 | 0.0565 | 335.41 |
| | D | 24.46 | 1000.57 | 1.1721 | 506 | 24.45 | 24.1297 | 1000.20 | 365173 | 1.2109 | 0.0559 | 335.44 |
| 80 | A | 24.57 | 1003.63 | 1.1753 | 548 | 24.60 | 24.2946 | 1003.58 | 365960 | 1.2173 | 0.0600 | 334.72 |
| | D | 24.51 | 1001.17 | 1.1726 | 543 | 24.51 | 24.2106 | 1000.96 | 365925 | 1.2143 | 0.0597 | 334.75 |
| 85 | A | 24.60 | 1003.35 | 1.1748 | 581 | 24.62 | 24.3148 | 1003.43 | 366720 | 1.2193 | 0.0633 | 334.03 |
| | D | 24.49 | 1001.93 | 1.1736 | 579 | 24.51 | 24.2224 | 1001.86 | 366694 | 1.2179 | 0.0634 | 334.05 |
| 90 | A | 24.59 | 1003.72 | 1.1753 | 605 | 24.61 | 24.3101 | 1003.29 | 367487 | 1.2216 | 0.0667 | 333.33 |
| | D | 24.58 | 1002.44 | 1.1739 | 607 | 24.52 | 24.2573 | 1002.30 | 367464 | 1.2204 | 0.0662 | 333.35 |
| 95 | | 24.59 | 1003.01 | 1.1745 | 639 | 24.62 | 24.3218 | 1002.76 | 368280 | 1.2234 | 0.0703 | 332.61 |
| Data used for pathlength calibration (the first zero step): $T_{SOS}$ = 24.2937 °C, $P$ = 1005.92 mbar, $t_m^0$ = 354029 ns, $W^0$ = 346.00 m/s. | | | | | | | | | | | | |

Table 122. Ethanol/dry air results (35 °C isotherm)

| $x_T$/%SAT | | Zero Step | | | $\Delta m_{read}$/µg | Non-Zero Step | | | | | | |
|---|---|---|---|---|---|---|---|---|---|---|---|---|
| | | $T_{DVS}$/°C | $P$/mbar | $\rho^0$/(kg/m$^3$) | | $T_{DVS}$/°C | $T_{SoS}$/°C | $P$/mbar | $t_m$/ns | $\rho$/(kg/m$^3$) | $x$ | $W_m$/(m/s) |
| 10 | A | 34.51 | 1002.31 | 1.1357 | 146 | 34.51 | 34.1039 | 1001.99 | 350968 | 1.1469 | 0.0170 | 348.37 |
| | D | 34.55 | 999.69 | 1.1326 | 153 | 34.56 | 34.1723 | 999.84 | 350933 | 1.1443 | 0.0171 | 348.40 |
| 20 | A | 34.49 | 1001.94 | 1.1354 | 280 | 34.49 | 34.0864 | 1001.83 | 353819 | 1.1568 | 0.0319 | 345.56 |
| | D | 34.52 | 999.73 | 1.1328 | 283 | 34.56 | 34.1673 | 999.83 | 353782 | 1.1544 | 0.0321 | 345.60 |
| 30 | A | 34.45 | 1001.82 | 1.1354 | 405 | 34.46 | 34.0581 | 1001.74 | 356470 | 1.1664 | 0.0460 | 342.99 |
| | D | 34.55 | 999.86 | 1.1328 | 402 | 34.51 | 34.1244 | 999.70 | 356428 | 1.1636 | 0.0455 | 343.03 |
| 40 | A | 34.50 | 1001.70 | 1.1351 | 529 | 34.53 | 34.1263 | 1001.57 | 359010 | 1.1756 | 0.0602 | 340.56 |
| | D | 34.58 | 1000.00 | 1.1328 | 528 | 34.57 | 34.1707 | 1000.04 | 358962 | 1.1733 | 0.0596 | 340.61 |
| 50 | A | 34.58 | 1001.55 | 1.1346 | 649 | 34.57 | 34.1708 | 1001.48 | 361475 | 1.1843 | 0.0733 | 338.24 |
| | D | 34.57 | 1000.44 | 1.1334 | 640 | 34.57 | 34.1665 | 1000.26 | 361418 | 1.1824 | 0.0727 | 338.29 |
| 60 | A | 34.54 | 1001.34 | 1.1345 | 756 | 34.53 | 34.1213 | 1001.36 | 363870 | 1.1925 | 0.0853 | 336.02 |
| | D | 34.56 | 1000.90 | 1.1339 | 753 | 34.58 | 34.1823 | 1000.64 | 363821 | 1.1916 | 0.0856 | 336.06 |
| 70 | A | 34.50 | 1001.42 | 1.1347 | 866 | 34.51 | 34.1037 | 1001.38 | 366255 | 1.2011 | 0.0979 | 333.83 |
| | D | 34.52 | 1001.25 | 1.1345 | 862 | 34.57 | 34.1702 | 1001.08 | 366193 | 1.2005 | 0.0980 | 333.88 |
| 80 | A | 34.47 | 1001.50 | 1.1349 | 972 | 34.47 | 34.0520 | 1001.56 | 368628 | 1.2094 | 0.1095 | 331.68 |
| | D | 34.54 | 1001.50 | 1.1347 | 977 | 34.50 | 34.1047 | 1001.34 | 368573 | 1.2095 | 0.1102 | 331.73 |
| 90 | A | 34.54 | 1001.77 | 1.1350 | 1090 | 34.58 | 34.1825 | 1001.99 | 371139 | 1.2185 | 0.1228 | 329.43 |
| | D | 34.55 | 1001.62 | 1.1348 | 1081 | 34.53 | 34.1355 | 1001.62 | 371076 | 1.2176 | 0.1218 | 329.49 |
| 95 | | 34.55 | 1001.90 | 1.1351 | 1134 | 34.56 | 34.1665 | 1001.84 | 372325 | 1.2220 | 0.1280 | 328.38 |
| Data used for pathlength calibration (the first zero step): $T_{SoS}$ = 34.1061 °C, $P$ = 1002.31 mbar, $t_m^0$ = 347672 ns, $W^0$ = 351.67 m/s. | | | | | | | | | | | | |

Table 123. Ethanol/dry air results (45 °C isotherm)

| $x_T$/%SAT | | Zero Step | | | $\Delta m_{read}$/µg | Non-Zero Step | | | | | | |
|---|---|---|---|---|---|---|---|---|---|---|---|---|
| | | $T_{DVS}$/°C | $P$/mbar | $\rho^0$/(kg/m³) | | $T_{DVS}$/°C | $T_{SoS}$/°C | $P$/mbar | $t_m$/ns | $\rho$/(kg/m³) | $x$ | $W_m$/(m/s) |
| 10 | A | 44.03 | 1011.18 | 1.1113 | 259 | 44.00 | 43.6505 | 1011.13 | 347959 | 1.1311 | 0.0298 | 351.20 |
| | D | 43.96 | 1013.80 | 1.1144 | 253 | 43.98 | 43.6223 | 1013.70 | 347867 | 1.1338 | 0.0294 | 351.30 |
| 20 | A | 43.99 | 1011.11 | 1.1114 | 482 | 43.99 | 43.6400 | 1011.33 | 352672 | 1.1483 | 0.0553 | 346.51 |
| | D | 43.93 | 1013.99 | 1.1147 | 470 | 43.96 | 43.5957 | 1013.83 | 352518 | 1.1507 | 0.0545 | 346.66 |
| 30 | A | 44.00 | 1011.48 | 1.1117 | 689 | 43.94 | 43.6200 | 1011.73 | 356918 | 1.1645 | 0.0787 | 342.39 |
| | D | 43.93 | 1013.83 | 1.1145 | 675 | 43.94 | 43.5887 | 1013.91 | 356733 | 1.1662 | 0.0775 | 342.57 |
| 40 | A | 43.92 | 1011.90 | 1.1125 | 873 | 43.90 | 43.5750 | 1012.05 | 360815 | 1.1794 | 0.1002 | 338.69 |
| | D | 44.00 | 1013.98 | 1.1145 | 867 | 44.01 | 43.6406 | 1013.99 | 360655 | 1.1809 | 0.0997 | 338.84 |
| 50 | A | 43.89 | 1012.25 | 1.1130 | 1055 | 43.94 | 43.5966 | 1012.44 | 364540 | 1.1938 | 0.1214 | 335.23 |
| | D | 44.02 | 1013.47 | 1.1139 | 1051 | 43.99 | 43.6215 | 1013.79 | 364352 | 1.1944 | 0.1202 | 335.40 |
| 60 | A | 43.93 | 1012.72 | 1.1133 | 1222 | 43.91 | 43.5458 | 1012.74 | 368020 | 1.2070 | 0.1404 | 332.06 |
| | D | 43.99 | 1013.23 | 1.1137 | 1216 | 43.98 | 43.6066 | 1013.30 | 367857 | 1.2069 | 0.1397 | 332.21 |
| 70 | A | 43.92 | 1012.86 | 1.1135 | 1392 | 43.97 | 43.5907 | 1013.07 | 371445 | 1.2202 | 0.1599 | 329.00 |
| | D | 43.95 | 1013.40 | 1.1140 | 1372 | 44.01 | 43.5832 | 1013.32 | 371210 | 1.2191 | 0.1581 | 329.21 |
| 80 | A | 43.97 | 1012.92 | 1.1134 | 1544 | 43.92 | 43.5732 | 1012.85 | 374720 | 1.2317 | 0.1773 | 326.12 |
| | D | 43.92 | 1013.37 | 1.1141 | 1538 | 43.99 | 43.6308 | 1013.36 | 374616 | 1.2320 | 0.1771 | 326.21 |
| 90 | A | 43.90 | 1012.89 | 1.1136 | 1700 | 43.98 | 43.5968 | 1013.08 | 377978 | 1.2439 | 0.1953 | 323.31 |
| | D | 43.96 | 1013.08 | 1.1136 | 1695 | 43.93 | 43.5985 | 1013.37 | 377847 | 1.2435 | 0.1940 | 323.42 |
| 95 | | 43.97 | 1013.19 | 1.1137 | 1774 | 44.00 | 43.6340 | 1013.27 | 379538 | 1.2497 | 0.2037 | 321.98 |
| Data used for pathlength calibration (the first zero step): $T_{SoS}$ = 43.6622 °C, $P$ = 1011.18 mbar, $t_m^0$ = 342210 ns, $W^0$ = 357.11 m/s. | | | | | | | | | | | | |

Table 124. Ethanol/dry air results (55 °C isotherm)

| $x_T$/%SAT | | Zero Step | | | $\Delta m_{read}$/µg | Non-Zero Step | | | | | | |
|---|---|---|---|---|---|---|---|---|---|---|---|---|
| | | $T_{DVS}$/°C | $P$/mbar | $\rho^0$/(kg/m³) | | $T_{DVS}$/°C | $T_{SoS}$/°C | $P$/mbar | $t_m$/ns | $\rho$/(kg/m³) | $x$ | $W_m$/(m/s) |
| 10 | A | 53.77 | 996.76 | 1.0627 | 469 | 53.78 | 53.4743 | 996.78 | 347439 | 1.0986 | 0.0567 | 351.43 |
| | D | 53.77 | 1003.02 | 1.0694 | 468 | 53.79 | 53.4805 | 1003.38 | 347227 | 1.1053 | 0.0557 | 351.65 |
| 20 | A | 53.78 | 997.03 | 1.0630 | 845 | 53.79 | 53.4757 | 996.92 | 355429 | 1.1277 | 0.1022 | 343.53 |
| | D | 53.77 | 1002.64 | 1.0690 | 832 | 53.79 | 53.4782 | 1002.72 | 355002 | 1.1327 | 0.0998 | 343.95 |
| 30 | A | 53.76 | 997.14 | 1.0631 | 1176 | 53.75 | 53.4394 | 997.49 | 362126 | 1.1532 | 0.1411 | 337.18 |
| | D | 53.79 | 1002.13 | 1.0684 | 1155 | 53.76 | 53.4597 | 1002.31 | 361594 | 1.1568 | 0.1381 | 337.68 |
| 40 | A | 53.74 | 997.70 | 1.0638 | 1471 | 53.79 | 53.4747 | 997.85 | 367992 | 1.1765 | 0.1771 | 331.80 |
| | D | 53.84 | 1001.50 | 1.0675 | 1450 | 53.80 | 53.5037 | 1001.78 | 367411 | 1.1787 | 0.1733 | 332.33 |
| 50 | A | 53.80 | 998.05 | 1.0640 | 1736 | 53.81 | 53.4928 | 998.22 | 373217 | 1.1971 | 0.2087 | 327.16 |
| | D | 53.82 | 1000.87 | 1.0669 | 1712 | 53.85 | 53.5267 | 1001.19 | 372623 | 1.1981 | 0.2050 | 327.68 |
| 60 | A | 53.79 | 998.27 | 1.0643 | 1972 | 53.81 | 53.4912 | 998.34 | 377860 | 1.2154 | 0.2370 | 323.14 |
| | D | 53.82 | 1000.34 | 1.0664 | 1945 | 53.82 | 53.5129 | 1000.59 | 377241 | 1.2154 | 0.2329 | 323.67 |
| 70 | A | 53.81 | 998.41 | 1.0643 | 2197 | 53.81 | 53.4926 | 998.64 | 382112 | 1.2327 | 0.2635 | 319.54 |
| | D | 53.82 | 999.71 | 1.0657 | 2172 | 53.84 | 53.5321 | 1000.00 | 381582 | 1.2321 | 0.2602 | 319.99 |
| 80 | A | 53.80 | 998.66 | 1.0646 | 2397 | 53.81 | 53.4863 | 998.83 | 386028 | 1.2483 | 0.2874 | 316.30 |
| | D | 53.85 | 999.41 | 1.0653 | 2379 | 53.84 | 53.5245 | 999.48 | 385660 | 1.2476 | 0.2852 | 316.60 |
| 90 | A | 53.84 | 998.93 | 1.0648 | 2591 | 53.84 | 53.5263 | 999.07 | 389656 | 1.2633 | 0.3105 | 313.36 |
| | D | 53.84 | 999.34 | 1.0652 | 2579 | 53.86 | 53.5388 | 999.37 | 389470 | 1.2629 | 0.3093 | 313.51 |
| 95 | | 53.83 | 999.21 | 1.0651 | 2674 | 53.83 | 53.5221 | 999.23 | 391266 | 1.2700 | 0.3205 | 312.07 |
| Data used for pathlength calibration (the first zero step): $T_{SoS}$ = 53.4733 °C, $P$ = 996.76 mbar, $t_m^0$ = 336742 ns, $W^0$ = 362.60 m/s. | | | | | | | | | | | | |

## A6.13 Isopropanol/dry air

Table 125. Isopropanol/dry air results (5 °C isotherm)

| $x_T$/%SAT | | Zero Step | | | $\Delta m_{read}$/µg | Non-Zero Step | | | | | | |
|---|---|---|---|---|---|---|---|---|---|---|---|---|
| | | $T_{DVS}$/°C | $P$/mbar | $\rho^0$/(kg/m$^3$) | | $T_{DVS}$/°C | $T_{SoS}$/°C | $P$/mbar | $t_m$/ns | $\rho$/(kg/m$^3$) | $x$ | $W_m$/(m/s) |
| 10 | A | 5.18 | 1004.11 | 1.2580 | 17 | 5.19 | 5.0924 | 1003.29 | 366029 | 1.2593 | 0.0017 | 334.12 |
| | D | 5.31 | 1004.43 | 1.2578 | 30 | 5.34 | 5.2173 | 1004.42 | 365942 | 1.2601 | 0.0018 | 334.19 |
| 20 | A | 5.18 | 1003.00 | 1.2566 | 55 | 5.20 | 5.0981 | 1002.97 | 366545 | 1.2609 | 0.0032 | 333.64 |
| | D | 5.31 | 1004.77 | 1.2583 | 56 | 5.32 | 5.2063 | 1004.56 | 366458 | 1.2625 | 0.0033 | 333.72 |
| 30 | A | 5.18 | 1003.16 | 1.2568 | 89 | 5.20 | 5.1021 | 1003.46 | 367054 | 1.2637 | 0.0048 | 333.18 |
| | D | 5.30 | 1005.24 | 1.2589 | 79 | 5.32 | 5.2146 | 1004.94 | 366958 | 1.2650 | 0.0048 | 333.27 |
| 40 | A | 5.17 | 1003.83 | 1.2577 | 113 | 5.20 | 5.1058 | 1004.05 | 367557 | 1.2664 | 0.0062 | 332.73 |
| | D | 5.30 | 1005.24 | 1.2589 | 109 | 5.31 | 5.2080 | 1005.32 | 367466 | 1.2673 | 0.0061 | 332.81 |
| 50 | A | 5.19 | 1004.42 | 1.2584 | 140 | 5.21 | 5.1076 | 1004.67 | 368062 | 1.2691 | 0.0077 | 332.27 |
| | D | 5.29 | 1006.12 | 1.2601 | 129 | 5.30 | 5.1968 | 1005.84 | 367975 | 1.2699 | 0.0075 | 332.35 |
| 60 | A | 5.21 | 1005.09 | 1.2591 | 169 | 5.22 | 5.1245 | 1005.50 | 368549 | 1.2721 | 0.0091 | 331.83 |
| | D | 5.29 | 1006.57 | 1.2606 | 160 | 5.32 | 5.2067 | 1006.52 | 368470 | 1.2729 | 0.0091 | 331.90 |
| 70 | A | 5.22 | 1006.10 | 1.2603 | 194 | 5.23 | 5.1339 | 1006.42 | 369042 | 1.2752 | 0.0106 | 331.39 |
| | D | 5.28 | 1006.70 | 1.2608 | 188 | 5.31 | 5.1972 | 1006.78 | 368978 | 1.2753 | 0.0106 | 331.45 |
| 80 | A | 5.22 | 1006.83 | 1.2613 | 214 | 5.23 | 5.1330 | 1006.88 | 369556 | 1.2777 | 0.0120 | 330.93 |
| | D | 5.21 | 1006.99 | 1.2615 | 208 | 5.25 | 5.1460 | 1006.82 | 369529 | 1.2775 | 0.0120 | 330.95 |
| 90 | A | 5.22 | 1006.82 | 1.2613 | 240 | 5.23 | 5.1327 | 1006.88 | 370084 | 1.2797 | 0.0134 | 330.45 |
| | D | 5.21 | 1007.02 | 1.2615 | 236 | 5.23 | 5.1282 | 1006.90 | 370073 | 1.2796 | 0.0134 | 330.46 |
| 95 | | 5.21 | 1007.02 | 1.2616 | 250 | 5.22 | 5.1317 | 1006.98 | 370350 | 1.2807 | 0.0141 | 330.22 |
| Data used for pathlength calibration (the first zero step): $T_{SoS}$ = 5.0681 °C, $P$ = 1004.11 mbar, $t_m^0$ = 365493 ns, $W^0$ = 334.61 m/s. | | | | | | | | | | | | |

Table 126. Isopropanol/dry air results (15 °C isotherm)

| $x_T$/%SAT | | Zero Step | | | $\Delta m_{read}$/µg | Non-Zero Step | | | | | | |
|---|---|---|---|---|---|---|---|---|---|---|---|---|
| | | $T_{DVS}$/°C | $P$/mbar | $\rho^0$/(kg/m³) | | $T_{DVS}$/°C | $T_{SoS}$/°C | $P$/mbar | $t_m$/ns | $\rho$/(kg/m³) | $x$ | $W_m$/(m/s) |
| 10 | A | 15.14 | 1022.83 | 1.2371 | 55 | 15.16 | 14.8815 | 1022.55 | 361062 | 1.2412 | 0.0034 | 339.45 |
| | D | 14.97 | 1022.52 | 1.2374 | 56 | 14.98 | 14.6984 | 1022.55 | 361153 | 1.2417 | 0.0032 | 339.36 |
| 20 | A | 15.17 | 1022.35 | 1.2364 | 108 | 15.11 | 14.8518 | 1022.12 | 362081 | 1.2447 | 0.0062 | 338.49 |
| | D | 14.98 | 1022.14 | 1.2369 | 109 | 14.99 | 14.7000 | 1022.33 | 362143 | 1.2453 | 0.0061 | 338.44 |
| 30 | A | 15.08 | 1021.88 | 1.2362 | 151 | 15.09 | 14.8214 | 1021.77 | 363079 | 1.2478 | 0.0088 | 337.56 |
| | D | 14.99 | 1021.95 | 1.2367 | 158 | 14.99 | 14.7140 | 1022.01 | 363118 | 1.2488 | 0.0090 | 337.53 |
| 40 | A | 15.10 | 1021.68 | 1.2359 | 211 | 15.11 | 14.8363 | 1021.75 | 364023 | 1.2521 | 0.0121 | 336.69 |
| | D | 15.01 | 1021.91 | 1.2365 | 205 | 15.00 | 14.7210 | 1021.83 | 364067 | 1.2523 | 0.0118 | 336.65 |
| 50 | A | 15.09 | 1021.72 | 1.2359 | 257 | 15.10 | 14.8195 | 1021.92 | 364973 | 1.2556 | 0.0146 | 335.81 |
| | D | 15.01 | 1022.10 | 1.2368 | 250 | 15.02 | 14.7311 | 1021.94 | 365013 | 1.2559 | 0.0145 | 335.78 |
| 60 | A | 15.09 | 1022.10 | 1.2364 | 303 | 15.08 | 14.8044 | 1022.05 | 365931 | 1.2596 | 0.0173 | 334.93 |
| | D | 14.94 | 1022.42 | 1.2375 | 294 | 15.01 | 14.7036 | 1022.29 | 365966 | 1.2600 | 0.0172 | 334.90 |
| 70 | A | 15.09 | 1022.16 | 1.2365 | 354 | 15.06 | 14.7950 | 1022.22 | 366891 | 1.2636 | 0.0201 | 334.06 |
| | D | 15.01 | 1022.66 | 1.2374 | 349 | 15.02 | 14.7338 | 1022.53 | 366913 | 1.2642 | 0.0201 | 334.04 |
| 80 | A | 15.03 | 1022.37 | 1.2370 | 401 | 15.01 | 14.7447 | 1022.30 | 367873 | 1.2677 | 0.0229 | 333.16 |
| | D | 14.98 | 1022.93 | 1.2379 | 393 | 15.03 | 14.7317 | 1022.80 | 367885 | 1.2680 | 0.0227 | 333.15 |
| 90 | A | 15.02 | 1022.45 | 1.2371 | 449 | 15.05 | 14.7488 | 1022.68 | 368898 | 1.2716 | 0.0256 | 332.24 |
| | D | 15.02 | 1022.89 | 1.2377 | 447 | 15.00 | 14.7174 | 1022.93 | 368893 | 1.2719 | 0.0255 | 332.24 |
| 95 | | 15.03 | 1022.82 | 1.2375 | 471 | 14.98 | 14.7160 | 1022.76 | 369388 | 1.2736 | 0.0268 | 331.80 |
| Data used for pathlength calibration (the first zero step): $T_{SoS}$ = 14.8570 °C, $P$ = 1022.83 mbar, $t_m^0$ = 359993 ns, $W^0$ = 340.46 m/s. | | | | | | | | | | | | |

Table 127. Isopropanol/dry air results (25 °C isotherm)

| $x_T$/%SAT | | Zero Step | | | $\Delta m_{read}$/µg | Non-Zero Step | | | | | | |
|---|---|---|---|---|---|---|---|---|---|---|---|---|
| | | $T_{DVS}$/°C | $P$/mbar | $\rho^0$/(kg/m³) | | $T_{DVS}$/°C | $T_{SoS}$/°C | $P$/mbar | $t_m$/ns | $\rho$/(kg/m³) | $x$ | $W_m$/(m/s) |
| 5 | A | 24.69 | 1021.96 | 1.1963 | 57 | 24.71 | 24.3360 | 1021.96 | 355094 | 1.2006 | 0.0034 | 344.95 |
| | D | 24.64 | 1020.32 | 1.1946 | 56 | 24.63 | 24.2795 | 1020.36 | 355104 | 1.1988 | 0.0032 | 344.94 |
| 10 | A | 24.70 | 1022.10 | 1.1964 | 105 | 24.70 | 24.3332 | 1022.14 | 356052 | 1.2045 | 0.0062 | 344.02 |
| | D | 24.65 | 1020.22 | 1.1944 | 104 | 24.66 | 24.2987 | 1020.27 | 356067 | 1.2024 | 0.0061 | 344.01 |
| 15 | A | 24.69 | 1022.25 | 1.1966 | 152 | 24.72 | 24.3420 | 1022.48 | 356998 | 1.2083 | 0.0089 | 343.11 |
| | D | 24.65 | 1020.49 | 1.1947 | 145 | 24.66 | 24.3019 | 1020.28 | 357016 | 1.2059 | 0.0088 | 343.09 |
| 20 | A | 24.68 | 1022.60 | 1.1971 | 198 | 24.69 | 24.3203 | 1022.65 | 357931 | 1.2122 | 0.0117 | 342.22 |
| | D | 24.66 | 1020.78 | 1.1950 | 193 | 24.67 | 24.3088 | 1020.53 | 357944 | 1.2098 | 0.0117 | 342.20 |
| 25 | A | 24.68 | 1022.66 | 1.1971 | 246 | 24.70 | 24.3241 | 1022.91 | 358844 | 1.2160 | 0.0143 | 341.35 |
| | D | 24.65 | 1020.84 | 1.1951 | 240 | 24.66 | 24.3018 | 1020.69 | 358859 | 1.2136 | 0.0144 | 341.33 |
| 30 | A | 24.68 | 1022.75 | 1.1972 | 289 | 24.69 | 24.3179 | 1022.84 | 359745 | 1.2194 | 0.0170 | 340.49 |
| | D | 24.66 | 1020.96 | 1.1952 | 286 | 24.67 | 24.3085 | 1020.88 | 359760 | 1.2172 | 0.0171 | 340.48 |
| 35 | A | 24.68 | 1022.76 | 1.1972 | 330 | 24.69 | 24.3177 | 1022.69 | 360624 | 1.2225 | 0.0196 | 339.66 |
| | D | 24.67 | 1020.95 | 1.1952 | 332 | 24.66 | 24.3067 | 1020.99 | 360634 | 1.2206 | 0.0196 | 339.65 |
| 40 | A | 24.68 | 1022.66 | 1.1971 | 376 | 24.67 | 24.3135 | 1022.50 | 361491 | 1.2260 | 0.0224 | 338.85 |
| | D | 24.66 | 1020.94 | 1.1952 | 374 | 24.68 | 24.3154 | 1020.92 | 361508 | 1.2239 | 0.0222 | 338.83 |
| 45 | A | 24.67 | 1022.48 | 1.1970 | 415 | 24.67 | 24.3012 | 1022.27 | 362356 | 1.2288 | 0.0247 | 338.04 |
| | D | 24.65 | 1020.78 | 1.1950 | 418 | 24.66 | 24.3010 | 1020.74 | 362365 | 1.2271 | 0.0248 | 338.03 |
| 50 | A | 24.65 | 1022.07 | 1.1966 | 458 | 24.66 | 24.2893 | 1021.84 | 363216 | 1.2317 | 0.0273 | 337.24 |
| | D | 24.67 | 1020.71 | 1.1949 | 463 | 24.66 | 24.3081 | 1020.84 | 363218 | 1.2304 | 0.0273 | 337.23 |
| 55 | A | 24.64 | 1021.61 | 1.1961 | 505 | 24.66 | 24.2857 | 1021.38 | 364084 | 1.2348 | 0.0301 | 336.43 |
| | D | 24.66 | 1020.37 | 1.1945 | 508 | 24.68 | 24.3233 | 1020.49 | 364077 | 1.2334 | 0.0300 | 336.44 |
| 60 | A | 24.66 | 1021.36 | 1.1957 | 550 | 24.66 | 24.2930 | 1021.46 | 364923 | 1.2378 | 0.0325 | 335.66 |
| | D | 24.66 | 1019.98 | 1.1941 | 551 | 24.68 | 24.3179 | 1020.14 | 364933 | 1.2363 | 0.0326 | 335.65 |

| | | | | | | | | | | | | |
|---|---|---|---|---|---|---|---|---|---|---|---|---|
| 65 | A | 24.65 | 1021.55 | 1.1960 | 593 | 24.66 | 24.2935 | 1021.68 | 365769 | 1.2414 | 0.0350 | 334.88 |
| | D | 24.67 | 1019.78 | 1.1938 | 592 | 24.68 | 24.3191 | 1019.81 | 365784 | 1.2392 | 0.0351 | 334.87 |
| 70 | A | 24.64 | 1021.74 | 1.1962 | 635 | 24.65 | 24.2858 | 1021.88 | 366636 | 1.2449 | 0.0375 | 334.09 |
| | D | 24.67 | 1019.98 | 1.1941 | 629 | 24.67 | 24.3109 | 1019.81 | 366655 | 1.2423 | 0.0374 | 334.07 |
| 75 | A | 24.64 | 1021.89 | 1.1964 | 677 | 24.64 | 24.2746 | 1022.08 | 367480 | 1.2483 | 0.0399 | 333.32 |
| | D | 24.68 | 1020.18 | 1.1942 | 678 | 24.68 | 24.3229 | 1019.94 | 367516 | 1.2462 | 0.0404 | 333.29 |
| 80 | A | 24.63 | 1022.29 | 1.1969 | 715 | 24.65 | 24.2741 | 1022.15 | 368349 | 1.2517 | 0.0424 | 332.54 |
| | D | 24.69 | 1020.32 | 1.1944 | 721 | 24.70 | 24.3367 | 1020.45 | 368378 | 1.2497 | 0.0426 | 332.51 |
| 85 | A | 24.64 | 1021.91 | 1.1964 | 759 | 24.64 | 24.2746 | 1021.99 | 369235 | 1.2546 | 0.0448 | 331.74 |
| | D | 24.69 | 1020.96 | 1.1951 | 759 | 24.70 | 24.3367 | 1020.76 | 369262 | 1.2532 | 0.0451 | 331.72 |
| 90 | A | 24.64 | 1021.94 | 1.1965 | 805 | 24.67 | 24.2938 | 1022.03 | 370129 | 1.2582 | 0.0476 | 330.94 |
| | D | 24.68 | 1021.38 | 1.1956 | 800 | 24.70 | 24.3280 | 1021.19 | 370140 | 1.2569 | 0.0476 | 330.93 |
| 95 | | 24.67 | 1021.94 | 1.1964 | 842 | 24.68 | 24.3101 | 1021.77 | 371008 | 1.2608 | 0.0500 | 330.15 |
| Data used for pathlength calibration (the first zero step): $T_{SOS}$ = 24.3154 °C, $P$ = 1021.96 mbar, $t_m^0$ = 354002 ns, $W^0$ = 346.01 m/s. | | | | | | | | | | | | |

Table 128. Isopropanol/dry air results (35 °C isotherm)

| $x_T$/%SAT | | Zero Step | | | $\Delta m_{read}$/µg | Non-Zero Step | | | | | | |
|---|---|---|---|---|---|---|---|---|---|---|---|---|
| | | $T_{DVS}$/°C | $P$/mbar | $\rho^0$/(kg/m³) | | $T_{DVS}$/°C | $T_{SoS}$/°C | $P$/mbar | $t_m$/ns | $\rho$/(kg/m³) | $x$ | $W_m$/(m/s) |
| 10 | A | 34.30 | 1017.58 | 1.1538 | 186 | 34.32 | 34.0322 | 1017.30 | 351610 | 1.1680 | 0.0117 | 347.72 |
| | D | 34.46 | 1017.70 | 1.1533 | 190 | 34.48 | 34.1515 | 1017.61 | 351588 | 1.1679 | 0.0118 | 347.74 |
| 20 | A | 34.30 | 1017.25 | 1.1534 | 358 | 34.31 | 34.0276 | 1017.24 | 355028 | 1.1809 | 0.0220 | 344.37 |
| | D | 34.46 | 1017.80 | 1.1535 | 358 | 34.46 | 34.1246 | 1017.87 | 355025 | 1.1809 | 0.0220 | 344.38 |
| 30 | A | 34.31 | 1017.29 | 1.1534 | 520 | 34.32 | 34.0295 | 1017.30 | 358250 | 1.1933 | 0.0319 | 341.28 |
| | D | 34.46 | 1017.97 | 1.1536 | 526 | 34.46 | 34.1283 | 1017.98 | 358251 | 1.1939 | 0.0323 | 341.27 |
| 40 | A | 34.32 | 1017.36 | 1.1535 | 681 | 34.34 | 34.0422 | 1017.64 | 361312 | 1.2057 | 0.0416 | 338.38 |
| | D | 34.48 | 1017.86 | 1.1535 | 680 | 34.48 | 34.1451 | 1017.86 | 361322 | 1.2056 | 0.0417 | 338.37 |
| 50 | A | 34.33 | 1017.71 | 1.1539 | 829 | 34.36 | 34.0509 | 1017.68 | 364285 | 1.2174 | 0.0510 | 335.62 |
| | D | 34.47 | 1017.71 | 1.1533 | 834 | 34.47 | 34.1303 | 1017.83 | 364302 | 1.2172 | 0.0510 | 335.61 |
| 60 | A | 34.36 | 1017.71 | 1.1537 | 978 | 34.38 | 34.0736 | 1017.82 | 367187 | 1.2287 | 0.0599 | 332.97 |
| | D | 34.46 | 1017.53 | 1.1531 | 982 | 34.46 | 34.1331 | 1017.62 | 367190 | 1.2284 | 0.0602 | 332.97 |
| 70 | A | 34.38 | 1017.91 | 1.1539 | 1124 | 34.40 | 34.0915 | 1017.92 | 370043 | 1.2400 | 0.0690 | 330.40 |
| | D | 34.45 | 1017.06 | 1.1526 | 1131 | 34.47 | 34.1350 | 1017.47 | 370050 | 1.2393 | 0.0691 | 330.39 |
| 80 | A | 34.40 | 1017.83 | 1.1537 | 1272 | 34.43 | 34.1132 | 1017.85 | 372927 | 1.2512 | 0.0781 | 327.84 |
| | D | 34.43 | 1016.99 | 1.1527 | 1270 | 34.44 | 34.1097 | 1017.03 | 372924 | 1.2500 | 0.0779 | 327.85 |
| 90 | A | 34.43 | 1017.86 | 1.1537 | 1412 | 34.44 | 34.1234 | 1017.81 | 375790 | 1.2619 | 0.0866 | 325.35 |
| | D | 34.43 | 1017.30 | 1.1530 | 1409 | 34.43 | 34.1028 | 1017.15 | 375766 | 1.2610 | 0.0866 | 325.37 |
| 95 | | 34.42 | 1017.57 | 1.1533 | 1481 | 34.43 | 34.1100 | 1017.48 | 377180 | 1.2668 | 0.0909 | 324.15 |
| Data used for pathlength calibration (the first zero step): $T_{SoS}$ = 34.0188 °C, $P$ = 1017.58 mbar, $t_m^0$ = 347709 ns, $W^0$ = 351.62 m/s. | | | | | | | | | | | | |

Table 129. Isopropanol/dry air results (45 °C isotherm)

| $x_T$/%SAT | | Zero Step | | | $\Delta m_{read}$/µg | Non-Zero Step | | | | | | |
|---|---|---|---|---|---|---|---|---|---|---|---|---|
| | | $T_{DVS}$/°C | $P$/mbar | $\rho^0$/(kg/m³) | | $T_{DVS}$/°C | $T_{SoS}$/°C | $P$/mbar | $t_m$/ns | $\rho$/(kg/m³) | $x$ | $W_m$/(m/s) |
| 10 | A | 44.00 | 1016.53 | 1.1173 | 335 | 44.03 | 43.6838 | 1016.48 | 349179 | 1.1430 | 0.0214 | 349.84 |
| | D | 43.90 | 1014.26 | 1.1151 | 335 | 43.88 | 43.5779 | 1014.34 | 349201 | 1.1408 | 0.0211 | 349.82 |
| 20 | A | 44.02 | 1016.38 | 1.1170 | 632 | 43.99 | 43.6799 | 1016.37 | 355098 | 1.1654 | 0.0400 | 344.01 |
| | D | 43.90 | 1014.33 | 1.1152 | 625 | 43.94 | 43.6124 | 1014.28 | 355120 | 1.1631 | 0.0399 | 343.99 |
| 30 | A | 43.95 | 1016.42 | 1.1173 | 903 | 43.93 | 43.6240 | 1016.42 | 360491 | 1.1865 | 0.0572 | 338.86 |
| | D | 43.99 | 1014.48 | 1.1151 | 902 | 43.95 | 43.6454 | 1014.34 | 360532 | 1.1842 | 0.0573 | 338.83 |
| 40 | A | 43.94 | 1016.46 | 1.1174 | 1169 | 43.96 | 43.6380 | 1016.55 | 365500 | 1.2070 | 0.0740 | 334.22 |
| | D | 44.00 | 1014.65 | 1.1152 | 1164 | 43.99 | 43.6689 | 1014.61 | 365543 | 1.2044 | 0.0739 | 334.18 |
| 50 | A | 43.92 | 1016.59 | 1.1176 | 1413 | 43.90 | 43.5737 | 1016.67 | 370186 | 1.2259 | 0.0893 | 329.99 |
| | D | 44.01 | 1014.61 | 1.1151 | 1417 | 44.01 | 43.6883 | 1014.65 | 370283 | 1.2237 | 0.0899 | 329.90 |
| 60 | A | 43.88 | 1016.69 | 1.1179 | 1646 | 43.90 | 43.5705 | 1016.58 | 374642 | 1.2440 | 0.1043 | 326.06 |
| | D | 44.00 | 1014.55 | 1.1151 | 1654 | 44.03 | 43.6937 | 1014.57 | 374750 | 1.2418 | 0.1050 | 325.97 |
| 70 | A | 43.87 | 1016.40 | 1.1176 | 1870 | 43.89 | 43.5551 | 1016.12 | 378880 | 1.2609 | 0.1186 | 322.42 |
| | D | 44.00 | 1014.51 | 1.1150 | 1879 | 43.99 | 43.6639 | 1014.53 | 378964 | 1.2591 | 0.1191 | 322.35 |
| 80 | A | 43.89 | 1015.86 | 1.1169 | 2099 | 43.92 | 43.5799 | 1015.66 | 383108 | 1.2778 | 0.1331 | 318.86 |
| | D | 43.96 | 1014.50 | 1.1152 | 2104 | 44.03 | 43.6578 | 1014.50 | 383112 | 1.2764 | 0.1336 | 318.86 |
| 90 | A | 43.93 | 1015.55 | 1.1164 | 2318 | 43.91 | 43.5873 | 1015.36 | 387136 | 1.2941 | 0.1468 | 315.54 |
| | D | 43.94 | 1014.81 | 1.1156 | 2317 | 43.90 | 43.6048 | 1014.62 | 387113 | 1.2932 | 0.1468 | 315.56 |
| 95 | | 43.92 | 1015.20 | 1.1161 | 2429 | 43.94 | 43.6270 | 1015.07 | 389158 | 1.3022 | 0.1540 | 313.90 |
| Data used for pathlength calibration (the first zero step): $T_{SoS}$ = 43.6673 °C, $P$ = 1016.53 mbar, $t_m^0$ = 342073 ns, $W^0$ = 357.11 m/s. | | | | | | | | | | | | |

Table 130. Isopropanol/dry air results (55 °C isotherm)

| $x_T$/%SAT | | Zero Step | | | $\Delta m_{read}$/µg | Non-Zero Step | | | | | | |
|---|---|---|---|---|---|---|---|---|---|---|---|---|
| | | $T_{DVS}$/°C | $P$/mbar | $\rho^0$/(kg/m³) | | $T_{DVS}$/°C | $T_{SoS}$/°C | $P$/mbar | $t_m$/ns | $\rho$/(kg/m³) | $x$ | $W_m$/(m/s) |
| 10 | A | 53.71 | 1017.81 | 1.0854 | 612 | 53.72 | 53.4358 | 1017.88 | 349721 | 1.1323 | 0.0399 | 349.16 |
| | D | 53.72 | 1020.24 | 1.0879 | 605 | 53.72 | 53.4310 | 1020.00 | 349683 | 1.1343 | 0.0396 | 349.20 |
| 20 | A | 53.71 | 1017.89 | 1.0855 | 1123 | 53.70 | 53.4248 | 1018.14 | 359755 | 1.1715 | 0.0730 | 339.42 |
| | D | 53.77 | 1020.45 | 1.0880 | 1118 | 53.75 | 53.4649 | 1020.47 | 359605 | 1.1737 | 0.0727 | 339.56 |
| 30 | A | 53.68 | 1018.38 | 1.0861 | 1583 | 53.69 | 53.4083 | 1018.51 | 368391 | 1.2074 | 0.1030 | 331.46 |
| | D | 53.72 | 1020.64 | 1.0883 | 1553 | 53.77 | 53.4835 | 1020.53 | 368187 | 1.2074 | 0.1012 | 331.65 |
| 40 | A | 53.62 | 1018.72 | 1.0866 | 1996 | 53.70 | 53.4059 | 1019.02 | 375913 | 1.2396 | 0.1299 | 324.83 |
| | D | 53.79 | 1020.43 | 1.0879 | 1993 | 53.76 | 53.4815 | 1020.55 | 375735 | 1.2406 | 0.1293 | 324.98 |
| 50 | A | 53.70 | 1019.22 | 1.0869 | 2387 | 53.70 | 53.4221 | 1019.18 | 382803 | 1.2698 | 0.1553 | 318.98 |
| | D | 53.81 | 1020.36 | 1.0878 | 2384 | 53.81 | 53.5195 | 1020.41 | 382605 | 1.2704 | 0.1549 | 319.15 |
| 60 | A | 53.68 | 1019.29 | 1.0871 | 2746 | 53.71 | 53.4186 | 1019.63 | 388929 | 1.2975 | 0.1782 | 313.96 |
| | D | 53.76 | 1020.08 | 1.0876 | 2737 | 53.79 | 53.5074 | 1020.04 | 388732 | 1.2973 | 0.1780 | 314.12 |
| 70 | A | 53.70 | 1019.88 | 1.0876 | 3084 | 53.71 | 53.4246 | 1020.07 | 394627 | 1.3239 | 0.2001 | 309.43 |
| | D | 53.71 | 1020.06 | 1.0878 | 3066 | 53.75 | 53.4529 | 1020.07 | 394361 | 1.3227 | 0.1992 | 309.63 |
| 80 | A | 53.70 | 1020.11 | 1.0878 | 3403 | 53.70 | 53.4244 | 1020.07 | 399984 | 1.3486 | 0.2209 | 305.28 |
| | D | 53.69 | 1020.16 | 1.0879 | 3384 | 53.70 | 53.4258 | 1020.07 | 399696 | 1.3473 | 0.2198 | 305.50 |
| 90 | A | 53.68 | 1020.20 | 1.0880 | 3691 | 53.62 | 53.3662 | 1020.15 | 404762 | 1.3709 | 0.2393 | 301.68 |
| | D | 53.71 | 1020.20 | 1.0879 | 3694 | 53.71 | 53.4349 | 1020.05 | 404824 | 1.3710 | 0.2398 | 301.63 |
| 95 | | 53.69 | 1020.24 | 1.0880 | 3843 | 53.70 | 53.4248 | 1020.14 | 407171 | 1.3826 | 0.2494 | 299.89 |
| Data used for pathlength calibration (the first zero step): $T_{SoS}$ = 53.4323 °C, $P$ = 1017.81 mbar, $t_m^0$ = 336778 ns, $W^0$ = 362.58 m/s. | | | | | | | | | | | | |

## A6.14 Dichloromethane/dry air

Table 131. Dichloromethane/dry air results (5 °C isotherm)

| $x_T$/%SAT | | Zero Step | | | $\Delta m_{read}$/µg | Non-Zero Step | | | | | | |
|---|---|---|---|---|---|---|---|---|---|---|---|---|
| | | $T_{DVS}$/°C | $P$/mbar | $\rho^0$/(kg/m$^3$) | | $T_{DVS}$/°C | $T_{SoS}$/°C | $P$/mbar | $t_m$/ns | $\rho$/(kg/m$^3$) | $x$ | $W_m$/(m/s) |
| 10 | A | 5.30 | 1014.56 | 1.2706 | 1017 | 5.32 | 5.2299 | 1014.34 | 377912 | 1.3485 | 0.0318 | 323.63 |
| | D | 5.26 | 1012.22 | 1.2678 | 1028 | 5.28 | 5.2248 | 1012.57 | 377977 | 1.3466 | 0.0319 | 323.58 |
| 20 | A | 5.33 | 1014.22 | 1.2700 | 1907 | 5.35 | 5.2534 | 1014.05 | 388622 | 1.4161 | 0.0594 | 314.71 |
| | D | 5.25 | 1011.50 | 1.2670 | 1911 | 5.27 | 5.2139 | 1011.92 | 388670 | 1.4134 | 0.0593 | 314.67 |
| 30 | A | 5.34 | 1014.03 | 1.2698 | 2723 | 5.36 | 5.2595 | 1013.66 | 398349 | 1.4785 | 0.0849 | 307.03 |
| | D | 5.23 | 1011.08 | 1.2665 | 2726 | 5.25 | 5.1999 | 1011.34 | 398377 | 1.4754 | 0.0848 | 307.01 |
| 40 | A | 5.33 | 1013.63 | 1.2693 | 3496 | 5.34 | 5.2538 | 1013.48 | 407286 | 1.5372 | 0.1087 | 300.29 |
| | D | 5.24 | 1010.67 | 1.2660 | 3491 | 5.25 | 5.1904 | 1010.86 | 407327 | 1.5335 | 0.1086 | 300.26 |
| 50 | A | 5.32 | 1013.47 | 1.2691 | 4207 | 5.32 | 5.2392 | 1013.09 | 415538 | 1.5915 | 0.1309 | 294.33 |
| | D | 5.23 | 1010.45 | 1.2657 | 4207 | 5.25 | 5.1831 | 1010.65 | 415592 | 1.5881 | 0.1309 | 294.29 |
| 60 | A | 5.30 | 1012.91 | 1.2685 | 4881 | 5.32 | 5.2328 | 1012.65 | 423202 | 1.6425 | 0.1518 | 289.00 |
| | D | 5.24 | 1010.19 | 1.2654 | 4881 | 5.25 | 5.1833 | 1010.44 | 423228 | 1.6394 | 0.1518 | 288.98 |
| 70 | A | 5.29 | 1012.34 | 1.2679 | 5533 | 5.29 | 5.2094 | 1012.51 | 430386 | 1.6918 | 0.1718 | 284.17 |
| | D | 5.24 | 1011.09 | 1.2665 | 5514 | 5.25 | 5.1796 | 1010.63 | 430439 | 1.6891 | 0.1718 | 284.14 |
| 80 | A | 5.26 | 1012.70 | 1.2684 | 6142 | 5.27 | 5.1967 | 1012.65 | 437159 | 1.7391 | 0.1907 | 279.77 |
| | D | 5.24 | 1011.49 | 1.2670 | 6135 | 5.25 | 5.1779 | 1011.33 | 437192 | 1.7372 | 0.1908 | 279.75 |
| 90 | A | 5.24 | 1012.45 | 1.2682 | 6719 | 5.26 | 5.1850 | 1012.18 | 443509 | 1.7831 | 0.2088 | 275.76 |
| | D | 5.23 | 1011.97 | 1.2677 | 6712 | 5.25 | 5.1762 | 1011.70 | 443496 | 1.7820 | 0.2086 | 275.77 |
| 95 | | 5.24 | 1012.05 | 1.2677 | 7008 | 5.26 | 5.1838 | 1012.06 | 446572 | 1.8047 | 0.2176 | 273.87 |
| Data used for pathlength calibration (the first zero step): $T_{SoS}$ = 5.2050 °C, $P$ = 1014.56 mbar, $t_m^0$ = 365426 ns, $W^0$ = 334.69 m/s. | | | | | | | | | | | | |

Table 132. Dichloromethane/dry air results (15 °C isotherm)

| $x_T$/%SAT | | Zero Step | | | $\Delta m_{read}$/µg | Non-Zero Step | | | | | | |
|---|---|---|---|---|---|---|---|---|---|---|---|---|
| | | $T_{DVS}$/°C | $P$/mbar | $\rho^0$/(kg/m$^3$) | | $T_{DVS}$/°C | $T_{SoS}$/°C | $P$/mbar | $t_m$/ns | $\rho$/(kg/m$^3$) | $x$ | $W_m$/(m/s) |
| 10 | A | 14.42 | 1004.46 | 1.2179 | 1743 | 14.39 | 14.0312 | 1004.26 | 382138 | 1.3515 | 0.0565 | 320.50 |
| | D | 14.39 | 1003.80 | 1.2172 | 1736 | 14.40 | 14.0295 | 1004.01 | 382008 | 1.3502 | 0.0562 | 320.61 |
| 20 | A | 14.35 | 1003.93 | 1.2176 | 3169 | 14.37 | 13.9947 | 1003.58 | 399582 | 1.4604 | 0.1030 | 306.50 |
| | D | 14.40 | 1003.70 | 1.2171 | 3156 | 14.40 | 14.0337 | 1003.68 | 399368 | 1.4589 | 0.1023 | 306.67 |
| 30 | A | 14.36 | 1003.36 | 1.2168 | 4422 | 14.37 | 13.9993 | 1003.21 | 414373 | 1.5556 | 0.1434 | 295.56 |
| | D | 14.40 | 1003.48 | 1.2168 | 4408 | 14.41 | 14.0406 | 1003.57 | 414176 | 1.5546 | 0.1428 | 295.70 |
| 40 | A | 14.37 | 1002.77 | 1.2161 | 5547 | 14.38 | 14.0141 | 1002.73 | 427345 | 1.6412 | 0.1798 | 286.59 |
| | D | 14.37 | 1003.64 | 1.2171 | 5524 | 14.42 | 14.0380 | 1003.61 | 427094 | 1.6404 | 0.1790 | 286.76 |
| 50 | A | 14.37 | 1002.54 | 1.2158 | 6548 | 14.38 | 14.0120 | 1002.27 | 438741 | 1.7176 | 0.2123 | 279.15 |
| | D | 14.42 | 1003.86 | 1.2172 | 6532 | 14.43 | 14.0558 | 1003.82 | 438437 | 1.7177 | 0.2114 | 279.34 |
| 60 | A | 14.38 | 1003.20 | 1.2166 | 7464 | 14.38 | 14.0080 | 1003.56 | 448702 | 1.7886 | 0.2412 | 272.95 |
| | D | 14.41 | 1004.03 | 1.2174 | 7442 | 14.43 | 14.0501 | 1003.86 | 448550 | 1.7877 | 0.2408 | 273.04 |
| 70 | A | 14.36 | 1003.72 | 1.2172 | 8295 | 14.37 | 13.9996 | 1004.51 | 457659 | 1.8529 | 0.2675 | 267.61 |
| | D | 14.41 | 1004.29 | 1.2177 | 8278 | 14.43 | 14.0512 | 1004.20 | 457650 | 1.8521 | 0.2676 | 267.61 |
| 80 | A | 14.36 | 1004.78 | 1.2185 | 9057 | 14.35 | 13.9829 | 1005.06 | 465826 | 1.9126 | 0.2921 | 262.92 |
| | D | 14.42 | 1004.47 | 1.2179 | 9053 | 14.42 | 14.0394 | 1004.28 | 465960 | 1.9117 | 0.2925 | 262.84 |
| 90 | A | 14.35 | 1004.96 | 1.2188 | 9766 | 14.35 | 13.9759 | 1005.03 | 473358 | 1.9672 | 0.3149 | 258.73 |
| | D | 14.40 | 1004.64 | 1.2182 | 9761 | 14.38 | 14.0109 | 1004.62 | 473423 | 1.9662 | 0.3149 | 258.70 |
| 95 | | 14.33 | 1005.04 | 1.2190 | 10125 | 14.42 | 14.0223 | 1004.94 | 477236 | 1.9949 | 0.3268 | 256.63 |
| Data used for pathlength calibration (the first zero step): $T_{SoS}$ = 14.0370 °C, $P$ = 1004.46 mbar, $t_m^0$ = 360249 ns, $W^0$ = 339.97 m/s. | | | | | | | | | | | | |

Table 133. Dichloromethane/dry air results (25 °C isotherm)

| $x_T$/%SAT | | Zero Step | | | $\Delta m_{read}$/µg | Non-Zero Step | | | | | | |
|---|---|---|---|---|---|---|---|---|---|---|---|---|
| | | $T_{DVS}$/°C | $P$/mbar | $\rho^0$/(kg/m$^3$) | | $T_{DVS}$/°C | $T_{SoS}$/°C | $P$/mbar | $t_m$/ns | $\rho$/(kg/m$^3$) | $x$ | $W_m$/(m/s) |
| 5 | A | 24.34 | 1003.84 | 1.1765 | 1995 | 24.35 | 23.9061 | 1003.89 | 379643 | 1.3293 | 0.0670 | 322.53 |
| | D | 24.31 | 1010.58 | 1.1845 | 1933 | 24.33 | 23.8815 | 1010.69 | 378480 | 1.3326 | 0.0644 | 323.52 |
| 10 | A | 24.34 | 1003.72 | 1.1763 | 3449 | 24.37 | 23.9209 | 1003.63 | 397422 | 1.4406 | 0.1158 | 308.10 |
| | D | 24.22 | 1010.48 | 1.1847 | 3323 | 24.31 | 23.8466 | 1010.51 | 395660 | 1.4393 | 0.1109 | 309.47 |
| 15 | A | 24.35 | 1003.64 | 1.1762 | 4701 | 24.37 | 23.9262 | 1004.00 | 412621 | 1.5364 | 0.1574 | 296.75 |
| | D | 24.32 | 1010.51 | 1.1843 | 4516 | 24.28 | 23.8558 | 1010.51 | 409824 | 1.5304 | 0.1503 | 298.78 |
| 20 | A | 24.36 | 1004.19 | 1.1768 | 5854 | 24.37 | 23.9267 | 1004.69 | 425808 | 1.6254 | 0.1958 | 287.56 |
| | D | 24.33 | 1010.30 | 1.1841 | 5595 | 24.33 | 23.8751 | 1010.23 | 422435 | 1.6128 | 0.1863 | 289.86 |
| 25 | A | 24.35 | 1005.00 | 1.1777 | 6816 | 24.36 | 23.9181 | 1005.25 | 436692 | 1.7001 | 0.2278 | 280.40 |
| | D | 24.31 | 1010.22 | 1.1840 | 6538 | 24.33 | 23.8750 | 1010.23 | 433164 | 1.6851 | 0.2176 | 282.68 |
| 30 | A | 24.36 | 1005.32 | 1.1781 | 7695 | 24.36 | 23.9128 | 1005.44 | 446503 | 1.7678 | 0.2571 | 274.23 |
| | D | 24.30 | 1010.21 | 1.1841 | 7359 | 24.32 | 23.8635 | 1010.27 | 442363 | 1.7480 | 0.2448 | 276.80 |
| 35 | A | 24.33 | 1005.74 | 1.1787 | 8481 | 24.35 | 23.9009 | 1005.94 | 455157 | 1.8286 | 0.2831 | 269.02 |
| | D | 24.31 | 1009.71 | 1.1834 | 8123 | 24.33 | 23.8717 | 1009.98 | 450802 | 1.8059 | 0.2700 | 271.62 |
| 40 | A | 24.34 | 1005.98 | 1.1789 | 9211 | 24.34 | 23.8979 | 1005.99 | 463056 | 1.8848 | 0.3074 | 264.43 |
| Data used for pathlength calibration (the first zero step): $T_{SoS}$ = 23.8788 °C, $P$ = 1003.84 mbar, $t_m^0$ = 354138 ns, $W^0$ = 345.76 m/s. | | | | | | | | | | | | |

## A6.15 Chloroform/dry air

Table 134. Chloroform/dry air results (5 °C isotherm)

| $x_T$/%SAT | | Zero Step | | | $\Delta m_{read}$/µg | Non-Zero Step | | | | | | |
|---|---|---|---|---|---|---|---|---|---|---|---|---|
| | | $T_{DVS}$/°C | $P$/mbar | $\rho^0$/(kg/m$^3$) | | $T_{DVS}$/°C | $T_{SoS}$/°C | $P$/mbar | $t_m$/ns | $\rho$/(kg/m$^3$) | $x$ | $W_m$/(m/s) |
| 10 | A | 5.44 | 1006.66 | 1.2600 | 613 | 5.46 | 5.3198 | 1006.75 | 372985 | 1.3070 | 0.0119 | 327.87 |
| | D | 5.37 | 1011.06 | 1.2659 | 609 | 5.40 | 5.2899 | 1011.24 | 372999 | 1.3126 | 0.0118 | 327.86 |
| 20 | A | 5.45 | 1006.95 | 1.2604 | 1171 | 5.47 | 5.3291 | 1007.05 | 379961 | 1.3501 | 0.0227 | 321.85 |
| | D | 5.38 | 1010.70 | 1.2654 | 1172 | 5.39 | 5.2833 | 1010.84 | 379948 | 1.3552 | 0.0226 | 321.86 |
| 30 | A | 5.46 | 1007.07 | 1.2605 | 1720 | 5.48 | 5.3391 | 1007.26 | 386644 | 1.3923 | 0.0333 | 316.29 |
| | D | 5.37 | 1010.48 | 1.2651 | 1714 | 5.38 | 5.2784 | 1010.67 | 386552 | 1.3965 | 0.0331 | 316.36 |
| 40 | A | 5.48 | 1007.37 | 1.2608 | 2246 | 5.50 | 5.3518 | 1007.40 | 393027 | 1.4329 | 0.0436 | 311.15 |
| | D | 5.37 | 1010.35 | 1.2650 | 2232 | 5.39 | 5.2800 | 1010.31 | 392847 | 1.4360 | 0.0432 | 311.29 |
| 50 | A | 5.48 | 1007.45 | 1.2608 | 2762 | 5.49 | 5.3538 | 1007.65 | 399147 | 1.4725 | 0.0535 | 306.38 |
| | D | 5.38 | 1010.05 | 1.2646 | 2747 | 5.39 | 5.2796 | 1010.29 | 398908 | 1.4751 | 0.0530 | 306.56 |
| 60 | A | 5.49 | 1007.83 | 1.2613 | 3260 | 5.49 | 5.3535 | 1008.10 | 404962 | 1.5111 | 0.0631 | 301.98 |
| | D | 5.36 | 1010.07 | 1.2647 | 3232 | 5.38 | 5.2723 | 1010.04 | 404697 | 1.5123 | 0.0625 | 302.18 |
| 70 | A | 5.47 | 1008.15 | 1.2618 | 3744 | 5.49 | 5.3519 | 1008.49 | 410625 | 1.5487 | 0.0725 | 297.82 |
| | D | 5.38 | 1010.30 | 1.2649 | 3719 | 5.38 | 5.2740 | 1010.30 | 410346 | 1.5499 | 0.0719 | 298.02 |
| 80 | A | 5.48 | 1008.58 | 1.2623 | 4224 | 5.49 | 5.3543 | 1008.90 | 416129 | 1.5860 | 0.0817 | 293.88 |
| | D | 5.39 | 1009.89 | 1.2644 | 4204 | 5.39 | 5.2817 | 1010.16 | 415876 | 1.5865 | 0.0812 | 294.06 |
| 90 | A | 5.47 | 1009.11 | 1.2630 | 4691 | 5.46 | 5.3358 | 1009.39 | 421417 | 1.6225 | 0.0907 | 290.19 |
| | D | 5.41 | 1009.79 | 1.2641 | 4678 | 5.42 | 5.2984 | 1009.88 | 421340 | 1.6226 | 0.0904 | 290.24 |
| 95 | | 5.42 | 1009.56 | 1.2638 | 4913 | 5.43 | 5.3124 | 1009.68 | 423930 | 1.6403 | 0.0950 | 288.47 |
| Data used for pathlength calibration (the first zero step): $T_{SoS}$ = 5.2987 °C, $P$ = 1006.66 mbar, $t_m^0$ = 365325 ns, $W^0$ = 334.74 m/s. | | | | | | | | | | | | |

Table 135. Chloroform/dry air results (15 °C isotherm)

| $x_T$/%SAT | | Zero Step | | | $\Delta m_{read}$/µg | Non-Zero Step | | | | | | |
|---|---|---|---|---|---|---|---|---|---|---|---|---|
| | | $T_{DVS}$/°C | $P$/mbar | $\rho^0$/(kg/m$^3$) | | $T_{DVS}$/°C | $T_{SoS}$/°C | $P$/mbar | $t_m$/ns | $\rho$/(kg/m$^3$) | $x$ | $W_m$/(m/s) |
| 10 | A | 14.72 | 1013.46 | 1.2276 | 994 | 14.69 | 14.4634 | 1013.44 | 372291 | 1.3038 | 0.0198 | 328.69 |
| | D | 14.69 | 1005.69 | 1.2183 | 1007 | 14.69 | 14.4717 | 1005.48 | 372612 | 1.2954 | 0.0203 | 328.41 |
| 20 | A | 14.72 | 1013.55 | 1.2277 | 1890 | 14.71 | 14.4830 | 1013.30 | 383483 | 1.3725 | 0.0378 | 319.10 |
| | D | 14.71 | 1006.30 | 1.2189 | 1898 | 14.70 | 14.4794 | 1005.94 | 383759 | 1.3644 | 0.0382 | 318.87 |
| 30 | A | 14.70 | 1013.32 | 1.2275 | 2739 | 14.72 | 14.4815 | 1013.18 | 393784 | 1.4374 | 0.0547 | 310.75 |
| | D | 14.70 | 1006.87 | 1.2196 | 2742 | 14.71 | 14.4835 | 1006.58 | 394030 | 1.4298 | 0.0551 | 310.56 |
| 40 | A | 14.73 | 1012.84 | 1.2268 | 3541 | 14.76 | 14.5137 | 1012.67 | 403354 | 1.4981 | 0.0707 | 303.38 |
| | D | 14.73 | 1007.40 | 1.2201 | 3542 | 14.72 | 14.4975 | 1007.06 | 403612 | 1.4916 | 0.0711 | 303.19 |
| 50 | A | 14.73 | 1012.69 | 1.2266 | 4309 | 14.75 | 14.5129 | 1012.54 | 412336 | 1.5568 | 0.0860 | 296.77 |
| | D | 14.71 | 1007.97 | 1.2209 | 4310 | 14.73 | 14.5041 | 1007.71 | 412623 | 1.5512 | 0.0865 | 296.57 |
| 60 | A | 14.75 | 1012.44 | 1.2262 | 5039 | 14.73 | 14.5031 | 1012.02 | 420808 | 1.6123 | 0.1006 | 290.80 |
| | D | 14.70 | 1008.35 | 1.2214 | 5035 | 14.72 | 14.4936 | 1008.25 | 420980 | 1.6073 | 0.1009 | 290.68 |
| 70 | A | 14.72 | 1011.72 | 1.2254 | 5748 | 14.73 | 14.4982 | 1011.35 | 428938 | 1.6659 | 0.1148 | 285.29 |
| | D | 14.75 | 1008.84 | 1.2218 | 5744 | 14.71 | 14.4976 | 1008.62 | 429044 | 1.6620 | 0.1150 | 285.22 |
| 80 | A | 14.72 | 1010.88 | 1.2244 | 6439 | 14.74 | 14.5020 | 1010.54 | 436763 | 1.7179 | 0.1287 | 280.17 |
| | D | 14.74 | 1009.29 | 1.2224 | 6437 | 14.72 | 14.4962 | 1009.07 | 436801 | 1.7157 | 0.1288 | 280.15 |
| 90 | A | 14.73 | 1010.21 | 1.2236 | 7120 | 14.74 | 14.5047 | 1010.09 | 444265 | 1.7692 | 0.1423 | 275.44 |
| | D | 14.71 | 1009.44 | 1.2227 | 7104 | 14.71 | 14.4800 | 1009.29 | 444203 | 1.7671 | 0.1420 | 275.48 |
| 95 | | 14.71 | 1009.77 | 1.2231 | 7440 | 14.73 | 14.4977 | 1009.70 | 447813 | 1.7932 | 0.1487 | 273.26 |
| Data used for pathlength calibration (the first zero step): $T_{SoS}$ = 14.4777 °C, $P$ = 1013.46 mbar, $t_m^0$ = 359666 ns, $W^0$ = 340.23 m/s. | | | | | | | | | | | | |

Table 136. Chloroform/dry air results (25 °C isotherm)

| $x_T$/%SAT | | Zero Step | | | $\Delta m_{read}$/µg | Non-Zero Step | | | | | | |
|---|---|---|---|---|---|---|---|---|---|---|---|---|
| | | $T_{DVS}$/°C | $P$/mbar | $\rho^0$/(kg/m$^3$) | | $T_{DVS}$/°C | $T_{SoS}$/°C | $P$/mbar | $t_m$/ns | $\rho$/(kg/m$^3$) | $x$ | $W_m$/(m/s) |
| 5 | A | 24.41 | 1001.60 | 1.1735 | 882 | 24.43 | 23.9953 | 1001.48 | 365638 | 1.2411 | 0.0185 | 334.80 |
| | D | 24.27 | 1003.71 | 1.1765 | 881 | 24.27 | 23.8392 | 1003.79 | 365772 | 1.2440 | 0.0183 | 334.67 |
| 10 | A | 24.41 | 1001.47 | 1.1734 | 1657 | 24.43 | 23.9931 | 1001.46 | 375544 | 1.3003 | 0.0346 | 325.97 |
| | D | 24.27 | 1003.64 | 1.1765 | 1635 | 24.28 | 23.8462 | 1003.72 | 375507 | 1.3018 | 0.0340 | 326.00 |
| 15 | A | 24.46 | 1001.77 | 1.1735 | 2397 | 24.46 | 24.0281 | 1001.81 | 384860 | 1.3572 | 0.0500 | 318.08 |
| | D | 24.28 | 1003.30 | 1.1760 | 2363 | 24.27 | 23.8365 | 1003.49 | 384578 | 1.3571 | 0.0491 | 318.31 |
| 20 | A | 24.46 | 1001.90 | 1.1737 | 3097 | 24.48 | 24.0448 | 1001.99 | 393520 | 1.4110 | 0.0646 | 311.08 |
| | D | 24.27 | 1003.04 | 1.1758 | 3048 | 24.29 | 23.8521 | 1003.25 | 393053 | 1.4094 | 0.0634 | 311.45 |
| 25 | A | 24.39 | 1001.95 | 1.1740 | 3740 | 24.36 | 23.9500 | 1001.98 | 401425 | 1.4606 | 0.0779 | 304.95 |
| | D | 24.26 | 1002.70 | 1.1754 | 3712 | 24.36 | 23.8862 | 1002.84 | 401162 | 1.4599 | 0.0773 | 305.15 |
| 30 | A | 24.35 | 1002.08 | 1.1743 | 4373 | 24.34 | 23.9267 | 1002.10 | 409044 | 1.5094 | 0.0911 | 299.27 |
| | D | 24.25 | 1002.15 | 1.1748 | 4329 | 24.27 | 23.8304 | 1002.41 | 408546 | 1.5066 | 0.0901 | 299.64 |
| 35 | A | 24.36 | 1002.00 | 1.1742 | 4995 | 24.43 | 23.9819 | 1001.93 | 416397 | 1.5570 | 0.1042 | 293.99 |
| | D | 24.25 | 1002.00 | 1.1746 | 4924 | 24.27 | 23.8309 | 1002.03 | 415665 | 1.5520 | 0.1025 | 294.50 |
| 40 | A | 24.35 | 1002.16 | 1.1744 | 5551 | 24.33 | 23.9092 | 1002.37 | 422892 | 1.5998 | 0.1154 | 289.47 |
| | D | 24.27 | 1001.97 | 1.1745 | 5507 | 24.29 | 23.8489 | 1001.94 | 422551 | 1.5965 | 0.1147 | 289.70 |
| 45 | A | 24.32 | 1002.50 | 1.1749 | 6124 | 24.33 | 23.9073 | 1002.66 | 429488 | 1.6442 | 0.1274 | 285.03 |
| | D | 24.28 | 1002.10 | 1.1746 | 6066 | 24.28 | 23.8503 | 1002.06 | 428962 | 1.6395 | 0.1263 | 285.37 |
| 50 | A | 24.33 | 1002.82 | 1.1753 | 6662 | 24.32 | 23.9030 | 1002.83 | 435675 | 1.6858 | 0.1385 | 280.98 |
| | D | 24.31 | 1002.32 | 1.1748 | 6612 | 24.31 | 23.8798 | 1002.21 | 435186 | 1.6815 | 0.1376 | 281.29 |
| 55 | A | 24.31 | 1002.91 | 1.1755 | 7187 | 24.31 | 23.8945 | 1003.07 | 441563 | 1.7262 | 0.1494 | 277.23 |
| | D | 24.39 | 1002.73 | 1.1749 | 7145 | 24.33 | 23.9170 | 1002.51 | 441159 | 1.7225 | 0.1486 | 277.48 |
| 60 | A | 24.30 | 1003.16 | 1.1758 | 7690 | 24.30 | 23.8736 | 1003.23 | 447198 | 1.7651 | 0.1598 | 273.74 |
| | D | 24.37 | 1002.63 | 1.1749 | 7668 | 24.40 | 23.9522 | 1002.69 | 446983 | 1.7625 | 0.1595 | 273.87 |

| | | | | | | | | | | | | |
|---|---|---|---|---|---|---|---|---|---|---|---|---|
| 65 | A | 24.29 | 1003.24 | 1.1759 | 8185 | 24.31 | 23.8714 | 1003.32 | 452702 | 1.8031 | 0.1700 | 270.41 |
| | D | 24.38 | 1002.68 | 1.1749 | 8151 | 24.38 | 23.9429 | 1002.55 | 452403 | 1.7995 | 0.1696 | 270.59 |
| 70 | A | 24.29 | 1003.18 | 1.1759 | 8667 | 24.29 | 23.8642 | 1003.03 | 458099 | 1.8400 | 0.1801 | 267.22 |
| | D | 24.39 | 1003.02 | 1.1753 | 8645 | 24.40 | 23.9573 | 1002.80 | 457853 | 1.8378 | 0.1798 | 267.37 |
| 75 | A | 24.29 | 1002.95 | 1.1756 | 9142 | 24.30 | 23.8699 | 1002.93 | 463281 | 1.8762 | 0.1900 | 264.23 |
| | D | 24.37 | 1003.22 | 1.1756 | 9123 | 24.39 | 23.9451 | 1003.12 | 462975 | 1.8747 | 0.1896 | 264.41 |
| 80 | A | 24.29 | 1002.87 | 1.1755 | 9585 | 24.28 | 23.8579 | 1002.74 | 468062 | 1.9100 | 0.1992 | 261.54 |
| | D | 24.35 | 1003.39 | 1.1759 | 9585 | 24.37 | 23.9308 | 1003.35 | 467938 | 1.9104 | 0.1991 | 261.60 |
| 85 | A | 24.27 | 1002.79 | 1.1755 | 10039 | 24.28 | 23.8540 | 1002.72 | 472877 | 1.9448 | 0.2086 | 258.87 |
| | D | 24.28 | 1003.28 | 1.1760 | 10050 | 24.36 | 23.9002 | 1003.34 | 472900 | 1.9461 | 0.2088 | 258.86 |
| 90 | A | 24.27 | 1002.67 | 1.1753 | 10478 | 24.30 | 23.8564 | 1002.73 | 477538 | 1.9783 | 0.2177 | 256.35 |
| | D | 24.26 | 1003.00 | 1.1758 | 10455 | 24.24 | 23.8207 | 1003.26 | 477155 | 1.9770 | 0.2169 | 256.55 |
| 95 | | 24.36 | 1002.76 | 1.1751 | 10915 | 24.30 | 23.8852 | 1002.92 | 481973 | 2.0116 | 0.2265 | 253.99 |
| Data used for pathlength calibration (the first zero step): $T_{SoS}$ = 23.9821 °C, $P$ = 1001.60 mbar, $t_m^0$ = 353986 ns, $W^0$ = 345.82 m/s. | | | | | | | | | | | | |

Table 137. Chloroform/dry air results (35 °C isotherm)

| $x_T$/%SAT | | Zero Step | | | $\Delta m_{read}$/µg | Non-Zero Step | | | | | | |
|---|---|---|---|---|---|---|---|---|---|---|---|---|
| | | $T_{DVS}$/°C | $P$/mbar | $\rho^0$/(kg/m$^3$) | | $T_{DVS}$/°C | $T_{SoS}$/°C | $P$/mbar | $t_m$/ns | $\rho$/(kg/m$^3$) | $x$ | $W_m$/(m/s) |
| 10 | A | 34.59 | 1017.23 | 1.1523 | 2835 | 34.61 | 34.2395 | 1016.95 | 384085 | 1.3696 | 0.0603 | 318.39 |
| | D | 34.55 | 1015.01 | 1.1499 | 2843 | 34.58 | 34.1888 | 1015.13 | 384236 | 1.3678 | 0.0605 | 318.27 |
| 20 | A | 34.60 | 1016.84 | 1.1518 | 5125 | 34.61 | 34.2407 | 1016.62 | 411846 | 1.5446 | 0.1089 | 296.93 |
| | D | 34.49 | 1015.01 | 1.1502 | 5073 | 34.49 | 34.1180 | 1015.07 | 411241 | 1.5389 | 0.1079 | 297.37 |
| 30 | A | 34.60 | 1016.43 | 1.1514 | 7137 | 34.63 | 34.2545 | 1016.28 | 434955 | 1.6983 | 0.1516 | 281.15 |
| | D | 34.53 | 1014.85 | 1.1499 | 7038 | 34.52 | 34.1692 | 1014.89 | 433888 | 1.6892 | 0.1496 | 281.84 |
| 40 | A | 34.63 | 1016.26 | 1.1511 | 8887 | 34.63 | 34.2676 | 1016.28 | 454289 | 1.8321 | 0.1886 | 269.19 |
| | D | 34.54 | 1014.69 | 1.1496 | 8755 | 34.54 | 34.1800 | 1014.80 | 452998 | 1.8206 | 0.1860 | 269.96 |
| 50 | A | 34.61 | 1016.21 | 1.1511 | 10416 | 34.59 | 34.2351 | 1016.15 | 470814 | 1.9493 | 0.2210 | 259.74 |
| | D | 34.55 | 1015.05 | 1.1500 | 10306 | 34.56 | 34.1946 | 1014.79 | 469745 | 1.9398 | 0.2190 | 260.33 |
| 60 | A | 34.59 | 1016.04 | 1.1510 | 11819 | 34.58 | 34.2232 | 1016.17 | 485453 | 2.0566 | 0.2505 | 251.91 |
| | D | 34.54 | 1015.54 | 1.1506 | 11690 | 34.55 | 34.1917 | 1015.32 | 484262 | 2.0464 | 0.2481 | 252.53 |
| 70 | A | 34.59 | 1016.19 | 1.1511 | 13103 | 34.60 | 34.2427 | 1016.44 | 498613 | 2.1553 | 0.2776 | 245.26 |
| | D | 34.52 | 1015.90 | 1.1511 | 12962 | 34.54 | 34.1713 | 1015.73 | 497270 | 2.1444 | 0.2749 | 245.92 |
| 80 | A | 34.58 | 1016.64 | 1.1517 | 14274 | 34.62 | 34.2508 | 1016.76 | 510289 | 2.2456 | 0.3022 | 239.65 |
| | D | 34.53 | 1016.20 | 1.1514 | 14141 | 34.53 | 34.1681 | 1016.05 | 509078 | 2.2350 | 0.2996 | 240.22 |
| 90 | A | 34.61 | 1016.79 | 1.1517 | 15362 | 34.61 | 34.2548 | 1016.74 | 520933 | 2.3289 | 0.3251 | 234.75 |
| | D | 34.61 | 1016.55 | 1.1515 | 15275 | 34.55 | 34.2041 | 1016.39 | 520126 | 2.3220 | 0.3233 | 235.11 |
| 95 | | 34.61 | 1016.67 | 1.1516 | 15853 | 34.62 | 34.2609 | 1016.73 | 525702 | 2.3665 | 0.3355 | 232.62 |
| Data used for pathlength calibration (the first zero step): $T_{SoS}$ = 34.2241 °C, $P$ = 1017.23 mbar, $t_m^0$ = 347669 ns, $W^0$ = 351.74 m/s. | | | | | | | | | | | | |

## A6.16 1,2-Dichloroethane/dry air

Table 138. 1,2-Dichloroethane/dry air results (5 °C isotherm)

| $x_T$/%SAT | | Zero Step | | | $\Delta m_{read}$/µg | Non-Zero Step | | | | | | |
|---|---|---|---|---|---|---|---|---|---|---|---|---|
| | | $T_{DVS}$/°C | $P$/mbar | $\rho^0$/(kg/m$^3$) | | $T_{DVS}$/°C | $T_{SoS}$/°C | $P$/mbar | $t_m$/ns | $\rho$/(kg/m$^3$) | $x$ | $W_m$/(m/s) |
| 10 | A | 5.31 | 1014.74 | 1.2708 | 158 | 5.33 | 5.2391 | 1014.66 | 367520 | 1.2829 | 0.0040 | 332.73 |
| | D | 5.35 | 1016.12 | 1.2723 | 161 | 5.35 | 5.2653 | 1016.09 | 367522 | 1.2847 | 0.0040 | 332.73 |
| 20 | A | 5.33 | 1014.56 | 1.2705 | 309 | 5.35 | 5.2522 | 1014.65 | 369558 | 1.2941 | 0.0077 | 330.90 |
| | D | 5.39 | 1015.89 | 1.2719 | 315 | 5.37 | 5.2898 | 1016.19 | 369559 | 1.2960 | 0.0077 | 330.90 |
| 30 | A | 5.34 | 1014.75 | 1.2707 | 454 | 5.36 | 5.2697 | 1014.70 | 371557 | 1.3054 | 0.0113 | 329.12 |
| | D | 5.40 | 1015.91 | 1.2718 | 457 | 5.40 | 5.3093 | 1015.90 | 371559 | 1.3068 | 0.0113 | 329.12 |
| 40 | A | 5.35 | 1014.59 | 1.2704 | 599 | 5.38 | 5.2829 | 1014.66 | 373509 | 1.3163 | 0.0149 | 327.40 |
| | D | 5.41 | 1015.94 | 1.2718 | 601 | 5.41 | 5.3219 | 1016.05 | 373506 | 1.3179 | 0.0149 | 327.40 |
| 50 | A | 5.37 | 1014.61 | 1.2703 | 743 | 5.38 | 5.2880 | 1014.71 | 375441 | 1.3273 | 0.0184 | 325.71 |
| | D | 5.40 | 1016.03 | 1.2720 | 741 | 5.42 | 5.3223 | 1015.87 | 375441 | 1.3288 | 0.0185 | 325.71 |
| 60 | A | 5.37 | 1014.99 | 1.2708 | 885 | 5.38 | 5.2929 | 1015.23 | 377327 | 1.3386 | 0.0219 | 324.09 |
| | D | 5.39 | 1015.90 | 1.2719 | 884 | 5.41 | 5.3196 | 1015.90 | 377329 | 1.3396 | 0.0220 | 324.08 |
| 70 | A | 5.38 | 1015.32 | 1.2712 | 1027 | 5.39 | 5.3020 | 1015.55 | 379195 | 1.3499 | 0.0254 | 322.49 |
| | D | 5.40 | 1016.20 | 1.2722 | 1023 | 5.41 | 5.3184 | 1016.09 | 379208 | 1.3506 | 0.0255 | 322.48 |
| 80 | A | 5.38 | 1015.95 | 1.2720 | 1167 | 5.39 | 5.3036 | 1016.18 | 381072 | 1.3614 | 0.0289 | 320.90 |
| | D | 5.38 | 1016.37 | 1.2725 | 1165 | 5.40 | 5.3089 | 1016.37 | 381078 | 1.3618 | 0.0289 | 320.90 |
| 90 | A | 5.38 | 1016.25 | 1.2723 | 1312 | 5.39 | 5.3064 | 1016.51 | 382931 | 1.3729 | 0.0324 | 319.34 |
| | D | 5.38 | 1016.56 | 1.2727 | 1305 | 5.39 | 5.3117 | 1016.39 | 382941 | 1.3728 | 0.0325 | 319.34 |
| 95 | | 5.39 | 1016.70 | 1.2729 | 1371 | 5.39 | 5.3104 | 1016.64 | 383822 | 1.3779 | 0.0340 | 318.60 |
| Data used for pathlength calibration (the first zero step): $T_{SoS}$ = 5.2147 °C, $P$ = 1014.74 mbar, $t_m^0$ = 365368 ns, $W^0$ = 334.69 m/s. | | | | | | | | | | | | |

Table 139. 1,2-Dichloroethane/dry air results (15 °C isotherm)

| $x_T$/%SAT | | Zero Step | | | $\Delta m_{read}$/µg | Non-Zero Step | | | | | | |
|---|---|---|---|---|---|---|---|---|---|---|---|---|
| | | $T_{DVS}$/°C | $P$/mbar | $\rho^0$/(kg/m$^3$) | | $T_{DVS}$/°C | $T_{SoS}$/°C | $P$/mbar | $t_m$/ns | $\rho$/(kg/m$^3$) | $x$ | $W_m$/(m/s) |
| 10 | A | 14.39 | 1016.64 | 1.2328 | 254 | 14.41 | 14.0370 | 1016.52 | 363765 | 1.2523 | 0.0066 | 336.61 |
| | D | 14.39 | 1008.93 | 1.2234 | 250 | 14.40 | 14.0442 | 1008.53 | 363793 | 1.2426 | 0.0066 | 336.58 |
| 20 | A | 14.40 | 1016.57 | 1.2327 | 495 | 14.41 | 14.0412 | 1016.50 | 367104 | 1.2706 | 0.0127 | 333.55 |
| | D | 14.39 | 1009.64 | 1.2243 | 491 | 14.40 | 14.0448 | 1009.28 | 367181 | 1.2619 | 0.0128 | 333.47 |
| 30 | A | 14.39 | 1016.42 | 1.2325 | 728 | 14.42 | 14.0435 | 1016.39 | 370368 | 1.2883 | 0.0187 | 330.61 |
| | D | 14.40 | 1010.54 | 1.2254 | 723 | 14.39 | 14.0386 | 1010.08 | 370439 | 1.2808 | 0.0188 | 330.54 |
| 40 | A | 14.40 | 1016.12 | 1.2321 | 958 | 14.42 | 14.0450 | 1016.16 | 373498 | 1.3055 | 0.0246 | 327.83 |
| | D | 14.41 | 1011.63 | 1.2266 | 949 | 14.42 | 14.0595 | 1011.11 | 373581 | 1.2994 | 0.0247 | 327.76 |
| 50 | A | 14.39 | 1016.08 | 1.2321 | 1177 | 14.40 | 14.0353 | 1015.88 | 376549 | 1.3223 | 0.0303 | 325.18 |
| | D | 14.42 | 1012.22 | 1.2273 | 1176 | 14.42 | 14.0607 | 1011.90 | 376634 | 1.3175 | 0.0304 | 325.11 |
| 60 | A | 14.39 | 1015.79 | 1.2318 | 1400 | 14.40 | 14.0354 | 1015.83 | 379547 | 1.3390 | 0.0359 | 322.61 |
| | D | 14.40 | 1012.97 | 1.2283 | 1393 | 14.42 | 14.0589 | 1012.60 | 379606 | 1.3351 | 0.0360 | 322.56 |
| 70 | A | 14.37 | 1015.71 | 1.2318 | 1613 | 14.39 | 14.0131 | 1015.60 | 382483 | 1.3554 | 0.0414 | 320.13 |
| | D | 14.41 | 1013.71 | 1.2292 | 1613 | 14.42 | 14.0601 | 1013.28 | 382557 | 1.3528 | 0.0416 | 320.07 |
| 80 | A | 14.39 | 1015.59 | 1.2316 | 1836 | 14.40 | 14.0353 | 1015.69 | 385384 | 1.3722 | 0.0470 | 317.72 |
| | D | 14.41 | 1014.45 | 1.2301 | 1830 | 14.42 | 14.0600 | 1014.11 | 385432 | 1.3703 | 0.0471 | 317.68 |
| 90 | A | 14.40 | 1015.75 | 1.2317 | 2049 | 14.38 | 14.0350 | 1015.59 | 388248 | 1.3887 | 0.0526 | 315.38 |
| | D | 14.41 | 1014.77 | 1.2305 | 2056 | 14.42 | 14.0608 | 1014.64 | 388302 | 1.3880 | 0.0528 | 315.34 |
| 95 | | 14.40 | 1015.35 | 1.2312 | 2157 | 14.42 | 14.0573 | 1014.99 | 389703 | 1.3965 | 0.0555 | 314.20 |
| Data used for pathlength calibration (the first zero step): $T_{SoS}$ = 14.0166 °C, $P$ = 1016.64 mbar, $t_m^0$ = 360178 ns, $W^0$ = 339.96 m/s. | | | | | | | | | | | | |

Table 140. 1,2-Dichloroethane/dry air results (25 °C isotherm)

| $x_T$/%SAT | | Zero Step | | | $\Delta m_{read}$/µg | Non-Zero Step | | | | | | |
|---|---|---|---|---|---|---|---|---|---|---|---|---|
| | | $T_{DVS}$/°C | $P$/mbar | $\rho^0$/(kg/m$^3$) | | $T_{DVS}$/°C | $T_{SoS}$/°C | $P$/mbar | $t_m$/ns | $\rho$/(kg/m$^3$) | $x$ | $W_m$/(m/s) |
| 5 | A | 24.36 | 1016.19 | 1.1909 | 226 | 24.39 | 23.9430 | 1016.04 | 357203 | 1.2082 | 0.0061 | 342.62 |
| | D | 24.26 | 1015.81 | 1.1908 | 225 | 24.29 | 23.8483 | 1015.63 | 357224 | 1.2080 | 0.0061 | 342.60 |
| 10 | A | 24.38 | 1016.04 | 1.1906 | 432 | 24.30 | 23.8941 | 1015.94 | 360117 | 1.2237 | 0.0114 | 339.85 |
| | D | 24.19 | 1016.07 | 1.1914 | 425 | 24.21 | 23.7698 | 1015.98 | 360146 | 1.2240 | 0.0113 | 339.82 |
| 15 | A | 24.26 | 1015.89 | 1.1909 | 623 | 24.26 | 23.8388 | 1015.67 | 362962 | 1.2386 | 0.0166 | 337.18 |
| | D | 24.19 | 1016.39 | 1.1918 | 622 | 24.21 | 23.7613 | 1016.30 | 362957 | 1.2394 | 0.0166 | 337.19 |
| 20 | A | 24.25 | 1015.61 | 1.1906 | 825 | 24.26 | 23.8349 | 1015.86 | 365713 | 1.2538 | 0.0218 | 334.65 |
| | D | 24.18 | 1016.61 | 1.1921 | 811 | 24.20 | 23.7611 | 1016.46 | 365682 | 1.2542 | 0.0216 | 334.67 |
| 25 | A | 24.22 | 1016.02 | 1.1912 | 1011 | 24.24 | 23.8011 | 1016.20 | 368368 | 1.2686 | 0.0267 | 332.23 |
| | D | 24.31 | 1016.88 | 1.1919 | 1007 | 24.23 | 23.8169 | 1016.64 | 368341 | 1.2691 | 0.0267 | 332.26 |
| 30 | A | 24.23 | 1016.35 | 1.1915 | 1199 | 24.26 | 23.8178 | 1016.58 | 370961 | 1.2834 | 0.0317 | 329.91 |
| | D | 24.30 | 1017.06 | 1.1921 | 1199 | 24.31 | 23.8722 | 1017.10 | 370977 | 1.2840 | 0.0318 | 329.90 |
| 35 | A | 24.24 | 1016.71 | 1.1919 | 1377 | 24.25 | 23.8160 | 1016.72 | 373477 | 1.2975 | 0.0365 | 327.69 |
| | D | 24.30 | 1017.18 | 1.1923 | 1381 | 24.32 | 23.8730 | 1017.21 | 373512 | 1.2981 | 0.0366 | 327.66 |
| 40 | A | 24.22 | 1016.70 | 1.1920 | 1557 | 24.24 | 23.8043 | 1016.79 | 375934 | 1.3113 | 0.0412 | 325.55 |
| | D | 24.31 | 1017.16 | 1.1922 | 1564 | 24.33 | 23.8784 | 1017.23 | 375995 | 1.3120 | 0.0414 | 325.49 |
| 45 | A | 24.23 | 1016.65 | 1.1919 | 1730 | 24.24 | 23.8037 | 1016.50 | 378374 | 1.3245 | 0.0459 | 323.45 |
| | D | 24.28 | 1017.13 | 1.1923 | 1739 | 24.31 | 23.8631 | 1017.19 | 378422 | 1.3255 | 0.0461 | 323.41 |
| 50 | A | 24.23 | 1016.56 | 1.1918 | 1905 | 24.25 | 23.8045 | 1016.39 | 380765 | 1.3378 | 0.0506 | 321.42 |
| | D | 24.30 | 1017.05 | 1.1921 | 1913 | 24.30 | 23.8555 | 1017.01 | 380798 | 1.3387 | 0.0507 | 321.39 |
| 55 | A | 24.22 | 1016.21 | 1.1914 | 2077 | 24.23 | 23.7965 | 1016.02 | 383090 | 1.3506 | 0.0551 | 319.47 |
| | D | 24.29 | 1016.87 | 1.1919 | 2089 | 24.30 | 23.8566 | 1016.94 | 383135 | 1.3520 | 0.0553 | 319.43 |
| 60 | A | 24.21 | 1015.84 | 1.1910 | 2247 | 24.21 | 23.7767 | 1015.93 | 385367 | 1.3632 | 0.0595 | 317.58 |
| | D | 24.28 | 1017.01 | 1.1921 | 2257 | 24.29 | 23.8390 | 1016.90 | 385425 | 1.3651 | 0.0598 | 317.53 |

| | | | | | | | | | | | | |
|---|---|---|---|---|---|---|---|---|---|---|---|---|
| 65 | A | 24.20 | 1015.84 | 1.1911 | 2416 | 24.20 | 23.7637 | 1015.95 | 387613 | 1.3762 | 0.0640 | 315.74 |
| | D | 24.17 | 1016.91 | 1.1925 | 2414 | 24.24 | 23.7641 | 1016.93 | 387610 | 1.3774 | 0.0640 | 315.74 |
| 70 | A | 24.19 | 1015.98 | 1.1913 | 2586 | 24.20 | 23.7625 | 1016.08 | 389884 | 1.3894 | 0.0685 | 313.90 |
| | D | 24.20 | 1017.11 | 1.1926 | 2581 | 24.19 | 23.7572 | 1017.04 | 389834 | 1.3904 | 0.0683 | 313.94 |
| 75 | A | 24.19 | 1016.28 | 1.1916 | 2751 | 24.20 | 23.7626 | 1016.32 | 392076 | 1.4025 | 0.0729 | 312.14 |
| | D | 24.31 | 1017.07 | 1.1921 | 2764 | 24.25 | 23.8380 | 1017.14 | 392126 | 1.4039 | 0.0731 | 312.10 |
| 80 | A | 24.18 | 1016.55 | 1.1920 | 2916 | 24.21 | 23.7636 | 1016.71 | 394245 | 1.4155 | 0.0772 | 310.43 |
| | D | 24.31 | 1016.91 | 1.1919 | 2934 | 24.32 | 23.8773 | 1017.11 | 394372 | 1.4167 | 0.0776 | 310.33 |
| 85 | A | 24.29 | 1016.81 | 1.1919 | 3098 | 24.31 | 23.8591 | 1016.71 | 396568 | 1.4293 | 0.0821 | 308.61 |
| | D | 24.31 | 1017.08 | 1.1921 | 3098 | 24.32 | 23.8777 | 1017.14 | 396557 | 1.4295 | 0.0820 | 308.62 |
| 90 | A | 24.30 | 1016.70 | 1.1917 | 3268 | 24.31 | 23.8692 | 1016.95 | 398720 | 1.4421 | 0.0864 | 306.94 |
| | D | 24.31 | 1017.19 | 1.1922 | 3267 | 24.33 | 23.8799 | 1017.12 | 398741 | 1.4425 | 0.0865 | 306.93 |
| 95 | | 24.30 | 1017.10 | 1.1921 | 3425 | 24.31 | 23.8666 | 1017.13 | 400789 | 1.4546 | 0.0907 | 305.36 |
| Data used for pathlength calibration (the first zero step): $T_{SOS}$ = 23.9127 °C, $P$ = 1016.19 mbar, $t_m^0$ = 353938 ns, $W^0$ = 345.78 m/s. | | | | | | | | | | | | |

Table 141. 1,2-Dichloroethane/dry air results (35 °C isotherm)

| $x_T$/%SAT | | Zero Step | | | $\Delta m_{read}$/µg | Non-Zero Step | | | | | | |
|---|---|---|---|---|---|---|---|---|---|---|---|---|
| | | $T_{DVS}$/°C | $P$/mbar | $\rho^0$/(kg/m$^3$) | | $T_{DVS}$/°C | $T_{SoS}$/°C | $P$/mbar | $t_m$/ns | $\rho$/(kg/m$^3$) | $x$ | $W_m$/(m/s) |
| 10 | A | 34.61 | 1016.15 | 1.1510 | 715 | 34.60 | 34.2377 | 1016.20 | 358115 | 1.2058 | 0.0196 | 341.47 |
| | D | 34.48 | 1013.56 | 1.1486 | 714 | 34.49 | 34.1078 | 1013.25 | 358230 | 1.2033 | 0.0198 | 341.36 |
| 20 | A | 34.61 | 1016.15 | 1.1510 | 1354 | 34.63 | 34.2710 | 1015.89 | 367254 | 1.2548 | 0.0373 | 332.97 |
| | D | 34.50 | 1014.20 | 1.1492 | 1347 | 34.50 | 34.1205 | 1013.87 | 367294 | 1.2525 | 0.0372 | 332.94 |
| 30 | A | 34.60 | 1015.89 | 1.1508 | 1956 | 34.58 | 34.2329 | 1015.89 | 375636 | 1.3007 | 0.0537 | 325.54 |
| | D | 34.53 | 1014.40 | 1.1493 | 1952 | 34.51 | 34.1438 | 1014.31 | 375649 | 1.2989 | 0.0537 | 325.53 |
| 40 | A | 34.56 | 1015.81 | 1.1508 | 2523 | 34.56 | 34.2132 | 1015.91 | 383422 | 1.3442 | 0.0692 | 318.93 |
| | D | 34.55 | 1014.49 | 1.1494 | 2521 | 34.56 | 34.1798 | 1014.44 | 383460 | 1.3425 | 0.0693 | 318.90 |
| 50 | A | 34.57 | 1015.87 | 1.1509 | 3073 | 34.62 | 34.2616 | 1015.85 | 390826 | 1.3863 | 0.0844 | 312.89 |
| | D | 34.58 | 1014.49 | 1.1493 | 3073 | 34.58 | 34.2006 | 1014.52 | 390828 | 1.3847 | 0.0844 | 312.89 |
| 60 | A | 34.51 | 1015.72 | 1.1509 | 3581 | 34.50 | 34.1734 | 1015.70 | 397606 | 1.4253 | 0.0982 | 307.56 |
| | D | 34.58 | 1014.40 | 1.1492 | 3591 | 34.59 | 34.2066 | 1014.43 | 397760 | 1.4244 | 0.0986 | 307.44 |
| 70 | A | 34.49 | 1015.77 | 1.1510 | 4088 | 34.49 | 34.1532 | 1015.58 | 404264 | 1.4643 | 0.1122 | 302.49 |
| | D | 34.58 | 1014.46 | 1.1492 | 4097 | 34.58 | 34.2060 | 1014.32 | 404373 | 1.4632 | 0.1126 | 302.41 |
| 80 | A | 34.48 | 1015.59 | 1.1509 | 4581 | 34.49 | 34.1446 | 1015.48 | 410593 | 1.5019 | 0.1257 | 297.83 |
| | D | 34.56 | 1014.50 | 1.1493 | 4590 | 34.58 | 34.1997 | 1014.36 | 410761 | 1.5011 | 0.1261 | 297.71 |
| 90 | A | 34.50 | 1015.38 | 1.1506 | 5058 | 34.50 | 34.1450 | 1015.34 | 416651 | 1.5381 | 0.1387 | 293.50 |
| | D | 34.56 | 1014.94 | 1.1499 | 5071 | 34.56 | 34.2010 | 1014.77 | 416823 | 1.5385 | 0.1392 | 293.38 |
| 95 | | 34.55 | 1015.30 | 1.1503 | 5307 | 34.56 | 34.2087 | 1015.16 | 419747 | 1.5570 | 0.1456 | 291.33 |
| Data used for pathlength calibration (the first zero step): $T_{SoS}$ = 34.2187 °C, $P$ = 1016.24 mbar, $t_m^0$ = 347665 ns, $W^0$ = 351.74 m/s. | | | | | | | | | | | | |

Table 142. 1,2-Dichloroethane/dry air results (45 °C isotherm)

| $x_T$/%SAT | | Zero Step | | | $\Delta m_{read}$/µg | Non-Zero Step | | | | | | |
|---|---|---|---|---|---|---|---|---|---|---|---|---|
| | | $T_{DVS}$/°C | $P$/mbar | $\rho^0$/(kg/m$^3$) | | $T_{DVS}$/°C | $T_{SoS}$/°C | $P$/mbar | $t_m$/ns | $\rho$/(kg/m$^3$) | $x$ | $W_m$/(m/s) |
| 10 | A | 43.97 | 1014.78 | 1.1154 | 1134 | 43.96 | 43.6965 | 1014.50 | 358481 | 1.2023 | 0.0322 | 340.35 |
| | D | 44.09 | 1012.15 | 1.1122 | 1168 | 44.09 | 43.7791 | 1012.34 | 358776 | 1.2016 | 0.0331 | 340.07 |
| 20 | A | 43.98 | 1014.31 | 1.1149 | 2130 | 44.04 | 43.7302 | 1014.26 | 372547 | 1.2781 | 0.0605 | 327.50 |
| | D | 43.98 | 1012.29 | 1.1127 | 2130 | 44.04 | 43.7132 | 1012.33 | 372605 | 1.2759 | 0.0605 | 327.45 |
| 30 | A | 43.98 | 1014.14 | 1.1147 | 3030 | 43.97 | 43.6956 | 1014.31 | 384977 | 1.3469 | 0.0858 | 316.93 |
| | D | 44.02 | 1011.80 | 1.1120 | 3033 | 44.00 | 43.7133 | 1011.96 | 384987 | 1.3444 | 0.0860 | 316.92 |
| 40 | A | 43.96 | 1014.36 | 1.1150 | 3858 | 44.04 | 43.7233 | 1013.84 | 396262 | 1.4107 | 0.1096 | 307.90 |
| | D | 44.10 | 1011.93 | 1.1119 | 3857 | 44.05 | 43.7453 | 1011.54 | 396174 | 1.4074 | 0.1096 | 307.97 |
| 50 | A | 43.99 | 1014.74 | 1.1153 | 4631 | 43.99 | 43.7092 | 1013.62 | 406432 | 1.4702 | 0.1316 | 300.20 |
| | D | 44.02 | 1012.05 | 1.1123 | 4633 | 44.06 | 43.7425 | 1011.91 | 406299 | 1.4673 | 0.1316 | 300.30 |
| 60 | A | 44.01 | 1014.17 | 1.1146 | 5364 | 43.99 | 43.7113 | 1013.79 | 415635 | 1.5257 | 0.1520 | 293.55 |
| | D | 44.01 | 1011.63 | 1.1119 | 5360 | 44.07 | 43.7463 | 1011.75 | 415554 | 1.5226 | 0.1521 | 293.61 |
| 70 | A | 44.06 | 1013.45 | 1.1137 | 6070 | 44.03 | 43.7388 | 1013.60 | 424363 | 1.5788 | 0.1717 | 287.51 |
| | D | 44.02 | 1011.87 | 1.1121 | 6033 | 44.00 | 43.6905 | 1011.65 | 424152 | 1.5744 | 0.1712 | 287.66 |
| 80 | A | 44.02 | 1013.53 | 1.1139 | 6723 | 43.99 | 43.7174 | 1013.46 | 432527 | 1.6291 | 0.1903 | 282.09 |
| | D | 44.00 | 1012.30 | 1.1126 | 6688 | 43.99 | 43.6938 | 1011.83 | 432310 | 1.6251 | 0.1898 | 282.23 |
| 90 | A | 43.99 | 1013.26 | 1.1137 | 7321 | 43.98 | 43.6819 | 1012.62 | 439962 | 1.6748 | 0.2076 | 277.32 |
| | D | 44.05 | 1012.11 | 1.1122 | 7338 | 43.99 | 43.7153 | 1012.28 | 439992 | 1.6746 | 0.2077 | 277.30 |
| 95 | | 44.07 | 1012.45 | 1.1125 | 7649 | 44.04 | 43.7427 | 1012.65 | 443681 | 1.6987 | 0.2165 | 274.99 |
| Data used for pathlength calibration (the first zero step): $T_{SoS}$ = 43.6880 °C, $P$ = 1014.78 mbar, $t_m^0$ = 341648 ns, $W^0$ = 357.12 m/s. | | | | | | | | | | | | |

Table 143. 1,2-Dichloroethane/dry air results (55 °C isotherm)

| $x_T$/%SAT | | Zero Step | | | $\Delta m_{read}$/µg | Non-Zero Step | | | | | | |
|---|---|---|---|---|---|---|---|---|---|---|---|---|
| | | $T_{DVS}$/°C | $P$/mbar | $\rho^0$/(kg/m$^3$) | | $T_{DVS}$/°C | $T_{SoS}$/°C | $P$/mbar | $t_m$/ns | $\rho$/(kg/m$^3$) | $x$ | $W_m$/(m/s) |
| 10 | A | 53.69 | 1014.10 | 1.0815 | 1890 | 53.74 | 53.4455 | 1014.12 | 364337 | 1.2263 | 0.0553 | 334.62 |
| | D | 53.77 | 1015.55 | 1.0827 | 1907 | 53.77 | 53.4843 | 1015.49 | 364497 | 1.2289 | 0.0557 | 334.48 |
| 20 | A | 53.71 | 1014.08 | 1.0814 | 3427 | 53.72 | 53.4342 | 1013.89 | 385812 | 1.3440 | 0.1002 | 316.00 |
| | D | 53.73 | 1015.57 | 1.0829 | 3413 | 53.71 | 53.4113 | 1015.51 | 385544 | 1.3444 | 0.0995 | 316.22 |
| 30 | A | 53.67 | 1013.97 | 1.0814 | 4758 | 53.65 | 53.3735 | 1013.89 | 403599 | 1.4460 | 0.1389 | 302.07 |
| | D | 53.75 | 1015.57 | 1.0829 | 4764 | 53.74 | 53.4453 | 1015.58 | 403470 | 1.4479 | 0.1388 | 302.17 |
| 40 | A | 53.70 | 1013.96 | 1.0813 | 5985 | 53.73 | 53.4264 | 1014.13 | 419272 | 1.5399 | 0.1746 | 290.78 |
| | D | 53.72 | 1015.49 | 1.0829 | 5919 | 53.68 | 53.3885 | 1015.54 | 418351 | 1.5365 | 0.1723 | 291.42 |
| 50 | A | 53.68 | 1014.23 | 1.0817 | 7072 | 53.74 | 53.4411 | 1014.38 | 432776 | 1.6236 | 0.2062 | 281.70 |
| | D | 53.72 | 1015.57 | 1.0829 | 7012 | 53.72 | 53.4257 | 1015.53 | 431956 | 1.6203 | 0.2042 | 282.24 |
| 60 | A | 53.74 | 1014.71 | 1.0820 | 8052 | 53.73 | 53.4389 | 1014.92 | 444594 | 1.6990 | 0.2344 | 274.22 |
| | D | 53.73 | 1015.49 | 1.0828 | 7982 | 53.74 | 53.4389 | 1015.43 | 443719 | 1.6945 | 0.2324 | 274.76 |
| 70 | A | 53.70 | 1015.08 | 1.0825 | 8940 | 53.72 | 53.4322 | 1015.25 | 455072 | 1.7676 | 0.2601 | 267.90 |
| | D | 53.76 | 1015.48 | 1.0827 | 8902 | 53.75 | 53.4662 | 1015.46 | 454536 | 1.7649 | 0.2590 | 268.22 |
| 80 | A | 53.74 | 1015.49 | 1.0828 | 9790 | 53.75 | 53.4494 | 1015.70 | 464857 | 1.8331 | 0.2846 | 262.26 |
| | D | 53.72 | 1015.49 | 1.0828 | 9726 | 53.75 | 53.4430 | 1015.29 | 464284 | 1.8282 | 0.2830 | 262.59 |
| 90 | A | 53.75 | 1015.58 | 1.0829 | 10554 | 53.73 | 53.4346 | 1015.60 | 473590 | 1.8916 | 0.3067 | 257.43 |
| | D | 53.73 | 1015.76 | 1.0831 | 10531 | 53.74 | 53.4470 | 1015.75 | 473281 | 1.8901 | 0.3060 | 257.60 |
| 95 | | 53.71 | 1015.49 | 1.0829 | 10909 | 53.74 | 53.4540 | 1015.69 | 477509 | 1.9189 | 0.3169 | 255.32 |
| Data used for pathlength calibration (the first zero step): $T_{SoS}$ = 53.3947 °C, $P$ = 1014.10 mbar, $t_m^0$ = 336267 ns, $W^0$ = 362.56 m/s. | | | | | | | | | | | | |

## A6.17 m-Xylene/dry air

Table 144. m-Xylene/dry air results (30 °C isotherm)

| $x_T$/%SAT | Zero Step | | | $\Delta m_{read}$/µg | Non-Zero Step | | | | | | |
|---|---|---|---|---|---|---|---|---|---|---|---|
| | $T_{DVS}$/°C | $P$/mbar | $\rho^0$/(kg/m$^3$) | | $T_{DVS}$/°C | $T_{SoS}$/°C | $P$/mbar | $t_m$/ns | $\rho$/(kg/m$^3$) | $x$ | $W_m$/(m/s) |
| 10 | 29.57 | 1006.25 | 1.1588 | 66 | 29.57 | 29.1779 | 1006.48 | 351334 | 1.1639 | 0.0015 | 347.79 |
| 20 | 29.55 | 1006.53 | 1.1592 | 124 | 29.57 | 29.1628 | 1006.91 | 352333 | 1.1687 | 0.0029 | 346.80 |
| 30 | 29.55 | 1007.13 | 1.1599 | 179 | 29.55 | 29.1325 | 1007.45 | 353310 | 1.1736 | 0.0043 | 345.85 |
| 40 | 29.57 | 1007.41 | 1.1602 | 231 | 29.59 | 29.1910 | 1007.42 | 354243 | 1.1779 | 0.0057 | 344.93 |
| 50 | 29.59 | 1007.61 | 1.1603 | 288 | 29.60 | 29.2074 | 1007.66 | 355188 | 1.1824 | 0.0071 | 344.02 |
| 60 | 29.59 | 1007.53 | 1.1602 | 343 | 29.57 | 29.1737 | 1007.59 | 356140 | 1.1865 | 0.0084 | 343.10 |
| 70 | 29.54 | 1007.57 | 1.1605 | 394 | 29.55 | 29.1433 | 1007.44 | 357084 | 1.1907 | 0.0098 | 342.19 |
| 80 | 29.55 | 1007.49 | 1.1603 | 449 | 29.59 | 29.1399 | 1007.53 | 358019 | 1.1948 | 0.0111 | 341.30 |
| 90 | 29.67 | 1007.52 | 1.1599 | 512 | 29.74 | 29.3105 | 1007.60 | 358908 | 1.1991 | 0.0127 | 340.45 |
| 95 | 29.71 | 1007.66 | 1.1599 | 531 | 29.66 | 29.2787 | 1007.70 | 359303 | 1.2006 | 0.0130 | 340.08 |
| Data used for pathlength calibration (the first zero step): $T_{SoS}$ = 29.1826 °C, $P$ = 1006.25 mbar, $t_m^0$ = 350280 ns, $W^0$ = 348.84 m/s. | | | | | | | | | | | |

Table 145. m-Xylene/dry air results (40 °C isotherm)

| $x_T$/%SAT | Zero Step | | | $\Delta m_{read}$/µg | Non-Zero Step | | | | | | |
|---|---|---|---|---|---|---|---|---|---|---|---|
| | $T_{DVS}$/°C | $P$/mbar | $\rho^0$/(kg/m$^3$) | | $T_{DVS}$/°C | $T_{SoS}$/°C | $P$/mbar | $t_m$/ns | $\rho$/(kg/m$^3$) | $x$ | $W_m$/(m/s) |
| 10 | 39.20 | 1009.75 | 1.1269 | 106 | 39.20 | 38.8478 | 1010.01 | 346412 | 1.1350 | 0.0026 | 352.54 |
| 20 | 39.21 | 1010.37 | 1.1276 | 202 | 39.23 | 38.8637 | 1010.74 | 348079 | 1.1431 | 0.0050 | 350.86 |
| 30 | 39.22 | 1010.91 | 1.1281 | 292 | 39.18 | 38.8183 | 1011.02 | 349730 | 1.1505 | 0.0073 | 349.20 |
| 40 | 39.18 | 1011.05 | 1.1284 | 384 | 39.17 | 38.7932 | 1011.15 | 351334 | 1.1579 | 0.0097 | 347.61 |
| 50 | 39.23 | 1011.24 | 1.1285 | 474 | 39.20 | 38.8152 | 1011.30 | 352887 | 1.1648 | 0.0120 | 346.08 |
| 60 | 39.17 | 1011.44 | 1.1289 | 562 | 39.20 | 38.8062 | 1011.61 | 354424 | 1.1720 | 0.0142 | 344.57 |
| 70 | 39.25 | 1011.75 | 1.1290 | 660 | 39.28 | 38.9158 | 1011.81 | 355950 | 1.1795 | 0.0168 | 343.10 |
| 80 | 39.18 | 1011.91 | 1.1294 | 740 | 39.18 | 38.8359 | 1012.01 | 357445 | 1.1861 | 0.0187 | 341.66 |
| 90 | 39.14 | 1012.23 | 1.1299 | 828 | 39.22 | 38.8430 | 1012.26 | 358950 | 1.1934 | 0.0211 | 340.23 |
| 95 | 39.25 | 1012.40 | 1.1297 | 875 | 39.23 | 38.8770 | 1012.52 | 359647 | 1.1968 | 0.0221 | 339.57 |
| Data used for pathlength calibration (the first zero step): $T_{SoS}$ = 38.8488 °C, $P$ = 1009.75 mbar, $t_m^0$ = 344619 ns, $W^0$ = 354.38 m/s. | | | | | | | | | | | |

Table 146. m-Xylene/dry air results (50 °C isotherm)

| $x_T$/%SAT | Zero Step | | | $\Delta m_{read}$/µg | Non-Zero Step | | | | | | |
|---|---|---|---|---|---|---|---|---|---|---|---|
| | $T_{DVS}$/°C | $P$/mbar | $\rho^0$/(kg/m$^3$) | | $T_{DVS}$/°C | $T_{SoS}$/°C | $P$/mbar | $t_m$/ns | $\rho$/(kg/m$^3$) | $x$ | $W_m$/(m/s) |
| 10 | 48.98 | 1016.25 | 1.0996 | 166 | 49.01 | 48.6202 | 1016.41 | 342090 | 1.1124 | 0.0043 | 356.78 |
| 20 | 49.00 | 1016.69 | 1.1001 | 319 | 48.98 | 48.6106 | 1016.96 | 344816 | 1.1245 | 0.0082 | 353.96 |
| 30 | 49.01 | 1017.14 | 1.1005 | 468 | 49.02 | 48.6812 | 1017.31 | 347441 | 1.1363 | 0.0121 | 351.28 |
| 40 | 49.04 | 1017.49 | 1.1008 | 612 | 49.05 | 48.6815 | 1017.63 | 349984 | 1.1477 | 0.0159 | 348.73 |
| 50 | 49.01 | 1017.74 | 1.1012 | 751 | 49.05 | 48.6615 | 1017.68 | 352468 | 1.1587 | 0.0196 | 346.28 |
| 60 | 49.00 | 1017.72 | 1.1012 | 892 | 49.05 | 48.6461 | 1017.72 | 354883 | 1.1695 | 0.0233 | 343.92 |
| 70 | 49.05 | 1017.78 | 1.1011 | 1038 | 49.09 | 48.7241 | 1017.74 | 357276 | 1.1806 | 0.0271 | 341.62 |
| 80 | 49.07 | 1017.86 | 1.1011 | 1181 | 49.05 | 48.7001 | 1017.82 | 359646 | 1.1916 | 0.0307 | 339.36 |
| 90 | 49.01 | 1018.00 | 1.1014 | 1323 | 49.06 | 48.6656 | 1018.36 | 361960 | 1.2028 | 0.0343 | 337.19 |
| 95 | 49.06 | 1018.62 | 1.1019 | 1393 | 49.09 | 48.7315 | 1018.85 | 363084 | 1.2087 | 0.0361 | 336.15 |
| Data used for pathlength calibration (the first zero step): $T_{SoS}$ = 48.6167 °C, $P$ = 1016.25 mbar, $t_m^0$ = 339133 ns, $W^0$ = 359.89 m/s. | | | | | | | | | | | |

## A6.18 o-Xylene/dry air

Table 147. o-Xylene/dry air results (30 °C isotherm)

| $x_T$/%SAT | Zero Step | | | $\Delta m_{read}$/µg | Non-Zero Step | | | | | | |
|---|---|---|---|---|---|---|---|---|---|---|---|
| | $T_{DVS}$/°C | $P$/mbar | $\rho^0$/(kg/m$^3$) | | $T_{DVS}$/°C | $T_{SoS}$/°C | $P$/mbar | $t_m$/ns | $\rho$/(kg/m$^3$) | $x$ | $W_m$/(m/s) |
| 10 | 29.71 | 1002.95 | 1.1545 | 53 | 29.74 | 29.4227 | 1003.01 | 351005 | 1.1586 | 0.0013 | 348.10 |
| 20 | 29.73 | 1003.11 | 1.1546 | 100 | 29.73 | 29.4316 | 1003.22 | 351820 | 1.1623 | 0.0024 | 347.30 |
| 30 | 29.73 | 1003.32 | 1.1549 | 144 | 29.73 | 29.4259 | 1003.33 | 352633 | 1.1659 | 0.0036 | 346.50 |
| 40 | 29.71 | 1003.18 | 1.1548 | 191 | 29.71 | 29.4003 | 1003.40 | 353441 | 1.1694 | 0.0046 | 345.70 |
| 50 | 29.69 | 1003.10 | 1.1547 | 234 | 29.69 | 29.3668 | 1003.04 | 354248 | 1.1727 | 0.0058 | 344.92 |
| 60 | 29.67 | 1002.81 | 1.1545 | 277 | 29.66 | 29.3305 | 1002.76 | 355046 | 1.1757 | 0.0069 | 344.14 |
| 70 | 29.62 | 1002.33 | 1.1541 | 321 | 29.64 | 29.2994 | 1002.23 | 355838 | 1.1787 | 0.0080 | 343.38 |
| 80 | 29.63 | 1002.17 | 1.1539 | 363 | 29.61 | 29.2795 | 1001.90 | 356622 | 1.1817 | 0.0091 | 342.62 |
| 90 | 29.64 | 1001.91 | 1.1536 | 411 | 29.66 | 29.3233 | 1001.93 | 357363 | 1.1851 | 0.0102 | 341.91 |
| 95 | 29.62 | 1001.92 | 1.1537 | 427 | 29.63 | 29.2803 | 1002.06 | 357696 | 1.1864 | 0.0106 | 341.59 |
| Data used for pathlength calibration (the first zero step): $T_{SoS}$ = 29.3832 °C, $P$ = 1002.95 mbar, $t_m^0$ = 350151 ns, $W^0$ = 348.95 m/s. | | | | | | | | | | | |

Table 148. o-Xylene/dry air results (40 °C isotherm)

| $x_T$/%SAT | Zero Step | | | $\Delta m_{read}$/µg | Non-Zero Step | | | | | | |
|---|---|---|---|---|---|---|---|---|---|---|---|
| | $T_{DVS}$/°C | $P$/mbar | $\rho^0$/(kg/m$^3$) | | $T_{DVS}$/°C | $T_{SoS}$/°C | $P$/mbar | $t_m$/ns | $\rho$/(kg/m$^3$) | $x$ | $W_m$/(m/s) |
| 10 | 39.21 | 1010.69 | 1.1279 | 82 | 39.13 | 38.8675 | 1010.51 | 346024 | 1.1342 | 0.0021 | 352.88 |
| 20 | 39.09 | 1010.66 | 1.1283 | 158 | 39.09 | 38.8125 | 1010.69 | 347428 | 1.1404 | 0.0040 | 351.46 |
| 30 | 39.07 | 1010.70 | 1.1284 | 232 | 39.15 | 38.8374 | 1010.54 | 348773 | 1.1462 | 0.0060 | 350.10 |
| 40 | 39.19 | 1010.24 | 1.1275 | 310 | 39.20 | 38.9160 | 1010.11 | 350076 | 1.1513 | 0.0079 | 348.80 |
| 50 | 39.16 | 1009.78 | 1.1271 | 379 | 39.19 | 38.9160 | 1009.53 | 351391 | 1.1561 | 0.0098 | 347.49 |
| 60 | 39.19 | 1009.24 | 1.1264 | 449 | 39.11 | 38.8517 | 1008.76 | 352677 | 1.1608 | 0.0115 | 346.22 |
| 70 | 39.12 | 1008.27 | 1.1256 | 525 | 39.18 | 38.8760 | 1007.94 | 353962 | 1.1658 | 0.0136 | 344.97 |
| 80 | 39.15 | 1007.63 | 1.1247 | 595 | 39.16 | 38.8838 | 1007.11 | 355257 | 1.1703 | 0.0154 | 343.71 |
| 90 | 39.09 | 1006.60 | 1.1238 | 671 | 39.07 | 38.8049 | 1006.62 | 356508 | 1.1752 | 0.0171 | 342.50 |
| 95 | 39.05 | 1006.42 | 1.1237 | 699 | 39.13 | 38.8279 | 1006.18 | 357101 | 1.1773 | 0.0180 | 341.94 |
| Data used for pathlength calibration (the first zero step): $T_{SoS}$ = 38.9135 °C, $P$ = 1010.69 mbar, $t_m^0$ = 344526 ns, $W^0$ = 354.42 m/s. | | | | | | | | | | | |

Table 149. o-Xylene/dry air results (50 °C isotherm)

| $x_T$/%SAT | Zero Step | | | $\Delta m_{read}$/µg | Non-Zero Step | | | | | | |
|---|---|---|---|---|---|---|---|---|---|---|---|
| | $T_{DVS}$/°C | $P$/mbar | $\rho^0$/(kg/m$^3$) | | $T_{DVS}$/°C | $T_{SoS}$/°C | $P$/mbar | $t_m$/ns | $\rho$/(kg/m$^3$) | $x$ | $W_m$/(m/s) |
| 10 | 48.90 | 1014.35 | 1.0979 | 136 | 48.89 | 48.5446 | 1014.72 | 341508 | 1.1083 | 0.0034 | 357.29 |
| 20 | 48.95 | 1014.97 | 1.0984 | 264 | 48.97 | 48.6618 | 1015.28 | 343738 | 1.1186 | 0.0068 | 354.97 |
| 30 | 48.97 | 1015.53 | 1.0989 | 379 | 48.95 | 48.6388 | 1015.64 | 345957 | 1.1280 | 0.0098 | 352.69 |
| 40 | 48.94 | 1015.87 | 1.0994 | 500 | 48.98 | 48.6559 | 1016.09 | 348088 | 1.1377 | 0.0130 | 350.53 |
| 50 | 48.97 | 1016.16 | 1.0996 | 619 | 48.96 | 48.6300 | 1016.54 | 350179 | 1.1470 | 0.0160 | 348.44 |
| 60 | 48.94 | 1016.37 | 1.0999 | 728 | 48.95 | 48.6155 | 1016.34 | 352203 | 1.1557 | 0.0190 | 346.44 |
| 70 | 48.97 | 1016.04 | 1.0994 | 844 | 48.98 | 48.6547 | 1015.78 | 354239 | 1.1641 | 0.0221 | 344.45 |
| 80 | 48.93 | 1015.80 | 1.0993 | 958 | 48.93 | 48.5933 | 1015.58 | 356244 | 1.1728 | 0.0250 | 342.51 |
| 90 | 49.00 | 1015.40 | 1.0987 | 1081 | 49.00 | 48.7008 | 1015.15 | 358246 | 1.1815 | 0.0283 | 340.59 |
| 95 | 48.97 | 1015.15 | 1.0985 | 1129 | 48.94 | 48.6317 | 1014.92 | 359179 | 1.1850 | 0.0295 | 339.71 |
| Data used for pathlength calibration (the first zero step): $T_{SoS}$ = 48.5546 °C, $P$ = 1014.35 mbar, $t_m^0$ = 339070 ns, $W^0$ = 359.86 m/s. | | | | | | | | | | | |

## A6.19 p-Xylene/dry air

Table 150. p-Xylene/dry air results (30 °C isotherm)

| $x_T$/%SAT | Zero Step | | | $\Delta m_{read}$/µg | Non-Zero Step | | | | | | |
|---|---|---|---|---|---|---|---|---|---|---|---|
| | $T_{DVS}$/°C | $P$/mbar | $\rho^0$/(kg/m$^3$) | | $T_{DVS}$/°C | $T_{SoS}$/°C | $P$/mbar | $t_m$/ns | $\rho$/(kg/m$^3$) | $x$ | $W_m$/(m/s) |
| 10 | 29.72 | 1016.44 | 1.1700 | 65 | 29.77 | 29.3817 | 1016.58 | 351048 | 1.1750 | 0.0016 | 347.87 |
| 20 | 29.79 | 1016.75 | 1.1701 | 131 | 29.71 | 29.3841 | 1016.93 | 352072 | 1.1801 | 0.0030 | 346.85 |
| 30 | 29.65 | 1017.08 | 1.1710 | 190 | 29.65 | 29.2962 | 1017.47 | 353134 | 1.1856 | 0.0045 | 345.81 |
| 40 | 29.62 | 1017.82 | 1.1720 | 244 | 29.63 | 29.2713 | 1018.05 | 354143 | 1.1907 | 0.0059 | 344.83 |
| 50 | 29.62 | 1017.95 | 1.1721 | 303 | 29.64 | 29.2840 | 1018.08 | 355137 | 1.1953 | 0.0074 | 343.86 |
| 60 | 29.65 | 1018.20 | 1.1723 | 361 | 29.65 | 29.2981 | 1018.23 | 356122 | 1.1999 | 0.0088 | 342.91 |
| 70 | 29.62 | 1018.27 | 1.1725 | 422 | 29.64 | 29.2771 | 1018.36 | 357110 | 1.2048 | 0.0103 | 341.96 |
| 80 | 29.61 | 1018.24 | 1.1725 | 479 | 29.62 | 29.2595 | 1018.26 | 358088 | 1.2092 | 0.0117 | 341.03 |
| 90 | 29.64 | 1018.47 | 1.1726 | 537 | 29.71 | 29.3194 | 1018.59 | 359030 | 1.2138 | 0.0131 | 340.13 |
| 95 | 29.70 | 1018.77 | 1.1728 | 569 | 29.75 | 29.3735 | 1019.28 | 359442 | 1.2164 | 0.0138 | 339.74 |
| Data used for pathlength calibration (the first zero step): $T_{SoS}$ = 29.3497 °C, $P$ = 1016.44 mbar, $t_m^0$ = 349972 ns, $W^0$ = 348.94 m/s. | | | | | | | | | | | |

Table 151. p-Xylene/dry air results (40 °C isotherm)

| $x_T$/%SAT | Zero Step | | | $\Delta m_{read}$/µg | Non-Zero Step | | | | | | |
|---|---|---|---|---|---|---|---|---|---|---|---|
| | $T_{DVS}$/°C | $P$/mbar | $\rho^0$/(kg/m$^3$) | | $T_{DVS}$/°C | $T_{SoS}$/°C | $P$/mbar | $t_m$/ns | $\rho$/(kg/m$^3$) | $x$ | $W_m$/(m/s) |
| 10 | 39.15 | 1018.23 | 1.1366 | 103 | 39.16 | 38.8478 | 1018.08 | 346293 | 1.1444 | 0.0027 | 352.47 |
| 20 | 39.15 | 1017.98 | 1.1363 | 207 | 39.16 | 38.8362 | 1018.09 | 348042 | 1.1521 | 0.0052 | 350.70 |
| 30 | 39.15 | 1018.33 | 1.1367 | 303 | 39.14 | 38.8254 | 1018.32 | 349741 | 1.1599 | 0.0076 | 349.00 |
| 40 | 39.15 | 1018.38 | 1.1367 | 398 | 39.14 | 38.8168 | 1018.29 | 351394 | 1.1672 | 0.0100 | 347.36 |
| 50 | 39.14 | 1018.30 | 1.1367 | 488 | 39.19 | 38.8412 | 1017.97 | 353022 | 1.1741 | 0.0125 | 345.75 |
| 60 | 39.19 | 1017.92 | 1.1361 | 586 | 39.19 | 38.8541 | 1017.85 | 354608 | 1.1810 | 0.0148 | 344.21 |
| 70 | 39.18 | 1017.39 | 1.1355 | 674 | 39.16 | 38.8313 | 1016.98 | 356184 | 1.1872 | 0.0171 | 342.68 |
| 80 | 39.18 | 1017.09 | 1.1352 | 777 | 39.21 | 38.8995 | 1016.98 | 357791 | 1.1947 | 0.0197 | 341.14 |
| 90 | 39.12 | 1016.82 | 1.1351 | 869 | 39.13 | 38.8366 | 1017.04 | 359331 | 1.2017 | 0.0219 | 339.68 |
| 95 | 39.12 | 1017.26 | 1.1356 | 909 | 39.12 | 38.8170 | 1017.08 | 360069 | 1.2053 | 0.0230 | 338.99 |
| Data used for pathlength calibration (the first zero step): $T_{SoS}$ = 38.8580 °C, $P$ = 1018.23 mbar, $t_m^0$ = 344424 ns, $W^0$ = 354.38 m/s. | | | | | | | | | | | |

Table 152. p-Xylene/dry air results (50 °C isotherm)

| $x_T$/%SAT | Zero Step | | | $\Delta m_{read}$/µg | Non-Zero Step | | | | | | |
|---|---|---|---|---|---|---|---|---|---|---|---|
| | $T_{DVS}$/°C | $P$/mbar | $\rho^0$/(kg/m$^3$) | | $T_{DVS}$/°C | $T_{SoS}$/°C | $P$/mbar | $t_m$/ns | $\rho$/(kg/m$^3$) | $x$ | $W_m$/(m/s) |
| 10 | 48.97 | 1013.51 | 1.0967 | 178 | 48.95 | 48.6386 | 1013.77 | 342085 | 1.1104 | 0.0045 | 356.63 |
| 20 | 48.95 | 1013.63 | 1.0969 | 331 | 48.96 | 48.6356 | 1013.61 | 344949 | 1.1222 | 0.0086 | 353.67 |
| 30 | 48.97 | 1013.75 | 1.0970 | 490 | 48.99 | 48.6686 | 1014.04 | 347704 | 1.1345 | 0.0127 | 350.87 |
| 40 | 48.99 | 1013.89 | 1.0971 | 632 | 48.98 | 48.6611 | 1013.55 | 350350 | 1.1455 | 0.0166 | 348.22 |
| 50 | 48.99 | 1013.27 | 1.0964 | 787 | 49.00 | 48.6925 | 1013.09 | 352959 | 1.1567 | 0.0206 | 345.64 |
| 60 | 49.00 | 1013.01 | 1.0961 | 931 | 48.99 | 48.6754 | 1012.73 | 355485 | 1.1674 | 0.0244 | 343.19 |
| 70 | 48.97 | 1012.52 | 1.0957 | 1079 | 49.00 | 48.6828 | 1012.33 | 357965 | 1.1783 | 0.0283 | 340.81 |
| 80 | 49.00 | 1011.78 | 1.0947 | 1224 | 48.93 | 48.6368 | 1011.47 | 360435 | 1.1885 | 0.0320 | 338.47 |
| 90 | 48.93 | 1011.15 | 1.0943 | 1371 | 48.95 | 48.6609 | 1010.80 | 362900 | 1.1993 | 0.0360 | 336.17 |
| 95 | 48.95 | 1010.74 | 1.0938 | 1447 | 48.96 | 48.6455 | 1010.88 | 364082 | 1.2047 | 0.0378 | 335.08 |
| Data used for pathlength calibration (the first zero step): $T_{SoS}$ = 48.6456 °C, $P$ = 1013.51 mbar, $t_m^0$ = 338971 ns, $W^0$ = 359.91 m/s. | | | | | | | | | | | |

## A6.20 Ethylbenzene/dry air

Table 153. Ethylbenzene/dry air results (30 °C isotherm)

| $x_T$/%SAT | Zero Step | | | $\Delta m_{read}$/µg | Non-Zero Step | | | | | | |
|---|---|---|---|---|---|---|---|---|---|---|---|
| | $T_{DVS}$/°C | $P$/mbar | $\rho^0$/(kg/m$^3$) | | $T_{DVS}$/°C | $T_{SoS}$/°C | $P$/mbar | $t_m$/ns | $\rho$/(kg/m$^3$) | $x$ | $W_m$/(m/s) |
| 10 | 29.59 | 1019.62 | 1.1742 | 70 | 29.63 | 29.3257 | 1019.59 | 351511 | 1.1795 | 0.0018 | 347.72 |
| 20 | 29.64 | 1019.83 | 1.1742 | 140 | 29.65 | 29.3646 | 1019.98 | 352629 | 1.1850 | 0.0034 | 346.62 |
| 30 | 29.68 | 1020.03 | 1.1743 | 204 | 29.70 | 29.4028 | 1019.91 | 353740 | 1.1899 | 0.0050 | 345.53 |
| 40 | 29.68 | 1019.93 | 1.1742 | 267 | 29.69 | 29.3863 | 1019.91 | 354837 | 1.1946 | 0.0065 | 344.46 |
| 50 | 29.69 | 1019.83 | 1.1740 | 332 | 29.70 | 29.3821 | 1019.83 | 355854 | 1.1995 | 0.0081 | 343.48 |
| 60 | 29.68 | 1019.73 | 1.1740 | 401 | 29.68 | 29.3653 | 1019.79 | 356902 | 1.2047 | 0.0098 | 342.47 |
| 70 | 29.65 | 1019.78 | 1.1741 | 459 | 29.67 | 29.3703 | 1019.53 | 357923 | 1.2093 | 0.0113 | 341.49 |
| 80 | 29.67 | 1019.34 | 1.1735 | 526 | 29.68 | 29.3720 | 1019.20 | 358994 | 1.2138 | 0.0129 | 340.47 |
| 90 | 29.67 | 1019.18 | 1.1734 | 590 | 29.66 | 29.3433 | 1019.21 | 360057 | 1.2186 | 0.0144 | 339.47 |
| 95 | 29.63 | 1019.07 | 1.1734 | 616 | 29.64 | 29.3032 | 1019.21 | 360549 | 1.2206 | 0.0150 | 339.01 |
| Data used for pathlength calibration (the first zero step): $T_{SoS}$ = 29.2797 °C, $P$ = 1019.62 mbar, $t_m^0$ = 350330 ns, $W^0$ = 348.89 m/s. | | | | | | | | | | | |

Table 154. Ethylbenzene/dry air results (40 °C isotherm)

| $x_T$/%SAT | Zero Step | | | $\Delta m_{read}$/µg | Non-Zero Step | | | | | | |
|---|---|---|---|---|---|---|---|---|---|---|---|
| | $T_{DVS}$/°C | $P$/mbar | $\rho^0$/(kg/m$^3$) | | $T_{DVS}$/°C | $T_{SoS}$/°C | $P$/mbar | $t_m$/ns | $\rho$/(kg/m$^3$) | $x$ | $W_m$/(m/s) |
| 10 | 39.15 | 1021.35 | 1.1401 | 115 | 39.16 | 38.8767 | 1021.35 | 346683 | 1.1489 | 0.0029 | 352.32 |
| 20 | 39.14 | 1021.64 | 1.1404 | 226 | 39.06 | 38.8172 | 1021.74 | 348594 | 1.1577 | 0.0055 | 350.39 |
| 30 | 39.06 | 1021.79 | 1.1409 | 328 | 39.06 | 38.7936 | 1021.72 | 350453 | 1.1660 | 0.0083 | 348.53 |
| 40 | 39.05 | 1021.64 | 1.1407 | 434 | 39.05 | 38.7858 | 1021.69 | 352250 | 1.1740 | 0.0109 | 346.75 |
| 50 | 39.07 | 1021.68 | 1.1407 | 535 | 39.12 | 38.8169 | 1021.62 | 354012 | 1.1817 | 0.0135 | 345.03 |
| 60 | 39.13 | 1021.81 | 1.1406 | 637 | 39.10 | 38.8310 | 1021.74 | 355737 | 1.1894 | 0.0160 | 343.35 |
| 70 | 39.13 | 1021.72 | 1.1406 | 737 | 39.11 | 38.8604 | 1021.41 | 357452 | 1.1971 | 0.0186 | 341.71 |
| 80 | 39.05 | 1021.37 | 1.1404 | 837 | 39.04 | 38.7823 | 1021.30 | 359147 | 1.2046 | 0.0210 | 340.09 |
| 90 | 39.13 | 1021.22 | 1.1400 | 945 | 39.08 | 38.8021 | 1021.28 | 360846 | 1.2124 | 0.0236 | 338.49 |
| 95 | 39.08 | 1021.33 | 1.1403 | 993 | 39.15 | 38.8519 | 1021.46 | 361681 | 1.2164 | 0.0250 | 337.71 |
| Data used for pathlength calibration (the first zero step): $T_{SoS}$ = 38.8735 °C, $P$ = 1021.35 mbar, $t_m^0$ = 344654 ns, $W^0$ = 354.39 m/s. | | | | | | | | | | | |

Table 155. Ethylbenzene/dry air results (50 °C isotherm)

| $x_T$/%SAT | Zero Step | | | $\Delta m_{read}$/µg | Non-Zero Step | | | | | | |
|---|---|---|---|---|---|---|---|---|---|---|---|
| | $T_{DVS}$/°C | $P$/mbar | $\rho^0$/(kg/m$^3$) | | $T_{DVS}$/°C | $T_{SoS}$/°C | $P$/mbar | $t_m$/ns | $\rho$/(kg/m$^3$) | $x$ | $W_m$/(m/s) |
| 10 | 48.94 | 1021.50 | 1.1055 | 189 | 49.03 | 48.7181 | 1021.61 | 342477 | 1.1199 | 0.0050 | 356.40 |
| 20 | 49.01 | 1021.81 | 1.1056 | 366 | 49.00 | 48.7147 | 1022.14 | 345578 | 1.1336 | 0.0093 | 353.20 |
| 30 | 49.00 | 1022.37 | 1.1062 | 529 | 48.98 | 48.6785 | 1022.48 | 348576 | 1.1468 | 0.0136 | 350.16 |
| 40 | 48.98 | 1022.58 | 1.1065 | 693 | 48.96 | 48.6547 | 1022.62 | 351443 | 1.1596 | 0.0179 | 347.31 |
| 50 | 48.97 | 1022.67 | 1.1066 | 854 | 48.99 | 48.6568 | 1022.71 | 354240 | 1.1721 | 0.0221 | 344.57 |
| 60 | 49.00 | 1022.77 | 1.1066 | 1015 | 49.03 | 48.7302 | 1022.65 | 356958 | 1.1844 | 0.0263 | 341.94 |
| 70 | 49.03 | 1022.77 | 1.1065 | 1174 | 49.05 | 48.7471 | 1022.66 | 359631 | 1.1965 | 0.0305 | 339.40 |
| 80 | 49.05 | 1022.54 | 1.1062 | 1339 | 49.04 | 48.7318 | 1022.80 | 362279 | 1.2088 | 0.0345 | 336.92 |
| 90 | 49.05 | 1022.71 | 1.1064 | 1496 | 49.10 | 48.7960 | 1022.59 | 364923 | 1.2210 | 0.0388 | 334.48 |
| 95 | 49.10 | 1022.89 | 1.1064 | 1572 | 49.10 | 48.8012 | 1022.71 | 366188 | 1.2269 | 0.0408 | 333.32 |
| Data used for pathlength calibration (the first zero step): $T_{SoS}$ = 48.6284 °C, $P$ = 1021.50 mbar, $t_m^0$ = 339149 ns, $W^0$ = 359.90 m/s. | | | | | | | | | | | |

## A6.21 n-Butylamine/dry air

Table 156. n-Butylamine/dry air results (25 °C isotherm)

| $x_T$/%SAT | Zero Step | | | $\Delta m_{read}$/µg | Non-Zero Step | | | | | | |
|---|---|---|---|---|---|---|---|---|---|---|---|
| | $T_{DVS}$/°C | $P$/mbar | $\rho^0$/(kg/m$^3$) | | $T_{DVS}$/°C | $T_{SoS}$/°C | $P$/mbar | $t_m$/ns | $\rho$/(kg/m$^3$) | $x$ | $W_m$/(m/s) |
| 10 | 24.49 | 1019.21 | 1.1938 | 344 | 24.54 | 24.1071 | 1019.43 | 360328 | 1.2202 | 0.0143 | 339.41 |
| 20 | 24.55 | 1019.58 | 1.1940 | 648 | 24.54 | 24.1334 | 1019.60 | 366214 | 1.2437 | 0.0271 | 333.96 |
| 30 | 24.50 | 1019.90 | 1.1946 | 940 | 24.51 | 24.1091 | 1020.19 | 371545 | 1.2666 | 0.0391 | 329.16 |
| 40 | 24.50 | 1020.17 | 1.1949 | 1213 | 24.50 | 24.1094 | 1020.16 | 376565 | 1.2879 | 0.0507 | 324.78 |
| 50 | 24.48 | 1020.33 | 1.1952 | 1482 | 24.50 | 24.0997 | 1020.39 | 381291 | 1.3088 | 0.0619 | 320.75 |
| 60 | 24.45 | 1020.73 | 1.1958 | 1737 | 24.45 | 24.0607 | 1020.93 | 385669 | 1.3289 | 0.0723 | 317.11 |
| 70 | 24.44 | 1021.01 | 1.1962 | 1987 | 24.45 | 24.0520 | 1021.00 | 389921 | 1.3484 | 0.0829 | 313.65 |
| 80 | 24.43 | 1021.40 | 1.1967 | 2237 | 24.44 | 24.0509 | 1021.36 | 394025 | 1.3681 | 0.0933 | 310.39 |
| 90 | 24.43 | 1021.77 | 1.1971 | 2489 | 24.43 | 24.0482 | 1022.09 | 397928 | 1.3879 | 0.1034 | 307.34 |
| 95 | 24.42 | 1022.33 | 1.1978 | 2611 | 24.45 | 24.0576 | 1022.59 | 399831 | 1.3979 | 0.1085 | 305.88 |
| Data used for pathlength calibration (the first zero step): $T_{SoS}$ = 24.0655 °C, $P$ = 1019.21 mbar, $t_m^0$ = 353601 ns, $W^0$ = 345.87 m/s. | | | | | | | | | | | |

Table 157. n-Butylamine/dry air results (35 °C isotherm)

| $x_T$/%SAT | Zero Step | | | $\Delta m_{read}$/µg | Non-Zero Step | | | | | | |
|---|---|---|---|---|---|---|---|---|---|---|---|
| | $T_{DVS}$/°C | $P$/mbar | $\rho^0$/(kg/m$^3$) | | $T_{DVS}$/°C | $T_{SoS}$/°C | $P$/mbar | $t_m$/ns | $\rho$/(kg/m$^3$) | $x$ | $W_m$/(m/s) |
| 10 | 34.29 | 1023.16 | 1.1602 | 566 | 34.32 | 33.8931 | 1023.51 | 358908 | 1.2035 | 0.0242 | 340.53 |
| 20 | 34.30 | 1023.77 | 1.1608 | 1049 | 34.33 | 33.8927 | 1023.73 | 368050 | 1.2412 | 0.0452 | 332.07 |
| 30 | 34.39 | 1023.49 | 1.1602 | 1518 | 34.44 | 34.0094 | 1023.36 | 376338 | 1.2765 | 0.0655 | 324.75 |
| 40 | 34.40 | 1023.33 | 1.1600 | 1947 | 34.41 | 33.9899 | 1023.29 | 383749 | 1.3092 | 0.0838 | 318.48 |
| 50 | 34.39 | 1023.10 | 1.1597 | 2352 | 34.40 | 33.9723 | 1022.97 | 390572 | 1.3400 | 0.1013 | 312.92 |
| 60 | 34.39 | 1022.57 | 1.1591 | 2729 | 34.40 | 33.9638 | 1022.02 | 396850 | 1.3683 | 0.1178 | 307.97 |
| 70 | 34.38 | 1022.00 | 1.1585 | 3100 | 34.37 | 33.9429 | 1021.85 | 402614 | 1.3961 | 0.1335 | 303.56 |
| 80 | 34.34 | 1021.61 | 1.1582 | 3450 | 34.33 | 33.9049 | 1021.49 | 408074 | 1.4226 | 0.1485 | 299.50 |
| 90 | 34.40 | 1021.41 | 1.1578 | 3808 | 34.40 | 33.9693 | 1021.27 | 413427 | 1.4496 | 0.1640 | 295.62 |
| 95 | 34.40 | 1021.16 | 1.1575 | 3975 | 34.41 | 33.9795 | 1021.13 | 415811 | 1.4621 | 0.1711 | 293.93 |
| Data used for pathlength calibration (the first zero step): $T_{SoS}$ = 33.8762 °C, $P$ = 1023.16 mbar, $t_m^0$ = 347662 ns, $W^0$ = 351.54 m/s. | | | | | | | | | | | |

Table 158. n-Butylamine/dry air results (45 °C isotherm)

| $x_T$/%SAT | Zero Step | | | $\Delta m_{read}$/µg | Non-Zero Step | | | | | | |
|---|---|---|---|---|---|---|---|---|---|---|---|
| | $T_{DVS}$/°C | $P$/mbar | $\rho^0$/(kg/m$^3$) | | $T_{DVS}$/°C | $T_{SoS}$/°C | $P$/mbar | $t_m$/ns | $\rho$/(kg/m$^3$) | $x$ | $W_m$/(m/s) |
| 10 | 43.83 | 1017.11 | 1.1185 | 931 | 43.90 | 43.5195 | 1017.14 | 360732 | 1.1898 | 0.0417 | 338.43 |
| 20 | 43.88 | 1017.58 | 1.1188 | 1712 | 43.91 | 43.5479 | 1017.67 | 374975 | 1.2501 | 0.0764 | 325.58 |
| 30 | 43.89 | 1017.49 | 1.1187 | 2399 | 43.91 | 43.5579 | 1017.31 | 386885 | 1.3026 | 0.1072 | 315.56 |
| 40 | 43.89 | 1017.40 | 1.1186 | 3009 | 43.92 | 43.5407 | 1017.33 | 396920 | 1.3492 | 0.1343 | 307.58 |
| 50 | 43.97 | 1017.00 | 1.1179 | 3583 | 43.91 | 43.5552 | 1017.01 | 405907 | 1.3924 | 0.1596 | 300.77 |
| 60 | 43.90 | 1016.86 | 1.1180 | 4087 | 43.89 | 43.5395 | 1016.64 | 413715 | 1.4312 | 0.1823 | 295.09 |
| 70 | 43.87 | 1016.37 | 1.1176 | 4558 | 43.87 | 43.5219 | 1016.19 | 420701 | 1.4669 | 0.2032 | 290.19 |
| 80 | 43.85 | 1016.01 | 1.1172 | 5002 | 43.85 | 43.5081 | 1015.94 | 427085 | 1.5005 | 0.2229 | 285.85 |
| 90 | 43.86 | 1015.83 | 1.1170 | 5404 | 43.94 | 43.5286 | 1015.99 | 432742 | 1.5311 | 0.2408 | 282.12 |
| 95 | 43.95 | 1016.21 | 1.1171 | 5598 | 43.92 | 43.5537 | 1016.42 | 435198 | 1.5461 | 0.2490 | 280.52 |
| Data used for pathlength calibration (the first zero step): $T_{SoS}$ = 43.4565 °C, $P$ = 1017.11 mbar, $t_m^0$ = 341980 ns, $W^0$ = 356.99 m/s. | | | | | | | | | | | |

## A6.22 Limonene/dry air

Table 159. Limonene/dry air results (25 °C isotherm)

| $x_T$/%SAT | Zero Step | | | $\Delta m_{read}$/µg | Non-Zero Step | | | | | | |
|---|---|---|---|---|---|---|---|---|---|---|---|
| | $T_{DVS}$/°C | $P$/mbar | $\rho^0$/(kg/m$^3$) | | $T_{DVS}$/°C | $T_{SoS}$/°C | $P$/mbar | $t_m$/ns | $\rho$/(kg/m$^3$) | $x$ | $W_m$/(m/s) |
| 10 | 24.35 | 1009.92 | 1.1835 | 13 | 24.39 | 23.9494 | 1010.06 | 353907 | 1.1845 | 0.00023 | 345.63 |
| 20 | 24.34 | 1009.98 | 1.1836 | 33 | 24.35 | 23.9213 | 1010.60 | 354107 | 1.1862 | 0.00041 | 345.44 |
| 30 | 24.29 | 1009.94 | 1.1838 | 37 | 24.31 | 23.8710 | 1010.17 | 354319 | 1.1866 | 0.00060 | 345.23 |
| 40 | 24.31 | 1010.04 | 1.1838 | 51 | 24.35 | 23.8955 | 1010.47 | 354479 | 1.1877 | 0.00081 | 345.07 |
| 50 | 24.33 | 1010.79 | 1.1846 | 55 | 24.35 | 23.9028 | 1011.00 | 354643 | 1.1889 | 0.00093 | 344.91 |
| 60 | 24.32 | 1011.21 | 1.1852 | 67 | 24.37 | 23.9178 | 1011.46 | 354808 | 1.1903 | 0.00114 | 344.75 |
| 70 | 24.36 | 1011.58 | 1.1854 | 66 | 24.38 | 23.9327 | 1010.97 | 354956 | 1.1905 | 0.00133 | 344.61 |
| 80 | 24.35 | 1011.45 | 1.1853 | 91 | 24.36 | 23.9177 | 1012.08 | 355109 | 1.1923 | 0.00143 | 344.46 |
| 90 | 24.29 | 1012.69 | 1.1870 | 95 | 24.34 | 23.8890 | 1013.16 | 355221 | 1.1943 | 0.00157 | 344.35 |
| 95 | 24.28 | 1013.40 | 1.1879 | 95 | 24.28 | 23.8384 | 1013.91 | 355264 | 1.1952 | 0.00152 | 344.31 |
| Data used for pathlength calibration (the first zero step): $T_{SoS}$ = 23.8978 °C, $P$ = 1009.92 mbar, $t_m^0$ = 353764 ns, $W^0$ = 345.77 m/s. | | | | | | | | | | | |

Table 160. Limonene/dry air results (35 °C isotherm)

| $x_T$/%SAT | Zero Step | | | $\Delta m_{read}$/µg | Non-Zero Step | | | | | | |
|---|---|---|---|---|---|---|---|---|---|---|---|
| | $T_{DVS}$/°C | $P$/mbar | $\rho^0$/(kg/m$^3$) | | $T_{DVS}$/°C | $T_{SoS}$/°C | $P$/mbar | $t_m$/ns | $\rho$/(kg/m$^3$) | $x$ | $W_m$/(m/s) |
| 10 | 34.21 | 1018.29 | 1.1550 | 23 | 34.26 | 33.9053 | 1018.44 | 348010 | 1.1567 | 0.00042 | 351.20 |
| 20 | 34.29 | 1018.71 | 1.1551 | 48 | 34.30 | 33.9331 | 1019.18 | 348349 | 1.1588 | 0.00074 | 350.86 |
| 30 | 34.31 | 1019.24 | 1.1557 | 63 | 34.33 | 33.9608 | 1019.36 | 348688 | 1.1604 | 0.00110 | 350.52 |
| 40 | 34.23 | 1019.63 | 1.1564 | 76 | 34.31 | 33.9434 | 1019.82 | 349045 | 1.1622 | 0.00137 | 350.16 |
| 50 | 34.31 | 1019.87 | 1.1564 | 95 | 34.35 | 33.9920 | 1019.71 | 349365 | 1.1636 | 0.00177 | 349.84 |
| 60 | 34.37 | 1019.80 | 1.1561 | 115 | 34.40 | 34.0554 | 1019.66 | 349675 | 1.1649 | 0.00212 | 349.53 |
| 70 | 34.39 | 1019.52 | 1.1557 | 139 | 34.41 | 34.0652 | 1019.62 | 350006 | 1.1663 | 0.00247 | 349.20 |
| 80 | 34.41 | 1019.75 | 1.1559 | 156 | 34.43 | 34.0734 | 1019.92 | 350337 | 1.1678 | 0.00276 | 348.87 |
| 90 | 34.41 | 1020.15 | 1.1563 | 169 | 34.28 | 33.9367 | 1020.07 | 350691 | 1.1693 | 0.00293 | 348.52 |
| 95 | 34.28 | 1020.37 | 1.1570 | 175 | 34.36 | 33.9876 | 1020.53 | 350774 | 1.1705 | 0.00315 | 348.43 |
| Data used for pathlength calibration (the first zero step): $T_{SoS}$ = 33.8541 °C, $P$ = 1018.29 mbar, $t_m^0$ = 347685 ns, $W^0$ = 351.53 m/s. | | | | | | | | | | | |

Table 161. Limonene/dry air results (45 °C isotherm)

| $x_T$/%SAT | Zero Step | | | $\Delta m_{read}$/µg | Non-Zero Step | | | | | | |
|---|---|---|---|---|---|---|---|---|---|---|---|
| | $T_{DVS}$/°C | $P$/mbar | $\rho^0$/(kg/m$^3$) | | $T_{DVS}$/°C | $T_{SoS}$/°C | $P$/mbar | $t_m$/ns | $\rho$/(kg/m$^3$) | $x$ | $W_m$/(m/s) |
| 10 | 43.85 | 1020.37 | 1.1220 | 33 | 43.87 | 43.5225 | 1020.27 | 342766 | 1.1245 | 0.00064 | 356.34 |
| 20 | 43.88 | 1020.36 | 1.1219 | 69 | 43.91 | 43.5048 | 1020.55 | 343404 | 1.1272 | 0.00125 | 355.68 |
| 30 | 43.94 | 1020.52 | 1.1219 | 104 | 43.94 | 43.5676 | 1020.53 | 344003 | 1.1298 | 0.00190 | 355.06 |
| 40 | 43.94 | 1020.40 | 1.1217 | 132 | 43.94 | 43.5851 | 1020.16 | 344608 | 1.1318 | 0.00248 | 354.43 |
| 50 | 43.93 | 1020.06 | 1.1214 | 164 | 43.93 | 43.5856 | 1019.73 | 345228 | 1.1339 | 0.00310 | 353.80 |
| 60 | 43.88 | 1019.71 | 1.1212 | 197 | 43.88 | 43.5525 | 1019.49 | 345838 | 1.1362 | 0.00367 | 353.17 |
| 70 | 43.87 | 1019.44 | 1.1209 | 226 | 43.88 | 43.5362 | 1019.10 | 346450 | 1.1383 | 0.00426 | 352.55 |
| 80 | 43.90 | 1018.67 | 1.1200 | 271 | 43.88 | 43.5261 | 1018.79 | 347058 | 1.1407 | 0.00494 | 351.93 |
| 90 | 43.87 | 1018.58 | 1.1200 | 299 | 43.92 | 43.5711 | 1018.49 | 347624 | 1.1429 | 0.00557 | 351.36 |
| 95 | 43.90 | 1018.51 | 1.1198 | 303 | 43.84 | 43.5182 | 1018.29 | 347849 | 1.1430 | 0.00559 | 351.13 |
| Data used for pathlength calibration (the first zero step): $T_{SoS}$ = 43.5101 °C, $P$ = 1020.37 mbar, $t_m^0$ = 342112 ns, $W^0$ = 357.02 m/s. | | | | | | | | | | | |

## A6.23 α-Pinene/dry air

Table 162. α-Pinene/dry air results (25 °C isotherm)

| $x_T$/%SAT | Zero Step | | | $\Delta m_{read}$/µg | Non-Zero Step | | | | | | |
|---|---|---|---|---|---|---|---|---|---|---|---|
| | $T_{DVS}$/°C | $P$/mbar | $\rho^0$/(kg/m$^3$) | | $T_{DVS}$/°C | $T_{SoS}$/°C | $P$/mbar | $t_m$/ns | $\rho$/(kg/m$^3$) | $x$ | $W_m$/(m/s) |
| 10 | 24.38 | 1018.91 | 1.1939 | 44 | 24.41 | 24.0484 | 1019.32 | 354187 | 1.1973 | 0.00067 | 345.28 |
| 20 | 24.42 | 1019.60 | 1.1946 | 69 | 24.45 | 24.0773 | 1019.71 | 354751 | 1.1999 | 0.00119 | 344.73 |
| 30 | 24.42 | 1019.61 | 1.1946 | 98 | 24.42 | 24.0593 | 1019.53 | 355328 | 1.2021 | 0.00171 | 344.17 |
| 40 | 24.41 | 1019.50 | 1.1945 | 130 | 24.43 | 24.0607 | 1019.36 | 355886 | 1.2045 | 0.00230 | 343.63 |
| 50 | 24.41 | 1019.10 | 1.1941 | 159 | 24.44 | 24.0692 | 1018.84 | 356428 | 1.2062 | 0.00284 | 343.11 |
| 60 | 24.41 | 1018.87 | 1.1938 | 190 | 24.41 | 24.0457 | 1018.58 | 356990 | 1.2083 | 0.00335 | 342.57 |
| 70 | 24.39 | 1018.65 | 1.1936 | 225 | 24.40 | 24.0316 | 1018.68 | 357534 | 1.2109 | 0.00389 | 342.05 |
| 80 | 24.37 | 1018.32 | 1.1933 | 259 | 24.40 | 24.0249 | 1018.59 | 358073 | 1.2131 | 0.00443 | 341.53 |
| 90 | 24.36 | 1018.67 | 1.1938 | 285 | 24.38 | 24.0135 | 1018.71 | 358589 | 1.2156 | 0.00493 | 341.04 |
| 95 | 24.34 | 1018.91 | 1.1941 | 294 | 24.35 | 23.9956 | 1018.99 | 358794 | 1.2167 | 0.00508 | 340.85 |
| Data used for pathlength calibration (the first zero step): $T_{SoS}$ = 24.0275 °C, $P$ = 1018.91 mbar, $t_m^0$ = 353607 ns, $W^0$ = 345.85 m/s. | | | | | | | | | | | |

Table 163. α-Pinene/dry air results (35 °C isotherm)

| $x_T$/%SAT | Zero Step | | | $\Delta m_{read}$/µg | Non-Zero Step | | | | | | |
|---|---|---|---|---|---|---|---|---|---|---|---|
| | $T_{DVS}$/°C | $P$/mbar | $\rho^0$/(kg/m$^3$) | | $T_{DVS}$/°C | $T_{SoS}$/°C | $P$/mbar | $t_m$/ns | $\rho$/(kg/m$^3$) | $x$ | $W_m$/(m/s) |
| 10 | 34.32 | 1018.69 | 1.1550 | 65 | 34.32 | 33.9343 | 1018.94 | 348706 | 1.1600 | 0.00109 | 350.51 |
| 20 | 34.36 | 1019.36 | 1.1556 | 121 | 34.38 | 33.9855 | 1019.63 | 349707 | 1.1649 | 0.00211 | 349.50 |
| 30 | 34.39 | 1019.93 | 1.1561 | 173 | 34.43 | 34.0126 | 1020.05 | 350700 | 1.1694 | 0.00308 | 348.51 |
| 40 | 34.42 | 1020.22 | 1.1563 | 234 | 34.42 | 33.9942 | 1020.41 | 351698 | 1.1742 | 0.00411 | 347.52 |
| 50 | 34.41 | 1020.54 | 1.1567 | 281 | 34.42 | 33.9906 | 1020.55 | 352661 | 1.1782 | 0.00501 | 346.58 |
| 60 | 34.38 | 1020.36 | 1.1567 | 334 | 34.46 | 34.0375 | 1020.30 | 353618 | 1.1822 | 0.00604 | 345.64 |
| 70 | 34.41 | 1020.49 | 1.1567 | 388 | 34.41 | 33.9806 | 1020.52 | 354576 | 1.1864 | 0.00691 | 344.70 |
| 80 | 34.40 | 1020.54 | 1.1568 | 445 | 34.41 | 33.9709 | 1020.82 | 355526 | 1.1909 | 0.00787 | 343.78 |
| 90 | 34.41 | 1021.10 | 1.1574 | 495 | 34.42 | 33.9776 | 1021.15 | 356464 | 1.1953 | 0.00882 | 342.88 |
| 95 | 34.40 | 1021.45 | 1.1578 | 516 | 34.41 | 33.9663 | 1021.61 | 356860 | 1.1974 | 0.00916 | 342.50 |
| Data used for pathlength calibration (the first zero step): $T_{SoS}$ = 33.9330 °C, $P$ = 1018.69 mbar, $t_m^0$ = 347648 ns, $W^0$ = 351.57 m/s. | | | | | | | | | | | |

Table 164. α-Pinene/dry air results (45 °C isotherm)

| $x_T$/%SAT | Zero Step | | | $\Delta m_{read}$/µg | Non-Zero Step | | | | | | |
|---|---|---|---|---|---|---|---|---|---|---|---|
| | $T_{DVS}$/°C | $P$/mbar | $\rho^0$/(kg/m$^3$) | | $T_{DVS}$/°C | $T_{SoS}$/°C | $P$/mbar | $t_m$/ns | $\rho$/(kg/m$^3$) | $x$ | $W_m$/(m/s) |
| 10 | 43.83 | 1021.73 | 1.1236 | 102 | 43.82 | 43.4792 | 1021.88 | 343935 | 1.1314 | 0.0018 | 355.17 |
| 20 | 43.84 | 1022.18 | 1.1240 | 191 | 43.90 | 43.5093 | 1022.38 | 345633 | 1.1387 | 0.0035 | 353.42 |
| 30 | 43.89 | 1022.55 | 1.1243 | 281 | 43.87 | 43.5398 | 1022.61 | 347284 | 1.1458 | 0.0051 | 351.74 |
| 40 | 43.86 | 1022.54 | 1.1244 | 370 | 43.88 | 43.5495 | 1022.64 | 348910 | 1.1527 | 0.0068 | 350.10 |
| 50 | 43.85 | 1022.60 | 1.1245 | 452 | 43.91 | 43.5025 | 1022.57 | 350508 | 1.1591 | 0.0084 | 348.51 |
| 60 | 43.90 | 1022.61 | 1.1243 | 544 | 43.90 | 43.5260 | 1022.50 | 352077 | 1.1660 | 0.0100 | 346.95 |
| 70 | 43.87 | 1022.35 | 1.1241 | 626 | 43.88 | 43.5129 | 1022.20 | 353617 | 1.1721 | 0.0115 | 345.44 |
| 80 | 43.86 | 1022.07 | 1.1239 | 715 | 43.84 | 43.5140 | 1021.92 | 355155 | 1.1787 | 0.0132 | 343.95 |
| 90 | 43.87 | 1021.89 | 1.1236 | 804 | 43.83 | 43.4986 | 1021.92 | 356678 | 1.1852 | 0.0147 | 342.48 |
| 95 | 43.83 | 1022.22 | 1.1241 | 840 | 43.83 | 43.5011 | 1022.37 | 357348 | 1.1885 | 0.0154 | 341.84 |
| Data used for pathlength calibration (the first zero step): $T_{SoS}$ = 43.4971 °C, $P$ = 1021.73 mbar, $t_m^0$ = 342157 ns, $W^0$ = 357.01 m/s. | | | | | | | | | | | |